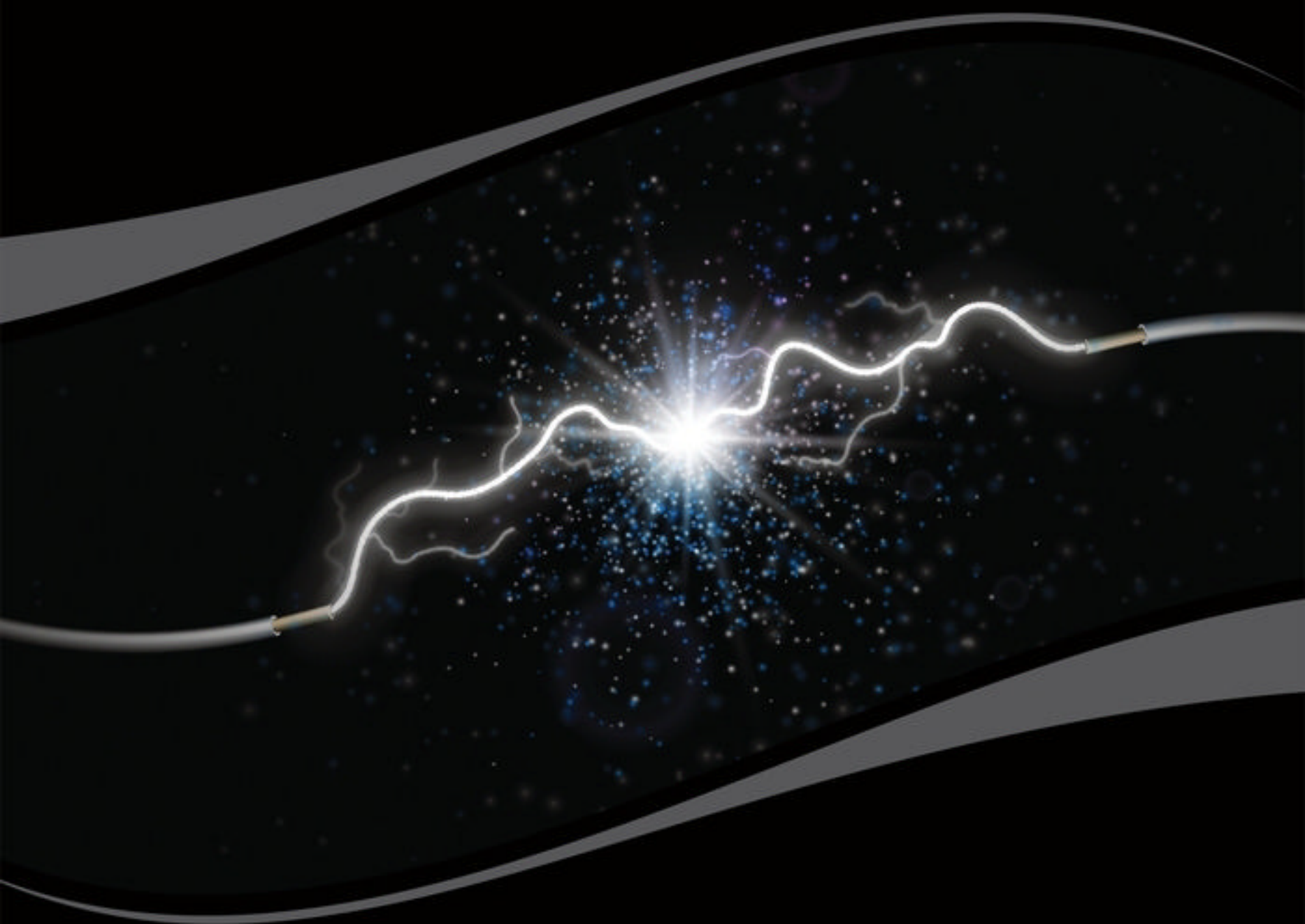


Premier Reference Source

Applications, Challenges, and Advancements in Electromyography Signal Processing



Ganesh R. Naik



Applications, Challenges, and Advancements in Electromyography Signal Processing

Ganesh R. Naik
University of Technology Sydney (UTS), Australia

A volume in the Advances in Medical
Technologies and Clinical Practice (AMTCP) Book
Series

Medical Information Science
REFERENCE

An Imprint of IGI Global

Managing Director: Lindsay Johnston
Production Editor: Jennifer Yoder
Development Editor: Allison McGinniss
Acquisitions Editor: Kayla Wolfe
Typesetter: James Knapp
Cover Design: Jason Mull

Published in the United States of America by
Medical Information Science Reference (an imprint of IGI Global)
701 E. Chocolate Avenue
Hershey PA 17033
Tel: 717-533-8845
Fax: 717-533-8661
E-mail: cust@igi-global.com
Web site: <http://www.igi-global.com>

Copyright © 2014 by IGI Global. All rights reserved. No part of this publication may be reproduced, stored or distributed in any form or by any means, electronic or mechanical, including photocopying, without written permission from the publisher. Product or company names used in this set are for identification purposes only. Inclusion of the names of the products or companies does not indicate a claim of ownership by IGI Global of the trademark or registered trademark.

Library of Congress Cataloging-in-Publication Data

Applications, challenges, and advancements in electromyography signal processing / Ganesh R. Naik, editor.
p. ; cm.

Includes bibliographical references and index. Summary: "This book provides an updated overview of signal processing applications and recent developments in EMG from a number of diverse aspects and various applications in clinical and experimental research"--Provided by publisher.

ISBN 978-1-4666-6090-8 (hardcover) -- ISBN 978-1-4666-6091-5 (ebook) -- ISBN 978-1-4666-6093-9 (print & perpetual access) I. Naik, Ganesh R., editor. [DNLM: 1. Electromyography. 2. Models, Biological. 3. Musculoskeletal Physiological Processes. WE 500]

RC77.5

616.7'407547--dc23

2014008006

This book is published in the IGI Global book series Advances in Medical Technologies and Clinical Practice (AMTCP) (ISSN: 2327-9354; eISSN: 2327-9370)

British Cataloguing in Publication Data

A Cataloguing in Publication record for this book is available from the British Library.

All work contributed to this book is new, previously-unpublished material. The views expressed in this book are those of the authors, but not necessarily of the publisher.

For electronic access to this publication, please contact: eresources@igi-global.com.



Advances in Medical Technologies and Clinical Practice (AMTCP) Book Series

Srikanta Patnaik
SOA University, India

Priti Das
S.C.B. Medical College, India

ISSN: 2327-9354
EISSN: 2327-9370

MISSION

Medical technological innovation continues to provide avenues of research for faster and safer diagnosis and treatments for patients. Practitioners must stay up to date with these latest advancements to provide the best care for nursing and clinical practices.

The **Advances in Medical Technologies and Clinical Practice (AMTCP) Book Series** brings together the most recent research on the latest technology used in areas of nursing informatics, clinical technology, biomedicine, diagnostic technologies, and more. Researchers, students, and practitioners in this field will benefit from this fundamental coverage on the use of technology in clinical practices.

COVERAGE

- Biomedical Applications
- Clinical Data Mining
- Clinical High-Performance Computing
- Clinical Studies
- Diagnostic Technologies
- E-Health
- Medical Imaging
- Neural Engineering
- Nursing Informatics
- Patient-Centered Care

IGI Global is currently accepting manuscripts for publication within this series. To submit a proposal for a volume in this series, please contact our Acquisition Editors at Acquisitions@igi-global.com or visit: <http://www.igi-global.com/publish/>.

The Advances in Medical Technologies and Clinical Practice (AMTCP) Book Series (ISSN 2327-9354) is published by IGI Global, 701 E. Chocolate Avenue, Hershey, PA 17033-1240, USA, www.igi-global.com. This series is composed of titles available for purchase individually; each title is edited to be contextually exclusive from any other title within the series. For pricing and ordering information please visit <http://www.igi-global.com/book-series/advances-medical-technologies-clinical-practice/73682>. Postmaster: Send all address changes to above address. Copyright © 2014 IGI Global. All rights, including translation in other languages reserved by the publisher. No part of this series may be reproduced or used in any form or by any means – graphics, electronic, or mechanical, including photocopying, recording, taping, or information and retrieval systems – without written permission from the publisher, except for non commercial, educational use, including classroom teaching purposes. The views expressed in this series are those of the authors, but not necessarily of IGI Global.

Titles in this Series

For a list of additional titles in this series, please visit: www.igi-global.com

Enhancing the Human Experience through Assistive Technologies and E-Accessibility

Christos Kouroupetroglou (Caretta-Net Technologies, Greece)

Medical Information Science Reference • copyright 2014 • 345pp • H/C (ISBN: 9781466661301) • US \$265.00 (our price)

Applications, Challenges, and Advancements in Electromyography Signal Processing

Ganesh R. Naik (University of Technology Sydney (UTS), Australia)

Medical Information Science Reference • copyright 2014 • 323pp • H/C (ISBN: 9781466660908) • US \$235.00 (our price)

Innovative Technologies to Benefit Children on the Autism Spectrum

Nava R. Siltan (Marymount Manhattan College, USA)

Medical Information Science Reference • copyright 2014 • 343pp • H/C (ISBN: 9781466657922) • US \$195.00 (our price)

Assistive Technology Research, Practice, and Theory

Boaventura DaCosta (Solers Research Group, USA) and Soonhwa Seok (Korea University, South Korea)

Medical Information Science Reference • copyright 2014 • 342pp • H/C (ISBN: 9781466650152) • US \$200.00 (our price)

Assistive Technologies and Computer Access for Motor Disabilities

Georgios Kouroupetroglou (University of Athens, Greece)

Medical Information Science Reference • copyright 2014 • 433pp • H/C (ISBN: 9781466644380) • US \$200.00 (our price)

Disability Informatics and Web Accessibility for Motor Limitations

Georgios Kouroupetroglou (University of Athens, Greece)

Medical Information Science Reference • copyright 2014 • 443pp • H/C (ISBN: 9781466644427) • US \$200.00 (our price)

Medical Advancements in Aging and Regenerative Technologies Clinical Tools and Applications

Andriani Daskalaki (Max Planck Institute for Molecular Genetics, Germany)

Medical Information Science Reference • copyright 2013 • 598pp • H/C (ISBN: 9781466625068) • US \$245.00 (our price)



www.igi-global.com

701 E. Chocolate Ave., Hershey, PA 17033

Order online at www.igi-global.com or call 717-533-8845 x100

To place a standing order for titles released in this series, contact: cust@igi-global.com

Mon-Fri 8:00 am - 5:00 pm (est) or fax 24 hours a day 717-533-8661

List of Reviewers

Emilia Ambrosini, *Politecnico di Milano*, Italy
Parveen Bawa, *Simon Fraser University*, Canada
Sébastien Boyas, *Université du Maine*, France
Varsha Chorsiya, *National Institute of Occupational Health*, India
Simona Ferrante, *Politecnico di Milano*, Italy
P. Geethanjali, *VIT University*, India
İmran Göker, *Istanbul Arel University*, Turkey
Dianne M. Ikeda, *University of Waterloo*, Canada
Kelvin E Jones, *University of Alberta*, Canada
Johann P. Kultz-Buschbeck, *Christian-Albrechts-University Kiel*, Germany
Le Li, *Sun Yat-sen University*, China
Sérgio Marta, *Universidade de Lisboa*, Portugal
Alessandra Pedrocchi, *Politecnico di Milano*, Italy
Angkoon Phinyomark, *University Joseph Fourier, France & University of Grenoble*, France
Daniel Robbins, *University of Bedfordshire*, UK
Andrés Felipe Ruiz-Olaya, *Antonio Nariño University*, Colombia

Table of Contents

Preface	xv
----------------------	----

Section 1 **EMG Basics and Motor Unit Action Potentials**

Chapter 1

Neural Control of Muscle	1
<i>Parveen Bawa, Simon Fraser University, Canada</i>	
<i>Kelvin E. Jones, University of Alberta, Canada</i>	

Chapter 2

New Advances in Single Fiber Electromyography	28
<i>Javier Rodriguez-Falces, Public University of Navarra, Spain</i>	

Chapter 3

Detection and Conditioning of EMG	58
<i>İmran Göker, Istanbul Arel University, Turkey</i>	

Chapter 4

An Introduction to EMG Signal Processing Using MatLab and Microsoft Excel.....	95
<i>Daniel Robbins, University of Bedfordshire, UK</i>	

Section 2 **EMG Signal Modeling and Signal Processing**

Chapter 5

Modeling the Human Elbow Joint Dynamics from Surface Electromyography	114
<i>Andrés Felipe Ruiz-Olaya, Antonio Nariño University, Colombia</i>	

Chapter 6

Arm Swing during Human Gait Studied by EMG of Upper Limb Muscles	129
<i>Johann P. Kuhtz-Buschbeck, Christian-Albrechts-University Kiel, Germany</i>	
<i>Antonia Frenzel, Christian-Albrechts-University Kiel, Germany</i>	
<i>Bo Jing, Christian-Albrechts-University Kiel, Germany</i>	

Chapter 7

- Using in Vivo Subject-Specific Musculotendon Parameters to Investigate Voluntary Movement Changes after Stroke: An EMG-Driven Model of Elbow Joint 161
Hujing Hu, First Affiliated Hospital, Sun Yat-sen University, China & Guangdong Provincial Work Injury Rehabilitation Center, China
Le Li, First Affiliated Hospital, Sun Yat-sen University, China

Chapter 8

- Study and Interpretation of Neuromuscular Patterns in Golf 181
Sérgio Marta, CIPER, Faculdade de Motricidade Humana, Universidade de Lisboa, Portugal
João Rocha Vaz, CIPER, Faculdade de Motricidade Humana, Universidade de Lisboa, Portugal
Luís Silva, CIPER, Faculdade de Motricidade Humana, Universidade de Lisboa, Portugal
Maria António Castro, Coimbra Health School, Instituto Politécnico de Coimbra, Portugal & Mechanical Engineering Research Center, University of Coimbra, Portugal
Pedro Pezarat Correia, CIPER, Faculdade de Motricidade Humana, Universidade de Lisboa, Portugal

Section 3

EMG: Endurance, Stability, and Muscle Activities

Chapter 9

- Assessing Joint Stability from Eigenvalues Obtained from Multi-Channel EMG: A Spine Example 203
Dianne M. Ikeda, University of Waterloo, Canada
Stuart M. McGill, University of Waterloo, Canada

Chapter 10

- Endurance Time Prediction using Electromyography 219
Sébastien Boyas, Université du Maine, France
Arnaud Guével, Université de Nantes, France

Chapter 11

- EMG Activation Pattern during Voluntary Bending and Donning Safety Shoes 234
P. K. Nag, National Institute of Occupational Health, India
Varsha Chorsiya, National Institute of Occupational Health, India
Anjali Nag, National Institute of Occupational Health, India

Chapter 12

- Tongue Movement Estimation Based on Suprahyoid Muscle Activity 257
Makoto Sasaki, Iwate University, Japan

Section 4

EMG for Prosthetic and HCI Applications

Chapter 13

- Design of Myocontrolled Neuroprosthesis: Tricks and Pitfalls 275
Emilia Ambrosini, Politecnico di Milano, Italy
Simona Ferrante, Politecnico di Milano, Italy
Alessandro Pedrocchi, Politecnico di Milano, Italy

Chapter 14

- Design and Development of EMG Conditioning System and Hand Gesture Recognition Based on Principal Component Analysis Feature Reduction Technique..... 304
P. Geethanjali, VIT University, India

Chapter 15

- The Relationship between Anthropometric Variables and Features of Electromyography Signal for Human–Computer Interface 321
Angkoon Phinyomark, University Joseph Fourier, France & University of Grenoble, France
Franck Quaine, University Joseph Fourier, France
Yann Laurillau, University of Grenoble, France

- Compilation of References** 354

- About the Contributors** 396

- Index**..... 402

Detailed Table of Contents

Preface	xv
----------------------	----

Section 1 **EMG Basics and Motor Unit Action Potentials**

Chapter 1

Neural Control of Muscle	1
<i>Parveen Bawa, Simon Fraser University, Canada</i>	
<i>Kelvin E. Jones, University of Alberta, Canada</i>	

Chapter 1 is titled “Neural Control of Muscle”. In this chapter, ParveenBawa and Kelvin Jones explain the ideas and concepts about the manner in which the central nervous system controls muscle contraction. The populations of motor units comprising a skeletal muscle have a diverse range of physiological and anatomical properties. The Size Principle of motor unit recruitment is a concept that proposes a simple strategy for exploiting the diversity of the motor unit population to produce graded force output. The Size Principle has a great deal of empirical support, but also faces criticism about the extent of generalization to all types and forms of movement. As the key principles of motor units are discussed, methods of measuring and methodology for analysing motor unit activity and whole muscle activities are introduced.

Chapter 2

New Advances in Single Fiber Electromyography	28
<i>Javier Rodriguez-Falces, Public University of Navarra, Spain</i>	

Chapter 2 is titled “New Advances in Single Fibre Electromyography”. In this chapter, Javier Rodriguez-Falces explains a general perspective of SFEMG together with a description of the anatomical, physiological, and technical aspects that are involved in the recording of single fibre action potentials (SFAPs). First, a simulation model that relates analytically the intracellular action potential (IAP) and SFAP mathematical expressions is described. Second, the most recent findings regarding the shape features of human SFAPs are outlined. Third, a description of how different types of needle electrodes affect the characteristics of the recorded potential is detailed. Fourth, an explanation of the most important effects of filtering on the SFAP characteristics is provided. Finally, a description of the principles of jitter estimation together with the most important sources of errors is presented.

Chapter 3

Detection and Conditioning of EMG	58
<i>İmran Göker, Istanbul Arel University, Turkey</i>	

Chapter 3 is titled “Detection and Conditioning of EMG”. In this chapter, İmran Göker explains the monitoring of the electrical activity of skeletal muscles. The main components of the detection and conditioning of the EMG signals are explained in the sense of the biomedical instrumentation. At first,

a brief description of EMG generation is introduced. Next, the hardware components of the general instrumentation system used in the acquisition of EMG signal such as amplifier, filters, analog-to-digital converter are discussed in detail. Subsequently, different types of electrodes used in different EMG techniques are mentioned. Then, various EMG signals that can be detected and monitored via EMG systems are described and their clinical importance are discussed in detail. Finally, different EMG techniques used in clinical studies and their purposes are highlighted.

Chapter 4

An Introduction to EMG Signal Processing Using MatLab and Microsoft Excel..... 95

Daniel Robbins, University of Bedfordshire, UK

Chapter 4 is titled “An Introduction to Signal Processing using MatLab and Microsoft Excel”. In this chapter, Daniel Robbins explains the fundamentals of biological signal analysis and processing, using EMG signals to illustrate the process. The areas covered within the chapter include: frequency analysis using the Fast Fourier Transform, identifying noise within a signal, signal smoothing via root mean square (RMS) processing and signal filtering with both low-pass and high-pass filters. Guidelines for the application of the processes covered are included in conjunction with step by step examples using both MathWorks MatLab and Microsoft Excel software. Following the examples therefore allows the reader to practice the processes described to promote and reinforce their learning.

Section 2

EMG Signal Modeling and Signal Processing

Chapter 5

Modeling the Human Elbow Joint Dynamics from Surface Electromyography 114

Andrés Felipe Ruiz-Olaya, Antonio Nariño University, Colombia

Chapter 5 is titled “Modeling the Human Elbow Joint Dynamics From Surface Electromyography”. In this chapter, Andrés Felipe Ruiz-Olaya describes an approximation for non-invasive biomechanical modelling of the elbow joint dynamics from electromyographic information. A case study presents results obtained aimed at deriving a relationship between the dynamic behaviour of the human elbow joint and surface Electromyography (sEMG) information in postural control. A set of experiments were carried out to measure bioelectrical (sEMG) and biomechanics information from human elbow joint, during postural control (i.e. isometric contractions) and correlate them with mechanical impedance at elbow joint. Estimates of elbow impedance were obtained by applying torque perturbations to the forearm. Results demonstrate that it is possible to estimate human joint dynamics from sEMG. The obtained results can contribute to the field of human motor control and also to its application in robotics and other engineering applications through the definition, specification and characterization of properties associated with the human upper limb and strategies used by people to command it.

Chapter 6

Arm Swing during Human Gait Studied by EMG of Upper Limb Muscles 129

Johann P. Kutzt-Buschbeck, Christian-Albrechts-University Kiel, Germany

Antonia Frendel, Christian-Albrechts-University Kiel, Germany

Bo Jing, Christian-Albrechts-University Kiel, Germany

Chapter 6 is titled “Arm Swing during Human Gait Studied by EMG of Upper Limb Muscles”. In this chapter, Kutzt-Buschbeck, Frendel and Jing explain the research conducted on arm swing during human gait for upper limb muscles. Initially, Electromyography (EMG) was performed with normal subjects to

describe patterns of arm and shoulder muscle activity in different gait conditions. These included normal forward walking, walking with immobilized arms, backward walking, power walking with accentuated arm swing, running, and load carriage. Complementary kinematic data are presented, too. Rhythmic muscle activity persists to some extent when both arms are immobilized during walking. Forward and backward walking involve dissimilar patterns of muscle activity, although the limb movements are very similar in both conditions. Likewise, power walking and running are characterized by different curves of EMG activity. Unimanual load carriage during walking affects muscle activities of both the loaded and the non-loaded arm. Research on normal arm swing provides a basis for clinical investigations of gait disorders.

Chapter 7

Using in Vivo Subject-Specific Musculotendon Parameters to Investigate Voluntary Movement

Changes after Stroke: An EMG-Driven Model of Elbow Joint 161

*Hujing Hu, First Affiliated Hospital, Sun Yat-sen University, China & Guangdong Provincial
Work Injury Rehabilitation Center, China*

Le Li, First Affiliated Hospital, Sun Yat-sen University, China

Chapter 7 is titled as “Using In Vivo Subject-Specific Musculotendon Parameters to Investigate Voluntary Movement Changes After Stroke: An EMG-Driven Model of Elbow Joint”. In this chapter, Hujing Hu and Le Li explain the feasibility of using ultrasonography to measure the musculotendon parameters of elbow muscles. These parameters help to build a subject-specific EMG-driven model, which could predict the individual muscle force and elbow voluntary movement trajectory using the input of EMG signal without any trajectory fitting procedure involved. The results demonstrated the feasibility of using EMG-driven neuromusculoskeletal modeling with ultrasound-measured data for prediction of voluntary elbow movement for both unimpaired subjects and persons after stroke.

Chapter 8

Study and Interpretation of Neuromuscular Patterns in Golf 181

*Sérgio Marta, CIPER, Faculdade de Motricidade Humana, Universidade de Lisboa,
Portugal*

*João Rocha Vaz, CIPER, Faculdade de Motricidade Humana, Universidade de Lisboa,
Portugal*

Luís Silva, CIPER, Faculdade de Motricidade Humana, Universidade de Lisboa, Portugal

*Maria Ant3nio Castro, Coimbra Health School, Instituto Polit3cnico de Coimbra, Portugal
& Mechanical Engineering Research Center, University of Coimbra, Portugal*

*Pedro Pezarat Correia, CIPER, Faculdade de Motricidade Humana, Universidade de
Lisboa, Portugal*

Chapter 8 is titled “Study and Interpretation of Neuromuscular Patterns in Golf”. In this chapter, Sérgio Marta et al. reports the golf swing EMG studies using amplitude, timing parameters and approaches to neuromuscular patterns recognition through EMG. The golf swing is a dynamic multi-joint movement. During each swing phase different activation levels occur, the combination of each muscle in amplitude provides an increased club head speed for the ball to travel to the hole. The timing when the maximum peak of each muscle occurs can be an important factor to understand the injury related mechanics and to prescribe strength programs. Most muscle studies describe their maximum activation level during the forward swing and acceleration phases, providing a controlled antigravity movement and acceleration of the club. The initial contraction time corresponds to the onset that can be used to describe the organization of the neuromuscular patterns during a task. This time parameter was used in golf to relate injuries to

skilled or less skilled golfers. The way to retrieve these time parameters may be reached through new approaches but no gold standard algorithm definition has been found yet. To better understand the neuromuscular patterns new algorithms based on the dynamical systems theory are now used.

Section 3 **EMG: Endurance, Stability, and Muscle Activities**

Chapter 9

Assessing Joint Stability from Eigenvalues Obtained from Multi-Channel EMG: A Spine Example 203

Dianne M. Ikeda, University of Waterloo, Canada

Stuart M. McGill, University of Waterloo, Canada

Chapter 9 is titled as “Assessing Joint Stability from Eigenvalues Obtained from Multi-Channel EMG: A Spine Example”. In this chapter, Ikeda and McGill explain the role of EMG signals to assess joint stability. Low back pain assessment and treatment interventions often involve the concepts of stability and/or joint stiffness. Using muscle activation and lumbar spine posture to calculate segmental stiffness and potential energy of the spine, eigenvalues can be linked to quantitative stability. It was reasoned that if a relationship exists between eigenvalues and individual muscles, then this approach could guide customized clinical intervention for people with defined spine instability.

Chapter 10

Endurance Time Prediction using Electromyography 219

Sébastien Boyas, Université du Maine, France

Arnaud Guével, Université de Nantes, France

Chapter 10 is titled “Endurance Time Prediction using Electromyography”. In this chapter, Sébastien Boyas and Arnaud Guével present the methodology used to predict Tlim from early changes in EMG signal and the factors that may influence its feasibility and reliability. It also presents the possible uses and benefits of the Tlim prediction. The purpose of endurance time (Tlim) prediction is to determine the exertion time of a fatiguing muscle contraction before it occurs. Tlim prediction would then allow the evaluation of muscle capacities while limiting fatigue and deleterious effects associated with exhaustive exercises. Fatigue is a progressive phenomenon which manifestations can be observed since the beginning of the exercise using electromyography (EMG). Studies have reported significant relationships between Tlim and changes in EMG signal suggesting that Tlim could be predicted from early EMG changes recorded during the first half of the fatiguing contraction. However some methodological factors can influence the reliability of the relationships between Tlim and EMG changes.

Chapter 11

EMG Activation Pattern during Voluntary Bending and Donning Safety Shoes 234

P. K. Nag, National Institute of Occupational Health, India

Varsha Chorsiya, National Institute of Occupational Health, India

Anjali Nag, National Institute of Occupational Health, India

Chapter 11 is titled “EMG Activation Pattern During Voluntary Bending and Donning Safety Shoes”. In this chapter, P. K. Nag, Varsha Chorsiya and Anjali Nag present a research study conducted on occupational health and safety at workplaces. Posture control is a well-coordinated interplay of sensory-motor system and forms the basis of voluntary movements. The daily activities and occupational task involves voluntary bending in different direction, which if falls beyond the limit of stability can cause

slipping, tripping, and falling. Further, these accidents are quite common in industries where workers have to wear safety shoes to protect their feet from the hazards of work environment. The study elucidates the muscular activation patterns in light of electromyographic (EMG) findings for voluntary bending within limits of stability and with donning of safety shoes. The present findings have implications regarding the viability of muscle adaptability as a putative postural control in preventing postural instability and avoiding injuries.

Chapter 12

Tongue Movement Estimation Based on Suprahyoid Muscle Activity 257
Makoto Sasaki, Iwate University, Japan

Chapter 12 is titled “Tongue Movement Estimation Based on Suprahyoid Muscle Activity”. In this chapter, Makoto Sasaki introduces a novel method for tongue movement estimation based on analysis of surface electromyography (EMG) signals from the suprahyoid muscles, which usually function to open the mouth and to control the hyoid position. The motor function of the tongue often remains intact even in cases of severe movement paralysis. Therefore, tongue movements offer great potential for the design of highly efficient human-machine interfaces for alternative communication and control.

Section 4

EMG for Prosthetic and HCI Applications

Chapter 13

Design of Myocontrolled Neuroprosthesis: Tricks and Pitfalls 275
Emilia Ambrosini, Politecnico di Milano, Italy
Simona Ferrante, Politecnico di Milano, Italy
Alessandro Pedrocchi, Politecnico di Milano, Italy

Chapter 13 is titled “Design of Myocontrolled Neuroprosthesis: Tricks and Pitfalls”. In this chapter, Ambrosini, Ferrante and Pedrocchi explain myocontrolled neuroprosthesis and related tricks and pitfalls. Recent studies suggest that the therapeutic effects of Functional Electrical Stimulation (FES) are maximized when the patterned electrical stimulation is delivered in close synchrony with the attempted voluntary movement. FES systems that modulate stimulation parameters based on the residual volitional muscle activity assure this combination. However, the development of such a system might be not trivial both from hardware and a software point of view. This chapter provides an extensive overview of devices and filtering solutions proposed in the literature to estimate the residual volitional EMG signal in the presence of electrical stimulation. Different control strategies to modulate FES parameters as well as the results of the first studies involving neurological patients are also presented. This chapter provides some guidelines to help people who want to design innovative myocontrolled neuroprostheses and might favor the spread of these solutions in clinical environments.

Chapter 14

Design and Development of EMG Conditioning System and Hand Gesture Recognition Based on Principal Component Analysis Feature Reduction Technique..... 304
P. Geethanjali, VIT University, India

Chapter 14 is titled “Design and Development of EMG Conditioning System for Hand Gesture Recognition Based on Principal Component Analysis Feature Reduction Technique”. In this chapter, P. Geethanjali presents design and development of surface Electromyogram (EMG) signal detection and conditioning

system along with the issues of gratuitous spurious signals such as power line interference, artifacts, and so forth which make signals which are just as plausible. In order to construe the recognition of hand gestures from EMG signals, time domain features were extracted. The extracted features were diminished using the principal component analysis (PCA) to alleviate the burden of the classifier. Furthermore, the chapter discusses the motion control of a prosthetic hand drive through continuous EMG acquisition, classification and the actuation of the DC drive using a TMS2407eZdsp digital signal controller.

Chapter 15

The Relationship between Anthropometric Variables and Features of Electromyography Signal for Human–Computer Interface 321

Angkoon Phinyomark, University Joseph Fourier, France & University of Grenoble, France

Franck Quaine, University Joseph Fourier, France

Yann Laurillau, University of Grenoble, France

Chapter 15 is titled “Relationship between Anthropometric Variables and Features of Electromyography Signal for Human–Computer Interface”. In this chapter, Phinyomark, Quaine and Laurillau explain the Muscle-computer interfaces (MCIs) based on surface electromyography (EMG) pattern recognition have been developed based on two consecutive components: feature extraction and classification algorithms. Many features and classifiers are proposed and evaluated, which yield the high classification accuracy and the high number of discriminated motions under a single-session experimental condition. However, there are many limitations to use MCIs in the real-world contexts, such as the robustness over time, noise, or low-level EMG activities. Although the selection of the suitable robust features can solve such problems, EMG pattern recognition has to design and train for a particular individual user to reach high accuracy. Due to different body compositions across users, a feasibility to use anthropometric variables to calibrate EMG recognition system automatically/semi-automatically is proposed. This chapter presents the relationships between robust features extracted from actions associated with surface EMG signals and twelve related anthropometric variables. The strong and significant associations presented in this chapter could benefit a further design of the MCIs based on EMG pattern recognition.

Compilation of References 354

About the Contributors 396

Index..... 402

Preface

BACKGROUND AND MOTIVATION

Electromyography (EMG) is a procedure for evaluating and recording the electrical activity produced by skeletal muscles. EMG has several clinical and prosthetic applications, which include the diagnosis of neuromuscular problems, biomechanical and motor control deficits, and other functional disorders. Moreover, it can be used as a control signal for interfacing with orthotic and/or prosthetic devices. This book aims at providing an updated overview of the recent developments in EMG from diverse aspects and various applications in clinical and experimental research. It will provide readers with a detailed introduction to EMG signal processing techniques and applications, while presenting several new results and explanation of existing algorithms.

INTENDED READERSHIP

This book brings the state-of-the-art of some of the most important current research related to EMG. The book is partly a textbook and partly a monograph. It is a textbook because it gives a detailed introduction to EMG techniques and applications. It is simultaneously a monograph because it presents several new results, concepts, and further developments. As a result of its twofold character, the book is likely to be of interest to undergraduate and postgraduate students. This book can also be used as handbook to engineers and scientists in the field of biomedical and biological engineering. One can read this book through sequentially, but it is not necessary since each chapter is essentially self-contained, with as few cross-references as possible.

As an editor and also an author in this field, I am honoured to be editing a book with such fascinating and exciting content, written by a selected group of gifted researchers. I would like to thank the authors, who have committed so much towards the publication of this work.

THE ORGANISATION OF CHAPTERS

The book is organized in four sections. In Section 1, “EMG Basics and Motor Unit Action Potentials,” basics of EMG and MUAP are dealt in detail. Chapters in this section combine hypothesis-driven experimentation with computer-based modelling and simulation to analyse MUAP functions and real EMG behaviours.

Section 2, titled “EMG Signal Modeling and Signal Processing,” presents mathematical and analytical techniques for modelling EMG systems and provides insights on how these can be exploited further in real-world applications. Advances in applied mathematics have facilitated the extension and development of analytical approaches and techniques, which are frequently supported by computer simulation, in order to tackle some challenging real problems in this research area.

Section 3, titled “EMG: Endurance, Stability, and Muscle Activities,” focuses on endurance, fatigue, and stability of EMG muscles and MUAPs. It proposes representation models that incorporate EMG signal processing techniques.

Finally, Section 4, titled “EMG for Prosthetic and HCI Applications,” presents methods and EMG systems and provides insights on how these can be exploited further in real-world applications. Moreover, real world applications that are employed to evaluate the effectiveness of the EMG-based systems are also presented in detail.

Below, an overview of the book chapters is presented.

Section 1: EMG Basics and Motor Unit Action Potentials

Chapter 1 is titled “Neural Control of Muscle.” In this chapter, Bawa and Kelvin Jones explain the ideas and concepts about how the central nervous system controls muscle contraction. The populations of motor units comprising a skeletal muscle have a diverse range of physiological and anatomical properties. The Size Principle of motor unit recruitment is a concept that proposes a simple strategy for exploiting the diversity of the motor unit population to produce graded force output. The Size Principle has a great deal of empirical support, but also faces criticism about the extent of generalization to all types and forms of movement. As the key principles of motor units are discussed, methods of measuring and methodology for analysing motor unit activity and whole muscle activities are introduced.

Chapter 2 is titled “New Advances in Single Fiber Electromyography.” In this chapter, Javier Rodriguez-Falces explains general perspective of EMG together with a description of the anatomical, physiological, and technical aspects that are involved in the recording of Single Fiber Action Potentials (SFAPs). First, a simulation model that relates analytically the Intracellular Action Potential (IAP) and SFAP mathematical expressions is described. Second, the most recent findings regarding the shape features of human SFAPs are outlined. Third, a description of how different types of needle electrodes affect the characteristics of the recorded potential is detailed. Fourth, an explanation of the most important effects of filtering on the SFAP characteristics is provided. Finally, a description of the principles of jitter estimation together with the most important sources of errors are presented.

Chapter 3 is titled “Detection and Conditioning of EMG.” In this chapter, İmran Göker explains the monitoring of the electrical activity of skeletal muscles. The main components of the detection and conditioning of the EMG signals are explained in the sense of the biomedical instrumentation. At first, a brief description of EMG generation is introduced. Next, the hardware components of the general instrumentation system used in the acquisition of EMG signals, such as amplifier, filters, analog-to-digital converter, are discussed in detail. Subsequently, different types of electrodes used in different EMG techniques are mentioned. Then, various EMG signals that can be detected and monitored via EMG systems are described, and their clinical importance is discussed in detail. Finally, different EMG techniques used in clinical studies and their purposes are highlighted.

Chapter 4 is titled “An Introduction to Signal Processing using MatLab and Microsoft Excel.” In this chapter, Daniel Robbins explains the fundamentals of biological signal analysis and processing, using

EMG signals to illustrate the process. The areas covered within the chapter include: frequency analysis using the Fast Fourier Transform, identifying noise within a signal, signal smoothing via Root Mean Square (RMS) processing, and signal filtering with both low-pass and high-pass filters. Guidelines for the application of the processes covered are included in conjunction with step-by-step examples using both MathWorks MatLab and Microsoft Excel software. Following the examples allows the reader to practice the processes described to promote and reinforce their learning.

Section 2: EMG Signal Modeling and Signal Processing

Chapter 5 is titled “Modeling the Human Elbow Joint Dynamics from Surface Electromyography.” In this chapter, Andrés Felipe Ruiz-Olaya describes an approximation for non-invasive biomechanical modelling of the elbow joint dynamics from electromyographic information. A case study presents results obtained aimed at deriving a relationship between the dynamic behaviour of the human elbow joint and surface Electromyography (sEMG) information in postural control. A set of experiments were carried out to measure bioelectrical (sEMG) and biomechanics information from human elbow joint, during postural control (i.e. isometric contractions) and correlate them with mechanical impedance at elbow joint. Estimates of elbow impedance were obtained by applying torque perturbations to the forearm. Results demonstrate that it is possible to estimate human joint dynamics from sEMG. The obtained results can contribute to the field of human motor control and also to its application in robotics and other engineering applications through the definition, specification, and characterization of properties associated with the human upper limb and strategies used by people to command it.

Chapter 6 is titled “Arm Swing during Human Gait Studied by EMG of Upper Limb Muscles.” In this chapter, Kutz-Buschbeck, Frenkel, and Jing explain the research conducted on arm swing during human gait for upper limb muscles. Initially, Electromyography (EMG) was performed with normal subjects to describe patterns of arm and shoulder muscle activity in different gait conditions. These included normal forward walking, walking with immobilized arms, backward walking, power walking with accentuated arm swing, running, and load carriage. Complementary kinematic data are presented, too. Rhythmic muscle activity persists to some extent when both arms are immobilized during walking. Forward and backward walking involve dissimilar patterns of muscle activity, although the limb movements are very similar in both conditions. Likewise, power walking and running are characterized by different curves of EMG activity. Unimanual load carriage during walking affects muscle activities of both the loaded and the non-loaded arm. Research on normal arm swing provides a basis for clinical investigations of gait disorders.

Chapter 7 is titled “Using In Vivo Subject-Specific Musculotendon Parameters to Investigate Voluntary Movement Changes after Stroke: An EMG-Driven Model of Elbow Joint.” In this chapter, Hujing Hu and Le Li explain the feasibility of using ultrasonography to measure the musculotendon parameters of elbow muscles. These parameters help to build a subject-specific EMG-driven model, which could predict the individual muscle force and elbow voluntary movement trajectory using the input of EMG signal without any trajectory fitting procedure involved. The results demonstrate the feasibility of using EMG-driven neuromusculoskeletal modeling with ultrasound-measured data for prediction of voluntary elbow movement for both unimpaired subjects and persons after stroke.

Chapter 8 is titled “Study and Interpretation of Neuromuscular Patterns in Golf.” In this chapter, Sérgio Marta et al. report the golf swing EMG studies using amplitude, timing parameters, and approaches to neuromuscular patterns recognition through EMG. The golf swing is a dynamic multi-joint

movement. During each swing, phase different activation levels occur; the combination of each muscle in amplitude provides an increased club head speed for the ball to travel to the hole. The timing when the maximum peak of each muscle occurs can be an important factor to understand the injury-related mechanics and to prescribe strength programs. Most muscle studies describe their maximum activation level during the forward swing and acceleration phases, providing a controlled antigravity movement and acceleration of the club. The initial contraction time corresponds to the onset that can be used to describe the organization of the neuromuscular patterns during a task. This time parameter was used in golf to relate injuries to skilled or less-skilled golfers. The way to retrieve these time parameters may be reached through new approaches, but no gold standard algorithm definition has been found yet. To better understand the neuromuscular patterns, new algorithms based on the dynamical systems theory are now used.

Section 3: EMG: Endurance, Stability, and Muscle Activities

Chapter 9 is titled “Assessing Joint Stability from Eigenvalues Obtained from Multi-Channel EMG: A Spine Example.” In this chapter, Ikeda and McGill explain the role of EMG signals to assess joint stability. Low back pain assessment and treatment interventions often involve the concepts of stability and/or joint stiffness. Using muscle activation and lumbar spine posture to calculate segmental stiffness and potential energy of the spine, eigenvalues can be linked to quantitative stability. It was reasoned that if a relationship exists between eigenvalues and individual muscles, then this approach could guide customized clinical intervention for people with defined spine instability.

Chapter 10 is titled “Endurance Time Prediction using Electromyography.” In this chapter, Sébastien Boyas and Arnaud Guével present the methodology used to predict Tlim from early changes in EMG signal and the factors that may influence its feasibility and reliability. It will also present the possible uses and benefits of the Tlim prediction. The purpose of endurance time (Tlim) prediction is to determine the exertion time of a fatiguing muscle contraction before it occurs. Tlim prediction would then allow the evaluation of muscle capacities while limiting fatigue and deleterious effects associated with exhaustive exercises. Fatigue is a progressive phenomenon whose manifestations can be observed from the beginning of the exercise using Electromyography (EMG). Studies have reported significant relationships between Tlim and changes in EMG signal suggesting that Tlim could be predicted from early EMG changes recorded during the first half of the fatiguing contraction. However, some methodological factors can influence the reliability of the relationships between Tlim and EMG changes.

Chapter 11 is titled “EMG Activation Pattern during Voluntary Bending and Donning Safety Shoes.” In this chapter, P. K. Nag, Varsha Chorsiya, and Anjali Nag present a research study conducted on occupational health and safety at workplaces. Posture control is a well-coordinated interplay of sensory-motor system and forms the basis of voluntary movements. The daily activities and occupational task involves voluntary bending in different directions, which, if beyond the limit of stability, can cause slips, trips, and falls. Further, these accidents are common in industries where workers have to wear safety shoes to protect their feet from hazards of the work environment. The study elucidates the muscular activation patterns in light of Electromyographic (EMG) findings for voluntary bending within limits of stability and with donning of safety shoes. The present findings have implication regarding the viability of muscle adaptability as a putative postural control in preventing postural instability and avoiding injuries.

Chapter 12 is titled “Tongue Movement Estimation Based on Suprahyoid Muscle Activity.” In this chapter, Makoto Sasaki introduces a novel method for tongue movement estimation based on analysis of

surface Electromyography (EMG) signals from the suprahyoid muscles, which usually function to open the mouth and to control the hyoid position. The motor function of the tongue often remains intact even in cases of severe movement paralysis. Therefore, tongue movements offer great potential for the design of highly efficient human-machine interfaces for alternative communication and control.

Section 4: EMG for Prosthetic and HCI Applications

Chapter 13 is titled “Design of Myocontrolled Neuroprosthesis: Tricks and Pitfalls.” In this chapter, Ambrosini, Ferrante, and Pedrocchi explain myocontrolled neuroprosthesis: tricks and pitfalls. Recent studies suggest that the therapeutic effects of Functional Electrical Stimulation (FES) are maximized when the patterned electrical stimulation is delivered in close synchrony with the attempted voluntary movement. FES systems that modulate stimulation parameters based on the residual volitional muscle activity assure this combination. However, the development of such a system might be not trivial both from hardware and a software point of view. This chapter provides an extensive overview of devices and filtering solutions proposed in the literature to estimate the residual volitional EMG signal in the presence of electrical stimulation. Different control strategies to modulate FES parameters as well as the results of the first studies involving neurological patients are also presented. This chapter provides some guidelines to help people who want to design innovative myocontrolled neuroprostheses and might favor the spread of these solutions in clinical environments.

Chapter 14 is titled “Design and Development of EMG Conditioning System for Hand Gesture Recognition using Principal Component Analysis.” In this chapter, P. Geethanjali presents design and development of surface Electromyogram (EMG) signal detection and conditioning system along with the issues of gratuitous spurious signals such as power line interference, artefacts, etc., which make signals plausible. In order to construe the recognition of hand gestures from EMG signals, time domain features were extracted. The extracted features were diminished using the Principal Component Analysis (PCA) to alleviate the burden of the classifier. The chapter discusses the motion control of a prosthetic hand through continuous EMG acquisition, classification, and the actuation of the DC drive using a TMS2407eZdsp digital signal controller.

Chapter 15 is titled “Relationship between Anthropometric Variables and Features of Electromyography Signal for Human-Computer Interface.” In this chapter, Phinyomark, Quaine, and Laurillau explain the relationships between robust features extracted from actions associated with surface EMG signals and 12 related anthropometric variables. Muscle-Computer Interfaces (MCIs) based on surface Electromyography (EMG) pattern recognition have been developed based on 2 consecutive components: feature extraction and classification algorithms. Many features and classifiers are proposed and evaluated, which yield the high classification accuracy and the high number of discriminated motions under a single-session experimental condition. However, there are many limitations to use MCIs in the real-world contexts, such as the robustness over time, noise, or low-level EMG activities. Although the selection of the suitable robust features can solve such problems, EMG pattern recognition has to design and train for a particular individual user to reach high accuracy. Due to different body compositions across users, a feasibility to use anthropometric variables to calibrate EMG recognition system automatically/semi-automatically is proposed. The strong and significant associations presented in this chapter could benefit further design of the MCIs based on EMG pattern recognition.

Ganesh R. Naik
University of Technology Sydney (UTS), Australia

Section 1

EMG Basics and Motor Unit Action Potentials

Chapter 1

Neural Control of Muscle

Parveen Bawa

Simon Fraser University, Canada

Kelvin E. Jones

University of Alberta, Canada

ABSTRACT

The purpose of this chapter is to introduce the reader to the development of ideas and concepts about the manner in which the central nervous system controls muscle contraction. The motor unit, the quantum of muscle contraction, is fundamental to concepts of the neural control of muscle and will be the focus of discussion. The population of motor units comprising a skeletal muscle have a diverse range of physiological and anatomical properties. The Size Principle of motor unit recruitment is a concept that proposes a simple strategy for exploiting the diversity of the motor unit population to produce graded force output. The Size Principle has a great deal of empirical support, but also faces criticism about the extent of generalization to all types and forms of movement. As the key principles of motor units are discussed, methods of measuring and methodology for analysing motor unit activity and whole muscle activities are introduced.

INTRODUCTION

The central nervous system receives inputs via many sensory pathways. This information is integrated, perceived and leads to an output; which for the purposes of this chapter is via the musculoskeletal system. The motor actions generated by the output of the musculoskeletal system range from simple reflexes to complex voluntary movements. In his 1904 address to the British Association for the Advancement of Science, Sherrington defined a few terms including the

“neurone” and “final common path.” The term “final common path” alluded to the idea that all reflex and descending motor commands converge on to the motoneurons whose axons provide the final link between neural and muscle tissue that leads to movement. With respect to the differences between reflexive and voluntary movements, it is difficult to separate different levels of control of the muscle (Prochazka et al., 2000). Here we will use the classical terminology for voluntary (willed) and reflex activities (automatic and generally resistant to conscious will).

DOI: 10.4018/978-1-4666-6090-8.ch001

BACKGROUND

Muscle and Its Motoneuron Pool

Skeletal muscle is composed of thousands of muscle fibres; each fibre a multi-nucleated cell. In this chapter we will concern ourselves with muscles of the limbs, which generally have a simpler structure; motoneurons innervating them lie in the spinal cord of vertebrates. The geometry of muscle fiber orientation relative to the long axis of the muscle and tendon varies in limb muscles. Muscle fibres can lie in parallel to the long axis of the muscle; all active fibres contract together with the force vector along the principal axis. A typical example of a parallel geometry is the biceps brachii (Loeb & Gans, 1986). In pennate (or pinnate) muscles, fibres attach to the tendon at an angle, called the angle of pennation. The force exerted along the line of action is less than if the fibres contracted along the main axis of the muscle. The directions of contraction of muscle fibres in different regions of large muscles are important for interpreting motor unit recruitment data (Staudenmann et al., 2009). Most of the muscles are multifunctional and their muscle fibres contribute different amounts of force in various directions (Jones et al., 1993; Ter Haar Romeny et al., 1984).

Motoneurons

The contraction of a muscle is controlled by a pool of alpha motoneurons¹ in the spinal cord. The morphology and electrophysiology of motoneurons within a pool vary over a wide range. The physiology of each motoneuron is well matched to the properties of the muscle fibres it innervates (Henneman, 1985; Henneman & Mendell, 1981; Kernell et al., 1999). The cell body, also referred to as the soma or perikaryon, and dendrites of a limb motoneuron lie in the ventral horn of the spinal cord. A long myelinated axon exits the spinal

cord through the ventral spinal root and travels to the muscle where it enters the muscle, divides into branches and terminals that make synaptic connections with muscle fibres. In a healthy adult, each muscle fibre receives input from a single motoneuron. A single motoneuron with all its muscle fibres is what Sherrington defined as the motor unit in 1925. All the muscle fibres innervated by the same motoneuron, the muscle unit (Burke, 1981), are of a uniform fibre type; and the number of muscle fibres connected to one motoneuron is the innervation ratio. Innervation ratio has been shown to be as high as 2000 in the cat gastrocnemius muscle which means that an action potential in the motoneuron results in 2000 synchronous muscle fiber action potentials in a large motor unit. This is an example of a system with high amplification.

Motoneurons that innervate limb muscles are typically in a resting inactive state until synaptic inputs excite them to an active state; this process is called recruitment. The number of motoneurons active at any time is associated with the force requirements, more motoneurons are recruited when more force is required. When a motoneuron is recruited to an active state for a long period, action potentials are generated at rates ranging roughly from 5- 30 impulses/s depending on the muscle and the force level. The time between action potentials, called the interspike interval (ISI), is not constant. The distribution of ISIs for an active motoneuron is unimodal with a variance resulting from various sources of probabilistic noise and electrophysiological properties (Jones & Bawa, 1997; Matthews, 1996). Motoneurons that are active simultaneously generate action potentials that are mostly independent of action potentials of other motoneurons. There is some level of synchronization of motorneuron action potentials in limb muscles that likely result from common input sources (Keen et al., 2012; Mochizuki et al., 2005).

Structure and Activation of Muscle Fibres

For many years, anatomists and physiologists recognized that skeletal muscles differed in appearance and speed of contraction to electrical stimulation. Muscles that appeared red in colour were associated with slower contractions compared to muscles that appeared white. Currently, mammalian muscle fibres are categorized into different types based on contractile protein expression (i.e. myosin heavy chain isoforms) and metabolic enzymes, from oxidative to glycolytic. There are four major fiber types based on myosin composition, though not all types are expressed in all species (Schiaffino and Reggiani, 2011). Three muscle fibre types are generally recognized in human limb muscles: slow oxidative (SO) or Type 1, fast-oxidative-glycolytic (FOG) or Type 2A, and fast glycolytic (FG) or Type 2X. The muscles of the body develop with different proportions of the major fiber types and these proportions are modified by activity and hormonal influences. The soleus muscle in the lower leg contains a high percentage of type 1 muscle fibres while its synergist medial gastrocnemius contains a much higher percentage of type 2 fibres (Johnson et al., 1973). In humans there are no muscles which contain either all Type 1 fibres, or all Type 2; each muscle is mixed. However, muscle fibres comprising a motor unit are of the same type.

The two main proteins responsible for contraction of a muscle fibre are myosin and actin. Molecules of myosin form the thick filaments and those of actin form the thin filaments. At one end of each myosin molecule is a mobile head which, under resting conditions, is not attached to thin filament. A thin filament has regularly spaced sites on it where the mobile heads of the thick filament can attach when Ca^{++} and ATP are available. Sufficient depolarisation (~ 50 mV) of the cell membrane releases Ca^{++} from sarcoplasmic reticulum (SR) which allows the thick filament to

“walk along” the surrounding thin filaments by attaching and detaching its mobile heads to the binding sites on the thin filaments. The mobile head of myosin attached to actin is called a cross bridge. The attached cross bridges are the sources of force output. Each cross bridge acts like a small spring; the net force is produced by the number of attached cross bridges. The movement of the thick filaments past the thin filaments shortens the contractile part (the active part) of the muscle fibre which in turn pulls on the passive parts such as the muscle tendon. If the tendon is fixed to a rigid device, the tendon is moderately stretched and the contraction is defined as isometric. When the tendon is free to move or lightly loaded, the contraction is non-isometric. Note that the term contraction does not mean shortening of the muscle; it applies to the active sliding of thick and thin filaments past each other in the presence of Ca^{++} and ATP molecules. For the whole muscle, the action of the contracting muscle depends on the load attached to the tendon. If the load is infinite, that is, the tendon is attached to a rigid frame, the muscle is said to be contracting isometrically. Shortening or concentric contraction occurs when load on the tendon is less than the maximum force the muscle can develop. When a person lifts something light with their hand, biceps brachii muscle contracts and shortens. Active lengthening, also known as an eccentric contraction, refers to the context when the muscle is contracting but is being lengthened (the load is larger than the force being produced by the muscle).

Electrical Activity of a Muscle Fibre and Motor Unit

Each terminal branch of a motoneuron makes a synapse with a muscle fibre of the motor unit at a region called the neuromuscular junction (NMJ). On the motoneuron side of this junction, the nerve terminal contains vesicles of acetylcholine (ACh) that will be released in response to the action

potential that was initiated in the spinal cord and conducted along the axon to the terminal. In the muscle fiber this region is also referred to as the end-plate region, which is distinguished by the high density of ACh receptors. The sequence of events from the arrival of the action potential in the motoneuron terminal to contraction of the muscle fibers is schematically illustrated in Figure 1.

Under normal conditions, when a motoneuron discharges an action potential, each terminal is depolarised by the action potential (Figure 1A) resulting in an influx of calcium from the extracellular medium into the terminal which causes the release of hundreds of ACh vesicles, each of which contains thousands of ACh molecules. The ACh molecules diffuse across a small gap in the NMJ and bind to nicotinic ACh receptors on the muscle fibre. When two molecules of ACh bind to an ACh receptor, the receptor changes its configuration creating a temporary pore (open for 1-2 ms) that permits the flux of Na^+ and K^+ ions along their electrochemical gradients, through the same pore. The flux of Na^+ ions inward is greater than K^+ ions going out, resulting in a net depolarization, or excitation of the muscle fibre, called the end-plate potential (EPP). The end-plate potential generated by ionic flux through the ACh receptor/pore complex can have a peak potential up to 70 mV, which is large enough to open voltage gated Na^+ channels that in turn produce an action potential in the muscle fibre (Figure. 1B). This action potential is conducted along the membrane of the muscle fibre away from the NMJ towards the two ends of the muscle fibre. Depolarization of the muscle membrane by the action potential triggers the release of calcium from sarcoplasmic reticulum, which results in a transient increase in Ca^{++} concentration inside the muscle fibre (Figure 1C). The increased Ca^{++} inside the muscle interacts with proteins on the thin filaments that then permit the penultimate interaction of the actin and myosin leading to the transient mechanical contraction of the muscle fibre (Figure 1D). There

is a high degree of synchrony across all terminals of a motoneuron and therefore near synchronous generation of action potentials in all the muscle fibres of the motor unit. This results in summation of the mechanical contraction of individual muscle fibers and generation of the motor unit twitch. The conventional measures of the motor unit twitch include the peak magnitude, the time from the onset of increasing tension to the peak value, i.e. the contraction time (CT), and the interval of time from the peak tension until the tension decreases to half the peak value, i.e. half-relaxation time. There is a strong positive correlation between CT and the half-relaxation time of a motor unit twitch that is associated with the dynamics of different muscle fiber types.

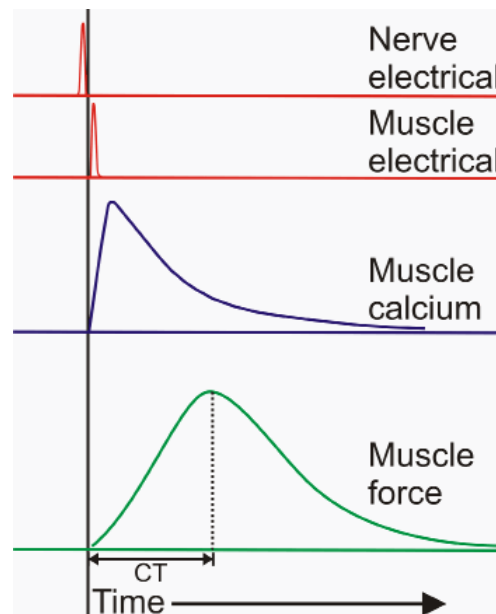
Motor Unit Classification

R.E. Burke (1981) classified motor units into three types (Figure. 2): S (slow, fatigue resistant), FR (fast contracting and resistant to fatigue), FF (fast, fatigable). S motor units innervate SO type muscle fibres, FR motor units innervate FOG type muscle fibres and FF motor units innervate FG type muscle fibres. (It should be remembered that motor units classification is for convenience since motor unit properties form a continuum). S motor units have small innervations ratios, generate small forces but fatigue less. At the other extreme, FF motor units have very high innervations ratios, generate large forces, but fatigue quickly. Muscle fibres belonging to one motor unit are scattered over a large cross section and length of the muscle (Bodine-Fowler et al., 1990; Monti et al., 2001; Vieira et al., 2011). In the cat, conduction velocity of alpha motor axons ranges from 50 to 110 meters/sec and that of muscle fibres ranges from 2-5 m/s. The slow CV of muscle fibres is due to large the capacitance of muscle membrane (Adrian, 1976).

Since a range of motor units properties exist for one muscle, the question arose on how the central nervous system utilized motor units

Neural Control of Muscle

Figure 1. Steps in the production of muscle fibre twitch. (A) Action potential travelling down the terminal branch of the motoneuron depolarises the presynaptic terminal at the neuromuscular junction. This releases ACh from the presynaptic terminal. (B) Binding of ACh to the receptors at the end plate region of the NMJ results in EPP which leads to an action potential in the muscle fibre. (C) The action potential releases Ca^{++} from sarcoplasmic reticulum (SR), Ca^{++} concentration reaches a peak within 3-4 ms, subsequently it is pumped back into SR by an ATP dependent pump. (D) Ca^{++} enables the formation of cross bridges between the thick and thin filaments. Making and breaking of cross bridges results in sliding of filaments past each other eliciting a mechanical response called muscle fibre twitch. Twitch is the profile of the force that is produced by one action potential in the muscle fibre



with heterogeneous speeds and force generating capabilities. This question has been addressed for simple muscles by many researchers and their findings are generalized to understand and raise questions about the contraction of more complex muscles. The following sections will present some Methods and Results before discussing the past literature and proposing future directions.

STUDIES ON MOTOR UNITS

In order to reach the most accurate possible conclusions in research, correct methods for recording and data analysis are imperative. Measurement of muscle output typically involves electrical

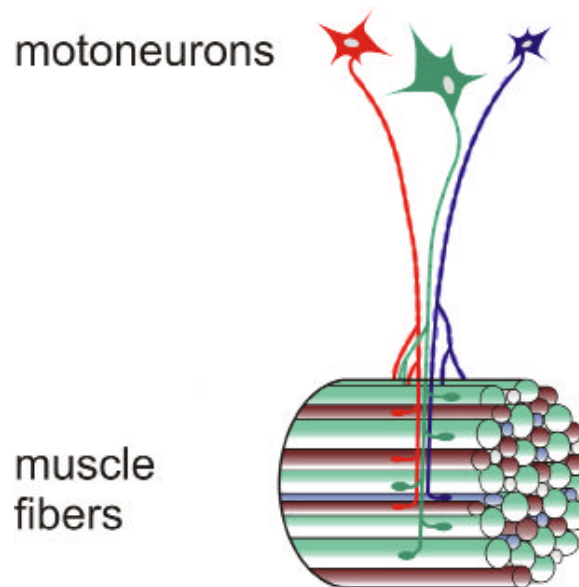
activity and force, though complementary measures of mechanical activity and length changes are becoming increasingly common. Since the properties of transducers used for measurement are of prime importance, the basic methods for recording and data analysis of motor units and whole muscle are reviewed.

Equipment

Population Activity

To record the electrical activity of the muscle or single motor units, different types of electrodes are used. The simplest recording is the population activity recorded with two surface EMG electrodes

Figure 2. The figure illustrates three motor units with different innervation ratios. The muscle fibres of the three motor units are interspersed rather than congregating together in clumps. The green motoneuron innervates the greatest number of muscle fibres, and is a schematic representation of an FF motor unit. Whereas the blue motoneuron and its smaller number of innervated muscle fibres represents an S type motor unit



as shown in Figure 3A for differential recording. Differential amplification eliminates the noise signal common to both electrodes thus maximizing the signal to noise ratio. The recording area of the electrode used depends on the size of the muscle; most commercial ones vary in size from 4-10 mm in diameter. Surface EMG electrodes are available in single-use disposable and re-usable configurations. Re-usable Ag/AgCl electrodes require a conducting gel placed between the surface of the electrode and thoroughly cleaned skin overlying the muscle of interest. The two electrodes are taped approximately 2 diameters apart, or roughly 2-3 cm between the centres of the two electrodes in line with the direction of the muscle fibres (De Luca et al., 2012). With surface electrodes cross-talk between muscles is a common problem; electrodes placed over one muscle can easily pick up activity of distant muscles (De Luca et al., 2012). Under such conditions, intramuscular EMG electrodes may be employed. These are also

available commercially but can be made easily in the laboratory. Two flexible insulated stainless wires, 75-100 μm in diameter, are inserted in a 25- 27 gauge hypodermic needle. Insulation is removed for 3-4 mm at both ends of the insulated wires; the ends of the wires near the tip of the needles are bent into a hook as illustrated in Figure 3B. Following insertion into the muscle, the needle is gently withdrawn while the bared wires remain within the muscle. The other ends of the surface or intramuscular electrodes are connected to preamplifiers. The commercially available preamplifiers make available variable gains and filters (De Luca et al., 2010). For population EMG, a gain of about 1000 is generally used, but this depends on the data acquisition system used. For example, if your data acquisition system allows ± 10 V input, set the gain to use as much of that range as possible without exceeding the limits. Besides the preamplifier, additional conditioning amplifiers may be used to adjust gain. Filtering at

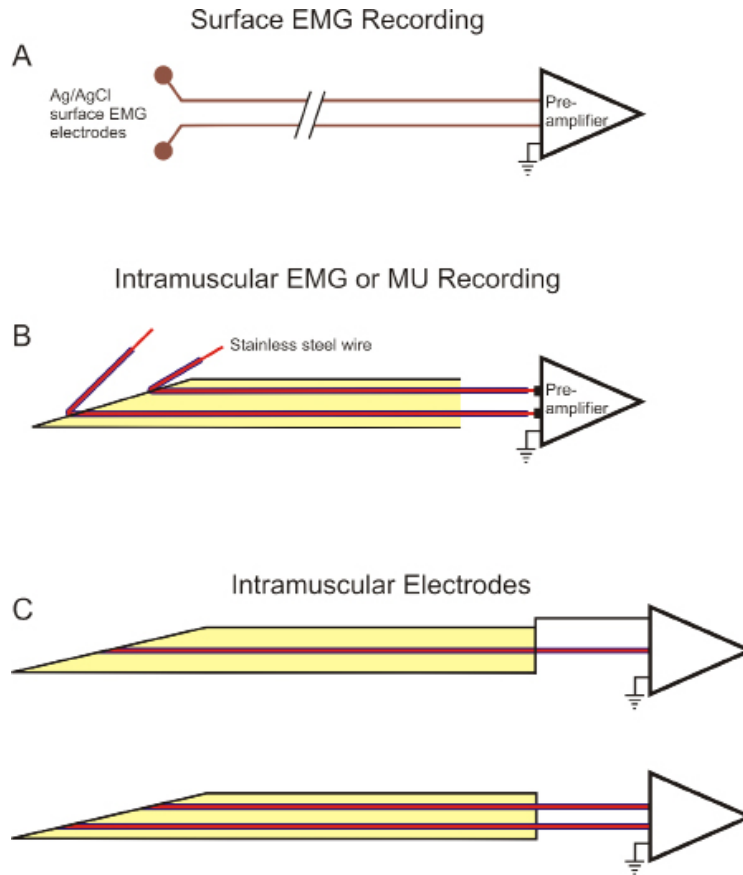
Neural Control of Muscle

band pass of 20Hz – 5KHz should be available; the lower limit of frequency (20-30 Hz) minimizes movement artifact. The cables and wires should be stabilised (wrapped and taped around the limb) to eliminate any movement of the wires carrying signal from the muscle to the preamplifier. Stability of electrodes and wires between the muscle and the preamplifiers cannot be over emphasized. One of the main requirements of a preamplifier is its input resistant (20-50 M Ω). For any amplifier, the internal noise should be very low (1-2 μ V). Battery operated preamplifiers have a lower internal noise. If you are going to use the same preamplifiers for surface EMG, intramuscular EMG and motor unit activity, it is better to have gain of the order of x2000 and filters in the range 20 Hz – 10 KHz available at the first stage of EMG and MU recordings. Population EMG, which represents activity of all active muscle fibres, has a much higher power at lower frequencies, and negligible power above 1KHz. Therefore, a higher cut off frequency at 1 KHz serves the purpose. On the other hand, single motor unit potentials have a higher frequency spectrum. In order to differentiate one motor unit potential from the other, 100 Hz is better suited for the lower frequency cut off and 10 KHz for the high frequency cut off.

Motor unit recording is done using intramuscular electrodes with very small recording surface area, which means high input resistance. Depending on the experimental protocol, various types of MU electrodes have been used. Properties of some these electrodes are discussed in Merletti and Farina (2009). For very low threshold motor units (recorded at minimal forces), researchers have used surface EMG electrodes; such recording can be stable for hours (Matthews, 1996). The other extreme is the recording of very high threshold motor units (when almost all MUs are active). Bigland-Ritchie's group used tungsten microelectrodes, which are also used to record from single axons and cortical neurons, to record discharge rates of the fast units (Bellemare et al., 1983). Under low to moderate forces, bipolar

electrodes shown in Figures 3B and 3C are used. Hook electrodes with insulated stainless steel wires (20-50 μ m diameter) are one option for stable recording, especially when movement is involved. At the recording end of the hook electrode, just the transverse surface of the wire is exposed for recording. For a wire of 50 μ m diameter, the recording area would then be 0.002 mm². However, once in place, these electrodes cannot be advanced deeper into the muscle to sample additional motor units. But the electrodes can be slowly withdrawn to sample more superficial units. If one wants to sample a number of motor units during one experimental session, needles with embedded wires (termed needle electrodes) are more suitable (Figure 3C). Bipolar or monopolar needle electrodes are available commercially but are a bit heavy. Lighter ones can be made in the laboratory (Bawa and Tatton, 1979). Small recording area of the recording wires presents a very high resistance and is able to detect very small currents. With a bipolar recording, the electrodes are able to record currents from active muscle fibres in the immediate vicinity of the tips of electrodes. Since the innervation ratio of larger MUs is high, one expects motor unit potentials to be of greater amplitude for large compared to small motor units. However, the size of an intramuscularly recorded MU spike does not necessarily represent the size of the motor unit (Henneman et al., 1976). The tip of the microelectrode samples currents only from a few muscle fibres in its vicinity; it may be closest to a muscle fibre of a small motor unit, and relatively far from muscle fibres of a large motor unit. Under these conditions a larger spike will be observed for a smaller motor unit. Furthermore, the MU spike recorded by the microelectrode does not look like an intracellular action potential of a muscle fibre or an axon. The shape and duration depend on how muscle fibres of a MU are distributed around the tip of the electrode. Relative sizes and shapes of two MU spikes recorded tell us nothing about the properties of the MUs, the only information we can derive is on the num-

Figure 3. Electrode types. A: Surface EMG electrodes are pasted on cleaned skin overlying the muscle of interest. Wires from the electrodes are connected to two inputs of a preamplifier for differential recording. B: An intramuscular hook electrode. For population EMG recording, 3-5 mm of the wire is bared of its insulation. For single MU recording, no insulation is removed; under these conditions the bare transverse surface of the insulated wires record electrical activity of a few muscle fibres in their vicinity. C: Intramuscular electrodes for motor unit recording. These electrodes are available commercially, or can be custom made in the laboratory



ber of units that are active around the tip of the electrode and about their relative firing times. In order to determine the size of the motor unit, the spike-triggered averaging technique may be used to extract associated motor unit action potential (MUAP) from surface EMG and/or twitch force from the AC force record as described below (Stein et al., 1972). If force can be recorded, then extraction of twitch force is preferred.

During voluntary contraction, auditory and visual feedback is often provided so that partici-

pants can maintain a constant firing rate. If auditory feedback of the discharge of a single MU is essential to the experimental design, additional equipment may be needed. When more than two MUs are firing, participants will have difficulty maintaining the firing rate of the third unit while the first two are also firing in the background. In this case, an analog window discriminator may be used to detect a target motor unit in real-time and provide isolated feedback. Alternatively, this can be done with real-time processors and software

Neural Control of Muscle

available from some commercial neurophysiology vendors.

Force recording can be done with commercially available transducers or a custom-built system. Signal conditioning of these data depends on which aspect of the muscle contraction is of interest. The magnitude of steady-state force generated by a muscle, or DC force, uses low pass filtering at 100 Hz (band pass DC-100 Hz). If the measured force is to be used for spike-triggered averaging of twitch profiles, a low pass at 500 Hz is more appropriate (Calancie & Bawa, 1986). If twitch profiles are to be extracted, the signal is high pass filtered at 0.1 Hz to provide a record of AC force (Figure 4 and Figure 5).

Data acquisition and analysis systems can be bought or custom built. Before investing in a system, check how limited or how expandable the system is. If you are interested in a system which comes with electrodes, preamplifiers, data acquisition and analysis boards, it may be very convenient for immediate use, but in the future it might limit you to expand the experimental protocols used in the laboratory. There are other systems available, which are also ready for immediate use, but give you the flexibility of choosing electrodes, preamplifiers, additional amplifiers and filters. It also depends on whether you want a mobile wireless system, or use a desktop that will stay in one room.

Procedures

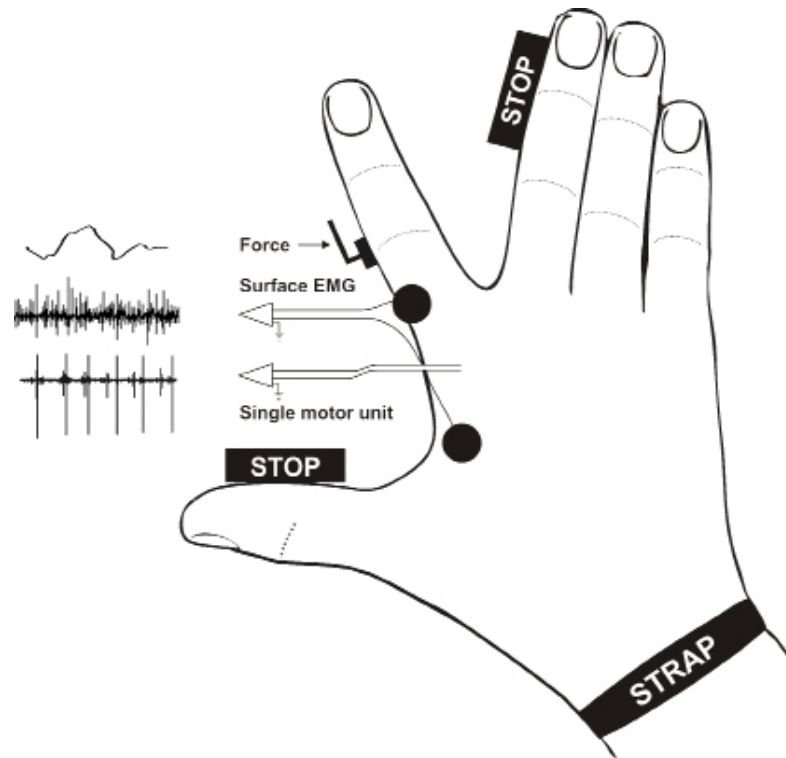
Once we have the equipment to record EMG, MU activity, force, along with the data acquisition system, we are ready to do experiments.

Procedures to Test Voluntary Recruitment of Motor Units

Figure 4 illustrates the set up used to record MUs from human first dorsal interosseous muscle, which abducts the index finger (Milner-Brown et al., 1973a). EMG is recorded with two small

surface EMG electrodes, one placed on the belly of the muscle and the second near the tendon (in a larger muscle both electrodes are placed on the belly of the muscle). The hand is stabilized to isolate force measurement from only the index finger. Once the hand is secured, a needle electrode is inserted in the muscle; the other end of the wires from the needle are connected to a preamplifier (gain x1000-2000; band pass filter 100Hz – 10 KHz). Both the subject and the experimenter should be able to hear the output of the preamplifier on an audio amplifier. Figure 5 illustrates schematically a sequence of events for measuring recruitment and DC force in three MUs. At stage 1, the participant is relaxed, no MU is active. At time 2, the participant is asked to slowly increase the force of abduction against the force transducer until the first clear MU spike is observed and heard (red solid vertical lines indicate spikes). The DC force at stage 3 indicates the recruitment threshold of the first MU. The participant is then asked to discharge the MU at the lowest possible tonic rate (e.g. <10 impulses/s, generally 5-6 imp/s). It is very important that the subject holds the DC force steady during this period and does not make sudden changes in force; sharp changes in force affect the filtered AC force and will preclude extracting the twitch profile of the unit. Once enough spikes are collected to extract a twitch (1-2 minutes between times 3 and 4 results in >350 spikes), the participant is verbally instructed to slowly increase their force until a new MU starts to discharge, at time 5. The firing rate of the first recruited motor unit will usually increase as the DC force level increases. The level of DC force at point 5 is the recruitment threshold of the second MU. The participant is then asked to maintain the discharge of this unit at a low firing rate with a steady DC force level, to collect sufficient data for twitch extraction, prior to increasing the force to recruit the third MU. Three to five motor units can be monitored from one position of the needle electrode as long as each of the units can be discriminated and

Figure 4. FDI recording. This is a classic set up to study recruitment order of MUs during abduction of the index finger in human subjects. The whole hand and forearm are stabilised to prevent movement. The index finger is held against a force transducer, the rest of the hand and fingers are prevented from contributing force to the transducer with appropriate stops. Isometric force, surface EMG and single motor units are recorded at different levels of effort



auditory feedback of discharge rate is available to the participant. If it is not possible to discern individual MUs, move the electrode slightly and repeat the above procedure. One expects to record new MUs in the new position, but the probability of recording from some of the same units is not ruled out; one is collecting a statistical sample of MUs from the muscle. To prevent the problem of aliasing, data acquisition should be done at appropriate rates; 20KHz would be typical for MU spikes. Aliasing of the intramuscular needle EMG for MU recording alters the size and shape of spikes, which in turn causes problems for discrimination of different MUs. This experimental protocol will provide data that can be used to infer the relationship between the recruitment threshold

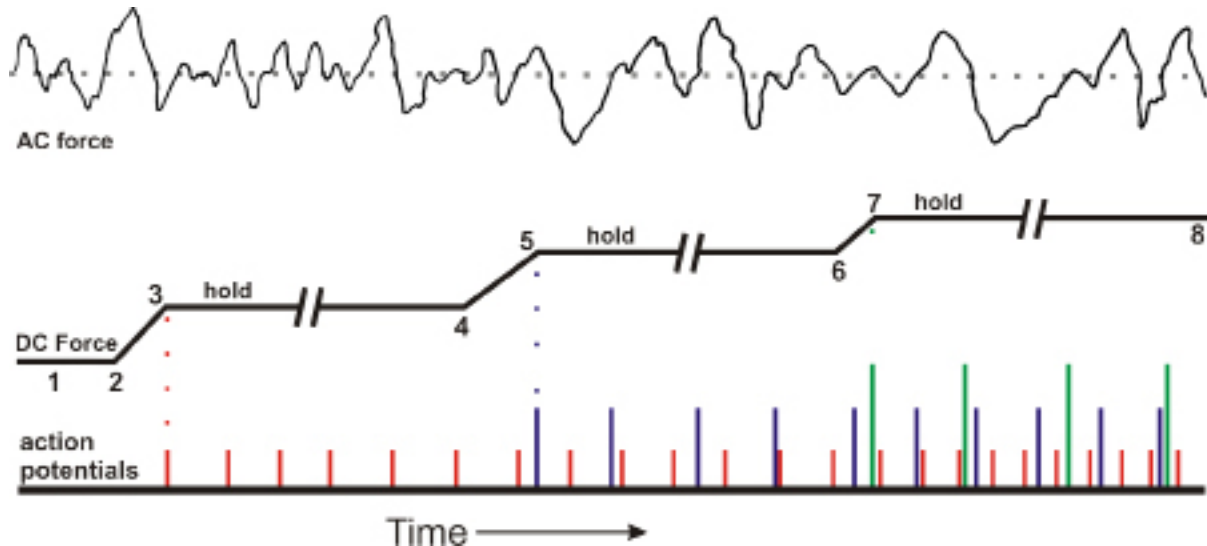
and twitch amplitude during voluntary isometric muscle contractions.

Phasic Recruitment During H-Reflex and Cortical Stimulation

In the above discussion we have dealt with tonic EMG and MU activities. Tonic activity means prolonged continuous activity at least one second in duration. Phasic activity refers to short duration signal such as a muscle twitch, EMG or motor unit response to a single stimulus. For tonic activity one can assess the average activity of the signal over time. For phasic activity, the average has to be obtained from the summation of successive individual responses. Study of recruitment order

Neural Control of Muscle

Figure 5. The three panels above illustrate, from bottom to top: MU spikes, DC and AC force. Note that the recorded MU spike amplitude is not necessarily related to the actual MU size, it is used to distinguish the three MUs. When extracting the twitch profile using spike triggered averaging (STA), the MU firing rate should be maintained at the lowest possible rhythmic firing rate. For example, between time points 3 and 4, the participant maintains a constant DC force and low discharge rate for the red MU, while the simultaneously measured AC force data are used for STA. This procedure is repeated for the remaining two motor units between time points 5-6 and 7-8



of MUs with Ia input is easily done in the soleus muscle in the leg or flexor carpi radialis (FCR) muscle in the forearm. In adults, it is possible to elicit H-reflexes in these two muscles without much interference from large M-waves. With transcranial magnetic stimulation (TMS), the stimulus threshold to recruit MUs is much lower in FCR than in soleus as the density of cortico-motoneuronal connections is much higher in the forearm motoneurons compared to soleus motoneurons. Here, we will describe the procedures to study the recruitment order of FCR MUs during voluntary isometric versus involuntary phasic excitation as illustrated in Figure 6.

Participants are asked to voluntarily recruit two MUs similar to the procedures outlined above for abduction of the index finger. We assume that during slow voluntary isometric contractions the recruitment of units is orderly and follows the size principle. The procedure works best when the two

MUs have clearly different voluntary recruitment thresholds. Therefore, the relative recruitment thresholds should be verified three or four times with slow changes in voluntary isometric force. The participant is then asked to maintain a relatively constant voluntary force near recruitment threshold for the lower threshold MU. A phasic excitation to the motoneuron pool is produced by stimulation: either H-reflex input by stimulating the peripheral nerve, or Transcranial Magnetic Stimulation (TMS) applied over the appropriate area of the primary motor cortex (Bawa and Lemon, 1993; Calancie and Bawa 1985). The strength of the stimulus should be adjusted so that the lower threshold unit responds to seven or eight stimuli out of every ten, then 50-100 stimuli of fixed intensity are given and the responses recorded. The probability of response of each MU to phasic stimuli is measured from their peri stimulus time histograms (PSTHs). If the MU

with the lower voluntary threshold has a greater response probability compared to the second higher threshold MU, then the inference is that the two units have the same order of recruitment to voluntary and phasic involuntary excitation.

Analysis

Population EMG

SEMG can be used for several purposes, and it is always a good idea to record it even if one does not see an immediate need for it. SEMG can be used to provide feedback to participants to enable them to maintain a steady contraction level. For this use, the filtered SEMG signal from the preamplifier, is further low pass filtered (5 – 10 Hz) and is visually displayed in front of the subject on a computer screen or an oscilloscope. If SEMG is going to be used together with spike triggered averaging to generate a MUAP, the preamplifier filters should be set at 30 Hz – 10 KHz. The higher cut off frequency of 10 KHz provides a better differentiation of single motor unit potentials (MUAPs)

To assess the response of a muscle to phasic stimulation using SEMG, a minimum of 75-100 stimuli are typically needed. Multiple stimuli are required because the responses of the motoneurons are probabilistic and vary from trial-to-trial. The response of the motoneurons to a phasic excitatory stimulus will result in short-term synchronization, which is detected as peaks in the SEMG signal (e.g. H-reflexes). With strong synchronous excitation, the trials are averaged with respect to the stimulus at time zero and the magnitude of the response measured from the peaks (e.g. peak-to-peak amplitude). Clear repetitive responses are rare and hence summation of successive responses can lead to error. To measure the response to the phasic stimulus at different levels of background SEMG activity, the signal should be rectified. Rectification is also necessary when phasic responses are spread out in time and shapes vary among succes-

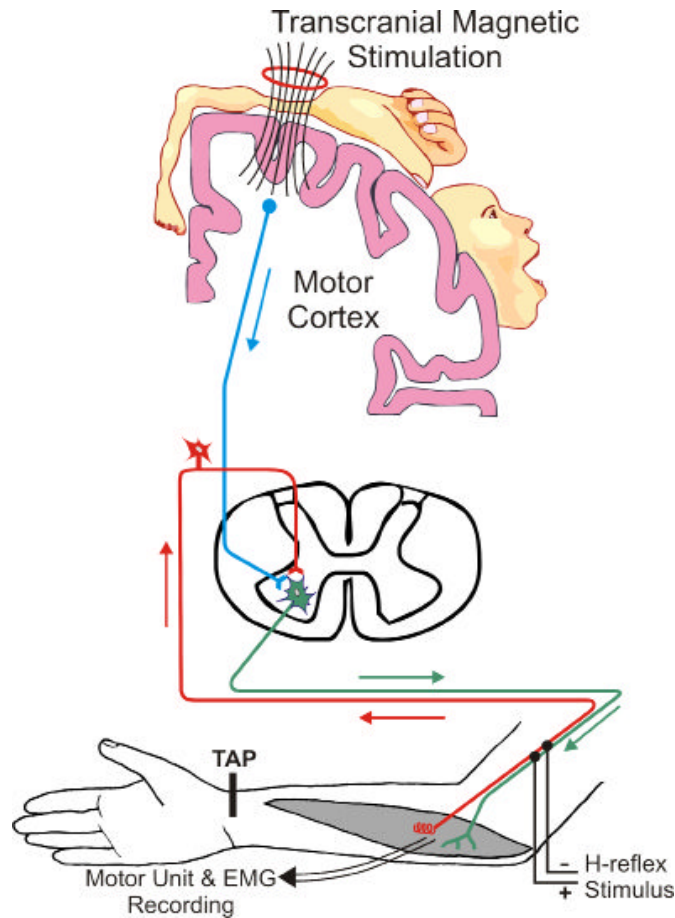
sive responses. Some of the examples are: motor evoked potentials (MEPs), cutaneous reflexes, and stretch reflexes (Figure 7). The SEMG is rectified before averaging, making sure to eliminate any DC bias or offset introduced by electronic hardware used for rectification. After rectification, the responses are averaged and quantified by measuring the area (Figure 7). When quantifying rectified SEMG by measuring the area, the background must be subtracted to estimate the magnitude of the evoked response. To obtain an accurate estimate of background SEMG, averaging is performed on data acquired 50-100 ms prior to the stimulus as well as times after the stimulus at the latency of the evoked response. The average background also helps to obtain values of onset and offset of the evoked activity (Figure7, Manning et al., 2012). Mean and standard deviation (SD) of the background are measured and a horizontal cursor is placed at Mean + 3SD as indicated in Figure 7. Intersection of this horizontal cursor with the evoked peak will give you the values of the onset and termination of the averaged evoked response. The magnitude of the response is measured above the horizontal cursor and between the onset and termination of the response.

Spike Sorting and Analysis

Once spikes have been recorded, we can determine the firing characteristics of each of the recorded MUs, and compute the response of each unit to phasic stimuli. Several discernible MU spikes are recorded by one electrode; spikes from any one MU have the same shape and size, but it is different from spike profiles of the other MUs discharging simultaneously. Different profiles help to separate spikes belonging to different MUs. An example is shown in Figure 8 where two motor units were recorded in a human hand muscle. The smaller spike has been separated and its TTL pulses transferred to channel A while the TTL pulses corresponding to the larger spike have been transferred to channel B. There are several

Neural Control of Muscle

Figure 6. Stimulation to produce involuntary phasic excitation of MUs in wrist flexor muscles. Electrical stimulation of Ia afferents in the median nerve at the elbow produces an H-reflex in FCR. Stimulation of the forearm area of the contralateral motor cortex, with a transcranial magnetic stimulator, generates an MEP in the wrist muscles

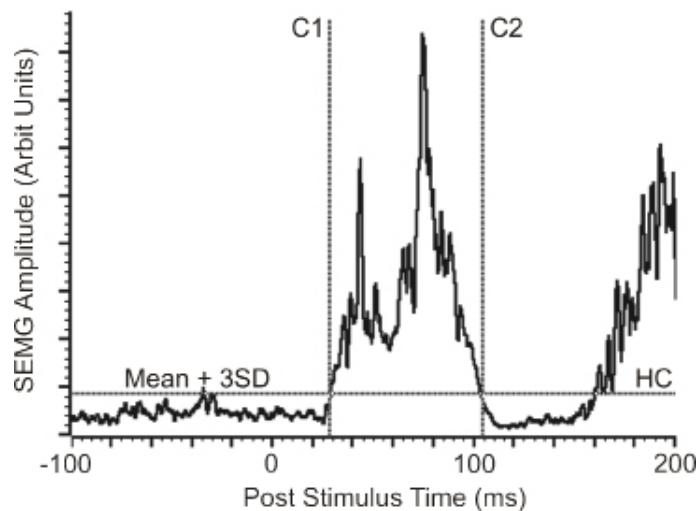


spike sorting algorithms available, or one can use a window discriminator to convert the spike into a TTL pulse; all data are analysed using these TTL pulses as point events in time. If there were a stimulus being applied to study responses of MUs, the time of stimuli would have been placed as TTL pulses on another channel.

First order interval histogram (INTH) provides information on the mean discharge rate of the motor unit and on the variability of inter spike interval (ISI). The histogram is constructed by binning all available intervals in the spike train of interest. A peri stimulus time histogram (PSTH) provides

information on the effect of the stimulus on motoneuron discharge. The histogram is constructed between the TTL pulses of the stimulus and those of the MU of interest. For a tonically firing MU, the histogram will have random events before the stimulus, the spikes will then accumulate during a restricted response time period after the stimulus. There will be MUs which are not active tonically and respond only phasically to the stimulus; their PSTHs will show zero background activity, and a peak will be observed at the time of the response. In a PSTH of a phasically responding MU, an occasional spike outside the response time may

Figure 7. Rectification of signal, measurement of response onset and area. This is an example of stretch reflexes recorded from human wrist flexors with surface EMG electrodes. The wrist was stretched with a torque motor, 20 trials were recorded. SEMG was amplified $\times 1000$, band pass filtered 30 Hz – 3KHz. DC bias was removed, the signal was rectified, and the 20 trials were averaged. The average is shown in the figure. Mean background was computed for 100 ms before the stimulus (time zero), the horizontal cursor (HC) was placed at Mean + 3SD. The vertical cursors C1 and C2 intersected the HC at 29 ms and 104 ms which give the onset and termination times of the reflex response. Area of the response lies between C1, C2 and HC



be observed; it results from synaptic noise. Note: There are non-synaptic sources of noise which can be mistaken for spikes, for example, noise from cell phones, capacitive discharges, spikes from dying muscle fibres, etc. With experience one can distinguish MU spikes from noise.

Spike Triggered Averaging Technique

STA technique is used to average out very small signals time locked to a stimulus from a large time varying signal. For example, if we have data for SEMG and a MU spike from a contracting muscle, we can obtain an estimate of the size of the whole MU from SEMG. Convert the MU spike train to its TTL train, this TTL is used as a stimulus for averaging of correlated MUAP or twitch force from the corresponding population activity. Trigger the computer with TTLs of spike train and average unrectified SEMG. Depending

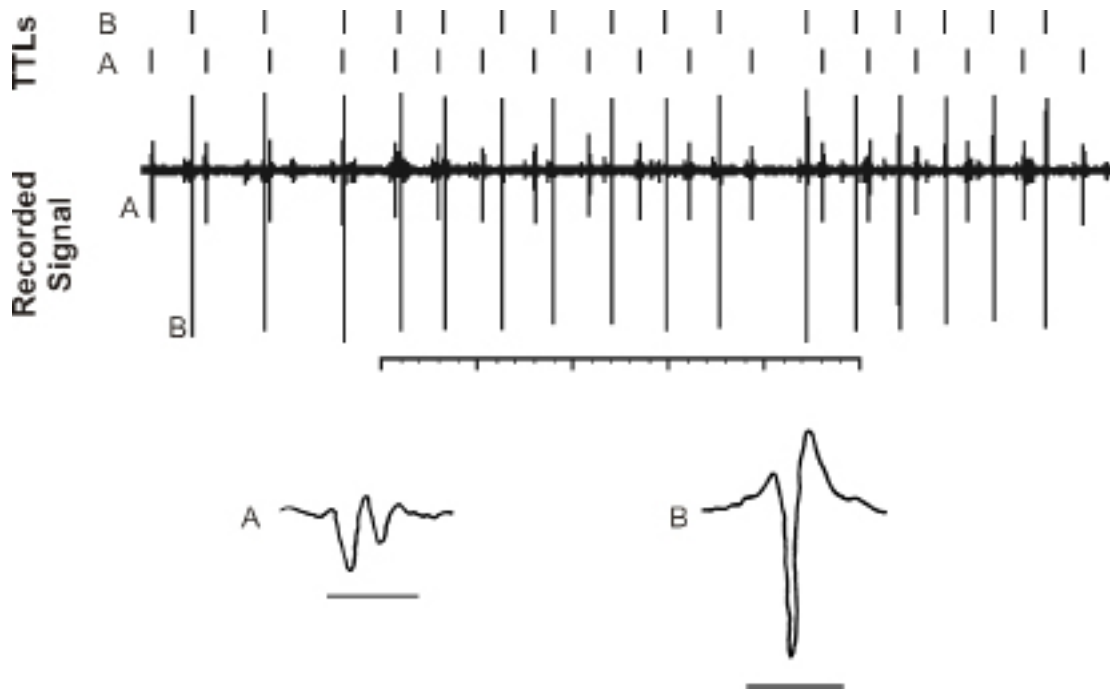
on the size of the MU and the background activity of the active muscle, you will need anywhere from 100 – 1000 triggers. Make your averaging window around 50 ms wide, 25 ms before and 25 ms after the trigger at time zero. The average will give you MUAP. To average twitch force, you need the TTL train of a MU and AC force when the motor unit is discharging at the lowest possible tonic rate (Fig. 5). For averaging, you need a window about 400 ms wide, 50 ms before and 350 ms after the TTL trigger, and 100 – 200 triggers to obtain a clean twitch profile, less for larger motor units (Calancie & Bawa 1986; Stein et al., 1972).

Behaviour of a Population of Motor Units

The description given above deals with 2-5 simultaneously recorded MU spikes in order to come

Neural Control of Muscle

Figure 8. A recording of motor unit signals is shown. The two motor units (A and B) recorded simultaneously with the same electrode are separated into two trains of TTL pulses. The separation is based on their shapes and sizes as shown at the bottom on an expanded time scale. Time bar = 1 sec for the recorded MU signal. For each spike profile, time bar = 2 ms



to conclusions about spike times and recruitment order. Such recordings tell us nothing about muscle fibre distribution for any one motor unit, concentration of MU types in different parts of the muscle and about the architecture of the muscle. More complex EMG array recording electrodes and decomposition techniques, both intracellular and surface recordings, have revealed relative firing behaviours of multiple motor units. For details of these techniques refer to publications by De Luca, Farina, McGill, Merletti, Stålberg and Stashuk, a few references are provided here (De Luca et al., 2006; McGill et al., 2005; Merletti & Farina, 2009; Parsaei et al., 2010; Stålberg et al. 1995; Vieira et al., 2011).

Results

Initial experiments which established the orderly recruitment of motor units were done on hind limb muscles of the cat; stretch of muscles excited Ia afferents which synaptically excited the homonymous and heteronymous motoneuron pools (Henneman 1985; Henneman et al., 1974; Henneman and Mendell 1981; Henneman et al., 1965). In these reduced preparations, reflex activity was recorded either from ventral roots or motor units within the muscle. Human experiments expanded our understanding of MU recruitment when synaptic inputs to motoneurons occurred during voluntary and reflex contractions under more physiological conditions.

Recruitment During Voluntary Contractions

Orderly recruitment, from small to large motor units, was first demonstrated in humans by Stein's group (Milner-Brown et al., 1973). Employing the STA technique to extract twitch profiles of motor units, these researchers showed that MUs with small twitch forces were recruited at lower force thresholds while stronger MUs were recruited at higher voluntary forces. These results for slow isometric voluntary contractions have been shown to be true for a large number of human muscles, see Calancie and Bawa (1990) for detailed references. For very fast voluntary contractions Grimby and Hannerz (1968) suggested a flexible recruitment order which was later refuted by careful studies carried out by Desmedt and Godaux (1977). Similar observations of orderly recruitment have been reported during non-isometric contractions. During functional tasks carried out by the FDI muscle, Jones et al. (1994) demonstrated that the order of recruitment was the same irrespective of the task performed by the subject.

One of the major exceptions to the size principle were reported from those muscles which have been defined anatomically as distinct muscles but functionally they are not. For example, sartorius, which is defined as a single muscle, consists of three functionally distinct subgroups of MUs (Hoffer et al., 1987). The authors suggested orderly recruitment within each subgroup. Such subgrouping and orderly recruitment within each subgroup was clearly demonstrated by Riek and Bawa (1992) for the extensor digitorum communis (EDC) in humans. When EDC acts as a wrist extensor, size-ordered recruitment occurs within the whole motoneuron pool. For extension of the fingers, EDC motoneuron pool is divided into sub-pools, and orderly recruitment takes place within each subgroup of MUs. These studies should not automatically imply that every muscle which is multifunctional has subgrouping of MUs for each task. Jones et al. (1993) tested the recruitment order of MUs in flexor carpi ulnaris (FCU) muscle while

subjects contracted the muscle during isometric and non-isometric wrist flexion, ulnar deviation and co-contraction. They reported that the same motor units contributed to each of the four tasks, and the order of recruitment was the same for all tasks. FCU motoneuron pool, therefore, is not fractionated into subgroups as originally suggested by Denny-Brown (1949).

Another exception to the size principle, which was accepted for a long period, was recruitment during lengthening contractions (Nardone et al. 1989). Bawa and Jones (1999) reinterpreted the data published by Nardone et al. (1989) and came to alternative conclusions. Orderly recruitment of MUs during lengthening contractions was later demonstrated in the upper limb (Søgaard et al. 1996; Stotz and Bawa 2001) and in lower limb muscles (Pasquet et al. 2006) in human subjects.

Recruitment and Rate Coding

Increase in force is produced by two mechanisms, recruitment of additional MUs and rate coding. When a motoneuron pool is excited at a level where it just discharges one MU, any additional excitation increases the firing rate of the first recruited unit while another unit is recruited. The change in firing rate is called rate coding. Recruitment and rate coding go hand in hand to increase muscle force smoothly (De Luca and Erim, 1994; Milner-Brown et al., 1973b; Monster and Chan, 1977; Tanji and Kato, 1973). In small hand muscles, recruitment of most of the MUs takes place at low forces, further increase in force occurs by rate coding. When Kukulka and Clamman (1981) compared activation of the small hand muscle adductor pollicis with the larger proximal muscle biceps brachii, they reported that the vast majority of MUs in the adductor pollicis were recruited at forces <30% MVC (maximum voluntary contraction) while in biceps brachii, recruitment occurred over 0-90% of MVC. Thus rate coding is important for large muscles at all force levels while recruitment is important for small muscles at lower force levels. At higher force levels, small

Neural Control of Muscle

muscles increase force mostly by rate coding. Because of this recruitment pattern, MUs with distinct spike profiles are difficult to record in small muscles; too many MUs become active at quite low levels of force and the potentials start to interfere with each other. Irrespective of the muscle, when a unit is just recruited, it fires at a low rate, thereafter it increases to a maximum rate. The maximum tonic rates in humans vary for slow and fast muscles; in slow soleus the highest tonic rates are around 15 imp/s, while for faster muscles firing rates in the range 30-60 have been reported (Bellemare et al., 1981; De Luca and Erim, 1994; Grimby et al. 1981; Kukulka and Clamman, 1981; Person and Kudina, 1972). During extremely fast contractions, instantaneous firing rates can easily exceed 100 imp/s, but the motoneuron fires only 2-3 spikes at high rates before it slows down (Bawa and Calancie, 1983; Desmedt, 1981; Tanji and Kato, 1972).

Recruitment During Reflexes and Transcranial Stimulation

The test of recruitment order during voluntary contractions involves tonic synaptic inputs to the motoneuron pool and the experimenter records hundreds of successive spikes of a MU. Noise in the neurons varies the instantaneous rate, but one deals with an average firing rate in impulses/s (imp/s). On the other hand when we deal with recruitment in response to a single stimulus, every response is affected by noise. Single response is probabilistic, noise might increase or decrease the probability of MU firing; one might come to wrong conclusions by observing 1-2 responses. One needs to average the response by applying the stimulus multiple times. The average is measured by constructing PSTHs for each MU. One of the main precautions to take in measuring response probability is the background firing rate of the motor unit; the response probability decreases with increase in background firing rate (Jones and Bawa, 1999). With tendon taps applied to the first and second dorsal interosseous muscles, Buller et

al. (1980) showed that MUs which were recruited first during voluntary contractions, were also the ones which responded with higher probability to tendon taps. The same is true for electrically elicited H-reflex in the soleus; MUs recorded first with voluntary effort were also the first ones to respond to Ia input from soleus muscle (Desmedt and Godaux, 1978). The stretch of upper limb muscles activate at least two clear reflex pathways, one spinal and the other transcortical. Surface EMG response consists of a short latency peak M1 (25-55 ms), and a longer latency peak M2 (55 – 100 ms) (Manning et al., 2012; Matthews 1991). Recruitment of motor units is more complex with stretch reflexes. For the wrist extensors and flexors, the transcortical reflex pathway has a much higher gain. In a detailed study of motor unit firing patterns during M1 and M2, Calancie and Bawa (1985) first recorded the voluntary recruitment order of 2-3 motor units and then observed their responses with stretch reflexes. The authors concluded that a motor unit that is recruited first during voluntary contraction is also the one that is recruited first during the stretch reflex response. When the stretch was small or the unit was not facilitated, it preferred to fire during M2 period. If the amplitude of stretch was increased, or the MU was made to fire tonically, the unit now responded at M1 time. Since the M1 reflex pathway has a lower gain, either the motoneuron excitability had to be increased or the synaptic input had to increase for the motoneuron to respond during M1 period. Size ordered recruitment order has also been reported during transcranial electrical stimulation (Calancie et al., 1987) and transcranial magnetic stimulation (Bawa and Lemon, 1993; Hess et al. 1987).

Preferential Recruitment of Motor Units and Explanations of Controversial Results

Though the orderly recruitment pattern of motor units from small to large is quite well established, there are studies which still believe in preferential

recruitment of larger motor units. Clear and repeated observations of selective recruitment are missing. However, there are examples in which very strict order of recruitment breaks down. With prolonged firing, motoneurons tend to fatigue, their firing thresholds increase. A small increase in synaptic input does not maintain firing of these motoneurons but is capable of recruiting new motoneurons. After a while, when the originally fatigued motoneurons recover after rest, the substituting motoneurons drop out to maintain a constant level of motoneuron activity. This phenomenon of substitution of fatigued motoneurons by freshly recruited motoneurons, and resumption of firing of the original motoneurons is called rotation. Rotation occurs among motoneurons which are quite close in thresholds (Manning et al., 2010; Westgaard and De Luca 1999). Another condition in which recruitment order might weaken is during pain. When experimental pain is induced, firing rates of lower threshold units decrease, while higher threshold units are recruited to maintain force (Tucker et al., 2009). There does not appear to be a clear pattern of derecruitment or recruitment in their data.

DISCUSSION

According to Henneman's size principle, the central nervous system employs a simple strategy to recruit motor units of a muscle or a task group. With experimental support from reduced preparations, he argued on theoretical grounds that if CNS had to pick the most appropriate motor units for every task, the computations involved and the time taken to pick just the right type and right number of MUs would make the CNS very inefficient (Henneman et al., 1974). Similarly, using information theory, Senn et al. (1997) provided a strong support for the size principle. They argued that size ordered, "non-selective" recruitment requires minimal neuronal hardware for computation of motor output. The rate of information

transmission between the motoneurons and the muscle is maximized and the error between the command signal to the motoneurons and the force output is minimized.

To explain the size-ordered recruitment, the simplest model is to consider the somata of motoneurons of a pool to be spheres of different diameters. The smallest sphere has the highest input resistance (IR) and IR decreases with increase in diameter of the sphere [considering resistance per unit area (specific resistance) to be the same for each motoneuron]. If the same magnitude of synaptic current arrives at every motoneuron, the smallest motoneuron would depolarize the most, and this depolarization would decrease with increasing size of the motoneuron (De Luca & Erim, 1994). Consequently, the small motoneuron would require the least amount of synaptic current to reach threshold for firing and the larger motoneurons would require more current to start discharging. However, the above assumed uniform membrane properties of motoneurons and uniform synaptic currents are not universally true; additional observations with non-uniform properties have also been reported. For spindle Ia afferents, it has been shown that every afferent gives synaptic input to each homonymous motoneuron, but the input is not uniformly distributed according to motoneuron size. Each afferent makes strongest connections with the motoneurons which are located near its entry zone in the spinal cord (Henneman, 1985; Henneman and Mendell, 1981). Yet, the overall effect of Ia afferent input is to recruit small motoneurons first. Further, it has been reported that small motoneurons have higher specific resistance, an observation which would further increase the IR of smaller motoneurons, and hence increase the probability of them firing with lower currents (Burke et al., 1982). The spike generating region and mechanism may also vary such that the smaller motoneurons fire easily (Gustaffson & Pinter, 1985). Besides variation in intrinsic properties of motoneurons, there is also non-uniformity of synaptic inputs. For example, for homonymous

Neural Control of Muscle

In synaptic inputs to motoneurons, Heckman and Binder (1988) demonstrated larger synaptic currents to small motoneurons, which again favours the size principle. On the other hand, there are inputs which do not favour the size principle. Some inhibitory inputs are stronger onto small motoneurons and under such conditions one might expect the larger MUs to fire without including the small ones (Powers and Binder, 2001). No such observations have been made in behaving, normal animals or humans. It has been proposed that the non-uniformity of synaptic inputs does not necessarily imply preferential recruitment of large units, but it determines gain of the input-output curve of the motoneuron pool (Kernell and Hultborn, 1990). When there is a stronger inhibitory synaptic input to the small motoneurons, or a stronger excitatory input of the larger motoneurons, the slope of the gain curve increases which makes it easier for the larger MUs to participate in force production (Burke, 1981; Heckman & Binder, 1988). Participation of larger MUs occurs also during fast synaptic inputs. Synaptic current, with higher rate of rise, recruits extra larger MUs which fire 1-2 spikes; these extra spikes enhance the rate of rise of force at the start of the contraction (Smith et al., 1995).

All carefully done experiments to date have shown motor units to be recruited according to Henneman's size principle, the small MUs recruited before larger ones. The most important point we want to make here is that size is not a perfect determinant in a normal animal or human subjects due to the presence of noise in the neuromuscular system. Small deviations, from perfect size relationship cannot be interpreted as exceptions to the size principle. An exception would imply that a small subgroup of larger MUs is recruited preferentially for each particular task without necessarily activating S type units. There are no experiments which have unequivocally shown such results. Furthermore, a contraction where larger units are recruited before small ones would be imprecise (Senn et al. 1997). A common

exception brought forward is the derecruitment of small motor units with electrical stimulation of cutaneous nerves in a reduced cat preparation (Kanda et al., 1977); however, this was later shown not to be true (Clarke et al. 1993). Other cases in which the size principle weakens is during pain and fatigue (rotation). This is not surprising. One of the fundamental advantages of orderly recruitment by size is that it allows precision of movement or contraction. Size principle is not very robust after reinnervation of a muscle after injury (Gordon et al. 2004). Death of motoneurons during ageing is accompanied by reinnervation of the orphaned muscle fibres, increase in motor unit sizes and molecular changes in muscle proteins (Chan et al. 2001). During conditions of fatigue, intense pain, reinnervation or ageing, we surely do not expect great precision of movement.

CONCLUSION

There are two points that we would like to make on motor unit studies: first, on order of recruitment, and second, on the questions still unresolved that can be handled by new technologies.

Recruitment of motoneurons according to Henneman's size principle seems to be a simplified strategy used by the central nervous system in order to produce force fast and with most precision. The precision is further enabled by rate coding. Selective recruitment of larger motor units has not been observed. The slowing of firing rates of already firing MUs and recruitment of additional, slightly higher threshold MUs with pain stimulus does not imply selective recruitment of large motor units. Similarly, rotation among motor units does not indicate a breakdown of size principle. During pain, fatigue or clinical injury, sufficient force output rather than extreme precision of force output become more relevant.

The second point we want to make is with regard to the future studies. In this Chapter we have described motor unit techniques which were based

on 1-2 intramuscular electrodes from which one can deduce discharge behaviour of few simultaneously firing motor units. Recruitment order at the level spinal cord translates into similar recruitment order in terms of force only for small muscles with parallel fibres. How does recruitment order related to force output in muscles with complex architectures, for example, human soleus (Agur et al. 2003; Sinha et al., 2011) or gastrocnemius muscles (Martin et al. 2001; Vieira et al. 2012). Monti et al. (2001) have described a variety of sophisticated muscle fibre distributions in various muscles which would affect the force output of each motor unit differently. In order to understand the interaction of various motor units in a complex muscle (muscle fibre distribution with respect to orientation, in-parallel or in-series placement with fibres of other motor units, placement of a muscle unit within the muscle), more sophisticated electrode configurations are needed. Even though the multi-electrode arrays are relatively new; they can provide information about the distribution of small versus large motor units within a muscle. Models of muscle contraction that include recruitment and rate coding, muscle fibre distribution, angle of pennation, types of muscle fibres, and other architectural and cellular characteristics can be challenging but can help us understand the contribution of each factor in cases where experimental data are not possible (Fuglevand et al., 1993 ; Röhrle et al., 2012). The non-invasive, multi-array SEMG electrodes can be very useful to investigate how muscles develop during childhood, change during ageing, and what happens during various neuromuscular diseases.

REFERENCES

- Adrian, R. H. (1976). The propagation of excitation in striated muscle. (1976). Voluntary control of human motor units. In M. Shahani (Ed.), *The motor system: Neurophysiology and muscle mechanisms* (pp. 15–24). Amsterdam, The Netherlands: Elsevier.
- Agur, A. M., Ng-Thow-Hing, V., Ball, K. A., Fiume, E., & McKee, N. H. (2003). Documentation and three-dimensional modelling of human soleus muscle architecture. *Clinical Anatomy (New York, N.Y.)*, 16(4), 285–293. doi:10.1002/ca.10112 PMID:12794910
- Bawa, P., & Calancie, B. (1983). Repetitive doublets in human flexor carpi radialis muscle. *Journal of Physiology, (London)*, 339, 123-132.
- Bawa, P., & Jones, K. E. (1999). Do lengthening contractions represent a case of preferential recruitment of large motor units. *Progress in Brain Research*, 123, 215–220. doi:10.1016/S0079-6123(08)62858-7 PMID:10635718
- Bawa, P., & Lemon, R. N. (1993). Recruitment of motor units in response to transcranial magnetic stimulation in man. *Journal of Physiology, (London)*, 471, 445-464.
- Bawa, P., Pang, P., Olesen, K., & Calancie, B. (2006). Rotation of motoneurons during prolonged isometric contractions in humans. *Journal of Neurophysiology*, 96(3), 1135–1140. doi:10.1152/jn.01063.2005 PMID:16775202
- Bawa, P., & Tatton, W. G. (1979). Motor units responses in muscles stretched by imposed displacements of the monkey wrist. *Experimental Brain Research*, 37, 417–438. doi:10.1007/BF00236815 PMID:118044

Neural Control of Muscle

- Bellemare, F., Woods, J. J., Johansson, R., & Bigland-Ritchie, B. (1983). Motor-unit discharge rates in maximal voluntary contractions of three human muscles. *Journal of Neurophysiology*, *50*(6), 1380–1392. PMID:6663333
- Bodine-Fowler, S., Garfinkel, A., Roland, R. R., & Edgerton, V. R. (1990). Spatial distribution of muscle fibres within the territory of a motor unit. *Muscle & Nerve*, *13*(12), 1133–1145. doi:10.1002/mus.880131208 PMID:1702521
- Brinkman, R. S. A., & Türker, K. S. (2003). A method for quantifying reflex responses from intra-muscular and surface electromyogram. *Journal of Neuroscience Methods*, *122*, 179–193. doi:10.1016/S0165-0270(02)00321-7 PMID:12573477
- Buller, N. P., Garnett, R., & Stephens, J. A. (1980). The reflex responses of single motor units in human hand muscles following muscle afferent stimulation. *The Journal of Physiology*, *193*, 141–160. PMID:7431236
- Burke, R. E. (1981). Motor units: Anatomy, physiology, and functional organization. In V. B. Brooks (Ed.), *Handbook of physiology* (Vol. I, pp. 345–422). Bethesda, MD: American Physiological Society.
- Burke, R. E., Dum, R. P., Fleshman, J. W., Glenn, L. L., Lev-Tov, A., O'Donovan, M. J., & Pinter, M. J. (1982). An HRP study of the relation between cell size and motor unit type in cat ankle extensor motoneurons. *The Journal of Comparative Neurology*, *209*, 17–28. doi:10.1002/cne.902090103 PMID:7119171
- Calancie, B., & Bawa, P. (1985). Voluntary and reflexive recruitment of flexor carpi radialis motor units in man. *Journal of Neurophysiology*, *53*, 1194–1200. PMID:3998806
- Calancie, B., & Bawa, P. (1986). Limitations of the spike triggered averaging technique for obtaining motor unit twitch profiles. *Muscle & Nerve*, *9*, 78–83. doi:10.1002/mus.880090113 PMID:3951484
- Calancie, B., & Bawa, P. (1990). Motor unit recruitment in humans. In M. D. Binder, & L. M. Mendell (Eds.), *The segmental motor system* (pp. 75–111). New York: Oxford University Press.
- Calancie, B., Nordin, M., Wallin, U., & Hagbarth, K.-E. (1987). Motor-unit responses in human wrist flexor and extensor muscles to transcranial cortical stimuli. *Journal of Neurophysiology*, *58*, 1168–1185. PMID:3694249
- Chan, K. M., Doherty, T. J., & Brown, W. F. (2001). Contractile properties of human motor units in health, aging, and disease. *Muscle & Nerve*, *24*(9), 1113–1133. doi:10.1002/mus.1123 PMID:11494264
- Clark, B. D., Dacko, S. M., & Cope, T. C. (1993). Cutaneous stimulation fails to alter motor units recruitment in the decerebrate cat. *Journal of Neurophysiology*, *70*(4), 1433–1439. PMID:8283206
- De Luca, C. J., Adam, A., Wotiz, R., Gilmore, L. D., & Nawab, S. H. (2006). Decomposition of surface EMG signals. *Journal of Neurophysiology*, *96*(3), 1646–1657. doi:10.1152/jn.00009.2006 PMID:16899649
- De Luca, C. J., & Erim, Z. (1994). Common drive of motor units in the regulation of muscle force. *Trends in Neurosciences*, *17*(7), 299–305. doi:10.1016/0166-2236(94)90064-7 PMID:7524216
- De Luca, C. J., Gilmore, L. D., Kuznetsov, M., & Roy, S. H. (2010). Filtering the surface EMG signal: Movement artifact and baseline noise contamination. *Journal of Biomechanics*, *43*(8), 1573–1579. doi:10.1016/j.jbiomech.2010.01.027 PMID:20206934

- De Luca, C. J., Kuznetsov, M., Gilmore, L. D., & Roy, S. H. (2012). Inter-electrode spacing of surface EMG sensors: Reduction of crosstalk contamination during voluntary contractions. *Journal of Biomechanics*, *45*(3), 555–561. doi:10.1016/j.jbiomech.2011.11.010 PMID:22169134
- Denny-Brown, D. (1949). Interpretation of the electromyogram. *Archives of Neurology and Psychiatry*, *61*(2), 99–128. doi:10.1001/archneur-psyc.1949.02310080003001 PMID:18152778
- Desmedt, J. E. (1981). The size principle of motoneuron recruitment in ballistic or ramp voluntary contractions in man. In J. E. Desmedt (Ed.), *Motor unit types, recruitment and plasticity in health and disease* (Progress in clinical neurophysiology, Vol. 9) (pp. 97-136). Basel, Switzerland: Karger.
- Desmedt, J. E., & Godaux, E. (1977). Fast motor units are not preferentially activated in rapid voluntary contractions in man. *Nature*, *267*(5613), 717–719. doi:10.1038/267717a0 PMID:876393
- Desmedt, J. E., & Godaux, E. (1978). Mechanism of the vibration paradox: Excitatory and inhibitory effects of tendon vibration on single soleus motor units in man. *Journal of Physiology*, (London), *285*, 197-207.
- Ellaway, P. H. (1978). Cumulative sum technique and its application to the analysis of peristimulus time histograms. *Electroencephalography and Clinical Neurophysiology*, *45*, 302–304. doi:10.1016/0013-4694(78)90017-2 PMID:78843
- Fuglevand, A. J., Winter, D. A., & Patla, A. E. (1993). *Journal of Neurophysiology*, *70*(6), 2470–2488. PMID:8120594
- Gordon, T., Thomas, C. K., Munson, J. B., & Stein, R. B. (2004). The resilience of the size principle in the organization of motor unit properties in normal and reinnervated adult skeletal muscle. *Canadian Journal of Physiology and Pharmacology*, *82*(8-9), 645–661. doi:10.1139/y04-081 PMID:15523522
- Grimby, L., & Hannerz, J. (1968). Recruitment order of motor units in voluntary contractions: Changes induced by proprioceptive afferent activity. *Journal of Neurology, Neurosurgery, and Psychiatry*, *31*(6), 565–564. doi:10.1136/jnnp.31.6.565 PMID:5709842
- Grimby, L., Hannerz, J., & Hedman, B. (1981). The fatigue and voluntary discharge properties of single motor units in man. *The Journal of Physiology*, *316*, 545–554. PMID:7320881
- Gustaffson, B., & Pinter, M. J. (1985). On factors determining orderly recruitment of motor units: a role for intrinsic membrane properties. *Trends in Neurosciences*, *8*, 431–433. doi:10.1016/0166-2236(85)90152-3
- Heckman, C. J., & Binder, M. D. (1988). Analysis of effective synaptic currents generated by homonymous Ia afferent fibers in motoneurons of the cat. *Journal of Neurophysiology*, *60*(6), 1946–1966. PMID:3236057
- Henneman, E. (1985). The size principle: A deterministic output emerges from a set of probabilistic connections. *The Journal of Experimental Biology*, *115*, 105–112. PMID:3161974
- Henneman, E., Clamann, H. P., Gillies, J. D., & Skinner, R. D. (1974). Rank order of motoneurons within a pool: Law of combination. *Journal of Neurophysiology*, *37*(6), 1338–1349. PMID:4436704
- Henneman, E., & Mendell, L. M. (1981). Functional organization of motoneuron pool and its inputs. In V. B. Brooks (Ed.), *Handbook of physiology* (Vol. I, pp. 423–507). Bethesda, MD: American Physiological Society.
- Henneman, E., Shahani, B. T., & Young, R. R. (1976). Voluntary control of human motor units. In M. Shahani (Ed.), *The motor system: Neurophysiology and muscle mechanisms* (pp. 73–78). Amsterdam, The Netherlands: Elsevier.

Neural Control of Muscle

- Henneman, E., Somjen, G., & Carpenter, D. (1965). Functional significance of cell size in spinal motoneurons. *Journal of Neurophysiology*, 28, 599–620. PMID:5835487
- Hess, C. W., Mills, K. R., & Murray, N. M. (1987). Responses in small hand muscles from magnetic stimulation of the human brain. *Journal of Physiology*, (London), 388, 397-419.
- Hoffer, J. A., Loeb, G. E., Sugano, N., Marks, W. B., O'Donovan, M. J., & Pratt, C. A. (1987). Cat hindlimb motoneurons during locomotion. III. Functional segregation in Sartorius. *Journal of Neurophysiology*, 57(2), 554–562. PMID:3559692
- Johnson, M. A., Polgar, J., Weightman, D., & Appleton, D. (1973). Data on the distribution of fibre types in thirty-six human muscles. An autopsy study. *Journal of the Neurological Sciences*, 18, 111–129. doi:10.1016/0022-510X(73)90023-3 PMID:4120482
- Jones, K. E., & Bawa, P. (1997). Computer simulations of responses of human motoneurons to composite Ia EPSPs: Effects of background firing rate. *Journal of Neurophysiology*, 77, 405–420. PMID:9120581
- Jones, K. E., & Bawa, P. (1999). A comparison of human motoneuron data to simulated data using cat motoneuron models. *Journal of Physiology, Paris*, 93, 43–59. doi:10.1016/S0928-4257(99)80135-1 PMID:10084708
- Jones, K. E., Bawa, P., & McMillan, A. S. (1993). Recruitment of motor units in human flexor carpi ulnaris. *Brain Research*, 602, 354–356. doi:10.1016/0006-8993(93)90702-O PMID:8448677
- Jones, K. E., Lyons, M., Bawa, P., & Lemon, R. N. (1994). Recruitment of motoneurons during various behavioural tasks. *Experimental Brain Research*, 100(3), 503–508. doi:10.1007/BF02738409 PMID:7813686
- Kanda, K., Burke, R. E., & Walmsley, B. (1977). Differential control of fast and slow twitch motor units in the decerebrate cat. *Experimental Brain Research*, 29(1), 57–74. doi:10.1007/BF00236875 PMID:891681
- Kanda, K., & Desmedt, J. E. (1983). Cutaneous facilitation of large motor units and motor control of human fingers in precision grip. In J. E. Desmedt (Ed.), *Motor control mechanisms in health and disease*. (Advances in neurology, vol. 39) (pp. 253-261). New York: Raven Press.
- Keen, D. A., Chou, L.-W., Nordstrom, M. A., & Fuglevand, A. J. (2012). Short-term synchrony in diverse motor nuclei presumed to receive different extents of direct cortical input. *Journal of Neurophysiology*, 108, 3264–3275. doi:10.1152/jn.01154.2011 PMID:23019009
- Kernell, D., Bakels, R., & Copray, J. C. (1999). Discharge properties of motoneurons: How are they matched to the properties and use of their muscle units? *Journal of Physiology, Paris*, 93, 87–96. doi:10.1016/S0928-4257(99)80139-9 PMID:10084712
- Kernell, D., & Hultborn, H. (1990). Synaptic effects on recruitment gain: A mechanism of importance for the input-output relations of motoneuron pools? *Brain Research*, 507, 176–179. doi:10.1016/0006-8993(90)90542-J PMID:2302576
- Kukulka, C. G., & Clamann, H. P. (1981). Comparison of the recruitment and discharge properties of motor units in human brachial biceps and adductor pollicis during isometric contractions. *Brain Research*, 219, 45–55. doi:10.1016/0006-8993(81)90266-3 PMID:7260629

- Manning, C. D., Miller, T. A., Burnham, M. L., Murnaghan, C. D., Calancie, B., & Bawa, P. (2010). Recovery of human motoneurons during rotation. *Experimental Brain Research*, *204*, 139–144. doi:10.1007/s00221-010-2295-2 PMID:20490783
- Manning, C. D., Tolhurst, S. A., & Bawa, P. (2012). Proprioceptive reaction times and long-latency reflexes in humans. *Experimental Brain Research*, *221*, 155–166. doi:10.1007/s00221-012-3157-x PMID:22766848
- Martin, D. C., Medri, M. K., Chow, R. S., Oxorn, V., Leekam, R. N., Agur, A. M., & McKee, N. H. (2001). Comparing human skeletal muscle architectural parameters of cadavers with in vivo ultrasonographic measurements. *Journal of Anatomy*, *199*(4), 429–434. doi:10.1046/j.1469-7580.2001.19940429.x PMID:11693303
- Matthews, P. B. C. (1991). The human stretch reflex and the motor cortex. *Trends in Neurosciences*, *14*, 87–91. doi:10.1016/0166-2236(91)90064-2 PMID:1709536
- Matthews, P. B. C. (1996). Relationship of firing intervals of human motor units to the trajectory of post-spike after-hyperpolarization and synaptic noise. *The Journal of Physiology*, *492*(2), 597–628. PMID:9019553
- McGill, K. C., Lateva, Z. C., & Marateb, H. R. (2005). EMGLAB: An interactive EMG decomposition program. *Journal of Neuroscience Methods*, *149*(2), 121–133. doi:10.1016/j.jneumeth.2005.05.015 PMID:16026846
- Merletti, R., & Farina, D. (2009). Analysis of intramuscular electromyogram signals. *Philosophical Transactions of the Royal Society A*, *367*, 357–368. doi:10.1098/rsta.2008.0235
- Milner-Brown, H. S., Stein, R. B., & Yemm, R. (1973a). The orderly recruitment of human motor units during voluntary isometric contractions. *The Journal of Physiology*, *230*, 359–370. PMID:4350770
- Milner-Brown, H. S., Stein, R. B., & Yemm, R. (1973b). Changes in firing rate of human motor units during linearly changing voluntary contractions. *The Journal of Physiology*, *230*, 371–390. PMID:4708898
- Mochizuki, G., Ivanova, T. D., & Garland, S. J. (2005). Synchronization of motor units in human soleus muscle during standing postural tasks. *Journal of Neurophysiology*, *94*, 62–69. doi:10.1152/jn.01322.2004 PMID:15744004
- Monster, A. W., & Chan, H. (1977). Isometric force production by motor units of the extensor digitorum communis muscle in man. *Journal of Neurophysiology*, *40*, 1432–1443. PMID:925737
- Monti, R. J., Roy, R. R., & Edgerton, V. R. (2001). Role of motor unit structure in defining function. *Muscle & Nerve*, *24*(7), 848–866. doi:10.1002/mus.1083 PMID:11410913
- Nardone, A., Romanò, C., & Schieppatti, A. (1989). Selective recruitment of high-threshold human motor units during voluntary isotonic lengthening of active muscles. *The Journal of Physiology*, *409*, 451–471. PMID:2585297
- Oya, T., Riek, S., & Cresswell, A. G. (2009). Recruitment and rate coding organisation for soleus motor units across entire range of voluntary isometric plantar flexions. *The Journal of Physiology*, *587*(19), 4737–4748. doi:10.1113/jphysiol.2009.175695 PMID:19703968
- Parsaei, H., Stashuk, D. W., Rasheed, S., Farkas, C., & Hamilton-Wright, A. (2010). Intramuscular EMG signal decomposition. *Critical Reviews in Biomedical Engineering*, *38*(5), 435–465. doi:10.1615/CritRevBiomedEng.v38.i5.20 PMID:21175408

Neural Control of Muscle

- Pasquet, B., Carpentier, A., & Duchateau, J. (2006). Specific modulation of motor unit discharge for a similar change in fascicle length during shortening and lengthening contractions in humans. *The Journal of Physiology*, *577*(2), 753–765. doi:10.1113/jphysiol.2006.117986 PMID:16959853
- Person, R. S., & Kudina, L. P. (1972). Discharge frequency and discharge pattern of human motor units during voluntary contraction of muscle. *Electroencephalography and Clinical Neurophysiology*, *32*, 471–483. doi:10.1016/0013-4694(72)90058-2 PMID:4112299
- Powers, R. K., & Binder, M. D. (2001). Input-output functions of mammalian motoneurons. *Reviews of Physiology, Biochemistry and Pharmacology*, *143*, 137–263. doi:10.1007/BFb0115594 PMID:11428264
- Prochazka, G. L., Clarac, F., Loeb, G. E., Rothwell, J. C., & Wolpaw, J. R. (2000). What do reflex and voluntary mean? Modern views on an ancient debate. *Experimental Brain Research*, *130*(4), 417–432. doi:10.1007/s002219900250 PMID:10717785
- Riek, S., & Bawa, P. (1992). Recruitment of motor units in human forearm extensors. *Journal of Neurophysiology*, *68*, 100–108. PMID:1517816
- Röhrle, O., Davidson, J. B., & Pullan, A. J. (2012). A physiologically based, multi-scale model of skeletal muscle structure and function. *Frontiers in Physiology*, *3*, 1–14. doi:10.3389/fphys.2012.00358 PMID:22275902
- Schiaffino, S., & Reggiani, C. (2011). Fiber types in mammalian skeletal muscles. *Physiological Reviews*, *91*(4), 1447–1531. doi:10.1152/physrev.00031.2010 PMID:22013216
- Senn, W. K., Wyler, K., Clamann, H. P., Kleinle, J., Lüscher, H.-R., & Müller, L. (1997). Size principle and information theory. *Biological Cybernetics*, *76*, 11–22. doi:10.1007/s004220050317 PMID:9050202
- Sinha, U., Sinha, S., Hodgson, J. A., & Edgerton, R. V. (2011). Human soleus muscle architecture at different ankle joint angles from magnetic resonance diffusion tensor imaging. *Journal of Applied Physiology*, *110*(3), 807–819. doi:10.1152/jappphysiol.00923.2010 PMID:21164150
- Smith, L. C., Zhong, T., & Bawa, P. (1995). Dynamic properties of human motoneurons. *Canadian Journal of Physiology and Pharmacology*, *73*, 113–123. doi:10.1139/y95-016 PMID:7600441
- Søgaard, K., Christensen, H., Jansen, B. R., Finsen, L., & Sjøgaard, G. (1996). Motor control and kinetics during low level concentric and eccentric contractions in man. *Electroencephalography and Clinical Neurophysiology*, *101*(5), 453–460. doi:10.1016/0924-980X(96)95629-5 PMID:8913200
- Stålberg, E., Falck, B., Sonoo, M., Stålberg, S., & Aström, M. (1995). Multi-MUP EMG analysis—A two year experience in daily clinical work. *Electroencephalography and Clinical Neurophysiology*, *97*(3), 145–154. doi:10.1016/0924-980X(95)00007-8 PMID:7607102
- Staudenmann, D., Kingma, I., Daffertshofer, A., Stegeman, D. F., & van Dieën, J. H. (2009). Heterogeneity of muscle activation in relation to force direction: A multi-channel surface electromyography study on the triceps surae muscle. *Journal of Electromyography and Kinesiology*, *19*, 882–895. doi:10.1016/j.jelekin.2008.04.013 PMID:18556216

Stein, R. B., French, A. S., Mannard, A., & Yemm, R. (1972). New methods for analyzing motor function in man and animals. *Brain Research*, 40(1), 187–192. doi:10.1016/0006-8993(72)90126-6 PMID:5033795

Stotz, P. J., & Bawa, P. (2001). Motor unit recruitment during lengthening contractions of human wrist flexors. *Muscle & Nerve*, 24(11), 1535–1541. doi:10.1002/mus.1179 PMID:11745957

Tanji, J., & Kato, M. (1972). Discharges of single motor units at voluntary contractions of abductor digiti minimi muscle in man. *Brain Research*, 45, 590–593. doi:10.1016/0006-8993(72)90488-X PMID:4634329

Tanji, J., & Kato, M. (1973). Firing rate of individual motor units in voluntary contractions of abductor digiti minimi muscle in man. *Experimental Neurology*, 40, 771–783. doi:10.1016/0014-4886(73)90111-8 PMID:4353259

Ter Haar Romeny, B. M., Danier van der Gon, J. J., & Gielen, C. C. A. M. (1984). Relation between location of a motor unit in the human biceps brachii and its critical firing levels for different tasks. *Experimental Neurology*, 85, 631–650. doi:10.1016/0014-4886(84)90036-0 PMID:6468581

Tucker, K., Butler, J., Graven-Nielsen, T., Riek, S., & Hodges, P. (2009). Motor unit recruitment strategies are altered during deep-tissue pain. *The Journal of Neuroscience*, 29(35), 10820–10826. doi:10.1523/JNEUROSCI.5211-08.2009 PMID:19726639

Vieira, T. M., Loram, I. D., Muceli, S., & Merletti, R., & Farina. (2011). Postural activation of the human gastrocnemius muscle: Are the muscle units spatially localised. *The Journal of Physiology*, 589(2), 431–443. doi:10.1113/jphysiol.2010.201806 PMID:21115645

Westgaard, R. H., & De Luca, C. J. (1999). Motor unit substitution in long-duration contractions of the human trapezius muscle. *Journal of Neurophysiology*, 82, 501–504. PMID:10400978

ADDITIONAL READING

Binder, M. D., & Mendell, L. M. (Eds.). (1990). *The Segmental Motor System*. New York: Oxford University Press.

Desmedt, J. E. (Ed.). (1981). *Motor unit types, recruitment and plasticity in health and disease*. *Progress in Clinical Neurophysiology* (Vol. 9). Basel: Karger.

Enoka, R. (2008). *Neuromechanics of human movement* (4th ed.). Champaign, IL: Human Kinetics.

Geddes, L. A., & Baker, L. E. (1975). *Principles of Applied Biomedical Instrumentation*. New York: Wiley-Interscience.

Heckman, C. J., & Enoka, R. M. (2012). Motor unit. *Comprehensive Physiology*, 2, 2629–2682. PMID:23720261

Kernell, D. (2006). *The motoneurone and its muscle fibres*. Oxford: Oxford University Press. doi:10.1093/acprof:oso/9780198526551.001.0001

Loeb, G. L., & Gans, C. (1986). *Electromyography for Experimentalists*. Chicago, Illinois: University of Chicago Press.

Robertson, D. G. E., Caldwell, G. E., Hamill, J., Kamen, G., & Whittlesey, S. N. (2004). *Research Methods in Biomechanics*. Champaign, IL: Human Kinetics.

KEY TERMS AND DEFINITIONS

Acquisition Rate: The sampling rate at which the computer acquires the physiological signal. The rate (Hz) is inverse of sampling interval (sec). It should be at least twice the highest frequency contained in the signal being sampled.

Action Potential (AP): The rapid change in membrane potential of a neuron or muscle fibre. Compound action potential (CAP) is the potential generated by the superposition of more than one AP. It is almost impossible to exactly superimpose two APs, therefore a CAP is longer in duration than a single AP.

Electromyography (EMG): The technique used to record and study population activity, for both surface (SEMG) and intramuscular (IEMG) recordings. Though invasive, intramuscular recording has been more accurate.

Firing Rate, Expressed As Impulses/s (imp/s): The number of action potentials generated in one second; many publications use Hz rather than imp/s. We will retain Hz when referring to data in the frequency domain. Instantaneous firing rate between two spikes is the inverse of interval between the two spikes. If the interval between two spikes is t sec, the instantaneous firing rate is $1/t$ imp/s.

Motor Unit (MU) Activity as Measured: Comprises the spikes or potentials recorded with intramuscular micro electrodes. The electrode samples the activity of a few muscle fibres of

each MU which are located in the vicinity of its tip. Thus a MU spike is a CAP.

Motor Unit Action Potential (MUAP): Generated by the whole motor unit, during almost synchronous firing all muscles fibres of MU, cannot be recorded. Since the onset times of APs in muscles fibres of a MU vary, the duration of MUAP is much longer than a typical AP, MUAP is a CAP. The representative motor unit potential (MUP) can be recorded with surface EMG electrodes during weak contractions, or is often extracted from SEMG by spike triggered averaging (STA) technique.

Single Fibre Action Potential (SFAP): The extracellular action potential generated by a single muscle fibre.

Spike Triggered Averaging: This procedure is used to extract a small signal time locked to a spike, from a large time varying signal which is produced by a number of other spikes which occur randomly with respect to the spike in question.

TTL or Transistor-Transistor-Logic Pulse: Will be use for a brief (100 μ s) pulse, 4-5 V in amplitude. It is an event which can be used as a stimulus, or for spike train analysis.

ENDNOTES

- ¹ Motoneuron will be used throughout rather than alpha motorneuron

Chapter 2

New Advances in Single Fiber Electromyography

Javier Rodriguez-Falces
Public University of Navarra, Spain

ABSTRACT

The aim of this chapter is to present a general perspective of SFEMG together with a description of the anatomical, physiological, and technical aspects that are involved in the recording of single fibre action potentials (SFAPs). First, a simulation model that relates analytically the intracellular action potential (IAP) and SFAP mathematical expressions is described. Second, the most recent findings regarding the shape features of human SFAPs are outlined. Third, a description of how different types of needle electrodes affect the characteristics of the recorded potential is detailed. Fourth, an explanation of the most important effects of filtering on the SFAP characteristics is provided. Finally, a description of the principles of jitter estimation together with the most important sources of errors is presented.

1. INTRODUCTION

The advent of single fibre electromyography (SFEMG) allowed investigators to record potentials produced by single muscle fibres (i.e., the so-called SFAPs). Characterization of the shape peculiarities of the SFAP (i.e., the SFAP morphologic features) is essential as it enables to extract information about the characteristics of human intracellular action potentials (IAPs). This is highly valuable as knowledge about the

characteristics of human IAPs is still incomplete (Rodriguez-Falces et al., 2012a, 2012b).

Over the years, SFEMG has been developed to study the microphysiology of the motor unit, such as the propagation velocity of individual muscle fibres (Stålberg, 1966), the distribution of muscle fibres within individual motor units (Sanders & Stålberg, 1996), and, most remarkably, the neuromuscular jitter (Stålberg & Trontelj, 1979). Nowadays, estimation of the neuromuscular jitter is the most reliable test to evaluate the function-

DOI: 10.4018/978-1-4666-6090-8.ch002

New Advances in Single Fiber Electromyography

ing of neuromuscular transmission in vivo and SFEMG has become a useful technique for the diagnosis of a great variety of neuromuscular disorders.

Buchthal was the first to analyze extensively the characteristics of extracellular potentials produced by the activation of human skeletal muscle fibres (Buchthal & Pinelli, 1953; Buchthal et al., 1954a, 1954b). However, the large recording surface of the electrodes he used prevented him to record electrical activity from individual muscle fibres. It was not until the advent of SFEMG, promoted by Ekstedt (1964) and Stålberg (1966), that the identification of SFAPs was possible. Therefore, the feature that makes the SFEMG technique unique is its high selectivity, which is provided by the small recording surface of the single-fiber (SF) electrode, approximately 25 μm in diameter (Stålberg & Trontelj, 1979). This selectivity is further enhanced by using a high-pass filter with a typical cut-off frequency of 500 Hz.

As established by Ekstedt (1964), the conditions for recording an SFAP in a voluntarily activated muscle are:

1. That the fibre is close to the electrode, and
2. That the other fibres of the motor unit that have coincident action potentials are remote enough from the electrode to make their contribution small.

Based on these conditions, Ekstedt (1964) established the criteria to select true SFAPs:

1. Have a clean and smooth biphasic spike and
2. Present identical shape at consecutive discharges when the recording system has a time resolution of 10 μs (these days much shorter acquisition times are possible).

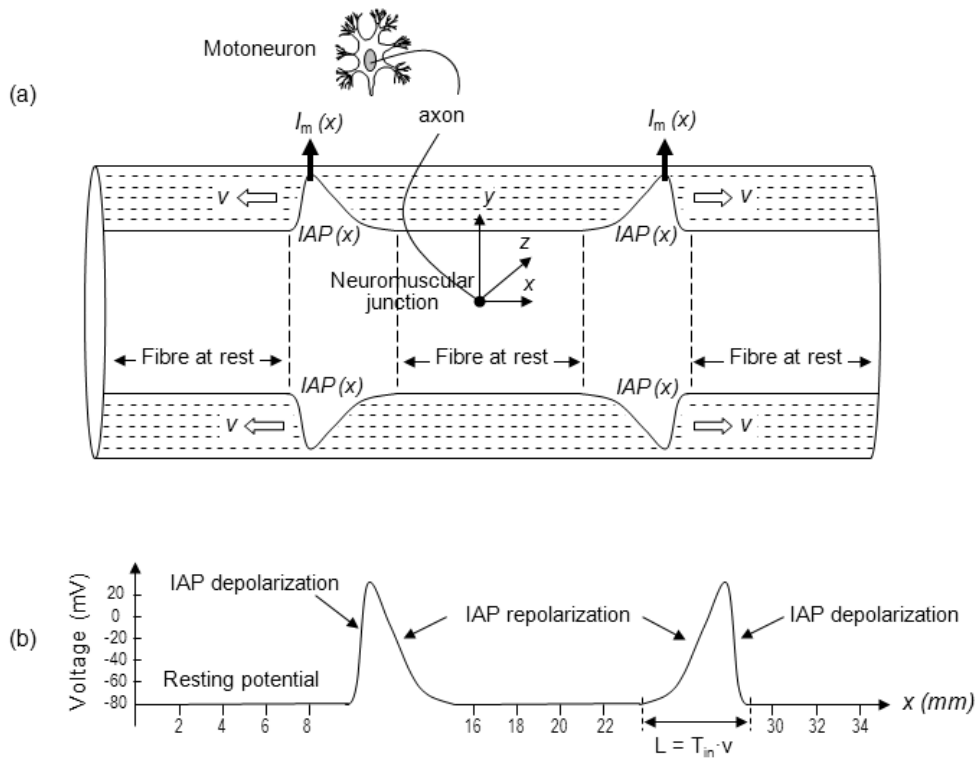
In the context of clinical neurophysiology studies, the most appreciated feature of SFAPs is the

fact that they show a constant shape at consecutive discharges (Ekstedt, 1964) and so they are ideal “time events” with which to estimate jitter. The study of the pure morphologic features of SFAPs has received little attention from investigators. There are several reasons for the relative lack of research in this direction:

1. The extremely high sensitivity of the SFAP characteristics to minor changes in the position of the electrode,
2. The difficulty to establish when, and to what extent, the time-course of an SFAP is contaminated by distant electrical activity from the same motor unit, and
3. Other technical problems related to SFEMG (inappropriate filter settings, contribution from the needle cannula, baseline fluctuation, physical noise, etc) (Dumitru et al., 1994).

The objective of this chapter is manifold. First, we will present a simulation model that relates mathematically the IAP and SFAP functions and use this model to address both the “forward problem” (analyze the influence of the IAP parameters on the morphology of the SFAP) and the “inverse problem” (obtain information of the IAP using some quantitative and morphological characteristics of the SFAP). Secondly, we will report some of the most relevant findings regarding the characteristics of human SFAPs. Afterwards, we will describe the main characteristics of single-fibre and concentric needle electrodes in relation to the recorded potentials. In addition, we will show the most important effects of filtering on SFAPs with special emphasis in the distortion introduced in the shape of the SFAPs. Finally, we will present the principles of jitter estimation together with the most important errors associated with this estimation.

Figure 1. (a) Schematic representation of a portion of muscle fibre in which two excitation sources [IAP(x)] are propagating with velocity v from the neuromuscular junction to the fibre ends. The polarization of the fibre membrane is represented by several layers of negative signs. The transmembrane ionic electric current, $I_m(z)$, is also indicated. (b) Spatial profile of the intracellular action potential (IAP) with its depolarization and repolarization phases are shown in the lower figure



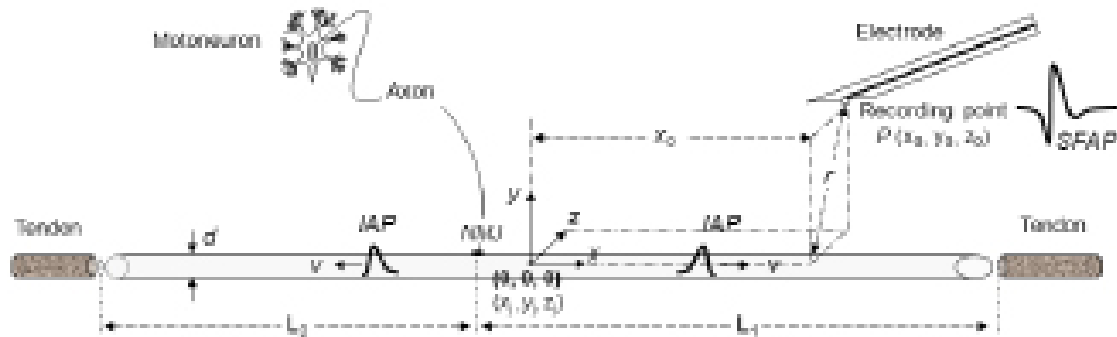
2. PHYSIOLOGICAL BASIS OF THE FORMATION OF THE INTRACELLULAR ACTION POTENTIAL (IAP)

Skeletal striated muscle is made up of individual components known as myocytes, or “muscle cells,” sometimes colloquially referred to a “muscle fibres.” Striated muscle fibres range from 10 to 90 μm in diameter (Lieber, 2010). These elongated, cylindrical cells contain actin and myosin filaments repeated as “sarcomere,” the basic functional unit of the muscle fibre and responsible for skeletal muscle’s striated appearance and forming

the basic machinery necessary for muscle contraction. Muscle contraction is generated by almost synchronous activation of several groups of muscle fibres, each group governed by a single motoneuron through its axon (Lieber, 2010). Figure 1 shows a portion of a muscle fibre synapsing with one of the terminal branches of the motoneuron at the neuromuscular junction (NMJ).

Three membrane potentials participate in the activation of the muscle fibre: namely, the resting membrane potential, the end plate potential, and the action potential. The membrane potential at rest is approximately -80 mV . When acetylcholine binds to the receptors at the neuromuscular junc-

Figure 2. Schematic representation of the neuromuscular junction (NMJ) where the intracellular action potential (IAP) is generated. The IAP travels with propagation velocity v . Due to volume conduction, currents arising from the propagating IAP can be recorded with a single fibre electrode to produce a SFAP. Thus a SFAP is a recorded representation of an IAP



tion, depolarization of the membrane potential occurs. This depolarization (normally called the end plate potential) reaches its maximum at the neuromuscular junction and decays exponentially away from it. The end plate potential is large enough to open voltage-gated Na^+ channels and initiates an action potential which travels away from the neuromuscular junction in both directions towards the tendons. In the present chapter this action potential is referred to as IAP. The ions involved in producing the IAP in the muscle fibre are the same as those for a typical axon, namely, sodium (Na^+) and potassium (K^+). However, the repolarization phase of the muscle IAP is different from that of axonal IAP. After repolarization, the axonal IAP is followed by a slight hyperpolarization while the muscle IAP has a delayed depolarization [see Figure 3]. In this chapter we will deal only with the IAP and not the resting membrane potential or the end plate potential.

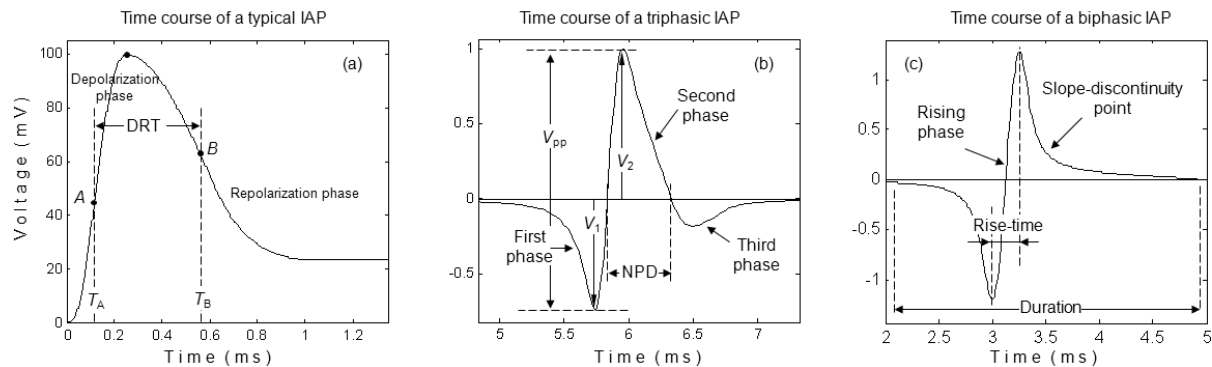
The plasma membrane of muscle fibre has the well-known property of actively maintaining a nearly constant potential difference between the intracellular and extracellular space. This voltage is normally referred to as the resting potential and has a value of about -80 mV [Figure 1]. The negative sign indicates that the interior is more

negative than the exterior (negative polarization). To illustrate this, in Figure 1 the polarization of the fibre membrane is represented by a number of layers of negative signs. As can be seen in this figure, when the fibre is at rest, the number of negative layers remains unchanged. A few milliseconds after the fibre activation, an IAP profile, or wave of excitation, exists at each side of the neuromuscular junction. In the representation of Figure 1 it can be seen that, along the spatial profile of the IAP, the number of negative-signed layers changes progressively with axial distance (the x -axis in Figure 1). This is consistent with the fact that the IAP profile has gradual depolarization and repolarization transitions, as shown in Figure 1.

3. GENERATION OF THE SINGLE FIBRE ACTION POTENTIAL (SFAP)

The propagation of the IAPs generated at the neuromuscular junction along the muscle fibre produces an electrical potential in the extracellular medium, the so-called single fiber action potential (SFAP), that can be recorded by an intramuscular electrode (Figure 2) (Plonsey, 1974).

Figure 3. (a) Time course of an IAP divided into the depolarization and repolarization phases. The time between the point of steepest rise (T_A) in the depolarization portion and the point of steepest decay (T_B) in the falling portion is the depolarization-to-repolarization time (DRT). (b) Typical example of a triphasic SFAP. The amplitude of the positive and negative phases (V_1 and V_2 , respectively), peak-to-peak amplitude (V_{pp}), and negative phase duration (NPD) are shown. (c) Typical example of a biphasic SFAP. Note that the declining negative phase has a slope-discontinuity point



If we assume that the shape of the IAP and the propagation velocity are approximately the same along the fibre, which is a reasonable assumption based on the observation of Buchthal et al., (1954) and Burke, (1981), the skeletal muscle fibre of finite length can be modeled as a linear and time-shift invariant system. This assumption is critical as it allows to express the SFAP as a convolution of the input signal (i.e. the real IAP) and impulse response (IR) of the corresponding system (The IR of a system is the output of the system when the input signal is the elementary delta function, see below for details) (Nandedkar & Stalberg 1983; Dimitrov & Dimitrova, 1998):

$$IAP(t) = 96t^3e^{-t} - 90$$

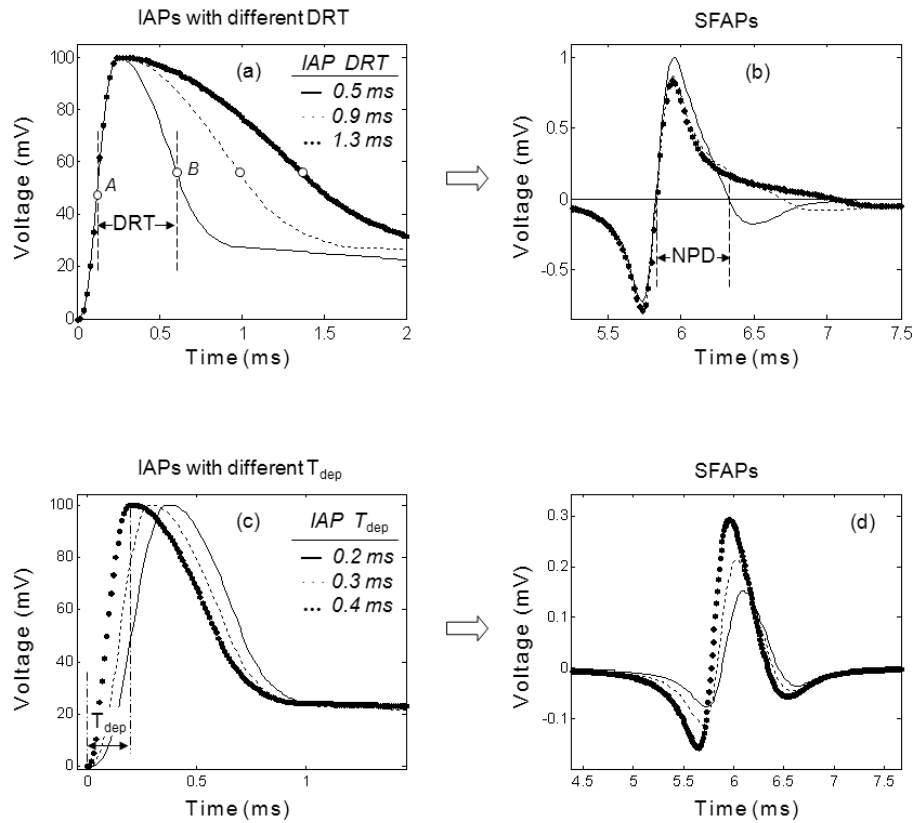
where C is a coefficient of proportionality that depends on the tissue conductivity (with a typical value of $0.01 \text{ s}\cdot\text{m}^{-1}$) and d is the fibre diameter (in mm). The input signal is the second temporal derivative of the intracellular action potential, $\partial^2 IAP(t)/\partial t$. The justification for this is as follows. During an IAP the membrane potential changes as a result of the exchange of sodium and potas-

sium ions between the inner and outer sides of the fibre membrane. The transmembrane ionic electric current, known to be proportional to $\partial^2 IAP(x)/\partial x^2$ (Clark & Plonsey, 1966), governs the exchange of these ions. Each of these ions carries a certain charge of current and therefore can be considered as a monopole of current. As a result, each infinitesimal portion of the muscle fibre affected by the IAP produces an electrical field equivalent to that generated by a lumped monopole of current. However, the IAP function is not a lumped (point) source, but a source distributed along the spatial extent of the fibre. Thus, the portion of the fibre affected by the IAP can be represented as a sequence of monopoles distributed equidistantly along its spatial profile (Rodriguez-Falces et al., 2011a). At a given position along the fibre, the strength and sign of each monopole is determined by the magnitude and sign of the function $\partial^2 IAP(x)/\partial x^2$, respectively, at this position (Dimitrova & Dimitrov, 2006).

One of the most used analytical functions for $IAP(t)$ is (Nandedkar and Stalberg 1983):

An impulse response of a system provides the output of the system to a brief impulse (a delta

Figure 4. Top row - simulation of the effects of changes in the IAP spike duration (DRT) (a) on the SFAP profile (b). A and B are the points of steepest rise and decay, respectively, along the IAP profile. The depolarization-to-repolarization times (DRTs) of the IAPs are indicated in the top right corner of (a). Bottom row - Simulation of the effects of changes in the IAP rising phase duration (T_{dep}) (c) on the SFAP profile (d). The T_{dep} values corresponding to the different IAPs are indicated in the top right corner of (a)



function). In time domain, the impulse response describes the properties of the system. For example, if one considers an action potential to be an impulse to the muscle, the resulting twitch force is the impulse response. Mathematical determination of the impulse response allows one to identify the parameters involved in producing the time dependent output. Moreover, once the impulse response has been determined, it is possible to convolve a more complex input function to the system to obtain the output.

In (1), the impulse response (IR) is computed as:

$$v(m/s) = 3.7 + 0.05 \cdot (d - 55)$$

In (3) the IR is calculated as the potential (at a detection point) by two current monopoles propagating along the fibre in opposite directions from the neuromuscular junction towards the fibre ends (Dimitrov & Dimitrova, 2006). Specifically, in (3) the first and second terms represent the potentials produced by the monopoles propagating rightwards and leftwards, respectively. Note that the longitudinal position of the origin of coordinates (x_j , i.e. the geometric centre of the fibre) does not necessarily coincide with the longitudinal position of the neuromuscular junction (x_{NMI}). The impulse response includes all the variables of the system:

- Anatomical properties of the fibre: right semilength, L_1 (in mm), left semilength, L_2 (in mm), and fibre diameter, d .
- Longitudinal position of the neuromuscular junction position, x_{NMJ} (in mm).
- Physiological properties of the fibre: propagation velocity, v (in m/s).
- Detection conditions: fibre-to-electrode distance, r (in mm), longitudinal position of the electrode in respect to the coordinate origin, x_0 (in mm).
- Duration properties: t_1 and t_2 represent the time (in ms) elapsed between the onset of IAP at the NMJ and its extinction at the right and left fibre-tendon junctions, respectively.

In (3), the propagation velocity (in m/s) and fibre diameter (in μm) are assumed to have a linear relationship (Nandedkar & Stalberg 1983) given by:

$$v \text{ (m / s)} = 3.7 + 0.05 (d - 55)$$

In (3), the radial distance (r) is calculated as:

$$r = \sqrt{(z_0 - z_j)^2 + (y_0 - y_j)^2}$$

where (x_0, y_0) and (x_j, y_j) are the coordinates of the electrode and the muscle fibre geometric centre, respectively. From (5), it is clear that the radial distance is the minimum distance from the electrode to a certain fibre (calculated within the muscle cross section $x = x_0$, as shown in Figure 2).

Before advancing to subsequent sections it is essential to emphasize the impact of radial distance on the relationship between the IAP and the SFAP functions. As shown in (3), the SFAP can be obtained as a convolution of the second derivative of IAP with IR. However, in close proximity to the fibre (i.e., radial distances shorter than approximately 0.2 mm), the SFAP can be considered proportional to the second derivative of IAP (Clark & Plonsey, 1966). This is explained

by the fact that, for such small radial distances, the impulse response is very narrow, with its shape approximating to a delta function. The shape similarity between the SFAP and the IAP second derivative can be appreciated in Figure 6.

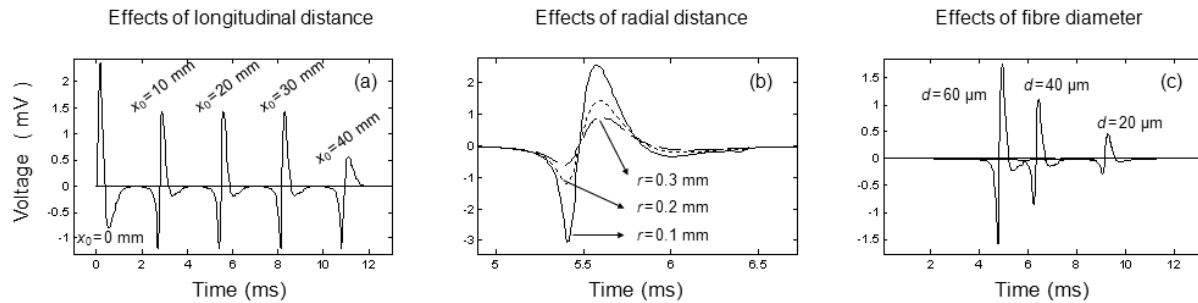
4. THE FORWARD PROBLEM: INFLUENCE OF THE EXCITATION AND SYSTEM PARAMETERS ON SFAP CHARACTERISTICS

The convolutional model described above is widely used and appreciated for its simplicity and computational efficiency. Perhaps the most remarkable advantage of this model is that it affords the possibility of making independent changes in excitation and impulse response functions. This allows the separation of the variables related to the system (represented in the impulse response) from those related to the source of excitation (i.e. the IAP). This flexibility enables study of the influence of the model's parameters on the waveform of the potential, providing insight into the relationships between the physiological and structural properties of the fibre and the characteristics of the potential. Thus, the proposed SFAP model is adequate to address the so-called "forward problem," that is, how specific mechanism and phenomena influence the recorded potentials. In the following, we will first introduce the most important parameters of the IAP and SFAP time-courses and then we will show the influence of the IAP and system parameters on the morphology of the SFAP.

4.1 Descriptions of IAP and SFAP

Intracellular Action Potential: It is necessary to emphasize that only Ludin (1973) recorded IAPs from human muscle fibres (intercostal muscle). Thus, knowledge about the characteristics of human IAPs is still incomplete. Nevertheless, a number of analytical expressions have been proposed over the years to model the time-

Figure 5. (a) Effect on the SFAP of changes in the longitudinal position of the electrode (x_0) relative to the neuromuscular junction. (b) Examples of three SFAPs simulated at three different fibre-to-electrode distances (r). (c) Examples of three SFAPs simulated with three different values of fibre diameter (d)



course of a mammalian IAP. Let us consider the IAP approximation proposed by Dimitrov and Dimitrova (1998) [Figure 3]. The rising phase models the depolarization process produced by the activation of the fibre. The point of steepest rise (A) along this phase occurs at T_A [Figure 3]. The falling portion of the IAP represents the repolarization process occurring at the membrane of the cell after the depolarization. The point of steepest decay (B) of the repolarization portion occurs at T_B [Figure 3]. The time interval between the points of steepest rise and decay of the IAP spike (T_A and T_B , respectively) will be referred to as *depolarization-to-repolarization time* (DRT). The DRT is normally taken as an estimation of the duration of IAP spike (Rodriguez-Falces et al., 2011a).

Single Fibre Action Potential: There is no unanimous consensus among scientists about the morphologic characteristics of human SFAPs (Dumitru, 1994; Rodriguez-Falces et al., 2012a, 2012b). Some researchers defend the contention that an SFAP recorded with an SFEMG electrode in optimal position (radial distance below 300 μm) is a roughly biphasic (positive-negative) spike [Figure 3] (Stålberg & Trontelj, 1979), whereas others alleged that it is not unusual to record SFAPs with three distinct phases (positive-negative-positive), i.e. with a terminal (positive) phase (Rodriguez-Falces et al., 2012a, 2012b) [Figure 3]. The filter settings chosen to record the SFAP

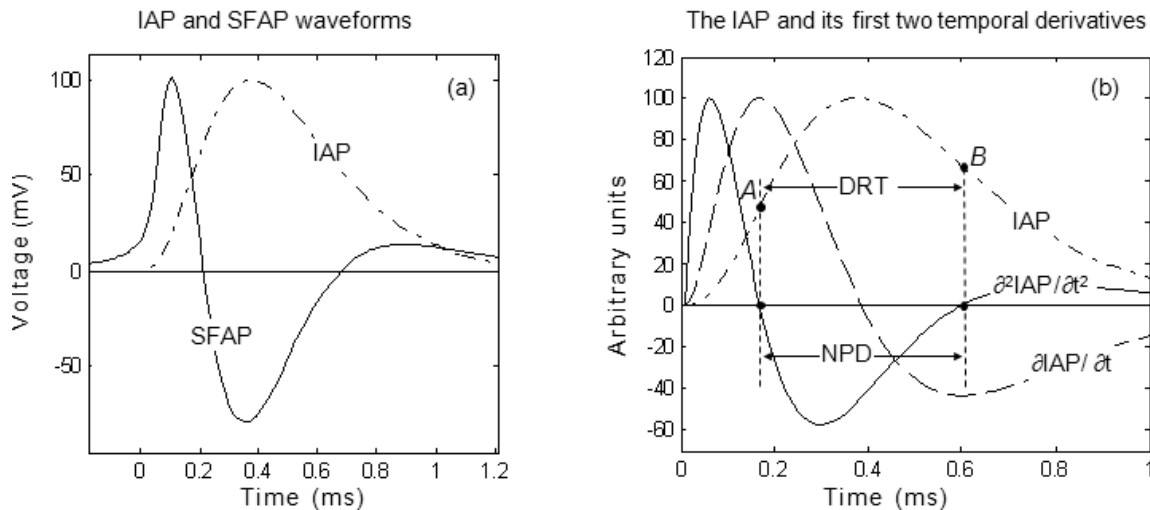
have a deep impact on the characteristics of the SFAP third phase (Dumitru, 1994), as it will be shown in next sections.

Studies dealing with SFAP analysis have been mainly interested in extracting quantitative information relative to certain parameters of the SFAP main spike. This includes the amplitudes of the first positive phase (V_1) and second negative phase (V_2), peak-to-peak voltage (V_{pp}), peak-to-peak duration (rise-time) and overall SFAP duration (Ekstedt, 1964; Miller-Larson, 1985; Piotrkiewicz et al., 1987). Recent studies have expanded the interest to other parameters, such as the ratio between V_1 and V_2 (the so-called peak-to-peak ratio, PPR) and the negative phase duration (NPD) (Rodriguez et al., 2011b; Rodriguez-Falces et al., 2012a, 2012b, 2012c). Moreover, recent works have drawn attention to some morphologic features of the SFAP time-course that had been traditionally overlooked, such as the slope discontinuity point (Rodriguez-Falces et al., 2012b).

4.2 Effects of the IAP Parameters on the SFAP Characteristics

Characteristics of SFAPs are strongly dependent on the shape of the IAP that propagates along the muscle fibre. Thus, any change in the IAP shape should translate, to some degree, into alterations of the SFAP waveform. It is well known that the IAP characteristics are very sensitive to neuromuscular

Figure 6. (a) Superimposed representation of the time-courses of the IAP and its corresponding SFAP. (b) Detail of the time course of an IAP together with its first two temporal derivatives. A and B are the points of steepest rise and decay, respectively, along the IAP profile. The depolarization-to-repolarization time (DRT), defined within the IAP profile, equals the negative phase duration (NPD), as measured in the IAP's second derivative. Note that in (a) and (b) the SFAP and the IAP's first and second derivatives have been normalized for the sake of clarity



disorders, such as muscle dystrophy, myopathy and myasthenia gravis (Stålberg & Trontelj, 1979). Thus, it is of interest to elucidate how changes in the IAP properties affect the characteristics of the detected SFAP. In the following we will show the effects on the SFAP characteristics resulting from changes in the IAP spike duration and IAP depolarization phase.

In the IAP series shown in Figure 4 there is a progressive broadening of the spike at the expense of a slowing of the IAP repolarization phase (the IAP depolarization phase is maintained constant). The effect of such widening on the corresponding SFAPs is an increase in the duration of the negative phase [i.e., the parameter NPD increases, Figure 4]. In the SFAPs of Figure 4 it is noteworthy that the rising phase varies only slightly, because this portion of the SFAP is essentially determined by the IAP rising phase (which is the same for the five IAPs simulated). Note also that the amplitude of the third phase of SFAPs (V_3) decreases as the NPD increases (the IAP spike becomes wider).

Figure 4 shows one set of IAPs with rising phases of different duration (i.e., different values of T_{dep}), but identical values of spike duration (i.e., same values of DRT). As can be seen, a slowing of the IAP rising phase brings about a decrease of the SFAP amplitude [Figure 4]. This is so because, for short radial distances, the SFAP main spikes is essentially produced by the IAP rising phase.

Sodium and potassium ions are released during each IAP and accumulate in both the interstitial space and within the transverse tubular system during contraction. The accumulation of K^+ ions in the interstitial space has received the attention of investigators as the extracellular concentration of these ions can rise up to 2–3 times as compared to the resting values (Sejersted & Sjogaard, 2000). Specifically, values of up to 15mM have been found in the interstitial medium following a sustained maximum voluntary contraction in humans. Experimental *in vitro* studies have provided evidence that increases in K^+ concentration bring about a reduction in muscle fiber conduction velocity, a

Table 1. Parameter values of one muscle fibre of the biceps brachii in different simulations

	L_1 (mm)	L_2 (mm)	NMJ (mm)	x_0 (mm)	r (mm)	d (μm)
Varying x_0	50	60	0	0 - 40 (step of 10)	0.20	50
Varying r	50	60	0	20	0.1 - 0.3 (step of 0.1)	50
Varying d	50	60	0	20	0.20	20 - 60 (step of 20)

broadening of the action potential and a reduction in action potential amplitude (Juel, 1988). The effects of potassium accumulation on the SFAP characteristics have been addressed in several publications (Dimitrova & Dimitrov, 2002, Fortune & Lowery, 2009; Rodriguez-Falces et al., 2011a).

When the muscle is fully contracted, the space between the adjacent muscle fibers (interstitial space) reduces significantly and the fluid that occupied this space is forced into the veins and lymphatic vessels. When the contraction stops, the muscle returns to its resting state (baseline length and baseline volume) and also the interstitial space expands to its resting value. This allows the interstitial space being filled with fresh blood plasma drawn from the arterial capillary bed. In these conditions, circulation is completely adequate to avoid the accumulation of “waste products” and, therefore, the onset of any disease process is avoided. The interstitial space and the exchange of oxygen and waste are functioning as they are supposed to. There are, however, several factors that can reduce the ability of the muscle to remove the waste products such as, muscle disease, reduced volume of the interstitial space, and squeezing of capillary beds and lymphatic vessels. These factors must be considered as they can noticeably affect the properties of the muscle conducting medium (and so parameters of the impulse response), thereby affecting the characteristics of SFAPs (Dimitrova & Dimitrov, 2006).

4.3 Effects of the System Parameters on SFAP Characteristics

One of the main interests of the electromyography (EMG) is to elucidate how the detection conditions (i.e., position of the recording electrode in respect to the active fibre) affect the characteristics of the recorded potential. This is a particularly important aspect in the context of single fibre electromyography (SFEMG) given the high sensitivity of some SFAP features (such as the amplitude) to changes in the needle position. Specifically, for the electromyographer it would be valuable to know how far the needle is from the active fibre (i.e., the fibre-to-electrode distance) and whether or not the needle is in the proximity of the neuromuscular junction or fibre-tendon junction (i.e., the longitudinal distance). In addition to the spatial location of the needle, it is also important to have an approximate value of the size of the fibre (i.e., its diameter) as well as its conduction velocity. Accordingly, in the following we will analyse the effect of changes in r , x_0 and d on the characteristics of the recorded SFAP.

For the sake of simplicity, the origin of coordinates (geometric centre of the fibre) was chosen to coincide with the longitudinal position of the neuromuscular junction (i.e., $x_j = x_{NMJ} = 0$). We will assess the effect of each parameter on the SFAP features in isolation of each other. The default values used for the parameters of the muscle fibre, together with the ranges of variation considered in each of the simulations are summarized in Table

1. The data shown in Table 1 represent real values that were obtained from a normal biceps brachii muscle (Lieber, 1992).

4.3.1 Effects of Varying the Electrode Longitudinal Distance

Figure 5 shows 5 SFAPs simulated at different longitudinal distances along the muscle fibre, from the neuromuscular junction ($x_0 = 0$ mm) to the fibre-tendon junction ($x_0 = 40$ mm). These SFAPs were simulated assuming $r = 0.2$ mm, and $d = 40$ μ m. Note that, when the electrode is sufficiently far from the end-plate and from fibre-tendon junction ($x_0 = 10, 20,$ and 30 mm), the amplitude of SFAP is constant, and its waveform have three phases. However, if the electrode is just above the endplate ($z_0 = 0$ mm) and/ or above the fibre-tendon junction ($z_0 = 40$ mm), the SFAP amplitude changes significantly and the SFAP becomes biphasic.

4.3.2 Effects of Varying the Radial Distance

Figure 5 shows 3 SFAPs simulated at different radial distances (assuming $d = 40$ μ m, and $x_0 = 20$ mm). As can be seen, SFAP amplitude exhibits an abrupt decline when the electrode is moved further away from the fibre. This is in agreement with Eq. (3), which predicts a decrement in the voltage of the EMG signal with increasing radial distance. In addition, it can be seen that, as the SFAP get smaller it also becomes longer.

4.3.3 Effects of Varying the Fibre Diameter

Figure 5 shows 3 SFAPs simulated with different fibre diameters (assuming $r = 0.2$ mm, and $x_0 = 20$ mm). As can be seen, SFAP amplitude increases with increasing diameter. This could be easily predicted from Eq. (1), where d acts as a scaling factor. This figure also reveals that differences

in the fibre diameter give rise to differences in the latencies (or delays) of the corresponding potentials. The explanation for this lies in the fact that changes in d not only has an influence on the SFAP amplitude, but also affects the propagation velocity of the IAP along the fibre, as established in (4). According to this equation, a high value of d (65 μ m) will result in an IAP travelling at a high conduction velocity ($v = 4.2$ m/s), which explains why the recorded SFAP exhibits a short latency [approximately 4.7 ms, as shown in Figure 5]. In contrast, a small fibre diameter (25 μ m) will make the IAP propagate at a slower velocity ($v = 2.2$ m/s), thereby generating an SFAP with longer latency.

5. THE INVERSE PROBLEM: USING THE SFAP CHARACTERISTICS TO OBTAIN INFORMATION ABOUT THE IAP

In the previous section we have shown some examples of how the SFAP convolutional model can be used to address the “forward problem.” In the present section we will focus on the so-called “inverse problem,” i.e., how the extracellular potentials provide information about the underlying mechanism and phenomena. When applied to our model, the inverse approach will be adopted to obtain information of the IAP using some quantitative and morphological information of the SFAP.

5.1 Motivation for Applying the Inverse Approach to the SFAP Convolutional Model

Surprisingly, most of the available information of IAPs has been obtained from *in vitro* and *in vivo* experiments conducted of IAPs from rats (Albuquerque and Thesleff, 1968; Hanson, 1974; Akaike, 1978; Mcardle et al., 1985; Wallinga et al., 1985) and frogs (Hanson and Persson, 1971;

Radicheva et al., 1986). In fact, knowledge about the characteristics of human IAPs is still limited, as only one author has been able to record IAPs from human muscles (Ludin, 1973) and the experiment was conducted under *in vitro* conditions. Some authors believe that the IAPs recorded under these *special* conditions should not be taken as representative of an IAP formed in the muscle fibre membrane surrounded by connective tissue (Wallinga et al., 1985; Van Veen et al., 1993). The main reason for this is the absence of protein in the artificial bathing medium in *in vitro* experiments (Hicks & McComas, 1989). From the above it follows that, to date, characterization of the human IAP is incomplete and so it is highly desirable to develop strategies to obtain information about the IAP characteristics by means of quantitative analysis of the corresponding SFAP, as shown next.

5.2 Limitations of the Inverse Approach in the SFAP Convolutional Model

Characteristics of single fibre action potentials (SFAPs) are strongly dependent on the shape of the intracellular potential that propagates along the muscle fibre (Clark & Plonsey, 1966, 1968; Plonsey, 1974; Fleisher, 1984; Dumitru, 1994). In fact, according to the core-conductor theory, in close proximity of the fibre, an SFAP can be assumed to be proportional to the IAP second derivative. Thus, changes in the IAP characteristics (for example, because of a pathological process or muscle fatigue) should be reflected, to some extent, into alterations of the SFAP waveform. However, there is an important obstacle to inferring data about IAP properties from the SFAP waveform: SFAP characteristics do not depend exclusively on the IAP profile but also on the distance from the needle to the fibre (i.e., the radial distance). Direct control of radial distance is not feasible with current technology (Albers et al., 1989; Van Veen et al., 1993). As a result,

traditional parameters used in quantitative EMG, such as the peak-to-peak amplitude and peak-to-peak interval, although useful for clinical diagnosis of neurogenic diseases and myopathic processes (Sonoo & Stålberg, 1993), are of limited use for glean information about the IAP shape since they vary significantly with positional changes of the electrode.

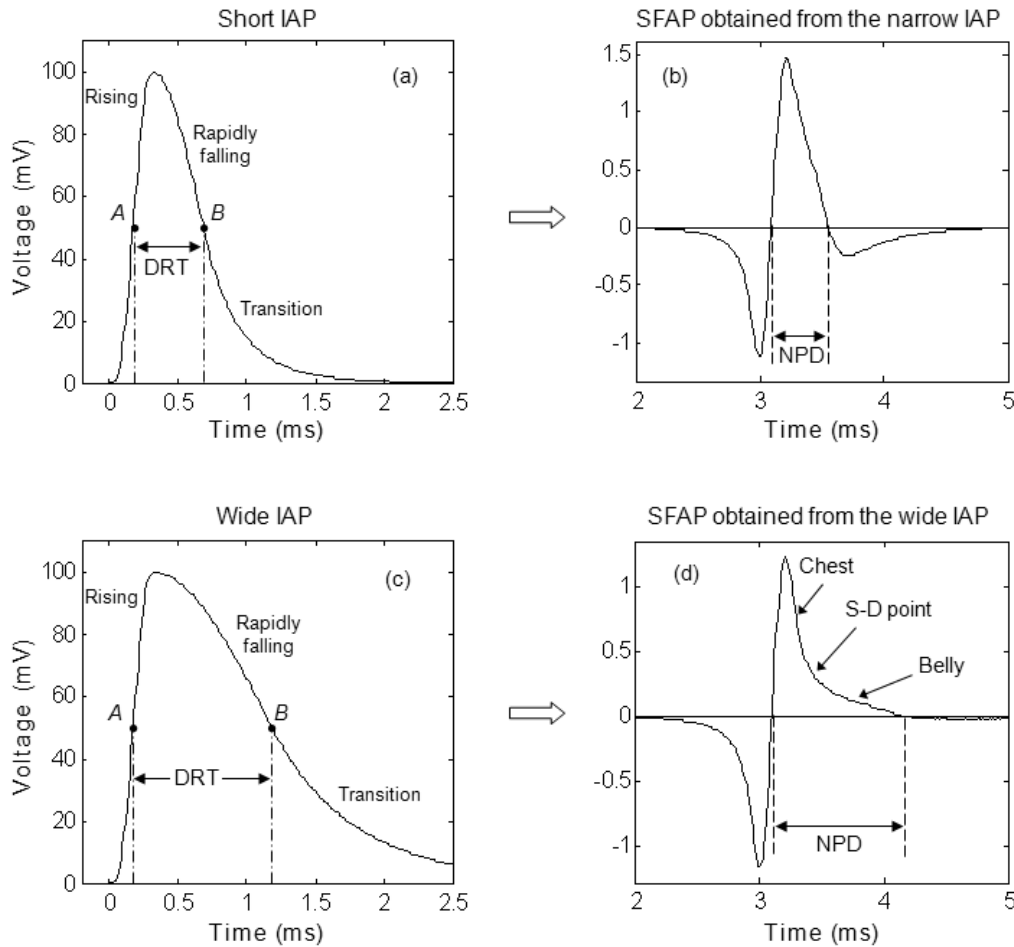
5.3 Procedures to Obtain Information of the IAP from the SFAP Waveform

From the foregoing, it is clear that we need to find a parameter of the SFAP waveform that: 1) is directly (or proportionally) related to some feature of the IAP waveform (preferably the T_{dep} or the DRT), and 2) does not depend on radial distance (at least for radial distances below 300 μm).

For the first condition to be fulfilled it would be highly desirable to relate the IAP and SFAP functions analytically, that is to determine a mathematical expression that links the IAP and SFAP waveforms. Specifically, it has been proposed that the SFAP approximately corresponds to the IAP second derivative (Plonsey, 1974) [Figure 6]. Such assertion is based on two assumptions: 1) the transmembrane current is proportional to the second derivative of the IAP, as predicted by the core-conductor theory [Figure 6] (Clark & Plonsey, 1966, 1968; Plonsey, 1974), and 2) in close proximity to the fibre, the SFAP can be considered proportional to the transmembrane current (Clark & Plonsey, 1966). Thus, the hypothesis that the SFAP can be approximated by the second derivative of IAP can be true only for very short radial distances (approximately below 200 μm), precisely the recording distances typical of SFEMG recordings.

Figure 6 shows the time course of an IAP, together with its first and second temporal derivatives. As can be seen, the time interval between the inflection points of the IAP spike (i.e., the DRT) coincides with the time interval between

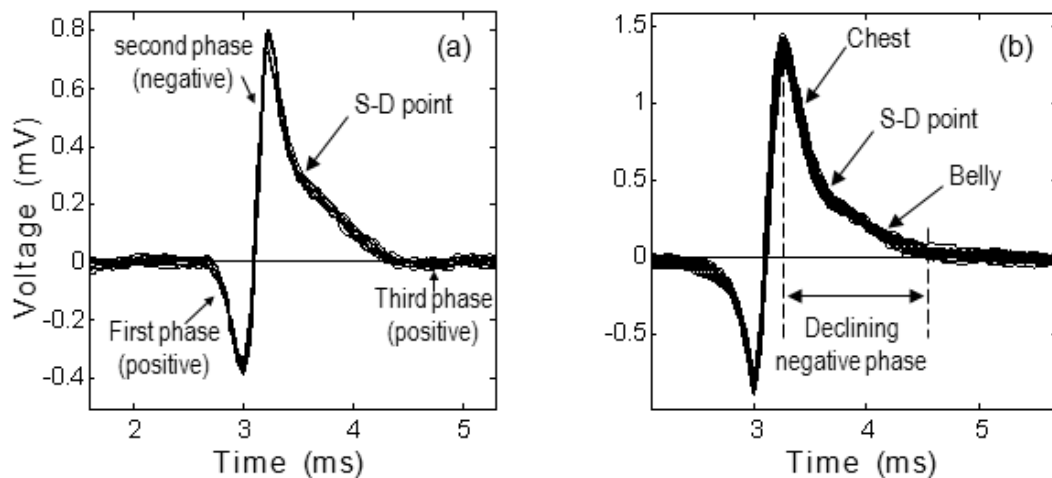
Figure 7. Simulation of IAPs with short (a) and long (c) spike durations and their corresponding SFAPs (b and d, respectively). The points of steepest rise (A) and decay (B) of the IAP spike and the depolarization-to-repolarization time (DRT) are indicated for both IAPs. Note that, for each SFAP, the duration of the negative phase (NPD) is very similar to the DRT of its corresponding IAP



the zero crossings of the IAP second derivative (i.e., the NPD). Since the shape of an SFAP can be regarded as being proportional to that of the corresponding IAP's second derivative, the NPD of a SFAP [Figure 6] should be approximately the same as the DRT of its corresponding IAP. In addition, recent publications have demonstrated, both by simulations and experimentally, that the SFAP NPD is largely unaffected by positional changes of the electrode (Rodriguez et al., 2011a). Thus, theoretical fundamentals predicts the equality

of IAP DRT and SFAP NPD, and so the spike duration of human intracellular potentials can, in principle, be estimated by direct measurements of the SFAP waveform. IAP characteristics (and especially the spike duration) are very sensitive to neuromuscular disorders, such as muscle dystrophy, myopathy and myasthenia gravis (Stålberg & Trontelj, 1979). Therefore, NPD parameter, as calculated in the SFAP, offers great potential in assisting the diagnosis of muscular myopathy and

Figure 8. Representations of 2 sets of consecutive SFAPs (shown superimposed) recorded from the tibialis anterior muscle using a single-fibre electrode. The three phases of an SFAP are indicated in (a), whereas the declining negative phase of an SFAP is depicted in (b). In both (a) and (b) it can be appreciated an abrupt change in the slope of the declining negative phase, the so-called slope-discontinuity point (S-D point)



dystrophy and also as an indicator of the changes in the IAP profile during fatiguing protocol.

The duration of the IAP spike (i.e., its DRT) does not only determine the NPD of its corresponding SFAP, but also influences significantly the shape characteristics of its final portion (i.e., the declining negative phase and terminal phase, see Figure 7). Specifically, a recent study has demonstrated that the shape of the declining negative phase of an SFAP is more dependent on the width of the corresponding IAP spike (i.e., its DRT) than on the specific outline of the IAP falling phase (Rodriguez-Falces et al., 2012c). The same study showed that characteristics of the SFAP third phase are more coupled to the specific profile (curvature) of the last part of the IAP falling phase (i.e., the transition phase, see Figure 3) than to the outline of its first part (i.e., the rapidly falling phase) or the IAP spike duration. It should be mentioned, however, that the curvature of the IAP transition phase is somewhat influenced by the IAP spike duration so long as narrow IAPs are normally associated with abrupt transitions

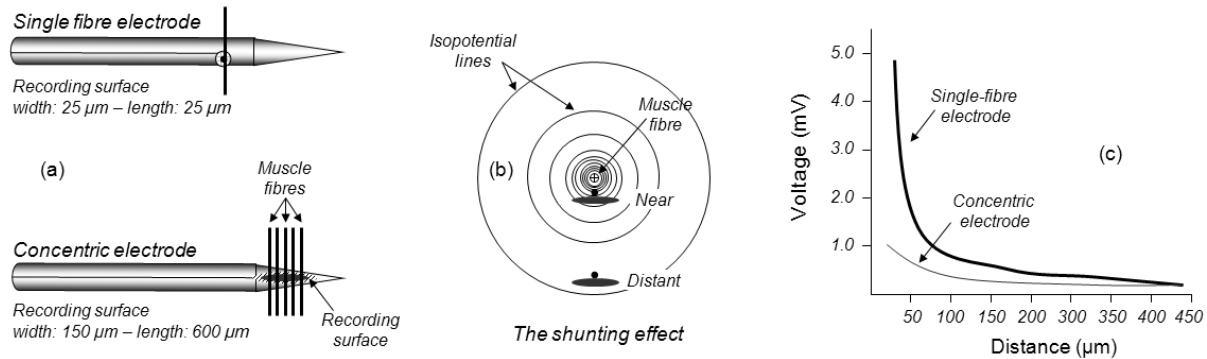
[Figure 7], whereas broad IAPs generally have slow transitions [Figure 7].

As an example, an IAP with a short spike duration [say DRT = 0.5 ms, Figure 7] would result in a SFAP whose the declining negative phase has and approximately constant slope and whose third phase is relative large and well-defined [Figure 7]. On the contrary, an IAP with a long spike duration [say DRT = 1.0 ms, Figure 7] would give rise to an SFAP with an abrupt change in the slope of the declining negative phase (the so-called slope-discontinuity point) and with a very small amplitude and prolonged duration [Figure 7].

6. CHARACTERISTICS OF HUMAN SFAP

The advent of single fibre electromyography (SFEMG) allowed investigators to analyze the shape peculiarities of the potentials produced by single muscle fibres (SFAPs) (Ekstedt, 1964; Stålberg, 1966, Stålberg & Trontelj, 1979).

Figure 9. (a) Schematic representation of a single fibre electrode (top) and a concentric electrode (bottom) together with the dimensions of their recording surfaces. Muscle fibres are represented superimposed to give an indication of their size relative to the recording surface of the electrode. (b) Electrical field (isopotential lines) generated by a muscle fibre (middle). The large electrode shunts the isopotential lines at short radial distances. (c) Decline of recorded amplitude of SFAP with increasing distance for the single fibre and concentric electrodes



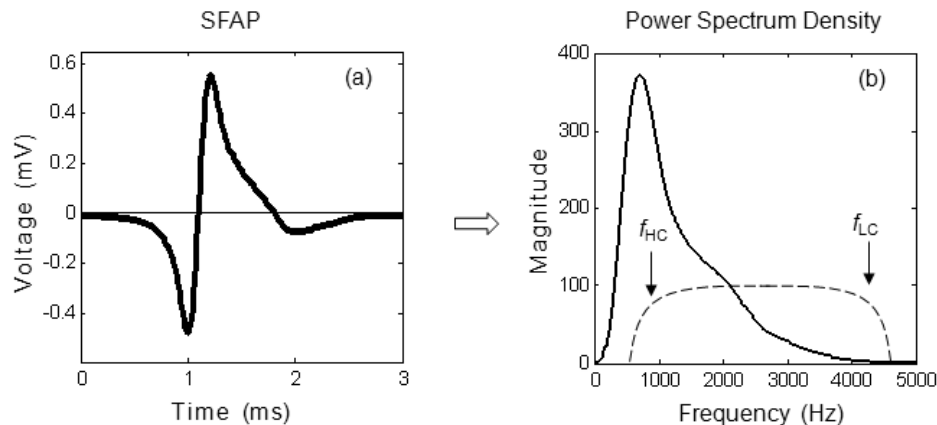
Stålberg and colleagues were mainly interested in characterizing the fundamental aspects of the SFAP main spike, its dependence with radial distance, and its shape variability at consecutive discharges. As such, the definition of the SFAP provided in the successive editions of the “Single Fibre Electromyography” by Stålberg and Trontelj (1979) includes these three aspects: 1) the SFAP recorded with the SFEMG electrode in optimal position is a biphasic spike with a positive-negative fast deflection and with a total duration of about one ms, 2) the SFAP shape is constant at consecutive discharges when the recording system has a resolution of 5 to 10 µs, and 3) the SFAP amplitude, which is positively correlated to the diameter of the muscle fibre, is extremely dependent on the recording distance. The radial attenuation of the AP amplitude is exponential (Gath & Stålberg, 1978).

Over the last 50 years, the above description of the SFAP has been relatively unchanged. This is not surprising in view of the fact that, in the context of clinical neurophysiology studies, the principal feature of the SFAP is not its waveform, but the fact that it shows a constant shape at consecutive discharges (Ekstedt, 1964). In

fact, in the clinical environment, the SFAP has been used as an auxiliary or reference element to assess the time-varying transmission at the neuromuscular junction, i.e. the neuromuscular jitter (Stålberg & Trontelj, 1979). After the initial characterization of the SFAP provided by Stålberg and Trontelj (1979), and despite the availability of single fibre electrodes, only a few studies have made progress in analysing the morphological aspects of experimental SFAPs in human fibres (Gydikov, 1991; Dumitru et al., 1994). There are several reasons for the relative lack of research in this direction: (1) the extremely high sensitivity of the SFAP characteristics (amplitude and shape) to minor changes in the position and orientation of the electrode, (2) the difficulty to establish when (and to what extent) the time-course of an SFAP is contaminated by distant electrical activity (Ekstedt, 1964; Dumitru et al., 1994), and (3) other technical problems related to SFEMG (physical noise, baseline fluctuation, background activity, etc).

Recent publications have revealed new morphologic features of human SFAPs (Rodriguez-Falces et al., 2012a, 2012b). Specifically, in SFAP recorded from the tibialis anterior muscle, the

Figure 10. Illustration of the slow and fast components of an SFAP (a) and its corresponding power spectrum density (b). In (b), the frequency response of a band-pass filter is shown with dashed-dotted line. The high-pass and low-pass cut-off frequencies of the filter (f_{HC} and f_{LC} , respectively) are also indicated



descending portion of the negative phase does not decrease at a constant rate; rather it starts declining steeply up to a certain point, where it suddenly changes its slope and continue decreasing at a much lower rate (Figure 8). The faster and slower portions of the declining negative phase have been referred to as the chest and belly, respectively (Figure 8). So, a remarkable feature of human SFAPs is an abrupt change in the slope of the declining negative phase of the SFAP (Figure 8). Such a feature, referred to as slope-discontinuity point (S-D point), can appear at different heights relative to the negative peak and be more or less apparent.

7. CHARACTERISTICS OF SINGLE-FIBRE ELECTRODES

The feature that makes the SFEMG technique particularly useful is its high selectivity, which permits identification of true SFAPs, namely, potentials produced by a single fibre close to the recording site of the electrode with no or negligible contamination from distant interfering fibres. The high selectivity of SFEMG is a consequence of the small recording surface of the single fibre (SF)

electrode. This recording area is much smaller as compared to that of concentric needle (CN) electrodes. In the following, we will present first the main important effects of needle electrodes on the recorded signal and compare afterwards the SF and CN in relation to the above effects.

7.1 Effects of Needle Electrodes on the Recorded Signal

When using needle electrodes to record the activity of muscle fibres, two distortion effects (shunting and wall effects) influence the characteristics (especially the amplitude) of the recorded potentials. First, the electrical field generated by an active fibre is shunted by the metallic recording surface of the electrode, and an average value of the isopotential lines crossing the electrode surface is recorded [Figure 9] (Stålberg & Trontelj, 1979). The larger the recording surface of the electrode, the more isopotential lines are involved in the averaging, and hence, more marked is the shunting effect [Figure 9]. Thus, the averaging of the isopotential lines will be much greater for concentric than for single-fibre electrodes. In addition, this distortion effect is most pronounced at small recording distances because, for these

distances, the isopotential lines have a smaller radius and the electrical field has a higher gradient. As the electrode is moved away from the fibre the distortion associated to the shunting effect gradually disappears. From the above, it follows that the shunting effect affects more markedly concentric electrodes at short radial distances. As a result, the characteristics of two SFAPs, one registered by a concentric electrode and the other by a single-fibre electrode, will be noticeable different if they are recorded in close proximity to the fibre, but will be very similar for longer radial distances [this can be appreciated in Figure 9].

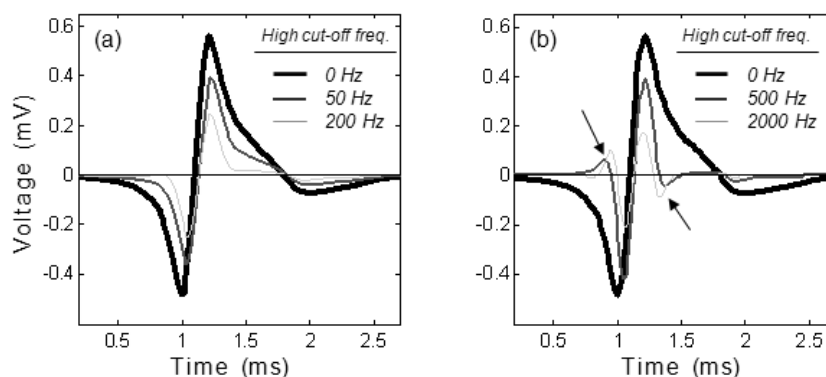
The second distortion effect (the wall effect) consists of an inherent amplification of the recorded potential caused by the specific features of the needle electrodes (Ekstedt, 1964; Nandedkar & Stålberg, 1983). This amplification is due to the fact that SFAPs are not recorded in an unlimited volume conductor but at the boundary of a volume conductor and an insulator: namely, the surface of the mould in which the electrodes were embedded. The effect of introducing a large insulating boundary in the plane of the electrodes is to increase any voltage by a factor of two. The wall effect does not affect the SFAP radial decline and so it is not as critical as the shunting effect.

There is another important aspect to take into account when analyzing needle electrodes: how big is the recording surface of the electrode in relation to the size of the muscle fibre diameter (which ranges between 10 and 90 μm). This is important because if the recording surface and fibre radius are of comparable size then, the active pole of the electrode can only be in close physical proximity to one. On the contrary, a recording surface of, say, five times the size of a given fibre would be in close physical proximity to various fibres at the same time.

7.2 Comparison between the Potentials Recorded by Single Fibre and Concentric Needle Electrodes

Both SF and CN electrodes consists of an insulated metal wire inside a hollow stainless steel canula (that serves as a reference). The metal wire exposes its end at a side port a few millimetres behind the tip [Figure 9] and is responsible for the detection of the electrical activity. The main difference between the SF and CN electrodes is in the area of their recording surfaces. A typical CN electrode has an oval recording surface with dimensions of 150 x 600 μm , whereas an ordinary

Figure 11. Simulation of the changes introduced in the SFAP time-course after high-pass filtering with cut-off frequencies of 50 Hz and 200 Hz (a) and 500 Hz and 2000 Hz (b). Arrows indicate the extra artifactual phases (ringing) that arise in the SFAP when strong high-pass filtering is performed



SF electrode has a circular recording surface with 25 μm in diameter [Figure 9].

There are two principal differences between SF and CN electrodes. The shunting effect of the electrical field around the muscle fibre is larger for CN than for SF electrodes due to the larger recording surface of the first electrodes. This difference is most notable at short radial distances. Specifically, for radial distances below 150 μm , the amplitude of the recorded SFAP is significantly smaller for CN than for SF electrodes [Figure 9]. With increasing radial distances the distortion associated to the shunting effect is less marked and, in fact, at 300 μm the amplitude of the recorded SFAP is comparable for CN than for SF electrodes.

The other discrepancy between SF and CN electrodes is also motivated by the difference in their recording surfaces. The 25- μm x 25- μm recording surface of a SF electrode can only be in close physical proximity to one fibre, whereas the recording area of a CN electrode can be in close physical proximity to at least 5 fibres [Figure 9]. This constitutes a significant disadvantage for the larger electrode, since more SFAPs from a given motor unit will be recorded as a summation signal. In fact, the most critical problem for using CN electrodes for jitter studies is the fact that it is difficult to determine if a simple spike recorded by a CN electrode is a truly single SFAP or superimposed SFAPs from two or more fibres (Stålberg and Sanders 2009).

8. EFFECTS OF FILTER SETTINGS ON SFAP RECORDINGS

The high selectivity provided by SF electrodes can be further enhanced if the high-pass cut-off frequency of the filter of the electromyograph is raised (for example up to 500 Hz as in ordinary jitter studies). Increasing the high-pass cut-off frequency (f_{HC}) of the filter on one hand attenuates the interference from remote active fibres (and reduces considerably the baseline fluctuation),

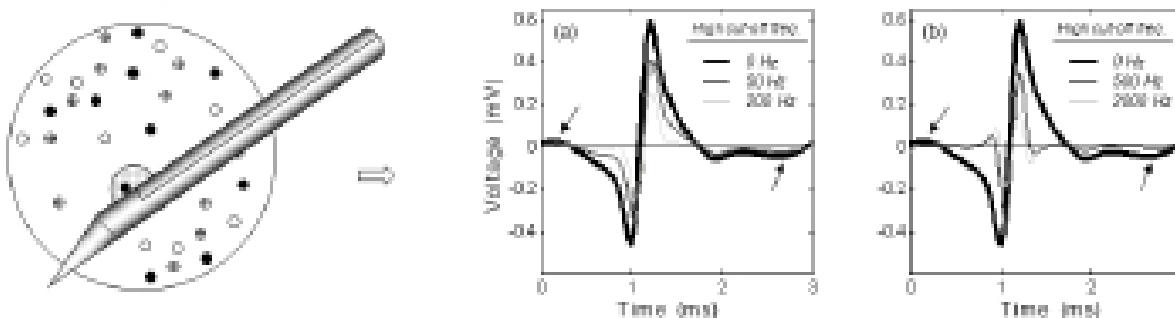
but on the other eliminates some of the most important frequency content of the SFAP. In the following we will discuss in more detail the effects on the SFAP morphology of applying filtering of different characteristics.

8.1 Frequency Range of the Power Spectrum of the SFAP

Figure 10 shows the time-course of an SFAP (a) simulated at a radial distance of 0.1 mm (typical of SFEMG recordings) and its corresponding power spectrum density (b). As can be seen, the power spectrum of the SFAP occupies frequencies ranging from almost 0 Hz up to 5000 Hz and has its maximum at approximately 600-700 Hz. The SFAP time-course contains certain portions which varies rather slowly, namely the initial positive deflection, the declining negative phase, and the third phase [Figure 10]. Such slow components contribute mainly to the lower frequency content of the spectrum (below 500 Hz). The fastest portion of the SFAP is the rising phase and it gives rise to frequency components covering a much wider range of the spectrum (from the lowest to the highest frequencies) (Dimitrova & Dimitrov, 2006).

Filters implemented in commercial EMG equipment are normally of band-pass type [Figure 10]. This means that the clinician must choose adequately both the high-pass cut-off frequency (f_{HC}) and the low-pass cut-off frequency (f_{LC}) of the filter before recording any signal. In SFEMG studies the recommendation is to use 10 kHz for the low-pass cut-off frequency (Stålberg & Sanders 2009), which implies that the high frequency content of the spectrum is normally well preserved. However, any high-pass frequency chosen (different from 0 Hz) will restrict the passage of most of the components of the signal below that frequency (in SFEMG studies, for example, the high-pass frequency is normally set to 500 Hz). This will bring about certain distortion of the time-course of the SFAP, as detailed next.

Figure 12. (a) Schematic representation of a SF electrode recording electrical activity from a single closest-main fibre (black circle) as well as from distant fibres from the same and different motor units. Distant fibres are responsible for the baseline fluctuation shown in (b) and (c). Simulation of the effects of applying high-pass filtering of different degrees on the baseline fluctuation



8.2 Effects of Moderate High-Pass Filtering on the SFAP

Different values of high-pass cut-off frequency will result in different degrees and types of distortion of the SFAP waveform. When using small high-pass frequencies (below 200 Hz), the most apparent effect of filtering is the attenuation of the slow components of the SFAP time-course and, in particular, of the SFAP third phase, as can be seen in the collection of SFAPs of Figure 11. In addition to third phase attenuation, moderate high-pass filtering also introduces some distortion in the shape of the declining negative phase of the SFAP. In fact, for a f_{HC} of 200 Hz, the belly of the declining negative phase is almost cancelled and, as a result, the slope-discontinuity point can hardly be recognized [Figure 11, thin grey line].

8.3 Effects of Strong High-Pass Filtering on the SFAP

When strong high-pass filtering is performed (high-pass frequencies of 500 Hz and beyond), much of the low-frequency content of the spectrum is lost and, as a result, the deformation introduced in the SFAP shape becomes rather pronounced. In fact, for such strong high-pass filtering, extra (artificial) phases arise in the time-course of

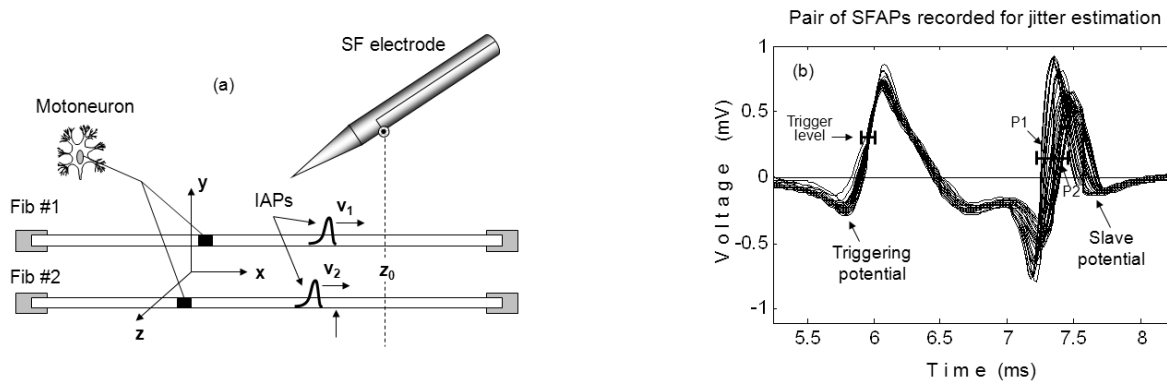
the SFAP. This is the so-called “ringing” which is a highly undesirable phenomenon as these extra phases can sometimes be mistaken for small SFAPs. Even worse, as a result of this “ringing,” an artificial positive phase appears just after the SFAP main spike [see arrow in Figure 11]. In the eyes of the unexpected observer, this positive phase could be mistaken for a real (physiological) phase of the SFAP and in fact, this is the reason why the SFAP has been wrongly considered by some as a triphasic waveform (Dumitru et al., 1994).

8.4 Benefits of High-Pass Filtering for SFEMG Studies

The idea of using high-pass filtering to select potentials from proximal sources and, at the same time, remove activity from distant fibres, was first introduced by Payan (1978) and is known as the “blanket principle.” The blanket principle was first applied to motor unit potentials (i.e., potentials that comprised the contribution from all fibres of the same motor unit) with the view of extracting the contribution from only the nearest fibres. Such idea is grounded on the observation that with progressively stronger high-pass filtering, the shape of the signal successively reflects the fast-rising components—like the derivative of the signal—and so, after filtering, only the

New Advances in Single Fiber Electromyography

Figure 13. (a) Typical scenario in jitter studies where the single-fibre (SF) electrode is recording activity mainly from two fibres of the same motor unit (fibre pair). (b) 25 superpositions of SFAPs (generated from a fibre pair) used to estimate jitter. The sweep is triggered on the triggering potential (and so the latency of this potential is constant). The variability in the latency of the slave potential, measured between points P1 and P2, represents jitter



contribution from most proximal fibres (well-defined SFAPs) remains.

When applied to potentials produced, theoretically, by a single fibre, strong high-pass filtering (as that performed in SFEMG studies) has the effect of enhancing the spiky components of the SFAP (i.e., the SFAP main spike) while removing its low frequency content. The deformation induced in the SFAP waveform by such strong filtering is so severe that the most important morphologic features of the original SFAP are lost. This, however, is not a problem for SFEMG studies. For example, in fibre density estimation, where the main goal is to count the number of single muscle fibres from one motor unit that falls within the uptake area of the SF electrode, strong filtering is advantageous in two ways: first, it enhances the potentials from the nearest fibres, and second it has the positive effect of largely eliminating the contribution from distant fibres (also reduces background activity and baseline fluctuation). In jitter studies, the SFAP is used as an auxiliary or reference spike to assess the time-varying transmission at the neuromuscular junction and so the specific morphologic features of that reference spike are not relevant at all. What

is really crucial for jitter studies is that the shape of this spike remains as unchanged as possible at consecutive discharges and such condition is best fulfilled by applying strong high-pass filtering to the SFAP.

As mentioned above, one of the main reasons for applying high-pass filtering while recording SFAPs is that it reduces activity from fibres from the same or different motor units (background activity), cannula potential, as well as interferences from other external sources. As a result, the so-called baseline fluctuation (or baseline drift) is largely attenuated. To illustrate this idea, Figure 12 shows a SF electrode recording activity from a single closest-main fibre (black circle within the uptake area) as well as from remote fibres from the same and different motor units. As can be seen in Figure 12, when potentials produced by distant activity add to the SFAP the slow components of this SFAP are significantly distorted (note that the SFAP third phase has an uneven return to the baseline and that the slope-discontinuity point has practically disappeared) [see arrows in Figure 12]. It could be said that the distortion introduced in the SFAP is the result of baseline fluctuation produced by distant activity.

As shown in Figure 12, applying filtering with high-pass cut-off frequencies below 200 Hz does not remove completely the drift in the baseline. In fact, strong high-pass filtering (cut-off frequencies of 500 Hz and beyond) is necessary to eliminate completely the baseline fluctuation [Figure 12]. Note that the cancellation of the baseline drift is achieved at the expense of severely distorting the SFAP shape.

8.5 Drawbacks of High-Pass Filtering for SFEMG Studies

From the above it is clear that the final portion of the SFAP, due to its low frequency content, is much more sensitive to high-pass filtering as compared to the SFAP main spike. In addition, the SFAP final portion (declining negative phase and third phase) has long duration and small amplitude and so it is much more affected by slow components, such as potentials from the cannula or from distant fibres (Rodriguez-Falces et al., 2012a). To make things worse, the frequency content corresponding to the declining negative phase and third phase of the SFAP largely overlaps with that of distant fibre potentials and cannula potential. As a result, in many EMG tests where moderate high-pass filtering is applied to reduce background activity and baseline fluctuation, the final portion of the SFAPs is systematically attenuated and distorted (Dumitru et al., 1994). For this reason, when SFAPs are collected for quantitative and/or morphological analysis the cut-off frequency should be kept around 2-5 Hz (Dumitru et al., 1994).

Recent simulation studies have attempted to elucidate the impact of distant-interfering fibres on the SFAP final portion (Rodriguez-Falces et al., 2012a). Additionally, an experimental study that recorded SFAPs with a very low high-pass cut-off frequency (2 Hz) has been conducted in order to analyze the true morphology of the SFAP final portion (Rodriguez-Falces et al., 2012b). As mentioned before, the most remarkable finding of

these studies is that the majority of SFAPs recorded from slow human muscle fibres have a declining negative phase with a slope-discontinuity point and a slow return towards the baseline. This return may be artificially elongated due to the contamination from interfering potentials, but the slope-discontinuity point seems to be a feature inherent to human SFAPs that has been traditionally overlooked. Future research is necessary to validate the observations reported in those studies.

9. JITTER ESTIMATION

Neuromuscular jitter is a phenomenon consisting in the time-varying transmission at the neuromuscular junction. Jitter is mainly caused by the variability in the characteristics of the end-plate potential at the neuromuscular junction. As a result of this variability, the time from the action potential in the nerve terminal to the action potential in the muscle fibre varies between consecutive discharges (Stålberg & Trontelj, 1979). In normal subjects, there are small changes in the size of the end plate potential (because the amount of acetylcholine released from the nerve terminal is rather stable) and so the variability in the time interval between the nerve action potential and the muscle action potential remains below a certain limit. Hence the jitter is small. Any disorder of neuromuscular transmission will increase the instability in the characteristics of the end-plate potential and this, in turn, will increase the variability in the time interval between the nerve and muscle action potentials.

Jitter is normally estimated taking as a reference two SFAPs (triggering and slave) recorded simultaneously from two fibres of a single motor unit (called fibre pair), as shown in Figure 13. Specifically, jitter is measured as the variability in the time interval between the triggering and slave potentials, termed as interpotential interval (IPI) variability [Figure 13] (Ekstedt et al., 1974; Stålberg et al., 1974; Stålberg & Trontelj, 1979).

Being a phenomenon of variability, jitter could be measured as the standard deviation of the interpotential interval, but because of the occasional occurrence of a gradual change in the mean IPI over time in one direction (i.e., a trend), jitter is normally obtained as the mean consecutive difference (MCD) of all the IPIs measured:

$$MCD = \frac{(IPI_1 - IPI_2) + (IPI_2 - IPI_3) + \dots + (IPI_{n-1} - IPI_n)}{n - 1}$$

where IPI_i is the interpotential interval of the i th discharge, and n is the number of pairs measured. To better understand the benefits of using the MCD over the standard deviation, let us assume the following IPI values for five consecutive fibre pairs: 95, 75, 65, 55, and 35 μ s. As can be readily seen, there is a decreasing trend in this sequence (typically caused by a concomitant change in the conduction velocity of the fibres). By applying the definition of MCD described in (6) we have:

$$SFAP(t) = C \cdot d^2 \cdot \frac{\partial^2 IAP(t)}{\partial t^2} * IR(t)$$

If we now compute the standard deviation corresponding to the above five IPIs we obtained 22.3 μ s. Thus, in the presence of a trend, the standard deviation provides an overestimation of the IPI variability as compared to the MCD index. Clearly, the MCD is a more reliable measure of jitter as it compensates for possible sources of IPI variability other than the neuromuscular jitter (such as changes in the conduction velocity of the fibres produced by the velocity recovery function).

The interpotential interval can be calculated using two approaches (algorithms): peak trigger and level trigger. In the former case, the IPI is measured between the negative peaks of the triggering and slave potentials, whereas in the latter, the measurement of the IPI is made between a point in the steep rising phase of the triggering

potential close to the baseline crossing and the corresponding point on the slave component [this is the algorithm shown in Figure 13].

The main requirements, essential for the reliable measurement of jitter and for the accurate interpretation of data are outlined next. First, use a SF electrode with a small recording surface (25 μ m in diameter). Second, select a high-pass cut-off frequency of 500 Hz in order to reduce the activity from fibres from the same or different motor units (background activity), cannula potential, as well as interferences from other external sources. Third, select SFAPs whose rise-time is shorter than 300 μ s and peak-to-peak amplitudes above 0.2 mV.

9.1 Errors in Jitter Estimation

As mentioned before, measurement of jitter is normally accomplished by estimating the variability in the time interval between the triggering and slave SFAPs (IPI variability). If we assume that the waveform of each of these SFAPs is exactly the same at consecutive discharges, then alterations in the IPI value would reflect only the time-varying transmission at the neuromuscular junction, i.e., the neuromuscular jitter. Any change in the shape of the triggering and slave SFAPs would result in additional variations of the IPI, which would alter the IPI variability produced by the end-plate transmission and therefore introduce false jitter. In fact, as demonstrated in a recent study, even the most spiky SFAPs exhibit a certain degree of shape variability at consecutive discharges (Rodriguez et al., 2011c). This is so mainly because of the interference from remote fibres of the same motor unit.

The contribution of distant fibres is not the only source responsible for the shape variability of SFEMG potentials. Indeed, clinicians are aware of the fact that technical problems related to SFEMG, such as background activity, needle movement and physical noise also compromise the stability of such potentials (Stålberg & Trontelj, 1979; Lange, 1992; Daube & Rubin, 2009). SFEMG is extremely sensitive to small movement of the SF electrode.

The ability to hold the SF electrode motionless is the greatest challenge in SFEMG. Minor angulation or rotation of the cannula often produces marked changes in the amplitude of the recorded SFAP. The second great technical challenge is to maintain low levels of muscle contraction, as excessive activation results in noise which may increase the baseline fluctuation and distort the SFAP of interest. The variability in the firing rate of SFAPs is also an issue in SFEMG as this variability affects the velocity recovery function of the muscle fibre. Finally, the shape of the IAP is not completely constant at consecutive discharges.

From the above it follows that there exists two sources of variability of the IPI that will give rise to two different components of jitter. The first source of IPI instability is the time-varying transmission at the neuromuscular junction, which will result in the so-called “neuromuscular” jitter. The second source of variation of the IPI resulted mainly from changes in the shape of the SFAPs caused by the technical problems encountered during acquisition of fibre pairs described above. This will give rise to the “technical” jitter. As a matter of fact, these two sources of IPI variability always coexist during SFEMG studies and the key point is to assess how the technical IPI variability affects the neuromuscular IPI variability, with a view to determining to what extent the technical jitter distorts the neuromuscular jitter. Such analysis has been performed in a recent study (Rodriguez et al., 2011c). Specifically, it was found that an increase of the technical IPI variability always results in an increase of the measured IPI variability, leading to an overestimation of the neuromuscular jitter. The artificial increase in the estimated jitter depends on the amount of neuromuscular jitter. Specifically, the impact of the technical IPI variability on the neuromuscular jitter becomes less important as the neuromuscular jitter increases. As an example, with voluntary activation and the peak trigger method, and for technical IPI variability values within 5 and 15 μ s, the jitter overestimation was 1.7–8.1, 0.3–5.6 and 0.1–3.5 μ s, for neuromuscular jitters of 20, 40 and 60 μ s, respectively.

It has been reported that different muscles have different upper limits for the normal jitter (Stålberg & Trontelj, 1979; Kimura, 1989). As an example, with voluntary activation, the reference jitter limits above which no more than 2 of 20 muscle fibre pairs are accepted as normal are 35, 44, 45, 45, 54, 55, 55 and 60 μ s for the biceps brachii, deltoid, frontalis, quadriceps, orbicularis oculi, orbicularis oris, extensor digitorum communis and tibialis anterior, respectively. Therefore, since the jitter distortion introduced by technical IPI variability is inversely proportional to the neuromuscular jitter, the impact of the technical IPI variability on the diagnosis of different disorders will be more important for the first four muscles above mentioned. The impact of technical IPI variability on the diagnosis will also depend on the severity and type of disorder considered. Because the jitter overestimation is always less than 8 μ s, it is expected that the technical IPI variability may not have great consequences in cases of acute myasthenia gravis who typically have a lot of jitter values well above the upper limits (Stålberg et al., 1974; Schwartz & Stålberg 1975; Sanders, 1979, 1987). However, when the jitter is increased only slightly, as in mild clinical manifestations of myasthenia gravis, early stages of reinnervation (Hakelius & Stålberg 1974; Stålberg and Trontelj, 1979), myopathies and Duchene dystrophies (Stålberg, 1977), technical IPI variability might be an important issue as even one more abnormal jitter value may be important for the diagnosis

10. FUTURE RESEARCH DIRECTIONS

In the last decades, the research effort in SFEMG studies has been mainly concentrated on the refinement of the technique to assess neuromuscular jitter more accurately. In fact, the sensitivity of jitter measurements made by the SFEMG technique is extraordinarily high. However, SF electrodes are expensive and, in addition, concern has been raised against reusing any material for invasive medical

procedures, including EMG. The most inexpensive direct alternative is to use conventional concentric needle electrodes. However, when using these new electrodes for jitter estimation, precise criteria for acceptable signals should be established, with special emphasis in filter settings.

The simulation model that relates analytically the IAP and SFAP functions is based on the hypothesis that the core-conductor theory is valid to accurately describe the generation of extracellular potentials. However, the core-conductor theory is grounded on two assumptions: the IAP is assumed to be distributed along the axis of the fibre and the influence of the extracellular potential field is neglected. In order to validate the assumptions of the core-conductor theory, it would be necessary to record, from the same muscle fibre, the IAP, the transmembrane current, and the SFAP and then relate their corresponding morphologic features as shown in the present chapter.

11. CONCLUSION

A general perspective of SFEMG has been presented together with a description of the anatomical, physiological, and technical aspects that are involved in the recording of SFAPs. This panoramic view comprises a simulation model that relates analytically the IAP and SFAP mathematical expressions, the most recent findings regarding the shape features of human SFAPs, a description of how different types of needle electrodes affects the characteristics of the recorded potential, an explanation of the most important effects of filtering on the SFAP characteristics, and a description of the principles of jitter estimation together with the most important sources of errors.

REFERENCES

- Akaike, N. (1978). Resting and action potentials in white muscle of potassium deficient rats. *Comparative Biochemistry and Physiology. Part A, Physiology*, 61, 629–633. doi:10.1016/0300-9629(78)90140-8
- Albers, B. A., Put, J. H., Wallinga, W., & Wirtz, P. (1989). Quantitative analysis of single muscle fiber action potentials recorded at known distances. *Electroencephalography and Clinical Neurophysiology*, 73(3), 245–253. doi:10.1016/0013-4694(89)90125-9 PMID:2475329
- Albuquerque, E. X., & Thesleff, S. (1968). A comparative study of membrane properties of innervated and chronically denervated fast and slow skeletal muscles of the rat. *Acta Physiologica Scandinavica*, 73, 471–480. PMID:5708174
- Buchthal, F., Guld, C., & Rosenfalck, P. (1954b). Action potential parameters in normal human muscle and their dependence on physical variables. *Acta Physiologica Scandinavica*, 32, 200–218. doi:10.1111/j.1748-1716.1954.tb01167.x PMID:13228109
- Buchthal, F., & Pinelli, P. (1953). Action potentials in muscular atrophy of neurogenic origin. *Neurology*, 3(8), 591–603. doi:10.1212/WNL.3.8.591 PMID:13087579
- Buchthal, F., Pinelli, P., & Rosenfalck, P. (1954a). Action potential parameters in normal human muscle and their physiological determinants. *Acta Physiologica Scandinavica*, 32(2), 219–229. doi:10.1111/j.1748-1716.1954.tb01168.x PMID:13228110
- Burke, R. E. (1981). Motor units: anatomy, physiology and functional organization. In *Handbook of physiology. The nervous system. Motor control* (pp. 345–422). Bethesda, MD: American Physiological Society.

- Clark, J., & Plonsey, R. (1966). A mathematical evaluation of the core conductor model. *Biophysical Journal*, 6(1), 95–112. doi:10.1016/S0006-3495(66)86642-0 PMID:5903155
- Clark, J., & Plonsey, R. (1968). The extracellular potential field of the single active nerve fibre in a volume conductor. *Biophysical Journal*, 8(7), 842–864. doi:10.1016/S0006-3495(68)86524-5 PMID:5699809
- Daube, J. R., & Rubin, D. I. (2009). *Needle electromyography (Contemporary neurology)* (pp. 475–492). Oxford, UK: Oxford University Press.
- Dimitrov, G. V., & Dimitrova, N. A. (1998). Precise and fast calculation of the motor unit potentials detected by a point and rectangular plate electrode. *Medical Engineering & Physics*, 20, 374–381. doi:10.1016/S1350-4533(09)00014-9 PMID:9773690
- Dimitrova, N. A., & Dimitrov, G. V. (2002). Amplitude-related characteristics of motor unit and M-wave potentials during fatigue. A simulation study using literature data on intracellular potential changes found in vitro. *Journal of Electromyography and Kinesiology*, 12, 339–349. doi:10.1016/S1050-6411(02)00046-9 PMID:12223166
- Dimitrova, N. A., & Dimitrov, G. V. (2006). Electromyography (EMG) modeling. In A. Metin (Ed.), *Wiley encyclopedia of biomedical engineering*. Hoboken, NJ: John Wiley & Sons. doi:10.1002/9780471740360.ebs0656
- Dumitru, D. (1994). The biphasic morphology of voluntary and spontaneous SFAPs. *Muscle & Nerve*, 17, 1301–1307. doi:10.1002/mus.880171109 PMID:7935552
- Ekstedt, J. (1964). Human single fibre action potentials. *Acta Physiologica Scandinavica*, 61(226), 1–96. PMID:14168041
- Ekstedt, J., Nilsson, G., & Stålberg, E. (1974). Calculation of the electromyographic jitter. *Journal of Neurology, Neurosurgery, and Psychiatry*, 37(5), 526–539. doi:10.1136/jnnp.37.5.526 PMID:4836748
- Fleisher, S. M. (1984). Comparative analysis of modeled extracellular potentials. *Medical & Biological Engineering & Computing*, 22, 440–447. doi:10.1007/BF02447704 PMID:6482532
- Fortune, E., & Lowery, M. M. (2009). Effect of extracellular potassium accumulation on muscle fiber conduction velocity: A simulation study. *Annals of Biomedical Engineering*, 37(10), 2105–2117. doi:10.1007/s10439-009-9756-4 PMID:19588250
- Gath, I., & Stålberg, E. (1978). The calculated radial decline of the extracellular action potential compared with in situ measurements in the human brachial biceps. *Electroencephalography and Clinical Neurophysiology*, 44(5), 547–552. doi:10.1016/0013-4694(78)90121-9 PMID:77760
- Gydikov, A. (1991). Biophysics of the skeletal muscle extracellular potentials. *Bulgarian Academy of Sciences*, 132, 60–100.
- Hakelius, L., & Stålberg, E. (1974). Electromyographical studies of free autogenous muscle transplants in man. *Scandinavian Journal of Plastic and Reconstructive Surgery*, 8, 211–219. doi:10.3109/02844317409084397 PMID:4458046
- Hanson, J. (1974). Effects of repetitive stimulation on membrane potentials and twitch in human and rat intercostal muscle fibres. *Acta Physiologica Scandinavica*, 92, 238–248. doi:10.1111/j.1748-1716.1974.tb05741.x PMID:4138188

New Advances in Single Fiber Electromyography

- Hanson, J., & Persson, A. (1971). Changes in the action potential and contraction of isolated frog muscle after repetitive stimulation. *Acta Physiologica Scandinavica*, *81*, 340–348. doi:10.1111/j.1748-1716.1971.tb04908.x PMID:5550516
- Hicks, A., & McComas, A. J. (1989). Increased sodium pump activity following repetitive stimulation of rat soleus muscles. *The Journal of Physiology*, *414*, 337–349. PMID:2558169
- Juel, C. (1988). Muscle action potential propagation velocity changes during activity. *Muscle & Nerve*, *11*(7), 714–719. doi:10.1002/mus.880110707 PMID:2457155
- Kimura, J. (1989). *Electrodiagnosis in diseases of nerve and muscle*. Philadelphia, PA: Davis.
- Lange, D.J. (1992). Single fiber electromyography in normal subjects: Reproducibility, variability, and technical considerations. *Electromyography and Clinical Neurophysiology*, *32*(7), 397–402. PMID:1526222
- Lieber, R. L. (2010). *Skeletal muscle structure, function, and plasticity*. Baltimore, MD: Lippincott Williams & Wilkins.
- Ludin, H. (1973). Action potentials of normal and dystrophic human muscle fibres. In J. E. Desmedt (Ed.), *New development in electromyography and clinical neurophysiology* (pp. 400–406). Basel, Switzerland: Karger.
- Mcardle, J., Michelson, L., & D'Alonzo, A. J. (1980). Action potentials in fast- and slow- twitch mammalian muscles during reinnervation and development. *The Journal of General Physiology*, *75*, 655–672. doi:10.1085/jgp.75.6.655 PMID:7391811
- Miller-Larsson, A. (1980). A model of spatial distribution of muscle fibres of a motor unit in normal human limb muscles. *Electroencephalography and Clinical Neurophysiology*, *20*, 281–298. PMID:7418648
- Nandedkar, S., & Stålberg, E. (1983). Simulation of single muscle fibre action potentials. *Medical & Biological Engineering & Computing*, *21*, 158–165. doi:10.1007/BF02441531 PMID:6887989
- Payan, J. (1978). The blanket principle: a technical note. *Muscle & Nerve*, *1*, 423–426. doi:10.1002/mus.880010517 PMID:263984
- Piotrkiewicz, M., & Miller-Larsson, A. (1987). A method of description of single muscle fiber activity. *Biological Cybernetics*, *56*, 237–245. doi:10.1007/BF00365218 PMID:3607099
- Plonsey, R. (1974). The active fibre in a volume conductor. *IEEE Transactions on Bio-Medical Engineering*, *21*, 371–381. doi:10.1109/TBME.1974.324406 PMID:4461667
- Plonsey, R., & Barr, R. C. (2000). *Bioelectricity. A quantitative approach*. New York: Kluwer Academic. doi:10.1007/978-1-4757-3152-1
- Radicheva, N., Gerilovsky, L., & Gydikov, A. (1986). Changes in the muscle fibre extracellular action potentials in long-lasting (fatiguing) activity. *European Journal of Applied Physiology and Occupational Physiology*, *55*(5), 545–552. doi:10.1007/BF00421651 PMID:3769911
- Rodriguez-Falces, J., Dimitrova, N., Dimitrov, G., & Gila, L. (2011c). Shape variability of potentials recorded by a single-fiber electrode and its effect on jitter estimation. *Annals of Biomedical Engineering*, *39*(2), 812–823. doi:10.1007/s10439-010-0207-z PMID:21108004
- Rodriguez-Falces, J., Gila, L., & Dimitrova, N. A. (2012a). The morphology of single muscle fibre potentials - Part I: Simulation study of the distortion introduced by the distant-interfering potentials. *Journal of Electromyography and Kinesiology*, *23*(1), 14–23. doi:10.1016/j.jelekin.2012.07.002 PMID:22863372

- Rodriguez-Falces, J., Gila, L., & Dimitrova, N. A. (2012b). The morphology of single muscle fibre potentials - Part II: Experimental findings. *Journal of Electromyography and Kinesiology*, 23(1), 24–32. doi:10.1016/j.jelekin.2012.07.003 PMID:22868038
- Rodriguez-Falces, J., Navallas, J., Gila, L., Dimitrova, N., & Malanda, A. (2011a). Estimating the duration of intracellular action potentials in muscle fibres from single-fibre extracellular potentials. *Journal of Neuroscience Methods*, 197, 221–230. doi:10.1016/j.jneumeth.2011.02.022 PMID:21396959
- Rodriguez-Falces, J., Navallas, J., Gila, L., Malanda, A., & Dimitrova, N. A. (2012c). Influence of the shape of intracellular potentials on the morphology of single-fiber extracellular potentials in human muscle fibers. *Medical & Biological Engineering & Computing*, 50(5), 447–460. doi:10.1007/s11517-012-0879-7 PMID:22447347
- Rodriguez-Falces, J., Navallas, J., Gila, L., Rodriguez, I., & Malanda, A. (2011b). The peak-to-peak ratio of single-fibre potentials is little influenced by changes in the electrode positions close to the muscle fibre. *Journal of Electromyography and Kinesiology*, 21, 423–432. doi:10.1016/j.jelekin.2010.04.001 PMID:20451410
- Sanders, D. B. (1987). The electrodiagnosis of myasthenia gravis. *Annals of the New York Academy of Sciences*, 505, 539–556. doi:10.1111/j.1749-6632.1987.tb51322.x PMID:2825576
- Sanders, D. B., Howard, J. F., & Johns, T. R. (1979). Single-fiber electromyography in myasthenia gravis. *Neurology*, 29(1), 68–76. doi:10.1212/WNL.29.1.68 PMID:218146
- Sanders, D. B., & Stålberg, E. (1996). Single-fibre electromyography. *Muscle & Nerve*, 19, 1069–1083. doi:10.1002/(SICI)1097-4598(199609)19:9<1069::AID-MUS1>3.0.CO;2-Y PMID:8761262
- Schwartz, M. S., & Stålberg, E. (1975). Myasthenia gravis with features of the myasthenic syndrome. An investigation with electrophysiologic methods including single-fiber electromyography. *Neurology*, 25(1), 80–84. doi:10.1212/WNL.25.1.80 PMID:1167410
- Sejersted, O. M., & Sjogaard, G. (2000). Dynamics and consequences of potassium shifts in skeletal muscle and heart during exercise. *Physiological Reviews*, 80(4), 1411–1481. PMID:11015618
- Sonoo, M., & Stålberg, E. (1993). The ability of MUP parameters to discriminate between normal and neurogenic MUPs in concentric EMG: analysis of the MUP thickness and the proposal of size index. *Electroencephalography and Clinical Neurophysiology*, 89(5), 291–303. doi:10.1016/0168-5597(93)90068-Z PMID:7691568
- Stålberg, E. (1966). Propagation velocity in human muscle fibres in situ. *Acta Physiologica Scandinavica*, 70(287), 1–112.
- Stålberg, E. (1977). Electrogenesis in human dystrophic muscle. In L. P. Rowland (Ed.), *Pathogenesis of human muscular dystrophies* (pp. 570–587). Amsterdam, The Netherlands: Excerpta Medica.
- Stålberg, E., Ekstedt, J., & Broman, A. (1974). Neuromuscular transmission in myasthenia gravis studied with single fibre electromyography. *Journal of Neurology, Neurosurgery, and Psychiatry*, 37(5), 540–547. doi:10.1136/jnnp.37.5.540 PMID:4366058
- Stålberg, E., & Sanders, D. B. (2009). Jitter recordings with concentric needle electrodes. *Muscle & Nerve*, 40(3), 331–339. doi:10.1002/mus.21424 PMID:19705424
- Stålberg, E., & Trontelj, J. (1979). *Single fibre electromyography*. Old Woking, UK: Raven Press.

Van Veen, B. K., Wolters, H., & Wallinga, W. (1993). The bioelectrical source in computing single muscle fibre action potentials. *Biophysical Journal*, *64*, 1492–1498. doi:10.1016/S0006-3495(93)81516-9 PMID:8324186

Wallinga, W., Gielen, F. L. H., Wirtz, P., de Jong, P., & Broenink, J. (1985). The different intracellular action potentials of fast and slow muscle fibres. *Electromyography and Clinical Neurophysiology*, *60*, 539–547. doi:10.1016/0013-4694(85)91115-0

ADDITIONAL READING

Andreassen, S., & Rosenfalck, A. (1981). Relationship of intracellular and extracellular action potentials of skeletal muscle fibres. *CRC Critical Reviews in Bioengineering*, *7*, 267–306.

Arabadzhiev, T., Dimitrov, G. V., Chakarov, V., Dimitrov, A., & Dimitrova, N. (2008). Effects of changes in intracellular action potential on potentials recorded by single-fibre, macro, and belly-tendon electrodes. *Muscle & Nerve*, *37*(6), 700–712. doi:10.1002/mus.21024 PMID:18506714

Baker, D. J., Cross, N. L., & Sedgwick, E. M. (1987). Normality of single fibre electromyographic jitter: a new approach. *Journal of Neurology, Neurosurgery, and Psychiatry*, *50*(4), 471–475. doi:10.1136/jnnp.50.4.471 PMID:3585360

Basmajian, J. V., & DeLuca, J. C. (1985). *Muscles alive. Their function revealed by Electromyography*. Baltimore, USA: Williams and Wilkinson.

Bromberg, M. B., & Scott, D. M. (1994). Single fiber EMG reference values: reformatted in tabular form. AD HOC Committee of the AAEM Single Fiber Special Interest Group. *Muscle & Nerve*, *17*, 820–821. doi:10.1002/mus.880170720 PMID:8008013

Dimitrova, N. (1987). Mathematical modelling of intra- and extracellular potentials generated by active structures: effects of a step change in structure diameter. *General Physiology and Biophysics*, *6*, 19–34. PMID:3596223

Duchêne, J., & Hogrel, J. Y. (2000). A model of EMG generation. *IEEE Transactions on Bio-Medical Engineering*, *47*, 192–201. doi:10.1109/10.821754 PMID:10721626

Dumitru, D. (1994). The biphasic morphology of voluntary and spontaneous SFAPs. *Muscle & Nerve*, *17*, 1301–1307. doi:10.1002/mus.880171109 PMID:7935552

Falces, J. R., Trigueros, A. M., Useros, L. G., Carreño, I. R., & Irujo, J. N. (2005). A mathematical analysis of SFAP convolutional models. *IEEE Transactions on Bio-Medical Engineering*, *52*(5), 769–783. doi:10.1109/TBME.2005.845045 PMID:15887526

Gath, I., & Stålberg, E. (1975). Frequency and time domain characteristics of single muscle fibre action potentials. *Electromyography and Clinical Neurophysiology*, *39*, 371–376. doi:10.1016/0013-4694(75)90100-5 PMID:51720

Goldstein, S. S., & Rall, W. (1974). Changes of action potential shape and velocity for changing core-conductor geometry. *Biophysical Journal*, *14*, 731–757. doi:10.1016/S0006-3495(74)85947-3 PMID:4420585

Gootzen, T., Stegeman, D., & Van Oosterom, A. (1991). Finite limb dimensions and finite muscle length in a model for the generation of electromyographic signals. *Electroencephalography and Clinical Neurophysiology*, *81*, 152–162. doi:10.1016/0168-5597(91)90008-L PMID:1708717

Håkansson, C. (1957). Action potentials recorded intra- and extracellularly from the isolated frog muscle fibre in Ringer's solution and in air. *Acta Physiologica Scandinavica*, 39, 291–312. doi:10.1111/j.1748-1716.1957.tb01430.x PMID:13444043

Hodgkin, A. L., & Huxley, A. F. (1952). A quantitative description of membrane current and its application to conduction and excitation in nerve. *The Journal of Physiology*, 117, 500–544. PMID:12991237

Lorente de Nó, R. (1947). Analysis of the distribution of action currents of nerve in volume conductors. *Studies from the Rockefeller Institute for Medical Research*, 132, 384–485. PMID:20261890

McGill, K. C., & Lateva, Z. C. (2001). A model of the muscle-fibre intracellular action potential waveform, including the slow repolarization phase. *IEEE Transactions on Bio-Medical Engineering*, 48, 1480–1483. doi:10.1109/10.966607 PMID:11759929

Nandedkar, S., & Sanders, D. B. (1988). Simulation of concentric needle EMG motor unit action potentials. *Muscle & Nerve*, 11, 151–159. doi:10.1002/mus.880110211 PMID:3343991

Rodríguez, J., Navallas, J., Gila, L., Latasa, I., & Malanda, A. (2012). Effects of changes in the shape of the intracellular action potential on the peak-to-peak ratio of single muscle fibre potentials. *Journal of Electromyography and Kinesiology*, 22(1), 88–97. doi:10.1016/j.jelekin.2011.06.005 PMID:21906960

Rodríguez-Falces, J., Malanda-Trigueros, A., Gila-Useros, L., Rodríguez-Carreño, I., & Navallas-Irujo, J. (2006). Modelling fibrillation potentials – a new analytical description for the muscle intracellular action potential. *IEEE Transactions on Bio-Medical Engineering*, 53, 581–592. doi:10.1109/TBME.2006.870257 PMID:16602564

Rosenfalck, P. (1969). Intra- and extracellular fields of active nerve and muscle fibres. A physico-mathematical analysis of different models. *Acta Physiologica Scandinavica*, 321, 1–168. PMID:5383732

Stålberg, E., & Antoni, L. (1980). Electrophysiological cross section of the motor unit. *Journal of Neurology, Neurosurgery, and Psychiatry*, 43, 464–474. doi:10.1136/jnnp.43.6.469 PMID:6968341

Stålberg, E., & Karlsson, L. (2001). Simulation of the normal concentric needle electromyogram by using a muscle model. *Clinical Neurophysiology*, 112, 464–471. doi:10.1016/S1388-2457(01)00459-X PMID:11222968

Stalberg, E., & Karlsson, L. (2001). Simulation of EMG in pathological situations. *Clinical Neurophysiology*, 112, 869–878. doi:10.1016/S1388-2457(01)00498-9 PMID:11336904

Stålberg, E., & Trontelj, J. (1992). Clinical neurophysiology: the motor unit in myopathy. In *Handbook of clinical neurology*, 49–84, Rowland LP. New York: Elsevier.

Stashuk, D. W. (1993). Simulation of electromyographic signals. *Journal of Electromyography and Kinesiology*, 3, 157–173. doi:10.1016/S1050-6411(05)80003-3 PMID:20719627

Trayanova, N. A., & Dimitrov, G. V. (1982). Extracellular potentials in the proximity of the excitable fibres. *Electromyography and Clinical Neurophysiology*, 22, 291–301. PMID:7084104

KEY TERMS AND DEFINITIONS

Concentric Electrodes: Needle electrode which has an oval recording surface in its tip, and the cannula serves as the reference. Typical dimensions of a single fibre electrode are: needle diameter of 0.46 mm, needle length of 37 mm, oval leading-off surface of 150 µm x 570 µm.

Filter Settings: Adjustments of the band-pass filter, normally integrated in commercial EMG equipment, which consists on selecting the cut-off frequencies for the high-pass and low-pass filter.

IAP Spike Duration: Time interval between the point of highest slope in the depolarization phases of the IAP and the point of highest slope in the repolarization phases of the IAP.

Intracellular Action Potential: Voltage measured inside the muscle fibre cell as a result of the transport of sodium and potassium ions through the membrane. In the present chapter, the intracellular action potential is assumed to be approximately the same as the transmembrane potential which is initiated at the neuromuscular junction and travels in both directions along the muscle towards the tendons.

Jitter Estimation: Quantification of the neuromuscular jitter (normally provided in μs), a phenomenon consisting in the time-varying transmission at the neuromuscular junction.

SFAP Morphology: Shape characteristics of the SFAP, which includes, among others: the number of phases, the polarity of each of the phases, the duration of the phases, and the ratio between the amplitudes of phases.

SFAP Third Phase: Last (positive) phase of the SFAP generated by the repolarization phase of the transmembrane voltage.

Single Fibre Action Potential: Potential generated in the extracellular medium surrounding the fibre cell by the propagation of the transmembrane voltage along a single muscle fibre.

Single Fibre Electrodes: Needle electrode which consists of an insulated metal wire inside a hollow stainless steel cannula (that serves as a reference). Typical dimensions of a single fibre electrode are: needle diameter of 0.46 mm, needle length of 37 mm, circular leading-off surface of 25- μm radius.

Chapter 3

Detection and Conditioning of EMG

İmran Göker

Istanbul Arel University, Turkey

ABSTRACT

In this chapter, the monitoring of the electrical activity of skeletal muscles is depicted. The main components of the detection and conditioning of the EMG signals is explained in the sense of the biomedical instrumentation. But, first, a brief description of EMG generation is introduced. The hardware components of the general instrumentation system used in the acquisition of EMG signal such as amplifier, filters, analog-to-digital converter are discussed in detail. Subsequently, different types of electrodes used in different EMG techniques are mentioned. Then, various EMG signals that can be detected and monitored via EMG systems are described and their clinical importance is discussed with detail. Finally, different EMG techniques used in clinical studies and their purposes are explained with detail.

INTRODUCTION

Electromyography (EMG) is an electrophysiological technique for displaying and for assessing the electrical activity generated by the skeletal muscles. These signals are analyzed to find medical abnormalities in peripheral nervous system and muscles, or to study the biomechanics of human or animal movement. As a result, EMG is commonly used in either the diagnosis or differential diagnosis of neuromuscular disorders. As the knowledge in neurophysiology has increased, specific EMG methods have been developed in

terms of the requirements of the clinical studies. With the advances in the hardware and software technology, various EMG systems, including some for electrophysiological methods such as Nerve Conductions Studies, have been manufactured. In this chapter, general principles of the instrumentation in EMG systems will be described. Then, various EMG electrode types will be introduced. Afterwards, different EMG signals and their clinical implications will be explained. Finally, different EMG techniques including not only conventional EMG used in routine examinations but also specific EMG techniques such as Single Fiber

DOI: 10.4018/978-1-4666-6090-8.ch003

Detection and Conditioning of EMG

EMG, Macro EMG, Scanning EMG, Quantitative EMG and Surface EMG will be depicted in details. The principles of these methods, the parameters measured by these methods, their applications, their purposes in clinical use will be discussed.

BACKGROUND

Movement in the living milieu is essential for many organisms in maintaining life. The musculoskeletal system is responsible not only in achieving the movements including locomotion but also in the maintenance of the posture and in the establishment of the gestures and speech by means of the actuators referred as skeletal muscles (Pozzo, Farina, & Merletti 2004; Moritani, Stegeman & Merletti 2004). In human beings, skeletal muscle has four functions which can be explained as follows.

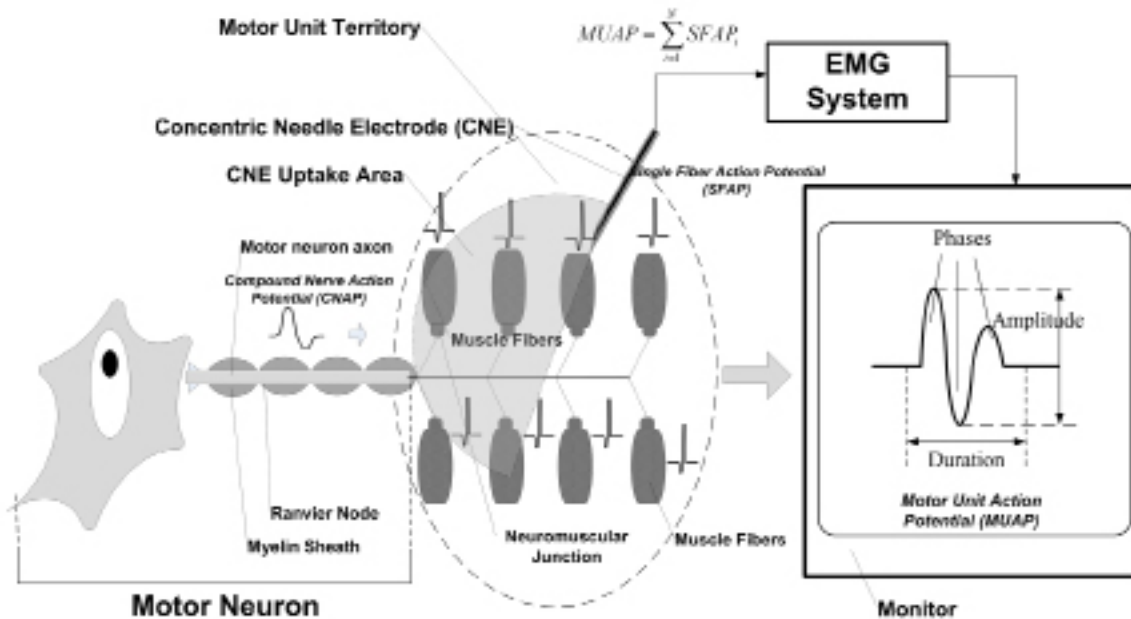
1. **Production of body movement:** In order to enable the organism to adapt rapidly to environmental changes, skeletal muscles have responsibilities for all locomotion including not only the movements playing role in displacement but also gestures and speech.
2. **Maintenance of Posture:** In the presence of gravity, equilibrium of the body is ensured by means of some skeletal muscles.
3. **Stabilization of Joints:** The joints such as shoulder and knee without complementary surface and hence with poor reinforcement can be stabilized with the help of the skeletal muscles
4. **Generation of Heat:** The skeletal muscles constituting 40% of body mass produce heat during their contractions which has a vital importance in maintaining normal body temperature (Marieb, 1995; Tortora, 2009; Tortora, 2010).

These functions are controlled by electrical signals transmitted from the nervous system to muscle fibers that bring about skeletal muscle contraction. (Henneberg, 2000, 2006). During the contractions the conversion of the chemical energy and electrical energy into mechanical energy takes place by the cleavage of ATP molecules in order to establish the motor activity (Guyton, 2002). Hence mechanical force is generated as the output of the motor system (Cotterill, 2002). The process of contribution of additional motor units to produce force at a certain level is referred as motor unit recruitment and it occurs in an orderly sequence based on the size of the motor units (Preston & Shapiro, 2005). According to the Henneman's Size Principles, as the contraction increases the small motor units are recruited first and then larger ones participate to this process (Loeb & Ghez, 2000).

Since it is not feasible in humans to insert force sensors in series on tendons, electrical activity of the muscles is used to assess muscle contraction (Pozzo, Farina, & Merletti 2004). These electrical activities are generated by the basic anatomical and functional unit of the skeletal muscle called as Motor Unit (MU). The concept of motor unit was first introduced by Sherrington in 1925 (Burke, 2001; Liddell & Sherrington, 1925). A motor unit consists of a motoneuron in anterior horn of the spinal cord, and all the muscle fibers innervated by this motor neuron (Preston & Shapiro, 2005).

Motor unit is a functional and anatomical unit and its different components such as nerve and muscle tissue achieve the movement in coordination by using the bioelectrical activity. The number of motor units in a muscle varies from muscle to muscle. The number muscle fiber contained in a motor unit can also vary in various muscles in human body (e.g. gastrocnemius muscle of the leg serving in coarse movements possesses up to 2000 muscle fibers per motor neuron whereas, extraocular muscles which generate fine-tuned movements may have three muscle fibers per motor neuron) (Cram & Kasman, 2001).

Figure 1. Schematic representation of the motor unit and the motor unit action potential (MUAP)



The electrical activity generated individually by the muscle fibers is referred as Single Fiber Action Potential (SFAP). Some of these SFAPs are superimposed in terms of amplitude while propagation within the volume conductor (i.e. muscle tissue) and this form of electrical activity being recorded by means of various electrodes is defined as Motor Unit Action Potential (MUAP). However, MUAP being acquired depending on the characteristics of the recording electrode is limited with the muscle fibers located within the uptake area of the electrode. MUAP is expressed by parameters such as amplitude, duration, number of phases etc. These parameters will be described with details in the following sections. These are represented in Figure 1. (Henneberg, 2006; Aminoff, 1992; Diószeghy, 2002).

The process of studying the electrical activity of muscles is referred as Electromyography (EMG) (Weiss, 2004). Although it implies the assessment (or evaluation) of peripheral nerve and muscle through the needle electrodes, “EMG” or

“Clinical EMG” is referred as the electrophysiologic examination including nerve conduction studies (NCS) as well by clinicians (Katirji, 2007). EMG is used as a major electrodiagnostic tools to detect and to characterize the disorders affecting the motor unit including muscle fibers, neuromuscular junctions, peripheral nerves and anterior horn cells (Aminoff, 1992; Rubin, 2009). In this context, EMG is beneficial in the clinical evaluation when the absolute localization of the lesion from where the symptoms originate is difficult to detect. Therefore, EMG is an auxiliary electrophysiological tool in the differential diagnosis of the neurogenic, myopathic and neuromuscular junction disorders (Aminoff, 1992; Kimura, 2001; Mills, 2005; Oh, 2003).

EMG signals are acquired by means of EMG instruments. In conjunction with these instruments, several EMG methods are used. Usually, conventional EMG is used in routine examinations. Even though the methods used for specific purposes such as Single Fiber EMG, Macro EMG,

Detection and Conditioning of EMG

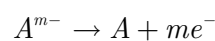
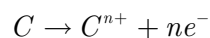
Scanning EMG and Surface EMG are performed with the same EMG instruments, special electrode types and software designed for these purposes are used.

ELECTRODES

The EMG signals are picked up through an electrode which is the passive electrical interface between the subject¹ and the equipment either during the voluntary contraction or at rest (Pozzo, Farina, & Merletti, 2004; Trontelj, Jabre & Mihelin, 2004). These EMG recordings can be performed either intramuscularly using various needle electrodes or by means of surface electrodes (see Figure 3).

Principles of Electrodes

Like other biopotential electrodes, the principles of the EMG electrodes are also based on the fact that the electrolytic solutions and tissues contain charged particles and ions. The biological signal detected by the EMG electrodes is generated by the transduction of the ionic current flowing through the body. This ionic current results in the electrical current being fed to the input stage of the EMG system by means of the electrodes. The generation of these ionic current yields from the reduction-oxidation at the interface between the electrode and the tissue in the double layer formed close to the electrode surface. This process can be represented by the following equations for the metal C forming the cathode and metal A forming the anode:



where n is the valence of cathode C and m is the valence of anode A (Neuman, 2010; Pozzo, Farina, & Merletti 2004).

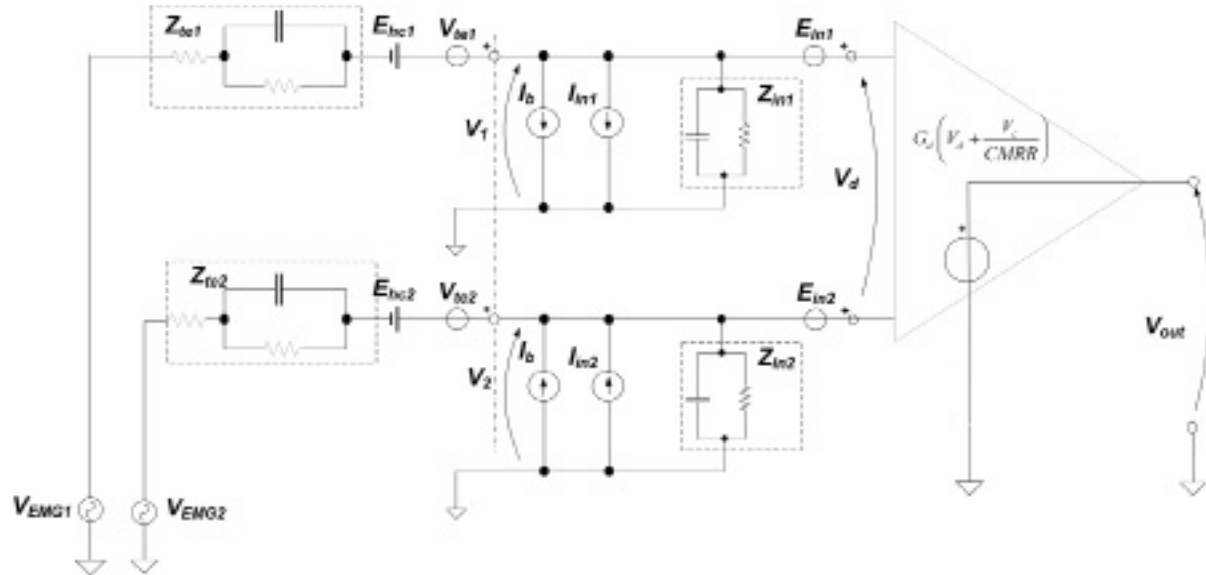
As a result, a half-cell potential (E) takes place when a metal is in contact with an ionic solution which can be represented as below by the Nernst equation

$$E = \frac{RT}{nF} \ln \left(\frac{a_1}{a_2} \right)$$

where R is the universal gas constant, T is the absolute temperature, n is the valence of the ion, and a_1 and a_2 are the activities of the ion on the two sides of the double layer (Neuman, 2010; Northtrope, 2002; Pozzo, Farina, & Merletti 2004; Togawa, Tamura, Öberg, 1997). The electrodes can be categorized into two categories such as polarizable and non-polarizable. Polarizability refers to the alteration of the half-cell potential due to the current passing through the membrane. It can be also called overvoltage and it is originated from the changes in charge distribution in the solution being in contact with the electrode. The electrical model of the tissue-electrode interaction is shown in Figure 2. V_c is the common mode input voltage that appears simultaneously and in phase on each of the instrument's inputs with respect to power ground. The common-mode rejection ratio (CMRR) is the rejection by the device of unwanted input signals common to both input leads, relative to the wanted difference signal. V_c and CMRR will be explained with detail in the following sections.

Perfectly polarizable electrodes demonstrate a capacitive behavior allowing a current flow between the electrode and electrolyte solution by changing the charge distribution in the electrolyte (i.e. body fluid). These electrodes are manufactured from noble metals such as platinum. Polarizability leads to motion artifact ranging from DC up to 20 Hz due to the changes in ion concentrations at the skin-electrode interface if the electrode moves with respect to the electrolyte. This is a challenge in surface EMG electrodes. On the other hand, in perfectly non-polarizable

Figure 2. Electrical Model of the tissue-electrode interaction and preamplifier stage; V_{EMG1} , V_{EMG2} : EMG signals; Z_{te1} , Z_{te2} : tissue-electrode impedances; E_{hc1} , E_{hc2} : Half-cell potentials; I_b : Amplifier input bias current; I_{in1} , I_{in2} : Amplifier input current noises; V_d : Differential input voltage; G_d : Differential gain; CMRR: Common mode rejection ratio; V_{CM} : common mode input voltage $[(V_1+V_2)/2]$



electrodes, current freely passes across the electrode-electrolyte interface without requiring energy. Therefore, non-polarizable electrodes (e. g. silver-silver chloride electrodes) are more suitable in surface EMG applications (Neuman, 2010a; Pozzo, Farina, & Merletti 2004).

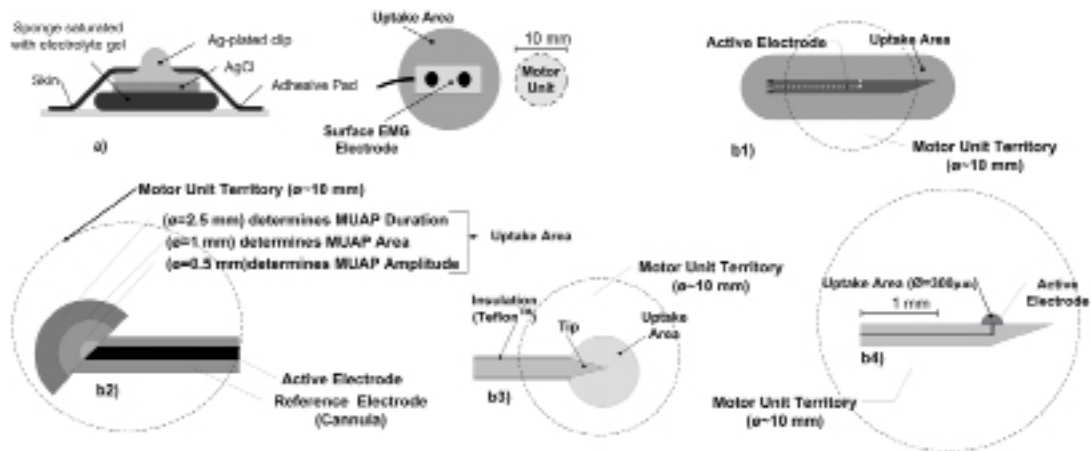
In addition to the challenges described in the previous paragraphs, several factors such as MU size, innervation ratio, temporal and spatial characteristics of the MUAP should be taken into the account while designing the electrodes. In that context, there exist several types of EMG electrodes. These are concentric needle electrode, monopolar electrode, single-fiber electrode, macro needle electrode and surface EMG electrode. The uptake areas of these electrodes differ from each other. The uptake area can be defined as the part of the MU where the bioelectrical activity recorded by the electrode. All of these electrodes are represented in Figure 3.

Concentric Needle Electrode (CNE)

The concentric needle electrode is used in the conventional needle EMG in clinical routine examinations. This electrode was first developed by Adrian and Bronk in 1929 (Henneberg, 2000; Trontelj, Jabre & Mihelin, 2004). It consists of a stainless-steel cannula and a wire made of nickel chrome or platinum. The diameters of this wire and the cannula measure 0.1-mm and 0.3-mm in diameter respectively. This wire is insulated with a resin layer. The beveled tip of the needle with a 15°-angle constitutes the active recording surface an oval shape in 150×600-μm dimensions. The impedance of this wire is approximately 50 kΩ (Kimura, 2001; Trontelj, Jabre & Mihelin, 2004). The uptake area of the concentric needle electrode is a semiglobe in 2.5-mm diameter. The MUAP duration is determined by muscle fibers within this area. The area under curve of the MUAP signal is determined by muscle fibers within the area with 1-mm diameter. The fibers within the uptake area

Detection and Conditioning of EMG

Figure 3. Schematic representation of the EMG electrodes in different types: (a) Surface EMG Electrode; (b) Macro EMG Electrode; (c) Concentric needle electrode; (d) Monopolar electrode; (e) Single fiber electrode



with 0.5-mm diameter contribute to the amplitude of the EMG signal of interest (Trontelj, Jabre & Mihelin, 2004). All these parameters such amplitude, duration, area etc. are illustrated in Figure 1 and Figure 7. Concentric needle electrode is illustrated in Figure 3c.

Monopolar Needle Electrode (MNE)

The monopolar needle electrode- made of stainless steel- is an insulated needle which is coated with Teflon™ except at the distal 0.2 to 0.4 mm. It has a fine point. This point is obtained by sharpening the tip of the electrode to conical shape. This tip, which is not insulated, has a conductive area of 0.15- to 0.25-mm² (Kimura, 2001; Oh, 2003; Trontelj, Jabre & Mihelin, 2004). The average diameter of the monopolar needle electrode with Teflon coating is 0.8-mm (Kimura, 2001; Oh, 2003; Stålberg & Falck, 1997; Trontelj, Jabre & Mihelin, 2004). The length ranges from 12 mm to 75 mm (Oh, 2003). The average impedance lies

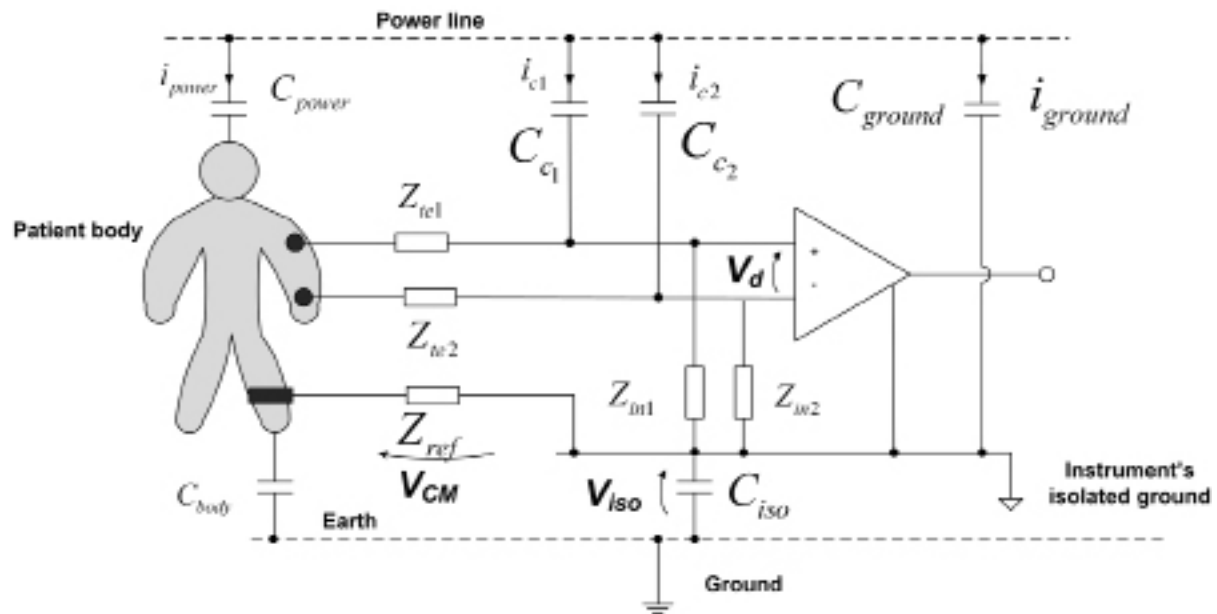
between 1.4 MΩ at 10 Hz to 6.6 kΩ at 10 kHz (Kimura, 2001).

In needle EMG studies, monopolar needle electrode may be used as the active electrode. A surface electrode or a second needle in the subcutaneous tissue is used as a reference electrode. A separate surface electrode placed on the skin is used as the ground electrode (Chan, & Hsu, 1991; Kimura, 2001; Oh, 2003; Trontelj, Jabre & Mihelin, 2004).

Monopolar needle electrode is less painful, less expensive and more sensitive in identifying EMG signals such as fibrillation and positive sharp waves than the concentric needle electrode (Oh, 2003). However, since it has a higher impedance, it is less stable and hence noisier (Kimura, 2001).

Monopolar needle electrode is also used as a stimulating electrode if the nerve trunk to be stimulated is located deep. It can also be used for intramuscular stimulation in activating only a single or a few motor units at a time (Oh, 2003; Trontelj, Jabre & Mihelin, 2004). Monopolar needle electrode is shown in Figure 3(d).

Figure 4. Sources of interferences when the patient, the electrodes and the amplifier of the emg system are connected to each other (i_{power} : displacement current flowing through the patient due to the power lines; c_{power} : capacitance between the patient's body and the power line; c_{body} : capacitance between patient's body and earth; i_{c1} , i_{c2} : displacement currents flowing through the electrodes due to the power lines; c_{c1} , c_{c2} : capacitances between the power lines and the electrodes; z_{te1} , z_{te2} : contact impedances of the electrodes; z_{ref} : contact reference electrode; z_{in1} , z_{in2} : amplifier input impedance; i_{ground} : displacement current flowing from the power lines toward the isolated ground. c_{ground} : capacitance between the power line and the isolated ground; v_d : differential input voltage; v_{cm} : common-mode input voltage; v_{iso} : isolation-mode voltage; c_{iso} : capacitance of the isolation barrier



Single Fiber Electrode (SFE)

Some clinical studies require recording from single muscle fibers, which necessitates a very selective electrode. (Kimura, 2001; Stålberg, Trontelji & Sanders, 2010). Since the diameter of the muscle fibers varies from 25 μm to 100 μm , SFE comprises a 25- μm platinum wire in diameter inside a cannula. The small recording surface of the platinum wire ensures selective recording of a single fiber action potential. An uptake area with 300- μm radius is created. This wire is insulated from the cannula by an epoxy resin and its tip is bent toward the side of the cannula. The cannula is the reference electrode with 0.5- to 0.6-mm

diameter (Kimura, 2001; Stålberg & Trontelji, 1994; Trontelji, Jabre & Mihelin, 2004). Single-fiber electrode is represented in Figure 3(e).

Macro Needle Electrode

Macro EMG electrode is an intramuscular needle electrode that is used to record the total electrical activity of all the muscle fibers belonging to same motor unit. It consists of a steel cannula and within a 25 micrometer platinum wire which bent in a side port which is used for recording a single fiber action potential in one channel to trigger the sweep of the second channel in which total activity of all muscle fibers from the same motor unit were

Detection and Conditioning of EMG

recorded and averaged (Trontelj, Jabre & Mihelin, 2004). The recording surface of the modified SFE is 7.5 mm from the tip of the electrode. Hence the recording surface is maintained as constant even if the needle is inserted into the deeper part of the MU. The cannula with a 0.55-mm-diameter and a 15-mm-exposed surface is used to record the electrical activity of the entire motor unit (Kimura, 2001; Stålberg & Falck, 1997).

In the limb muscle, the muscle fibers are distributed over a cross-sectional area with 5- to 10-mm diameter. The 15-mm recording area of the macro-EMG needle enables this electrode to perceive a motor unit over a cross-sectional area with 5- to 10-mm diameter (Smith, 2009). Macro needle electrode is illustrated in Figure 3(b).

Surface EMG Electrode

In contrast to the invasive intramuscular electrodes, surface electrodes do not penetrate the skin. They are fixed on the skin over the muscles of interest for the in vivo measurements of the EMG signals (Christe, 2009; Sawney, 2007). These electrodes are manufactured materials such as solid silver or gold, platinum, sintered silver and silver chloride, carbon, and sponge saturated with electrolyte gel or conductive hydrogel (Neuman, 2010). Surface electrodes have a large pick-up area.

They register electrical activity from a wider region depending on the size of the electrodes. They are non-selective. However, they record mass activity from a large proportion of a muscle, or from many muscles, depending on recording site (Kimura, 2001; Stålberg & Falck, 1997). Surface electrodes are usually used for monitoring voluntary muscle contraction during kinesiology studies and evoked compound nerve and muscle potentials (Kimura, 2001). Surface EMG electrode is shown in Figure 3(a).

GENERAL PRINCIPLES OF INSTRUMENTATION IN ELECTROMYOGRAPHY

Like other biopotentials, EMG signals should be also conditioned after the detection process via the convenient electrodes. Signal conditioning process includes amplification, filtering and converting into digital form. Therefore, the electrical activities can be monitored in a visible form that enables the clinicians to make any clinical interpretation. So the essential part of the EMG instruments is the biopotential readout circuits that establish the signal conditioning and the signal processing of the detected electric activities to display them in the readable form by the physicians. EMG signals are extremely small and require several stages of processing before they can be made understood and quantified (Aminoff, 1992; Nagel, 2006; Van Hoof & Puers, 2009). The instruments consist of preamplifiers, filters, circuits for noise reduction and connections to protect subjects from shocks (Pozzo, Farina & Merletti, 2004).

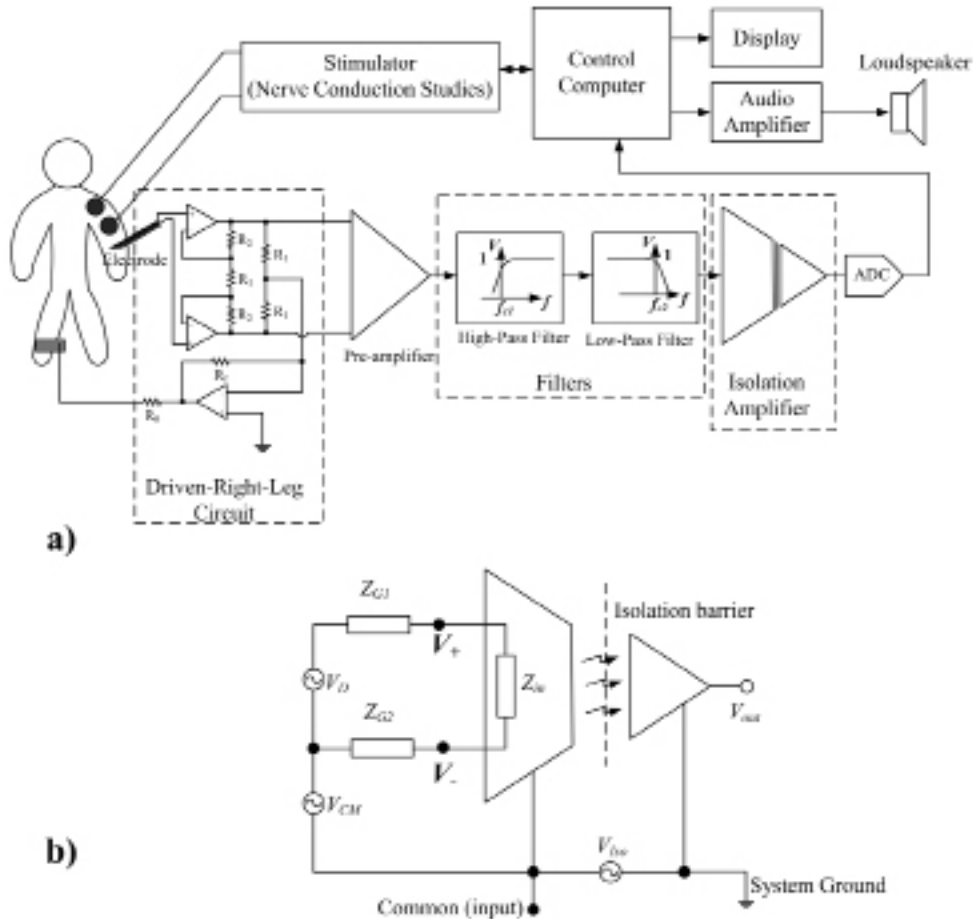
General Characteristics of EMG Signals

EMG signals recorded with concentric needle electrode during voluntary contraction of particular muscle include different MUAPs which are firing with their own frequencies. These EMG signals have a frequency range lying between 10 Hz to 10 kHz (Brown et al., 1999). The amplitudes of each MUAPs vary between 50 μ V and 20 to 30 mV. They have duration of 3 to 15 milliseconds. These parameters may depend on the recording characteristics of the electrode of interest (Aminoff, 1992; Bryan, 1998; Oh, 2003).

General Structure of EMG Systems

The general structure of the modern electromyography systems consist of input stage or ampli-

Figure 5. (a) Block diagram of the EMG system (b) equivalent circuit for the isolation amplifier



fier stage, filters, analog-to-digital converters, computer systems with specific software used to process the acquired signals for different electrophysiological applications and managing to storage and displaying these processed data, output devices such as a loud speaker in conjunction with an audio amplifier, a display to monitor the signal of interest and a printer for the hard copies of the reports.

Like other biopotential amplifiers, while designing the EMG systems tissue-electrode interactions and interferences originating from the ambient environment should be taken into

account. The general configuration of the EMG recording system is shown in Figure 5(a).

Tissue-Electrode Interactions

Tissue-electrode interface comprises contact impedance with resistive and capacitive components ranging from $10\text{ k}\Omega$ to $1\text{ M}\Omega$ which is related with the type of electrode, the half-cell potential at this interface which can be as 200 mV , the intrinsic noise of the tissue-electrode interface due to the thermal noise across the contact impedance the electrode contact noise due to the ionic exchange

Detection and Conditioning of EMG

at the tissue-electrode interface and the source of EMG signals (Pozzo, Farina, & Merletti, 2004). An EMG signal below the intrinsic electrode noise is masked by this noise. Therefore, since the input stage plays role in the final quality of the detected EMG signal, the lower boundary of the meaningful input range of an EMG amplifier should be determined by considering the intrinsic electrode noise (Pozzo, Farina, & Merletti, 2004).

Sources of Interferences and Noises

While operating, an EMG amplifier is usually exposed to noise leading to inferences that can considerably distort the quality of the signal of interest. Sources of interferences can be summarized as power line cables, HF interferences, ripples in the power supply of the amplifier and internally and externally generated magnetic and electrical fields. While designing such systems, these sources of interferences should be taken into account and the design of the equipment should aim to reduce the effects of these interactions.

One of the sources of interference is the capacitive coupling between the measurement cables connected to electrodes and the power line cables and the induced currents flowing through the body which can be expressed as follows:

$$V_d = i_c Z_{electrode} \left(\frac{\Delta Z_{electrode}}{Z_{electrode}} + \frac{\Delta i_c}{i_c} \right)$$

where

$$i_c \equiv \frac{i_{c1} + i_{c2}}{2}$$

$$\text{and } Z_{electrode} \equiv \frac{Z_{electrode1} + Z_{electrode2}}{2}$$

The resulting voltage is referred as differential input voltage V_d . Since this induced V_d voltage

is differential, it cannot be attenuated through Common-Mode Rejection Ratio (CMRR). Therefore, its effect can be reduced by minimizing the parasitic capacitances between power lines and measurements cables connected to the electrodes. This is achieved by making the connections between the electrodes and the input stage as short as possible and thus by placing the instrumentation amplifier circuit as close as possible to the electrodes. Besides, shielded cables with active guarding in which the shield is driven with a buffer possessing an input connected to common mode voltage is also an effective precaution.

Another source of interference takes place due to the common-mode voltage V_{CM} as a result of the power lines interferences. This voltage reveals between the differential voltage and the earth through the reference impedance due to the imperfections in differential amplifiers (Brown et al., 1999; Pozzo, Farina, & Merletti, 2004). The relationship between the differential input voltage and the common-mode voltage is called *potential divider effect* and it can be described by the following equations:

$$V_d = V_{CM} \frac{Z_{electrode}}{Z_i} \left(\frac{\Delta Z_{electrode}}{Z_{electrode}} + \frac{\Delta Z_i}{Z_i} \right)$$

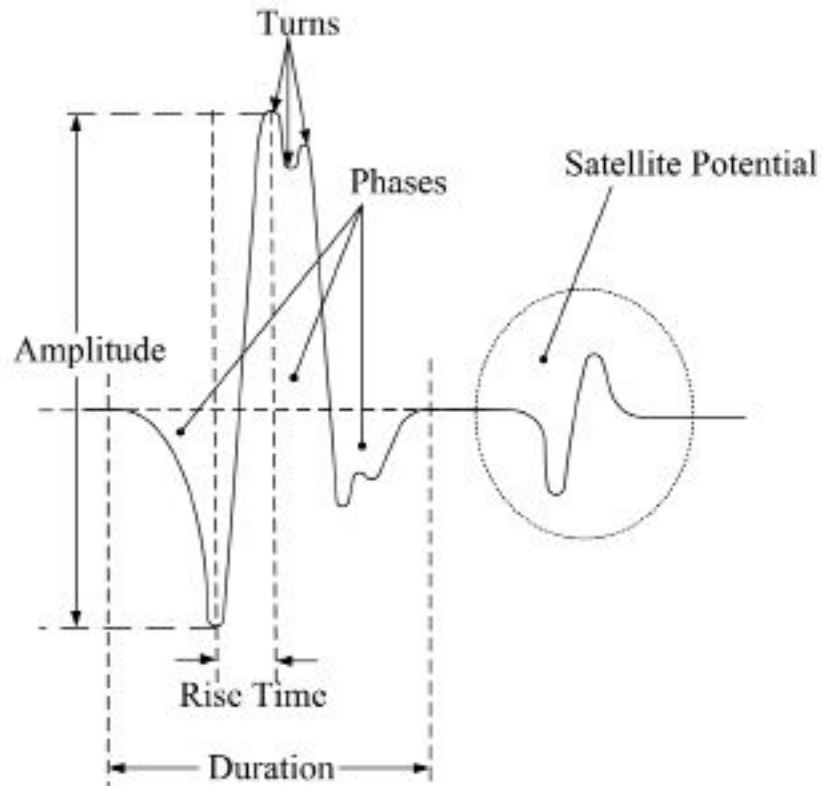
where

$$Z_{electrode} = \frac{Z_{electrode1} + Z_{electrode2}}{2}$$

$$\text{and } Z_i = \frac{Z_{i1} + Z_{i2}}{2}$$

The minimization of the common mode voltage is expressed by Common Mode Rejection Ratio (CMRR). Hence the power line interference can be minimized theoretically with a CMRR as much as possible.

Figure 6. Characteristic parameters of the motor unit action potential (MUAP)



High Frequency (HF) emissions emanating from the sources located in the vicinity of the EMG systems are other sources of interferences beside the high-frequency components of the signal of interest (van der Horst et al., 1998). This kind of interference can be eliminated by means of low-pass filter in the signal conditioning process. Occasionally, intrinsic rectifying effect of the input stage acting as an AM/FM demodulator may lead HF-induced interferences with the bandwidth of EMG signals. This can be prevented by inserting HF ceramic disc capacitor between the inputs and the reference (Grimbergen, Metting van Rijn & van der Horst, 1991; Pozzo, Farina, & Merletti, 2004).

Thermal noise (Johnson noise) is an intrinsic noise revealed at the tissue-electrode interface across the contact impedance. So, it is an electrical current resulting from the thermal movement of ions and electrons that generates a noise voltage. The magnitude of this noise can be expressed as follows;

$$V_{thermal,RMS} = \sqrt{4kTR\Delta f}$$

where k is the Boltzmann Constant (1.308×10^{-23} J/K), T is absolute temperature, R is the value of the resistance in Ohms and Δf is the bandwidth of the system in Hertz. The Johnson noise cannot be eliminated. But its magnitude should

Detection and Conditioning of EMG

be calculated in order to estimate the signals of interest.

Motion artifacts originate from two sources such as contact of electrode to tissue and connection cables between the electrodes and the input stage. The spectral range of this noise extends between DC and 20 Hz. It can be minimized by using high-pass filters with proper connection of cables (Lin et al., 1999; Pozzo, Farina, & Merletti, 2004; Sörnmo & Laguna, 2005).

Input Stage of the Amplifier

EMG signals have amplitudes of the order of millivolts. So their voltage should be amplified to readable levels by the displays and to be stored in computers. Like other biopotential amplifiers, those used in EMG input stages must have gains of at least 1000 (Prutchi & Norris, 2005). The gain is computed as follows;

$$Gain(dB) = 20 \log_{10}(\text{linear gain}) = 20 \log_{10} \left(\frac{V_{out}}{V_{in}} \right)$$

The input stage of an EMG system comprises *instrumentation amplifier (IA)* and *isolation amplifier*. The instrumentation amplifier which is also called preamplifier is used to match impedance and to realize the amplification and the conditioning of the biological signal acquired from the patient. On the other hand, the isolation amplifier is a safety device used to protect the patient from the line voltage (Nagel, 2006).

An electrode is connected to the pre-amplifier through cables and these cables are exposed to interference signals. But the interference occurs only on the input cables to the amplifier and it is not seen on the ground cable with "0" potential. In order to minimize noise, a differential amplifier can be used which takes the difference of two inputs and that amplifies this difference. In the presence of noise interference, this noise can be

cancelled out by this circuitry in symmetrical manner. It is difficult to make a differential amplifier with perfect subtraction. As a result, due to this imperfection, a common-mode voltage V_{CM} is created on human body by the displacement current i_D flowing through the impedance of reference electrode Z_r and the magnitude of this voltage is given as follows;

$$V_{CM} = \left(\frac{i_D}{2} \right) Z_r$$

The Common Mode Rejection Ratio (CMRR) which is the capability to reject common-mode signals could measure the accuracy of subtraction in each amplifier (Pozzo, Farina, & Merletti 2004; Prutchi & Norris, 2005). It is defined as the ratio between the gain of the common-mode signal (Nagel, 2006) and that of an equivalent differential signal and can be given as follows;

$$CMRR = 20 \log \left(\frac{G_d}{G_{CM}} \right)$$

where the differential gain G_d and the common-mode gain G_{CM} are as follows;

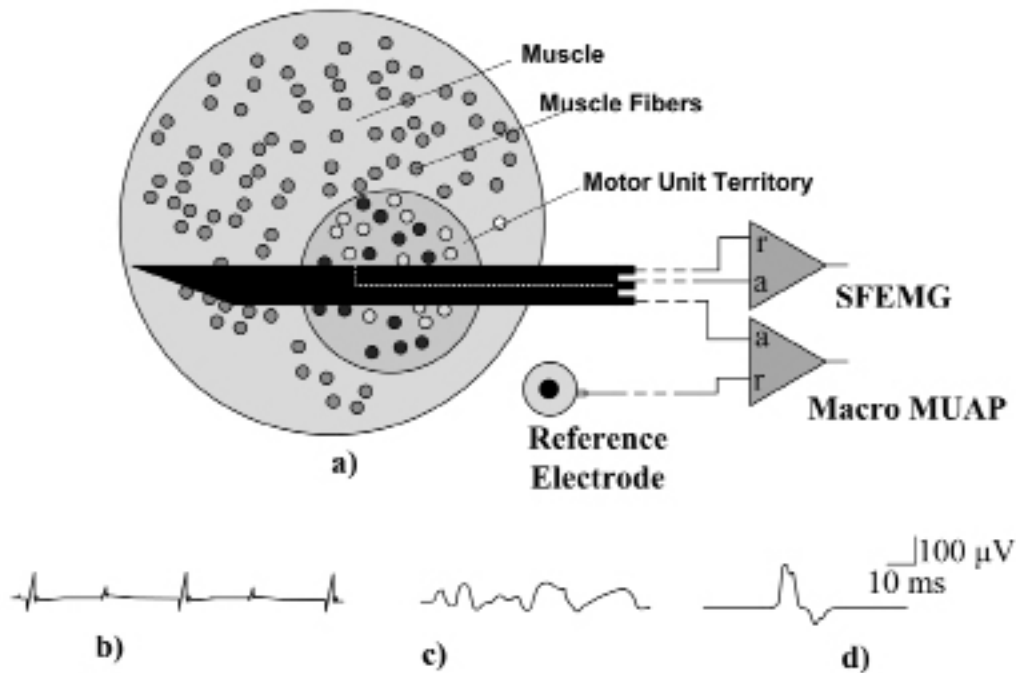
$$G_d = \left(\frac{V_{out}}{V_d} \right) \text{ and } G_{CM} = \left(\frac{V_{out}}{V_{CM}} \right)$$

In conclusion, the output voltage V_{out} of the instrumentation amplifier can be expressed as below;

$$V_{out} = G_d (V_1 - V_2) + \frac{G_d V_{CM}}{CMRR} + G_d V_{CM} \left(1 - \frac{Z_{in}}{Z_{in} + Z_{s1} - Z_{s2}} \right)$$

where Z_{in} is the inner impedance of the instrumentation amplifier. From this expression, it is obvious that as much as higher CMRR is preferable in the

Figure 7. (a) Configuration of macro electromyography (b) single fiber action potentials captured by the SFEMG electrode (c) potential captured by the outer cannula (Macro MUAP) (Macro MUAP)



design of such an amplifier (Brown et al., 1999; Pozzo, Farina, & Merletti, 2004).

Driven Right-Leg-Circuit

In order to reduce common-mode interference, a driven-right-leg circuit (DRL circuit) is added to the instrumentation amplifier of the EMG systems in the input stage (Winter & Webster, 1983). The patient's body can also behave like an antenna picking up electromagnetic interference especially yielded from 50/60-Hz noise of the power lines which can obscure the EMG signals of interest. In many modern biopotential amplifiers, the right

leg of the patient is connected to the auxiliary op-amp of the DRL circuit instead of grounding the patient directly. Hence the common-mode on the body is sensed by the two averaging resistors R_3 . Then, it is inverted, amplified and fed back to the right leg.

As a result, the negative feedback reduces the common-mode voltage. The patient's displacement current flows to the op-amp output circuit rather than to ground (Nagel, 2006; Neuman 2010b, Pozzo, Farina, & Merletti, 2004). Also, electrical safety can be ensured by saturating auxiliary op-amp provided that a high voltage takes place between the patient and the ground

due to an electrical leakage (Neuman 2010b). DRL circuit is shown in Figure 5a.

Isolation Amplifier

In order to protect the patient from the possible dangerous currents and voltages originating from the non-biomedical equipments, safety standards mandate to isolate the electrodes and the front-end circuits from the rest of the equipment (Jennings et al., 1995; Metting van Rijn et al., 1993).

Different methods such as transformer isolation, capacitor isolation, and opto-isolation are utilized in isolation amplifiers. A galvanic separation between the input side consisting of patient and input stage and the output side comprising all other equipments is established. Ideally, it is expected that no electric current will flow across this galvanic separation. On the other hand, an isolation-mode voltage may occur between the input common and output common across this barrier. That would imply that there is a leakage across the isolation barrier and this Isolation Mode Rejection Ratio (IMRR) is not finite. The output voltage V_{out} of the is isolation amplifier can be expressed as follows;

$$V_{out} = \frac{G}{Z_{G1} + Z_{G2} + R_{IN}} \left[V_D + \frac{V_{CM}}{CMRR} \right] + \frac{V_{iso}}{IMRR}$$

where A is the amplifier gain, V_D , V_{CM} , and V_{ISO} are differential, common mode, and isolation voltages, respectively, CMRR is the common mode rejection ratio for the amplifier and Z_{G1} , Z_{G2} , R_{IN} are the measurement electrode and reference electrode impedances and inner resistance of the isolation amplifier respectively. Transformer coupled amplifier is based on the inductive transmission of a carrier signal with amplitude modulated by the EMG signal. The signal is reconstructed at the output side by means of a synchronous demodulator (Nagel, 2006). Another way of obtaining

galvanic isolation is optical coupling the input side with the output side. This is achieved by using a single LED and photodiode combination. Since no resistive conductive path should exist between the input and output side, this system is supplied by transformer-isolated power supply (DC/DC converter) or a battery (Nagel, 2006; Pozzo, Farina & Merletti 2004). Isolation amplifier is represented in Figure (5b).

Filtering

Another stage of signal conditioning in an EMG system is filtering. The input stage is followed by a band-pass filter in which all the frequencies below and above preset cutoff values are rejected. In EMG, the cutoff frequencies for band-pass filter are 5 Hz and 10 kHz respectively (Prutchi & Norris, 2005); these values depend on the electrodes used and purpose of the recording. Half-cell potentials occurring at the electrode-tissue interface result in DC offsets. They could reduce the beneficial dynamic range of the signal. In addition, they could saturate the last stage of the amplifier. In order to remove these undesired DC offsets, a high-pass filter is required. Low-pass filter is required to remove the noise beyond the bandwidth leading a distortion in signal-to-noise ratio (SNR). The signal-to-noise ratio can be expressed in decibels (dB) as follows;

$$SNR = 20 \log \left(\frac{S}{N} \right)$$

where S is the amplitude of the signal and N of the noise (Pozzo, Farina, & Merletti, 2004; Sörnmo & Laguna, 2005).

Analogue-to-Digital (A/D) Conversion

After being conditioned by in the input stage, the signal of interest should be converted into digital form in order to process the EMG signals by the

computer of the EMG system for displaying and to store data (Jennings et al., 1995; Pozzo, Farina, & Merletti, 2004). The EMG signals acquired by the electrodes are time-varying analog signals usually in the form of voltage and these are converted into digital form by means of the circuitry called analogue-to-digital (A/D) converter (Christe, 2009; Shawhney, 2007). A/D Converter can be either implemented internally in the EMG systems or connected externally as a data acquisition board (Pozzo, Farina, & Merletti, 2004). By virtue of the progress in digital technology in terms of both hardware and software makes digital processing more efficient and flexible compared to analog processing. Digital processing has numerous advantages. Even complex algorithms which are used for special techniques can be easily implemented. The accuracy depends only on the truncation errors. Since they involve software rather than hardware modification design parameters can be easily altered (Mainardi, Bianchi & Cerutti, 2006).

The processes followed during the A/D conversion are sampling and quantization respectively. In sampling, the values of the EMG signal are acquired at uniformly spaced time intervals. These time intervals provide sampling frequency and they should be selected properly. Otherwise, the high frequencies are mistaken for low frequencies. This phenomenon is known as aliasing. As a result the reconstructed signal is corrupted and differs in frequency and phase from the original waveform leading to the false representation of the information. In order to overcome this problem, the Nyquist theorem should be satisfied. This theorem states that the original signal can be fully reconstructed from its samples provided that the sampling frequency is at least twice the maximum frequency present in EMG f_{max} and this is expressed mathematically as below;

$$f_s \geq 2.f_{max}$$

where f_s is the sampling frequency (inverse sampling interval) and f_{max} is the maximum frequency

of the EMG signal in question (Jennings et al., 1995; Mainardi, Bianchi & Cerutti, 2006; Pozzo, Farina, & Merletti 2004).

The process of converting the almost infinitely variable amplitude of an analog waveform to one of a finite series of discrete levels is called quantization. Following the sampling, the sampled values are rounded to the nearest values among finite values. Thus the analog value of the sampled signal is expressed in terms of digital words or steps with limited resolution. A least-significant-bit (LSB) is assigned to these sampled amplitudes. As expected, the original signal cannot be exactly reconstructed. Hence a quantization error takes place. This error can be minimized by dividing the difference between the minimum and maximum values of the signal by as many as possible levels (i.e. by reducing the step height) (Jennings et al., 1995; Pozzo, Farina, & Merletti 2004).

Output Devices

It is obvious that it is usually required to monitor the acquired signal in order to make interpretations in clinical sense. EMG instrumentation systems are controlled by means of the computer systems and they have output devices such as display, loudspeaker and printer for this purpose (Brown et al., 1999).

The waveform of the acquired MUAPs can be monitored by means of a visual display. In the previous generations of EMG systems, cathode ray tube (CRT) oscilloscopes were utilized to display this waveform pattern. With recent technologies, Liquid Crystal Displays (LCDs) of computers are implemented into the EMG systems (Brown et al., 1999).

Acquired EMG signals have also distinct auditory characteristics which clinicians sometimes utilize the auditory characteristics of these signals in different clinical states. After being conditioned these signals are fed to an audio-amplifier and then these are converted to audible signal via loudspeaker. Beside visually displayed waveforms

Detection and Conditioning of EMG

of these signals, the clinicians usually assess the characteristic sounds of various EMG patterns associated with different clinical cases (Brown et al., 1999).

In order to attach to the patient reports and to epicrisis, the hard copy of the acquired EMG signals can be required. Furthermore, interpretations about the signs of the related EMG signals made by the physician can be printed through the associated printer (Brown et al., 1999).

Electrodiagnostic Examination Systems Associated with EMG Systems

Although EMG is mainly concerned with the monitoring of the neuromuscular electrical activities related with the muscle contraction, neurophysiology examination systems such as stimulators for nerve conduction studies and evoked potential systems are integrated with the modern EMG systems.

Stimulators in Nerve Conductions Studies

A nerve conduction study (NCS) is a test commonly used to assess the ability of electrical conduction of the motor and sensory nerves of the human body.

Motor nerve conduction studies are performed by electrical stimulation of a peripheral nerve with a single supramaximal stimulus and recording compound muscle action potential (CMAP) from a muscle supplied by this nerve with a surface EMG electrode. The summation of the action potentials stimulated by electrical impulses and being transferred across the neuromuscular junction and the time needed to propagate from the stimulation site to the recording site measured in milliseconds (i.e. latency) are recorded. The amplitude of the summated action potentials is measured in millivolts (mV) (Aminoff, 1992; Preston & Shapiro, 2005; Oh, 2003).

Sensory nerve conduction studies are performed by electrical stimulation of a peripheral nerve and recording a compound nerve action potential (CNAP) from a purely sensory portion of the nerve, such as on a finger. Sensory latencies are also on the scale of milliseconds. Sensory amplitudes are much smaller than the motor amplitudes, usually in the microvolt (μV) range. The sensory nerve conduction velocity is calculated based upon the latency and the distance between the stimulating and recording electrodes. Large-diameter myelinated fibers can be stimulated with low-amplitude stimuli compared to small-diameter myelinated fibers (Aminoff, 1992; Oh, 2003, Preston & Shapiro, 2005).

The stimulus applied to the stimulating electrodes on the skin surface induces a current of short duration of 0.04 to 1 milliseconds in the fluid surrounding a nerve bundle. The stimulating current depolarizes the nerve under the cathode and hyperpolarizes it under the anode. Increasing the current to obtain a repeatable and maximal recorded response assures that essentially every nerve fiber in the bundle discharges. Surface electrode stimulation requires 50-500 V to drive currents of 5-50 mA, depending on skin impedance. The patients poorly tolerate the stimuli exceeding 1000 μsec . On the other hand, the rate of rise of the stimuli with less than 50 μsec is limited by tissue capacitances which prevent them to reach to effective amplitude. The stimulator equipment should also ensure control and timing of the stimuli for different types of measurements (Kimura, 2001).

Electrical stimulators are isolated from the input stage of the EMG system for safety and artifact reduction. Hence, the stimulation circuits have no conductive path to other circuits except through the patient's body in case that the stimulating and recording electrodes have been applied. This isolation leads that stimulus current flow only in the loop provided by the two stimulating electrodes. If the stimulator circuit has any connection to the input stage of the amplifier, then the stimulus

current distributed in the body can divide into additional paths, causing a large stimulus artifact, amplifier overload, or even spurious stimulation at non-targeted sites. Furthermore under conditions of component failure, these additional paths might conduct hazardous levels of current. Even though battery-powered stimulators may use optical coupling of the control signal stimulus isolation usually is achieved by magnetic coupling of energy to the stimulating circuits (Kimura, 2001).

EMG SIGNALS IN CLINICAL STUDIES

Neuromuscular disorders that result in the structural and functional impairments of the motor unit cause alterations in the waveform of the EMG signals. The characteristics of these abnormal waveforms may suggest particular pathological processes. These signals may exhibit normal spontaneous activity (End-plate Activity), normal voluntary activity (Normal Motor Unit Action Potentials), abnormal spontaneous activity such as Insertional Activity, Fibrillation Potentials, Myotonic Discharges, Complex Repetitive Discharges, Fasciculation Potentials, Myokymic Discharges, Neuromyotonic Discharges, Cramp Potentials, Synkinesis or abnormal voluntary electrical activity (Abnormal Motor Unit Action Potentials) (Kimura, 2001; Rubin, 2009).

Normal Spontaneous Activity

In normal muscle fibers, spontaneous electric activity is observed only in end-plate region which are also called miniature end plate potentials (MEPPs). MEPPs are randomly generated in this region due to spontaneous release of individual quanta of acetylcholine. These are irregular positive potentials with 10- to 50 μ V amplitude and with 1- to 3- millisecond duration. They have typical sound in the loudspeaker similar to seashell sound. MEPPs reflect the activity of motor end-

plates. Their amplitudes are so small and closely related to the positioning the needle electrode in muscle that they do not have any clinical relevance so far (Kimura, 2001; Rubin, 2009).

The action potentials of the individual muscle fibers recorded from the end-plate region as the brief spikes are called End-plate spikes. These are generated by the mechanical activation of a nerve terminal with a secondary discharge of a muscle fiber. These potentials are represented by the intermittent spikes with 100- to 200- μ V amplitude and with 3-to 4-millisecond duration firing irregularly at 5 to 50 Hz (Kimura, 2001; Preston & Shapiro, 2005; Rubin, 2009).

Abnormal Spontaneous Activity

Although end-plate activities and brief injury potentials occurring with the insertion of the needle can be recorded in a muscle at rest, no electrical activity is observed in a relaxed muscle. These abnormal spontaneous activities can be listed as increased insertional activity, fibrillation potentials, positive sharp waves, complex repetitive discharge, myotonic discharge.

Increased Insertional Activity

Since this electrical discharge yields from the injured muscle fibers it is also referred as injury potential. Under normal conditions, insertion of a needle into muscle or repositioning of a needle within the muscle results in the mechanical depolarization of the muscle fiber and it leads to brief burst of electrical activity with a duration of a few hundred milliseconds. This activity indicates the number of muscle fibers depolarizing due to the mechanical irritation. They are observed as positive or negative high frequency spikes. This electrical activity stops after the cessation of the needle movement. Increase in the amplitude of the insertional activity may point out to the early sign of denervation originating from an acute

Detection and Conditioning of EMG

neurogenic such as early radiculopathy, mono-neuropathy.

Decreased insertional activity may be revealed in cases where muscle fibers are unable to generate action potentials. This is observed in end-stage neuromuscular diseases in which the muscle is replaced by fat or connective tissue (Kimura, 2001; Preston & Shapiro, 2005; Rubin, 2009).

Fibrillation Potentials

Fibrillation potentials originate from the spontaneously twitching of single muscle fibers when innervation is lost. They have amplitude ranging from 20 to 500 μV and duration lying between 1 and 30 milliseconds. They have a regular firing pattern at rates of 0.5 to 15 Hz. They may be occasionally intermittent or irregular especially after an early denervating process like end-plate spikes. But their interspike interval longer than 70 milliseconds distinguishes them from the end-plate spikes (Kimura, 2001; Rubin, 2009). They have biphasic or triphasic waveforms with initial negative deflection. They are related with denervated muscle fibers. They usually occur in neurogenic disorders such as neuropathies, radiculopathies or motor neuron disease. However, they can be observed also in some myopathic disorders such as inflammatory myopathies and dystrophies and occasionally in neuromuscular junction (NMJ) disorders (e.g. botulism) (Kimura, 2001; Mills, 2005; Preston & Shapiro, 2005; Rubin, 2009).

Positive Sharp Waves

These are biphasic action potentials beginning with a positive deflection and then continuing with a negative phase and occur spontaneously after needle electrode movement. These are regular pattern at a firing frequency of 1 to 50 Hz in saw-tooth appearance. The positive initial deflection is rapid (< 1 millisecond) and the amplitude can reach up to 1 mV. The negative phase has longer duration of 10 to 100 milliseconds and low

amplitude (Preston & Shapiro, 2005). They may manifest active denervation. They can be seen in disorders such as radiculopathy and entrapment neuropathies (Kimura, 2001; Mills, 2005; Preston & Shapiro, 2005).

Complex Repetitive Discharge (CRD)

Complex repetitive discharges are the action potentials with 50- μV - to 1-mV-amplitude, varying between 50 to 100 milliseconds in amplitude discharging spontaneously in synchrony with regular and repetitive pattern at fast or slow rates ranging 3 to 100 Hz. They start suddenly and continue with constant firing frequency and then stop abruptly. One muscle fiber initiates these discharges serving as a pacemaker then, the ephaptic propagation of these action potentials along the muscle fibers located in the vicinity of the pacemaker fiber. These can be observed in myopathies including muscular dystrophy or polymyositis, in conditions with chronic denervation such as motor neuron disease, radiculopathy, chronic polyneuropathy, myxedema, and the Schwarz-Jampel syndrome (Kimura, 2001; Mills, 2005; Preston & Shapiro, 2005; Rubin, 2009).

Myotonic Discharges

Myotonic discharges are spontaneous activities generated by the single muscle fibers in a prolonged fashion after external excitation. These are firing regularly with a firing rate of 20 to 150 Hz and are characterized by waxing and waning pattern both in amplitude and frequency. They may have amplitudes ranging from 20 to 300 μV . They are typically observed in channelopathies such as dystrophia myotonica, congenital myotonias, proximal myotonic dystrophy, and hyperkalemic periodic paralysis and in several forms of myopathies such as acid maltase deficiency, polymyositis, myotubular myopathy (Kimura, 2001; Mills, 2005; Rubin, 2009).

Normal Voluntary Contractions (Normal MUAP)

Motor unit (MU) which is the basic functional unit of the skeletal muscle consists of the anterior horn cell, the motor neuron, the neuromuscular junction and the muscle fibers innervated by this motor neuron. It constitutes a bioelectric source located in a volume conductor consisting of other muscle fibers generating the Motor Unit Action Potential (MUAP) [8, 24, 50]. Motor Unit Action Potential is the sum of all the action potentials of the individual muscle fibers within the Motor Unit. In order to generate force in significant quantities, more than one motor unit should be activated. The process where additional motor units are contributed to generate a muscle contraction at certain level is referred as motor unit recruitment (Kimura, 2001; Milner-Brown, Stein & Yemm, 1973; Moritani, Stegeman & Merletti, 2005 ;Preston & Shapiro, 2005).

Motor Unit Action Potential is assessed by means of its recorded configuration. This configuration is characterized by its amplitude, duration, number of turns, number of phases, area under curve and rise time. All these characteristics are demonstrated in Figure 6. These are determined by technical, physiological and pathological factors. Technical factors can be listed as the type of needle electrode used for recording, the area of exposed surface of the active leads of the electrode, the characteristics of the metal recording surfaces, and the electric characteristics of the cables, preamplifier, and amplifier. Physiological factors affecting the configuration are age, the muscle under the investigation, the location of the needle electrode within the muscle, the degree of activation of the muscle (minimal voluntary contraction, maximal voluntary contraction, reflex activation, or electric stimulation), the temperature of the muscle. The pathological factors play roles according to the anatomical and histological changes during the loss or the remodeling of the motor unit (e.g. reinnervation in neurogenic disorders). These

anatomical and histologic changes take place in innervation ratio which implies number of muscle fibers in the motor unit, fiber density indicating number of muscle fibers in a unit cross-sectional area, the distance of the needle tip from the muscle fibers and from the end plate region, and the direction of the axis of the muscle fiber (Rubin, 2009).

The duration of a Motor Unit Action Potential can be defined as the time between the onset of the initial deflection from the baseline and the end of the return to the baseline. It reflects the number of muscle fibers being detected by the needle electrode. The duration for a normal motor unit action potential varies from 3 to 15 milliseconds (Dumitru, King & Rogers, 1999; Henneberg, 2006; Oh, 2003; Rubin, 2009).

The amplitude of a Motor Unit Action Potential is the voltage measured from peak to peak of the main spike of the signal. It depends on the size and on the density of the muscle fibers within the uptake area of the needle electrode and the synchrony of firing. The value of the amplitude ranges from 300 μ V to 3 mV in healthy subjects. It varies with muscle, muscle temperature and the patient's age (Dumitru, King & Rogers, 1999; Dumitru, 2000; Henneberg, 2006).

The rise time is the duration of the between the initial negative peak and the subsequent positive peak. It is the function of the distance of the muscle fibers from the electrodes. If the electrode is located in the vicinity of the muscle fiber, the measured rise time of a single fiber action potential is between 100 and 300 μ s. As the needle electrode moves away from the muscle fiber, the rise time will increase, on contrary, the amplitude and the duration of the motor unit may decrease (Dumitru, King & Rogers, 1999; Oh, 2003; Rubin, 2009).

A phase can be defined as the portion of a waveform between the deflection from the baseline and the return to the baseline. A motor unit action potential can have a monophasic, biphasic or triphasic configuration or it may have multiple phases. If a motor unit action potential has more than four phases, it is called polyphasic potential.

Detection and Conditioning of EMG

The percentage of the polyphasic motor unit action potentials should not be more than 15% of all normal potentials. These configurations vary according to the synchrony of firing of the muscle fibers within the uptake area of the needle electrode. Number of phases is a measure of complexity and the misalignment of the muscle fibers of the motor unit under investigation. In neurogenic diseases, polyphasic motor unit action potentials yield from the slow conduction of the new nerve sprouts in the reinnervated muscle fibers. In myopathic cases, the polyphasic motor unit action potentials are due to the variation in muscle fiber size (Henneberg, 2006; Rubin, 2009).

Turns are the serrated potentials indicating the directional changes in amplitude without crossing the baseline. These are the indicators of desynchronization among discharging muscle fibers (Dumitru, King & Rogers, 1999; Henneberg, 2006; Oh, 2003).

Abnormal Motor Unit Potentials

Abnormal Motor Unit Action Potentials can be summarized as fasciculation potentials, doublets (multiplets), myokymic discharges, neuromyotonic discharges, cramps and rest tremor.

Fasciculation Potentials

Fasciculation potentials are spontaneously firing involuntary motor unit action potentials with irregular pattern generated by a group of muscle fibers belonging to a part of a motor unit (Bryan, 1998; Kimura, 2001; Preston & Shapiro, 2005; Rubin, 2009). Since they can be either observed as a benign phenomenon such as eyelid twitching or be accompanied to a neurogenic disorder such as radiculopathies, polyneuropathies and entrapment neuropathies, peripheral nerve hyperexcitability syndrome they can be considered nonspecific in terms of clinical significance (Kimura, 2001; Rubin, 2009). They are firing with repetitive patterns very slowly less than 1 to 2 Hz with irregular

intervals in the order of several seconds. They may be also observed after the administration of the anticholinesterase medications or a depolarizing neuromuscular blocker (Mills, 2005; Preston & Shapiro, 2005; Rubin, 2009).

Doublets (Multiplets)

These are recurring firing of the same motor unit action potential in semirhythmic pattern two or more times at short intervals such as 10 to 30 milliseconds. They can be observed in hyperventilation, hypocalcemia or hyperexcitable nerve syndromes (Kimura, 2001; Preston & Shapiro, 2005; Rubin, 2009). The doublets recorded during voluntary contraction are considered as physiological MUAPs (Kudina and Andrieva, 2013). On the other hand, if they are recorded during the resting state of the muscle, they can be regarded as the sign of hyperexcitability such as hyperventilation, hypercalcemia and some peripheral nerve diseases (Kimura 2001).

Myokymic Discharges

These are the groups of spontaneously firing complex motor unit action potentials consisting of two to ten potentials in a recurring burst pattern (Kimura, 2001; Preston & Shapiro, 2005; Rubin, 2009). Each burst which has a regular pattern at 0.1 to 10 seconds being followed by a silent period has a firing frequency ranging from 5 to 60 Hz and they are not affected by the voluntary contraction (Aminoff, 1992; Kimura, 2001; Rubin, 2009). These discharges can be seen in patients with a prior history of radiotherapy due to the radiation-induced nerve damage which is also referred as radioation-induced plexopathy (Aminoff, 1992; Kimura, 2001; Preston & Shapiro, 2005). Also these may be observed in radiation myelopathy, radiculopathy, entrapment neuropathy, spinal cord lesions associated with demyelination and gold intoxication, acute inflammatory polyradiculoneuropathy and multiple sclerosis (Preston &

Shapiro, 2005). Myokimic discharges occur in facial muscles in the presence of brainstem lesions associated with multiple sclerosis, neoplasms such as pontine gliomas and vascular diseases and in 15% of the patients with Guillain-Barré syndrome (Aminoff, 1992; Preston & Shapiro, 2005). Myokymic burst of the peripheral can be aggravated in hypocalcemia induced by hyperventilation or with the use of acid-citrate-dextrose being an anti-coagulant which is given during plasma exchange (Kimura, 2001; Preston & Shapiro, 2005).

Neuromyotonic Discharges

These discharges are long continuous spontaneously occurring motor unit action potentials with shorter bursts. Their firing frequencies vary between 100 and 300 Hz (Kimura, 2001; Rubin, 2009). They result from the neuromyotonia being peripheral nerve hyperexcitability which is also referred as Isaac's syndrome as well as pseudomyotonia, neurotonia, normocalcemic tetany (Kimura, 2001; Preston & Shapiro, 2005). It can appear also in Morvan's syndrome which is a autoimmune anti-voltage gated potassium nerve axon channelopathy (Mills, 2005; Preston & Shapiro, 2005). Neuromyotonic discharges may accompany to generalized stiffness, hyperhidrosis and delayed muscle relaxation after contraction. They may be seen in chronic neuropathic disease especially in old poliomyelitis and adult spinal muscular atrophy (Preston & Shapiro, 2005).

Cramp Discharges

These are involuntary and sometimes irregularly firing motor unit action potentials at higher frequencies lying between 200 and 300 Hz identified by the quick recruitment related with a painful muscle cramp (Kimura, 2001; Preston & Shapiro, 2005; Rubin, 2009).

Cramp discharges may be seen healthy individuals in the form of benign nocturnal cramps or post-exercise cramps. On the other hand, they can

be detected in chronic disorders such as chronic radiculopathies, peripheral neuropathy, motor neuron disorders, in metabolic or electrolyte disturbances such as salt depletion, pregnancy, hypothyroidism, uremia in dialysis or in peripheral nerve hyperexcitability syndromes such as cramp fasciculation syndrome (Preston & Shapiro, 2005; Rubin, 2009).

ELECTROMYOGRAPHY (EMG) TECHNIQUES

Conventional Electromyography

Conventional Electromyography is the commonly EMG technique applied in clinical routine study for the examination of the neuromuscular disorders. It is usually performed by using concentric needle electrode to record either spontaneous or voluntary electrical activities. This electrode is inserted into the motor unit territory for this purpose (Stålberg & Falck, 1997; Trontelj, Jabre & Mihelin, 2004). These potentials are the sum of the single fiber action potentials generated by the muscle fibers located within the uptake area of the concentric needle electrode (Stålberg & Falck, 1997). Various parameters of EMG signals such as amplitude, duration, number of phases, rise time being utilized in the differential diagnosis of neuromuscular diseases are monitored by this technique (Henneberg, 2006; Kimura, 2001; Oh, 2003; Stålberg & Falck, 1997).

Single Fiber Electromyography (SFEMG)

In order to examine single muscle fibers rather than activities from the motor unit, motor end-plates, terminal axon branches a selective recording method is used (Stålberg & Trontelji, 1994). Single fiber EMG with an uptake area of 300 μm -radius is utilized for this purpose as a selective method (Kimura, 2001). Since it has a

Detection and Conditioning of EMG

small recording surface, the active electrode of the SFEMG electrode has higher impedance than a concentric needle electrode. Impedance values are on the order of several megaohms at 1 kHz for platinum needle. Therefore, amplifier should have higher input impedance of 100 M Ω to maintain a higher signal-to-noise ratio. As a result, the common mode rejection ratio (CMRR) greater than 200 is maintained (Kimura, 2001; Stålberg & Trontelji, 1994).

The single-fiber potential recorded through this technique is a biphasic spike with a rise-time varying between 75 μ sec to 200 μ sec. It has a total duration which is approximately 1 millisecond (Kimura, 2001). Despite it varies between 200 μ V and 20 mV, the peak-to-peak amplitude usually remains within the 1 to 7 millivolts (Kimura, 2001; Stålberg & Trontelji, 1994; Trontelj, Jabre & Mihelin, 2004). The frequency spectrum ranges from 100 Hz to 10 kHz with a peak at 1.61 ± 0.30 kHz (Kimura, 2001).

Several physiological and morphological parameters such as fiber density (FD), jitter, blocking and duration can be measured and quantified by means of Single-Fiber Electromyography

The degree of packing of muscle fibers within the uptake area of single fiber electrode is described by fiber density (FD). Therefore, it can be defined as the average number density of single fiber action potentials firing almost synchronously within this area (Harper, 2009; Kimura, 2001; Trontelj, Jabre & Mihelin, 2004). In measuring fiber density, the needle is adjusted until a single fiber action potential with a 500- μ s rise time is detected. The number of the time-locked single fiber action potentials being time-locked to the triggered potential with amplitudes greater than 200 μ V is counted. This procedure is repeated for 30 separate triggered potentials to calculate the mean fiber density for the muscle of interest. The mean fiber density varies between 1.3 and 1.8. By definition the lowest mean fiber density can be accepted as 1 (Harper, 2009; Kimura, 2001; Stålberg & Trontelji, 1994; Trontelj, Jabre

& Mihelin, 2004). Fiber density is used to detect slight changes in motor unit topography after collateral sprouting due to the reinnervation in neuropathies (Stålberg & Falck, 1997; Stålberg & Trontelji, 1994).

Jitter is the measure of the latency variability of muscle fiber action potentials within the same motor unit. Therefore, the variability in rise time of the end plate potential is reflected by this parameter. It provides a sensitive indicator for the defects of neuromuscular transmission. Jitter is increased in neuromuscular junction diseases beside the disorders associated with denervation and reinnervation (Chaudry & Crawford, 1999; Harper, 2009; Kimura, 2001; Padua et al., 1999).

Blocking is a measure demonstrating the intermittent loss of a regularly firing single fiber action potential within a motor unit. Hence, the failure of the end plate potential of reaching threshold in disorders with neuromuscular transmission. Blocking can be in disorders associated with denervation and reinnervation of muscle, and in neuropathies associated with impulse blocking in the nerve terminal (Harper, 2009; Kimura, 2001).

Duration represents the time between single fiber action potentials within recording distance of the electrode. This reflects differences in conduction time along the terminal axonal branch and muscle fiber. It is increased in neurogenic disease and in some chronic myopathies (Harper, 2009).

Single fiber EMG is the most sensitive technique in the diagnosis of the abnormalities of neuromuscular transmission (Spaans et al., 2003). Fiber density is used for the detection of the alteration in motor unit topography such as reinnervation in some neuromuscular disorders such as anterior horn cell. Jitter and blocking are used to investigate the disturbance in neuromuscular transmission. These are used for the diagnosis of the disorders concerning neuromuscular disorders such as Myasthenia Gravis, Lambert-Eaton Myasthenic Syndrome and Botulism (Stålberg & Falck, 1997; Stålberg & Trontelji, 1994; Padua et al., 1999; Weinberg et al., 1999).

Macro Electromyography (Macro EMG)

Macro Motor Unit Action Potential arises from almost all muscle fibers within the same motor unit. The special technique used for this purpose is called Macro Electromyography (Smith, 2009). This technique was first described and applied by Stålberg (Stålberg, 1986). In macro electromyography, two channels are used for recording. Activity acquired from the 15-mm bare shaft is recorded through the first channel with respect to a surface electrode used as reference. Activity acquired by the 25- μm wire electrode which is also a single fiber EMG signal is recorded with respect to the shaft through the second channel. The activity coming from this second channel is used as trigger and the activity from the first channel is average for 60 to 80 milliseconds after being recorded. In case of reinnervation followed by denervation in neurogenic diseases, the amplitude of the macro motor unit potentials are increased. In subacute myopathies, this amplitude may be decreased (Kimura, 2001; Smith, 2009; Stålberg & Falck, 1997). Macro Electromyography and the resulting signals are schematized in Figure 7.

Scanning Electromyography

Scanning EMG is an experimental technique enabling to study the spatial and temporal properties of a motor unit electrical activity to examine the topography of a motor unit (Aminoff, 1992; Stålberg & Falck, 1997; Stålberg & Trontelji, 1994). The electric activity of the motor unit can be illustrated as a electrophysiological cross-sectional map (Stalberg et al., 1986a; Stalberg, 1986b; Stalberg 1987). In this technique, a concentric needle electrode and a single fiber electrode are used. The single fiber electrode is inserted into the muscle in a fashion that a single fiber action potential is detected and recorded. This activity is used to trigger the sweep created by motor unit territory synchronous with the detected single

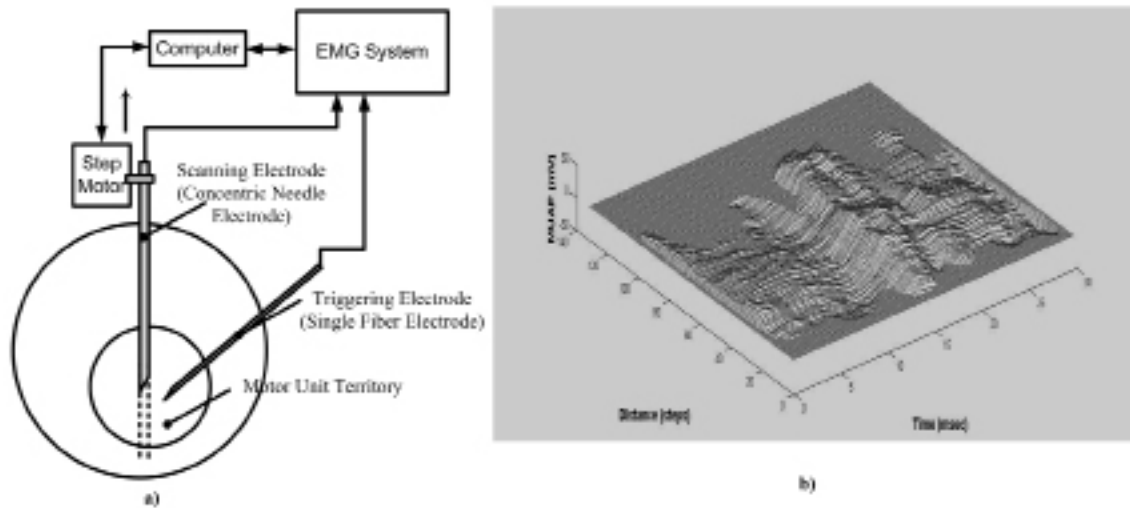
fiber action potential. Then, the concentric needle electrode is inserted close to this single fiber electrode and pulled upward mechanically until no electric is detected (Smith, 2009). Scanning Electromyography is illustrated schematized in Figure 8a.

Beside the parameters monitored with conventional needle electromyography such as amplitude and duration, additional parameters which also variation of shape of the motor unit action potential is illustrated are introduced with this technique. These are length of motor unit cross-section, fractions of motor unit, silent periods, polyphasic and complex portions of motor unit action potentials maximum duration and the maximum amplitude (Stålberg & Antoni, 1980; Stålberg & Dioszeghy 1991). The length of motor unit cross-section can be defined as the distance between the first and the last electrical activity recorded by the concentric needle electrode. The fractions of motor unit action potentials are the one or more separate area taking place with different latencies. They represent the groups of muscle fibers being innervated by different intramuscular axonal branch of the parent anterior horn cell. The silent periods representing the fat or connective tissues due to the proliferation are sections with electrical activities with less than 50- μV peak-to-peak amplitude along the upward movement of the concentric needle electrode during the recording process. The polyphasic and complex portions of motor unit action potential which can be detected only by chance via conventional electromyography can be presented during the upward movement of the recording electrode. Furthermore, the maximum amplitude and the maximum duration within the motor unit territory can be measured by virtue of this technique (Diozeghy, 2002; Stålberg & Antoni, 1980; Stålberg & Dioszeghy 1991).

Scanning electromyography is an experimental technique rather than being used in clinical routine studies. It has been used in several researches concerning the motor unit territory. It was first used to investigate the motor unit organization

Detection and Conditioning of EMG

Figure 8. (a) Configuration of scanning EMG (b) motor unit territory acquired by scanning EMG



by building electrophysiological cross-section of the motor unit (Stålberg & Antoni, 1980). Then, it was used to reveal that EMG changes in muscular dystrophies due to the loss of muscle fiber and neurogenic component of the regeneration and in macro motor unit potential (Hilton-Brown & Stålberg, 1983a; Hilton-Brown & Stålberg, 1983b). Scanning electromyography was also used to study mandibular motor system and length of cross-section of masseter was found less than large muscles. As a result, the fact that muscle performing fine movements have smaller motor unit territory and less muscle fibers (Stalberg & Eriksson, 1987). It was also used to study the rearrangement of the muscle fibers in abnormal muscles (Stålberg & Dioszeghy, 1991) and the structure of the human quadriceps muscle (Gootzen, Vingerhoest & Stegeman, 1992). In recent study, scanning electromyography was used to reveal to preponderance of the large motor units with normal structure in juvenile myoclonic epilepsy patients. In this study, a concentric needle electrode was used as triggering electrode instead of a single fiber electrode by setting the cut-off frequency of the low-pass filter to 2 kHz (Ertas

et al., 2000; Göker et al., 2009; Göker et al., 2010). Afterwards, the data obtained from this clinical study were used to classify by utilizing Feed-Forward Neural Networks, Support Vector Machines, Decision Trees, and Naïve Bayes methods (Göker et al., 2012).

Scanning EMG can be used for the characterization of the motor unit fractions to investigate the motor end-plate topography and branching pattern of the axon innervating the motor unit (Navallas & Stalberg, 2009). The electrophysiological cross-section obtained by scanning electromyography is shown in Figure 8b.

Quantitative Electromyography

Since subjective or semi-quantitative analysis of motor unit action potential activity is fast, efficient and accurate in reasonable degree if the findings are assessed by experienced electromyographers, inexperienced clinicians are prone to errors especially in differential diagnosis of the neuromuscular diseases. In quantitative electromyography, numerical values can be derived from the precise measurements of the motor unit action potentials.

It results in normative data which enables the examiners to compare with data obtained from the patients with suspected neuromuscular diseases. Reproducible results which can be compared at different time, by different clinicians, in different laboratories can be obtained. Furthermore, quantitative electromyography ensures to evaluate the prognosis of neuromuscular diseases (Kimura, 2001; Smith, 2009).

Most commonly used quantitative methods can be listed as Interference Pattern Analysis (IPA), Decomposition, Power Spectrum Analysis (PSA), Turn-Amplitude Analysis (TAA) and Motor Unit Number Estimation (MUNE).

Interference Pattern Analysis (IPA)

Motor unit action potentials can be distinguished and measured individually at minimal level of muscle contractions. As the level of force increased toward the maximal voluntary contraction, since the number and the firing rates of active motor unit increase number of spikes and amplitude in the electromyography signal is also increased becoming difficult to identify individual motor unit action potentials. The observed electromyography signal in which individual motor unit action potentials are superimposed resulting in a complex pattern due to the summation and cancellation of these motor unit action potential components is referred as interference pattern (Fuglsang-Frederiksen, 2000; Nandedkar & Sanders, 1990).

Concentric needle electrode is inserted into an area of the muscle where motor unit action potentials have short rise times. Test can be performed at different at fixed or variable percentages of maximum voluntary contractions or at the fixed forces of 2 to 5 kilograms. The measurement is made at 20 to 30 distinct sites. After the measurement, the number of turns is measured. Turns are defined as the change in signal direction at least $50\mu\text{V}$ and they indirectly represent the number of active motor unit action potentials the proportion of polyphasic motor unit action potentials and the

motor unit action potential firing rate. Amplitude is measured as the potential difference between successive turns. Cumulative amplitude is computed by summing amplitude of turns over a certain time interval. Mean amplitude is calculated by dividing the cumulative amplitude for a fixed time interval by the number of turns. By dividing the number of turns by the mean amplitude Turn/Amplitude (T/A) ratio is obtained (Fuglsang-Frederiksen, 2000; Nandedkar & Sanders, 1990).

Interference pattern analysis is beneficial in evaluating the recruitment of the motor units in order with respect to the size of the motor units. By inspection the fullness of the interference pattern reflects the number and firing rates of the component motor units and the amplitude of the interference pattern signals. Quantitatively, the spike density and the average amplitude of the summated response in interference pattern depend on number of motor neurons capable of discharging, firing frequency of each motor unit, waveform of individual potentials (Kimura, 2001).

In myopathic disorders, the interference pattern may have a full appearance with decreased amplitude at maximum voluntary contraction due to the loss of fibers. In neurogenic cases, the firing frequency at maximum voluntary contraction will be reduced despite the number of the recruited motor unit action potential is normal if the lesion is in the upper levels. On the other hand, if the lesion is at the level of peripheral nerve, there will a loss of motor unit action potential at the maximum voluntary contraction with normal firing frequencies (Finsterer, 2001; Fuglsang-Frederiksen, 2000; Nandedkar & Sanders, 1990).

Decomposition

The EMG signal recorded during the contraction is composed of the motor unit action potential trains (MUAPTs). Finally, the orderly-recruited motor units according to Henneman's size principle generate interference pattern at maximum voluntary contraction (Ganong, 2001; Smith, 2009)(Joynt

Detection and Conditioning of EMG

et al., 1991). Decomposition is a technique using pattern recognition methods in order to separate this interference pattern into MUAPTs (McGill et al., 1985)(McGill, 2002)(Stashuk,1999). The information obtained by means of this technique is used in the diagnosis of the neuromuscular disorders, in the evaluation of the muscle function and to investigate how motor units are controlled by motor neurons to generate force (De Luca & Contessa, 2012).

Turn-Amplitude Analysis (TAA)

Turns and Amplitude analysis is based on comparing the number of turns per unit time (T/S) with the amplitude of the activity between the turns (A/T). In myopathies, since the number muscle fibers contributing to motor unit action potential decreases and amplitude per turn will be decreased. In contrary, the turns per second decreases and the amplitude per turn increases due to the reinnervation resulted from the collateral sprouting. These parameters can be represented graphically in a scatter plot. Hence the need of controlling the force is discarded (Arabadzhiev et al., 2008, Diószeghy et al., 1996; Farrugia & Kenet, 2005; Smith, 2009).

Power Spectrum Analysis (PSA)

In this technique, interference pattern is decomposed into sinusoidal-waves of different phases which are harmonically related, frequency and amplitude. This is achieved by means of analysis methods such as analogue octave-band filtering (early PSA) or Fast Fourier transformation (FFT) using anti-aliasing filters and a Hanning window (Finsterer, 2001). Afterwards, the power spectrum of these harmonics is computed. Median and mean frequency values can be calculated for the interference pattern in question (Fuglsang-Frederiksen, 2000).

The highest peak observed during the maximal voluntary contraction ranges from 100 to 200 Hz

in normal subjects [Kimura, 2001]. The power spectrum shifts to higher frequencies in myopathic cases where as power is higher in lower frequencies in neuropathies (Fuglsang-Frederiksen, 2000; Fuglsang-Frederiksen, 2006; Kimura, 2001; Smith, 2009).

Motor Unit Number Estimate (MUNE)

Motor unit number reflects the number of motor neurons or motor axons in any disease involving injury or death. The estimation of motor unit number was first proposed by McComas et al. on in 1971 in order to detect the denervation in patients with normal electromyographic interference pattern.

Recruitment of successive motor units is established by the gradual intensity of the electrical stimulation to the nerve. Finally, all muscles innervated by a peripheral nerve are activated by the supramaximal stimulation of this nerve (Kimura, 2001). Motor unit number is estimated by comparing average motor unit parameter with the corresponding parameter of whole muscle (Arasaki et al., 1997; McComas, 1971; McComas, 1995).

Consequently, a compound muscle action potential (CMAP) which is also referred as M-Wave is obtained (McComas, 1991). Motor unit number estimate (MUNE) is computed by dividing the CMAP by the average value of single motor unit potentials (SMUPs) (Daube, 2006; Shefner, 2001).

FUTURE RESEARCH DIRECTIONS

Nowadays, electromyography is commonly used not only in clinical routine examinations as an auxiliary tool for the diagnosis and differential diagnosis of the neuromuscular diseases, but in scientific researches concerning several disciplines such as neurophysiology, kinesiology, sport medicine, ergonomics.

It is obvious that as the technological innovations take place in computer technology in terms

of hardware and software, these developments will be reflected to the instrumentation implemented into EMG systems. Developments in the material science will be utilized in the improvement of the electrode technologies to minimize the noise and interferences. In addition, the developments in microelectronics will enable to manufacture signal conditioning systems in EMG instruments which are influenced as less as possible from the interferences. The assessment of the acquired electrophysiological data will be more efficient and faster with the innovations in software technology adapted to the most commonly used electromyography techniques.

The signal processing technology used in electromyography will be improved by virtue of the implementation of new mathematical algorithms in parallel to the development of software technologies. This may result in the improvements in surface electromyography.

The developments in surface electromyography will make its use more effective in the fields in which it is used to acquire signals such as gait analysis, biomechanics, ergonomics. The improvements in surface EMG methods will also lead the effective use of EMG controlled prostheses.

The surface EMG electrode supported by microelectronics and RF systems that can be implemented into Wireless Body Area Networks (WBAN). Therefore, this can found application fields in aerospace technologies, sport technologies, sport medicine and even in military technologies.

CONCLUSION

Electromyography is used commonly in clinical routine as an auxiliary tool in the differential diagnosis of the neuromuscular diseases. In this chapter, the signal detection, signal acquisition and signal conditioning in electromyography have been explained not only in technical sense but also from the medical point of view. First,

how the electrical activity is generated by neuromuscular system has been briefly explained. Then, different types of electrodes used to detect and to acquire these activities and their principles have been introduced. Afterwards, the principles of biomedical instrumentation used for the signal conditioning such as amplification, filtering and analogue-to-digital conversion in electromyography have been described. Finally, different specific electromyography techniques have been depicted beside the conventional needle electromyography have been depicted.

ACKNOWLEDGMENT

I would like to express my sincere gratitude and special thanks to Prof. Dr. M. Barış Baslo from which, I have benefited from his broad academic and clinical experience for his continuous supervisions, for his valuable criticisms, for his patience of job throughout this manuscript.

REFERENCES

Aminoff, M. J. (1992). Clinical electromyography. In M. J. Aminoff (Ed.), *Electrodiagnosis in clinical neurology* (pp. 249–283). New York: Churchill Livingstone Inc.

Arabadzhiev, T. I., Dimitrov, G. V., Dimitrov, A. G., Chakarov, V. E., & Dimitrova, N. A. (2008). Factors affecting the turns analysis of the interference EMG signal. *Biomedical Signal Processing and Control*, 3(4), 145–153. doi:10.1016/j.bspc.2007.07.003

Arasaki, K., Tamaki, M., Hosoya, Y., & Kudo, N. (1997). Validity of electromyograms and tension as a means of motor unit number estimation. *Muscle & Nerve*, 20(5), 552–560. doi:10.1002/(SICI)1097-4598(199705)20:5<552::AID-MUS3>3.0.CO;2-8 PMID:9140361

Detection and Conditioning of EMG

Brown, B. H., Lawford, P. W., Smallwood, R. H., Hose, D. R., & Barber, D. C. (1999). *Medical physics and biomedical engineering*. London: IOP Publishing Ltd. doi:10.1887/0750303689

Bryan, A. (1998). Electromyography: Recording methods and signal processing techniques. *Current Anaesthesia and Critical Care*, 9(3), 110–116. doi:10.1016/S0953-7112(98)80003-3

Chan, R. C., & Hsu, T. C. (1991). Quantitative comparison of motor unit potential parameters between monopolar and concentric needles. *Muscle & Nerve*, 14(10), 1028–1032. doi:10.1002/mus.880141015 PMID:1944402

Chaudry, V., & Crawford, T. O. (1999). Stimulation single-fiber EMG in infant botulism. *Muscle & Nerve*, 22(10), 1698–1703. doi:10.1002/(SICI)1097-4598(199912)22:12<1698::AID-MUS12>3.0.CO;2-K PMID:10567083

Christe, B. L. (2009). *Introduction to biomedical instrumentation: the technology of patient Care*. New York: Cambridge University Press. doi:10.1017/CBO9780511808937

Cotterill, R. M. J. (2002). *Biophysics: An introduction*. Hoboken, NJ: John Wiley & Sons Inc.

Cram, J. R., & Kasman, G. S. (2001). The basics of surface electromyography. In E. Criswell (Ed.), *Cram's introduction to surface electromyography* (pp. 1–173). Sudbury, MA: Jones and Bartlett Publishers.

Daube, J. R. (2006). Motor unit number estimates—From A to Z. *Journal of the Neurological Sciences*, 242(1), 23–35. doi:10.1016/j.jns.2005.11.011 PMID:16423366

DeLuca, C. J., & Contessa, P. (2012). Hierarchical control of motor units in voluntary contractions. *Journal of Neurophysiology*, 107(1), 178–195. doi:10.1152/jn.00961.2010 PMID:21975447

Diószeghy, P. (2002). Scanning electromyography. *Muscle & Nerve*, 25(S11), S66–S71. doi:10.1002/mus.10150 PMID:12116288

Diószeghy, P., Egerhazi, A., Molnar, M., & Mechler, F. (1996). Turn-amplitude analysis in neuromuscular diseases. *Electromyography and Clinical Neurophysiology*, 36(8), 463–468. PMID:8985673

Dumitru, D., King, J. C., & Rogers, W. E. (1999). Motor unit action potential components and physiologic duration. *Muscle & Nerve*, 22(6), 733–741. doi:10.1002/(SICI)1097-4598(199906)22:6<733::AID-MUS10>3.0.CO;2-6 PMID:10366227

Dumitru, D., King, J. C., & Rogers, W. E. (2000). Physiologic basis of potentials recorded in electromyography. *Muscle & Nerve*, 23(11), 1667–1685. doi:10.1002/1097-4598(200011)23:11<1667::AID-MUS2>3.0.CO;2-H PMID:11054745

Ertaş, M., Baslo, M. B., Yıldız, N., Yazıcı, J., & Öge, E. (2000). Concentric needle electrode for neuromuscular jitter analysis. *Muscle & Nerve*, 23(5), 715–719. doi:10.1002/(SICI)1097-4598(200005)23:5<715::AID-MUS8>3.0.CO;2-V PMID:10797394

Farrugia, M. A., & Kenet, R. P. (2005). Turns amplitude analysis of the orbicularis oculi and oris muscles. *Clinical Neurophysiology*, 116(11), 2550–2559. doi:10.1016/j.clinph.2005.07.018 PMID:16221560

Finsterer, J. (2001). EMG-interference pattern analysis. *Journal of Electromyography and Kinesiology*, 11(4), 231–246. doi:10.1016/S1050-6411(01)00006-2 PMID:11532594

Fuglsang-Frederiksen, A. (2006). The role of different EMG methods in evaluating myopathy. *Clinical Neurophysiology*, 117(6), 1173–1189. doi:10.1016/j.clinph.2005.12.018 PMID:16516549

- Ganong, W. F. (2001). Review of medical physiology. New York: McGraw-Hill.
- Goker, I., Baslo, B., Ertas, M., & Ulgen, Y. (2009). Design of an experimental system for scanning electromyography method to investigate alterations of motor units in neurological disorders. *Digest Journal of Nanomaterials and Biostructures*, 4(1), 133–139.
- Goker, I., Baslo, B., Ertas, M., & Ulgen, Y. (2010). Large motor unit territories by scanning electromyography in patients with juvenile myoclonic epilepsy. *Journal of Clinical Neurophysiology*, 27(3), 212–215. doi:10.1097/WNP.0b013e3181e0b228 PMID:20461011
- Goker, I., Osman, O., Ozekes, S., Baslo, M. B., Ertas, M., & Ulgen, Y. (2012). Classification of juvenile myoclonic epilepsy data acquired through scanning electromyography with machine learning algorithms. *Journal of Medical Systems*, 36(5), 2705–2711. doi:10.1007/s10916-011-9746-6 PMID:21681512
- Gootzen, T. H. J. M., Vingerhoest, D. J. M., & Stegeman, D. F. (1992). A study of motor unit structure by means of scanning EMG. *Muscle & Nerve*, 15(3), 349–357. doi:10.1002/mus.880150314 PMID:1557083
- Grimbergen, C. A., Metting van Rijn, A. C., & Peper, A. (1991). Influence of isolation on interference in bioelectric recordings. *Annual International Conference of the IEEE Engineering in Medicine and Biology Society*, 13(4), 1720–1721.
- Guyton, A. C., & Hall, J. E. (2000). Textbook of medical physiology. West Philadelphia, PA: W. B. Saunders Company.
- Harper, M. C. (2009). Single fiber electromyography. In J. R. Daube, & D. I. Rubin (Eds.), *Clinical neurophysiology* (pp. 475–491). New York: Oxford University Press.
- Henneberg, K. A. (2000). Principles of electromyography. In J. D. Bronzino (Ed.), *The biomedical engineering handbook* (pp. 14.1–14.3). Boca Raton, FL: Taylor and Francis Group.
- Henneberg, K. A. (2006). Principles of electromyography. In J. D. Bronzino (Ed.), *The biomedical engineering handbook* (pp. 25.1–25.10). Boca Raton, FL: Taylor and Francis Group.
- Hilton-Brown, P., & Stålberg, E. (1983a). Motor unit size in muscular dystrophy, a macro EMG and scanning EMG study. *Journal of Neurology, Neurosurgery, and Psychiatry*, 46(11), 996–1005. doi:10.1136/jnnp.46.11.996 PMID:6655485
- Hilton-Brown, P., & Stålberg, E. (1983b). Motor unit size in muscular dystrophy, a single fiber EMG and scanning EMG study. *Journal of Neurology, Neurosurgery, and Psychiatry*, 46(11), 981–996. doi:10.1136/jnnp.46.11.981 PMID:6655484
- Jennings, D., Flint, A., Turton, B. C. H., & Nokes, L. D. M. (1995). *Introduction to medical electronics applications*. London: Hodder Headline PLC.
- Joynt, R. L., Erlandson, R. F., Wu, S. J., & Wang, C. M. (1991). Electromyography interference pattern decomposition. *Archives of Physical Medicine and Rehabilitation*, 72(8), 567–572. PMID:2059134
- Katirji, B. (2007). *Electromyography in clinical practice. A case study approach*. Philadelphia, PA: Mosby Elsevier.
- Kimura, J. (2001). *Electrodiagnosis in the disease of nerve and muscle*. New York: Oxford University Press.
- Lin, Y. D., Tsai, C. D., Huang, H. H., Chiou, D. C., & Wu, C. P. (1999). Preamplifier with a second-order high-pass filtering characteristic. *IEEE Transactions on Bio-Medical Engineering*, 46(5), 609–612. doi:10.1109/10.759062 PMID:10230140

Detection and Conditioning of EMG

- Loeb, G. E., & Ghez, C. (2006). The motor unit and muscle action. In E. R. Kandel, J. H. Schwartz, & T. M. Jessell (Eds.), *Principles of neural science* (pp. 674–695). New York: McGraw-Hill.
- Mainardi, L. T., Bianchi, A. M., & Cerutti, S. (2006). Digital biomedical signal acquisition and processing. In J. D. Bronzino (Ed.), *Medical devices and systems* (pp. 2–24). Boca Raton, FL: CRC Press Taylor & Francis Group. doi:10.1201/9781420003864.ch2
- Marieb, E. N. (1995). *Human anatomy and physiology*. Redwood City, CA: Benjamin/Cummings.
- McComas, A. J. (1995). Motor unit estimation: Anxieties and achievements. *Muscle & Nerve*, 18(4), 369–379. doi:10.1002/mus.880180402 PMID:7715621
- McCommas, et al. (1971). Electrophysiological estimation of the number of motor units within a human muscle. *Journal of Neurology, Neurosurgery, and Psychiatry*, 34(2), 121–131. doi:10.1136/jnnp.34.2.121 PMID:5571599
- McGill, K. C. (2002). Optimal resolution of superimposed action potentials. *IEEE Transactions on Bio-Medical Engineering*, 49(7), 640–650. doi:10.1109/TBME.2002.1010847 PMID:12083298
- McGill, K. C., Cummins, K. L., & Dorfman, L. J. (1985). Automatic decomposition of the clinical electromyogram. *IEEE Transactions on Bio-Medical Engineering*, 32(7), 470–477. doi:10.1109/TBME.1985.325562 PMID:3839488
- Metting van Rijn, A. C., Kuiper, A. P., Linnenbank, A. C., & Grimbergen, C. A. (1993). Patients isolation in multichannel bioelectric recordings by digital transmission through a single optical fiber. *IEEE Transactions on Bio-Medical Engineering*, 40(3), 302–307. doi:10.1109/10.216416 PMID:8335335
- Mills, K. R. (2005). The basics of electromyography. *Journal of Neurology, Neurosurgery, and Psychiatry*, 76(Supplement II), ii32–ii35. doi:10.1136/jnnp.2005.069211 PMID:15961866
- Moritani, T., Stegeman, D., & Merletti, R. (2004). Basic physiology and biophysics of EMG signal generation. In R. Merletti, & P. A. Parker (Eds.), *Electromyography, physiology, engineering and noninvasive applications* (pp. 1–27). Hoboken, NJ: John Wiley and Sons. doi:10.1002/0471678384.ch1
- Nagel, J. (2006). Biopotential amplifiers. In J. D. Bronzino (Ed.), *The biomedical engineering handbook, medical devices and systems* (pp. 52.1–52.14). Boca Raton, FL: CRC Press Taylor & Francis Group.
- Nandedkar, S. D., & Sanders, D. B. (1990). Measurement of the amplitude of the envelope. *Muscle & Nerve*, 13(10), 933–938. doi:10.1002/mus.880131008 PMID:2233851
- Navallas, J., & Stålberg, E. (2009). Studying motor end-plate topography by means of scanning-electromyography. *Clinical Neurophysiology*, 120(7), 1335–1341. doi:10.1016/j.clinph.2009.05.014 PMID:19535290
- Neuman, M. R. (2010). Biopotential amplifiers. In J. G. Webster (Ed.), *Medical instrumentation: Application and design* (pp. 241–292). Hoboken, NJ: John Wiley & Sons.
- Neuman, M. R. (2010). Biopotential electrodes. In J. G. Webster (Ed.), *Medical instrumentation: Application and design* (pp. 189–241). Hoboken, NJ: John Wiley & Sons.
- Northrop, R. B. (2002). *Noninvasive instrumentation and measurement in medical diagnosis*. Boca Raton, FL: CRC Press.
- Oh, S. J. (2003). *Clinical electromyography: Nerve conduction studies*. Philadelphia, PA: Lippincott Williams and Wilkins.

- Padua, L., Aprile, I., Monaco, M., Fenicia, L., Anniballi, F., Pauri, F., & Tonali, P. (1999). Neurophysiological assessment in the diagnosis of botulism: Usefulness of single-fiber EMG. *Muscle & Nerve*, 22(10), 1388–1392. doi:10.1002/(SICI)1097-4598(199910)22:10<1388::AID-MUS8>3.0.CO;2-3 PMID:10487905
- Pozzo, M., Farina, D., & Merletti, R. (2004). Electromyography: Detection, processing, and applications. In J. Moore, & G. Zouridakis (Eds.), *Biomedical technology and devices handbook* (pp. 4.1–4.60). Boca Raton, FL: CRC Press.
- Preston, D. C., & Shapiro, B. E. (2005). *Electromyography and neuromuscular disorders: Clinical-electrophysiologic correlation*. Philadelphia, PA: Butterworth-Heinemann.
- Prutchi, D., & Norris, M. (2005). *Design and development of medical electronic instrumentation: A practical perspective of the design, construction, and test of medical devices*. Hoboken, NJ: John Wiley & Sons. doi:10.1002/0471681849
- Rubin, D. I. (2009). Assessing the neuromuscular junction with repetitive stimulation studies. In J. R. Daube, & D. I. Rubin (Eds.), *Clinical neurophysiology* (pp. 401–451). New York: Oxford University Press.
- Sawhney, G. S. (2007). *Fundamentals of biomedical engineering*. New Delhi, India: New Age International (P) Ltd. Publisher.
- Shefner, J. M. (2001). Motor unit number estimation in human neurological diseases and animal models. *Clinical Neurophysiology*, 112(6), 955–964. doi:10.1016/S1388-2457(01)00520-X PMID:11377252
- Silver, J. (2004). What Is EMG? In L. Weiss, J. K. Silver, & J. Weiss (Eds.), *Easy EMG* (pp. 1–5). China: Butterworth-Heinemann. doi:10.1016/B978-0-7506-7431-7.50006-3
- Smith, B. E. (2009). Quantitative electromyography. In J. R. Daube, & D. I. Rubin (Eds.), *Clinical neurophysiology* (pp. 451–475). New York: Oxford University Press.
- Sörnmo, L., & Laguna, P. (2005). *Bioelectrical signal processing in cardiac and neurological application*. New York: Elsevier Academic Press.
- Spaans, F., Vredeveld, J. W., Morre, H. H. E., Jacobs, B. C., & Debaets, M. H. (2003). Dysfunction at the motor end-plate and axon membrane in Guillain-Barre´ Syndrome: A single-fiber EMG study. *Muscle & Nerve*, 27(4), 426–434. doi:10.1002/mus.10334 PMID:12661043
- Stålberg, E. (1986). Single fiber EMG, macro EMG, and scanning EMG. *New ways of looking at the motor unit*. *CRC Critical Reviews in Clinical Neurobiology*, 2(2), 125–167. PMID:3536309
- Stålberg, E. (1987). New EMG methods to study the motor unit. *Electroencephalography and Clinical Neurophysiology. Supplement*, 39, 38–49. PMID:3308420
- Stålberg, E., Andreassen, S., Falck, B., Lang, H., Rosenfalck, A., & Trojaborg, W. (1986). Quantitative analysis of individual motor unit potentials: A proposition for standardized terminology and criteria for measurement. *Journal of Clinical Neurophysiology*, 3(4), 313–348. doi:10.1097/00004691-198610000-00003 PMID:3332279
- Stålberg, E., & Antoni, L. (1980). Electrophysiological cross section of the motor unit. *Journal of Neurology, Neurosurgery, and Psychiatry*, 43(6), 469–474. doi:10.1136/jnnp.43.6.469 PMID:7205287
- Stålberg, E., & Dioszeghy, P. (1991). Scanning EMG in normal muscle and in neuromuscular disorders. *Electroencephalography and Clinical Neurophysiology*, 81(6), 403–416. doi:10.1016/0168-5597(91)90048-3 PMID:1721580

Detection and Conditioning of EMG

Stålberg, E., & Eriksson, P. O. (1987). A scanning electromyographic study of the topography of human masseter single motor units. *Archives of Oral Biology*, 32(11), 793–797. doi:10.1016/0003-9969(87)90005-7 PMID:3482348

Stålberg, E., & Falck, B. (1997). The role of EMG in neurology. *Electroencephalography and Clinical Neurophysiology*, 103(6), 579–598. doi:10.1016/S0013-4694(97)00138-7 PMID:9546485

Stålberg, E., & Trontelji, J. V. (1994). *Single fiber electromyography studies in healthy and diseased muscle*. New York: Raven Press.

Stålberg, E., Trontelji, J. V., & Sanders, D. B. (2010). *Single fiber electromyography studies in healthy and diseased muscle*. Fiskebäckskil, Sweden: Edshagen Publishing House.

Stashuk, D. W. (1999). Decomposition and quantitative analysis of clinical electromyographic signals. *Medical Engineering & Physics*, 21(6-7), 389–404. doi:10.1016/S1350-4533(99)00064-8 PMID:10624736

Togawa, T., Tamura, T., & Öberg, P. A. (1997). *Biomedical transducers and instruments*. Boca Raton, FL: CRC Press.

Tortora, G. J., & Derrickson, B. (2009). *Principles of anatomy and physiology*. Hoboken, NJ: John Wiley & Sons, Inc.

Tortora, G. J., & Derrickson, B. (2010). *Introduction to the human body*. Hoboken, NJ: John Wiley & Sons, Inc.

Trontelji, J. V., Jabre, J., & Mihelin, M. (2004). Basic physiology and biophysics of EMG signal generation. In R. Merletti, & P. A. Parker (Eds.), *Electromyography, physiology, engineering and noninvasive applications* (pp. 27–47). Hoboken, NJ: John Wiley and Sons.

van der Horst, M. J., Metting van Rijn, A. C., Peper, A., & Grimbergen, C. A. (1998). High frequency interference effects in amplifiers for biopotential recordings. *Proceedings of the 20th Annual International Conference of the IEEE Engineering in Medicine and Biology Society*, 20(6), 3309–3312.

Weinberg, D. H., Rizzo, J., Hayes, M. T., Knell, M. D., & Kelly, J. J. (1999). Ocular yasthenia gravis: Predictive value of single-fiber electromyography. *Muscle & Nerve*, 22(9), 1222–1227. doi:10.1002/(SICI)1097-4598(199909)22:9<1222::AID-MUS8>3.0.CO;2-R PMID:10454717

Winter, D., & Webster, J. G. (1983). Driven right leg circuit design. *IEEE Transactions on Bio-Medical Engineering*, 30(1), 62–66. doi:10.1109/TBME.1983.325168 PMID:6826188

Yazıcıoğlu, R. F., Van Hoof, C., & Puers, R. (2009). *Biopotential readout circuits for portable acquisition systems*. Dordrecht, The Netherlands: Springer.

ADDITIONAL READING

Aminoff, M. J. (1992). Clinical Electromyography. In M. J. Aminoff (Ed.), *Electrodiagnosis in Clinical Neurology* (pp. 249–283). New York, NY: Churchill Livingstone Inc.

Brown, B. H., Lawford, P. W., Smallwood, R. H., Hose, D. R., & Barber, D. C. (1999). *Medical Physics and Biomedical Engineering*. London, United Kingdom: IOP Publishing Ltd. doi:10.1887/0750303689

Bryan, A. (1998). Electromyography: recording methods and signal processing techniques. *Current Anaesthesia and Critical Care*, 9(3), 110–116. doi:10.1016/S0953-7112(98)80003-3

- Burke, R. (2001). The Structure and Function of Motor Units. In G. Karpati, D. Hilton-Jones, & R. C. Griggs (Eds.), *Disorder of Voluntary Muscle* (pp. 3–26). Cambridge, United Kingdom: University Press.
- Chan, R. C., & Hsu, T. C. (1991). Quantitative comparison of motor unit potential parameters between monopolar and concentric needles. *Muscle & Nerve*, 14(10), 1028–1032. doi:10.1002/mus.880141015 PMID:1944402
- Cram, J. R., & Kasman, G. S. (2001). The Basics of Surface Electromyography. In E. Criswell (Ed.), *Cram's Introduction to Surface Electromyography* (pp. 1–173). Sudbury, MA: Jones and Bartlett Publishers.
- DeLuca, C. J., & Contessa, P. (2012). Hierarchical control of motor units in voluntary contractions. *Journal of Neurophysiology*, 107(1), 178–195. doi:10.1152/jn.00961.2010 PMID:21975447
- Dumitru, D., King, J. C., & Rogers, W. E. (1999). Motor Unit Action Potential Components and Physiologic Duration. *Muscle & Nerve*, 22(6), 733–741. doi:10.1002/(SICI)1097-4598(199906)22:6<733::AID-MUS10>3.0.CO;2-6 PMID:10366227
- Dumitru, D., King, J. C., & Rogers, W. E. (2000). Physiologic Basis of Potentials Recorded in Electromyography. *Muscle & Nerve*, 23(11), 1667–1685. doi:10.1002/1097-4598(200011)23:11<1667::AID-MUS2>3.0.CO;2-H PMID:11054745
- Grimbergen, C. A., Metting van Rijn, A. C., & Peper, A. (1991). Influence of isolation on interference in bioelectric recordings. *Annual International Conference of the IEEE Engineering in Medicine and Biology Society*, 13(4), 1720–1721.
- Harper, M. C. (2009). Single Fiber Electromyography. In J. R. Daube, & D. I. Rubin (Eds.), *Clinical Neurophysiology* (pp. 475–491). New York, MA: Oxford University Press.
- Henneberg, K. A. (2000). Principles of Electromyography. In J. D. Bronzino (Ed.), *The Biomedical Engineering Handbook* (pp. 14.1–14.3). Boca Raton, FL: Taylor and Francis Group.
- Henneberg, K. A. (2006). Principles of Electromyography. In J. D. Bronzino (Ed.), *The Biomedical Engineering Handbook* (pp. 25.1–25.10). Boca Raton, FL: Taylor and Francis Group.
- Jennings, D., Flint, A., Turton, B. C. H., & Nokes, L. D. M. (1995). *Introduction to Medical Electronics Applications*. Bristol, United Kingdom: J.W. Arrowsmith Ltd.
- Katirji, B. (2007). *Electromyography in Clinical Practice. A Case Study Approach*. Suite, PA, USA: Mosby Elsevier.
- Kimura, J. (2001). *Electrodiagnosis in the Disease of Nerve and Muscle*. New York, NY: Oxford University Press.
- Liddell, E. G. T., & Sherrington, C. S. (1925). Recruitment and some other factors of reflex inhibition. *Proceedings of the Royal Society of London. Series B, Containing Papers of a Biological Character*, 97, 488–518. doi:10.1098/rspb.1925.0016
- Lin, Y. D., Tsai, C. D., Huang, H. H., Chiou, D. C., & Wu, C. P. (1999). Preamplifier with a second-order high-pass filtering characteristic. *IEEE Transactions on Bio-Medical Engineering*, 46(5), 609–612. doi:10.1109/10.759062 PMID:10230140
- Mainardi, L. T., Bianchi, A. M., & Cerutti, S. (2006). Digital Biomedical Signal Acquisition and Processing. In J. D. Bronzino (Ed.), *Medical Devices and Systems* (pp. 2-1–2-24). Boca Raton, FL: CRC Press Taylor & Francis Group. doi:10.1201/9781420003864.ch2
- Marieb, E. N. (1995). *Human Anatomy and Physiology*. Redwood City, CA: Benjamin/Cummings.

Detection and Conditioning of EMG

McCommas, et al. (1971). Electrophysiological estimation of the number of motor units within a human muscle. *Journal of Neurology, Neurosurgery, and Psychiatry*, 34(2), 121–131. doi:10.1136/jnnp.34.2.121 PMID:5571599

McGill, K. C. (2002). Optimal Resolution of Superimposed Action Potentials. *IEEE Transactions on Bio-Medical Engineering*, 49(7), 640–650. doi:10.1109/TBME.2002.1010847 PMID:12083298

McGill, K. C., Cummins, K. L., & Dorfman, L. J. (1985). Automatic Decomposition of the Clinical Electromyogram. *IEEE Transactions on Bio-Medical Engineering*, 32(7), 470–477. doi:10.1109/TBME.1985.325562 PMID:3839488

Metting van Rijn, A. C., Kuiper, A. P., Linnenbank, A. C., & Grimbergen, C. A. (1993). Patients isolation in multichannel bioelectric recordings by digital transmission through a single optical fiber. *IEEE Transactions on Bio-Medical Engineering*, 40(3), 302–307. doi:10.1109/10.216416 PMID:8335335

Millner-Brown, H. S., Stein, R. B., & Yemm, R. (1973). The Orderly Recruitment of Human Motor Units During Voluntary Isometric Contractions. *The Journal of Physiology*, 30(2), 359–370.

Mills, K. R. (2005). The basics of Electromyography. *Journal of Neurology, Neurosurgery, and Psychiatry*, 76(Supplement II), ii32–ii35. doi:10.1136/jnnp.2005.069211 PMID:15961866

Moritani, T., Stegeman, D., & Merletti, R. (2004). Basic Physiology and Biophysics of EMG Signal Generation. In R. Merletti, & P. A. Parker (Eds.), *Electromyography, Physiology, engineering and Noninvasive Applications* (pp. 1–27). Hoboken, New Jersey: John Wiley and Sons. doi:10.1002/0471678384.ch1

Nagel, J. (2006). Biopotential Amplifiers. In J. D. Bronzino (Ed.), *The Biomedical Engineering Handbook, Medical Devices and Systems* (pp. 52.1–52.14). Boca Raton, Florida: CRC Press Taylor & Francis Group.

Neuman, M. R. (2010). Biopotential Amplifiers. In J. G. Webster (Ed.) *Medical Instrumentation: Application and Design* (pp.241-292). Hoboken, NJ: John Wiley & Sons.

Neuman, M. R. (2010). Biopotential Electrodes. In J. G. Webster (Ed.), *Medical Instrumentation: Application and Design* (pp. 189–241). Hoboken, NJ: John Wiley & Sons.

Northrop, R. B. (2002). *Noninvasive Instrumentation and Measurement in Medical Diagnosis*. Boca Raton, USA: CRC Press.

Oh, S.J. (2003). *Clinical Electromyography: Nerve Conduction Studies*. Philadelphia, PA: Williams and Wilkins.

Pozzo, M., Farina, D., & Merletti, R. (2004). Electromyography: Detection, Processing, and Applications. In J. Moore, & G. Zouridakis (Eds.), *Biomedical Technology and Devices Handbook* (pp. 4.1–4.60). Boca Raton, FL: CRC Press.

Preston, D. C., & Shapiro, B. E. (2005). *Electromyography and neuromuscular disorders: clinical-electrophysiologic correlation*. Philadelphia, Pennsylvania: Butterworth-Heinemann.

Prutchi, D., & Norris, M. (2005). *Design and Development of Medical Electronic Instrumentation: A Practical Perspective of the Design, Construction, and Test of Medical Devices*. Hoboken, New Jersey: John Wiley & Sons. doi:10.1002/0471681849

Rubin, D. I. (2009). Assessing the Neuromuscular Junction with Repetitive Stimulation Studies. In J. R. Daube, & D. I. Rubin (Eds.), *Clinical Neurophysiology* (pp. 401–451). New York, NY: Oxford University Press.

- Sawhney, G. S. (2007). *Fundamentals of Biomedical Engineering*. New Delhi, India: New Age International (P) Ltd. Publisher.
- Silver, J. (2004). What Is EMG? In L. Weiss, J. K. Silver, & J. Weiss (Eds.), *Easy EMG* (pp. 1–5). China: Butterworth-Heinemann. doi:10.1016/B978-0-7506-7431-7.50006-3
- Smith, B. E. (2009). Quantitative Electromyography. In J. R. Daube, & D. I. Rubin (Eds.), *Clinical Neurophysiology* (pp. 451–475). New York, NY: Oxford University Press.
- Sörnmo, L., & Laguna, P. (2005). *Bioelectrical Signal Processing in Cardiac and Neurological Application*. New York, NY: Elsevier Academic Press.
- Stålberg, E. (1986). Single fiber EMG, macro EMG, and scanning EMG. New ways of looking at the motor unit. *CRC Critical Reviews in Clinical Neurobiology*, 2(2), 125–167. PMID:3536309
- Stålberg, E. (1987). New EMG methods to study the motor unit. *Electroencephalography and Clinical Neurophysiology. Supplement*, 39, 38–49. PMID:3308420
- Stålberg, E., Andreassen, S., Falck, B., Lang, H., Rosenfalck, A., & Trojaborg, W. (1986). Quantitative analysis of individual motor unit potentials: a proposition for standardized terminology and criteria for measurement. *Journal of Clinical Neurophysiology*, 3(4), 313–348. doi:10.1097/00004691-198610000-00003 PMID:3332279
- Stålberg, E., & Antoni, L. (1980). Electrophysiological Cross Section of the Motor Unit. *Journal of Neurology, Neurosurgery, and Psychiatry*, 43(6), 469–474. doi:10.1136/jnnp.43.6.469 PMID:7205287
- Stålberg, E., & Dioszeghy, P. (1991). Scanning EMG in normal muscle and in neuromuscular disorders. *Electroencephalography and Clinical Neurophysiology*, 81(6), 403–416. doi:10.1016/0168-5597(91)90048-3 PMID:1721580
- Stålberg, E., & Eriksson, P. O. (1987). A scanning electromyographic study of the topography of human masseter single motor units. *Archives of Oral Biology*, 32(11), 793–797. doi:10.1016/0003-9969(87)90005-7 PMID:3482348
- Stålberg, E., & Falck, B. (1997). The role of EMG in neurology. *Electroencephalography and Clinical Neurophysiology*, 103(6), 579–598. doi:10.1016/S0013-4694(97)00138-7 PMID:9546485
- Stålberg, E., & Trontelji, J. V. (1994). *Single Fiber Electromyography Studies in Healthy and Diseased Muscle*. New York, NY: Raven Press.
- Stålberg, E., Trontelji, J. V., & Sanders, D. B. (2010). *Single Fiber Electromyography Studies in Healthy and Diseased Muscle*. Fiskebäckskil, Sweden: Edshagen Publishing House.
- Togawa, T., Tamura, T., & Öberg, P. A. (1997). *Biomedical Transducers and Instruments*. Boca Raton, FL: CRC Press.
- Tortora, G. J., & Derrickson, B. (2009). *Principles of Anatomy and Physiology*. Hoboken, NJ: John Wiley & Sons, Inc.
- Tortora, G. J., & Derrickson, B. (2010). *Introduction to the Human Body*. Hoboken, NJ: John Wiley & Sons, Inc.
- Trontelj, J. V., Jabre, J., & Mihelin, M. (2004). Basic Physiology and Biophysics of EMG Signal Generation. In R. Merletti, & P. A. Parker (Eds.), *Electromyography, Physiology, engineering and Noninvasive Applications* (pp. 27–47). Hoboken, NJ: John Wiley and Sons.

Detection and Conditioning of EMG

van der Horst, M. J., Metting van Rijn, A. C., Peper, A., & Grimbergen, C. A. (1998). High frequency interference effects in amplifiers for Biopotential Recordings. In Proceedings of the 20th Annual International Conference of the IEEE Engineering in Medicine and Biology Society 20(6), 3309-3312.

Weinberg, D. H., Rizzo, J., Hayes, M. T., Knell, M. D., & Kelly, J. J. (1999). Ocular myasthenia gravis: predictive value of single-fiber electromyography. *Muscle & Nerve*, 22(9), 1222–1227. doi:10.1002/(SICI)1097-4598(199909)22:9<1222::AID-MUS8>3.0.CO;2-R PMID:10454717

Winter, D., & Webster, J. G. (1983). Driven Right Leg Circuit Design. *IEEE Transactions on Bio-Medical Engineering*, 30(1), 62–66. doi:10.1109/TBME.1983.325168 PMID:6826188

Yazıcıoğlu, R. F., Van Hoof, C., & Puers, R. (2009). *Biopotential Readout Circuits for Portable Acquisition Systems*. Dordrecht, Netherland: Springer.

KEY TERMS AND DEFINITIONS

Biomedical Instrumentation: The field of Biomedical Engineering focused on the engineering principles of medical instruments such as Biopotential Amplifiers (e.g. Electromyography), Medical Imaging Systems etc. Since it is concerned with the measurement of all the variables in the body for the diagnostic and therapeutic purposes, biomedical instrumentation is the subdivision of biomedical engineering mainly focused on how to acquire physiological signal from the living organisms.

Concentric Needle Electrode (CNE): A bipolar EMG electrode used in detecting and acquiring electrical activity of skeletal muscle via intramuscular measurements. It consists of two electrodes: one of them is the active electrode

located at the center of CNE and the other is the cannula functioning as a reference electrode. The signals acquired by both electrodes are fed to the front-end of the EMG instrument in order to detect the time-varying amplitude of the EMG signal under the investigation.

Conventional Electromyography: The most commonly used EMG technique in clinical routine for the diagnosis of the neuromuscular diseases. It is performed by means of the concentric needle electrode. The time-varying signal pattern of the Motor Unit Action Potential is monitored during the application of this technique.

Macro Electromyography: An electrophysiological technique used for the registration of macro motor unit potentials which arises from the entire motor unit using a cannula with relatively larger surface to capture the electrical activity from the majority of the muscle fibers within the motor unit territory and a single-fiber electrode to detect a triggering single muscle fiber action potential in order to average the same motor unit potential.

Motor Unit: The basic anatomical and functional unit of the skeletal muscle consisting of an anterior horn cell, its axon, the neuromuscular junctions, and the muscle fibers innervated by the motor neuron.

Motor Unit Action Potential: Spikes of electrical activity recorded during an EMG that is correlated with the number of the contributing motor units activated during the voluntary muscle contraction.

Quantitative Electromyography (QEMG): Electrophysiological techniques used in clinical routine to characterize motor unit action potential waveforms using statistical and probabilistic techniques that allow for greater objectivity and reproducibility via the normative data in supporting the diagnostic process.

Scanning Electromyography: An experimental electrophysiological technique used to build-up the electrophysiological cross-section of the motor unit territory by means of the temporal and spatial characteristics of the motor unit.

Single-Fiber Electromyography: Single-fiber electromyography (SFEMG) is a selective EMG recording technique enabling the detection of action potentials generated by a single muscle fiber. The selectivity of the technique results from the small recording surface (25 μm in diameter) exposed at a port on the side of the electrode which provides a 300- μm uptake area. The selectivity of the recording is further improved by using a high pass filter with a 500- Hz cut-off frequency.

Surface Electromyography: A non-invasive electrophysiological technique in which electrodes are placed on the skin overlying the muscle of interest to detect the electrical activity of this muscle.

ENDNOTES

- ¹ Although EMG signals are usually acquired from the patients for diagnostic purposes, they can be also acquired from healthy individuals in researches concerning sport medicine, biomechanics, ergonomics, biomedical engineering. Therefore, the term “subject” will be preferred throughout this chapter instead of “patient.”

Chapter 4

An Introduction to EMG Signal Processing Using MatLab and Microsoft Excel

Daniel Robbins
University of Bedfordshire, UK

ABSTRACT

This chapter provides the reader with an introduction to the fundamentals of biological signal analysis and processing, using EMG signals to illustrate the process. The areas covered within the chapter include: frequency analysis using the Fast Fourier Transform, identifying noise within a signal, signal smoothing via root mean square (RMS) processing and signal filtering with both low-pass and high-pass filters. Guidelines for the application of the processes covered are included in conjunction with step by step examples using both MathWorks MatLab and Microsoft Excel software. Following the examples therefore allows the reader to practice the processes described to promote and reinforce their learning.

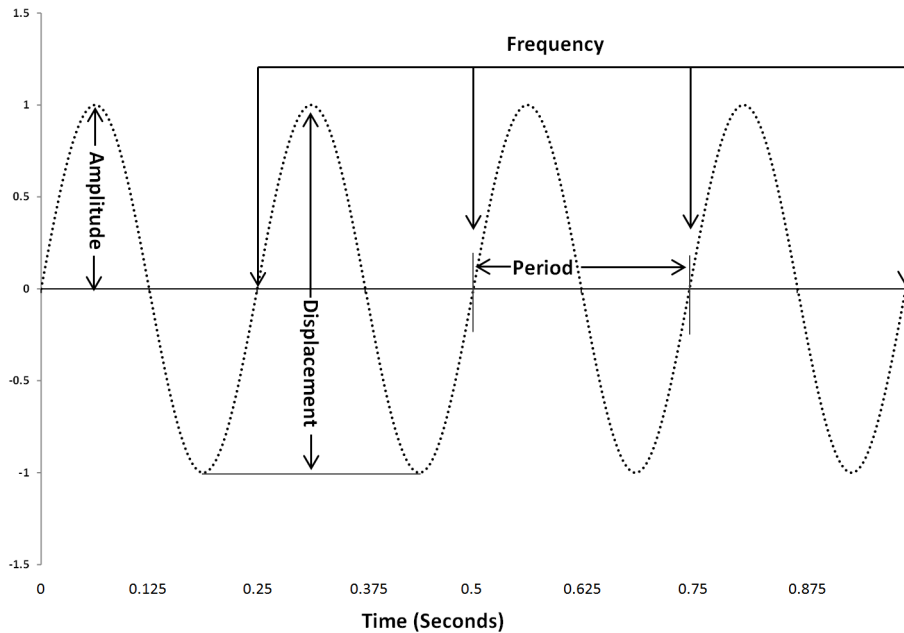
INTRODUCTION

In the previous chapter the basis for the myoelectrical signal was introduced. Now that the source of the signal has been covered, this chapter will introduce the reader to the basic concepts of signal processing i.e. *what to do with the signal once it has been obtained*. One unfortunate but unavoidable fact with regards to acquisition of biological electrical signals is that pure signals are very rarely, if ever, obtained. Typically in addition to the biological signals there will also be additional

signals or *noise* from other biological signals e.g. from the heart, from other electrical equipment in the vicinity or from moving wires during data collection. The combination of additional signals corrupts the desired biological signal resulting in a ‘noisy’ signal. The process of removing this noise is known as signal processing and is essentially a series of mathematical steps which attempt to strip away the noise and leave only the biological signal. Signal processing is a vast area, far too large to cover in one book chapter; therefore this chapter will focus on analogue signal filters

DOI: 10.4018/978-1-4666-6090-8.ch004

Figure 1. Parameters of signals



with examples applied to electromyographic signals (EMG). Once the maximum amount of noise possible has been removed the signal can be quantified, for example by its amplitude, power, or time to peak events. In addition to signal filters the *Fast Fourier Transform* (FFT) for displaying the frequency content of the signal will be considered, including details of how to apply the FFT and which signal types are suitable for FFT.

Working through the chapter content will provide an appreciation for the basics of signal processing whilst providing both the opportunity to complete analyses, without expensive software, and the foundation knowledge required to understand more complex procedures.

Introduction to Signal Parameters

Before beginning with signal processing it is important to establish a foundation with the language used to describe signals themselves. The simplest way to achieve an understanding in this area is to consider a simple sin wave (see figure one). A

sin wave can be described a periodic graph, in as much as it has a distinct pattern that continuously repeats. The distance from the baseline to the apex of a peak, or the lowest point of a trough, is known as the *amplitude*, this should not be confused with the *displacement* or *peak to peak amplitude* which is a measure of the distance between the apex of a peak to lowest point of a trough (see figure one).

The distance from the start to the end of section of a graph is defined as the point when the graph travels away from the zero line until it returns to from the zero line. The *period* or *wavelength* is generally measured in milliseconds (msec). The amount of times a wavelength occurs within one second is the frequency of the signal and is measured in Hertz (Hz). This relationship can be defined two ways; depending on whether you know the frequency value or the time value. If you know the frequency of the wavelength, the time period can be calculated via:

$$T = \frac{1}{F}$$

If you know the time period of the wavelength, the frequency can be calculated via:

$$F = \frac{1}{T}$$

where: T = the time period of one wavelength and F = the frequency of the signal.

Therefore longer time periods result in lower frequencies and higher frequencies result in lower time periods. As the waveforms are essentially rotating about zero, this relationship can also be described by the *angular frequency*. The angular frequency (ω) is a measure of rotation rates and can be described by the following equations:

$$\dot{\theta} = \frac{2\pi}{T} = 2\pi F$$

The angular frequency is used for filter design in signal processing and will be covered in more detail later in the chapter.

Starting Signal Processing

Before any type of filtering can be applied to the signal, the signal itself must be viewed. A key characteristic of the raw myoelectrical signal is that the signal is centred about zero i.e. there are equal and opposite amounts of values above and below the zero line creating a symmetrical graph in the vertical plane. Prior to any other action, signal symmetry about zero must be confirmed. Often data acquisition equipment or local electrical equipment can create signal changes which interfere with the biological signal and create what is known as *zero offset*. Zero offset is simply a graph which is not centred on the zero line i.e. the middle of the graph is slightly above or below the zero line. Any zero offset will create issues when filters are applied leading to inaccurate results. The simplest way to check for zero offset, other than to view it on a graph... is to calculate the

average value for the signal. A symmetrical signal which is truly centred on the zero line will have an average of zero. If the average of the signal is not zero the simplest correction is to subtract the average value from each data point in the signal (Haykin & Liu, 2009). This will correct any zero offset while maintaining the signal symmetry.

One issue that can affect this process is the presence of low frequency noise. Often hardware design will prevent the range of signal frequencies recorded to actually start at zero. The actual range available will depend on the equipment, but is likely to be something like 20-500 Hz or 10-1000 Hz. The majority of the EMG signal frequency concentration is between 20-200 Hz, with minor contributions potentially extending up to 1000 Hz (Winter, 2005). Therefore, very low frequencies e.g. 1-5 Hz in the signal is likely to be noise, and as such will need to be removed. The presence of low frequencies can be displayed in frequency spectrums, or potentially by simply plotting the raw signal. Once the presence of low frequencies is confirmed, filters to remove the frequencies must be applied.

When considering analogue filters there are two distinct categories:

1. High-pass filters, these are filters which attenuate low frequencies and retains high frequencies.

and

2. Low-pass filters, these are filters which attenuate high frequencies and retains low frequencies.

If there are abnormal low frequencies present then a high-pass filter should be applied, this will both attenuate low frequencies and correct any zero offset. The process for designing and applying filters will be reviewed in more detail later in the chapter.

To summarise, the first stage of EMG processing is to establish if there is any zero offset and if low frequencies are present. If only zero offset is present, the signal mean should be subtracted from each data point. If low frequencies are present a high-pass filter should be applied.

Signal Frequency Analysis

Before filters can be designed the frequency content of the signal must be considered. One approach to analyse the frequency of a signal is to use a *Fourier analysis*. A Fourier analysis is a process to determine the range of frequencies present in a signal – but not the time at which they occur. To consider the time-frequency relationship the short term Fourier transform (STFT) or wavelet analysis would need to be employed; however these are outside the scope of this chapter.

Typically the FFT is used to analyse frequency content of signals and as such is available in a wide variety of computer packages. However, there are some rules which must be followed for an FFT analysis to provide accurate data.

1. The data should come from periodic, stationary signals. In EMG terms this means that the signal should come from an isometric and isotonic contraction. Dynamic contractions should be analysed via other techniques such as wavelet analysis.
2. The data collection should have complied to the Nyquist theorem, which states that the data collection sampling frequency should be at least twice the highest frequency component of that being analysed (Prutchi & Norris, 2005).
3. The signal analysed should have a length that is equal to a power of two e.g. 256, 512, 1024, 2048, 4096, 8192 etc. If the sampling frequency of the data acquisition equipment is 2000 Hz, this would equate to 0.5 and 2.9 seconds of muscle contractions respectively.

If the signal length is not a power of two the signal can be padded with zeros to reach an appropriate length.

Note that of the three rules above, rules one and two both apply to the data collection and as such should be addressed during protocol design. Rule three is a post processing issue, and therefore can be addressed during data analysis.

The underlying mathematical principles are complex, for a detailed analysis see Chu & George (2010) or for a fun and simpler explanation see review by the Transnational College of LEX (2006). For the sake of simplicity this book will address the process of how to apply the FFT, not the mathematical principles of how it works. The easiest way to view the process is to first view the MatLab code for the process.

MatLab Code for Completing Frequency Analysis

N.B. the following code is a MatLab command; if the line starts with ‘%’ this is a note. When using MatLab a ‘%’ informs the software that the following text is programmer notes/comments and not part of the programme commands. Providing the user names data files correctly, the following code could be copied word for word to recreate the outputs displayed.

```
raw=xlsread('raw.xls')
```

```
% This command loads the raw data from an Excel file and creates a variable called 'raw'
```

```
Fs = 2000;
```

```
% This command saves the sampling frequency of the data acquisition.
```

```
nfft=2^(nextpow2(length(raw)));
```

% An important aspect of FFT analysis is to keep the dataset in a quantity which is an exact power of two. The line of code above identifies the maximum length the dataset can be before the length exceeds an exact power of 2. This value is saved as 'nfft'.

```
fft1=fft(raw,nfft);
```

% This command will perform the Fourier analysis on the raw data, truncating the dataset and if at the nfft value identified above if the raw signal is longer than this value.

```
fft_HalfLengthValue=ceil((nfft+1)/2);
```

% Frequency analysis only uses the first half of the values produced by an FFT analysis. This function counts the number of unique data points i.e. the first half and saves the count as variable 'fft_HalfLengthValue'.

```
fft_HalfLength=fft1(1:fft_HalfLength-Value);
```

% This command half's the size of fft1 and saves the result as 'fft_HalfLength'.

```
mag =abs(fft_HalfLength);
```

% The FFT function calculation outputs complex numbers, this converts to real numbers

```
power=mag.^2;
```

% While this is not always used for EMG studies, it is typical to square each data point and report the values as the signal power.

```
fscale=(fs/2)/length(power);
```

% This calculates the increments for the x axis of the output graph

```
frqscale=(0:fscale:(fs/2)-fscale);
```

% Calculates the range for the axis

```
FFTpowerSpec=[frqscale' power];
```

% This command produces a two column array which can be used to calculate median

% frequency or to plot the frequency spectrum
Plot(frqscale, power)

% This command plots the frequency spectrum

It is important to note that the above code is designed to analyse a complete individual signal i.e. one contraction. If the signal being analysed is a portion of a signal, as opposed to a complete signal, there is a risk that the signal portion may not represent the periodic nature of the signal. To account for this technique known as 'windowing' is applied to adjust the signal. There are many different types of 'windows that can be applied, such as a Hanning, Hamming, Welch or Blackman, for a review of FFT windows see (Kester, 2005).

In addition to producing a frequency spectrum, it is sometimes useful to calculate the *median frequency*. This has the advantage of providing a singular value for comparison across protocol stages, including calculation of confidence intervals and variance of obtained results which can be used during scientific reporting of findings. The median frequency is essentially based on a calculated value of half of the area under the frequency spectrum graph. The MatLab code to achieve this, based on the values obtained in the previous code, is as follows.

MatLab Code for Calculation of Median Frequency

```
Cumulative_Power= cumsum(power);
```

% This command calculates the cumulative summation of all the elements in the power previously calculated.


```
Half_cumulative_power= sum(power)/2;
```

% This command produces a single value for half of the summation of all elements the calculated power

```
[MINvalue index] =  
min(abs(Cumulative_Power - Half_cumulative_power));
```

% This creates a reference for the smallest difference between the cumulative summation of the power and the half cumulative power. The smallest difference represents the median frequency.

```
medfreq=frqscale(index)
```

% This command will use the above reference and the scale calculated in the previous code to display the median frequency in the workspace area.

Calculating Frequency Content in Excel

The frequency content can also be calculated in Microsoft Excel, though there is less opportunity for automation during the process. To complete the analysis the following steps will need to be completed:

1. Save the raw signal to column A
2. At the top of column B use the count function to determine how many data points there are e.g. =COUNT(A1:A1024). Alternatively simply look and note the amount of cells with numbers in.
3. Ensure the signal length is a power of 2 – if not pad with zeros to the next power of 2 signal length value, e.g. 512, 1024, 2048, 4096 etc.
4. Using the data analysis menu, select Fourier analysis

- a. Select all the raw signal data in column A
 - b. Select the output range to be column C
5. The Fourier analysis outputs complex numbers, convert these to an amplitude value in column D using the IMABS function e.g. =IMABS(C1)
 6. In column E take the square of the amplitude in column D e.g. =D1^2, this represents the power of the signal.
 7. In column F calculate the cumulative power e.g. F1=E1, F2=F1+E2, F3=F2+E3 etc.
 8. In column G calculate the frequency scale by cumulatively adding the result of the sampling frequency divided by the total number of data points in the raw signal e.g. G1=1000/4096, G2=G1+(1000/4096), G3=G2+(1000/4096) etc.
 9. As only half the values are used, the cell where the frequency scale is equal to half of the sampling frequency can be used to identify the maximum power in the frequency spectrum. For example, if the data was collected with a sample frequency of 1000 Hz, the formula =INDEX(F2:F1024,MATCH(500,G2:G1024)) would identify the maximum power in the frequency spectrum.
 10. The median frequency is the frequency at which half of the maximum cumulative power is obtained. This can be automatically located using the VLOOKUP function e.g. =VLOOKUP(H2,F2:G1024,2).

You can plot the data using either the amplitude (column D) or the power (column E) against the frequency scale (column B). Remember not plot the data past half the sampling frequency.

To summarise, the frequency spectrum will provide information about the weight of the frequency components. This provides two key benefits:

1. Both high and low-pass filters require parameters, such as cut-off frequency, to be selected. The frequency spectrum provides one source of information to base this selection on.
2. The median frequency, this can be used for estimation of physiological changes such as fatigue if the median frequency changes during the course of a contraction (De Luca, 1984) or following some sort of intervention.

Once the frequency spectrum has been analysed and potential cut off values have been identified the high-pass filters can be applied to the raw signal. Identification of the actual cut-off is a long debated issue, attempt to produce a quantifiable method to establish the cut-off value, such as residual analysis (Winter, 2005), the Jackson knee-method (Jackson, 1979) and the autocorrelation method (Challis, 1999) have been suggested, although no one technique has been found to be optimal. The above process could then be repeated following the application of different filter cut off selections to ensure the appropriate frequencies have been removed.

Removing Zero Offset

Prior to signal smoothing or filtering to remove signal corruption, the signal should be free from any zero offset. Recall that to remove any zero offset the signal mean is subtracted from each point in the signal. Not all acquired signals will have a zero offset, therefore it is important to plot the data and check whether offset correction is required. While attempting to correct a zero offset when it does not exist will not change the signal (as the signal mean will be zero), it will unnecessarily increase the amount of processing being completed.

To complete this process in MatLab you will need to input the following commands:

```
raw=xlsread('raw data.xls');  
  
% This command loads the raw data from an  
Excel file and creates a variable called 'raw'  
  
signal_mean=mean(raw);  
  
% This command calculates the signal mean  
  
signal_offset_corrected=raw-signal_  
mean;
```

% This command subtracts the mean from each point in the original signal.

To complete the process in excel you need to complete the following:

1. Enter the raw signal in column A
2. Enter the following formula in row B
 - a. $B1=A1-\text{mean}(A1:A4096)$
 - b. $B2=A2-\text{mean}(A1:A4096)$
 - c. $B3=A3-\text{mean}(A1:A4096)$ etc. for the duration of the signal.

N.B this example presumes the raw signal is contained in cells A1:A4096

Once this process has been applied the next stage of processing can be applied. Potentially, the signal may not require further filtering. Meticulous care during set up in areas shielded for signal corruption from electrical devices can yield signals that do not require much filtering. However, frequently further filtering will be required. The following sections provide an overview of filter structure and implementation.

Designing Filters

Recall that when considering signal filters there are two key classifications, the first is low pass filters which retain signal frequencies below the filter cut-off frequency and attenuate frequencies above the filter cut off frequency. The second

classification is high-pass filters which are filters which retain signal frequencies above the filter cut off frequency and attenuate frequencies below the filter cut off frequency. As high-pass filtering is applied prior to low-pass filters they will be addressed first.

The basic structure for filters is as follows:

$$X^1_{nT} = a_0 X_{nT} + a_1 X_{nT-T} + a_2 X_{nT-2T} + b_1 X^1_{nT-2T} + b_2 X^1_{nT-T}$$

X = Raw signal

X^1 = Filtered signal

nT = n th sample

$nT-T$ = $n-1$ th sample

$nT-2T$ = $n-2$ th sample

$a_0 \dots, b_2$ = filter coefficients.

In order to implement the above filter, the coefficients are required. The summed coefficients of a filter total one. Therefore the coefficients effectively weight each section of the filter and adjust the values to remove unwanted frequencies. The coefficients can either be obtained online, from a textbook, or calculated. In order to calculate the coefficients for filters there are some parameters which need to be established first. These include:

1. The sampling frequency during signal acquisition?
2. The desired cut off frequency?
3. The number of bi-directional passes will the filter make?

The first two of these parameters are fairly intuitive, the frequency of which the data was obtained and the desired point at which filtering should start. The third parameter is less obvious,

what is a ‘bi-directional pass’ and why would this be completed more than one time? Simply put, a bi-directional pass is where the direction of the filter is reversed and applied to the filtered producing a second filtered signal. Adapting the above equation results in the following equation:

$$X^2_{nT} = a_0 X^1_{nT} + a_1 X^1_{nT+T} + a_2 X^1_{nT+2T} + b_1 X^2_{nT+2T} + b_2 X^2_{nT+T}$$

X = Raw signal

X^1 = First filtered signal

X^2 = Second filtered signal

nT = n th sample

$nT+T$ = $n+1$ th sample

$nT+2T$ = $n+2$ th sample

$a_0 \dots, b_2$ = filter coefficients

The purpose of this process is twofold. Firstly filters introduce a delay in the signal. By reversing the filter and reapplying the filter, this lag is corrected therefore removing any errors in time to events/changes within the signal.

Secondly, the frequency at which the filter begins to attenuate the signal is not one specific frequency. The attenuation of frequencies by the filter increases over a range, this transition range is known as the ‘roll-off’. Increasing the number of bidirectional passes reduces the transition range. An ideal filter would not change the signal at all before the cut off frequency, and immediately start to filter signals above the cut off frequency; unfortunately this is not the case. The effectiveness of signal filter performance resulting from varying parameters, such as the order, is outside the scope of this chapter, for a review see (Robertson & Dowling, 2003).

To calculate the filter coefficients the first stage is an adjustment to the cut off frequency:

$$f_c Adjusted = f_s / 2 - f_{hp}$$

Where f_s = the sampling frequency, and f_{hp} = the cut off of the high-pass filter.

The angular frequency is then calculated:

$$\dot{u}_c = \left(\tan \left(\delta f_c Adjusted / f_s \right) \right)$$

The angular frequency is adjusted for the number of bidirectional passes:

$$\dot{u}_c Adjusted = \dot{u}_c / \sqrt{\left(2^{1/(2xn)} - 1 \right)}$$

Where n = the number of passes the filter makes over the data e.g. one bi-directional pass equates to $n = 2$.

For the coefficients the calculations are as follows:

$$K = 2\dot{u}_{c Adjusted}$$

$$K_2 = \dot{u}_c^2 Adjusted$$

$$a_0 = \frac{K_2}{(1 + K_1 + K_2)} \quad a_1 = -2a_0 \quad a_2 = a_0$$

$$b_1 = -(1 / K_2 - 1)^2 2a_0 \quad b_2 = 1 - (a_0 + a_1 + a_2 + b_1)$$

For a detailed review of high pass filter coefficient design see (Murphy & Robertson, 1994). Once the coefficients have been calculated, the filter can be applied to the signal.

MatLab Code for Applying a High-Pass Filter With a 40 Hz Cut-Off

When using MatLab the coefficients are automatically calculated. However, MatLab uses a normalised cut-off frequency. Therefore prior to inputting the signal parameters the cut-off frequency must be converted to normalised frequency using the following command:

```
Fnorm = 40 / (1024/2);
```

% Where 40 = the desired cut-off frequency and 1024 = the sampling frequency.

```
[b,a]=butter(2,Fnorm,'high');
signal_hp = filtfilt(b,a, signal_offset_corrected);
```

% The 'butter' command applies a high-pass 2nd order Butterworth filter, representing one pass over the signal. The 'filtfilt' command doubles the order producing a 4th order filter with a 40 Hz cut off frequency. The 'signal_offset_corrected' variable is obtained from the removing zero-offset correction section previously applied.

Excel Formulae for Applying a High-Pass Filter with a 40 Hz Cut-Off

To complete the process in excel the coefficients must first be calculated. For an overview of how to do this see table one.

After the coefficients have been calculated the filter can then be applied in excel. Table 1 represents a section of an excel spread sheet below that displayed in Table 2. Note the addition of the dollar sign '\$' in the cells. The '\$' fixes the cells that the formulae refers to, this allows the formula to be copied to additional cells without changing the cells the formula refers to. Note that the number of passes equals two, which is one in each direction or one bi-directional pass.

Table 1. Calculating high pass filter coefficients in Excel

	A	B
1	Sample frequency	1024
2	Cut off frequency	40
3	Number of passes	2
4		
5	Adjusted cut off	=B1/2-B2
6	\dot{E}_c	= (TAN((B5*PI())/B1))
7	\dot{E}_c Adjusted	=B6/(SQRT(2^(1/(2*B3))-1))
8		
9	K	=2*B7
10	K_2	=B7^2
11	a_0	=B10/(1+B9+B10)
12	a_1	=-2*B11
13	a_2	=B11
14	b_1	=(1/B10-1)*(2*B11)
15	b_2	=1-(B11+B12+B13+B14)

In Table 3 the filter is applied twice, achieving a bidirectional pass over the data resulting in zero-lag filter out put. Obviously a genuine signal would be much longer; however the basic process and Excel structure is essentially displayed. To create a useable spread sheet all that is needed is to extend the middle of the above table by increasing the number of cells with the formula included i.e. rows 20-23.

It should be noted that sometimes the high-pass filter does not always completely remove

a zero offset to the signal. In the case that this occurs, all that is needed to correct the signal is to simply subtract the mean of the total filtered signal from each data point within the filtered signal (as previously detailed in ‘removing zero offset’). This process will remove the zero offset and produce a signal that is symmetric about zero (see figure one). When developing a signal processing algorithm it is paramount to continuously check on the effect on the signal. While there are certain rules which must be followed, e.g. rectifying before applying a low-pass filter, there are also processes which can be applied at different times during the algorithm. For example the signal mean can be subtracted before or after the high-pass filter is applied, provided it is applied before rectification. It is only by plotting the signal that the appropriate next stage can be identified. An example of ‘noisy’ data filtered using the above techniques in Microsoft Excel is shown in figure two

Root Mean Square

The RMS of a signal is a technique of taking a portion of a signal, known as a *linear envelope* or *window* and converting all the signal values, both positive and negative, into a positive value representative of the signal power. The window length should be based on the speed of the movement and the length of the signal. Small windows will allow detection of rapid changes in EMG, yet will not result in much smoothing or the original EMG signal. Larger windows result in increased smoothing of the signal, but with the cost of loss of the original signal trends. Another approach is to combine the benefits of small and large windows by overlapping the windows i.e. including data points in more than one window which moves along the signal from start to finish.

To obtain the RMS the values within the window the square root of the averaged, squared values is calculated using the following equation:

Table 2. Applying a low-pass filter in Excel (forwards direction)

	A	B
18	Raw Signal	=A18
19	Raw Signal	=A19
20	Raw Signal	=A20*b\$12+A19*b\$13+A18* b\$14+B19* b\$15+B18* b\$16
21	Raw Signal	=A21*b\$12+A20*b\$13+A19* b\$14+B20* b\$15+B19* b\$16
22	Raw Signal	=A22*b\$12+A21*b\$13+A20* b\$14+B21* b\$15+B20* b\$16
23	Raw Signal	=A23*b\$12+A22*b\$13+A21* b\$14+B22* b\$15+B21* b\$16
24	Raw Signal	=A24* b\$12+A23*b\$13+A22* b\$14+B23* b\$15+B22* b\$16
25	Raw Signal	=A25* b\$12+A24*b\$13+A23* b\$14+B24* b\$15+B23* b\$16

$$RMS = \sqrt{\left(\frac{\text{Sum of data points within window}}{\text{Length of window}} \right)^2}$$

To complete this process in MatLab you will need to input the following commands:

```
signal_windows=buffer(signal_hp,128);
```

% This command takes the original signal and creates an array of the signal with 128 data points in each column. Presuming the sampling frequency was 1024 Hz this would equate to windows approximately 12.5 msec long. To convert this into

a window four times as long overlapping by 75%, the command would change to:

```
signal_windows=buffer(signal_hp,512,384);
```

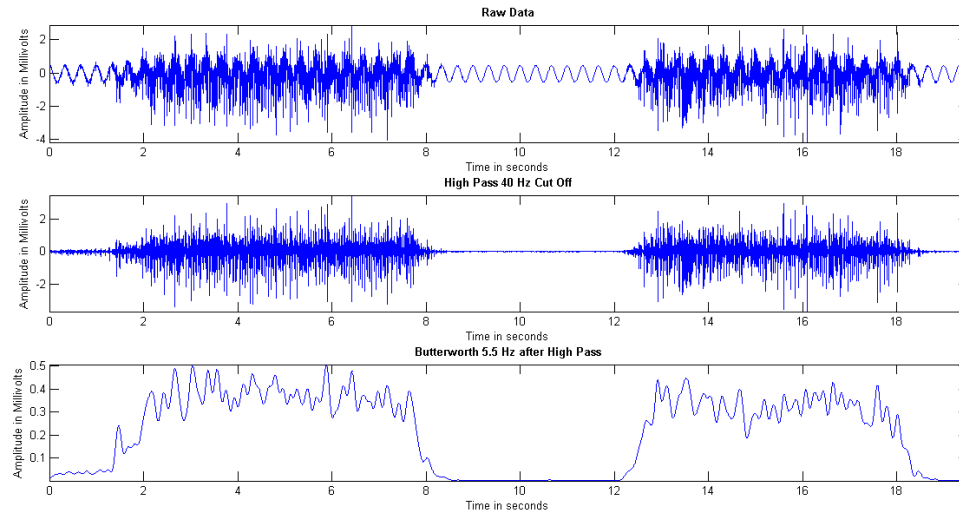
% NB There is no fixed rules for the size of the window or the amount of overlap, often parameter selection comes from plotting various window size and overlaps and establishing which best reflects the original signal.

```
RMS=zeros(1,length(signal_windows(1,:)));
```

Table 3.

	C
18	=B18*b\$12+B19* b\$13+B20* b\$14+C19* b\$15+C20* b\$16
19	=B19*b\$12+B20* b\$13+B21* b\$14+C20* b\$15+C21* b\$16
20	=B20*b\$12+B21* b\$13+B22* b\$14+C21* b\$15+C22* b\$16
21	=B21*b\$12+B22* b\$13+B23* b\$14+C22* b\$15+C23* b\$16
22	=B22*b\$12+B23* b\$13+B24* b\$14+C23* b\$15+C24* b\$16
23	=B23*b\$12+B24* b\$13+B25* b\$14+C24* b\$15+C25* b\$16
24	=B24
25	=B25

Figure 2.



% This command pre-allocates an array for the RMS values to be stored in. This is not an essential stage, but it is good practice to do so.

```
for i=1:length(signal_windows(1,:))
    RMS(i)= sqrt(mean(signal_
windows(:,i).^2));
end
```

% This command works along the array created by the ‘buffer’ command and calculates the RMS. The results are stored in the pre-allocated array created by the ‘zeros’ command.

To calculate the RMS without overlap in excel you need to complete the following:

1. Enter the raw signal in column A
2. Enter the following formula in row B
 - a. $B1 = \text{SQRT}(\text{mean}(A1:A128)^2)$
 - b. $B9 = \text{SQRT}(\text{mean}(A9:A136)^2)$
 - c. $B3 = \text{SQRT}(\text{mean}(A17:A144)^2)$ etc. for the duration of the signal.

With overlap column B changes to:

- a. $B1 = \text{SQRT}(\text{mean}(A1:A512)^2)$
- b. $B9 = \text{SQRT}(\text{mean}(A128:A640)^2)$
- c. $B3 = \text{SQRT}(\text{mean}(A256:A768)^2)$ etc. for the duration of the signal.

The RMS offers a form of signal processing which is easy to implement. However, if the signal contains noise that is corrupting the signal the RMS will not be able to remove the noise. Therefore in this instance further processing will be required. Recall that thus far the processing completed has removed any zero offset and attenuated low frequency noise components of the signal. The next stage is to deal with any high frequency noise components in the signal. Low-pass filters do not work effectively with signals symmetrical about the mean. Therefore before low-pass filters can be applied the signal must go through a process called *rectification*.

Rectification

Rectification is the process by which all the values below zero are removed. There are two techniques to achieve this aim.

1. **Half Wave Rectification:** This approach the values that equal less than zero are simply deleted. While this is very simple, it effectively halves the energy within the signal as half of the values are removed.
2. **Full Wave Rectification:** This approach takes each value, multiplies it by itself, then takes the square root of the answer i.e. takes the absolute value for each data point. This effectively changes all the negative values to positive values therefore creating twice as many positive values and therefore producing a signal with the same amount of energy as the original signal.

Rectifying Signals in MatLab

To complete full wave rectification in MatLab you will simply need to input the following command:

```
rectified_signal=signal_offset_cor-  
rected.^2;
```

Rectifying Signals in Microsoft Excel

1. Enter the raw signal in column A
2. Enter the following formula in row B
 - a. B1=A1^2
 - b. B9= A2^2
 - c. B3= A3^2 etc. for the duration of the signal.

Low-Pass Filters

Two commonly applied low-pass filters are the Butterworth filter and the critically damped filter, which are both based on the same equation as the high pass filter, though the coefficients are calculated differently.

First the correction factor for the number of bidirectional passes is required:

For a Butterworth filter this is:

$$C = \left(2^{(1/\text{number of passes})} - 1\right)^{0.25}$$

For a critically damped filter:

$$C = \left(2^{(1/(2 \times \text{number of passes}))} - 1\right)^{0.5}$$

Next the angular frequency of the coefficients:

$$\dot{u}_c = \frac{\left(\tan\left(\delta f_c / f_s\right)\right)}{C}$$

where:

f_c = the cut off frequency

f_s = the sampling frequency

The final difference between Butterworth and critically damped filter coefficients is the parameter 'K'.

For a Butterworth filter this is: $K = \sqrt{2\dot{u}_c}$

For a critically damped filter: $K = 2\dot{u}_c$

To calculate the coefficients:

$$K_2 = \dot{u}_c^2$$

$$a_0 = \frac{K_2}{(1 + K_1 + K_2)} \quad a_1 = 2a_0 \quad a_2 = a_0$$

$$K_3 = \frac{2a_0}{K_2}$$

$$b_1 = -2a_0 + K_3 \quad b_2 = 1 - 2a_0 - K_3$$

MatLab Code for Applying a Low-Pass Filter with a 5.5 Hz Cut-Off

To apply a low-pass filter in MatLab the follow code can be used:

```
lpcutoff=5.5/(1024/2);  
[b,a]=butter(2,lpcutoff,'low');  
signal_lp = filtfilt(b,a, signal_hp);
```

% Applies the low-pass Butterworth filter, representing one bidirectional pass over the signal. The process doubles the order producing a 4th order filter. The variable 'signal_hp' is obtained from the signal high-pass filtered in the section 'MatLab code for applying a high-pass filter with a 40 Hz cut-off'.

Excel Formulae for Applying a High-Pass Filter with a 5.5 Hz Cut-Off

The formulae to calculate these coefficients in Excel are displayed in the table three.

CONCLUSION

In summary this chapter has provided an insight in to the fundamental principles of filtering raw EMG signals using analogue filters and plotting both the filtered signals and the frequency spectrum. Often the use of 'black box' software prevents the user from truly understanding the underlying process completed when applying filters mathematical operations to biological signals. Without an appreciation of the mechanisms of the processes applied it is difficult to know when and how to accurately apply each stage of the filtering process. By working through this chapter and creating examples in Excel and MatLab the reader will be able to not only appreciate how the filters work, but will be able to create their own resources to process signals obtained in research and practice.

The filtering process previously described using was generated using MatLab 2013a with the signal processing toolbox. A combined recap of the code is displayed below with the results plotted in figure three.

MatLab Code for Signal Filtering

```
raw=xlsread('RMS');
```

% This command loads the raw data from an Excel file and creates a variable called 'raw'

```
signal_mean=mean(raw);
```

% This command calculates the signal mean

```
signal_offset_corrected=raw-signal_mean;
```

% This command subtracts the mean from each point in the original signal.

```
Fnorm = 40/(2000/2);
```

% Where 40 = the desired cut-off frequency and 1024 = the sampling frequency.

```
[b,a]=butter(2,Fnorm,'high');  
signal_hp = filtfilt(b,a, signal_offset_corrected);
```

% The 'butter' command applies a high-pass 2nd order Butterworth filter, representing one pass over the signal. The 'filtfilt' command doubles the order producing a 4th order filter with a 40 Hz cut off frequency. The 'signal_offset_corrected' variable is obtained from the removing zero-offset correction section previously applied.

```
signal_windows=buffer(signal_hp,128);
```

% This command takes the original signal and creates an array of the signal with 128 data points

Table 4. Low-pass filter coefficients

	A	B	C
1	Sample frequency	1024	
2	Cut off frequency	5.5	
3	Number of passes	2	
4			
5		Butterworth	Critically damped
6	Correction factor	$= (2^{1/B3}-1)^{0.25}$	$= (2^{1/(2*B3)}-1)^{0.5}$
7	\acute{E}_c	$= (\text{TAN}((B2*PI())/B1))/B6$	$= (\text{TAN}((B2*PI())/B1))/C6$
8			
9	K	$=\text{SQRT}(2)*B7$	$=2*C7$
10	K_2	$=B7^2$	$=C7^2$
11	K_3	$= (2*B12)/B10$	$= (2*C12)/C10$
12	a_0	$=B10/(1+B9+B10)$	$=C10/(1+C9+C10)$
13	a_1	$=2*B12$	$=2*C12$
14	a_2	$=B12$	$=C12$
15	b_1	$=(-2*B12+B11)$	$=(-2*C12+C11)$
16	b_2	$=1-(2*B12)-B11$	$=1-(2*C12)-C11$

in each column. Presuming the sampling frequency was 1024 Hz this would equate to windows approximately 12.5 msec long. To convert this into a window four times as long overlapping by 75%, the command would change to:

```
signal_windows=buffer(signal_offset_
corrected,512,384);
```

% NB There is no fixed rules for the size of the window or the amount of overlap, often parameter selection comes from plotting various window size

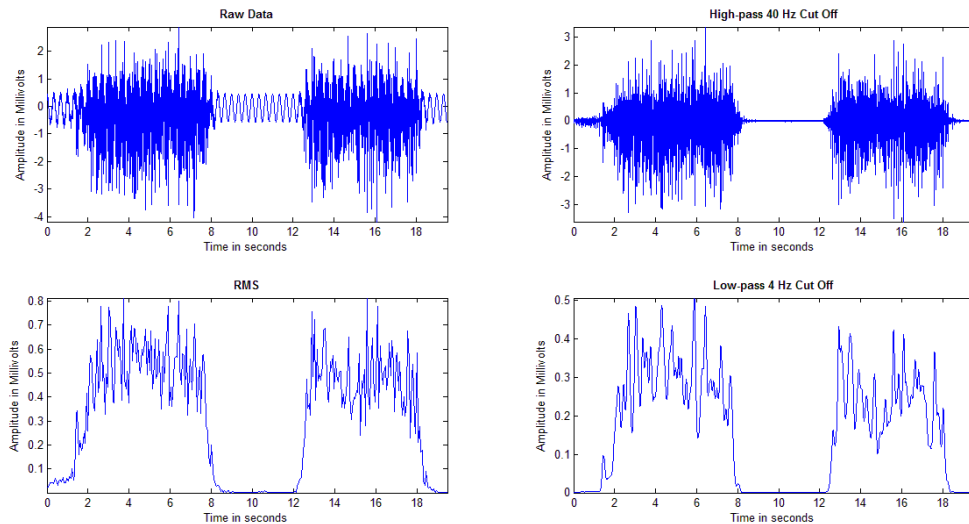
and overlaps and establishing which best reflects the original signal.

```
RMS=zeros(1,length(signal_wins
dows(1,:)));
```

% This command pre-allocates an array for the RMS values to be stored in. This is not an essential stage, but it is good practice to do so.

```
for i=1:length(signal_windows(1,:))
    RMS(i)=sqrt(mean(signal_
```

Figure 3.



```

windows(:,i).^2);
end
rectified_signal=signal_hp.^2;
lpcutoff=4/(2000/2);
[b,a]=butter(2,lpcutoff,'low');
signal_lp = filtfilt(b,a, rectified_
signal);

```

% Applies the low-pass Butterworth filter, representing one bidirectional pass over the signal. The process doubles the order producing a 4th order filter. The variable 'signal_hp' is obtained from the signal high-pass filtered in the section 'MatLab code for applying a high-pass filter with a 40 Hz cut-off'.

```
n=length(raw);
```

% Calculate the amount of data points in the signal

```

siglength=n/2000;
Xincrement=siglength/n;
Xscale=(0:Xincrement:siglength-Xin-
crement);

```

% Calculates the duration of the signal and the increment for the X axis

```
RMSn=length(RMS);
```

% Calculate the amount of data points in the signal

```

rmsXincrement=siglength/RMSn;
rmsXscale=(0:rmsXincrement:siglength-
rmsXincrement);

```

% Plotting the data, the following code plots the data as seen in figure two

```

subplot(4,1,1), plot(Xscale,raw)
title('Raw Data', 'FontWeight',
'bold')
axis tight
xlabel('Time in seconds')
ylabel('Amplitude in Millivolts')
subplot(4,1,2), plot(Xscale,siglap_
hp)
title('High-pass 40 Hz Cut Off',
'FontWeight', 'bold')

```

```
axis tight
xlabel('Time in seconds')
ylabel('Amplitude in Millivolts')
subplot(4,1,3), plot(rmsXscale,RMS)
title('RMS', 'FontWeight', 'bold')
axis tight
xlabel('Time in seconds')
ylabel('Amplitude in Millivolts')
subplot(4,1,4)
plot(Xscale,signal_lp)
title('Low-pass 4 Hz Cut Off',
'FontWeight', 'bold')
axis tight
xlabel('Time in seconds')
ylabel('Amplitude in Millivolts')
```

REFERENCES

Challis, J. (1999). A procedure for the automatic determination of filter cutoff frequency for the processing of biomechanical data. *Journal of Applied Biomechanics*, 15(3), 303–317.

Chu, E., & George, A. (2010). *Inside the FFT black box, serial and parallel fast Fourier transform algorithms*. Boca Raton, FL: CRC Press.

De Luca, C. J. (1984). Myoelectrical manifestations of localized muscular fatigue in humans. *Critical Reviews in Biomedical Engineering*, 11(4), 251–279. PMID:6391814

Haykin, S., & Liu, R. (2009). *Handbook on array processing and sensor networks*. Hoboken, NJ: John Wiley and Sons, Inc.

Jackson, K. M. (1979). Fitting of mathematical functions to biomechanical data. *IEEE Transactions on Bio-Medical Engineering*, BME-26(2), 122–124. doi:10.1109/TBME.1979.326551 PMID:761932

Kester, W. (2005). *The data conversion handbook*. Norwood, MA: Analog Devices, Inc.

Murphy, S., & Robertson, D. G. E. (1994). Construction of a high-pass digital filter from a low-pass digital filter. *Journal of Applied Biomechanics Biomechanics*, 10, 374–381.

Prutchi, D., & Norris, M. (2005). *Design and development of medical electronic instrumentation*. Hoboken, NJ: John Wiley and Sons, Inc. doi:10.1002/0471681849

Robertson, D. G. E., & Dowling, J. J. (2003). Design and responses of Butterworth and critically damped digital filters. *Journal of Electromyography and Kinesiology: Official Journal of the International Society of Electrophysiological Kinesiology*, 13(6), 569–573. doi:10.1016/S1050-6411(03)00080-4 PMID:14573371

Transnational College of LEX. (2006). *Who is Fourier? A mathematical adventure*. Language Research Foundation.

Winter, D. (2005). *Biomechanics and motor control of human movement* (3rd ed.). Hoboken, NJ: John Wiley and Sons, Inc.

ADDITIONAL READING

Palaniappan, R. (2010). *Biological Signal Analysis*. BookBoon.

Transnational College of LEX. (2006). *Who is Fourier? A Mathematical adventure*. Language Research Foundation.

Winter, D. (2005). *Biomechanics and Motor Control of Human Movement* (Third Edit.). John Wiley and Sons, Inc.

KEY TERMS AND DEFINITIONS

Amplitude: The amount of voltage between zero voltage and the signal peak.

Filter: A tool used to remove noise from a signal.

Frequency: The amount of times a repetitive signal pattern occurs.

Hertz: The amount of signal cycles/repetitions in one second.

Noise: Values from other sources being incorporated in to the acquired signal e.g. from nearby electrical equipment.

Period/Wavelength: The length of time taken for a signal to complete one cycle.

Rectification: The process of changing a signal from one with both positive and negative value to a signal with only positive values.

Roll-Off: The transition between an inactive and an active filter.

Signal: Values which represent physiological changes, e.g. the amount of muscle activity.

Window: A portion of the signal being analysed or a series of weighted values used to adjust a portion, or envelope, of a signal.

Zero Offset: The difference between the mean signal value and zero.

Section 2

EMG Signal Modeling and Signal Processing

Chapter 5

Modeling the Human Elbow Joint Dynamics from Surface Electromyography

Andrés Felipe Ruiz-Olaya
Antonio Nariño University, Colombia

ABSTRACT

Biomechanical modelling and analysis of human motion are main topics of interest for a number of disciplines, ranging from biomechanics to human movement science. There exist various experimental and theoretical techniques developed to model the biomechanics and human motor system. A classic way to characterize a system is done by perturbation analysis, through applying an external perturbation and the observation of changes in the dynamic of system. In literature, human joint dynamics has been studied mainly in relation to external perturbations. However, those perturbations interact with the natural human motor behaviour. This chapter describes an approximation for non-invasive biomechanical modelling of the elbow joint dynamics from electromyographic information. A case study presents results obtained aimed at deriving a relationship between the dynamic behaviour of the human elbow joint and Surface Electromyography (SEMG) information in postural control. A set of experiments were carried out to measure bioelectrical (SEMG) and biomechanics information from human elbow joint, during postural control (i.e. isometric contractions) and correlate them with mechanical impedance at elbow joint. Estimates of elbow impedance were obtained by applying torque perturbations to the forearm. The results demonstrate that it is possible to estimate human joint dynamics from SEMG. The obtained results can contribute to the field of human motor control and also to its application in robotics and other engineering applications through the definition, specification and characterization of properties associated with the human upper limb and strategies used by people to command it.

DOI: 10.4018/978-1-4666-6090-8.ch005

INTRODUCTION

It is well known phenomena that human skeletal muscle has elastic-like and viscous-like properties, which change widely with the level of muscle activation. Also, the human neuromuscular control system has highly developed self-adaptive properties. The dynamic response of a limb is largely insensitive to external forces in a wide range. It also appears that adaptive compensation for external changes occurs very rapidly in relation to the dominant dynamics of the limb/joint system and the dynamic behavior may include a feedback and a feedforward component (van der Helm et al., 2002). In literature, numerous studies have modeled the dynamic behavior of human body segments and joints as mechanical impedance (Dolan et al., 1993; Tsuji et al., 1995). Mechanical impedance in this context may be defined as the dynamic relationship between forces and position variations, and can be characterized by its stiffness, viscosity and inertia (which are functions of the muscle condition).

Measurement and understanding of these dynamics is important in several areas such as rehabilitation engineering, biomechanics, basic motor control research, bionics, humanoid robotics, among others (Tanaka et al., 2007). This understanding about the human limb/joint dynamics permits to develop bio-inspired control strategies to be implemented in new devices, such as prostheses and orthoses and to explore new therapies in disabled people by pathologies and disorders affecting the human motor system.

Human joints dynamics may be approximate as mechanical impedance (Dolan, 1993). Modulation of mechanical impedance provides the basis for several theories in human motor control such as the α -model and λ -model equilibrium point theories, the virtual trajectory theory, and dynamic interaction in manipulation, (Hogan, 1985). The general finding is that increasing joint impedance, both through co-contraction and reflex modulation, stabilises the limb to external force fields.

Quantification of the mechanical impedance of the human joints and the muscle-skeletal system has a long history (Kearney & Hunter, 1990). The mechanical impedance of a system is best described by its transfer function, which can have been estimated using continuous perturbations. In fact, in literature human joint dynamics has been studied mainly in relation to external perturbations (Acosta et al., 2000; Franklin et al., 2003; Xu & Hollerbach, 1999); however, such perturbations interact with the natural behaviour of the motor control system and disturb the task under study (Kirsch et al., 1994). It will be beneficial to estimate such mechanical impedance in a non-invasive way; in this context, electromyography may provide such non-invasive way. Recently, researchers have been studying the relationship between the Surface Electromyography (SEMG) and torque produced about a joint, as a means of non-invasively estimating the joint/musculoskeletal dynamics (Bru & Amarantini, 2008; Clancy et al., 2012).

This chapter describes a biomechanical modelling technique from EMG data to estimate the elbow joint dynamics. A detailed Case Study shows a set of experiments carried out to correlates SEMG to elbow joint dynamics, i.e. mechanical impedance. In those experiments, joint posture was disturbed by applying an external torque about the joint, and the resulting change in joint angle was measured along the EMG of muscles involved in joint movement. Specifically, EMG signals were measured from human agonist and antagonistic muscles at elbow joint level. Later, it was used a mathematical model to correlates SEMG signals to mechanical impedance. The elbow joint dynamic system was approximated with a second-order model. The elbow joint system is of much higher order; however, we were interested in the modulation of stiffness and damping using EMG data and not in their exact values. A direct estimate of stiffness and damping were required to quantify the magnitude of impedance modulation and to correlates EMG and imped-

ance. The methods applied in the present study cannot distinguish between the contributions of intrinsic muscle properties and spinal reflexes to the overall joint impedance.

BACKGROUND

Electromyography basically consists of the acquisition, record and analysis of the electric activity generated in nerves and muscles, through the utilisation of surface electrodes, thin-wire electrodes or implanted electrodes (De Luca, 2003). SEMG is a technique to measure muscle activity noninvasively using surface electrodes placed on the skin overlying the muscle. In literature, there are a lot of works to determine the scope of SEMG utility, its benefits and risks, and the extent to which SEMG techniques vary, and to assess SEMG's strengths and weaknesses for specific clinical and research applications (Kleissen et al., 1998).

Measurements extracted from SEMG provide valuable information about the physiology and muscle activation patterns. The information obtained from EMG reflects the forces that will be generated by the muscles and the intervention timing of motor commands (De Luca, 1997). For instance, a number of studies have investigated the relationship between surface electromyography (EMG) and torque exerted about a human joint. The relation of surface EMG to torque makes EMG an attractive alternative to direct muscle tension measurements, necessary in many physical assessments.

The dependence of the recorded EMG signal and muscle tension on mutual physiological factors inspires on-going research work to develop mathematical models relating EMG to torque and joint dynamics. The experimental studies have explored both linear and nonlinear models to achieve better accuracy. Some researchers have even built complex models that describe the details of muscles, however little or no improvement is seen in doing so.

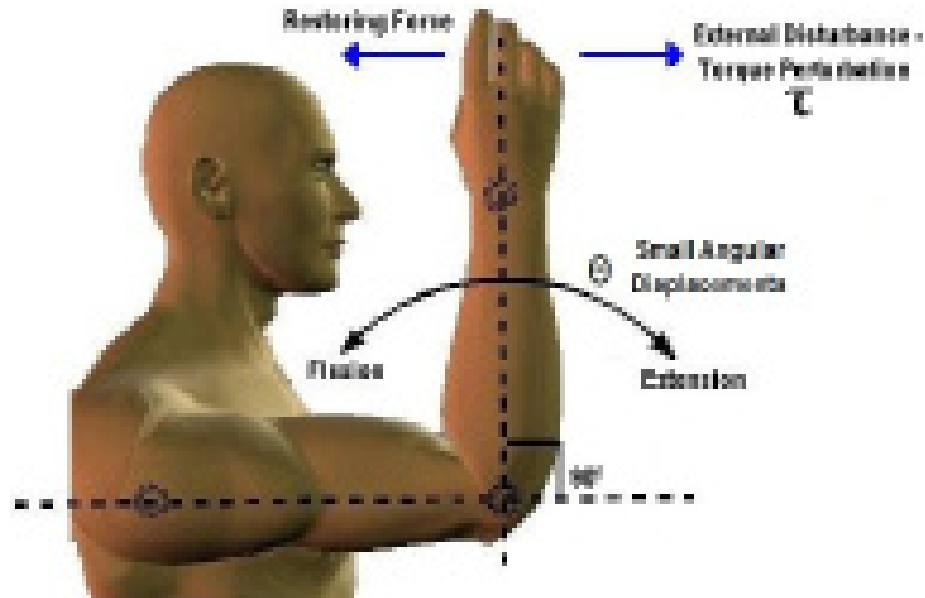
Modelling of the complex relationship between muscular activity and biomechanics parameters like torque and joint dynamics have been approached in two different methods; a priori (morphological) and a posteriori (black box) type of modelling techniques. The morphological modelling technique involves designing a model based on the physical characteristics of the system. The parameters are flexible and well adapted to the system itself. The drawback of this method is the large number of parameters that result in a high level of complexity. Additionally, it requires a thorough understanding of the system structure, while most of the times, the system is unknown and it is considered as a black box.

The black box type of modelling is referred to as system identification, and it is used to obtain a relationship between inputs and outputs, rather than determining the structure of the system. System identification is a study of the dynamics and physical behaviour of systems under external disturbances. Specifically, it is a set of standardized guides on building system mathematical models based on observations made on system reactions. The external data that can be manipulated and measured by the user are referred to as inputs and others as disturbances, even though most of the time their difference does not affect the modelling process. The measured/observed response of the system is referred to as its output (Ljung, 1999). Although this modelling technique is more practical than the first one, the results require careful interpretation and validation with the physical concepts.

MODULATION OF MECHANICAL IMPEDANCE IN HUMAN JOINTS

Several works on human motor control have demonstrated that when humans are subjected to a force field that systematically disturbs arm motion they are able to recover their original kinematic patterns, (Shadmehr & Mussa-Ivaldi,

Figure 1. Small-amplitude random perturbations to quantify the dynamic behaviour of the human elbow joint. An external torque disturbance (τ) generated small displacements (θ)



1994). This is accomplished by the adaptation of torques at their joints to compensate for the perturbing forces, (DeBicki & Gribble, 2004). When the perturbation force is abruptly removed, they exhibit error due to adaptation. Thus, there is a basic compensation and learning mechanism that exploits the viscoelastic properties of the neuromuscular system. The learning process is implicated in the development of internal models in the cerebellum, (Kawato, 1999).

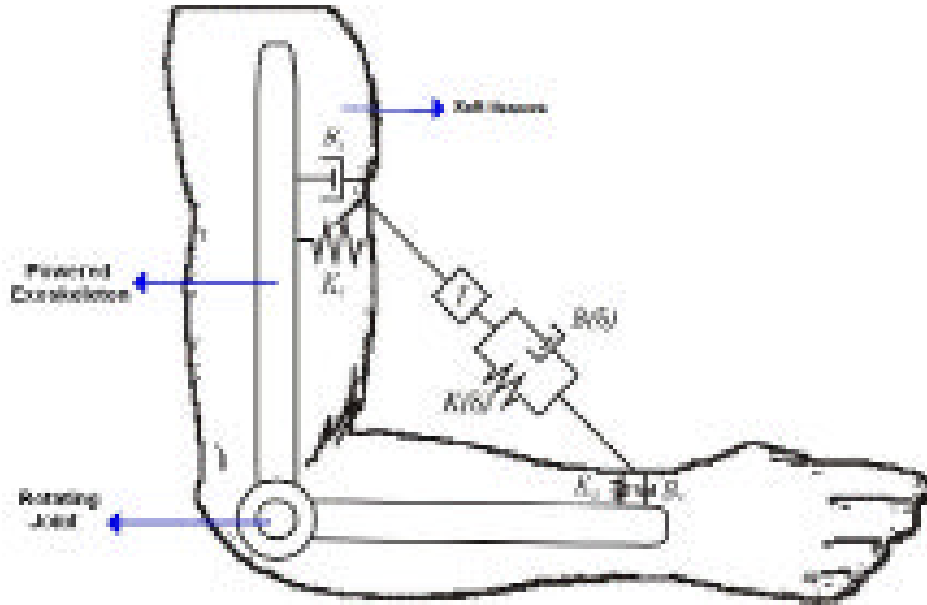
There are different theories about the neural control of human motion that have proposed different types of control models to understand the behaviour of the motor system, (Tsuji et al., 1995; Kawato, 1999). Several hypotheses suggested separating adaptation into two components: (1) a peripheral adaptation involving gain settings and dynamic control of the peripheral postural control system, and (2) a central prediction of input characteristics and a prefitting command signals for compensation.

The Central Nervous System (CNS) avoids the kind of complex computation involved in

motor control through the viscoelastic properties of neuro-muscular system, the muscles and the reflex loops. This viscoelasticity is able to generate restitution forces against external perturbations and may be considered as a control gain in the peripheral feedback. Humans can tune viscoelasticity by regulating the level of muscle co-contraction and the reflex gain. Control of the mechanical impedance (i.e. joint stiffness, viscosity and inertia) of the neuromuscular system is a form of adaptive behaviour that the CNS uses to accommodate perturbations from the environment, (Hogan, 1984).

In the human motor control field, to quantify mechanical impedance, small-amplitude random perturbations (zero mean) can be applied about the flexion-extension rotation axis at specific muscle contraction levels, such as showed in Figure 1, where an external disturbance (τ) is applied to elbow joint and a restoring force is generated. The relation between small displacements (θ) of joint system and the external torque (τ) associated with such displacements can be represented by a

Figure 2. Contribution of passive structures and elbow joint dynamics to the overall joint impedance. K_s and B_s denote the stiffness and viscosity of soft tissues.



linear transfer function which is usually named the mechanical impedance Z .

Under external perturbations, the intrinsic mechanical response of muscle is immediate. On the other hand, reflex responses and other responses that act by way of changes in muscle activation can only produce force after some delay with respect to the movements that trigger them. Using a simple linear control system, it is explained here how the components of the control system influence the mechanical impedance. The model is nonlinear and varies depending on factors such as torque bias and posture. Thus, in order to fit the data to a second-order linear model must be specified an operating point. The operating point consists of constant posture, constant force and non-fatiguing contractions for a particular task. Parameters in the model change as the operating point changes. Reflex gain also increases in parallel with muscle activation provided that the contraction is well below maximal. The linear model for the human elbow joint can be defined by the linear equation in 1.

$$\tau(t) = I \frac{\partial^2 \theta(t)}{\partial t^2} + B(\delta) \frac{\partial \theta(t)}{\partial t} + K(\delta) \theta(t) \quad (1)$$

where δ represents the operating point of the system. Equation (1) is useless when the operating point vary in a considerable way. For a more exact model, it could be required to account for the contribution of passive structures at the joint, while maintaining the simplicity of the model such as showed in figure 2, where K_s and B_s denote the stiffness and viscosity of soft tissues (skin, fat, fibrous tissues, etc.).

The visco-elastic properties of the human arm and joints vary in a wide range, (Zhang and Rymer, 1997; Stroeve, 1999). The relationship between the neural input to a muscle and its subsequent mechanical behaviour is highly complex. For a given neural input the contractile force of a muscle depends on the length of the muscle, its velocity of shortening, the type of muscle, its state of fatigue, and its history of exercise (or of

Modeling the Human Elbow Joint Dynamics from Surface Electromyography

Table 1. Factors that influence surface EMG (from Farina et al., 2004)

Factors That Influence the Surface EMG		
Nonphysiological		
	Anatomic	<ul style="list-style-type: none"> • Shape of the volume conductor • Thickness of the subcutaneous tissue layers • Tissue inhomogeneities • Distribution of the motor unit territories in the muscle • Size of the motor unit territories • Distribution and number of fibers in the motor unit territories • Length of the fibers • Spread of the endplates and tendon junctions within the motor units • Spread of the innervation zones and tendon regions among motor units • Presence of more than one pinnation angle
	Detection System	<ul style="list-style-type: none"> • Skin-electrode contact (impedance, noise) • Spatial filter for signal detection • Interelectrode distance • Electrode size and shape • Inclination of the detection system relative to muscle fiber orientation • Location of the electrodes over the muscle
	Geometrical	<ul style="list-style-type: none"> • Muscle fiber shortening • Shift of the muscle relative to the detection system
	Physical	<ul style="list-style-type: none"> • Conductivities of the tissues • Amount of crosstalk from nearby muscles
Physiological		
	Fiber membrane properties	<ul style="list-style-type: none"> • Average muscle fiber conduction velocity • Distribution of motor unit conduction velocities • Distribution of conduction velocities of the fibers within the motor units • Shape of the intracellular action potentials
	Motor unit properties	<ul style="list-style-type: none"> • Number of recruited motor units • Distribution of motor unit discharge rates • Statistics and coefficient of variation for discharge rate • Motor unit synchronization

electrical stimulation) amongst others. However, one fundamental observation is that the neural input to a muscle simultaneously determines the force and the stiffness of the muscle, i.e. its resistance to stretch.

ELECTROMYOGRAPHY FOR MODELLING THE HUMAN MOTOR SYSTEM

The contraction of muscle fibers generates electrical activity that can be measured by electrodes affixed to the skin surface on top of the muscle group. The recorded spikes of electrical activity

are referred to as the electromyography signal or “raw” EMG. The surface EMG signal recorded using surface electrodes that monitor the activity of multiple muscle fibers can be well modelled as a zero-mean time-varying stochastic process. Motor units are the smallest functional muscle group. It is observed that the standard deviation of the raw EMG signal is monotonically related to the number of the activated motor units and the rate of their activation. This standard deviation is used to approximate the magnitude of the muscular electrical activity referred to as EMG amplitude (Clancy & Hogan, 1997).

A number of studies have investigated the relationship between surface electromyography

(EMG) and torque exerted about a joint (Bru & Amarantini, 2008; Clancy et al., 2012). The relation of surface EMG to torque makes EMG an attractive alternative to direct muscle tension measurements, necessary in many physical assessments. However, the complexity of the EMG signal origin has been a barrier for developing a quantitative description of this relation. Interpretation of SEMG information is not easy to be accomplished due to some difficulties. First of all, SEMG signals are time-varying and highly nonlinear. Secondly, in literature it is identified that EMG signal are affected by noises, such as ECG crosstalk, electromagnetic induction from power lines, and arm and cable movements (artifacts). Third, there are other factors such as proximal muscle interference, physiological conditions (e.g. fatigue), and skin impedance, among others. Finally, the activity level of each muscle for a certain motion is different between each person.

Furthermore, the SEMG signal is complicated to use since properties of muscles, the control scheme of the peripheral nervous system, and the characteristics of instrumentation used to detect the SEMG signal affect them. SEMG provides information on the “quality” of contraction, i.e., whether it is continuous, phasic, or clonic, and also the ability to compare the timing of activity of several muscles. These activities or events are usually dynamic and impossible to view because they occur too quickly or are due to the activity of a group of muscles.

De Luca categorized the factors that effect EMG signal and force into three groups: causative, intermediate and deterministic factors (De Luca, 1997). The causative factors are the basis of EMG signal and they are both intrinsic and extrinsic. The extrinsic factors are related to the electrode structure and its placement on the skin overlying the muscle. Such instances include the electrode configuration, location, and the orientation of detection surfaces relative to the muscle fibers. On the other hand, the intrinsic causative factors are related to the physiological, anatomical and

biochemical character of EMG signals. These factors can not be controlled, but their knowledge and understanding help with the accuracy of EMG interpretation.

Table 1 represents a summary of the known effects to EMG interpretation. The presence of subcutaneous fatty tissues becomes a significant factor, because the loss of the high frequency components reduces the spectrum of the EMG signal. Besides the stability of the position of the electrodes and the stability of the Motor Unit firing rate, the issue of crosstalk is always present. Crosstalk is defined as the interference pattern recorded from a distant muscle when the electrodes are intended to monitor another muscle.

In literature, researchers have been studying the relationship between the SEMG and torque produced about a joint, as a means of non-invasively estimating musculoskeletal load and the dynamics of joints (Clancy et al., 2012). In this context, it is estimated EMG amplitude from the EMG waveform, and then it is developed an EMG-torque model that include mains characteristics. Using advanced methods for estimating EMG amplitude have been shown to provide better EMG-torque estimates.

The most common technique of detection for EMG amplitude is the rectification process followed by a smoothing step. The recorded EMG signal may be described as the product of a zero-mean stochastic process with the time-varying EMG intensity. Therefore the intensity of the EMG signal (EMG amplitude) can be obtained by proper rectification and smoothing. The early researchers in the field studied and utilized non-linear analog circuits, such as a full wave rectifier and a low pass filter made of simple passive components (resistors and capacitors), to detect the signal. This method eventually led to the use of the statistical moving average mean absolute value (MAV) and the moving average root mean square (RMS), equations 3 and 4, respectively.

Moving Average Mean Absolute Value:

$$MAV = \frac{1}{n} \sum_{i=1}^n |x_i| \quad (3)$$

Moving Average Root Mean Square:

$$RMS = \sqrt{\frac{1}{n} \sum_{i=1}^n x_i^2} \quad (4)$$

where in both expressions n is the number of samples in each smoothing window of the moving average filter; and x_i is the signal being smoothed in the time-domain.

There are many applications where it is useful to quantify the tension exerted by the muscle group during several activities, however direct measurements are unnatural, invasive, expensive, and they may also not be possible presently. The assumption of torque being related to the nervous excitation of the individual muscle or the muscle group, relates torque to the magnitude of electrical muscle activity (EMG signal). A relation between EMG and torque simplifies the situation, because EMG is readily obtained by either surface or wire electrodes depending upon whether the muscle group or individual muscle measurements are needed. Although many studies have made a great impact in the EMG field, there is no consensus on a standardized set of models that relate a specific muscle (muscle group) to tension (torque).

The development of a general prediction model has been less successful, perhaps due to variations in muscle composition. However, different procedures used to record and to analyze EMG also need to be considered when determining the relationship between muscular forces and the EMG signal. Several investigators have agreed that it is required to incorporate the control strategy for the muscles being investigated, including: the force generation rate, joint angle, muscle length, and muscular coactivation. It is also determined that changes in recording procedures, including

variations in electrode placement, recording configuration and limb position, significantly alter the EMG-torque relationship.

CASE STUDY: FEASIBILITY OF ESTIMATING HUMAN ELBOW JOINT DYNAMICS FROM MYOELECTRIC DATA IN POSTURAL CONTROL

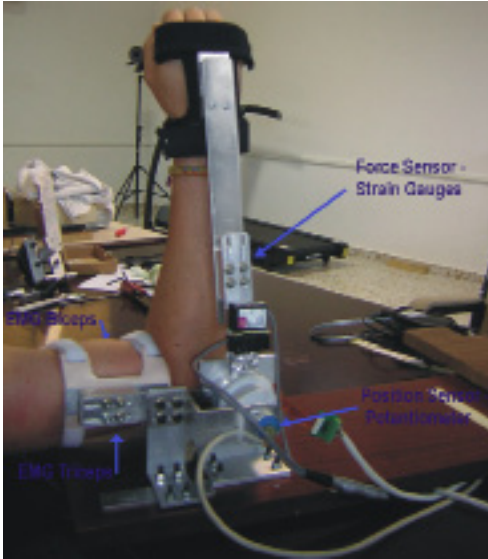
The protocol and experiments were designed to identify and characterise the human elbow joint dynamics in terms of mechanical impedance during a postural task. Moreover, it was obtained the EMG activation patterns in the adaptation process under dynamic conditions (torque perturbations).

Apparatus and Experimental Protocol

Four healthy adult volunteers (mean age 28 ± 3 , mean height 1.73 ± 0.04 m) were instrumented with surface EMG electrodes following the SENIAM recommendations (<http://www.seniam.org>). Two upper arm muscles were measured: the flexor (biceps brachii) and extensor (triceps brachii long head) muscles involved in the elbow joint movement. An experimental platform described in (Ruiz et al., 2008), was coupled to the upper limb of the subject. This platform permits to apply mechanical perturbations at elbow joint while simultaneously it is acquired bioelectric and biomechanical signals. Figure 3 show the experimental platform coupled to the upper limb of one subject.

Subjects produced constant-posture, non-fatiguing, force-varying contractions about the elbow while torque and biceps/triceps EMG were recorded. At one specific time instant, the experimental platform applied unexpectedly random torque perturbations on the forearm. Subjects were instructed to maintain the forearm posture while resisting external perturbations. In this case the

Figure 3. Experimental platform for characterization of mechanical impedance at elbow joint level



elbow joint does not move, i.e. a fixed position is being maintained, then the setpoint of the velocity feedback is zero and the setpoint of the position feedback is the equilibrium position. The feedback damping and stiffness will act to restore the joint to this state. Five repetitions were chosen for each experimental session and data were sampled at 1 kHz for biomechanical variables (kinetics and kinematics) and for the SEMG. In last trial, it were measured the SEMG of muscles to obtain the MVC (maximum voluntary contraction).

Data Analysis

Acquired signals were rectified, averaged, and smoothed. The kinematics and kinetics data were filtered through a four-pole Butterworth filter with a cut-off frequency of 10 Hz. Surface EMG signals were normalized respect to the MVC and were rectified and the envelope of the EMG signals extracted using a low pass filter with a cut-off frequency of 10 Hz. It was used a 5th order Butterworth filter for this propose. EMG

amplitude estimation was accomplished using its RMS magnitude:

$$RMS = \sqrt{\frac{1}{n} \sum_{i=1}^n x_i^2} \quad (5)$$

where x_i is the voltage value in the i -sample and n is the number of samples of the segment. The recorded data set was subdivided into smaller data sets. Moreover, individual “windows” overlap in time. Whole data set was separated in windows of 1024-samples length. There was overlapping of 128 samples with the adjacent windows. For each window, the elbow joint parameters, i.e. the mechanical impedance was estimated. Windows were overlapped to identify time trends and variations of impedance parameters. Figure 4 shows the recorded signals in an experimental section for one subject.

EMG to Elbow Joint Dynamics Relationship

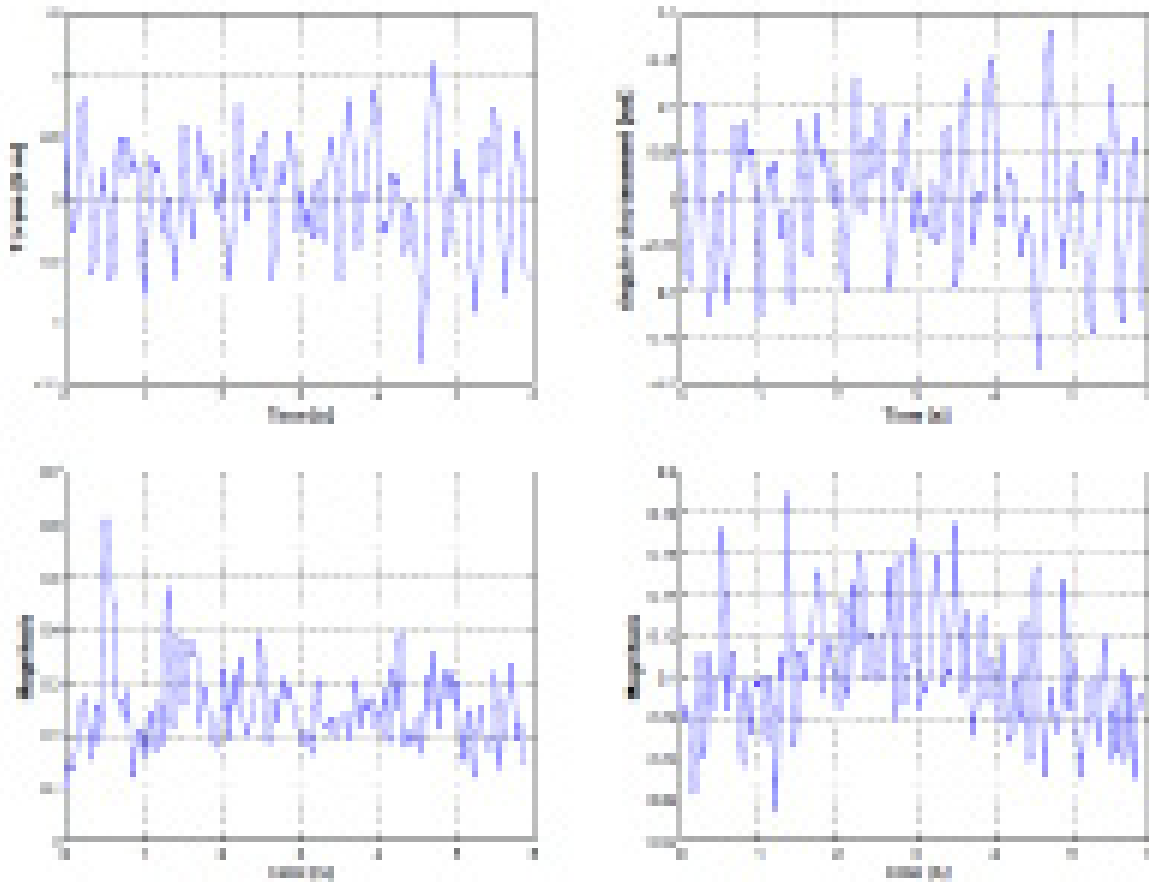
For experimental conditions that involve quasi-static and postural tasks, parameters are function of the EMG amplitude estimations (\hat{s}_E, \hat{s}_F). Linear second-order equation that relates EMG amplitude and angular displacement with changes of generated torque in joint can be modelled as:

$$\Delta\tau = I \cdot \Delta\ddot{\theta} + B(\hat{s}_E, \hat{s}_F) \cdot \Delta\dot{\theta} + K(\hat{s}_E, \hat{s}_F) \cdot \Delta\theta \quad (6)$$

where \hat{s}_E is the estimation of the EMG amplitude of extensor muscles, \hat{s}_F is the estimation of the EMG amplitude of flexor muscles, $\Delta\theta$ is the variation of angular displacement in the joint, $\Delta\tau$ is the variation of generated torque in the joint, $K(\hat{s}_E, \hat{s}_F)$ is the stiffness function, $B(\hat{s}_E, \hat{s}_F)$

Modeling the Human Elbow Joint Dynamics from Surface Electromyography

Figure 4. Recorded signals of one subject that correspond to torque (top, left), angular displacement (top, right), filtered-rectified EMG biceps brachii (bottom, left) and filtered-rectified EMG triceps brachii (bottom, right)



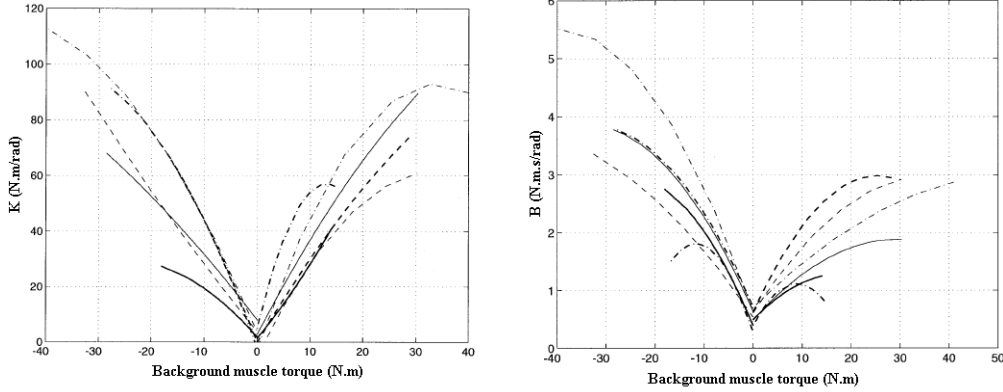
is the viscosity function and I is the inertial parameter.

As have been showed in literature, during an isometric contraction in which a subject voluntarily increases or decreases the joint torque by changing muscle activation, joint viscoelasticity has been shown to increase in parallel with joint torque, (Zhang and Rymer, 1997). Figure 5 shows values reported in literature related to joint viscoelasticity.

Thus, to evaluate joint viscoelasticity during the postural (isometric condition) experiments carried out, it was used previous studies which had suggested a linear relation between surface

EMG activity and joint torque and joint stiffness, (Osui et al., 2004). They defined a parameter called IMCJ (index of muscle co-contraction around the joint). The IMCJ was defined as the summation of the absolute values of agonistic and antagonistic muscle torques around the joint and computed from the linear relation between surface EMG and joint torque. IMCJ around elbow joint can be expressed as the equation 3, (Osui and Gomi 1999; Osui et al., 2004). s_{F1} and s_{E1} are the surface EMG activity of the elbow monoarticular flexor and extensor, respectively, and s_{F2} and s_{E2} denote

Figure 5. Magnitudes of elbow joint viscoelasticity in function of torque for isometric contractions. Adapted from (Zhang and Rymer, 1997)



surface EMG activity of bi-articular flexor and extensor, respectively.

$$\text{IMCJ} = a_1 s_{F1} + a_2 s_{E1} + a_3 s_{F2} + a_4 s_{E2} \quad (7)$$

In literature, human arm visco-elastic parameters are function of the muscular activation. For experimental conditions that involve isometric, quasi-static and postural tasks, it was validate the stiffness and viscosity parameters modelled as linear functions of the EMG amplitude estimations (\hat{s}_E, \hat{s}_F). Thus, it could be defined relations in equations 8 and 9.

$$B(\hat{s}_E, \hat{s}_F) = b_e \cdot \hat{s}_E + b_f \cdot \hat{s}_F \quad (8)$$

$$K(\hat{s}_E, \hat{s}_F) = k_e \cdot \hat{s}_E + k_f \cdot \hat{s}_F \quad (9)$$

Thus, as presented in equation 6, there is a second-order relationship involving EMG information in the visco-elastic parameters. Starting from equation 6, it were used $\Delta\theta$ and $\Delta\tau$ to estimate K, B and I. Next, it were used the EMG amplitude calculated as well as K and B values to correlates the information, using linear least squares.

Results

Figure 6 presents the estimation of K and B respectively, for all four subjects. Such parameters were obtained after calculating individual parameters of the overlapped windows.

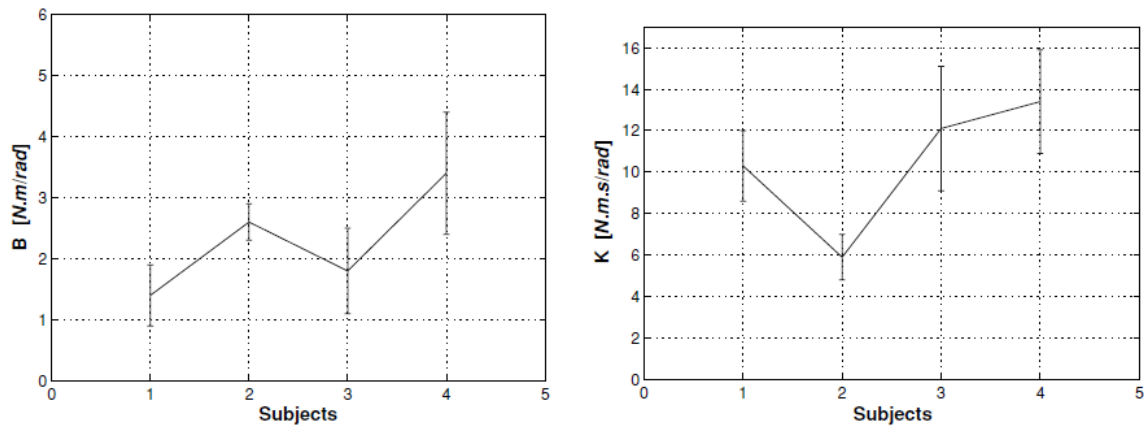
Estimated values in Figure 6, there are approximately constant parameters. Variations arise from the torque modulation generated by subjects in order to maintain the postural task. It were obtained magnitudes in the range of 2.5 a 4.7 N.m.s/rad for viscosity and 5.3 a 13.1 N.m/rad for stiffness parameters. Those values are in the range found in literature.

FUTURE RESEARCH DIRECTIONS

In order to obtain more accurate models of the joint dynamics, it is required to include the non-linearities and reflexes involved (soft tissues, muscular spindles, etc.).

The methods described in case study cannot distinguish between the contributions of intrinsic muscle properties and spinal reflexes to the overall joint impedance. It is required to implement experimental methods to identify those contributions.

Figure 6. Estimated parameters of viscosity (left side) and stiffness (right side) for all subjects



A future research direction relates to identify joint dynamics in execution of movement. SEMG may provide valuable information to reach this purpose.

CONCLUSION

The mechanical impedance of a system is best described by its transfer function, which can only be estimated using perturbations. However, those perturbations interact with the natural behaviour of the system being analyzed. In biomechanical modelling, it is useful to obtain a non-invasive technique for modelling purposes. This chapter presented the electromyography for biomechanical modelling of human elbow joint. A Case Study described a specific study to obtain the modulation and prediction of stiffness and damping using EMG data. Experiments carried out aimed to approximate the behavioural characteristics of the human elbow joint system by some mathematical expression. The compact and simple model presented in the Case Study was enough to characterize the main factors relating articular dynamics with muscular activation. In this approach, a second-order, linear model described the relationship between joint dynamics and position

well, provided that the position input was limited to small perturbations around a fixed mean position. The parameters of the second-order model varied strongly with the mean position, the level of background contraction, and the size of the perturbations.

The results presented in this chapter provide information to the field of human motor control and also to its application in robotics and other engineering applications. Thus, through the characterisation of mechanical properties associated with the human joints as well as strategies used by human beings to command it, exist a direct application to control devices based on EMG in a biologically inspired way, i.e. biomimetic control.

REFERENCES

Acosta, A. M., Kirsch, R. F., & Perreault, E. J. (2000). A robotic manipulator for the characterization of two-dimensional dynamic stiffness using stochastic displacement perturbations. *Journal of Neuroscience Methods*, 102(2), 177–186. doi:10.1016/S0165-0270(00)00307-1 PMID:11040414

- Bru, B., & Amarantini, D. (2008). Influence of sporting expertise on the EMG–torque relationship during isometric contraction in man. *Computer Methods in Biomechanics and Biomedical Engineering*, *11*(1), 43–44. doi:10.1080/10255840802296806
- Buchanan, T. S., Lloyd, D. G., Manal, K., & Bessier, T. F. (2004). neuromusculoskeletal modeling: estimation of muscle forces and joint moments and movements from measurements of neural command. *Journal of Applied Biomechanics*, *20*(4), 367–395. PMID:16467928
- Clancy, E. A., Bida, O., & Rancourt, D. (2006). Influence of advanced electromyogram (EMG) amplitude processors on EMG-to-torque estimation during constant-posture, force-varying contractions. *Journal of Biomechanics*, *36*(14), 2690–2698. doi:10.1016/j.jbiomech.2005.08.007 PMID:16243341
- Clancy, E. A., Lukai, L., Liu, P., & Moyer, D. V. Z. (2012). Identification of constant-posture EMG–torque relationship about the elbow using nonlinear dynamic models. *IEEE Transactions on Bio-Medical Engineering*, *59*(1), 205–212. doi:10.1109/TBME.2011.2170423 PMID:21968709
- De Luca, C. J. (1997). The use of surface electromyography in biomechanics. *Journal of Applied Biomechanics*, *13*(2), 135–163.
- De Luca, G. (2003). *Fundamental concepts in EMG signal acquisition*. Boston: DelSys Inc.
- de Vlugt, E., Schouten, A. C., & van der Helm, F. C. (2003). Closed-loop multivariable system identification for the characterization of the dynamic arm compliance using continuous force disturbances: a model study. *Journal of Neuroscience Methods*, *122*(2), 123–140. doi:10.1016/S0165-0270(02)00303-5 PMID:12573472
- Debicki, D. B., & Gribble, P. L. (2004). Inter-joint coupling strategy during adaptation to novel viscous loads in human arm movement. *Journal of Neurophysiology*, *92*(1), 754–765. doi:10.1152/jn.00119.2004 PMID:15056688
- Dolan, J. M., Friedman, M. B., & Nagurka, M. L. (1993). Dynamic and loaded impedance components in the maintenance of human arm posture. *IEEE Transactions on Systems, Man, and Cybernetics*, *23*(3), 698–709. doi:10.1109/21.256543
- Dolan, J. M., Friedman, M. B., & Nagurka, M. L. (1993). Dynamic and loaded impedance components in the maintenance of human arm posture. *IEEE Transactions on Systems, Man, and Cybernetics*, *23*(3), 698–709. doi:10.1109/21.256543
- Farina, D., Merletti, R., & Enoka, R. M. (2004). The extraction of neural strategies from the surface EMG. *Journal of Applied Physiology*, *96*(1), 1486–1495. doi:10.1152/jappphysiol.01070.2003 PMID:15016793
- Franklin, D. W., Leung, F., Kawato, M., & Milner, T. E. (2003). Estimation of multijoint limb stiffness from EMG during reaching movements. In *Proceedings of IEEE EMBS Asian-Pacific Conference on Biomedical Engineering* (pp. 224–225).
- Gomi, H., & Osu, R. (1998). Task-dependent viscoelasticity of human multijoint arm and its spatial characteristics for interaction with environments. *The Journal of Neuroscience*, *18*(21), 8965–8978. PMID:9787002
- Hogan, N. (1984). Adaptive control of mechanical impedance by coactivation of antagonist muscles. *IEEE Transactions on Automatic Control*, *29*(8), 681–690. doi:10.1109/TAC.1984.1103644
- Hogan, N. (1985). Impedance control: An approach to manipulation, parts i, ii, iii. *Transactions of the ASME. Journal of Dynamic Systems, Measurement, and Control*, *107*(1), 1–24. doi:10.1115/1.3140702

Modeling the Human Elbow Joint Dynamics from Surface Electromyography

- Kawato, M. (1999). Internal models for motor control and trajectory planning. *Current Opinion in Neurobiology*, 9(1), 718–727. doi:10.1016/S0959-4388(99)00028-8 PMID:10607637
- Kearney, R. E., & Hunter, I. W. (1990). System identification of human joint dynamics. *Critical Reviews in Biomedical Engineering*, 18, 55–87. PMID:2204515
- Kleissen, R. F. M., Buurke, J. H., Harlaar, J., & Zilvold, G. (1998). Electromyography in the biomechanical analysis of human movement and its clinical application. *Gait & Posture*, 8(2), 143–158. doi:10.1016/S0966-6362(98)00025-3 PMID:10200405
- Kutch, J. J., & Buchanan, T. S. (2001). Human elbow joint torque is linearly encoded in electromyographic signals from multiple muscles. *Neuroscience Letters*, 311(1), 97–100. doi:10.1016/S0304-3940(01)02146-2 PMID:11567787
- Ljung, L. (1999). *System identification: Theory for the user* (2nd ed.). Englewood Cliffs, NJ: Prentice-Hall.
- Osu, R., & Gomi, H. (1999). Multijoint muscle regulation mechanisms examined by measured human arm stiffness and EMG signals. *Journal of Neurophysiology*, 81(4), 1458–1468. PMID:10200182
- Osu, R., Kamimura, N., Iwasaki, H., Nakano, E., Harris, C. M., Wada, Y., & Kawato, M. (2004). Optimal impedance control for task achievement in the presence of signal-dependent noise. *Journal of Neurophysiology*, 92(2), 1199–1215. doi:10.1152/jn.00519.2003 PMID:15056685
- Perreault, E. J., Crago, P. E., & Kirsch, R. F. (2000). Estimation of intrinsic and reflex contributions to muscle dynamics: A modeling study. *IEEE Transactions on Bio-Medical Engineering*, 47(11), 1413–1421. doi:10.1109/TBME.2000.880092 PMID:11077734
- Ruiz, A. F., Brunetti, F. J., Rocon, E., Moreno, J. C., Bueno, L., & Pons, J. L. (2008). NeuroLab: A multimodal networked exoskeleton for neuromotor and biomechanical research. In *Proceedings of the International Conference on Biomedical Electronics and Devices - BioDevices*, 2, (pp. 68-73).
- Shadmehr, R., & Mussa-Ivaldi, F. A. (1994). Adaptive representation of dynamics during learning of a motor task. *The Journal of Neuroscience*, 14(1), 3208–3224. PMID:8182467
- Stroeve, S. (1999). Impedance characteristics of a neuromusculoskeletal model of the human arm I. Posture control. *Biological Cybernetics*, 81(5-6), 475–494. doi:10.1007/s004220050577 PMID:10592022
- Tanaka, Y., Onishi, T., Tsuji, T., Yamada, N., Takeda, Y., & Masamori, I. (2007). Analysis and modeling of human impedance properties for designing a human-machine control system. In *Proceeding of the IEEE International Conference on Robotics and Automation* (pp. 3627–3632).
- Tsuji, T., Morasso, P. G., & Ito, K. (1995). Human hand impedance characteristics during maintained posture. *Biological Cybernetics*, 74(1), 475–485. doi:10.1007/BF00199890 PMID:7612720
- van der Helm, F. C. T., Schouten, A. C., de Vlugt, E., & Brouwn, G. G. (2002). Identification of intrinsic and reflexive components of human arm dynamics during postural control. *Journal of Neuroscience Methods*, 119(1), 1–14. doi:10.1016/S0165-0270(02)00147-4 PMID:12234629
- Xu, Y. M., & Hollerbach, J. M. (1999). A robust ensemble data method for identification of human joint mechanical properties during movement. *IEEE Transactions on Bio-Medical Engineering*, 46(4), 409–419. doi:10.1109/10.752938 PMID:10217879

Zhang, L. Q., & Rymer, W. Z. (1997). Simultaneous and nonlinear identification of mechanical and reflex properties of human elbow joint muscles. *IEEE Transactions on Bio-Medical Engineering*, 44(12), 1192–1209. doi:10.1109/10.649991 PMID:9401219

ADDITIONAL READING

Baiqing, S., & Yanjun, L. (2009). Dynamics modeling of human elbow joints servicing for rehabilitation robots. *In Proceeding of the IEEE International Conference on Industrial Electronics and Applications*, 2566-2569.

Karniel, A., & Inbar, G. F. (2000). Human Motor Control: Learning to Control a Time-Varying, Nonlinear, Many-to-One System. *IEEE Transactions on Systems, Man and Cybernetics. Part C, Applications and Reviews*, 30(1), 1–11. doi:10.1109/5326.827449

Kistemaker, D. A., Van Soest, A. J., & Bobbert, M. F. (2007). A model of open-loop control of equilibrium position and stiffness of the human elbow joint. *Biological Cybernetics*, 96(3), 341–350. doi:10.1007/s00422-006-0120-6 PMID:17171564

Sepulveda, F., Wells, D. M., & Vaughan, C. L. (1993). A neural network representation of electromyography and joint dynamics in human gait. *Journal of Biomechanics*, 26(2), 101–109. doi:10.1016/0021-9290(93)90041-C PMID:8429053

Tözeren, A. (2000). *Human Body Dynamics: Classical Mechanics and Human Movement*. Springer-Verlag New York Inc.

Tsuji, T., Fukuda, O., Shigeyoshi, H., & Kaneko, M. (2000). Bio-mimetic impedance control of an emg-controlled prosthetic hand. *In Proceeding of the IEEE/RSJ International Conference on Intelligent Robots and Systems*, pp. 377-382.

Venture, G., Yamane, K., & Nakamura, Y. (2006, May). In-vivo Estimation of the Human Elbow Joint Dynamics during Passive Movements Based on the Musculo-skeletal Kinematics Computation. *In Proceedings of the IEEE International Conference on Robotics and Automation*, pp. 2960-2965.

Winter, D. A. (2009). *Biomechanics and Motor Control of Human Movement*. Wiley John & Sons. doi:10.1002/9780470549148

KEY TERMS AND DEFINITIONS

Applications of Surface Electromyography: Various uses of electromyographic signals.

Biomechanical Modelling: Process to develop models of the complex relationship between muscular activity, kinematics and kinetics of the human body.

Elbow Joint Dynamics: Viscoelastic properties of the single-joint.

Human Motor Control: Process by which humans organize and execute their actions.

Impedance Control: Approach to the control of dynamic interaction between a manipulator and its environment.

Mechanical Impedance: Dynamic relationship between forces and position variations.

Musculoskeletal System: System that provides form, support, stability, and movement to the body.

Chapter 6

Arm Swing during Human Gait Studied by EMG of Upper Limb Muscles

Johann P. Kuhtz-Buschbeck
Christian-Albrechts-University Kiel, Germany

Antonia Frenzel
Christian-Albrechts-University Kiel, Germany

Bo Jing
Christian-Albrechts-University Kiel, Germany

ABSTRACT

Arm swing during human gait has both passive and active components. The chapter presents a study conducted with normal subjects using electromyography (EMG) to describe patterns of arm and shoulder muscle activity in different gait conditions. These included normal forward walking, walking with immobilized arms, backward walking, power walking with accentuated arm swing, running, and load carriage. Complementary kinematic data are presented, too. Rhythmic muscle activity persists to some extent when both arms are immobilized during walking. Forward and backward walking involve dissimilar patterns of muscle activity, although the limb movements are very similar in both conditions. Likewise, power walking and running are characterized by different curves of EMG activity. Unimanual load carriage during walking affects muscle activities of both the loaded and the non-loaded arm. Research on normal arm swing provides a basis for clinical investigations of gait disorders.

INTRODUCTION

Arm swing is a typical, though not obligatory, feature of normal human gait. Since arm swing has no direct function for propulsion, it is unclear why this movement occurs (Meysns, Bruijn, & Duysens

2013); suggested reasons include improvement of stability, reduction of energy consumption, neural coupling of upper and lower limbs, and passive induction of arm swing by trunk movements, gravity, and inertia. Compared to the extensive research on leg muscle activity, EMG of upper

DOI: 10.4018/978-1-4666-6090-8.ch006

limb muscles during walking has received little attention. This study characterizes the activity of arm and shoulder muscles during different modes of human gait in healthy volunteers. We aimed to gain insight into neurophysiological mechanisms of gait (leg-arm coupling, adaptation of motor synergies to changing conditions) and to provide physiological EMG data, which might be useful for studies in patients with gait disorders, e.g. in Parkinson's disease.

The frequency of arm swing and the phase coupling between upper and lower limbs depend on the walking velocity (Wagenaar & van Emmerik, 2000). During slow walking (<0.8 m/s), both arms tend to swing back and forth together rather than alternately, at twice the stride frequency of the legs. During normal and fast walking and running, both arms swing in alternation and in phase with the contralateral legs, so the left arm swings forward along with the right leg and vice versa (Webb, Tuttle, & Baksh, 1994).

In their seminal EMG study, Ballesteros, Buchthal, and Rosenfalck (1965) concluded that swinging the arm from back to forth (forward arm swing) during walking is actuated by contractions of internal rotators of the upper arm (latissimus dorsi), while the posterior part of the deltoid muscle and the teres major are responsible for backswing. Others argued that forward arm swing is a passive movement (Hinrichs, 1990; Hogue, 1969). Possibly due to methodical limitations, the aforementioned studies found no EMG activity of upper arm muscles (triceps, biceps) during walking, whereas recent research detected such activity (Ivanenko, Cappellini, Poppele, & Lacquaniti, 2008; Kuhtz-Buschbeck & Jing, 2012). In brief, it has been shown that arm swing is not an entirely passive pendular movement, but the extent to which upper limb muscles actively drive arm swing during walking and running is not yet completely understood.

This chapter presents novel EMG data to characterize the activity of shoulder and arm muscles in normal subjects during various gait conditions. Activity of one paravertebral trunk

muscle (erector spinae) was recorded, too. First, normal forward walking (control condition) is described together with corresponding kinematic data of arm swing. In line with the concept that arm and leg muscle activations are coupled by a central motor program (Dietz, 2002; Nielsen, 2003), it was then hypothesized that some EMG activity of upper limb muscles would persist when both arms are immobilized during walking. We also examined whether deliberate suppression of persisting EMG signals is possible. Next, we compare EMG data of forward and backward walking. Although the limb movement trajectories are remarkably similar in both conditions (Thorstensson, 1986), we expected dissimilar patterns of upper limb muscle activity. Reciprocal arm swing was deliberately accentuated during power walking, which is a popular alternative to Nordic pole walking. Here it was hypothesized that rhythmical shoulder and upper arm muscle activations would increase above control values. However, since the basic biomechanical features of walking are preserved during power walking, we anticipated no major change in the activation profile of the erector spinae muscle. By contrast, we expected the EMG curves of both, upper limb and paravertebral muscles, to differ between walking and running. Furthermore we studied the EMG during treadmill walking with unimanual and bimanual load carriage (10% body weight). Here we anticipated differences between uni- and bimanual carriage and a possible involvement of the non-loaded arm during unilateral load carriage.

Taken together, the current EMG data have been collected in twenty normal subjects to outline the profiles of arm and shoulder muscle activity for different modes of gait on a treadmill (forward walking, walking with immobilized arms, backward walking, power walking, running, load carriage). The current data complement two previous related studies, which had been performed in the same laboratory, but with other subjects and other gait conditions (Kuhtz-Buschbeck, Brockmann, Gilster, Koch, & Stolze, 2008; Kuhtz-Buschbeck & Jing, 2012).

BACKGROUND

The following short review will first discuss passive and active components of arm swing during human gait. Then the pertinent neuronal circuitry of the spinal cord will be outlined, including central pattern generators (CPGs) that generate rhythmic muscle activity during locomotion. Possible benefits of natural arm swing are then weighed against the metabolic cost of this rhythmical movement. Finally, particular gait conditions such as walking backwards, load carriage, power walking and running will be discussed.

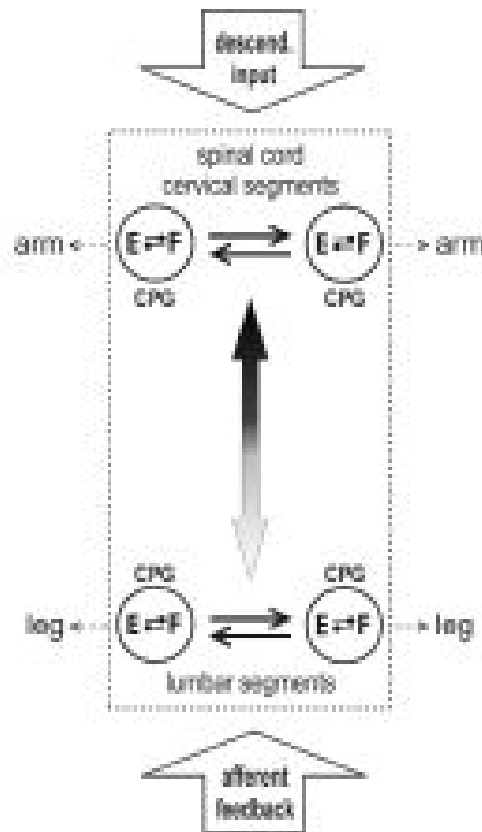
Arm swing: active or passive movement? Passive dynamics facilitate normal arm swing during human walking. The trunk does not move forward with constant speed, but with small cyclic changes superimposed upon a steady baseline velocity (Murray, 1967). The suspension points of the arms (glenohumeral joints) undergo horizontal and vertical accelerations during each step cycle, which induce passive pendular arm movements (Jackson, Joseph, & Wyard 1978, 1983a, 1983b). Elastic and frictional resistive forces develop as the swinging arms approach the turning points of their excursions (Kubo, Wagenaar, Saltzman, & Holt, 2004). It has recently been proposed that the arms act as passive mass dampers that diminish head and torso rotations during walking and running (Pontzer, Holloway, Raichlen, & Lieberman, 2009). According to this passive arm swing hypothesis, the swinging of the arms is indirectly powered by movements of the lower body rather than actively driven by shortening contractions of shoulder muscles. To demonstrate passive dynamics, Collins, Adamczyk and Kuo (2009) attached artificial arms made of rope to a yoke, which was placed on the shoulders of a person, who then walked with his real arms tied to his body. The artificial arms started to oscillate in a movement similar to natural arm swing. Moreover, these researchers constructed a mechanical walking model consisting of two curved feet, two straight legs and a pelvis to which two straight free-swinging arms were attached to. Masses of

the limbs were based on anthropometric data. The stance foot rolled along the floor, which had a slight downward inclination, thus providing the model with energy. Different modes of fully passive arm swing were observed with this mechanical walking model, including a reciprocal mode similar to natural arm swing of human walking.

However, arm swing during human gait has also active components. Already the first analysis of the angular momentum of the upper limbs showed that arm swing is not merely a passive pendular motion (Elftman, 1939). Ballesteros et al. (1965) later found rhythmical activity of arm and shoulder muscles during forward walking, illustrating their seminal study with selected original EMG recordings. Subsequent studies largely agree that backward arm swing is supported by contractions of shoulder extensor muscles (Hinrichs, 1990; Hogue, 1969; Jackson et al., 1978; Kuutz-Buschbeck & Jing, 2012). Yet, there is no consensus regarding both the contribution of shoulder flexor muscles to arm swing and the activity of upper arm muscles during this movement. Early EMG research was based on selected data of single steps, but averaged data of many step cycles describe the temporal pattern and amount of muscle activity more accurately (Frigo & Crenna, 2009). In the current study, EMG data of ~50 step cycles per subject and condition were averaged, amplitude-normalized and time-normalized. Individual EMG curves are shown to illustrate inter-subject variability. Complementary kinematic recordings help to distinguish between shortening muscle contractions, which drive a movement, and lengthening contractions, which may resist passively induced motions (Faulkner, 2003).

Functional organization of motor output: Walking and running involve simultaneous contractions of many muscles, and hence coordinated motor neuronal activity in the spinal cord. To illustrate this, EMG signals of specific muscles can be mapped onto spinal cord segments according to the locations of the respective motor neuron pools (Chiovetto, 2011). Leg muscle activity during human walking is associated with a cranio-caudal

Figure 1. Simplified diagram of the neuronal circuitry. Central pattern generators (CPG, circles) are groups of neurons in the spinal cord (dotted rectangle), which generate alternating activity of flexor and extensor muscles during locomotion. The respective motoneurons (F, E) of a CPG inhibit each other reciprocally via interneurons. Each limb has an own CPG. Horizontal arrows indicate that the CPGs of the same girdle are connected to ensure alternating movements of the left and right limbs. Long propriospinal connections (vertical arrow) couple the CPGs of the arms and legs. The influence of the legs on the arms is probably stronger than vice versa (grey shade in vertical arrow). The spinal circuitry is influenced by descending input from higher centers (e.g. brainstem, mesencephalon, cortex) and by afferent feedback



migration of motor neuronal activity within the lumbosacral spinal cord, which mirrors changes of kinetic energy due to motion of the center of body mass (Cappellini, Ivanenko, Dominici, Poppele, & Lacquaniti, 2010). Simultaneous EMG recordings at various levels of the trunk during human gait showed that long paravertebral muscles are sequentially activated by a motor command, which propagates along the spinal cord in cranio-caudal direction (Ceccato, de Sèze, Azevedo, & Cazalets, 2009). In this present study we monitored EMG

signals of muscles innervated by cervical segments (e.g. trapezius, deltoideus) and lumbar segments (erector spinae) of the spinal cord to allow detection of a possible similar temporal sequence of muscle activations.

Central motor program: Central pattern generators of locomotion (CPGs) are neuronal networks in the spinal cord (Figure. 1), which can generate the rhythmic muscle activity necessary for walking without higher brain centers and even without sensory feedback (Grillner, 1981). The existence

Arm Swing during Human Gait Studied by EMG

of such CPGs has been demonstrated with spinal animal preparations; walking recovers considerably after complete transection of the spinal cord in rats and cats. Most likely each limb has its own CPG. These pattern generators are connected via propriospinal neuronal pathways to ensure smooth inter-limb coordination. In a trotting animal the left and right limbs of the same girdle move in strict alternation, with a phase shift of half a step cycle. Diagonal limbs move in synchrony: the right hindlimb in phase with the left forelimb and the left hindlimb in phase with the right forelimb. The same phase coupling between legs and arms is typical for normal and fast human walking and also for running. There is evidence that also humans possess a spinal rhythm-generating network for arm and leg movements during locomotion, which depends, however, much more on intact supraspinal control than in animals (Grillner, 2011; Nielsen, 2003). Step-related EMG activity of leg muscles has been observed in patients with complete spinal cord lesions during treadmill training with body-weight support (Wirz, Colombo, & Dietz, 2001), although functional recovery of gait is hitherto not possible after such injuries.

Cyclic movements of the arms have been shown to influence leg muscle activity (and vice versa), indicating that CPGs of the upper and lower limbs are coupled via propriospinal pathways in humans as well (Zehr & Duysens, 2004). Concerning arm swing, Ballesteros et al. (1965) found that some step-related shoulder muscle activity persists when subjects walk with both arms loosely tied to the trunk (their Figure. 10A). To replicate and to extend their finding, we examined tight and loose immobilization of the arms during treadmill walking. Persistent rhythmical EMG signals of upper limb muscles would indicate that leg movements “automatically” trigger upper limb muscle activity in such conditions. We also asked the subjects to suppress residual muscle activity with the help of visual EMG feedback. A moderate or strong coupling between leg and arm muscle activations would impede such suppression, whereas a weak coupling would make suppression easy.

Benefits of arm swing during gait: The metabolic costs of natural arm swing are low, because the associated muscle contractions are weak (Kuitz-Buschbeck & Jing, 2012). Arm swing and shoulder rotation in the transverse plane counteract the angular momentum that is imparted by the swinging legs during walking and running (Collins, Adamczyk, & Kuo, 2009; Hamner, Seth, & Delp, 2010; Hinrichs, 1990). Thus, body rotation about the vertical axis (axial twist) is reduced, and trunk and head are stabilized. Moreover, arm swing can improve lateral balance during walking and running (Arellano & Kram, 2011; Ortega, Fehlman, & Farley, 2008). Although it is simple to walk with the hands in the pockets or clasped behind the trunk, walking without natural arm swing is less efficient. Maximum walking speed was found to be reduced when both arms are strapped to the body (Eke-Okoro, Gregoric, & Larsson, 1997). Here, velocity is gained mainly by increasing the step frequency (cadence), whereas the step length increases less than it would normally. Restriction of arm swing at a given gait velocity augments energy expenditure during walking by 5-10% (Collins et al., 2009; Ortega et al., 2008; Umberger, 2008). The whole-body angular momentum about the vertical axis increases in this situation (Collins et al., 2009), as does the free vertical moment between the foot and the ground (Li, Wang, Crompton, & Gunther, 2001; Park, 2008). Umberger (2008) found that the foot exerts higher external rotation moments onto the surface of a force plate in the second half of the stance phase when subjects walk without arm swing (his Figure. 2). This may augment energy expenditure, because additional contractions of leg and trunk muscles are probably necessary to counteract these ground reaction moments (Collins et al., 2009; Ortega et al., 2008). Therefore we expected paravertebral muscle activity to increase when subjects walked with immobilized arms in the present experiments.

Walking backwards: By time-reversing otherwise invariant kinematic patterns, healthy adults can instantly change from forward to backward

walking. Leg movements during forward and backward walking are strikingly similar; the feet travel along nearly the same path, though in reversed direction (Thorstensson, 1986; his Figure. 1). A kinematic study of arm movements shows that elbow joint excursions and shoulder joint extension are nearly identical in both conditions, while (anterior) flexion of the shoulder is somewhat reduced during backward walking (Kutzt-Buschbeck et al., 2008; their Figure. 2). Even though the kinematic templates are preserved across gait reversal, this does not necessarily indicate that the EMG patterns are invariant, too. Leg muscles activations of forward and backward walking are known to differ considerably (Grasso, Bianchi, & Lacquaniti, 1998). We have addressed this issue for the upper limbs in the present study.

Power walking and running: The current data characterize EMG patterns of both, power walking and running, and compare those with normal forward walking. Arm swing is deliberately emphasized during power walking. By comparison with Nordic walking, no poles are required. During power walking both arms are briskly moved back and forth (not side to side) close to the body (Meakin, 2003). The elbows maintain an angle of about ninety degrees. At the end of forward arm swing, the elbow is about level with the breastbone; at the end of backswing, the hand is near the hip. The head is kept up with the chin parallel to the ground and the eyes look straight ahead. The posture is kept upright with enhanced tension of abdominal and gluteal muscles. Since especially backward arm swing is accentuated during power walking, we expected enhanced activity of shoulder extensors in this gait condition. Up to now only one study has compared power walking with normal walking (Cho, Kim, & Kim, 2006). The step length was enlarged, shoulder joint excursions were bigger, the elbows more flexed, and especially ankle extensors (gastrocnemius, soleus) and elbow flexors (biceps brachii) were more active in the former condition. However, muscle activation patterns are not evident from that study (no EMG curves are shown).

Walking in general (i.e. also power walking) involves an inverted pendulum mechanism, where the center of mass of the body (COM) vaults over the supporting leg during the stance phase (Lacquaniti, Ivanenko, & Zago, 2012). The COM trajectory curves upward during stance to reach maximum height in the middle of this phase. Short double stance phases (= double support phases), where both feet are in contact with the ground, are characteristic for walking. By contrast, running is a bouncing gait in which the forward movement of the COM slows down and the COM trajectory is curved downward in the first half of the stance phase (Hamner & Delp, 2013), because the supporting leg acts as a spring that is loaded. In the second half of the stance phase (of running) the COM is accelerated upward and forward. At the switch from walking to running, ground reaction forces increase, the stance phase shortens, and stance and swing phases are separated by a float phase, in which there is no contact with the ground (Nicola & Jewison, 2012). No double stance phases exist during running. In line with these biomechanical differences between walking and running, we expected divergent EMG profiles of upper limb and paravertebral muscles.

Load carriage: Grocery bags, buckets, briefcases or other items are often carried with one or both hands during walking. One previous study examined the effects of loading on upper limb kinematics and deltoid muscle activity (Donker, Mulder, Nienhuis, & Duysens; 2002). The movement amplitude of the loaded arm during walking decreased when a 1.8 kg mass was attached to the wrist, while EMG signals of the deltoid muscle increased. In the present experiments we let the subjects carry a heavier load of 10% of their respective body weights (BW). This is typical for carrying school bags by hand (Brackley & Stevenson, 2004) and also for carrying tasks during agricultural work (Gillette, Stevermer, Miller, Meardon, & Schwab, 2010). The load was carried either unilaterally by one hand or bilaterally and evenly allocated to both hands (2 x 5% BW). Effects on the different arm and shoulder muscles

Arm Swing during Human Gait Studied by EMG

are described. Moreover, it is examined whether unimanual load carriage influences the EMG activity on the contralateral (non-loaded) side.

GAIT CONDITION - DEPENDENT PATTERNS OF MUSCLE ACTIVITY

Method: EMG of Upper Limb Muscles During Human Gait

Twenty healthy volunteers (10 men, 10 women) participated in the experiments. Their mean age was 26.2 ± 7.6 years (\pm SD), mean body height 178 ± 8 cm, weight 70.7 ± 11.4 kg and body mass index 22.3 ± 2.4 kg/m². Approval from the local ethics committee had been obtained and all participants gave informed consent. They wore tank tops, sweatpants (with pockets) and their personal running shoes. Experiments were performed on a treadmill with a belt surface of 170 cm in length and 44 cm in width (Woodway®, Germany). The different gait conditions were trained extensively during an initial practice phase of ~60 min. They comprised of:

1. Normal walking with natural unrestricted arm swing at a treadmill velocity of 6 km/h.
- 2-3. Bound condition (6 km/h) without and with feedback of the EMG signal: Walking with both arms immobilized by a brace and Velcro® straps that attached the upper arms, forearms and hands to the trunk (medi Arm fix® shoulder immobilization support, Bayreuth, Germany). The subjects were asked to keep both arms comfortably relaxed. A safety line connected them to an emergency stop switch. This condition was initially practiced without feedback of the EMG signals, and later performed with and without such feedback (see below).
- 4-6. Pocket conditions (6 km/h): Treadmill walking with loosely restricted arm movements. The left, right or both hands were put into trousers pockets.

7. Backward walking (4 km/h) on the treadmill, with unrestricted arm swing. This task was perceived as difficult, so a low treadmill velocity was chosen for safety reasons. Slow forward walking (4 km/h) served as control condition.
8. Power walking (6 km/h): Demonstrations, detailed instructions (Meakin, 2003), and short video clips were used to teach this walking style with accentuated arm swing. It was practiced until performance appeared to be smooth.
9. Slow running at 6 km/h (jogging) with free arm swing.
- 10-12. Load carriage (6 km/h): The volunteers walked forward while carrying a load (dumbbell, 10% of body weight) in the left hand, the right hand or with two smaller loads in both hands (2 x 5% of body weight).

Subsequent to the initial practice phase, self-adhering Ag-AgCl electrodes (Arbo®H124SG, Germany) were attached to the abraded skin above seven muscles on the right side of the body, with an inter-electrode distance of 2.5 cm. A bipolar surface EMG system was used (EMG MyoSystem 1400L, Noraxon, Scottsdale, AZ). The following muscles were studied (Figure. 2): upper trapezius (TRAP), electrodes on the middle of a line between C7 spinous process and acromion. Anterior deltoid (AD): electrodes ~ 4 cm anterior to acromion, on line to thumb. Posterior deltoid (PD): electrodes ~ 4 cm behind angle of acromion, on line to little finger. Biceps brachii (BIC): electrodes on line between acromion and fossa cubiti at ~1/3 from the fossa. Triceps brachii (TRI): electrodes on long head of the muscle, ~ 3 cm medial to central part of a line connecting the acromion and olecranon. Latissimus dorsi (LD): electrodes ~ 4 cm caudal of inferior scapular angle (arms hanging), oriented parallel to the muscle fibers. Lumbar erector spinae (ES): electrodes were placed ~3 cm lateral of the spinous process of vertebra L3.

After the EMG electrodes had been placed in line with published guidelines (Hermens, Freriks,

Disselhorst-Klug, & Rau, 2000), three static maximum voluntary contractions (MVC; duration ~ 3 s) were performed by each muscle of interest. AD, PD and LD were tested by flexion/extension of the shoulder against a fixed resistance, with the elbow extended. TRAP was tested by abduction of the extended arm in the frontal plane. TRI and BIC were contracted with the elbow flexed by ~90°. To test the ES, subjects lay in the prone position and extended the trunk (lordosis) against external resistance. For later normalization of the EMG signals obtained during gait, the data of each muscle were amplitude-normalized to the highest activity level (mean amplitude for 0.3 s) found in this set of maximum voluntary contractions (Burden, 2010; Konrad, Schmitz, & Denner, 2001). The aforementioned 12 gait trials (conditions) were then performed by each subject in randomized order. To allow for comparison of the various conditions, treadmill velocity was kept constant at 6 km/h, except during backward gait (4 km/h). Each trial lasted for one minute, but the Bound condition trials were extended by another ~2 minutes. After the first minute without EMG feedback, the subjects watched their own EMG signals on a monitor while walking with immobilized arms. We explained those signals to the volunteers and encouraged them to repress residual activity of arm and shoulder muscles with the help of this feedback. They had not been informed in advance about this additional task to ensure natural performance during the initial minute of the Bound condition, e.g. without premature explorations of suppression strategies or other distortions. Stance and swing phases were detected with an optical sensor system (virtual footswitch) working at a frequency of 1000 Hz and having an accuracy of 1 cm (Microgate Optogait®, Bolzano, Italy), which was mounted on the treadmill. All gait trials were filmed with a digital video camera. The experiments lasted for approximately 3 hours per volunteer (total duration).

EMG signals were recorded at a bandwidth of 10-500 Hz, A/D converted at 1000 Hz (12 bit

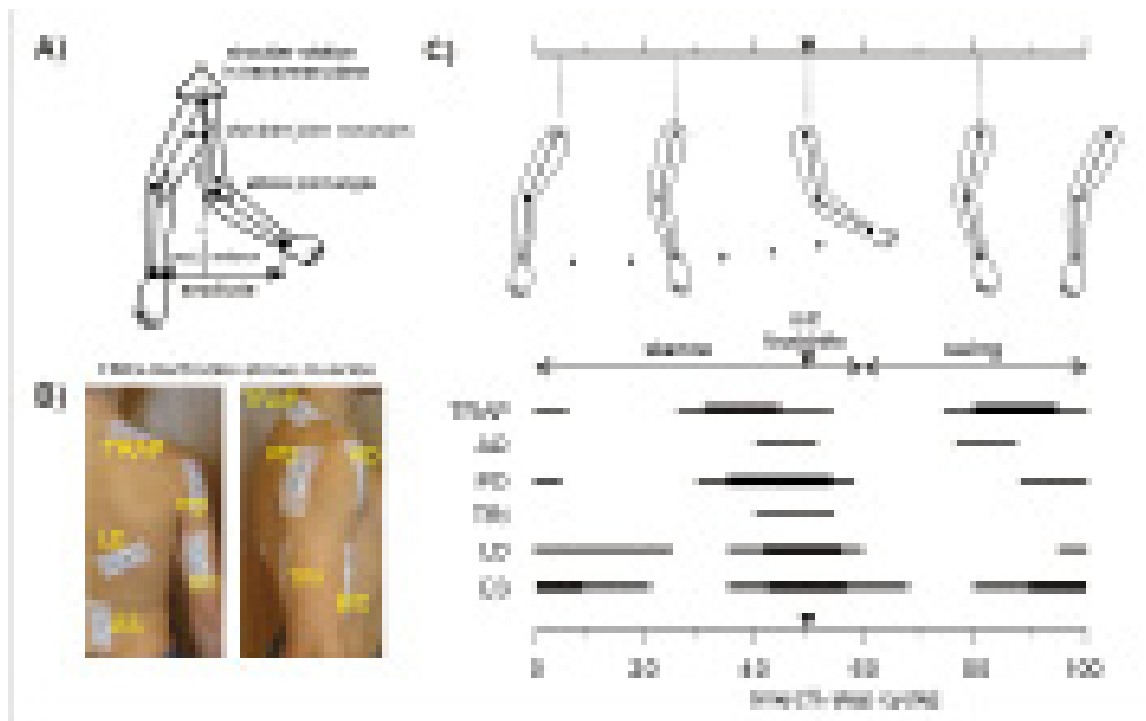
resolution) and stored together with synchronized footswitch and video data for later offline analysis. Appropriate software (Noraxon® MyoResearch XP, Master Edition 1.07) was used for digital filtering (FIR bandpass 20 - 250 Hz), full-wave rectification and smoothing (root mean square, window 50 ms). EMG signals of each muscle were amplitude-normalized (% MVC, see above). Data of ~50 step cycles per gait condition and subject were averaged to obtain individual EMG profiles, which are shown to demonstrate between-subject variability. As time axis, the step cycle of the right leg (ipsilateral to the EMG electrodes) was normalized from 0% (footstrike, onset of stance) to 100% (end of swing phase). Mean amplitudes of the rectified normalized EMG signals over the entire step cycle were calculated for each subject and condition to obtain average levels of muscle activity.

Analysis of the inter-subject variability of these activity levels indicated non-normal distribution for several muscles and conditions (Kolmogorov-Smirnov tests). Group data are therefore illustrated as median EMG curves of the 20 subjects with quartiles (whiskers: 25%, 75%). Non-parametric analyses of variance and Wilcoxon tests were calculated to detect significant differences in muscle activity between conditions, e.g. AD Normal vs. AD Bound. Tables with statistical results are provided as supplementary data (appendix).

EMG curves are arranged from top to bottom in figures, according to the segmental innervation of the muscles by the spinal cord: TRAP (segments C2-C4), AD and PD (C5-C6), BIC (C5-C7), TRI (C6-C8), LD (C6-C8) and ES (L3), see Schünke, Schulte, Schumacher, Voll, and Wesker (2010). To establish relationships between muscle activity and movements, video recordings (lateral view) and footswitch signals were examined together with synchronized EMG data in slow motion. Furthermore we draw on kinematic data of shoulder and elbow movements during human gait, which had been collected earlier (Kuhtz-Buschbeck et al., 2008). Lengthening (eccentric) and shortening

Arm Swing during Human Gait Studied by EMG

Figure 2. a. Typical arm swing excursion at a gait velocity of 6 km/h (adapted from Kutz-Buschbeck et al., 2008). b. EMG electrodes on muscles: TRAP, trapezius, pars descendens; AD, anterior deltoid; PD, posterior deltoid; BIC, biceps brachii; TRI, long biarticular head of triceps brachii; LD, latissimus dorsi; ES, lumbar erector spinae. c. Periods of muscle activity during forward walking (6 km/h) with natural arm swing. Data are based on median EMG profiles of the 20 participants. Thick bars (TRAP, PD, LD, ES) indicate that the median EMG activity of exceeds 4% MVC. Thin bars denote weaker EMG activity, i.e. >2% MVC for TRAP, PD, LD, ES, >1.5% MVC for TRI and >0.75% MVC for AD. Activity of the BIC (not shown) was irregular and very weak. Concomitant arm movements are depicted above; arrowheads denote movement direction. The time axis indicates a normalized step cycle of the right leg (0-100%)



(concentric) muscle contractions are described as defined by Faulkner (2003). During a lengthening contraction the muscle elongates while under tension, because the contractile muscular force is weaker than an opposing force.

Results: Muscle Activity during Normal Forward Walking

During walking and running the anterior reversal of the (right) arm swing takes place at ~50% of the step cycle of the ipsilateral leg (see Figures.

2, 3), coinciding with the onset of the contralateral stance phase (i.e. left footstrike). The posterior reversal falls together with the onset of the ipsilateral stance phase (right footstrike, 0% of the step cycle). A typical arm swing movement for a gait velocity of 6 km/h is shown in Figure. 2A (for details see Kutz-Buschbeck et al., 2008). The amplitude (= wrist displacement) is ~40 cm in anterior-posterior direction; excursions of the shoulder cover an angle of ~35°; elbow flexion reaches ~135° and elbow extension ~170°. Rotation of both shoulders in the transverse plane,

about the vertical axis of the body, amounts to $\sim 10^\circ$. Positions of the EMG electrodes (Figure. 2B) and periods of muscle activity in relation to arm swing kinematics (Figure. 2C) are shown. Individual curves and median EMG profiles of the twenty subjects are illustrated in Figure. 3 (left and middle panels) for normal walking.

The upper TRAP exhibited biphasic activity with a first peak at $\sim 40\%$ (late stance phase) and a second peak at $\sim 85\%$ of the step cycle (swing phase). This muscle abducts the arms so that they clear the side of the trunk and swing approximately parallel to the sagittal plane (Hogue, 1969). The TRAP may also control shoulder inclination in the frontal plane, which changes in a single oscillation per gait cycle (Ceccato et al., 2009). Rather weak shortening AD contractions ($<1\%$ MVC) supported the forward arm swing during the stance phase (at $\sim 45\%$), and slight lengthening AD contractions opposed shoulder extension in the swing phase (at $\sim 80\%$). Extensor (PD) activity was about three times higher than AD activity. PD and LD signals reached peaks at 50% of the step cycle, i.e. at heelstrike of the contralateral (left) foot. These contractions decelerated the forward arm swing and initiated the reversal to backswing; both PD and LD retract the upper arm. TRI contractions prevented excessive passive elbow flexion when the forward swing reached its anterior turning point. Backward arm swing was supported by shortening PD and LD contractions at the end of the step cycle (at $\sim 90\%$), which then continued as lengthening contractions, opposing forward swing during the early stance phase ($\sim 0-20\%$). ES activity reached distinctive peaks in the middle and at the end of the step cycle as reported by others (Anders et al., 2007). The lumbar ES stabilizes the pelvic girdle when the body weight is transferred from one leg onto the other leg. Its activity has been shown to be synchronized to an anterior pelvic tilt that occurs at each footstrike (Ceccato et al., 2009). Muscle activity was weak in relation to maximum voluntary contractions, which confirms that normal arm swing is facilitated by

passive dynamics (Collins et al., 2009). Median EMG activity levels (group data) were $\sim 7\%$ (ES), $\sim 3.5\%$ (TRAP), $\sim 2.5\%$ (PD, LD), $\sim 1.3\%$ (TRI), and $<1\%$ MVC (AD, BIC); see Table 1 (appendix) for details. BIC activity was irregular.

Shoulder and elbow extensor activity (LD, PD, TRI) was clearly (about threefold) stronger than flexor (AD, BIC) activity, and the EMG signals of extensor muscles exhibited definite peaks of activation. Compatible with this difference, Hinrichs (1990) postulated that backward arm swing is supported by extensor muscle activity (PD, LD), whereas forward arm swing is primarily passive, analogous to a child on a swing that is pushed from one direction. Accordingly, recent research found enhanced extensor activity (TRI, LD) when the arms were deliberately held still, parallel to the trunk, during walking (Kuhtz-Buschbeck & Jing, 2012). Especially the biarticular long head of the TRI contracted phasically, indicating that enhanced shoulder and elbow extensor activity is necessary to prevent passively induced forward arm swing. Lengthening contractions of extensor muscles (PD, LD, TRI) decelerate forward arm swing, which seems to be mostly passive, and initiate the reversal to backswing in the middle of the normal walking cycle. Interestingly, Barthelemy and Nielsen (2010) found that inhibition of the motor cortex by paired-pulse transcranial magnetic stimulation partly suppresses PD activity around the anterior turning point of the arm swing movement during treadmill walking. This indicates a corticospinal control of the deltoid muscle at that time, which may facilitate the combination of an “automatic” forward arm swing with voluntary goal-directed movements (e.g. pointing, reaching).

A passive arm swing hypothesis for upper body movement during human walking and running has been put forward, where the forces are derived from the legs and transmitted via the trunk to act through the shoulders on the arms (Pontzer et al., 2009). According to this model, deltoid muscle contractions do not drive the arm swing. Instead, anterior and posterior portions of

Arm Swing during Human Gait Studied by EMG

the deltoid (AD, PD) serve as spring-like elements that co-contrast simultaneously to stabilize the shoulder and to prevent excessive passive arm movements. We found frequent co-contractions of AD and PD, but extensor (PD) activity was clearly stronger. Inter-subject variability of AD activity was high (Figure. 3, left panel), possibly reflecting differences in walking styles (Weiss & St. Pierre, 1983). Moreover, shortening PD and LD contractions initiated and later actively completed the backward arm swing (Figure. 2C), which is not entirely in line with a passive arm swing model. Combined EMG and kinetic data (joint moments and torques) would be required to resolve this issue.

A cranio-caudal propagation of the EMG activity along the various portions of the erector spinae muscle during normal human walking has been described in a recent study (Ceccato et al., 2009). It corresponds to a descending “motor wave” that sequentially activates the different segments of the spinal cord (Falgairolle, de Sèze, Juvin, Morin, & Cazalets, 2006). Accordingly, the present data of normal walking (Figure. 3, left panel) show that the onset of TRAP activity (innervation by segments C3-C4) at ~30% is closely followed by PD and LD (C5-C8) activation onsets, whereas the steep rise of lumbar ES activity (L3) starts later, at ~40% of the step cycle. However, the variability and fluctuations of the EMG curves impede precise definitions of the onset times. The maxima of PD, LD, ES signals all coincided at contralateral footstrike (50%).

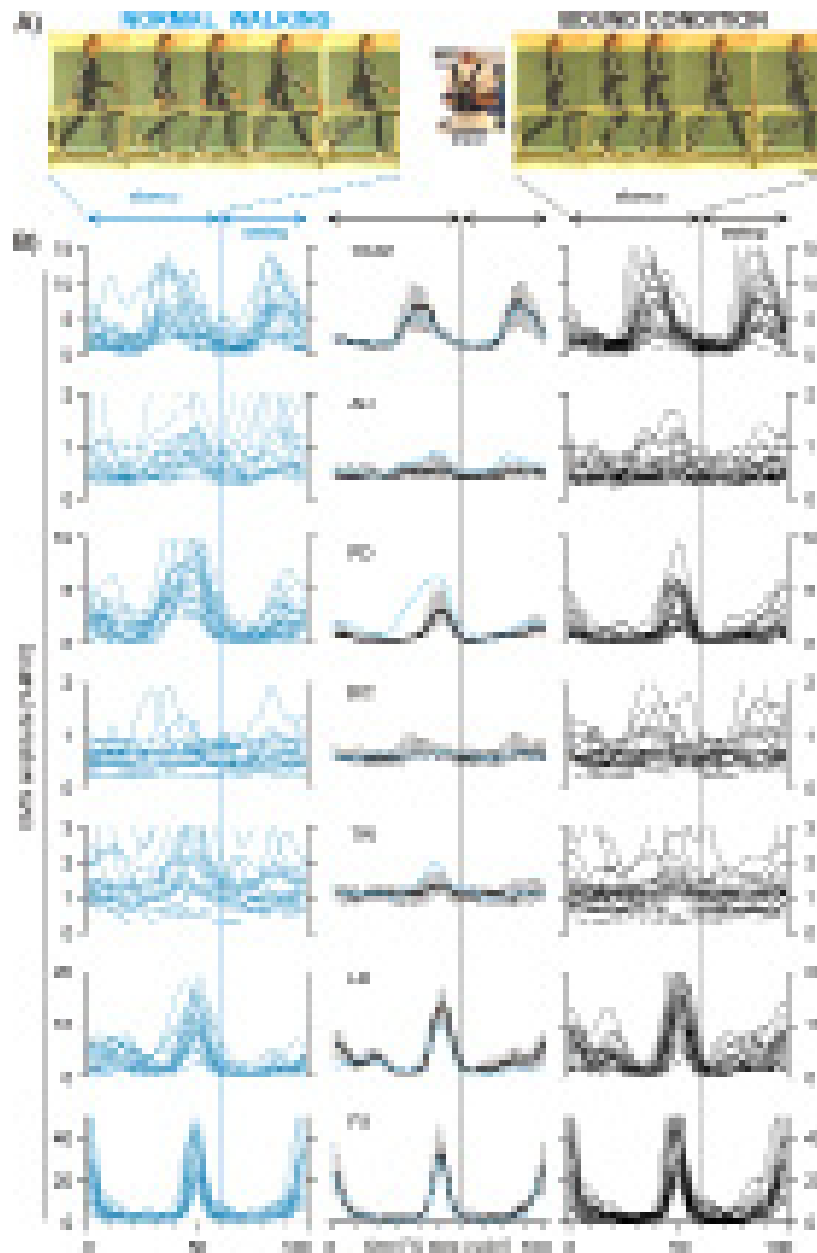
Muscle Activity during Gait with Restricted Arm Swing

Bound condition: Median EMG activities of the AD, PD and TRI decreased below control values when subjects walked with both arms immobilized by a brace (see *Table 1* in appendix). Nevertheless rhythmic activity with a temporal pattern similar to normal walking was still present (Figure. 3, right panel), especially in the TRAP, PD, LD and ES.

Since the brace prevented retraction and inward rotation of the upper arm, the phasic PD and LD activations could not produce movements. When visual feedback of the EMG signals was provided, many subjects were astonished about their ongoing rhythmic shoulder muscle activity (TRAP, PD, LD). Despite the feedback, they could not entirely suppress the EMG signals, as illustrated in Figure. 4 with data of a female volunteer. She managed to minimize TRAP activity by lowering the right shoulder, and could also reduce EMG signals of PD and LD. However, AD and TRI became more active during this attempt. Altogether, rhythmic EMG activity in the Bound condition was natural, while its suppression was difficult and ineffective. This coupling of lower and upper limb muscle activations supports the view that both are part of a centrally determined motor program (Balter & Zehr, 2007; Dietz & Michel, 2009; Zehr & Duysens, 2004). Leg movements during human walking “automatically” activate shoulder muscles.

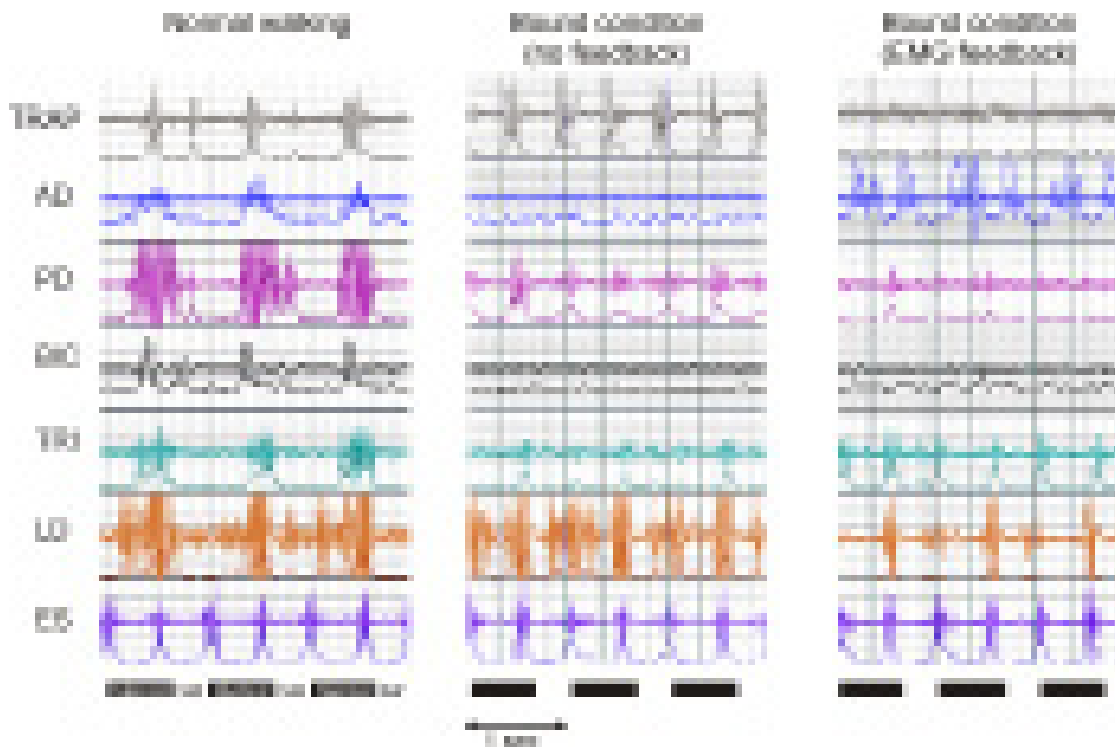
Restricting arm movements during walking has adverse effects, because arm swing normally counterbalances the angular momentum of the swinging legs and thereby helps to control the twisting motion of the trunk about its vertical axis (Hinrichs, 1990). Elftman (1939) stated “it is therefore possible for the legs to go through the movements necessary for walking, without imparting marked rotation to the body as a whole” (p. 531). EMG activities of LD and ES increased significantly (see *Table 1* in appendix) in the Bound condition of the present study. Congruently, Callaghan, Patla, and McGill (1999) found that trunk muscle activity (LD, ES, oblique abdominal muscles) and compressive loading of lower back intervertebral joints are augmented when arm swing during walking is restricted by crossing the arms over the abdomen. Although normal arm swing itself requires some muscle contractions, more energy-consuming techniques of gait stabilization (like enhanced trunk muscle activity) are needed without this movement, so

Figure 3. Normal walking and Bound condition. a. Limb movements of a stance phase during normal walking (left series of pictures) and walking with both arms immobilized by a brace (right picture series). Note the upward “bobbing” movement of head and trunk during stance. b. EMG curves with normalized amplitudes (%MVC) are shown in relation to a time-normalized gait cycle of the right leg (0-100%). Left panel (blue lines): Individual curves of normal walking. Right panel (black lines): Individual curves of the Bound condition. Each line shows the EMG activity of one subject, based on averaged data of ~50 step cycles. Middle panel: Group results, i.e. median EMG profiles of the 20 subjects during normal walking (blue broken line) and walking with immobilized arms (Bound condition, black solid line). The thin error bars denote quartiles (25%, 75%) for Bound condition



Arm Swing during Human Gait Studied by EMG

Figure 4. Remaining EMG activity in the Bound condition. Data of normal walking (control condition), walking with immobilized arms (without EMG feedback), and gait with immobilized arms plus EMG feedback are shown. Signals of TRAP, PD, and LD could be repressed, but AD and TRI activity increased in the latter condition. Raw unfiltered EMG data of one representative subject (note cable movement artefacts in BIC curves during normal walking). Stance (black bars) and swing (sw) phases are indicated below

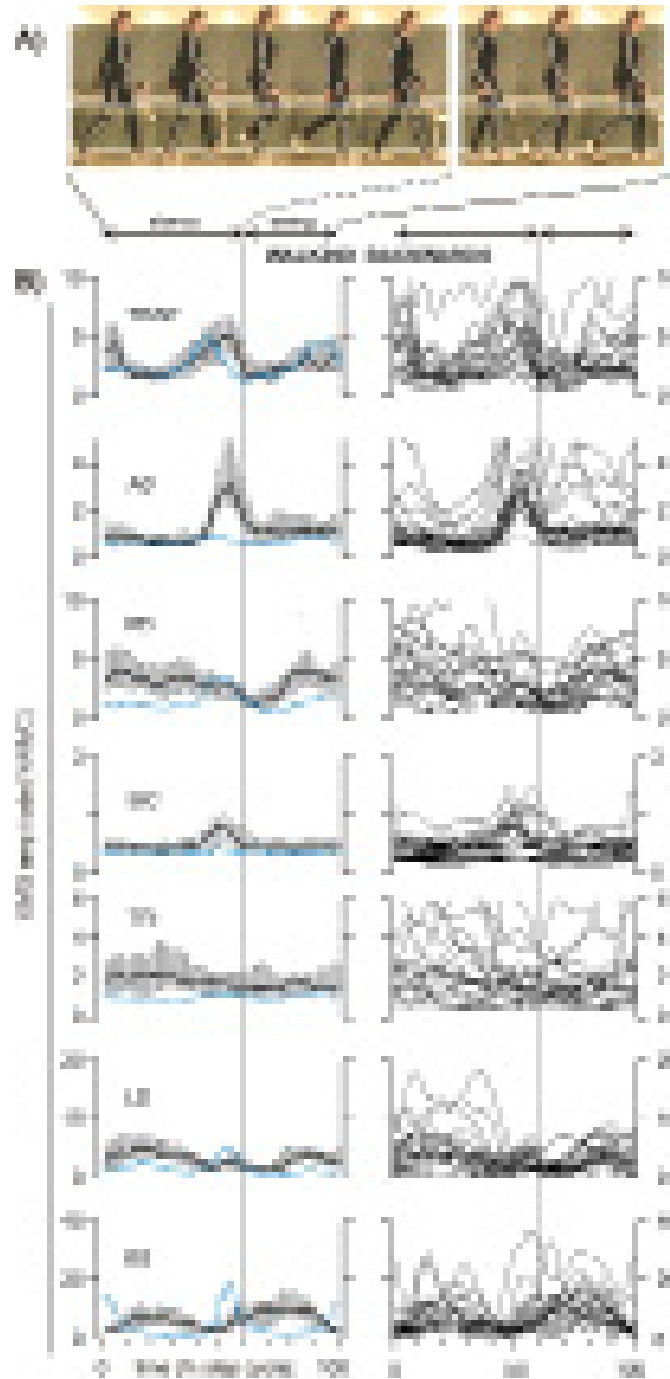


that the metabolic cost of walking increases (Collins et al., 2009; Ortega et al., 2008). Not only trunk muscles, but probably also leg muscles are involved, as the knee joint moment during stance is known to increase when subjects walk without arm swing (Umberger, 2008). Hence EMG of leg muscles in this condition may be an interesting topic for further research.

Pocket conditions: Ballesteros et al. (1965) demonstrated ongoing shoulder muscle activity in subjects who walked along a walkway with their arms loosely tied to the trunk. We could reproduce this result in subjects who walked with both hands in the pockets (not illustrated for the sake of brevity). When only one hand was put in the pocket, while the contralateral arm could swing

free, EMG signals of both sides changed (Table 2 in appendix). On the constrained (pocket) side, deltoid muscle activity decreased, while BIC, LD and ES signals increased above control values of normal walking. On the contralateral side, TRI activity of the free swinging right arm increased ~15% above control values. In accordance, a kinematic study found a noticeable increase of the non-constrained arm swing amplitude during gait with unilateral arm constraint (Ford, Wagenaar, & Newell, 2007).

Figure 5. Backward walking. a. Limb movements during backward walking. Stance and swing phases of the right leg are indicated by arrows. b. EMG curves. Left panel: Group results, i.e. median EMG profiles of the 20 subjects during normal walking (blue broken line) and backward walking (black solid line) at a treadmill velocity of 4 km/h. Error bars denote quartiles (25%, 75%) for walking backwards. Right panel: Individual EMG curves of the 20 participants during backward walking. Otherwise as in Figure. 3



Muscle Activity during Backward Gait

Obvious differences between the EMG patterns of forward and backward gait were found (Figure. 5). AD and BIC, both almost inactive during forward walking, showed distinct peaks of activity at the end of the stance phase during backward walking, which coincided with the posterior (in relation to the body, i.e. dorsal) turnaround of arm swing. These contractions may initiate reversal from shoulder extension to flexion; the BIC furthermore limits elbow extension. Typical features of forward walking, such as the sharp peak EMG signals of PD, LD and ES at ~50% of the step cycle, were missing during backward walking. Instead, these muscles showed smooth profiles of activity in the stance phase (~10-40%) and in the swing phase of the ipsilateral leg. No cranio-caudal sequence of the muscle activation onsets (i.e. TRAP first, ES last) was evident during backward walking. The median level of the EMG activity changed, too. All investigated muscles except the TRAP were significantly ($p < 0.01$) more active during backward than forward walking (Table 3, appendix).

Despite similar movement trajectories of forward and backward gait, reversal of the movement direction hence entails apparent changes of the EMG patterns of upper limb muscles. In accordance to the above others found divergent leg muscle synergies (Thorstensson, 1986; Grasso et al., 1998). Nevertheless a sequential activation of paravertebral muscles may occur in both conditions (De Sèze, Falgairolle, Viel, Assaïante, & Cazalets, 2008). In six out of nine subjects, these researchers found that the ES was activated with a cranio-caudal progression (from C7 to L4) of EMG activity during both forward and backward walking. Moreover, the dissimilar EMG profiles of forward and backward walking can be reconstructed as a weighted combination of a few underlying basic activation patterns, whose timing and weight change as a function of

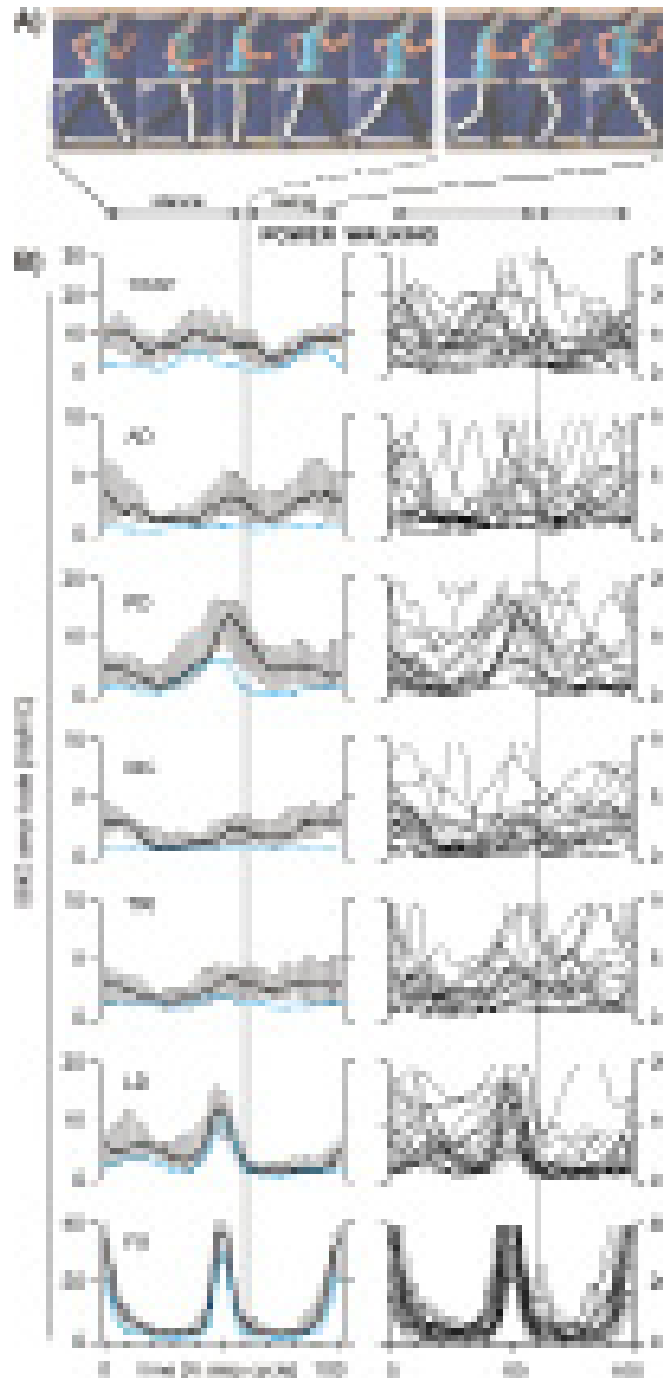
the walking direction, but whose waveforms are largely preserved (Lacquaniti et al., 2012).

Muscle Activity during Power Walking

Data of normal walking and power walking are contrasted in Figure 6. All investigated muscles were significantly ($p < 0.01$) more active in the latter condition (see Table 4 in appendix). Exaggerated arm swing was associated with nearly continuous TRAP activity during the entire step cycle, in contrast to the biphasic pattern of normal walking. Maximal PD activity was reached somewhat later than during normal walking, i.e. at ~55% of the step cycle, just after heelstrike of the contralateral foot. This PD contraction probably implemented powerful backward arm swing by shoulder extension, assisted by TRI activity. BIC and TRI were active together in the second half of the step cycle (50-100%) to probably stabilize the elbow joint. The reversal from backward to forward arm swing at the end of the step cycle was associated with AD and BIC contractions; the latter prevented excessive elbow extension. Minimum AD, PD, BIC and TRI signals were found during midstance (~30% of the step cycle), suggesting that forward arm swing is mostly passive at that time.

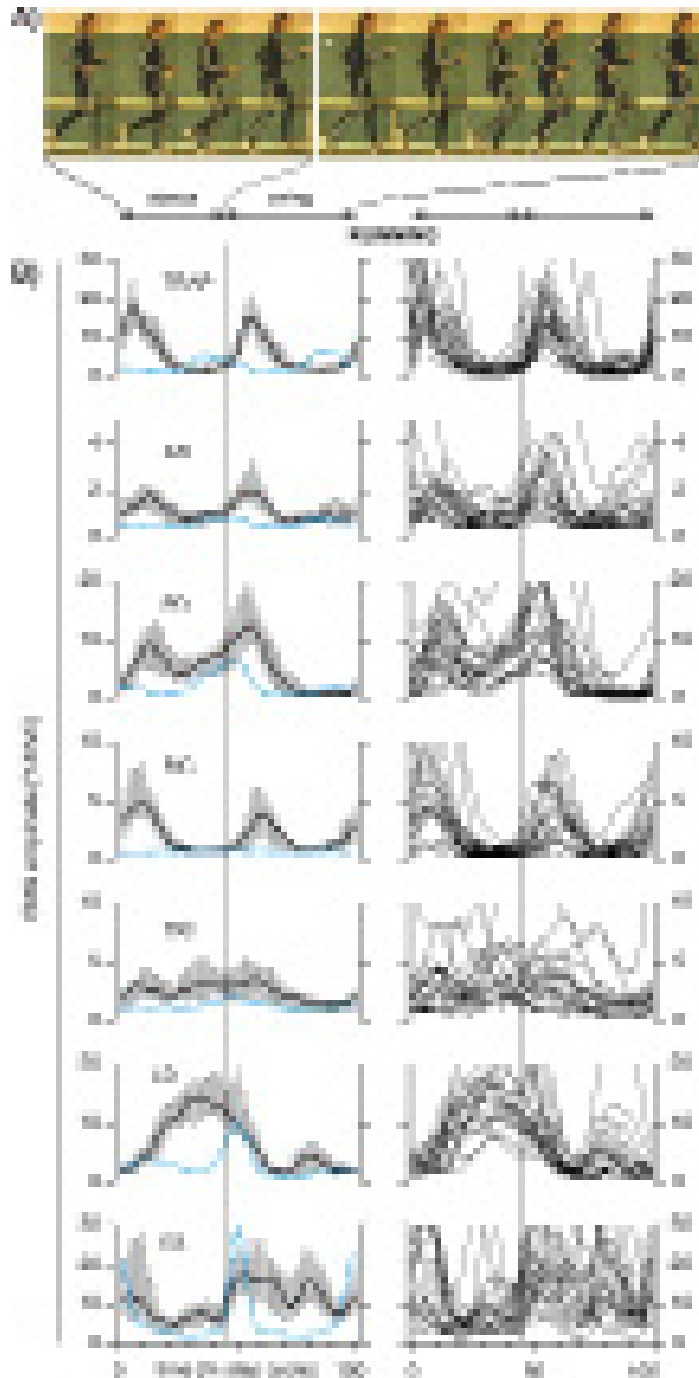
A high inter-subject variability of power walking performance is evident from the individual EMG curves, especially of the TRAP, AD, PD and TRI (Figure. 6, right panel). The volunteers had not been familiar with this walking technique prior to the experiments. They were instructed carefully and they practiced thoroughly prior to the EMG recordings. Nevertheless a uniform and stereotyped performance was obviously not reached. Future work could combine longer repeated training with kinematic and EMG analyses. The EMG profiles of LD and ES were very similar during normal walking and power walking, as basic biomechanical features are shared by both modes of gait (curvature of COM trajectory during stance,

Figure 6. Power walking. a. Limb movements during power walking with accentuation of arm swing. Stance and swing phase of the right leg are indicated. b. EMG curves. Left panel: Group results, i.e. median EMG profiles of the 20 subjects during normal walking (blue broken line) and power walking (black solid line). Treadmill velocity was 6 km/h. Error bars denote quartiles for power walking (25%, 75%). Right panel: Individual EMG curves of the 20 participants during power walking. Otherwise as in Figure. 3



Arm Swing during Human Gait Studied by EMG

Figure 7. Running. a. Movements during slow running (6 km/h). Stance and swing phase of the right leg are indicated. Note the downward “bobbing” of the head during mid-stance. White asterisk denotes the short float phase, where there is no ground contact. b. EMG curves. Left panel: Group results, i.e. median EMG profiles of the 20 subjects during normal walking (blue broken line) and running (black solid line). Error bars denote quartiles (25%, 75%) for running. Right panel: Individual EMG curves of the 20 participants during running. Otherwise as in Figure. 3



inverted pendulum mechanism). Conversely, the LD and ES activation profiles differ markedly between walking and running (see below).

Muscle Activity during Running

Compared to walking, the shoulders are more extended (upper arm retraction) and the elbows more flexed during running, and the anterior-posterior amplitude of arm swing is diminished (see kinematic data in Kuhtz-Buschbeck et al., 2008). Figure 7 shows EMG curves of both gait conditions, recorded at a treadmill speed of 6 km/h. All examined muscles were significantly more active ($p < 0.001$) during running than during walking (Table 4, appendix). The two peaks of TRAP activity were shifted towards the onset of the step cycle during running, occurring just after ground contact of each foot, i.e. at ~5% and 55% of the step cycle. Likewise, ankle extensor activity is known to shift from the second to the first half of the stance phase at the transition from walking to running (Cappellini, Ivanenko, Poppele, & Lacquaniti, 2006). AD, PD and BIC profiles all had two peaks during running, one in the early stance phase and another one in the early swing phase. The first peak had not been present during walking. Sharp peaks of LD activity in the middle of the step cycle, which are typical for walking, were not found during running. Instead, LD activity started in the early stance phase of running and continued into the swing phase (until ~60%). Hence a sustained lengthening LD contraction opposes forward arm swing during running and implements the reversal to backward arm swing in the middle of the step cycle. An analogous role of the LD has been described for quadrupedal walking in monkeys, where the main function of this muscle is to slow down the swinging forelimb in preparation for touchdown of the hand (Larson & Stern, 2007). Timing and amplitude of lumbar ES activity differed between walking and running, too. This muscle showed (rather variable) EMG activity in the swing phase of running and not a

clear peak at ~50% of the step cycle as during walking. Previous research of Thorstensson, Carlson, Zomlefer, and Nilsson (1982) found evidence that the lumbar ES controls trunk movements mainly in the sagittal plane during running, whereas it restricts mostly movements in the frontal plane during walking.

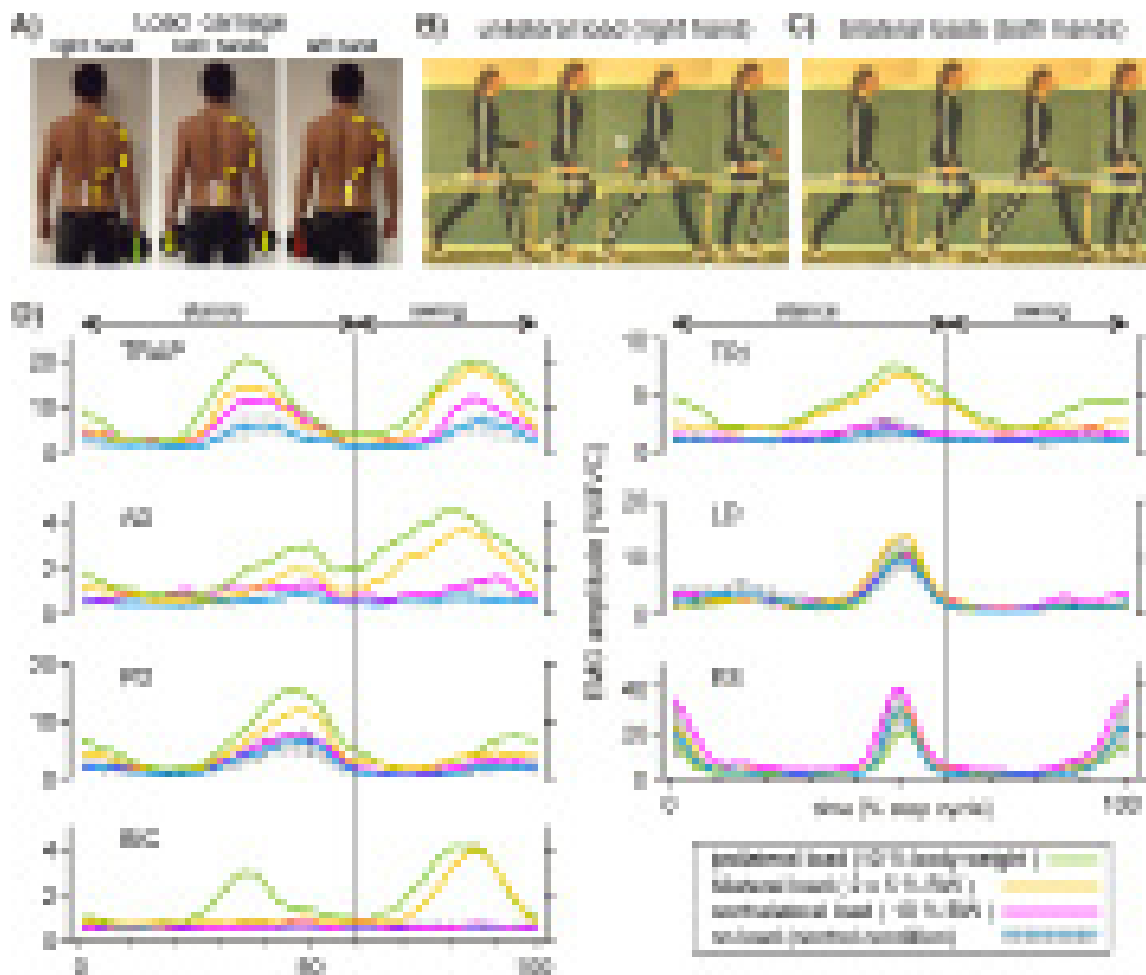
In summary, the EMG patterns of walking and running are dissimilar. Enhanced muscle activity (TRAP, AD, PD, BIC) in the early stance phase of the ipsilateral leg is characteristic for running. Forward movement of the COM (center of body mass) decelerates and the COM approaches the ground at that time (Hamner & Delp, 2013). The function of the supporting leg as a spring, which stores elastic energy, explains the analogous temporal shift of leg muscle activity towards the onset of the stance phase (Cappellini et al., 2006; Ivanenko et al., 2008). Activation peaks of LD and ES during phases of double stance, in which both feet contact the ground, are typical for walking, but not for running. As in walking, the arm swing during running is known to counterbalance the vertical angular momentum of the legs (Hamner & Delp, 2013), but the patterns of muscle activity needed to accomplish this function are different.

Muscle Activity during Load Carriage

The results of are displayed as median EMG curves of the twenty subjects for the three load conditions together with control data of normal walking without load (Figure. 8). Numerical values are listed in Table 5 (appendix). Bimanual load carriage (Figure. 8) increased the EMG activity of all investigated muscles above control values ($p < 0.01$). Phasic EMG signals were obvious, but the arm swing excursions were reduced. BIC activity reached a pronounced peak in the swing phase (at ~40%) in this condition. Unimanual load carriage with the right hand augmented the EMG signals of most ipsilateral muscles (TRAP, AD, PD, BIC, TRI) more than bimanual load carriage (see Table 5). The increases of TRAP, AD, and

Arm Swing during Human Gait Studied by EMG

Figure 8. Load carriage. a. Allocation of loads during unimanual carriage and bilateral carriage. White ellipsoids indicate straining of lumbar ES muscle(s) in each condition. Yellow dots denote positions of EMG electrodes (always on right side). b. Limb movements (stance phase) during unilateral carriage. Swinging of the loaded arm is diminished, swinging of the non-loaded arm is pronounced (white asterisk). c. Bimanual load carriage. d. Median EMG curves (group result of 20 subjects) of the four conditions, superimposed at the same scale for direct comparison. Blue lines with error bars (quartiles 25%, 75%) are curves of normal walking without load. Green lines: Right hand (ipsilateral to EMG electrodes) carries the load. Red lines: Left hand carries load. Yellow lines: Bimanual carriage. Treadmill velocity was always 6 km/h



TRI activities were most pronounced (more than threefold). However, activity of the ipsilateral ES, i.e. a paravertebral muscle, was reduced during unimanual load carriage.

The non-loaded side was affected by unilateral load carriage. When the load was carried with the

left hand (Figure. 8) contralateral muscle activity increased; especially the EMG signals of the right TRAP, AD and ES were higher (Table 5). In accordance with the above, other researchers found an increased movement amplitude of the non-loaded free arm during walking, which may

compensate for the reduced movements of the loaded arm (Donker et al., 2002). With more EMG leads (which were not available), it would have been possible to measure ipsi- and contralateral effects of unilateral load carriage simultaneously. Resultant asymmetries of lower extremity kinematics and ground reaction forces have been published elsewhere (Zhang, Ye, & Wang, 2010).

FUTURE RESEARCH DIRECTIONS

We studied the EMG patterns of (only) seven muscles due to technical limitations. Further research may include more muscles and also provide complementary kinematic data for the different gait conditions. Hof, Elzinga, Grimmius, and Halbertsma (2002) found that average EMG profiles of leg muscles vary in a predictable way with gait velocity, but this relationship has not yet been established in detail for upper limb muscles. Gait patterns and arm-leg coordination are somewhat different between treadmill and overground locomotion (Carpinella, Crenna, Rabuffetti, & Ferrarin, 2010; Stolze et al., 1997). The impact of these differences on upper limb EMG patterns is not yet known and may be a topic of further research. A considerable inter-individual variability of the arm and shoulder muscle EMG curves is evident from the current data. Individual styles of walking and running most likely shape the muscle activation patterns. Some people swing their arms nearly directly forward and back (parallel to gait direction), others swing them with some crossover in front of the chest, elbow flexion can vary etc. Asymmetrical behaviour of the lower limbs and side differences of arm swing occur during normal gait of able-bodied subjects (Kuhtz-Buschbeck et al., 2008; Sadeghi, Allard, Prince, & Labelle, 2000). How such individual features and asymmetries of gait influence the EMG activity is not known precisely, so that further study is warranted.

Explaining inter-individual differences may be one topic. On the other hand, it is also interesting

to identify basic patterns of muscle activity, which remain stable across subjects and gait conditions. Recent research has used component analyses to reconstruct the EMG profiles of a large set of muscles as a weighted combination of a few (i.e. four to five) basic underlying activation patterns (for review see Lacquaniti et al., 2012). Each of these patterns is timed at different periods of the gait cycle and weighted according to its relative contribution to the overall EMG profile. Timing and weighting of the basic patterns vary between gait conditions, which results in different EMG curves, but the waveforms of the patterns stay nearly constant. This approach has been mostly applied to EMG data of trunk and leg muscles, but it will certainly be relevant for upper limb muscles as well.

It is often assumed that if one moves the arms quickly and with power, the legs will also move more quickly and powerfully. If this was true, then significant correlations should exist between EMG signals of arm and leg muscles e.g. during power walking and running, which may be an issue of further research. For recumbent stepping it has been shown that rhythmic arm movements can enhance and shape the muscle activity of the legs (Ferris, Huang, & Kao, 2006). Possible influences of the arms on the legs are also interesting because rhythmic arm movements could be included in the rehabilitation of walking after neurological injuries (Klimstra, Thomas, Stoloff, Ferris, & Zehr, 2009). A recent study of stroke patients found that arm movements (performed on a treadmill with sliding handles) affect the kinematic and EMG patterns of the legs (Stevenson, de Serres, & Lamontagne, 2010). Potential benefits of such gait rehabilitation protocols are a point of current clinical research.

Reduced arm swing during walking, which is often asymmetrical, is a typical feature of Parkinson's disease. Quantitative evaluation of arm swing might be useful for early and differential diagnosis, and for tracking of disease progression (Lewek, Poole, Johnson, Halawa, & Huang, 2010).

Arm Swing during Human Gait Studied by EMG

The reduction of the arm excursion is related to abnormal activation of shoulder muscles (Buchthal & Fernandez-Ballesteros, 1965). These authors found a spectrum of EMG abnormalities that ranged from wrongly timed non-rhythmical muscle activity to continuous rhythmical activity, which had no relation to the gait cycle. The posterior deltoid muscle was most often involved. A recent kinematic study of the influence of the basal ganglia on upper limb locomotor synergies evaluated arm and leg movements during gait in Parkinson's disease patients under four conditions, namely (i) no treatment (baseline), (ii) therapeutic stimulation of the subthalamic nucleus, (iii) L-DOPA medication, and (iv) a combination of both treatments (Crenna et al., 2008). Interestingly, gait-related movements of the arms and legs showed different susceptibility to the therapeutic interventions. Leg movements (thigh excursion, step length) improved significantly more than arm swing, which remained small. This disparity may be related to different supraspinal influences on CPGs of upper and lower limb movements. Direct corticospinal control dominates arm and hand movements, whereas phylogenetically older pathways involving brainstem relay stations influence leg movements (Crenna et al., 2008; Chastan et al., 2009). Future EMG studies might confirm this concept, further elucidate the influence of the basal ganglia on locomotor synergies, and possibly help to optimize treatment of the gait disorder in Parkinson's disease. Control data of normal subjects provide a basis for such studies.

CONCLUSION

During normal and fast walking, both arms swing in alternation and in phase with the contralateral legs. We performed EMG recordings from upper limb muscles with healthy volunteers during different gait conditions on a treadmill. Free arm swing during normal forward walking is not an entirely passive movement; it is associated with rhythmi-

cal shortening and lengthening contractions of upper limb muscles. Lengthening contractions of elbow and shoulder extensor muscles curtail the forward arm swing and initiate the reversal of this movement in the middle of the step cycle, at the onset of the stance phase of the contralateral leg. Shortening contractions of these muscles then support the backward arm swing. Shoulder and elbow flexor muscles are generally less active than extensor muscles. The overall EMG activity of upper limb muscles during normal walking (at 6 km/h) with unrestricted arm swing is low (< 5% MVC) compared to maximum voluntary contractions. Passive dynamics make reciprocal arm swing easy.

Spinal locomotor pattern generators and neuronal pathways that couple hindlimb and forelimb movements have been demonstrated earlier in quadrupedal animals. We found that some phasic EMG activity of the posterior deltoid and of other muscles persists when both arms are immobilized with a brace during human walking. It is not possible to completely suppress this remaining rhythmic activity, even when biofeedback of the EMG signals is provided. This supports the concept that the leg movements of human walking automatically trigger simultaneous activity of arm and shoulder muscles.

Forward and backward walking are associated with different patterns of upper limb EMG activity, although both modes of gait have similar kinematic features. Likewise, the transition from walking to running induces pronounced changes of the EMG curves. Compared to normal walking, power walking with deliberate accentuation of arm swing is characterized by strong increases in the activities of the trapezius, biceps brachii, and of the anterior portion of the deltoid muscle. Unimanual load carriage during walking increases the muscle activities in both arms, i.e. the loaded and the non-loaded arm. Paravertebral muscle activity (erector spinae) on the side of the load is, however, reduced.

Studies of physiological EMG patterns in healthy volunteers provide a basis for research in patients with gait disorders that are associated with reduced and/or altered arm swing.

REFERENCES

- Anders, C., Wagner, H., Puta, C., Grassme, R., Petrovitch, A., & Scholle, H. C. (2007). Trunk muscle activation patterns during walking at different speeds. *Journal of Electromyography and Kinesiology*, *17*(2), 245–252. doi:10.1016/j.jelekin.2006.01.002 PMID:16517182
- Arellano, C. J., & Kram, R. (2011). The effects of step width and arm swing on energetic cost and lateral balance during running. *Journal of Biomechanics*, *44*(7), 1291–1295. doi:10.1016/j.jbiomech.2011.01.002 PMID:21316058
- Ballesteros, M. L. F., Buchthal, F., & Rosenfalck, P. (1965). The pattern of muscular activity during the arm swing of natural walking. *Acta Physiologica Scandinavica*, *63*, 296–310. doi:10.1111/j.1748-1716.1965.tb04069.x PMID:14329151
- Balter, J. E., & Zehr, E. P. (2007). Neural coupling between the arms and legs during rhythmic locomotor-like cycling movement. *Journal of Neurophysiology*, *97*(2), 1809–1818. doi:10.1152/jn.01038.2006 PMID:17065245
- Barthelemy, D., & Nielsen, J. B. (2010). Cortico-spinal contribution to arm muscle activity during human walking. *The Journal of Physiology*, *588*(6), 967–979. doi:10.1113/jphysiol.2009.185520 PMID:20123782
- Brackley, H. M., & Stevenson, J. M. (2004). Are children's backpack weight limits enough? A critical review of the relevant literature. *Spine*, *29*(19), 2184–2190. doi:10.1097/01.brs.0000141183.20124.a9 PMID:15454714
- Buchthal, F., & Fernandez-Ballesteros, M. L. (1965). Electromyographic study of the muscles of the upper arm and shoulder during walking in patients with Parkinson's disease. *Brain*, *88*, 875–896. doi:10.1093/brain/88.5.875 PMID:5864465
- Burden, A. (2010). How should we normalize electromyograms obtained from healthy participants? What we have learned from over 25 years of research. *Journal of Electromyography and Kinesiology*, *20*(6), 1023–1035. doi:10.1016/j.jelekin.2010.07.004 PMID:20702112
- Callaghan, J. P., Patla, A. E., & McGill, S. M. (1999). Low back three-dimensional joint forces, kinematics, and kinetics during walking. *Clinical Biomechanics (Bristol, Avon)*, *14*(3), 203–216. doi:10.1016/S0268-0033(98)00069-2 PMID:10619108
- Cappellini, G., Ivanenko, Y. P., Dominici, N., Poppele, R. E., & Lacquaniti, F. (2010). Migration of motor pool activity in the spinal cord reflects body mechanics in human locomotion. *Journal of Neurophysiology*, *104*(6), 3064–3073. doi:10.1152/jn.00318.2010 PMID:20881204
- Cappellini, G., Ivanenko, Y. P., Poppele, R. E., & Lacquaniti, F. (2006). Motor patterns in human walking and running. *Journal of Neurophysiology*, *95*(6), 3426–3437. doi:10.1152/jn.00081.2006 PMID:16554517
- Carpinella, I., Crenna, P., Rabuffetti, M., & Ferrarin, M. (2010). Coordination between upper- and lower-limb movements is different during over-ground and treadmill walking. *European Journal of Applied Physiology*, *108*(1), 71–82. doi:10.1007/s00421-009-1168-5 PMID:19756711
- Ceccato, J. C., de Sèze, M., Azevedo, C., & Cazalets, J. R. (2009). Comparison of trunk activity during gait initiation and walking in humans. *PLoS ONE*, *4*(12), e8193. doi:10.1371/journal.pone.0008193 PMID:19997606

Arm Swing during Human Gait Studied by EMG

- Chastan, N., Westby, G. W. M., Yelnik, J., Bardinet, E., Do, M. C., Agid, Y., & Welter, M. L. (2009). Effects of nigral stimulation on locomotion and postural stability in patients with Parkinson's disease. *Brain*, *132*(1), 172–184. doi:10.1093/brain/awn294 PMID:19001482
- Chiovetto, E. (2011). The motor system plays the violin: a musical metaphor inferred from the oscillatory activity of the α -motoneuron pools during locomotion. *Journal of Neurophysiology*, *105*(4), 1429–1431. doi:10.1152/jn.01119.2010 PMID:21273310
- Cho, K. K., Kim, Y. S., & Kim, E. J. (2006). The comparative analysis of kinematic and EMG on power walking and normal gait. *Korean Journal of Sport Biomechanics*, *16*(2), 85–95. doi:10.5103/KJSB.2006.16.2.085
- Collins, S. H., Adamczyk, P. G., & Kuo, A. D. (2009). Dynamic arm swinging in human walking. *Proceedings. Biological Sciences*, *276*, 3679–3688. doi:10.1098/rspb.2009.0664 PMID:19640879
- Crenna, P., Carpinella, I., Lopiano, L., Marzegan, A., Rabuffetti, M., & Rizzone, M. et al. (2008). Influence of basal ganglia on upper limb locomotor synergies. Evidence from deep brain stimulation and L-DOPA treatment in Parkinson's disease. *Brain*, *131*(12), 3410–3420. doi:10.1093/brain/awn272 PMID:18952669
- De Séze, M., Falgairolle, M., Viel, S., Assaiante, C., & Cazalets, J. R. (2008). Sequential activation of axial muscles during different forms of rhythmic behavior in man. *Experimental Brain Research*, *185*(2), 237–247. doi:10.1007/s00221-007-1146-2 PMID:17940760
- Dietz, V. (2002). Do human bipeds use quadrupedal coordination? *Trends in Neurosciences*, *25*(9), 462–467. doi:10.1016/S0166-2236(02)02229-4 PMID:12183207
- Dietz, V., & Michel, J. (2009). Human bipeds use quadrupedal coordination during locomotion. *Annals of the New York Academy of Sciences*, *1164*, 97–103. doi:10.1111/j.1749-6632.2008.03710.x PMID:19645886
- Donker, S. F., Mulder, T., Nienhuis, B., & Duyens, J. (2002). Adaptation in arm movements for added mass to wrist or ankle during walking. *Experimental Brain Research*, *145*, 26–31. doi:10.1007/s00221-002-1145-2
- Eke-Okoro, S. T., Gregoric, M., & Larsson, L. E. (1997). Alterations in gait resulting from deliberate changes of arm-swing amplitude and phase. *Clinical Biomechanics (Bristol, Avon)*, *12*(7-8), 516–521. doi:10.1016/S0268-0033(97)00050-8 PMID:11415762
- Elftman, H. (1939). The function of the arms in walking. *Human Biology*, *11*(4), 529–535.
- Falgairolle, M., de Séze, M., Juvin, L., Morin, D., & Cazalets, J. R. (2006). Coordinated network functioning in the spinal cord: an evolutionary perspective. *Journal of Physiology, Paris*, *100*(5-6), 304–316. doi:10.1016/j.jphysparis.2007.05.003 PMID:17658245
- Faulkner, J. A. (2003). Terminology for contractions of muscles during shortening, while isometric, and during lengthening. *Journal of Applied Physiology*, *95*(2), 455–459. PMID:12851415
- Ferris, D. P., Huang, H. J., & Kao, P. C. (2006). Moving the arms to activate the legs. *Exercise and Sport Sciences Reviews*, *34*(3), 113–120. doi:10.1249/00003677-200607000-00005 PMID:16829738
- Ford, M. P., Wagenaar, R. C., & Newell, K. M. (2007). Arm constraint and walking in healthy adults. *Gait & Posture*, *26*(1), 135–141. doi:10.1016/j.gaitpost.2006.08.008 PMID:16997561

- Frigo, C., & Crenna, P. (2009). Multichannel SEMG in clinical gait analysis: A review and state-of-the-art. *Clinical Biomechanics (Bristol, Avon)*, 24(3), 236–245. doi:10.1016/j.clinbiomech.2008.07.012 PMID:18995937
- Gillette, J. C., Stevermer, C. A., Miller, R. H., Meardon, S. A., & Schwab, C. V. (2010). The effects of age and type of carrying task on lower extremity kinematics. *Ergonomics*, 53(3), 355–364. doi:10.1080/00140130903402234 PMID:20191410
- Grasso, R., Bianchi, L., & Lacquaniti, F. (1998). Motor patterns for human gait: backward versus forward locomotion. *Journal of Neurophysiology*, 80(4), 1868–1885. PMID:9772246
- Grillner, S. (1981). Control of locomotion in bipeds, tetrapods, and fish. In V. Brooks (Ed.), *Handbook of physiology-the nervous system II* (pp. 1179–1236). Baltimore: Waverly Press.
- Grillner, S. (2011). Neuroscience. Human locomotor circuits conform. *Science*, 334(6058), 912–913. doi:10.1126/science.1214778 PMID:22096178
- Hamner, S. R., & Delp, S. L. (2013). Muscle contributions to fore-aft and vertical body mass center accelerations over a range of running speeds. *Journal of Biomechanics*, 46(4), 780–787. doi:10.1016/j.jbiomech.2012.11.024 PMID:23246045
- Hamner, S. R., Seth, A., & Delp, S. L. (2010). Muscle contributions to propulsion and support during running. *Journal of Biomechanics*, 43(14), 2709–2716. doi:10.1016/j.jbiomech.2010.06.025 PMID:20691972
- Hermens, H. J., Freriks, B., Disselhorst-Klug, C., & Rau, G. (2000). Development of recommendations for SEMG sensors and sensor placement procedures. *Journal of Electromyography and Kinesiology*, 10(5), 361–374. doi:10.1016/S1050-6411(00)00027-4 PMID:11018445
- Hinrichs, R. N. (1990). Whole body movement: Coordination of arms and legs in walking and running. In J. M. Winters, & S. L. Y. Woo (Eds.), *Multiple muscle systems: Biomechanics and movement organization* (pp. 694–705). New York: Springer. doi:10.1007/978-1-4613-9030-5_45
- Hof, A. L., Elzinga, H., Grimmius, W., & Halbertsma, J. P. (2002). Speed dependence of averaged EMG profiles in walking. *Gait & Posture*, 16(1), 78–86. doi:10.1016/S0966-6362(01)00206-5 PMID:12127190
- Hogue, R. E. (1969). Upper-extremity muscular activity at different cadences and inclines during normal gait. *Physical Therapy*, 49(9), 963–972. PMID:5802700
- Ivanenko, Y. P., Cappellini, G., Poppele, R. E., & Lacquaniti, F. (2008). Spatiotemporal organization of alpha-motoneuron activity in the human spinal cord during different gaits and gait transitions. *The European Journal of Neuroscience*, 27(12), 3351–3368. doi:10.1111/j.1460-9568.2008.06289.x PMID:18598271
- Jackson, K. M., Joseph, J., & Wyard, S. J. (1978). A mathematical model of arm swing during human locomotion. *Journal of Biomechanics*, 11(6-7), 277–289. doi:10.1016/0021-9290(78)90061-1 PMID:711777
- Jackson, K. M., Joseph, J., & Wyard, S. J. (1983a). The upper limbs during human walking. Part I: Sagittal movement. *Electromyography and Clinical Neurophysiology*, 23(6), 425–434. PMID:6641598
- Jackson, K. M., Joseph, J., & Wyard, S. J. (1983b). The upper limbs during human walking. Part 2: Function. *Electromyography and Clinical Neurophysiology*, 23(6), 435–446. PMID:6641599

Arm Swing during Human Gait Studied by EMG

- Klimstra, M. D., Thomas, E., Stoloff, R. H., Ferris, D. P., & Zehr E. P. (2009) Neuromechanical considerations for incorporating rhythmic arm movement in the rehabilitation of walking. *Chaos* 19(2), 026102 1-14.
- Konrad, P., Schmitz, K., & Denner, A. (2001). Neuromuscular evaluation of trunk-training exercises. *Journal of Athletic Training*, 36(2), 109–118. PMID:12937449
- Kubo, M., Wagenaar, R. C., Saltzman, E., & Holt, K. G. (2004). Biomechanical mechanism for transitions in phase and frequency of arm and leg swing during walking. *Biological Cybernetics*, 91(2), 91–98. doi:10.1007/s00422-004-0503-5 PMID:15351887
- Kuhtz-Buschbeck, J. P., Brockmann, K., Gilster, R., Koch, A., & Stolze, H. (2008). Asymmetry of arm-swing not related to handedness. *Gait & Posture*, 27(3), 447–454. doi:10.1016/j.gaitpost.2007.05.011 PMID:17616462
- Kuhtz-Buschbeck, J. P., & Jing, B. (2012). Activity of upper limb muscles during human walking. *Journal of Electromyography and Kinesiology*, 22(2), 199–206. doi:10.1016/j.jelekin.2011.08.014 PMID:21945656
- Lacquaniti, F., Ivanenko, Y. P., & Zago, M. (2012). Patterned control of human locomotion. *The Journal of Physiology*, 590(10), 2189–2199. doi:10.1113/jphysiol.2011.215137 PMID:22411012
- Larson, S. G., & Stern, J. T. (2007). Humeral retractor EMG during quadrupedal walking in primates. *The Journal of Experimental Biology*, 210(7), 1204–1215. doi:10.1242/jeb.002337 PMID:17371919
- Lewek, M. D., Poole, R., Johnson, J., Halawa, O., & Huang, X. (2010). Arm swing magnitude and asymmetry during gait in the early stages of Parkinson's disease. *Gait & Posture*, 31(2), 256–260. doi:10.1016/j.gaitpost.2009.10.013 PMID:19945285
- Li, Y., Wang, W., Crompton, R. H., & Gunther, M. M. (2001). Free vertical moments and transverse forces in human walking and their role in relation to arm-swing. *The Journal of Experimental Biology*, 204(1), 47–58. PMID:11104710
- Meakin, J. (2003). *The beginner's guide to power walking*. Hauppauge, NY: Barron's Educational Series.
- Meysns, P., Bruijn, S. M., & Duysens, J. (2013). (in press). The how and why of arm swing during human walking. *Gait & Posture*; Epub ahead of print. doi:10.1016/j.gaitpost.2013.02.006 PMID:23489950
- Murray, M. P. (1967). Gait as a total pattern of movement. *American Journal of Physical Medicine*, 46(1), 290–333. PMID:5336886
- Nicola, T. L., & Jewison, D. J. (2012). The anatomy and biomechanics of running. *Clinics in Sports Medicine*, 31(2), 187–201. doi:10.1016/j.csm.2011.10.001 PMID:22341011
- Nielsen, J. B. (2003). How we walk: Central control of muscle activity during human walking. *The Neuroscientist*, 9(3), 195–204. doi:10.1177/1073858403009003012 PMID:15065815
- Ortega, J. D., Fehلمان, L. A., & Farley, C. T. (2008). Effects of aging and arm swing on the metabolic cost of stability in human walking. *Journal of Biomechanics*, 41(16), 3303–3308. doi:10.1016/j.jbiomech.2008.06.039 PMID:18814873

- Park, J. (2008). Synthesis of natural arm swing motion in human bipedal walking. *Journal of Biomechanics*, *41*(7), 1417–1426. doi:10.1016/j.jbiomech.2008.02.031 PMID:18417138
- Pontzer, H., Holloway, J. H., Raichlen, D. A., & Lieberman, D. E. (2009). Control and function of arm swing in human walking and running. *The Journal of Experimental Biology*, *212*(4), 523–534. doi:10.1242/jeb.024927 PMID:19181900
- Sadeghi, H., Allard, P., Prince, F., & Labelle, H. (2000). Symmetry and limb dominance in able-bodied gait: A review. *Gait & Posture*, *12*(1), 34–45. doi:10.1016/S0966-6362(00)00070-9 PMID:10996295
- Schünke, M., Schulte, E., Schumacher, U., Voll, M., & Wesker, K. (2007). *Allgemeine Anatomie und Bewegungssystem. Prometheus. Lernatlas der Anatomie*. Stuttgart, Germany: Georg Thieme Verlag.
- Stephenson, J. L., De Serres, S. J., & Lamontagne, A. (2010). The effect of arm movements on the lower limb during gait after a stroke. *Gait & Posture*, *31*(1), 109–115. doi:10.1016/j.gaitpost.2009.09.008 PMID:19854654
- Stolze, H., Kutz-Buschbeck, J. P., Mondwurf, C., Boczek-Funcke, A., Jöhnk, K., Deuschl, G., & Illert, M. (1997). Gait analysis during treadmill and overground locomotion in children and adults. *Electroencephalography and Clinical Neurophysiology*, *105*(6), 490–497. doi:10.1016/S0924-980X(97)00055-6 PMID:9448652
- Thorstensson, A. (1986). How is the normal locomotor program modified to produce backward walking? *Experimental Brain Research*, *61*(3), 664–668. doi:10.1007/BF00237595 PMID:3956625
- Thorstensson, A., Carlson, H., Zomlefer, M. R., & Nilsson, J. (1982). Lumbar back muscle activity in relation to trunk movements during locomotion in man. *Acta Physiologica Scandinavica*, *116*(1), 13–20. doi:10.1111/j.1748-1716.1982.tb10593.x PMID:7158389
- Umberger, B. R. (2008). Effects of suppressing arm swing on kinematics, kinetics, and energetics of human walking. *Journal of Biomechanics*, *41*(11), 2575–2580. doi:10.1016/j.jbiomech.2008.05.024 PMID:18621376
- Wagenaar, R. C., & van Emmerik, R. E. (2000). Resonant frequencies of arms and legs identify different walking patterns. *Journal of Biomechanics*, *33*(7), 853–861. doi:10.1016/S0021-9290(00)00020-8 PMID:10831760
- Webb, D., Tuttle, R. H., & Baksh, M. (1994). Pendular activity of human upper limbs during slow and normal walking. *American Journal of Physical Anthropology*, *93*(4), 477–489. doi:10.1002/ajpa.1330930407 PMID:8048469
- Weiss, P. L., & St Pierre, D. (1983). Upper and lower extremity EMG correlations during normal human gait. *Archives of Physical Medicine and Rehabilitation*, *64*(1), 11–15. PMID:6849627
- Wirz, M., Colombo, G., & Dietz, V. (2001). Long term effects of locomotor training in spinal humans. *Journal of Neurology, Neurosurgery, and Psychiatry*, *71*(1), 93–96. doi:10.1136/jnnp.71.1.93 PMID:11413270
- Zehr, E. P., & Duysens, J. (2004). Regulation of arm and leg movement during human locomotion. *The Neuroscientist*, *10*(4), 347–361. doi:10.1177/1073858404264680 PMID:15271262

Zhang, X. A., Ye, M., & Wang, C. T. (2010). Effect of unilateral load carriage on postures and gait symmetry in ground reaction force during walking. *Computer Methods in Biomechanics and Biomedical Engineering*, 13(3), 339–344. doi:10.1080/10255840903213445 PMID:20521188

KEY TERMS AND DEFINITIONS

Angular Momentum: A vector quantity, which represents the product of a body's rotational inertia and rotational velocity. The angular momentum of a group of particles is the sum of the angular momentum of each particle. Often the angular momentum of a group of particles (e.g. human body) about their center of mass is calculated.

Center of Mass (COM) of the Body: The center of mass is the balance point of an object's mass (here human body); the distribution of the mass is balanced around the COM. A person's center of mass is slightly below his/her belly button.

Central Pattern Generator (CPG) for Locomotion: Neuronal network in the spinal cord that by itself can generate the rhythmic motor neuronal activity, which is necessary to activate the muscles so that stepping movements are elicited. Each limb has an own CPG.

Double Stance Phase (=Double Support Phase): Time interval in which the stance phases of the left and the right leg overlap, so that both feet are in contact with the ground. The double stance phase is a typical feature of walking; it does not exist in running.

Inter-Limb Coupling: Stereotyped co-ordination of upper and lower limb movements during locomotion. It ensures alternate movements of the right and left legs during walking, while the arms swing out of phase with the ipsilateral legs.

Maximum Voluntary Contraction (MVC): Maximum isometric (or nearly isometric) contraction of a muscle. Such contractions are used to normalize EMG amplitudes, which are then expressed as a percentage (%MVC) of the EMG signal during the MVC.

Propriospinal Pathways: Neuronal pathways within the spinal cord, which connect different centers (e.g. CPGs) of the spinal cord.

Step Cycle: Time interval between ground contact of one foot (footstrike) until the next ground contact of the same foot. The step cycle consists of a stance and a swing phase.

APPENDIX

Tables (Supplementary Data)

Table 1. Median EMG amplitudes during normal forward walking and walking with immobilized arms (Bound condition) at a treadmill velocity of 6 km/h

	Normal forward walking				Bound condition		
	Median	Percentiles			Median	Percentiles	
<i>Muscles</i>		25%	75%			25%	75%
<i>TRAP</i>	3.41	1.95	4.51		3.11	2.26	4.36
<i>% Change</i>	100%				- 9%		
<i>AD</i>	0.70	0.50	0.89		0.48 **	0.39	0.68
<i>% Change</i>	100%				- 31%		
<i>PD</i>	2.50	1.64	3.34		1.04 **	0.75	1.32
<i>% Change</i>	100%				- 58%		
<i>BIC</i>	0.64	0.47	0.78		0.63	0.54	0.76
<i>% Change</i>	100%				- 2%		
<i>TRI</i>	1.29	0.95	1.84		1.17 *	0.86	1.31
<i>% Change</i>	100%				- 10%		
<i>LD</i>	2.79	2.25	4.88		4.02 *	2.95	5.23
<i>% Change</i>	100%				+ 44%		
<i>ES</i>	7.08	5.61	8.61		8.00 **	6.16	10.19
<i>% Change</i>	100%				+ 13%		

Amplitude values of normalized EMG activity over the entire step cycle (unit % MVC) are given as median data of the 20 subjects, with percentiles describing inter-individual variability (quartiles, 25%, 75%). % Change: Values of normal walking (baseline) have been set to 100% to illustrate relative changes in Bound condition. *p<0.05, ** p<0.01 (Wilcoxon tests): Significant differences between Bound and Normal condition.

Arm Swing during Human Gait Studied by EMG

Table 2. Median EMG amplitude values during walking with the hands in the pockets (Pocket conditions) at a treadmill velocity of 6 km/h

	Normal gait	Left hand in pocket			Right hand in pocket			Both hands in pockets		
		Median	Percentiles		Median	Percentiles		Median	Percentiles	
Muscles			25%	75%		25%	75%		25%	75%
TRAP	3.41	3.84	2.44	5.00	3.85	2.26	4.95	3.58	2.48	5.04
% Change	100%	+13%			+13%			+5%		
AD	0.70	0.83	0.55	0.99	0.50 **	0.40	0.65	0.56 **	0.40	0.74
% Change	100%	+19%			-28%			-20%		
PD	2.50	2.57	2.04	3.04	1.67 **	1.09	2.54	2.15 *	1.24	2.79
% Change	100%	+3%			-33%			-14%		
BIC	0.64	0.62	0.46	0.83	0.70 *	0.55	0.87	0.78 **	0.59	0.98
% Change	100%	-4%			+10%			+21%		
TRI	1.29	1.52 *	1.03	1.92	1.54	1.16	1.82	1.77	1.25	2.21
% Change	100%	+18%			+19%			+37%		
LD	2.79	2.65	1.80	3.92	3.72 **	3.06	4.90	4.71 **	3.21	5.57
% Change	100%	-5%			+34%			+69%		
ES	7.08	7.74	5.25	8.31	7.91 *	5.41	8.64	7.73 **	5.61	9.09
% Change	100%	+9%			+12%			+9%		

Amplitude values of normalized EMG activity over the entire step cycle (unit %MVC) are given as median data of 20 subjects with percentiles (quartiles, 25%, 75%). %Change: Data of normal walking (baseline) have been set to 100% to illustrate the relative changes that occur in Pocket conditions. *p<0.05, ** p<0.01 (Wilcoxon tests): Significant differences between Normal and Pocket conditions.

Arm Swing during Human Gait Studied by EMG

Table 3. Median EMG amplitudes of forward walking and backward walking (at 4 km/h)

	Normal forward walking				Backward walking		
	Median	Percentiles			Median	Percentiles	
<i>Muscles</i>		25%	75%			25%	75%
<i>TRAP</i>	2.97	1.47	3.79		2.77	2.12	4.17
<i>% Change</i>	100%				- 7%		
<i>AD</i>	0.72	0.53	1.08		1.17 **	1.01	1.64
<i>% Change</i>	100%				+ 62%		
<i>PD</i>	1.71	1.08	2.41		3.19 **	2.25	4.45
<i>% Change</i>	100%				+ 87%		
<i>BIC</i>	0.56	0.43	0.70		0.76 **	0.59	0.95
<i>% Change</i>	100%				+ 35%		
<i>TRI</i>	1.05	0.77	1.36		1.84 **	1.49	2.82
<i>% Change</i>	100%				+ 74%		
<i>LD</i>	1.72	1.38	3.07		3.04 **	2.81	4.44
<i>% Change</i>	100%				+ 77%		
<i>ES</i>	5.16	4.27	7.25		7.50 **	4.91	9.98
<i>% Change</i>	100%				+ 45%		

Amplitude values of normalized EMG activity over the entire step cycle (unit %MVC) are given as median data of 20 subjects with percentiles (quartiles, 25%, 75%). %Change: Data of normal walking (control condition) have been set to 100% to illustrate relative changes during backward walking. ** p<0.01 (Wilcoxon tests): Significant differences between forward and backward walking

Arm Swing during Human Gait Studied by EMG

Table 4. Median EMG amplitudes for normal walking, power walking, and running at a treadmill velocity of 6 km/h

	Normal walking	Power walking		Running			
	Median	Median	Percentiles		Median	Percentiles	
<i>Muscles</i>			25%	75%		25%	75%
<i>TRAP</i>	3.41	9.51 *	5.53	11.38	# 6.72 *	5.63	8.29
% Change	100%	+179%			+97%		
<i>AD</i>	0.70	2.99 *	1.66	5.02	## 1.26 *	1.01	1.59
% Change	100%	+330%			+80%		
<i>PD</i>	2.50	5.88 *	4.25	9.17	5.54 *	3.65	7.94
% Change	100%	+136%			+122%		
<i>BIC</i>	0.64	2.31 *	1.44	3.39	2.38 *	1.37	3.29
% Change	100%	+261%			+272%		
<i>TRI</i>	1.29	2.97 *	1.73	4.85	2.45 *	1.86	3.70
% Change	100%	+131%			+90%		
<i>LD</i>	2.79	5.28 *	3.59	7.09	# 6.51 *	5.45	8.46
% Change	100%	+89%			+133%		
<i>ES</i>	7.08	10.80 *	8.13	14.49	13.29 *	7.84	14.44
% Change	100%	+53%			+88%		

Median amplitude values of the normalized EMG activity over the entire step cycle (unit % MVC) and relative changes of the amplitudes, compared to normal walking (see footnote of Table 1).

* Compared to normal walking (baseline), all EMG amplitudes were significantly (Wilcoxon tests, $p < 0.001$) increased during power walking, and also significantly increased during running.

$p < 0.05$, ## $p < 0.01$ (Wilcoxon tests): Significant differences between power walking and running.

Arm Swing during Human Gait Studied by EMG

Table 5. Median EMG amplitudes during walking with unimanual and bimanual carriage of a load (treadmill velocity 6 km/h)

	Normal gait	Load in left hand			Load in right hand			Load in both hands		
		Median	Percentiles		Median	Percentiles		Median	Percentiles	
<i>Muscles</i>			25%	75%		25%	75%		25%	75%
<i>TRAP</i>	3.41	5.13 **	4.51	7.67	11.06 **	7.16	16.2	# 8.41 **	5.61	10.8
% Change	100%	+50%			+224%			+147%		
<i>AD</i>	0.70	1.13 **	0.81	1.48	2.44 **	1.34	5.78	# 1.72 **	1.04	3.14
% Change	100%	+62%			+250%			+147%		
<i>PD</i>	2.50	2.92 **	2.02	4.06	6.37 **	3.66	10.5	# 4.81 **	3.25	6.75
% Change	100%	+17%			+155%			+93%		
<i>BIC</i>	0.64	0.67 *	0.52	0.85	1.95 **	1.41	2.84	# 1.26 **	0.75	2.50
% Change	100%	+5%			+205%			+97%		
<i>TRI</i>	1.29	1.70 **	1.13	2.37	4.37 **	2.63	6.36	# 3.42 **	2.64	5.28
% Change	100%	+32%			+239%			+165%		
<i>LD</i>	2.79	3.45 *	2.55	5.32	2.80	1.79	5.09	# 4.13 **	2.47	5.54
% Change	100%	+24%			+1%			+48%		
<i>ES</i>	7.08	12.0 **	9.56	14.2	5.68 *	4.20	7.73	# 8.40 **	6.57	9.48
% Change	100%	+69%			-20%			+19%		

Median amplitude values of normalized EMG activity over the entire step cycle (unit % MVC); group data of the 20 subjects. Relative changes (%) as compared to normal gait without load (baseline, 100%) are indicated (see footnote of Table 1).

* p<0.05, ** p<0.01 (Wilcoxon tests): Significant differences between load carriage condition and normal walking without any load. The loads (dumbbells) amounted to 10% of the body weight during unimanual carriage, and 2 x 5%, allocated to both hands, during bimanual carriage.

p< 0.05 (Wilcoxon tests): Significant differences between bimanual load carriage and unimanual load carriage with the right hand.

Chapter 7

Using in Vivo Subject-Specific Musculotendon Parameters to Investigate Voluntary Movement Changes after Stroke: An EMG-Driven Model of Elbow Joint

Hujing Hu

First Affiliated Hospital, Sun Yat-sen University, China & Guangdong Provincial Work Injury Rehabilitation Center, China

Le Li

First Affiliated Hospital, Sun Yat-sen University, China

ABSTRACT

Neuromusculoskeletal modeling provides insights into the muscular system which are not always obtained through experiment or observation alone. One of the major challenges in neuromusculoskeletal modeling is to accurately estimate the musculotendon parameters on a subject-specific basis. The latest medical imaging techniques such as ultrasound for the estimation of musculotendon parameters would provide an alternative method to obtain the muscle architecture parameters noninvasively. In this chapter, the feasibility of using ultrasonography to measure the musculotendon parameters of elbow muscles is validated. These parameters help to build a subject-specific EMG-driven model, which could predict the individual muscle force and elbow voluntary movement trajectory using the input of EMG signal without any trajectory fitting procedure involved. The results demonstrate the feasibility of using EMG-driven neuromusculoskeletal modeling with ultrasound-measured data for prediction of voluntary elbow movement for both unimpaired subjects and persons after stroke.

DOI: 10.4018/978-1-4666-6090-8.ch007

INTRODUCTION

Stroke: A Public Disease

The term ‘stroke’, or cerebro-vascular accident, refers to the neurological symptoms and signs, usually focal and acute, which result from diseases involving blood vessels. Stroke occurs when the blood supply to a part of the brain is cut off, and the brain cells in that part cannot function. Hemiparesis, partial weakness of the contralateral side of the body because of an injury to one side of the brain, commonly occurs after the onset of stroke. Strokes are either occlusive (due to occlusion of a blood vessel supplying the brain) or hemorrhagic (due to bleeding from a vessel). On average, occlusive strokes account for about 80% and hemorrhagic strokes for about 20% of all strokes (Westcott, 2000). There is a large population of humans that suffer from stroke. Stroke is one of the leading medical problems, mostly in elderly subjects (Popovic & Sinkjaer, 2000). In the U.S, there are approximately 730,000 new cases each year and an estimated 4 million survivors (Carr, 2003).

Therefore, there is a need to help stroke survivors to evaluate the disabilities and to regain their independence through rehabilitation as much as possible and, in addition, to reduce the burden of care on institutions and families.

Rationale and Scope of the Study

Cerebrovascular accident, or stroke, can cause significant impairment of neural or motor functions in survivors. Subsequent to these impairments, morphological changes in the architecture of the paretic muscles often occur, which affect the muscles’ functions. Previous studies have revealed a reduction in muscle volume, a shortening of muscle fiber, and a reduction in the number of motor units in the paretic muscles in people after stroke (Halar et al., 1978; Becher et al., 1998; Metoki et al., 2003). These muscle deformations are highly related to syndromes of paretic muscles,

such as muscle weakness, spasticity, contracture, etc (Patten et al., 2004; McCrea et al., 2002; Chae et al., 2002). Evaluating muscle structural variations in people after stroke is clinically important for both diagnosis and rehabilitation treatment.

Stroke rehabilitation often includes muscle strengthening, resistance training, constrained-induced therapy and robotic-assisted therapy. These are applied to counteract the muscle changes and the affected functions after stroke (Dean & Shepherd, 1997; Lum et al., 2004; Fasoli et al., 2003). In order to evaluate muscle impairment after stroke and the efficiency of different stroke rehabilitation programs, kinematics analysis and clinical scales have been used to evaluate neuromuscular changes and functional outcomes after interventions (Ju et al., 2002). Often, kinematics evaluations have focused on the results of motor execution (Yeh et al., 2004), while the clinical experiences of the examiners usually determined how clinical scales such as the Modified Ashworth Scale (MAS) were used (Pizzi et al., 2005; Bohannon & Smith, 1987). However, these evaluations do not reveal the specific changes at the level of muscle structure. Studies on skeletal muscle have shown that the moment across the joint generated by the associated muscle is highly related to the muscle’s architectural parameters, such as the cross-sectional area, moment arm and the muscle’s force–length behaviour (Huijing & Baan, 1992; Naici, 1999). Therefore, a technique that can measure these muscle architectural changes after the onset of stroke may help to evaluate the functional improvement of the affected muscle after an intervention program, and to enhance the understanding of the mechanism underlying the rehabilitation treatment.

BACKGROUND

Muscle Mechanics

It is known that, at constant levels of excitation, the amount of force generated isometrically is

a function of the length of the muscle under investigation (Gordon et al., 1966; Vredenberg & Rau, 1973). Muscles that operate on the ascending limb of the force-length relationship typically function in stretch-shortening cycle contractions, and muscles that operate on the descending limb typically function in shorten-stretch cycle contractions (McMahon, 1984). Fundamental theories behind the force-length relationship are sliding filament (Gordon et al., 1966) and cross-bridge theories (Huxley, 1957). Gordon assumed that the length changes in sarcomeres, fibers, and muscles are accomplished by relative sliding of the essentially inextensible myofilaments, actin and myosin, within a sarcomere. Huxley suggested that the relative sliding of actin and myosin is caused by independent force generators, i.e. the cross bridges.

Previously, most investigations were performed on single in vitro muscle fiber and in situ muscle of amphibians and small mammals (Gossman et al., 1982). There are still questions that how the classic force-length relationship (Gordon et al., 1966) is transferred to in vivo human muscle. The lack of this information is due to the difficulty of isolating individual muscles (Leedham & Dowling, 1995). Leedham and Dowling used electrical stimulation to isolate the torque-angle and force-length relationships of the biceps brachii, and found only the torque-angle had the classic inverted “U” pattern, but the force-length relationship displayed a monotonically increasing pattern in biceps brachii. Possible reasons could be that limitations of the elbow joint restrict the range of motion, which constrains the force-length relationship of in vivo biceps brachii to the ascending segment of the classic relationship of Gordon et al., (1966). These findings supported those of Lieber et al., (1990) and Murray et al., (2000) about the force-length relationship of the biceps brachii.

Zuurbier and Huijing (1995) used mean sarcomere length-force relations of intact rat fibers, multiplied by the number of sarcomeres in series, thought to be more appropriate for describing the

length-force relation of mammalian fiber and muscle (Zuurbier & Huijing, 1995). They provided this model to dispute the classic results by Gordon et al., (1966) that may have resulted in an overestimate of force at mean sarcomere lengths below, and an underestimate above optimum sarcomere lengths.

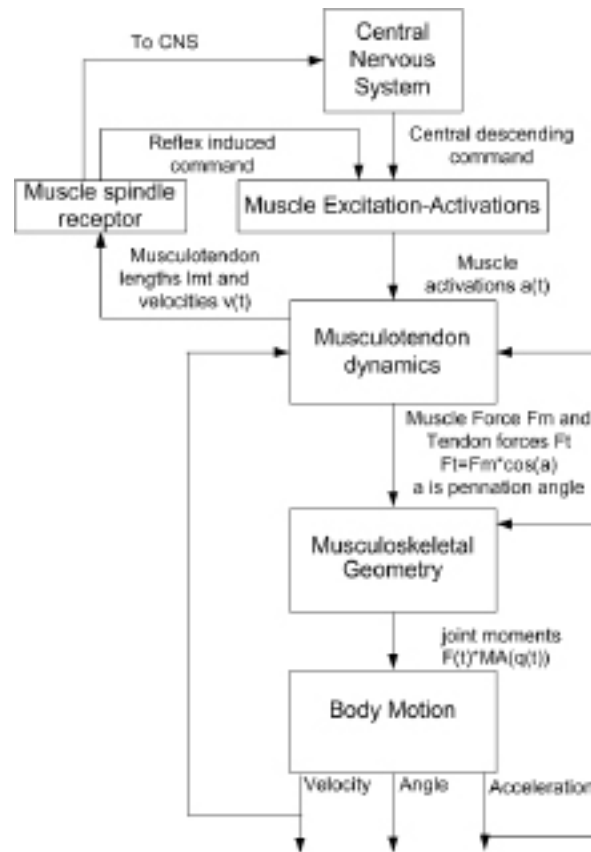
Neuromusculoskeletal Modeling

Neuromusculoskeletal (NMS) modeling (Figure 1) provides insights into the muscular system which are not always obtained through experiment or observation alone. (Buchanan et al., 2005; Gonzalez et al., 1996; Holzbaur et al., 2005; Li & Tong, 2011). However, the challenge is how to get the information accurately with this method. Koo et al., (2002) found that in order to enhance the accuracy and reliability of the model in evaluating muscle functions, accuracy and completeness of musculotendon parameters used in the model are important. Sensitivity and validation studies also have shown that the estimated values of the musculotendon parameters have significant effects on the simulation results (Huijing & Baan, 1992; Lieber et al., 1992; Murray et al., 2000).

Computational modeling and simulation of the NMS system provides both qualitative and quantitative insights into human movements (Pandy, 2001). In the past decades, computational modeling of the NMS system has been applied in many aspects. This modeling approach can provide more information on why and how the chain reaction of the NMS system occurs in order to produce all forms of functions. With the development of the computing technology and simulation resources available today, more complex and realistic models have been developed for studying human movement and other applications.

The NMS model can be defined as a set of equations which describe the dynamics of a neuromusculoskeletal system during generation of a function. The model is an idealized mathematical representation of the body, comprising the bones, muscles, joints, and passive structures in vary-

Figure 1. A schematic diagram of the neuromusculoskeletal system (modified from Martini, 1995)



ing degrees of complexity. The motor unit of the muscle fiber obtains the command from the nervous system and triggers the activation dynamics with muscle fiber contraction. The musculotendon force depends not only on the activation, but also on the architectural and biomechanical properties of the tendon and muscle fibers (Huijing & Baan, 1992). Various types of musculoskeletal models have been developed for human lower extremities (Neptune et al., 1998 and 2000; Anderson et al., 2001) and upper extremities (Giat et al., 1994; Maurel & Thalmann, 1998; Murray et al., 2000; Koo et al., 2002). Incorporated with dynamic analysis, this systematic approach to studying human movement can provide more accurate estimation and proper evaluation (Pandy, 2001).

Cadaveric-Scaled Parameters

Some of the previous modeling efforts directly applied cadaveric-scaled parameters to predict muscle force or joint trajectory (Chang et al., 1999; Giat et al., 1994). Cadaver data are limited in their usefulness because cadaver muscles undergo shrinking and could degrade during the course of storage. Such physiological changes could affect the measurement results. In addition, the fixed position of a cadaver limits investigation of dynamic changes in muscle architectures with a joint position, and these changes may have important implications in muscle function (Fukunaga et al., 1997; Maganaris et al., 1998). Moreover, most cadaver studies of muscle architecture were mainly conducted on subjects without impairment or disability.

Using in Vivo Subject-Specific Musculotendon Parameters

Musculotendon parameters can be regarded as anatomical or biomechanical properties that describe a skeletal muscle's force generating characteristics. Sensitivity studies have shown that selections of neuromusculoskeletal parameters have great effects on the modeling of NMS system (Lemay & Crago, 1996; Gonzalez et al., 1997). For example, when muscle does constant activation, its moment arm, physiological cross-section area (PCSA), and its operating range (how much and what portion of the isometric force-length curve the muscles uses during joint rotation) are the key factors that determine the maximum moment-generating capacity as a function of joint position (Huijing & Baan, 1992; Maganaris, 2004).

Ultrasonography of Musculotendon Parameter

Ultrasound technology has been applied in many aspects for measuring the musculoskeletal parameters in vivo. Accuracy of the ultrasound method in measuring muscle architecture features has also been demonstrated to show good agreement with direct anatomical measurement on cadaver (Narici et al., 1996; Martin et al., 2001). The pennation angle and muscle fascicle length are two architectural variables readily measured by using ultrasound imaging previously (Herbert et al., 1995; Maganaris et al., 2004; Kawakami et al., 1993; Hodges et al., 2003; Chleboun et al., 2001; Gao et al., 2009).

Recently, the feasibility of using ultrasonography to measure the musculotendon parameters of elbow muscles is validated (Li et al., 2007a). Ultrasound imaging technology has the advantages of being less expensive, relatively easier to incorporate with other instruments such as dynamometer, and feasible to test limb movements in a larger space. In addition, the measurement error of ultrasound imaging technology has been verified in comparison with direct anatomical measurements on specimens, with ultrasonography having a mean error of 7% for pennation angle and

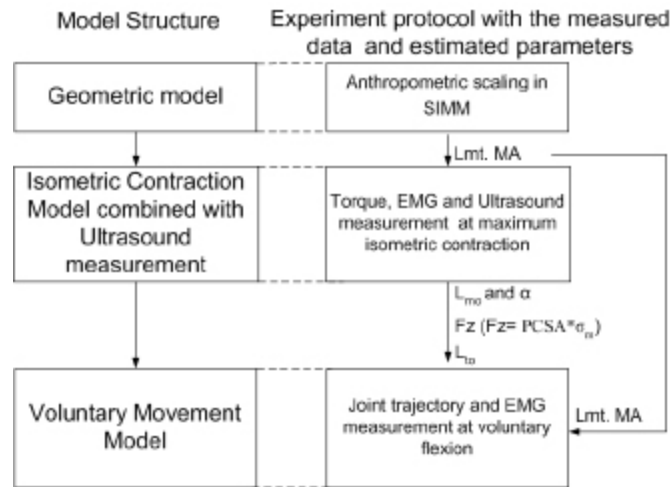
3.2% for fascicle length (Chardon et al., 2010). Thus, incorporating ultrasound-measured muscle architectural parameters in isometric contraction modeling for healthy subjects can be a good choice to collect the musculotendon parameters for the patients.

MAIN FOCUS OF THE CHAPTER

Model Structure

An EMG-driven model was built through combining the in vivo ultrasound measured musculotendon parameters to predict the joint trajectory (Figure 2). At first, a subject-specific isometric contraction model of the elbow joint was built, which incorporated an anthropometrically scaled geometrical model, a Hill-type musculotendon model. The isometric contraction model also included an optimization process and the model could be used to obtain muscle parameters and to evaluate the muscle properties in persons after stroke. In details, a subject-scaled geometrical model was used to calculate muscle moment arms (MA) and musculotendon lengths (l_{mt}) (Li et al., 2007b). These parameters were then used in the isometric contraction model and voluntary elbow flexion model (Figure 2). The ultrasound technique was employed to measure the pennation angle (α) at different joint angles and muscle optimal length (l_{mo}) of each prime elbow flexor and extensor, and these parameters were then inputted into the isometric contraction model to reduce the number of unknown parameters to be optimized. The optimizations were conducted to allow changes of individual maximum isometric muscle force by minimizing the root mean square difference between the predicted and measured isometric torque–angle curves. The tendon slack length (l_{to}) and the maximum muscle stress (δm) from the isometric contraction modeling together with the pennation angle and muscle optimal length of each muscle were then used

Figure 2. Modeling structure and corresponding experiment protocol with modeling parameters



in the voluntary modeling. The voluntary elbow flexion model was an EMG driven model, which relied on normalized EMG and the initial elbow joint position and velocity as inputs, to predict voluntary elbow flexion trajectory.

Experiment Protocol

Firstly, ultrasound technique was employed to measure the muscle optimal length and pennation angle of each prime elbow flexors (Biceps Brachii, Brachialis, Brachioradialis) and extensors (Three heads of Triceps brachii), and these architectural parameters were inputted into the model to reduce the number of unknown parameters to be optimized. The optimizations were conducted to allow changes of individual maximum isometric muscle force by minimizing the root mean square difference between the predicted and measured isometric torque-angle curves. The results showed that the prediction of joint torque fits quite well with the measured one. Then the voluntary movement control strategy was investigated through an EMG-driven musculoskeletal model, which could predict the individual muscle force and elbow voluntary movement trajectory using the input of EMG signal without any trajectory fitting procedure involved.

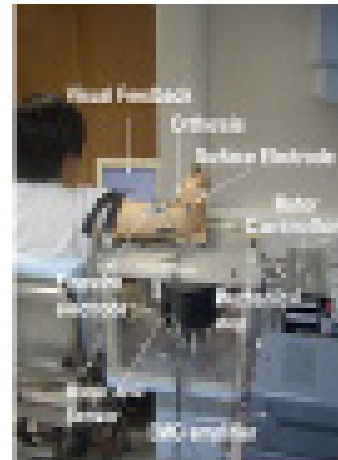
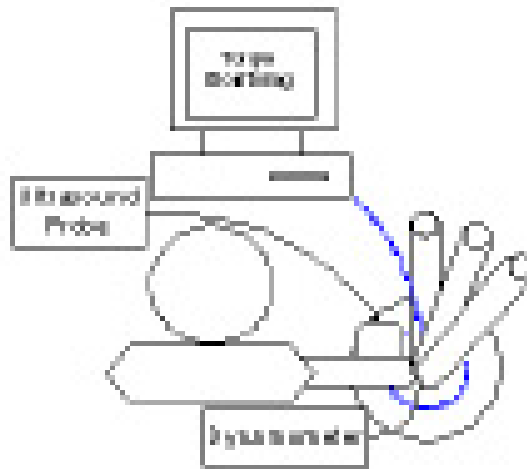
Then, the some patients who suffered from stroke were recruited in the modeling test. The selection criteria for the persons after stroke included:

1. hemiparesis resulting from a single unilateral lesion of the brain with the duration of stroke more than 2 years;
2. presence of spasticity with a modified Ashworth score (MAS) larger than one at the affected elbow joint;
3. sufficient passive range of motion ($>90^\circ$) at the affected elbow joint;
4. adequate mental capacity to attempt the elbow flexion movement as instructed;
5. no surgical procedure done on the upper limb of the affected side; and
6. absence of significant medical complications.

Experimental setup is shown in Figure 3. During the test, the subject sat on a height-adjusted chair with the upper arm in vertical position. The shoulder was orientated at 0° of flexion, 5° of abduction, and neutral rotation. The forearm was in a supinated position. Angular displacement of the elbow joint was monitored by a flexible electrogoniometer, which was attached on the median side of the arm when the forearm was in a fully

Using in Vivo Subject-Specific Musculotendon Parameters

Figure 3. Experiment setup. A dynamometer was used to measure and provide torque feedback, which was shown on a computer monitor to the subject being tested. A B-mode ultrasound probe was used to obtain a two-dimensional image of the muscle (Left). Surface and fine wire EMG electrodes were attached on the corresponding muscles. A qualified physician was inserting a pair of fine wire electrodes into the brachialis (Right)



supinated position. Surface EMG signals of the elbow prime flexors and prime elbow extensors and fine wire EMG from brachialis (BRA) muscles were recorded simultaneously. The voluntary elbow movement was under four testing conditions. These comprised voluntary elbow flexion with and without 1.13 kg sand pad strapped over the wrist and voluntary elbow extension with and without load condition. Prior to the test, the subject was instructed to be completely relaxed with his/her forearm in a fully extended position (i.e. 0°) for the test. The subject was then instructed to flex the elbow in his/her nature speed to a nearly full-flexed position (i.e. around 110°), hold 3-5 second, and then extended the elbow to original full extension position. Before the voluntary movement simulation, modeling parameters was obtained from an isometric contraction experiment combing ultrasound measurement and optimization calculation.

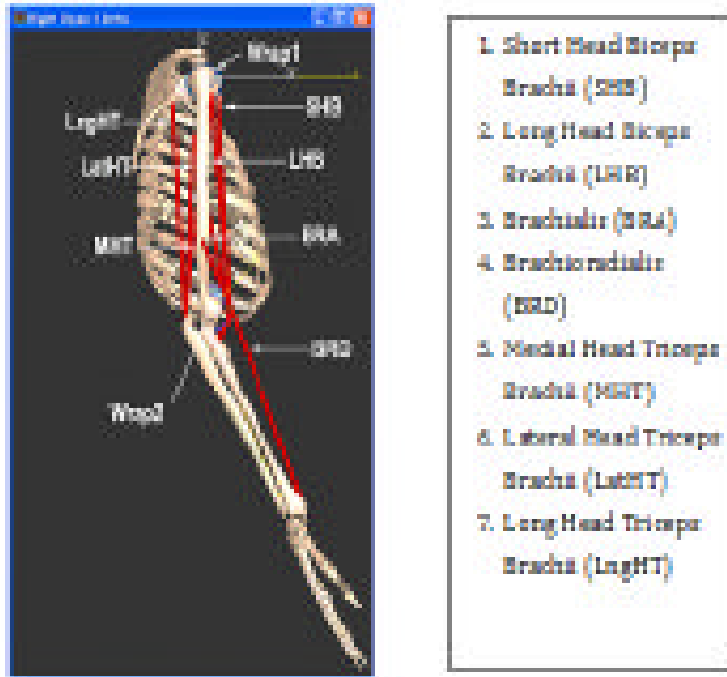
Finally, these measured pennation angle, estimated optimal muscle length, tendon slack length and maximum muscle stress were applied in this voluntary model for estimation of elbow trajectory.

Geometrical and Musculotendon Modeling

A generic interactive graphics-based model of the upper limb and its associated prime elbow flexors (LHB, SHB, BRA, BRD) and extensors (MHT, LatHT, LngHT) were developed using a musculo- skeletal modeling package (SIMM, MusculoGraphics, USA)

In the geometric model, the elbow joint was defined as a uniaxial hinge joint with its axis passing through the centers of the capitulum and trochlear sulcus (Figure 4). Each body segment was composed of graphical polyhedra that described the bone surfaces. Muscles were modeled as line segments connected from origin to insertion area

Figure 4. Geometric model for prime elbow flexors and wrap objects. Wrap1: a cylindrical-shaped object simulating the humeroulnar joint; wrap2: a spherical-shaped object for a glenohumeral joint; LHB: long head of biceps brachii; SHB: short head of brachii brachii; BRA: brachialis; BRD: brachioradialis



with intermediate points that allowed the muscle to wrap around bones and joints. Musculotendon length (l_{mt}) was determined by computing the sum of the lengths of the line segments on the muscle path, and moment arm (MA) was computed as the partial derivative of the musculotendon length (∂l_{mt}) with respect to the joint angle ($\partial \theta$). The generic geometric model was scaled to specific-subject models based on the segment ratio from the upper arm and fore- arm in SIMMs general model and of each subject. The model-generated l_{mt} and MA were then used in the musculotendon model to estimate the maximum isometric muscle stresses.

In a Hill-type musculotendon model, muscle dynamics could be described by a lumped-parameter model, which accounts for the force-length-velocity properties of the muscle and the elastic properties of the tendon (Figure 5). The

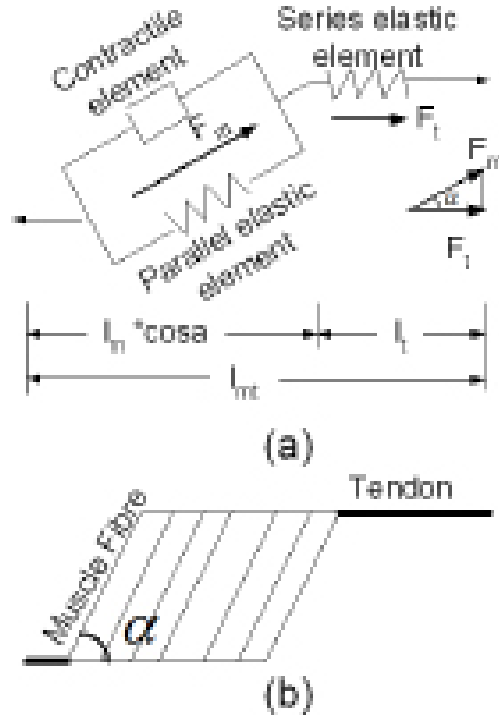
force generated by each musculotendon unit (F_t) can be represented by the following equations:

$$F_t = F_m * \cos \alpha = F_z [f_a(l)f(v)a(t) + f_p(l)] \cos \alpha \quad (1)$$

$$F_z = PCSA * \delta m \quad (2)$$

where $f_a(l)$ is the contractile element's force-length relationship, $f_p(l)$ is the parallel passive elastic muscle force (Giat et al., 1994), $a(t)$ is the activation level, $f(v)$ is the force-velocity relationship, and a is the pennation angle. Equations 1 and 2 describe the relationship between the force produced by the musculotendon unit and the related F_z . During maximum isometric voluntary flexion (MIVF) of the elbow joint, it is assumed that all the elbow flexors are fully activated (i.e., $a(t) = 1$) and their contraction velocities equal zero (i.e., $f(v) = 1$).

Figure 5. Schematic figure of Hill-type musculotendon model, consisting of a contractile element, a parallel passive elastic element, and a series elastic element, where F_m is muscle force and F_t is tendon force. (b) Simplified structure of a musculotendon actuator, where l_{mt} is muscle-tendon length, l_t is tendon length, l_m is muscle fascicle length, and α is pennation angle



The relationship between the length of the musculotendon unit, muscle fascicle and tendon can be stated in Equation 3. Tendon length (l_t) was calculated by subtracting muscle fascicle length (l_m) from l_{mt} , taking pennation angle (α) into account

$$l_t = l_{mt} - l_m \cos \alpha \quad (3)$$

During MIVF, the torque generated by the elbow could be estimated from the summation of each muscle's contribution, considering MA of each muscle

$$T(\theta) = \sum_{i=1}^4 F_i(\theta) \times MA_i(\theta)$$

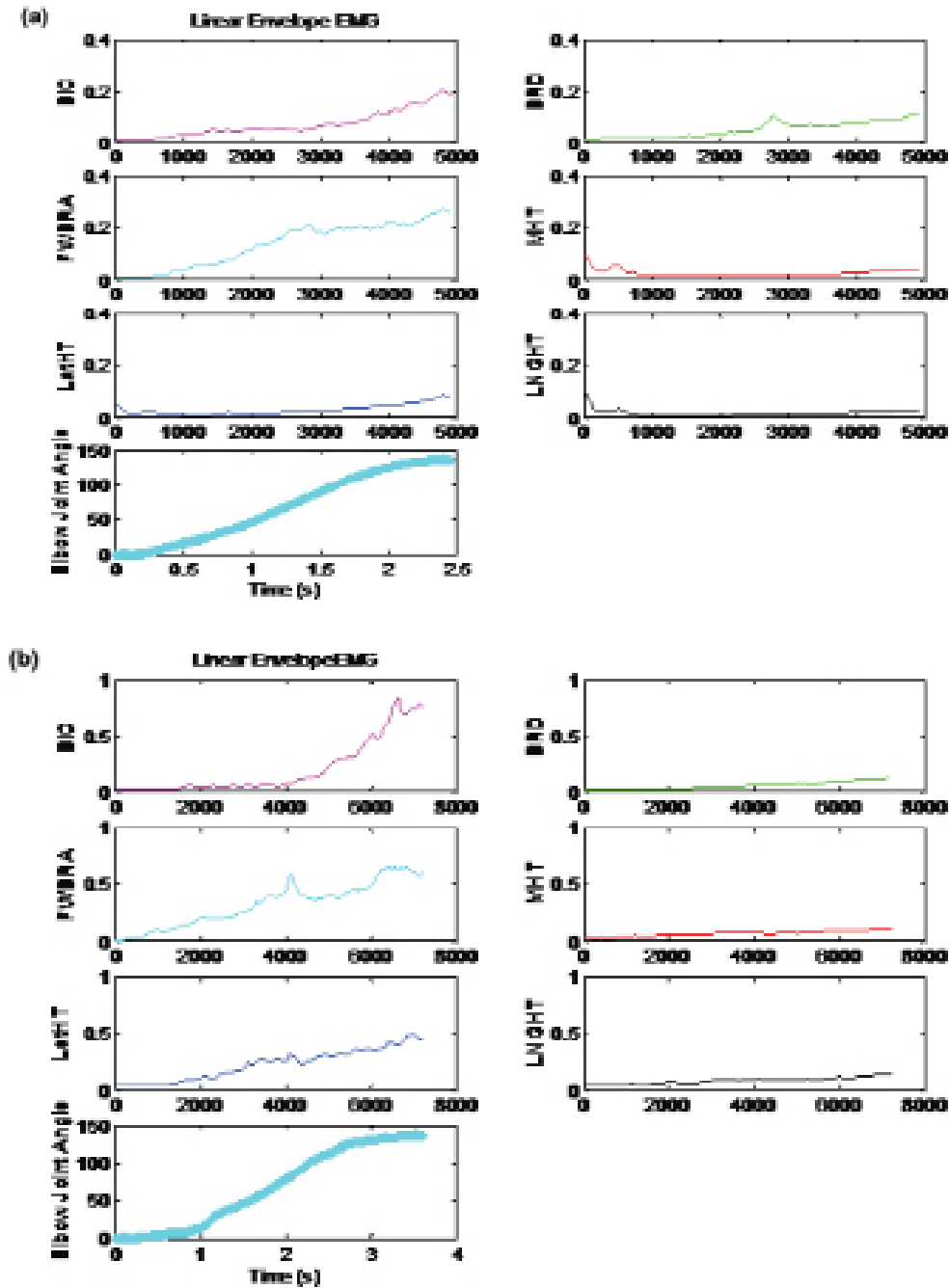
$$\sum_{i=1}^4 F_i(\theta) \times MA_i(\theta) \quad (4)$$

where $F_i(\theta)$ is the tendon force and $MA_i(\theta)$ is the moment arm of prime elbow flexor i (i.e., 1=SHB, 2=LHB, 3 = BRA, 4 = BRD) at position θ .

EMG-Activation Conversion and Linkage Dynamics

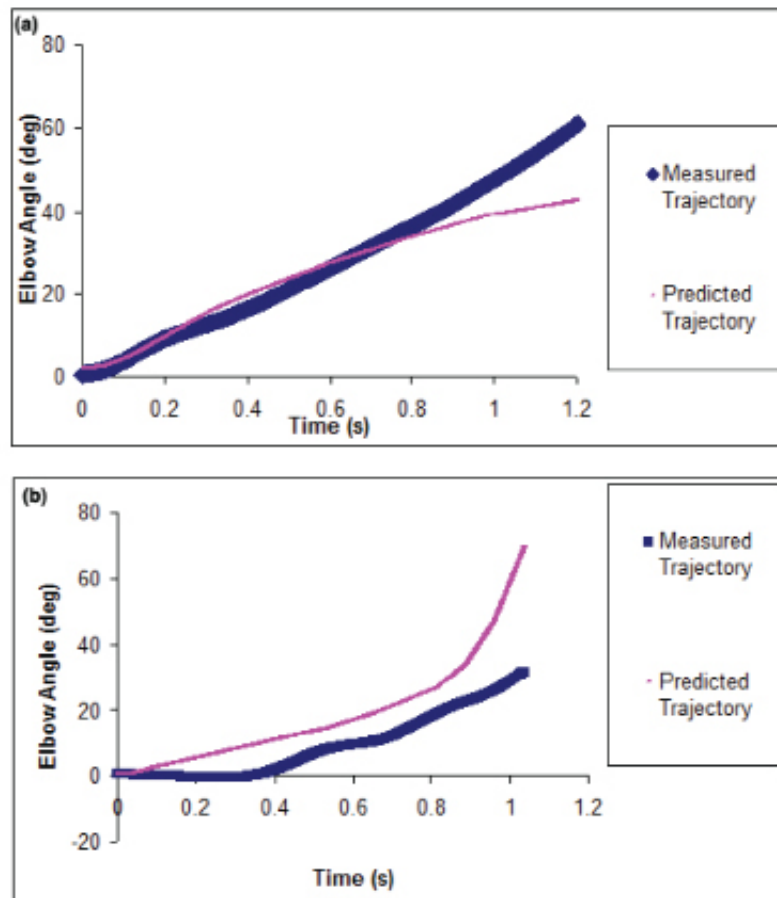
EMG to activation level conversion used the linear envelope method. Linear envelope processing can be regarded as an EMG processing scheme that converts the raw EMG signals to a linear envelope profile that mimics the muscle tension waveform during dynamic changes of isometric tension. The linear envelope profile was obtained by full-wave rectification of the band-pass filtered EMG

Figure 6. The normalized moving average EMG for the prime elbow flexors (BIC, BRA, BRD) and extensors (MHT, LatHT, LngHT) of one unimpaired subject(a) and one hemiparetic subject (b) during voluntary elbow flexion. The measured flexion trajectory is also plotted on the same figure



Using in Vivo Subject-Specific Musculotendon Parameters

Figure 7. Typical result of comparison of the measured (bold) and predicted (thin) voluntary elbow flexion trajectories of one unimpaired subject (a) and one hemiparetic subject (b)



signals (10–500 Hz for surface EMG, 10–1000 Hz for fine-wire EMG), followed by forward and backward low-pass filtering using a second-order Butterworth filter with a cut-off frequency of 3 Hz and then normalized by the corresponding MIVF/E EMG.

The linkage dynamics of the EMG-driven model described the flexion of the elbow joint in the sagittal plane. The voluntary flexion test was assumed to be a single degree of freedom movement and the upper extremity was treated as consisting of two rigid bodies — the upper arm and the forearm, the latter including the hand. The test configuration was the shoulder orientated at 0° flexion, 5° abduction, and neutral axial

rotation. The forearm in a supinated position and the hand in a loosely grasped position, with no relative movement at the wrist was involved throughout the entire movement. The flexion movement of the elbow joint was modeled as a frictionless hinge joint rotation of the ulna with respect to the humerus, with the axis of rotation passing through the centers of the capitellum and trochlear sulcus (Koo & Mak, 2005). The carrying angle of the elbow joint was assumed to be unchanged as the forearm flexed and extended around the elbow joint.

For each subject, the segment mass, moment of inertia, and location of the center of gravity of the forearm with respect to the flexion axis

were estimated using the formulas suggested by Winter (1990) and Dempster (1955). Then the angular displacement signals were low-pass filtered with a cut-off frequency of 10 Hz. The filtered EMG signals were rectified and normalized by the peak EMG amplitude measured during the MIVF/E tests.

Solutions and Recommendations

Typical linear envelope EMG profiles of the prime elbow flexors and extensors during voluntary elbow flexion were shown in Figure 6 for one control subject and one hemiparetic subject. The EMG profiles as well as the level of activation of each muscle group were phase-specific. It appeared that the flexion movement was mainly actuated by the BIC and BRA while the activation of BRD was relatively low. Coactivation of the three heads of triceps brachii was found to be minimal in the group of unimpaired subjects. However, the activation level of lateral head of triceps brachii in the hemiparetic group was increased in the elbow flexion movement and became comparable with the activation of BIC and BRA, which might indicate the muscle cocontraction in the paretic muscle.

Figure 7 shows the typical results of measured and predicted joint trajectories for the voluntary elbow flexion for one unimpaired subject (Figure 7). In the unimpaired group, the root mean square (RMS) error between the measured and predicted joint trajectory was $20.1^\circ \pm 6.0^\circ$ (Mean \pm SD, $n=4$). It seemed that the elbow flexion trajectories predicted by the EMG-driven model matched well with the measured trajectory. For one hemiparetic subject, the RMS error between the measured and predict trajectory was $34.1 \pm 26.4^\circ$ (Mean \pm SD, $n=4$). The general shape of the predicted trajectories followed the measured one well (Figure 7). But it seemed that the predicted elbow flexion trajectory ascend a little bit faster than the measured trajectory. It appeared that the RMS error of the hemiparetic group was larger as compare to the

results from the unimpaired group, although the difference was not statistically significant which might due to the smaller sample size.

By comparing the RMS error in the cadaveric data with the subject specific data, the result shows that the RMS error from the use of subject-specific data was significantly smaller than that from using the literature data. And the experimental trials were better than using cadaver data from the literature, with the significant effects clearly observable in the hemiparetic group data.

Based on ultrasound measured parameters and isometric contraction modeling results, an EMG driven model of human elbow for both the unimpaired subjects and persons after stroke has been built. This completed forward dynamics Hill-type model could predict the individual muscle force and elbow trajectory with the input of EMG signal. Importantly, our modeling approach needs not do any trajectory fitting procedure.

Forward dynamics model could predict forces within individual muscle elements, ligaments, and other soft tissues crossing joints and loads on the joint surfaces. In the last decade, EMG-driven modeling approach has been one promising trend of biomechanical modeling using forward dynamics (Benoit & Dowling, 2006; Manal et al., 2002; Buchanan, 2004). This technique develops computational musculoskeletal model which includes both agonists and antagonists of the joint and takes the following knowledge into account: the excitation-activation relationship of muscle, the nonlinear musculotendon properties, and the dynamics of the joint. The models which were developed for voluntary elbow flexion-extension movement in unimpaired subjects were discussed and compared with this study in the following paragraphs.

Manal and Buchanan (2005) proposed a detailed model of upper limbs to simulate the human arm and help to understand how muscle activation patterns changed in response to injury. They applied a Hill-type model and muscle forces of the prime elbow flexors and extensors were estimated

Using in Vivo Subject-Specific Musculotendon Parameters

from EMG. However, the tuning of their virtual arm to subject-specific model needs the training of the subject to control the virtual arm and the prediction results were different on highly-trained and control subjects. This limitation decreases the meaningful explanation of the results.

Benoit and Dowling (2006) measured the activation level of the biceps brachii to represent the whole elbow flexors during stretch-shortening cycle to predict the torque of the elbow. Although the simplified model could still estimate the torque, the model needs extra modeling parameters from previous literature based on experimental trial data (Benoit & Dowling, 2006). They found a decreased M-wave which indicates decreased biceps brachii activation under voluntary conditions. This finding is different from our isometric EMG data and the conclusion from van Zuylen (1988). The discrepancy might indicate the elbow flexor activation patterns are different in static and dynamic conditions.

FUTURE RESEARCH DIRECTIONS

In current studies, there is no subject-specific parameter in the simulation to take into account the effects of the inherent muscle property changes after the onset of stroke, such as the spasticity, which could be due to changes in muscle activation and in muscle stiffness (Becher et al., 1998). It was found that inherent muscle and joint properties are modified by alterations and immobilization induced after stroke and these in turn might change the parameters related to the moment of inertia (Yeh et al., 2004). According to the concept of mechanical impedance, the internal characteristics of a musculoarticular system are expressed by inertial, elastic and viscous parameters (Winters & Stark, 1988). However, such information for spastic muscle is lacking in the literature. Therefore, future study is needed to quantitatively measure the inherent properties of the moment of inertia in spastic muscle, which

could be helpful in the biomechanical modeling of persons after stroke to evaluate the effects of spasticity on the model.

CONCLUSION

An EMG-driven model was built through combining the in vivo ultrasound-measured musculotendon parameters to predict the joint trajectory during voluntary flexion and extension. The voluntary movement control strategy was investigated through an EMG-driven musculoskeletal model, which could predict the individual muscle force and elbow voluntary movement trajectory using the input of EMG signal without any trajectory fitting procedure involved. Our findings demonstrated the feasibility of using EMG-driven neuromusculoskeletal modeling with ultrasound-measured data for prediction of voluntary elbow movement for both unimpaired subjects and persons after stroke. In addition, the results revealed that the prediction of voluntary flexion in the hemiparetic group using ultrasound measured parameters was better than that of using the cadaver data from literature.

ACKNOWLEDGMENT

The project was supported by the National Natural Science Foundation of China (No.31100669), the Fundamental Research Funds for the Central Universities of China (No.11yRpy22) and partly supported by Guangdong Provincial Medical Research Fund (B2013331).

REFERENCES

Anderson, F. C., & Pandy, M. G. (2001). Dynamic optimization of human walking. *Journal of Biomechanical Engineering: ASME*, 123, 381–390. doi:10.1115/1.1392310 PMID:11601721

- Becher, J. G., Harlaar, J., Lankhorst, G. J., & Vogelaar, T. W. (1998). Measurement of impaired muscle function of the gastrocnemius, soleus, and tibialis anterior muscles in spastic hemiplegia: A preliminary study. *Journal of Rehabilitation Research and Development*, *35*, 314–326. PMID:9704315
- Benoit, D. L., & Dowling, J. J. (2006). In vivo assessment of elbow flexor work and activation during stretch-shortening cycle tasks. *Journal of Electromyography and Kinesiology*, *16*, 352–364. doi:10.1016/j.jelekin.2004.07.006 PMID:16263310
- Bohannon, R. W., & Smith, M. B. (1987). Interrater reliability of a modified Ashworth scale of muscle spasticity. *Physical Therapy*, *67*, 206–207. PMID:3809245
- Buchanan, T. S., Lloyd, D. G., Manal, K., & Besier, T. F. (2004). Neuromusculoskeletal modeling: Estimation of muscle forces and joint moments and movements from measurements of neural command. *Journal of Applied Biomechanics*, *20*, 367–395. PMID:16467928
- Buchanan, T. S., Lloyd, D. G., Manal, K., & Besier, T. F. (2005). Estimation of muscle forces and joint moments using a forward-inverse dynamics model. *Medicine and Science in Sports and Exercise*, *37*, 1911–1916. doi:10.1249/01.mss.0000176684.24008.6f PMID:16286861
- Carr, H. J. (2003). *Stroke rehabilitation guidelines for exercise and training to optimize motor skill*. New York: Elsevier Science Ltd.
- Chae, J., Yang, G., Park, R. K., & Labatia, I. (2002). Muscle weakness and cocontraction in upper limb hemiparesis: Relationship to motor impairment and physical disability. *Neurorehabilitation and Neural Repair*, *16*, 241–248. doi:10.1177/154596830201600303 PMID:12234087
- Chang, Y. W., Su, F. C., Wu, H. W., & An, K. N. (1999). Optimum length of muscle contraction. *Clinical Biomechanics (Bristol, Avon)*, *14*, 537–542. doi:10.1016/S0268-0033(99)00014-5 PMID:10521638
- Chardon, M. K., Suresh, N. L., & Rymer, W. Z. (2010). An evaluation of passive properties of spastic muscles in hemiparetic stroke survivors. In *Conference Proceedings 32th IEEE Engineering Medical Biology Society*, (pp. 2993–2996).
- Chleboun, G. S., France, A. R., Crill, M. T., Braddock, H. K., & Howell, J. N. (2001). In vivo measurement of fascicle length and pennation angle of the human biceps femoris muscle. *Cells, Tissues, Organs*, *169*, 401–409. doi:10.1159/000047908 PMID:11490120
- Dean, C. M., & Shepherd, R. B. (1997). Task-related training improves performance of seated reaching tasks after stroke. *Stroke*, *28*, 722–728. doi:10.1161/01.STR.28.4.722 PMID:9099186
- Dempster, W. T. (1955). *Space requirements of the seated operator: Geometrical, kinematics, and mechanical aspects of the body with special reference to the limbs* (Wright Air Development Center Tech. Rep. No. 55-159). Dayton, OH: Wright-Patterson Air Force Base, WADC. (National Technical Information Service No. AD-087892).
- Fasoli, S. E., Krebs, H. I., Stein, J., Frontera, W. R., & Hogan, N. (2003). Effects of robotic therapy on motor impairment and recovery in chronic stroke. *Archives of Physical Medicine and Rehabilitation*, *84*, 477–482. doi:10.1053/apmr.2003.50110 PMID:12690583
- Fukunaga, T., Kawakami, Y., Kuno, S., Funato, K., & Fukashiro, S. (1997). Muscle architecture and function in humans. *Journal of Biomechanics*, *30*, 457–463. doi:10.1016/S0021-9290(96)00171-6 PMID:9109557

Using in Vivo Subject-Specific Musculotendon Parameters

- Gao, F., Grant, T. H., Roth, E. J., & Zhang, L. Q. (2009). Changes in passive mechanical properties of the gastrocnemius muscle at the muscle fascicle and joint levels in stroke survivors. *Archives of Physical Medicine and Rehabilitation*, *90*, 819–826. doi:10.1016/j.apmr.2008.11.004 PMID:19406302
- Giat, Y., Mizrahi, J., Levine, W. A., & Chen, J. (1994). Simulation of distal tendon transfer of the biceps brachii and the brachialis muscles. *Journal of Biomechanics*, *27*, 1005–1014. doi:10.1016/0021-9290(94)90217-8 PMID:8089155
- Gonzalez, R. V., Buchanan, T. S., & Delp, S. L. (1997). How muscle architecture and moment arms affect wrist flexion-extension moment. *Journal of Biomechanics*, *30*, 705–712. doi:10.1016/S0021-9290(97)00015-8 PMID:9239550
- Gonzalez, R. V., Hutchins, E. L., Barr, R. E., & Abraham, L. D. (1996). Development and evaluation of a musculoskeletal model of the elbow joint complex. *Journal of Biomechanical Engineering: ASME*, *118*, 32–40. doi:10.1115/1.2795943 PMID:8833072
- Gordon, A. M., Huxley, A. F., & Julian, F. J. (1996). The variation in isometric tension with sarcomere length in vertebrate muscle fibres. *The Journal of Physiology*, *184*, 170–192.
- Gossman, M. R., Sahrmann, S. A., & Rose, S. J. (1982). Review of length-associated changes in muscle: experimental evidence and clinical implications. *Physical Therapy*, *62*, 1799–1808. PMID:6755499
- Halar, E. M., Stolov, W. C., Venkatesh, B., Brozovich, F. V., & Harley, J. D. (1978). Gastrocnemius muscle belly and tendon length in stroke patients and able-bodied persons. *Archives of Physical Medicine and Rehabilitation*, *59*, 476–484. PMID:718411
- Herbert, R. D., & Gandevia, S. C. (1995). Changes in pennation with joint angle and muscle torque: in vivo measurements in human brachialis muscles. *The Journal of Physiology*, *484*, 523–532. PMID:7602542
- Hodges, P. W., Pengel, L. H. M., Herbert, R. D., & Gandevia, S. C. (2003). Measurement of muscle contraction with ultrasound imaging. *Muscle & Nerve*, *27*, 682–692. doi:10.1002/mus.10375 PMID:12766979
- Holzbour, K. R. S., Murray, W. R., & Delp, S. L. (2005). A model of the upper extremity for simulating musculoskeletal surgery and analyzing neuromuscular control. *Annals of Biomedical Engineering*, *33*, 829–840. doi:10.1007/s10439-005-3320-7 PMID:16078622
- Huijing, P. A., & Baan, G. S. (1992). Stimulation level dependent length-force and architecture characteristics of rat gastrocnemius muscle. *Journal of Electromyography and Kinesiology*, *2*, 112–120. doi:10.1016/1050-6411(92)90022-B PMID:20719604
- Huxley, A. F. (1957). Muscle structure and theories of contraction. *Progress in Biochemistry and Biophysics*, *7*, 255–318. PMID:13485191
- Ju, M. S., Lin, C. C. K., Chen, J., Cheng, H. S., & Lin, C. W. (2002). Performance of elbow tracking under constant torque disturbance in normotonic stroke patients and normal subjects. *Clinical Biomechanics (Bristol, Avon)*, *17*, 640–649. doi:10.1016/S0268-0033(02)00131-6 PMID:12446160
- Kawakami, Y., Abe, T., & Fukunaga, T. (1993). Muscle-fiber pennation angle are greater in hypertrophied than in normal muscles. *Journal of Applied Physiology*, *74*, 2740–2744. PMID:8365975

- Koo, T. K. K., & Mak, A. F. T. (2005). Feasibility of using EMG driven neuromusculoskeletal model for prediction of dynamic movement of the elbow. *Journal of Electromyography and Kinesiology*, *15*, 12–26. doi:10.1016/j.jelekin.2004.06.007 PMID:15642650
- Koo, T. K. K., Mak, A. F. T., & Hung, L. K. (2002). In vivo determination of subject-specific musculodenton parameters: Applications to the prime elbow flexors in normal and hemiparetic subject. *Clinical Biomechanics (Bristol, Avon)*, *17*, 390–399. doi:10.1016/S0268-0033(02)00031-1 PMID:12084544
- Leedham, J. S., & Dowling, J. J. (1995). Force-length, torque-angle and EMG-joint angle relationships of the human in vivo biceps brachii. *Archives of Physical Medicine and Rehabilitation*, *70*, 421–426. PMID:7671877
- Lemay, M. A., & Crago, P. E. (1996). A dynamic model for simulating movements of the elbow, forearm, and wrist. *Journal of Biomechanics*, *29*, 1319–1330. doi:10.1016/0021-9290(96)00026-7 PMID:8884477
- Li, L., & Tong, K. Y. (2011). An introduction to biomechatronics. In K. Y. Tong (Ed.), *Biomechatronics in medicine and health care* (pp. 1–8). Singapore: Pan Stanford Publishing Pte Ltd. doi:10.1201/b11402-2
- Li, L., Tong, K. Y., & Hu, X. L. (2007a). The effect of poststroke impairments on brachialis muscle architecture as measured by ultrasound. *Archives of Physical Medicine and Rehabilitation*, *88*, 243–250. doi:10.1016/j.apmr.2006.11.013 PMID:17270524
- Li, L., Tong, K. Y., Song, R., & Koo, T. K. K. (2007b). Is maximum isometric muscle stress the same among prime elbow flexors? *Clinical Biomechanics (Bristol, Avon)*, *22*, 874–883. doi:10.1016/j.clinbiomech.2007.06.001 PMID:17681653
- Lieber, R. L., Fazeli, B. M., & Botte, M. J. (1990). Architecture of selected wrist flexor and extensor muscles. *The Journal of Hand Surgery*, *15A*, 244–250. doi:10.1016/0363-5023(90)90103-X PMID:2324452
- Lieber, R. L., Jacobson, M. D., Fazeli, B. M., Abrams, R. A., & Botte, M. J. (1992). Architecture of selected muscles of the arm and forearm: Anatomy and implications for tendon transfer. [American Volume]. *The Journal of Hand Surgery*, *17A*, 787–798. doi:10.1016/0363-5023(92)90444-T PMID:1401782
- Lum, P. S., Taub, E., Schwandt, D., Postman, M., Hardin, P., & Uswatte, G. (2004). Automated constraint-induced therapy extension (AutoC-ITE) for movement deficits after stroke. *Journal of Rehabilitation Research and Development*, *41*, 249–258. doi:10.1682/JRRD.2003.06.0092 PMID:15543442
- Maganaris, C. N. (2004). A predictive model of moment-angle characteristics in human skeletal muscle: Application and validation in muscles across the ankle joint. *Journal of Theoretical Biology*, *230*, 89–98. doi:10.1016/j.jtbi.2004.04.025 PMID:15276003
- Maganaris, C. N., Baltzopoulos, V., & Sargeant, A. J. (1998). In vivo measurement of the triceps surae complex architecture in man: implications for muscle function. *The Journal of Physiology*, *512*, 603–614. doi:10.1111/j.1469-7793.1998.603be.x PMID:9763648
- Manal, K., & Buchanan, T. S. (2005). Use of an EMG-driven biomechanical model to study virtual injuries. *Medicine and Science in Sports and Exercise*, *37*, 1917–1923. doi:10.1249/01.mss.0000176685.35442.6b PMID:16286862

Using in Vivo Subject-Specific Musculotendon Parameters

- Martin, D. C., Medri, M. K., Chow, R. S., Oxorn, V., Leekam, R. N., Agur, A. M., & Mckee, N. H. (2001). Comparing human skeletal muscle architectural parameters of cadavers with in vivo ultrasonographic measurements. *Journal of Anatomy*, 199, 429–434. doi:10.1046/j.1469-7580.2001.19940429.x PMID:11693303
- Martini, F. H. (1995). *Fundamentals of anatomy and physiology*. Englewood, NJ: Prentice Hall.
- Maurel, W., & Thalman, D. (1998). A case study on human upper limb modelling for dynamic simulation. *Computer Methods in Biomechanics and Biomedical Engineering*, 2, 65–82. doi:10.1080/10255849908907979 PMID:11264819
- Mccrea, P. H., Eng, J. J., & Hodgson, A. J. (2003). Time and magnitude of torque generation is impaired in both arms following stroke. *Muscle & Nerve*, 28, 46–53. doi:10.1002/mus.10397 PMID:12811772
- McMahon, T. A. (1984). *Muscles, reflexes, and locomotion*. Princeton, NJ: Princeton University Press.
- Metoki, N., Sato, Y., Satoh, K., Okumura, K., & Iwamoto, J. (2003). Muscular atrophy in the hemiplegic thigh in patients after stroke. *American Journal of Physical Medicine & Rehabilitation*, 82, 862–865. doi:10.1097/01.PHM.0000091988.20916.EF PMID:14566154
- Murray, W. M., Buchanan, T. S., & Delp, S. L. (2000). The isometric functional capacity of muscles that cross the elbow. *Journal of Biomechanics*, 33, 943–952. doi:10.1016/S0021-9290(00)00051-8 PMID:10828324
- Narici, M. V., Binzoni, T., Hiltbrand, E., Fasel, J., Terrier, F., & Cerretelli, P. (1996). In vivo human gastrocnemius architecture with changing joint angle at rest and during graded isometric contraction. *The Journal of Physiology*, 496, 287–297. PMID:8910216
- Neptune, R. R., Kautz, S. A., & Hull, M. L. (1998). Evaluation of performance criteria for simulation of submaximal steady-state cycling using a forward dynamic model. *Journal of Biomechanical Engineering: ASME*, 120, 334–341. doi:10.1115/1.2797999 PMID:10412400
- Neptune, R. R., Kautz, S. A., & Zajac, F. E. (2000). Muscle contributions to specific biomechanical functions do not change in forward versus backward pedaling. *Journal of Biomechanics*, 33, 155–164. doi:10.1016/S0021-9290(99)00150-5 PMID:10653028
- Pandy, M. G. (2001). Computer modeling and simulation of human movement. *Annual Review of Biomedical Engineering*, 3, 245–273. doi:10.1146/annurev.bioeng.3.1.245 PMID:11447064
- Patten, C., Lexell, J., & Brown, H. E. (2004). Weakness and strength training in persons with poststroke hemiplegia: Rationale, method, and efficacy. *Journal of Rehabilitation Research and Development*, 41, 293–312. doi:10.1682/JRRD.2004.03.0293 PMID:15543447
- Pizzi, A., Carlucci, G., Falsini, C., Verdesca, S., & Grippo, A. (2005). Application of a volar static splint in poststroke spasticity of the upper limb. *Archives of Physical Medicine and Rehabilitation*, 86, 1855–1859. doi:10.1016/j.apmr.2005.03.032 PMID:16181954
- Popovic, D., & Sinkjaer, T. (2000). *Control of movement for the physically disabled*. London: Springer-Verlag. doi:10.1007/978-1-4471-0433-9
- Van Zuylen, E. J., Cielen, C. C., & Denier van der Gon, J. J. (1988). Coordination and inhomogeneous activation of human muscles during isometric torques. *Journal of Neurophysiology*, 60, 1523–1548. PMID:3199172

Vredenberg, J., & Rau, G. (1973). Surface electromyography in relation to force, muscle length and endurance. In J. E. Desmede (Ed.), *New developments in EMG and clinical neurophysiology* (pp. 607–622). Basel, Switzerland: Karger.

Westcott, P. (2000). *Stroke-questions and answers*. London: The Stroke Association.

Winter, D. A. (1990). *Biomechanics and motor control of human movement*. New York: Wiley.

Winters, J. M., & Stark, L. (1988). Estimated mechanical properties of synergistic muscles involved in movements of a variety of human joints. *Journal of Biomechanics*, *21*, 1027–1041. doi:10.1016/0021-9290(88)90249-7 PMID:2577949

Yeh, C. Y., Chen, J. J. J., & Tsai, K. H. (2004). Quantitative analysis of ankle hyper-tonia after prolonged stretch in subjects with stroke. *Journal of Neuroscience Methods*, *137*, 305–314. doi:10.1016/j.jneumeth.2004.03.001 PMID:15262075

Zuurbier, C. J., & Huijing, P. A. (1992). Influence of muscle geometry on shortening speed of fibre, aponeurosis and muscle. *Journal of Biomechanics*, *25*, 1017–1026. doi:10.1016/0021-9290(92)90037-2 PMID:1517262

ADDITIONAL READING

Au, A. T. C., & Kirsch, R. F. (2000). EMG-based prediction of shoulder and elbow kinematics in able-bodied and spinal cord injured individuals. *IEEE Transactions on Rehabilitation Engineering*, *8*, 471–480. doi:10.1109/86.895950 PMID:11204038

Buchanan, T. S., Moniz, M. J., Dewald, J. P. A., & Rymer, Z. W. (1993). Estimation of muscle forces about the wrist joint during isometric tasks using an EMG coefficient method. *Journal of Biomechanics*, *26*, 547–560. doi:10.1016/0021-9290(93)90016-8 PMID:8478356

Chae, J., Yang, G., Park, B. K., & Labatia, L. (2002). Muscle weakness and cocontraction in upper limb hemiparesis: relationship to motor impairment and physical disability. *Neurorehabilitation and Neural Repair*, *16*(3), 241–248. doi:10.1177/154596830201600303 PMID:12234087

Fang, L. D., Jia, X. H., & Wang, R. C. (2007). Modeling and simulation of muscle forces of trans-tibial amputee to study effect of prosthetic alignment. *Clinical Biomechanics (Bristol, Avon)*, *22*, 1115–1131. doi:10.1016/j.clinbiomech.2007.07.017 PMID:17942203

Feng, J., Mak, A. F. T., & Koo, T. K. K. (1999). A surface EMG driven musculoskeletal model of the elbow flexion-extension movement in normal subjects and in subjects with spasticity. *Journal of Musculoskeletal Research*, *3*, 109–123. doi:10.1142/S0218957799000129

Heine, R., Manal, K., & Buchanan, T. S. (2003). Using Hill-type muscle models and EMG data in a forward dynamic analysis of joint moment: Evaluation of critical parameters. *Journal of Mechanics in Medicine and Biology*, *3*, 169–186. doi:10.1142/S0219519403000727

Hof, A. L., & Van Den Berg, J. (1981). EMG to force processing I: An electrical analogue of the Hill muscle model. *Journal of Biomechanics*, *14*, 747–758. doi:10.1016/0021-9290(81)90031-2 PMID:7334035

Using in Vivo Subject-Specific Musculotendon Parameters

- Hof, A. L., & Van Den Berg, J. (1981). EMG to force processing III: Estimation of model parameters for the human triceps surae muscle and assessment of the accuracy by means of a torque plate. *Journal of Biomechanics*, *14*, 771–785. doi:10.1016/0021-9290(81)90033-6 PMID:7334037
- Ichinose, Y., Kanehisa, H., Ito, M., Kawakami, Y., & Fukunaga, T. (1998). Morphological and functional differences in the elbow extensor muscle between highly trained male and female athletes. *European Journal of Applied Physiology*, *78*(2), 109–114. doi:10.1007/s004210050394 PMID:9694308
- Koo, T. K. K., & Mak, A. F. T. (2006). A neuromusculoskeletal model to simulate the constant angular velocity elbow extension test of spasticity. *Medical Engineering & Physics*, *28*, 60–69. doi:10.1016/j.medengphy.2005.03.012 PMID:15908257
- Langenderfer, J., Lascalza, S., Mell, A., Carpenter, J. E., Kuhn, J. E., & Hughes, R. E. (2005). An EMG-driven model of the upper extremity and estimation of long head biceps force. *Computers in Biology and Medicine*, *35*, 25–39. doi:10.1016/j.compbiomed.2003.12.002 PMID:15567350
- Li, L., Tong, K. Y., Hu, X. L., Hung, L. K., & Koo, T. K. K. (2009). Incorporating Ultrasound-measured musculotendon parameters to subject-specific EMG-Driven model to simulate voluntary elbow flexion for persons after Stroke. *Clinical Biomechanics (Bristol, Avon)*, *24*, 101–109. doi:10.1016/j.clinbiomech.2008.08.008 PMID:19012998
- Lloyd, D. G., & Besier, T. F. (2003). An EMG-driven musculoskeletal model to estimate muscle forces and knee joint moment in vivo. *Journal of Biomechanics*, *36*, 765–776. doi:10.1016/S0021-9290(03)00010-1 PMID:12742444
- Maganaris, C. N., & Baltzopoulos, V. (1999). Predictability of in vivo changes in pennation angle of human tibialis anterior muscle from rest to maximum isometric dorsiflexion. *European Journal of Applied Physiology*, *79*(3), 294–297. doi:10.1007/s004210050510 PMID:10048637
- McCrea, P. H., Eng, J. J., & Hodgson, A. J. (2002). Biomechanics of reaching: clinical implications for individuals with acquired brain injury. *Disability and Rehabilitation*, *24*(10), 534–541. doi:10.1080/09638280110115393 PMID:12171643
- Pandy, M. G., & Andriacchi, T. P. (2010). Muscle and joint function in human locomotion. *Annual Review of Biomedical Engineering*, *12*, 401–433. doi:10.1146/annurev-bioeng-070909-105259 PMID:20617942
- Potvin, J. R., Norman, R. W., & McGill, S. M. (1996). Mechanically corrected EMG for the continuous estimation of erector spinae muscle loading during repetitive lifting. *European Journal of Applied Physiology and Occupational Physiology*, *74*, 119–132. doi:10.1007/BF00376504 PMID:8891510
- Qi, S., Macleod, T. D., Manal, K., & Buchanan, T. S. (2011). Estimation of ligament loading and anterior tibial translation in healthy and ACL-Deficient knees during gait and the influence of increasing tibial slope using EMG-driven approach. *Annals of Biomedical Engineering*, *39*, 110–121. doi:10.1007/s10439-010-0131-2 PMID:20683675
- Ryan, A. S., Dobrovolny, C. L., Smith, G. V., Silver, K. H., & Macko, R. F. (2002). Hemiparetic muscle atrophy and increased intramuscular fat in stroke patients. *Archives of Physical Medicine and Rehabilitation*, *83*, 1703–1707. doi:10.1053/apmr.2002.36399 PMID:12474173

Sunnerhagen, K. S., Svantesso, U., Lonn, L., Krotkiewski, M., & Grimby, G. (1999). Upper motor neuron lesions: their effect on muscle performance and appearance in stroke patients with minor motor impairment. *Archives of Physical Medicine and Rehabilitation*, *80*, 155–161. doi:10.1016/S0003-9993(99)90113-2 PMID:10025489

Vredenberg, J., & Rau, G. (1973). Surface electromyography in relation to force, muscle length and endurance. In J. E. Desmede (Ed.), *New developments in EMG and Clinical Neurophysiology* (pp. 607–622). Basel: Karger.

Wang, L., & Buchanan, T. S. (2002). Prediction of joint moments using a neural network model of muscle activations from EMG signals. *IEEE Transactions on Neural Systems and Rehabilitation Engineering*, *10*, 30–37. doi:10.1109/TNSRE.2002.1021584 PMID:12173737

Yoshida, N., Domen, K., Koike, Y., & Kawato, M. (2002). A method for estimating torque-vector direction of shoulder muscles using surfaces EMG. *Biological Cybernetics*, *86*, 167–177. doi:10.1007/s00422-001-0286-x

Zajac, F.E. (1989). Muscle and tendon: properties, models, scaling, and application to biomechanics and motor control. *Critical Reviews™ in Biomedical Engineering*, *17*(4), 359-411.

Zheng, N., Fleisig, G. S., Escamilla, R. F., & Barrentine, S. W. (1998). An analytical model of the knee for estimation of internal forces during exercise. *Journal of Biomechanics*, *31*, 963–967. doi:10.1016/S0021-9290(98)00056-6 PMID:9840764

Motor Control: The process by which humans and animals organize and execute their actions.

Musculotendon Parameters: Parameters to define the structural and force-related characteristics of a muscle-tendon complex.

Neuromusculoskeletal (NMS) Model: The NMS model can be defined as a set of equations which describe the dynamics of a neuromusculoskeletal system during generation of a function.

Stroke: A cerebro-vascular accident refers to the neurological symptoms and signs, usually focal and acute, which result from the blood supply to a part of the brain is cut off, and the brain cells in that part cannot function.

Ultrasonography: Ultrasonography is an ultrasound-based diagnostic imaging technique used for visualizing subcutaneous body structures including tendons, muscles, joints, vessels and internal organs for possible pathology or lesions.

KEY TERMS AND DEFINITIONS

Electromyography(EMG): Technique for assessing the electrical activity of muscles.

EMG-Driven Model: Using the input of EMG signal to a biomechanical model to predict the individual muscle force and trajectory.

Chapter 8

Study and Interpretation of Neuromuscular Patterns in Golf

Sérgio Marta

CIPER, Faculdade de Motricidade Humana, Universidade de Lisboa, Portugal

João Rocha Vaz

CIPER, Faculdade de Motricidade Humana, Universidade de Lisboa, Portugal

Luís Silva

CIPER, Faculdade de Motricidade Humana, Universidade de Lisboa, Portugal

Maria António Castro

Coimbra Health School, Instituto Politécnico de Coimbra, Portugal & Mechanical Engineering Research Center, University of Coimbra, Portugal

Pedro Pezarat Correia

CIPER, Faculdade de Motricidade Humana, Universidade de Lisboa, Portugal

ABSTRACT

This chapter reports the golf swing EMG studies using amplitude, timing parameters and approaches to neuromuscular patterns recognition through EMG. The golf swing is a dynamic multi-joint movement. During each swing phase different activation levels occur, the combination of each muscle in amplitude provides an increased club head speed for the ball to travel to the hole. The timing when the maximum peak of each muscle occurs can be an important factor to understand the injury related mechanics and to prescribe strength programs. Most muscle studies describe their maximum activation level during the forward swing and acceleration phases, providing a controlled antigravity movement and acceleration of the club. The initial contraction time corresponds to the onset that can be used to describe the organization of the neuromuscular patterns during a task. This time parameter was used in golf to relate injuries to skilled or less skilled golfers. The way to retrieve this time parameter may be reached through new approaches but no gold standard algorithm definition has been found yet. To better understand the neuromuscular patterns new algorithms based on the dynamical systems theory are now used.

DOI: 10.4018/978-1-4666-6090-8.ch008

INTRODUCTION

Golf is a sport accessible to all ages and levels of physical condition. The number of golf courses and players has increased and golf has become a popular sport all over the world in the last fifty years. The recreational player tends to be older because practice demands time and the high performance and skill are not age limited. The golf swing is the most complex and predominant technique of the game and is associated to the majority of golf related injuries (Cabri, Sousa, Kots, & Barreiros, 2009). The injury rate varies between amateurs and professionals and is associated to the increased hours of play per day with a prevalence of nearly 88% (Therriault & Lanchance, 1998). The golf player's characteristics are poorly known and present potential for injuries (McHardy, Pollard, & Luo, 2006), either through lack of structured exercise programs and practice, specific morphological and functional properties, or through the nature of the sports activity. Nevertheless, health benefits and golf practice-related risks have not been fully explored and there is still controversy in the literature (Cabri et al., 2009).

The application of EMG in golf can describe how the Nervous Central System organizes the neuromuscular patterns during a dynamic movement. The amplitude parameter is the most studied one (Bechler, Jobe, Pink, Perry, & Ruwe, 1995; Bulbulian, Ball, & Seaman, 2001; Cole & Grimshaw, 2008a; Farber, Smith, Kvitne, Mohr, & Shin, 2009; Glazebrook, Curwin, Islam, Kozey, & Stanish, 1994; Jobe, Moynes, & Antonelli, 1986; Jobe, Perry, & Pink, 1989; Kao, Pink, Jobe, & Perry, 1995; Marta, Silva, Vaz, Bruno, Pezarat-Correia, 2013; Pink, Jobe, & Perry, 1990; Pink, Perry, & Jobe, 1993; Watkins, Uppal, Perry, Pink, & Dinsay, 1996). This parameter describes the muscle activation levels during each phase and was the most used to study the golf swing. The temporal parameter retrieves the instant of muscle activation related to the impact of the ball (Cole & Grimshaw, 2008b; Horton, Lindsay, &

Macintosh, 2001; Silva, Marta, Vaz, Fernandes, Castro, & Pezarat-Correia, 2013).

These parameters are used to set new physical condition and rehabilitation programs for coaches and physical therapists but there is still a lack of field studies on this topic and more should be carried out.

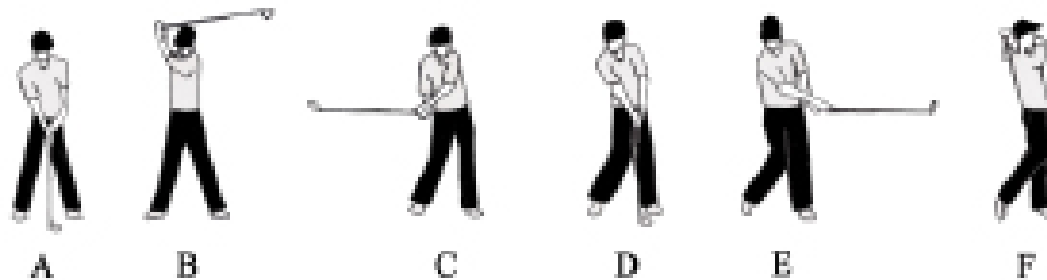
The objective of this chapter is to report studies and share EMG data by presenting different approaches concerning the use of EMG in sport sciences and the importance of its physiological meaning, specifically during the golf swing.

BACKGROUND

The first study of EMG in golf dates from 1948 (Slater-Hammel, 1948). From then on not many studies have been done, though they have been more frequent in the last five years. Most of these studies focused on the intensity levels of the trunk muscles (Bulbulian et al., 2001; Cole & Grimshaw, 2008a,b; Horton et al., 2001; Marta et al., 2013; Pink et al., 1993; Watkins et al., 1996) and shoulders (Jobe et al., 1986, 1989; Kao et al., 1995; Pink et al., 1990;). Only one study centered its attention on the lower limbs (Bechler et al., 1995) and two studies evaluated the forearm muscles (Farber et al., 2009; Glazebrook et al., 1994), respectively. Five studies were literature reviews in EMG patterns: two dedicated specifically to EMG in golf (Marta et al., 2012; McHardy & Pollard, 2005a); two retrieving the upper limb (Escamilla & Andrews, 2009) and one on the shoulder muscles (Moynes, Perry, Antonelli, & Jobe, 1986). Besides these previous studies three epidemiology reports (Cabri et al., 2009; Kim, Millet, Warner, & Jobe, 2004; McHardy & Pollard, 2005b) presented data about the injury and muscle activity patterns in golfers.

In general the studies dedicated their attention to professional golfers. Recent literature is more aware of the possible differences between professional and recreational players. Another point of

Figure 1. Golf swing phases



interest in golf research is golfers' injuries, i.e. low back pain related (Horton et al., 2001; Cole & Grimshaw, 2008a,b) and medial epicondylitis (Glazebrook et al., 1994). The majority of the studies concentrate on the male players but two studies (Jobe et al., 1989; Pink et al., 1990) analyze differences between women golfers.

The EMG golf studies divided the golf swing according to the geometric position of the club in five phases: (Bechler et al., 1995; Farber et al., 2009; Jobe et al., 1989; Kao et al., 1995; Marta et al., 2013; Pink et al., 1990, 1993; Watkins et al., 1996;):

1. **Backswing:** From address to top of swing (A-B);
2. **Forward Swing:** From the top of swing to horizontal positioning of the golf club (early part of downswing) (B-C);
3. **Acceleration:** From horizontal club position to ball impact (late part of downswing) (C-D);
4. **Early Follow-Through:** from impact to a horizontal club positioning (D-E);
5. **Late Follow-Through:** From horizontal club position to completion of the swing (E-F).

This chapter focuses its attention on understanding the neuromuscular information to

improve the golfers' physical conditioning and preventing injury mechanisms by retrieving the available literature concerning the golf swing through electromyography (EMG).

EMG AMPLITUDE PARAMETERS IN GOLF SWING: STATE OF THE ART

The identification of neuromuscular patterns through EMG recording can provide important information for different study fields such as performance, injury prevention, management of muscle conditioning, skill improvement, motor control and learning. The muscle activation (intensity and timing) can be extracted from the EMG profile and is used to identify changes in muscle coordination (Hug, 2011). The EMG muscles activation could be studied by the mean of the intensity in the different swing phases. The changes in motor unit action potentials are detected through EMG and then normalized using an isometric maximal voluntary contraction (MVC) task, originally called Manual Muscle Test (MMT), to compare different subjects and studies. However, a few limitations are related to the inter-individual variability (Hug, 2011), heterogeneity in the golfers, and lack of informa-

tion about previously used EMG methods (Marta et al., 2012).

Neuromuscular activity studies about golf focused in several parts of the body. In order to analyze the amplitude parameters the body segments were divided into four subheads:

1. Shoulder;
2. Forearm;
3. Trunk;
4. Lower Limbs

To compare amplitude studies all EMG data was converted to a new scale of muscular levels. Therefore, each (+) corresponds to approximately 20% MMT/MVC.

Shoulder

The activity of the shoulder muscles was reported in four studies (Jobe et al., 1986, 1989; Kim et al., 2004; Pink et al., 1990;). The EMG shoulder studies were performed with fine wire methodology and described that participants were right-handed male professional golfers (handicap <5). However, Jobe et al., (1989) compared the men and women's neuromuscular patterns but no significant differences were found, as similar firing patterns and amplitudes were found. Despite that, women tended to have slightly more activity during the backswing and forward swing phase, while men tended to have it in the other phases. This fact is related to men being stronger than women and having longer arms, thereby increasing the club speed, particularly during the acceleration phase.

Table 1 summarizes the electromyographic studies performed in the shoulder muscles during the golf swing.

During the backswing the right supraspinatus muscle reached its peak with significant levels of activity above 40% (Jobe et al., 1986, 1989; Pink et al., 1990) - contributing to the rotation to the right of the shoulder girdle, and the abduction

flexion and external rotation of the arm. The left subscapularis registered high values of activity (40-80% MVC) during all the phases involved in the continuous internal rotation of the arm and specially to stabilize the shoulder but no significant differences were found between phases. In the forward swing and acceleration phases the shoulder muscles exhibited their activation peak. In these phases the club head speed increases to transmit velocity to the ball. The pectoralis major, subscapularis and latissimus dorsi muscles from both sides had high levels of activity, which exceeded 40% MVC (Jobe et al., 1986, 1989; Pink et al., 1990) during these phases. Thus, they increased the anti-clock rotation of the shoulder girdle, scapular rotation and it can be related to the left shoulder injury (Kim et al., 2004). During the early follow-through phase the left infraspinatus, right subscapularis and pectoralis major developed significant high activity levels (above 60% MVC) as they continued the action, as in the previous phase. In the late follow-through phase the left and right subscapularis, left and right pectoralis major, right latissimus dorsi, left supraspinatus, left infraspinatus, left subscapularis and the pectoralis major decreased their levels of activity reporting 40 – 60% MVC to decelerate and stop the movement.

All studies showed minimum to low levels of activation of the deltoids (below 20% MVC), bilaterally during the golf swing (Jobe et al., 1986, 1989; Pink et al., 1990), which can be related to limited elevation of the arm. Nevertheless, the right anterior deltoid is the most active portion during the forward swing phase and appears to be assisting the flexing and rising of the arm. This muscle is considered the arm prime mover and can function independently to perform the golf swing when adequately strengthened (Jobe et al., 1986).

The scapular muscles are responsible for the dynamic stability of the glenohumeral joint (rotation and protraction in the right arm) and play an important role in positioning and stabilizing

Study and Interpretation of Neuromuscular Patterns in Golf

Table 1. Activation levels of the shoulder muscles in EMG studies from both sides

Side	Authors	Muscles	BS	FS	ACC	EFT	LFT	FT
Right	Jobe et al. (1989) Pink et al. (1990)	SU	++	+	+	+	+	
		IS	++	+	+	+	+	
		SS	+	+++	++++	++++	+++	
		LD	+	+++	+++	++	++	
		PM	+	++++	+++++	++++	++	
		AD	+	++	+	+	+	
		MD	+	+	+	+	+	
		PD	+	+	+	+	+	
	Jobe et al. (1986)	SU	+++	+	++			+
		IS	++	++	++			+
		SS	+	+++	++++			+++++
		LD	+	+++	+++++			+++
		PM	+	+++	+++++			+++
		DL	+	+	+			+
Left	Jobe et al. (1989) Pink et al. (1990)	SU	++	++	+	++	++	
		IS	+	+	++	++++	++	
		SS	++	++	+++	++	++	
		LD	+	+++	++	++	+	
		PM	++	+	+++++	++++	++	
		AD	+	+	+	++	++	
		MD	+	+	+	+	+	
		PD	+	++	+	+	+	
	Jobe et al. (1986)	SU	+	+	++			++
		IS	+	++	+			++
		SS	+++++	+++	+++++			+++++
		LD	+	++	+++++			+++
		PM	++	++	+++++			+++
		DL	+	++	+			+

Legend: SU – Supraspinatus; IS – Infraspinatus; SS – Subscapularis; LD – Latissimus Dorsi; PM – Pectoralis Major; DL – Deltoid; AD – Anterior Deltoid; MD – Middle Deltoid; PD – Posterior Deltoid; BS – Backswing; FS – Forward Swing; ACC – Acceleration; EFT – Early Follow-Through; LFT – Late Follow-Through; FT – Follow-Through; + corresponds to 20% MMT/MVC

the humerus in the athlete’s shoulder (Blevins, 1997; Kao et al., 1995), especially if repeated movements are performed with great amplitude and velocity. These muscles must synchronically fire to provide intermuscular coordination and protect the glenohumeral complex with specific roles for different muscles and these neuromuscular patterns are related with overuse injuries of the professional golfers (Cabri et al., 2009). Only one study (Kao et al., 1995) described the scapular muscle patterns on normalized EMG values with

fine wire methodology but no statistical information was provided.

Table 2 summarizes the electromyographic studies performed in the scapular muscles during the golf swing.

In the backswing, in right-handed golfers, the right trapezius muscle presented its highest activity level, above 40% MVC, particularly in the trapezius lower portion, to elevate the arm. The left upper and lower serratus anterior showed medium activity levels (above 20%) allowing the protraction and abduction of the scapula on this side. The forward

Table 2. Activation levels of the scapular muscles in EMG studies from both sides

Author	Side	Muscles	BS	FS	ACC	EFT	LFT
Kao et al. (1995)	Right	LS	++	++	++	+	+
		RH	++	+++	++	++	+
		UT	++	+	+	++	+
		MT	++	+	+	++	+
		LT	+++	+	+	++	+
		USA	+	+++	++++	+++	++
		LSA	+	++	+++	+++	++
		LS	+	+++	++++	++	++
		RH	+	++++	+++	++	++
		LIT	+	++	+++	++	++

Legend: LS – Levator Scapulae RH – Rhomboid; UT – Upper Trapezius; MT – Middle Trapezius; LT – Lower Trapezius; USA – Upper Serratus Anterior; LSA – Lower Serratus Anterior; BS – Backswing; FS – Forward Swing; ACC – Acceleration; EFT – Early Follow-Through; LFT – Late Follow-Through; + corresponds to 20% MMT/MVC

swing and acceleration phases were the most active. The right serratus anterior muscle, mainly the upper portion, was the most active especially during the acceleration phase, with values higher than 60% MVC, probably due to scapula abduction. The left serratus anterior muscles decreased their activity (below 20% MVC) in the forward swing but increased it in the acceleration phase (above 20% MVC). The left levator scapular attained its peak during the acceleration phase with high levels of activity (above 60% MVC) to help the scapular elevation, retraction, and stabilization of the arm. The rhomboids muscles reached their peak during the forward swing phase with values above 40% MVC, and have firing patterns similar to the levator scapulae muscle. The left trapezius also reached its peak with levels of activity above 40% EMG. Therefore, the left scapular adductors were the most active muscles during these phases, indicating a major role in stabilization to assist control of the scapula rotation and protraction of the left arm. During the follow-through phase the right serratus anterior maintained high levels

of activity (above 40% MVC) and decreased to medium levels (above 20% MVC) in the late follow-through phase. The right rhomboids and right trapezius exhibited medium levels of activity (above 20% MVC) to adduct and stabilize the scapula in the first part of the follow-through phase. The left levator scapulae, left rhomboid, left trapezius and left serratus anterior showed medium levels of activity (above 20% MVC) to stabilize the scapula and to support the activation of the shoulder muscles.

The described consistent tonic activity suggests that the muscles with a scapula stabilizing function assume the primary role during the golf swing and can lead to fatigue and, consequently, to injury, especially on the right side. The rhomboid and levator scapulae are end-range muscles being easily injured with a lower intermuscular coordination. The golf swing does not require high levels of muscular activity from the glenohumeral muscles, so the success of this movement depends mostly on the balance of these muscles, i.e. neuromuscular synchrony.

Forearm

The only two studies (Faber et al., 2009; Glazebrook et al., 1994) that investigated the forearm were reported on right-handed male groups divided by handicap or injury (medial epicondylitis). Farber et al., (2009) compared the EMG of the forearm between professional and amateur golfers, while Glazebrook et al., (1994) compared an injury between handicaps. The EMG methodological differences were the fine wire and surface for Farber et al. (2009) and Glazebrook et al., (1994), respectively. Both articles reported that the forward swing and acceleration phases presented the highest levels of muscle activity in the forearm.

Table 3 summarizes the electromyographic studies performed in the forearm muscles during the golf swing.

In the backswing phase the right extensor carpi radialis brevis showed high levels of activity (above 40% MVC) in both groups to extend the wrist. The amateur group had also activated (above 20% MVC) the right pronator teres and the right flexor carpi ulnaris, which can be related to poor mechanics in this phase. The left extensor carpi radialis and left pronator teres had medium levels of activity (above 20% MVC) in both groups to extend the left wrist. The left flexors showed no significant differences between groups but the professionals exhibited higher levels of activity in the flexor carpi ulnaris and lower levels of activity in the flexor carpi radialis. During the forward swing and acceleration phases the muscles reached their maximum level of activity. Farber et al. (2009) reported high EMG activity, exceeding 100% MVC, as in the flexor carpi ulnaris muscle of the right forearm during the forward swing phase. This high level of activation is probably related to the wrist flexion and ulnar deviation presented during impact that concludes the proximal to distal kinetic chain developed during the downswing. Higher levels of activity in the extensor carpi radialis brevis were also reported in amateur

golfers during all swing phases, except during the takeaway. The right pronator teres muscle presented a higher level of activity during the acceleration phase in professionals (professionals - 88% MVC; amateurs - 36% MVC). On the left side, amateur golfers showed higher muscle activity in the pronator teres during the forward swing phase (professionals - 57% MVC; amateurs - 121% MVC). After comparing professional to amateur golfers, significant differences occurred in the pronator teres muscle during the forward swing and acceleration phases for the right and left sides, respectively. These high levels of activity of the pronator muscle in amateurs could be associated with the development of medial epicondylitis in the right arm (especially at impact) and to a superior technique of the professional golfers in the left arm. This technical difference occurs as a protective mechanism – the professional golfer pulls the golf club through the swing arc by using the lead arm – but it can also increase the risk of medial epicondylitis on this side. The follow-through phases were less demanding and with no significant differences between groups. Still, higher levels of activity were exhibited by all the studied muscles (above 20% MVC), especially in the early follow-through phase.

Glazebrook et al., (1994) compared asymptomatic and symptomatic golfers and their handicaps but by retrieving instants of the swing, except in the so called “swing phase,” which made it difficult to compare. The right wrist posterior muscles reached their peak activity at 60% MVC in the contact phase while the right wrist anterior muscles demonstrated moderate activity during the first two phases but increased to 91% MVC at contact (referred by the authors as “the flexor burst”). The symptomatic golfers showed higher levels of activity with significant differences in the asymptomatic players during address, backswing and downswing phases, but no significant differences were located between handicap groups.

Table 3. Activation levels of the forearm muscles in EMG studies from both sides

Author	Side	Group	Muscles	Address	Swing	Contact	Post Contact	
Glazebrook et al. (1994)	Right		AMF	++	++	+++++	++++	
			PMF	++	+++	++++	++++	
		ASYG	AMF	+	+	+++++	+++	
		SYG		+++	+++	+++++	++++	
Author	Side	Muscles	Group	BS	FS	ACC	EFT	LFT
Farber et al. (2009)	Right	ECRB	Prof	+++	++	++	++	+
			Amt	+++	++++	+++++	+++	+
		PT	Prof	+	+++	+++	++	+
			Amt	+++	+++++	+++++	+++	++
		FCR	Prof	+	+++++	++++	+++	++
			Amt	+	+++++	+++++	+++	++
		FCU	Prof	+	+++++	++++	+++	++
	Amt		++	+++++	+++++	+++	++	
	Left	ECRB	Prof	++	+++	+++	++	+
			Amt	++	+++	++++	++	++
		PT	Prof	++	++	++++	+++	+
			Amt	++	++	++	++	+
		FCR	Prof	+	+++	+++	++	+
			Amt	++	+++	+++	++	++
FCU		Prof	+++	++++	++++	+++	++	

Legend: ASYG – Asymptomatic group; SYG – Symptomatic Group; AMF – Anterior Muscles of the Forearm; PMF – Posterior Muscles of the Forearm; Prof – Professionals; Amt – Amateurs; ECRB – Extensor Carpi Radialis Brevis; PT – Pronator Teres; FCR – Flexor Carpi Radialis; FCU – Flexor Carpi Ulnaris; BS – Backswing; FS – Forward Swing; ACC – Acceleration; EFT – Early Follow-Through; LFT – Late Follow-Through; + corresponds to 20% MMT/MVC

Trunk

The trunk is the most EMG studied body part in golf with five articles focusing on the muscles' amplitude parameters (Bulbulian et al., 2001; Cole & Grimshaw, 2008a; Marta et al., 2013; Pink et al., 1993; Watkins et al., 1996). The most studied groups were the right-handed professional golfers, yet two articles investigated the recreational golfers (Bulbulian et al., 2001; Cole & Grimshaw, 2008a) and one had one female participant (Bulbulian et al., 2001). Trunk muscles have a high muscular solicitation during trunk rotation by both the professional and the recreational golfers.

Table 4 summarizes the electromyographic studies performed in the trunk muscles during the golf swing.

During the backswing phase the trunk rotates to the right and hyperextends with moderate levels of activity in the external oblique and erector spinae (above 20% MVC) in both sides. The downswing phase intends to drive power to the ball (Watkins et al., 1996) to achieve the desired distance. Commonly designated as “controlled fall” of the club, it increases the velocity of the club head with the trunk rotation and transfers kinetic energy to the ball (Pink et al., 1993). The trunk muscle activity increases during the forward swing and the acceleration phase, mainly in the right erector spinae

Study and Interpretation of Neuromuscular Patterns in Golf

Table 4. Activation levels of the trunk muscles in EMG studies from both sides

Side	Authors	Muscles	BS	FS	ACC	EFT	LFT
Right	Pink et al. (1993)	ES	+	++++	+++	++	++
		AO	+	++++	++++	+++	+++
	Watkins et al. (1996)	ES	+	+++	++	+	+
		AO	++	+++	+++	+++	++
		URA	+	++	++	++	+
		LRA	+	++	++	++	+
	Marta et al. (2013)	RA	+	++	+	++	+
		ES	++	++	++	+	+
		EO	++	+++	+++	+++	++
Left	Pink et al. (1993)	ES	++	++	+++	++	++
		AO	++	+++	+++	++	+++
	Watkins et al. (1996)	ES	++	++	+++	++	+
		AO	++	++++	++	++	++
	Marta et al. (2013)	RA	+	++	+	+	+
		ES	++	++	++	+	+
		EO	++	++	++	++	++

Legend: ES – Erector Spinae; AO – Abdominal Oblique; URA – Upper Rectus Abdominis; LRA – Lower Rectus Abdominis; RA – Rectus Abdominis; EO – External Oblique; BS – Backswing; FS – Forward Swing; ACC – Acceleration; EFT – Early Follow-Through; LFT – Late Follow-Through; + corresponds up to 20% MMT/MVC.

and oblique abdominal muscles with values above 40% MVC (Marta et al., 2013; Pink et al., 1993; Watkins et al., 1996). Therefore, the counteraction of gravity depends on the back muscles while the trunk rotation relies on the external oblique muscles. The balance of the intermuscular coordination between these muscles might be associated with injuries, due to high levels of activity in the erector spinae muscle and overuse syndrome in amateurs' and professional golfers, respectively. In the early and late follow-through phases the levels of activation were maintained (above 20% MVC) and decreased (below 20% MVC) for the erector spinae and external oblique.

Trunk injuries, especially low back pain (LBP), represent the most common musculoskeletal complaint during all swing phases, mainly at the end of the backswing (Cabri et al., 2009). The golf swing overuse practices may increase pain in the low back area in symptomatic subjects (Horton et

al., 2001). LBP is the most common musculoskeletal injury in golfers but little is known about the specific mechanisms responsible for it (Lindsay & Horton, 2002). Additionally, it is unclear if golf practice is causing, aggravating or inducing high skilled golfers. It is commonly accepted that low muscular coordination and low endurance could symbolize a significant risk factor to the occurrence of LBP, especially low resistance to fatigue of the abdominal and back muscles (Lindsay & Horton, 2002). Researchers found that, when comparing the control group with LBP golfers, important differences were presented in spine movement (Lindsay, Horton, & Vandervoot, 2000) and in the intensity and timing in trunk muscles EMG activation, i.e. lumbar erector spinae and abdominal oblique muscles (Cole & Grimshaw, 2008a,b; Horton et al., 2001). Those differences were obvious especially during the backswing and downswing in the erector spinae recruitment in

the beginning of the backswing, as was observed by Cole and Grimshaw (2008a,b), and were interpreted as a lumbar spine stabilizer. The higher external oblique activity can contribute to spinal instability by changing muscles coordination patterns (Marta et al., 2013; Pink et al., 1993; Watkins et al., 1996;). Grimshaw and Burden (2000) applied a conditioning program and coach intervention during a three-month period of training. Results showed a lesser level of activity from the left erector spinae muscle during the downswing. So, it was suggested in this case study that an improved technique modification and physical conditioning are related with low back pain, but no data were retrieved from the external oblique and shoulder muscles. The deep spine and pelvis muscles stabilizers must be studied with fire wire EMG and are considered to be operational previous to rapid movements of the upper and lower limbs (Marshall & Murphy, 2003), but no data were found concerning the iliopsoas, transversus abdominis and multifidus muscles that supposedly play an important role in lumbar dynamics. The difficulty to obtain data on these deep fascia muscles is due to its localization and to the high-speed movement.

The trunk clockwise rotation during the backswing stretches the trunk muscles, thus facilitating their action in the forward swing phase (Pink et al., 1993), but accumulates kinetic energy. The final stage of the stretches, i.e. the end of the backswing and start of forward swing, is mentioned as the moment when pain complaints are reported especially due to over-rotation (Cabri et al., 2009). This move is usually accomplished by high level golfers and is believed to maximize ball distance by generating high club head speed, but probably origins abnormal load in the lumbar spine and rises the injuries risk. Bulbulian et al., (2001) stated that a shorter backswing showed lower abdominal and lumbar muscles activation levels; however, a higher activation occurs in the latissimus dorsi and pectoralis major, during the downswing. So, during a task, the body had to

find a new balance in the swing mechanics to accomplish its goal. Results showed that during a shorter backswing, no significant differences were found in the club head velocity or stroke accuracy. This backswing changes suggest that less spinal rotation occurs but they increased the muscle activity on the shoulder muscles. The relationship between the EMG activity patterns and the X-factor magnitude has not been studied yet.

Lower Limbs

The foot/ankle is the third most injured area in golfer players (McHardy et al., 2006) but only one study (Bechler et al., 1995) was done focusing on the EMG activity in the hip and knee joints but by using fire wire EMG. Other studies (Marta et al., 2013; Watkins et al., 1996;) focused on the gluteus maximus with surface electromyography but were mostly heeded on trunk muscle activation.

Table 5 summarizes the electromyographic studies performed in the lower limb muscles during the golf swing.

In the backswing the right gluteus medius, right semimembranosus, right vastus lateralis and left and right biceps femoris showed medium levels of activity, above 20% MVC, as the body weight is located on that side. During the forward swing and acceleration phases, the right lower limb demonstrated higher muscle activity when compared to the left one, especially in the forward swing phase. The right gluteus maximus showed moderate to high activity levels (40-100% MVC) in the forward swing phase and the left gluteus maximus presented moderate to high levels in the acceleration phase (above 40% MVC) being the most active muscle in the lower limb and contributing to pelvis rotate. The weight transfer from right to left (in right-handed golfers) is very clear in the transition from the forward swing to acceleration of the EMG muscle activity. The right biceps femoral and semimembranosus muscles also showed high activation levels (above 40% MVC) during the forward swing and acceleration

Study and Interpretation of Neuromuscular Patterns in Golf

Table 5. Activation levels of the lower limbs muscles in EMG studies from both sides

Side	Authors	Muscles	BS	FS	ACC	EFT	LFT
Right	Bechler et al. (1995)	ADM	+	++	++	++	+
		UGM	+	+++++	++	+	+
		LGM	+	+++++	++	+	+
		GMED	++	++++	+++	+++	++
		BF	++	++++	+	+	+
		SM	++	++++	+	+	+
		VL	++	++	++	++	++
	Watkins et al. (1996)	GM	+	++++	++	+	+
	Marta et al. (2013)	GM	+	++	++	+	+
	Left	Bechler et al. (1995)	ADM	+	++++	+++	++
UGM			+	+++	+++	+++	++
LGM			+	+++	+++	++	+
GMED			+	++	++	+	++
BF			++	+++	++++	+++	+++
SM			+	++	+++	+++	+++
VL			+	+++++	+++	+++	+++
Watkins et al. (1996)		GM	+	++	+++	++	+
Marta et al. (2013)		GM	+	+	+++	++	+

Legend: ADM – Adductor Magnus; UGM – Upper Gluteus Maximus; LGM – Lower Gluteus Maximus; GMED – Gluteus Medius; BF – Biceps Femoris; SM – Semimembranosus; VL – Vastus Lateralis; GM – Gluteus Maximus; BS – Backswing; FS – Forward Swing; ACC – Acceleration; EFT – Early Follow-Through; LFT – Late Follow-Through; + corresponds to 20% MMT/MVC

phases. The left adductor magnus peaked during forward swing (above 60% MVC), increasing the pelvic rotation by pulling back the left hip. The left vastus lateralis muscle reached its peak (above 80% MVC) during the forward swing phase and maintained its activity levels (above 40%) during the follow up phases. This muscle contributes to stabilize the left knee and helps the pelvis rotation by providing a fulcrum. The follow-through phases were less active than the later phases. Nevertheless, the left hamstrings, left vastus lateralis, right upper gluteus maximus and left gluteus medius muscles showed activity levels

above 20% MVC to extend the hip and knee and stabilize the pelvis. The lower limbs muscles had high activity levels but further studies are needed, especially in the leg.

EMG ONSET: DIFFICULTIES, BARRIERS, AND PHYSIOLOGICAL MEANING

The study of EMG timing parameters provides information about activation time and muscle sequence contraction. The most known variable is

the *onset*, which can be defined as the beginning of the action potential of the motor units (Solnik, Rider, Steinweg, DeVita, & Hortobágyi, 2010). The study of the *onset* muscle activity can inform us on how the Central Nervous System (CNS) controls a set of muscles while performing a task. The study of muscle activation time – *onset* - is of major importance. The *onset muscle* activity can present information concerning the muscles temporal organization and coordination during a motor skill (De Luca, 1997) such as the golf swing.

The golf swing is a complex motor skill and associates power and precision synchronization. The increased speed of the distal segments is supported by the energy transferred from the core muscles, especially in explosive and accurate motor skills (Hirashima, Kadota, Sakurai, Kudo, & Ohtsuki, 2002). So the motor program of the central nervous system output will depend on specific sequence, intensity and activation time of the used muscles. For instance, in complex motor abilities the reaction time of abdominal muscles is crucial and tends to increase in subjects with low back pain due to postural organization (Hodges, 2001).

A wide variety of approaches has been used to detect EMG muscle *onset* but there is no standardized method and its application is usually done in motor skills with isometric contraction (Farina & Merletti, 2000) normally reported to present better reproducibility (Lee, Jung, & Kim, 2011). The dynamic and complex skills are characterized by EMG signals with higher level of instability and less reliability. So, the *onset* determination in those tasks is more demanding in terms of the involved methods. This is probably the reason why only two papers (Cole and Grimshaw, 2008b; Horton et al., 2001) studied the *onset* of muscle activity in the golf swing.

Cole and Grimshaw (2008b) and Horton et al., (2001) compared abdominal muscle activation in subjects with and without chronic low back pain. Horton et al., (2001) studied the abdominal muscle activation of professional golfers in five

maximal shots before and after a typical 50 min practice session. The external oblique and rectus abdominis muscles of both sides (lead and trail) showed similar activity levels in both groups. Only one significant difference was reported between groups: injured golfers exhibited EMG *onset* times in the lead external oblique occurring significantly later during the backswing. The control group activated its lead external oblique 17 ms (before practice) and 42 ms (after practice) after the start of the backswing. The chronic low back pain group activated the same muscle 56 ms (before practice) and 67 ms (after practice) after the beginning of the backswing. Cole and Grimshaw (2008b) compared trunk and abdominal muscles timing parameters in golfers with and without low back pain. The used threshold algorithm was calculated through the average baseline activity when it exceeded one SD during a 50 ms window for both *onset* and *offset* parameters. The muscle activation pattern of the golfer with low back pain showed statistical differences in the ES muscle just prior to the initiation of the backswing. This difference is explained by the hypothesis of the poor functioning of the deeper spinal stabilization muscles. Silva et al., (2013) described timing parameters on the trunk muscles by comparing club types. The maximum activation tends to occur simultaneously during the forward swing and acceleration phases for the rectus abdominis, erector spinae, internal oblique and external oblique muscles. The *onset* tends to occur simultaneously during the backswing, but no differences were reported between club types.

Onset detection can be performed with visual inspection or detection algorithms (Vaisman, Zariffa, & Popovic, 2010). Visual inspection (VI) is highly time-consuming and depends on the researcher's expertise, so it can be considered a subjective process (Jöllenbeck, 2000). Conversely, the lack of a *goldstandard* measurement used for algorithms validation leads to using visual inspection to confirm threshold algorithms. Previous literature generally organized the detection algorithms into threshold algorithms (Allison,

2003; Hodges & Bui, 1996; Jöllenbeck, 2000; Van Boxtel, Geraats, Van de Berg-Lenssen, & Brunia, 1993) and statistically optimized algorithms (Micera, Sabatini, & Dario, 1998; Staude, Flachenecker, & Wolf, 2001), such as maximum likelihood, wavelet transform (Vannozzi, Conforto, & D'Alessio, 2010) and Teager-Kaiser energy operator (Li, Zhou, & Aruin, 2007; Solnik, DeVita, Rider, Long, & Hortobágyi, 2008; Solnik et al., 2010).

The *onset* algorithm detection precision is influenced by background activity level, signal-to-noise ratio activity (Hodges & Bui, 1996; Staude et al., 2001) and *onset* rate of signal amplitude (Allison, 2003). Hug (2011) states that, generally, used threshold algorithms variation is: 1, 2, and 3 SD or between 15 to 25% of maximum activity peak. Other threshold algorithm approaches have considered the use of the signal voltage/intensity by exceeding the upper limit of the confidence interval during a stationary number of samples (Van Boxtel et al., 1993).

Hodges and Bui (1996) have reported *onset* detection algorithms combined with different background activity levels of diverse variables, such as low pass filters (10, 50, 500 Hz), sampling windows (10, 25, 50 ms) and standard deviations (1, 2, 3 SD). The results showed that the most accurate combinations for low pass filter, sample window and SD were: 50 Hz / 25 ms / 3 SD and 50 Hz / 50 ms / 1 SD. Consequently, it's clear that smoothing is an important issue that can interfere with the use of *onset* detection algorithms. Although excessive smoothing may facilitate information losses and inaccurate identification, insufficient smoothing is normally associated with a delay on *onset* detection (Hodges & Bui, 1996).

Besides *onset* detection in dynamic tasks, the meaning of the signal and relation with its task are not well described in literature. As a result, several authors have explained the movement analysis through descriptive and qualitative approaches (Hirashima et al., 2002; McGill, Chaimberg, Frost, & Fenwick, 2010; Silva et al., 2013). Figure 2

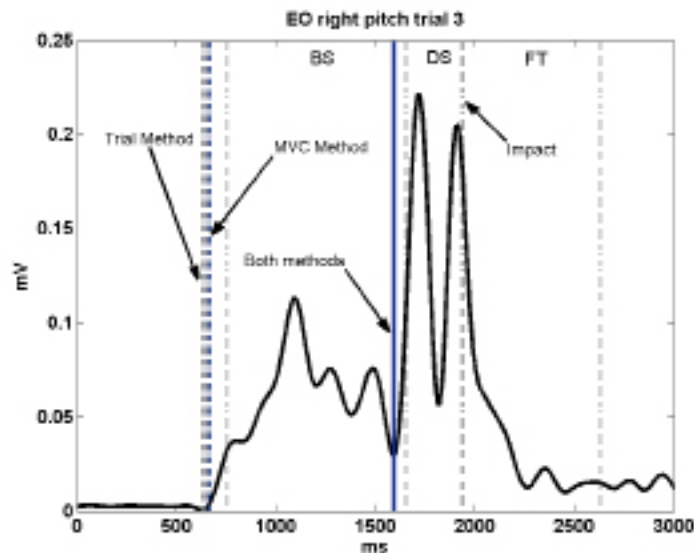
shows the external oblique EMG muscle activity during the swing phases. Two methods were used for *onset* detection by differing the threshold determination. The trial method consisted in determination of the threshold by using the mean EMG activity for 1000 ms before the 500 ms prior to the start of the backswing. In the MVC method, threshold was determined by the baseline activity between two MVC. From restriction to different mechanical actions of the swing phases, the *onset* search had to start before the backswing and the downswing. Two activation instants were found: the first before the downswing and the second before the backswing. Obviously, in this example the baseline had a very favorable signal to noise-ratio. In the erector spinae muscle the baseline was very high due to the trunk flexion during the address but a peak occurs immediately before impact. Then the timing parameters studies should regard the physiological meaning in dynamic tasks, trying to explain how the CNS recruits muscles to achieve a certain mechanical output.

For complex dynamic motor tasks, such as golf swing, the nature of EMG signals is quite different from those registered during isometric contractions. Apart from the used method, when studying temporal parameters of EMG signals in dynamic tasks we should be able to identify and describe the physiological phenomenon and its interpretation.

Solutions and Recommendations

To collect EMG signal the electrodes placement must be correct and well described in papers, especially in small muscles, so comparison between studies may represent new approaches. Data collection procedures must be well planned to diminish the time spent during the task and in signal processing. EMG signal should be task related and normalized through isometric maximum voluntary contraction with specific exercises. In dynamic tasks, such as golf swing, more complications can happen: time consumption to prepare

Figure 2. Onset detection using two methods during a golf swing



the participant for the task, difficulty to retrieve a huge amount of muscles at the same time, and use of kinematic points needed to divide the swing phases. Nevertheless, an organized plan and a good laboratory group can work against adversities and retrieve the EMG signal sooner.

FUTURE RESEARCH DIRECTIONS

In future studies the activation patterns of lower limb and the distal portion of upper limb should be characterized because those regions are injury related and there is a lack of EMG research performed with those muscle groups.

The club kinematic and club head velocity differs according to the used club type, so differences in muscular activity patterns can occur.

Studies must investigate the amateur's level golfers and special group population (i.e. different handicap) since some differences can be found between skilled and less skilled golfers, as the latter ones are in a larger number.

Most studies have focused their attention on male golfers, but some differences can occur in

female golfers since they show differences in muscle profile and strength capacity, mainly in upper limb muscles, and they have a different body composition (i.e. more body fat).

Studies should relate the kinematic with EMG (e.g. the X-factor with EMG activity patterns of the trunk muscles) in order to understand their connection to injuries.

There is a lack of research on EMG timing parameters during the golf swing and this kind of approach is important to characterize how the central nervous system controls the temporal organization and coordination during the swing and how it adapts to different constraints. For this research topic an objective and uniform definition of criteria for timing parameters definition is necessary.

Muscle synergies extraction on EMG signals has been being used in sports science and rehabilitation field (Hug, Turpin, Couturier, & Dorel, 2011; Hug, Turpin, Guével, & Dorel, 2010; Turpin, Guével, Durand, & Hug, 2011). This technique allows a better understanding on how Central Nervous System controls a lot of muscles at the same time (Safavynia, Torres-Oviedo, & Ting,

2011), i.e., it gives insights about motor program. Thus, studying how such muscle synergies differ in golfer's handicap or different club use might give interesting information to trainers and therapists. Future studies should also encompass this kind of analyses.

CONCLUSION

This chapter is aimed to describe the EMG muscular activity of a golf swing in different body regions. The intensity parameters were the first to be studied and more have followed. However, they focused specially on trunk and shoulders. Therefore, distal regions must be studied, especially the lower limbs. Additionally, some studies have been completed to report frequent injuries in golfers, mainly the low back pain. The timing parameters studies could allow additional information about musculoskeletal injuries in golf, and they can be used to describe differences between special groups. New approaches have been presented and discussed to understand how time parameters determination should contribute, in the future, to the research about neuromuscular function in golf. However, no *goldstandard* algorithm definition has consensus in the scientific community. Consequently, there is need for further studies on golfers' injury mechanisms, and on prescription of training programs and rehabilitation in order to understand such a complex motor task as the golf swing.

ACKNOWLEDGMENT

The project “*Neuromuscular activity in the golf swing with implications for the practice and in the prevention of overuse injuries*” was supported by the Portuguese Foundation for Science and Technology fund (PTDC/DES/105176/2008).

REFERENCES

- Abernethy, B., Neal, R. J., Moran, M. J., & Parker, A. W. (1990). Science and golf: Proceedings of the First World Scientific Congress of Golf. In A. J. Cochran (Ed.), *Expert-novice differences in muscle activity during the golf swing* (pp. 54-60). London: E. & F. N. Spon.
- Allison, G. T. (2003). Trunk muscle onset detection technique for EMG signals with ECG artefact. *Journal of Electromyography and Kinesiology*, 13(3), 209–216. doi:10.1016/S1050-6411(03)00019-1 PMID:12706601
- Bechler, J., Jobe, F., Pink, M., Perry, J., & Ruwe, P. (1995). Electromyographic analysis of the hip and knee during the golf swing. *Clinical Journal of Sport Medicine*, 5(3), 162–165. doi:10.1097/00042752-199507000-00005 PMID:7670971
- Blevins, F. (1997). Rotator cuff pathology in athletes. *Sports Medicine (Auckland, N.Z.)*, 24(3), 205–220. doi:10.2165/00007256-199724030-00009 PMID:9327536
- Bulbulian, R., Ball, K., & Seaman, D. (2001). The short golf backswing effects on performance and spinal health implications. *Journal of Manipulative Physiological Therapeutics*, 24(9), 569–575. doi:10.1067/mmt.2001.118982 PMID:11753330
- Cabri, J., Sousa, J. P., Kots, M., & Barreiros, J. (2009). Injuries in golf: A systematic review. *European Journal of Sport Science*, 9(6), 353–366. doi:10.1080/17461390903009141
- Cole, M. H., & Grimshaw, P. N. (2008a). Electromyography of the trunk and abdominal muscles in golfers with and without low back pain. *Journal of Science and Medicine in Sport*, 11(2), 174–181. doi:10.1016/j.jsams.2007.02.006 PMID:17433775

- Cole, M. H., & Grimshaw, P. N. (2008b). Trunk muscle onset and cessation in golfers with and without low back pain. *Journal of Biomechanics*, *41*(13), 2829–2833. doi:10.1016/j.jbiomech.2008.07.004 PMID:18718596
- De Luca, C. J. (1997). The use of surface electromyography in biomechanics. *Journal of Applied Biomechanics*, *13*, 135–163.
- Escamilla, R., & Andrews, J. (2009). Shoulder muscle recruitment patterns and related biomechanics during upper extremity sports. *Sports Medicine (Auckland, N.Z.)*, *39*(7), 569–590. doi:10.2165/00007256-200939070-00004 PMID:19530752
- Farber, A., Smith, J., Kvitne, R., Mohr, K., & Shin, S. (2009). Electromyographic analysis of forearm muscles in professional and amateur golfers. *The American Journal of Sports Medicine*, *37*(2), 396–401. doi:10.1177/0363546508325154 PMID:19022991
- Farina, D., & Merletti, R. (2000). Comparison of algorithms for estimation of EMG variables during voluntary isometric contractions. *Journal of Electromyography and Kinesiology*, *10*(5), 337–349. doi:10.1016/S1050-6411(00)00025-0 PMID:11018443
- Glazebrook, M., Curwin, S., Islam, M., Kozey, J., & Stanish, W. (1994). Medial epicondylitis. An electromyographic analysis and an investigation of intervention strategies. *The American Journal of Sports Medicine*, *22*(5), 674–679. doi:10.1177/036354659402200516 PMID:7810792
- Grimshaw, P., & Burden, A. (2000). Case report: Reduction of low back pain in professional golfer. *Medicine & Science in Sports & Exercise*, *32*(10), 1667–1673.
- Hirashima, M., Kadota, H., Sakurai, S., Kudo, K., & Ohtsuki, T. J. (2002). Sequential muscle activity and its functional role in the upper extremity and trunk during overarm throwing. *Sports Science*, *20*(4), 301–310. doi:10.1080/026404102753576071 PMID:12003275
- Hodges, P. W. (2001). Changes in motor planning of feedforward postural responses of the trunk muscles in low back pain. *Experimental Brain Research*, *141*(2), 261–266. doi:10.1007/s002210100873 PMID:11713638
- Hodges, P. W., & Bui, B. H. (1996). A comparison of computer-based methods for the determination of onset of muscle contraction using electromyography. *Electroencephalography and Clinical Neurophysiology*, *101*(6), 511–519. doi:10.1016/S0013-4694(96)95190-5 PMID:9020824
- Horton, J. F., Lindsay, D. M., & Macintosh, B. R. (2001). Abdominal muscle activation of elite male golfers with chronic low back pain. *Medicine and Science in Sports and Exercise*, *33*(10), 1647–1654. doi:10.1097/00005768-200110000-00006 PMID:11581547
- Hug, F. (2011). Can muscle coordination be precisely studied by surface electromyography? *Journal of Electromyography and Kinesiology*, *21*, 1–12. doi:10.1016/j.jelekin.2010.08.009 PMID:20869882
- Hug, F., Turpin, N. A., Couturier, A., & Dorel, S. (2011). Consistency of muscle synergies during pedaling across different mechanical constraints. *Journal of Neurophysiology*, *106*(1), 91–103. doi:10.1152/jn.01096.2010 PMID:21490282
- Hug, F., Turpin, N. A., Guével, A., & Dorel, S. (2010). Is interindividual variability of EMG patterns in trained cyclists related to different muscle synergies? *Journal of Applied Physiology*, *108*(6), 1727–1736. doi:10.1152/jappphysiol.01305.2009 PMID:20299611

Study and Interpretation of Neuromuscular Patterns in Golf

- Jobe, F., Moynes, D., & Antonelli, D. (1986). Rotator cuff functions during a golf swing. *The American Journal of Sports Medicine*, 14(5), 388–392. doi:10.1177/036354658601400509 PMID:3777315
- Jobe, F., Perry, J., & Pink, M. (1989). EMG shoulder activity in men and women professional golfers. *The American Journal of Sports Medicine*, 17(6), 782–787. doi:10.1177/036354658901700611 PMID:2624291
- Jöllenbeck, J. (2000). Methodological limitations of EMG-based bio-mechanical motion analysis. In *ISBS Conference Proceedings Archive, 18th International Symposium on Biomechanics in Sports*. Hong Kong, China.
- Kao, J., Pink, M., Jobe, F., & Perry, J. (1995). EMG analysis of the scapular muscles during a golf swing. *The American Journal of Sports Medicine*, 23(1), 19–23. doi:10.1177/036354659502300104 PMID:7726345
- Kim, D., Millett, P., Warner, J., & Jobe, F. (2004). Shoulder injuries in golf. *The American Journal of Sports Medicine*, 32(5), 1324–1330. doi:10.1177/0363546504267346 PMID:15262661
- Lee, J., Jung, M. Y., & Kim, S. H. (2001). Reliability of spike and turn variables of surface EMG during isometric voluntary contractions of the biceps brachii muscle. *Journal of Electromyography and Kinesiology*, 21(1), 119–127. doi:10.1016/j.jelekin.2010.08.008 PMID:20833563
- Li, X., Zhou, P., & Aruin, A. S. (2007). Teager-Kaiser energy operation of surface EMG improves muscle activity onset detection. *Annual Biomedical Engineering*, 35(9), 1532–153. doi:10.1007/s10439-007-9320-z PMID:17473984
- Lindsay, D., & Horton, J. (2002). Comparison of spine motion in elite golfers with and without low back pain. *Journal of Sports Sciences*, 20(8), 599–605. doi:10.1080/026404102320183158 PMID:12190279
- Lindsay, D., Horton, J., & Vandervoort, A. (2000). A review of injury characteristics, aging factors and prevention programmes for the older golfer. *Sports Medicine (Auckland, N.Z.)*, 30(2), 89–103. doi:10.2165/00007256-200030020-00003 PMID:10966149
- Marshall, P., & Murphy, B. (2003). The validity and reliability of surface EMG to assess the neuromuscular response of the abdominal muscles to rapid limb movement. *Journal of Electromyography and Kinesiology*, 13, 477–489. doi:10.1016/S1050-6411(03)00027-0 PMID:12932422
- Marta, S., Silva, L., Castro, M. A., Pezarat-Correia, P., & Cabri, J. (2012). Electromyography variables during the golf swing: A literature review. *Journal of Electromyography and Kinesiology*, 22(6), 803–813. doi:10.1016/j.jelekin.2012.04.002 PMID:22542769
- Marta, S., Silva, L., Vaz, J., Bruno, P., & Pezarat-Correia, P. (2013). Electromyographic analysis of trunk muscles during the golf swing performed with two different clubs. *Annual Review of Golf Coaching supplement of the International Journal of Sports Science & Coaching*.
- McGill, S. M., Chaimberg, J. D., Frost, D. M., & Fenwick, C. M. (2010). Evidence of a double peak in muscle activation to enhance strike speed and force: an example with elite mixed martial arts fighters. *Journal of Strength and Conditioning Research*, 24(2), 348–357. doi:10.1519/JSC.0b013e3181cc23d5 PMID:20072065
- McHardy, A., & Pollard, H. (2005a). Muscle activity during the golf swing. *British Journal of Sports Medicine*, 39(11), 799–804. doi:10.1136/bjism.2005.020271 PMID:16244187

- McHardy, A., & Pollard, H. (2005b). Golf and upper limb injuries: A summary and review of the literature. *Chiropractic & Osteopathy*, *13*(7). PMID:15967021
- McHardy, A., Pollard, H., & Luo, K. (2006). Golf injuries: A review of the literature. *Sports Medicine (Auckland, N.Z.)*, *36*, 171–187. doi:10.2165/00007256-200636020-00006 PMID:16464124
- Micera, S., Sabatini, A. M., & Dario, P. (1998). An algorithm for detecting the onset of muscle contraction by EMG signal processing. *Medicine Engennier Physical*, *20*(3), 211–215. doi:10.1016/S1350-4533(98)00017-4 PMID:9690491
- Moynes, D., Perry, J., Antonelli, D., & Jobe, F. (1986). Electromyography and motion analysis of the upper extremity in sports. *Physical Therapy*, *66*(12), 1905–1911. PMID:3786421
- Pink, M., Jobe, F., & Perry, J. (1990). Electromyographic analysis of the shoulder during the golf swing. *The American Journal of Sports Medicine*, *18*(2), 137–140. doi:10.1177/036354659001800205 PMID:2343980
- Pink, M., Perry, J., & Jobe, F. (1993). EMG analysis of the trunk in golfers. *The American Journal of Sports Medicine*, *21*(3), 385–388. doi:10.1177/036354659302100310 PMID:8346752
- Safavynia, S. A., Torres-Oviedo, G., & Ting, L. H. (2011). Muscle Synergies: Implications for Clinical Evaluation and Rehabilitation of Movement. *Topics in Spinal Cord Injury Rehabilitation*, *17*(1), 16–24. doi:10.1310/sci1701-16 PMID:21796239
- Silva, L., Marta, S., Vaz, J., Fernandes, O., Castro, M. A., & Pezarat-Correia, P. (2013). Trunk muscle activation during golf swing: Baseline and threshold. *Journal of Electromyography and Kinesiology*, *23*(5), 1174–1182. doi:10.1016/j.jelekin.2013.05.007 PMID:23816264
- Slater-Hammel, A. T. (1948). Action current study of contraction-movement relationship in golf stroke. *Research Quarterly*, *19*(3), 164–177. PMID:18887614
- Solnik, S., DeVita, P., Rider, P., Long, B., & Hortobágyi, T. (2008). Teager-Kaiser Operator improves the accuracy of EMG onset detection independent of signal-to-noise ratio. *Acta Bioengennier Bio-mechanics*, *10*(2), 65–68. PMID:19032000
- Solnik, S., Rider, P., Steinweg, K., DeVita, P., & Hortobágyi, T. (2010). Teager-Kaiser energy operator signal conditioning improves EMG onset detection. *European Journal of Applied Physiology*, *110*(3), 489–498. doi:10.1007/s00421-010-1521-8 PMID:20526612
- Staude, G., Flachenecker, C., & Wolf, W. (2001). Onset detection in surface electromyographic signals: A systematic comparison of methods. *EURASIP Journal on Applied Signal Processing*, *2*, 67–81. doi:10.1155/S1110865701000191
- Therriault, G., & Lachance, P. (1998). Golf injuries. An overview. *Sports Medicine (Auckland, N.Z.)*, *26*(1), 43–57. doi:10.2165/00007256-199826010-00004 PMID:9739540
- Turpin, N. A., Guével, A., Durand, S., & Hug, F. (2011). No evidence of expertise-related changes in muscle synergies during rowing. *Journal of Electromyography and Kinesiology*, *21*(6), 1030–1040. doi:10.1016/j.jelekin.2011.07.013 PMID:21856171
- Vaisman, L., Zariffa, J., & Popovic, M. R. (2010). Application of singular spectrum-based change-point analysis to EMG-onset detection. *Journal of Electromyography and Kinesiology*, *20*(4), 750–760. doi:10.1016/j.jelekin.2010.02.010 PMID:20303784

Study and Interpretation of Neuromuscular Patterns in Golf

Van Boxtel, G. J., Geraats, L. H., Van den Berg-Lenssen, M. M., & Brunia, C. H. (1993). Detection of EMG onset in ERP research. *Psychophysiology*, *30*(4), 405–412. doi:10.1111/j.1469-8986.1993.tb02062.x PMID:8327626

Vannozzi, G., Conforto, S., & D'Alessio, T. (2010). Automatic detection of surface EMG activation timing using a wavelet transform based method. *Journal of Electromyography and Kinesiology*, *20*(4), 767–772. doi:10.1016/j.jelekin.2010.02.007 PMID:20303286

Watkins, R., Uppal, G., Perry, J., Pink, M., & Dinsay, J. (1996). Dynamic electromyographic analysis of trunk musculature in professional golfers. *The American Journal of Sports Medicine*, *24*(4), 535–538. doi:10.1177/036354659602400420 PMID:8827315

ADDITIONAL READING

Basmajian, J. (1985). *Muscles alive. Theirs functions revealed by electromyography* (5th ed.). Baltimore: William & Wilkins.

Beck, T. W., Stock, M. S., & Defreitas, J. M. (2011). Paired Pattern Classification of Electromyographic Intensity Patterns During Concentric and Eccentric Muscle Actions. *Clinical Kinesiology*, *65*(4), 76–82.

Bernstein, N. A. (1967). *The co-ordination and regulation of movements*. Oxford: Pergamon Press.

Bosco, G. (2010). Principal component analysis of electromyographic signals: An overview. *Open Rehabilitation Journal*, *3*, 127–131. doi:10.2174/1874943701003010127

Cappellini, G., Ivanenko, Y., Poppele, R., & Lacquaniti, F. (2006). Motor Patterns in Human Walking and Running. *Journal of Neurophysiology*, *95*, 3426–3437. doi:10.1152/jn.00081.2006 PMID:16554517

Chen, X., Zhu, X., & Zhang, D. (2010). A discriminant bispectrum feature for surface electromyogram signal classification. *Medical Engineering & Physics*, *32*(2), 126–135. doi:10.1016/j.medengphy.2009.10.016 PMID:19955011

Chu, Y., Sell, T., & Lephart, S. (2010). The relationship between biomechanical variables and driving performance during the golf swing. *Journal of Sports Sciences*, *28*(11), 1251–1259. doi:10.1080/02640414.2010.507249 PMID:20845215

d'Avella, A., & Bizzi, E. (2005). Shared and specific muscle synergies in natural motor behaviors. *Proceedings of the National Academy of Sciences of the United States of America*, *102*, 3076–3081. doi:10.1073/pnas.0500199102 PMID:15708969

De Luca, C. (1997). The use of surface electromyography in biomechanics. *Journal of Applied Biomechanics*, *13*, 135–163.

Egret, C., Vincent, O., Weber, J., Dujardin, F., & Chollet, D. (2003). Analysis of 3D kinematics concerning three different clubs in golf swing. *International Journal of Sports Medicine*, *24*(6), 465–470. doi:10.1055/s-2003-41175 PMID:12905097

Englehart, K., Hudgins, B., & Member, S. (2003). A Robust, Real-Time Control Scheme for Multifunction Myoelectric Control. *IEEE Transactions on Bio-Medical Engineering*, *50*(7), 848–854. doi:10.1109/TBME.2003.813539 PMID:12848352

Frère, J., Gopfert, B., Slawinski, J., & Touny-Chollet, C. (2012). Effect of the upper limbs muscles activity on the mechanical energy gain in pole vaulting. *Journal of Electromyography and Kinesiology*, *22*(2), 207–214. doi:10.1016/j.jelekin.2011.11.007 PMID:22133664

Frère, J., & Hug, F. (2012). . . *Frontiers in Computational Neuroscience*, *6*, 99. doi:10.3389/fncom.2012.00099 PMID:23293599

- Gosheger, G., Liem, D., Ludwig, K., Greshake, O., & Winkelmann, W. (2003). Injuries and overuse syndromes in golf. *The American Journal of Sports Medicine*, 31(3), 438–443. PMID:12750140
- Hosea, T. M., & Gatt, C. J. (1996). Back pain in golf. *Clinics in Sports Medicine*, 15(1), 37–53. PMID:8903708
- Hudgins, B., Parker, P., & Scott, R. N. (1993). A new strategy for multifunction myoelectric control. *IEEE Transactions on Bio-Medical Engineering*, 40(1), 82–94. doi:10.1109/10.204774 PMID:8468080
- Hume, P. A., Koegh, J., & Reid, D. (2005). The role of biomechanics in maximizing distance and accuracy of golf shots. *Sports Medicine (Auckland, N.Z.)*, 35(5), 429–449. doi:10.2165/00007256-200535050-00005 PMID:15896091
- Khushaba, R. N., Kodagoda, S., Takruri, M., & Dissanayake, G. (2012). Expert Systems with Applications Toward improved control of prosthetic fingers using surface electromyogram (EMG) signals. *Expert Systems with Applications*, 39(12), 10731–10738. doi:10.1016/j.eswa.2012.02.192
- McHardy, A., & Pollard, H. (2005c). Lower back pain in golfers: a review of the literature. *Journal of Chiropractic Medicine*, 4(3), 135–143. doi:10.1016/S0899-3467(07)60122-0 PMID:19674655
- McHardy, A., Pollard, H., & Bayley, G. (2006). A comparison of the modern and classical golf swing: A clinician's perspective. *The American Journal of Sports Medicine*, 18(3), 80–92.
- McHardy, A., Pollard, H., & Luo, K. (2007). One-year follow-up study on golf injuries in Australian amateur golfers. *The American Journal of Sports Medicine*, 35(8), 1354–1360. doi:10.1177/0363546507300188 PMID:17387218
- Oskoei, A. M., & Hu, H. (2007). Myoelectric control systems - A survey. *Biomedical Signal Processing and Control*, 2(4), 275–294. doi:10.1016/j.bspc.2007.07.009
- Oskoei, M. A., & Hu, H. Support vector machine-based classification scheme for myoelectric control applied to upper limb. *IEEE Trans Biomed Eng.* 55(8):1956-65. doi: 10.1109/TBME.2008.919734.
- Oskoei, M.A., & Hu, H. (2008). Support Vector Machine-Based Classification Scheme for Myoelectric Control Applied to Upper
- Park, S. H., & Lee, S. P. (1998). EMG pattern recognition based on artificial intelligence techniques. *IEEE transactions on rehabilitation engineering : a publication of the IEEE Engineering in Medicine and Biology Society*, 6(4), 400-405.
- Phinyomark, a., Nuidod, a., Phukpattaranont, P., & Limsakul, C. (2012). Feature Extraction and Reduction of Wavelet Transform Coefficients for EMG Pattern Classification. *Electronics and Electrical Engineering*, 122(6), 27-32.
- Rainoldi, A., Bullock-Saxton, J., Cavarretta, F., & Hogan, N. (2001). Repeatability of maximal voluntary force and of surface EMG variables during voluntary isometric contraction of quadriceps muscles in healthy subjects. *Journal of Electromyography and Kinesiology*, 11(6), 425–438. doi:10.1016/S1050-6411(01)00022-0 PMID:11738955
- Schölkopf, B., Smola, A. J., Williamson, R. C., & Bartlett, P. L. (2000). New Support Vector Algorithms. *Neural Computation*, 12, 1207–1245. doi:10.1162/089976600300015565 PMID:10905814
- Tkach, D., Huang, H., & Kuiken, T. (2010). Study of stability of time-domain features for electromyographic pattern recognition. *Journal of Neuroengineering and Rehabilitation*, 7(21), 1–13. PMID:20064261

Study and Interpretation of Neuromuscular Patterns in Golf

Wakeling, J. M., & Horn, T. (2009). Neuromechanics of Muscles Synergy During Cycling. *Journal of Neurophysiology*, *101*, 843–854. doi:10.1152/jn.90679.2008 PMID:19073812

Zecca, M., Micera, S., Carrozza, M. C., & Dario, P. (2002). Control of multifunctional prosthetic hands by processing the electromyographic signal. *Critical Reviews in Biomedical Engineering*, *30*(4-6), 459–485. doi:10.1615/CritRevBiomedEng.v30.i456.80 PMID:12739757

Swing: A multi-dynamic and complex movement used in golf in order to hit the ball.

Threshold: Value used to calculate limits to start the *onset* or *offset*, generally, by using percentage or standard deviation.

Trail: The right side (upper or lower limb) on a right-handed golfer.

KEY TERMS AND DEFINITIONS

Club: The object used by golfers to hit the ball.

Lead: The left side (upper or lower limb) on a right-handed golfer.

Low Back Pain: The most frequent golf injury located in the posterior and low trunk.

Muscle Synergies: Low-dimensional modules formed by muscles activated in synchrony.

Offset: The time that corresponds to the final contraction of the muscle.

Onset: The time that corresponds to initial contraction of the muscle.

Phases: The division of a task into parts to better describe the swing, which normally is divided in five.

Section 3

EMG:

Endurance, Stability, and Muscle Activities

Chapter 9

Assessing Joint Stability from Eigenvalues Obtained from Multi-Channel EMG: A Spine Example

Dianne M. Ikeda

University of Waterloo, Canada

Stuart M. McGill

University of Waterloo, Canada

ABSTRACT

Electromyographic (EMG) signals have many uses. This chapter addresses the role of EMG signals to assess joint stability. Low back pain assessment and treatment interventions often involve the concepts of stability and/or joint stiffness. Using muscle activation and lumbar spine posture to calculate segmental stiffness and potential energy of the spine, eigenvalues can be linked to quantitative stability. It is reasoned that if a relationship exists between eigenvalues and individual muscles, then this approach can guide customized clinical intervention for people with defined spine instability.

INTRODUCTION

EMG can be used to obtain force and stiffness estimates from which stability of joints can be estimated. Using the lumbar spine as an example, EMG from the trunk muscles can be used to calculate joint stiffness, which is recognized as universally enhancing stability and the ability to withstand a perturbation. The flexible column does not have sufficient stiffness to support the

weight of the upper body without buckling unless muscles are activated and stiffened around the column (Lucas & Bresler, 1961). Perturbed muscle activation patterns leading to instability have been shown to be both a cause and consequence of low back pain. Addressing the perturbed patterns with corrective exercise appears, at least in some patients, to reduce or eliminate their pain immediately. Insufficient stability is thought to allow micro movements in the spine motion seg-

DOI: 10.4018/978-1-4666-6090-8.ch009

ments resulting in painful stress concentrations of innervated tissues (McGill, 2007). Further understanding of quantitative spine stability could potentially assist in clinical interventions of individuals with spine instability.

Some investigations of spine stability use a potential energy approach to evaluate the eigenvalues (EV) derived from the segmental stiffness and potential energy of the spinal column and joints. However, it is unknown whether specific muscles can be represented by specific EVs, obtained from EMG, such that their evaluation could guide clinical approaches to modify muscle activation/stiffness and thus the stability state of the joint. This chapter will examine this and establish a theoretical framework for understanding the links between posture and muscle activity, which results in force and ultimately spine load and stability/stiffness. It was hypothesized that:

1. Individual muscles affect specific EVs, but no one muscle can be associated with one EV level
2. Specific muscles do affect specific planes of stability/stiffness
3. EVs are affected by posture
4. Overactivating muscles by increasing muscle activation to 100% maximum voluntary contraction (MVC) negatively affects the EVs
5. The relationship between muscles and specific EVs obtained during simulation remains with real subjects performing loaded tasks.

The hypotheses were evaluated in two stages. First, synthetic muscle activation levels enabled a sensitivity analysis of the variables that affect the EVs. Second, the sensitivity analysis was repeated with actual muscle activation and spine posture data obtained from a carrying task.

BACKGROUND

Quantifying joint stability, particularly that of the spine, involves the interpretation of stiffness enhancing the ability to survive a perturbation. Some investigations using this potential energy based approach evaluate the EVs derived from the segmental stiffness and potential energy of the column and joints. Thus, stability was defined as the ability of the spinal column to withstand perturbation while resisting buckling behavior. Joint stiffness is recognized as universally enhancing stability and is the second derivative of potential energy. EVs, when positive, indicate a sufficiently stiff state to prevent unstable behavior in the elastic spinal column. The number of EVs corresponds to the degrees of freedom (in this study, the number of spinal levels, multiplied by the three rotational orthopedic axes of each joint – i.e. six lumbar levels by three axes of flexion/extension, lateral bend and twist renders 18 EVs). Beyond indicating whether a stable state is present or not, this study attempted to probe the EVs for any additional information content, including whether specific muscles are better reflected in specific EVs. If this is true, then the value of the EVs for a given patient could provide clues when choosing optimal muscle based interventions.

Anders Bergmark (1989) pioneered the potential energy approach to assess spine stability with joint stiffness and 40 muscle stiffness coefficients to calculate energy minima from total joint stiffness. Bergmark simplified the potential energy approach conceptually by using the analogy of a ball rolling on a surface. The ball seeks a state of minimum potential energy by rolling and eventually coming to rest in the bottom of a local “bowl.” The steeper the sides of the bowl, the greater the external perturbation is required to influence the ball out of the bowl and therefore, it is more stable. The system is potentially unstable if the perturbation is large enough to cause the ball to roll out of the bowl and into the next “energy well”

or local bowl. In the case of the spinal system, the slope of the bowl sides represents the joint and muscle stiffness, which offers resistance to the applied force. The width of the flatter region at the bottom of the bowl represents joint laxity (McGill, 2007).

While the previous example illustrates the relationships between the potential energy state of a system and its stability, it needs expanding for relevance to a musculoskeletal system of joints. The potential energy of a joint system is a function of the elastic energy in the muscles, modeled as linear springs and the elastic energy in the passive tissues, modeled as torsional springs, which is challenged by the work performed by an external load or perturbation. Examples of this modeling approach include the lumbar spine models of Stokes and Gardner-Morse (Stokes & Gardner-Morse, 2001) and Cholewicki and McGill (1996). The second partial derivatives of the potential energy of the system is calculated for each joint (6 lumbar) and axis (3, flexion/extension, lateral bend and axial twist) combination and arranged into an 18x18 Hessian matrix. Global stability could be calculated as the determinant of the Hessian matrix, where the system is considered stable if the determinant is positive and unstable if the determinant is negative (Howarth, Allison, Grenier, Cholewicki, & McGill, 2004). Gardner-Morse et al. (2006) have suggested that a second way to calculate stability is to diagonalize the Hessian matrix to determine the 18 EVs, using the lowest EV as the stability index under the assumption that the spine will buckle at the point of lowest potential energy. The EVs represent the degree of curvature of the surface, from the previous bowl analogy, at each joint/axis combination. Howarth et al. (2004) suggested that examining the determinant and lowest EV methods together may provide more information than simply whether the system is stable or not.

MAIN FOCUS OF THE CHAPTER

Methods

The analysis of stability was performed using an EMG-assisted anatomically detailed spine model. A brief description of the model is provided here, with a flow chart of the steps shown in figure 1, although the interested reader may refer elsewhere for a detailed description (Cholewicki, McGill, & Norman, 1995; Cholewicki & McGill, 1994, 1996; Grenier & McGill, 2007; McGill & Norman, 1986; McGill, 1992).

This model consisted of three interdependent models: (1) a 3-dimensional linked segment model, (2) a 'lumbar spine model' and (3) a 'distribution-moment muscle model' (D-M muscle model). The lumbar spine model incorporated the 3-dimensional anatomy and segmental movement according to the subject movement. Five lumbar vertebrae were joined with non-linear elastic elements representing rotational motion between a rigid pelvis/sacrum and a rigid ribcage. Muscles and tendons were modeled with linear stiffness elements. Eleven bilateral muscle groups were divided into 59 muscle fascicles, for a total of 118 muscle fascicles. Muscle lengths and velocities from the lumbar spine model were input to the D-M muscle model together with the normalized muscle activation profiles of seven electrode sites per body side to calculate individual muscle force and stiffness profiles. They were then used to calculate the L4/L5 muscle forces and moments.

EMG was used to drive estimation of muscle force. Muscle force can be calculated using the equation

$$F_m = G[(EMG/EMG_m)^{1/1.3}(P_0)(\Omega)(\delta) + F_{pec}] \quad (1)$$

where:

F_m = Muscle force (N)

G = Gain factor, calculated through an EMG-Assisted optimization routine
 EMG = EMG amplitude
 EMG_m = MVC EMG amplitude
 P_0 = Maximum isometric force (N)
 Ω = Coefficient for velocity variation
 δ = Coefficient for length variation
 F_{pec} = Force due to the passive elastic component (McGill & Norman, 1986).

Muscle force was then used to estimate muscle stiffness using the equation

$$k_m = (q)(F_m/L_m) \quad (2)$$

where:

k_m = Muscle stiffness (N/m)
 q = Coefficient fitting the relationship between muscle force and stiffness
 F_m = Muscle force (N)
 L_m = Muscle length (m)
 (Brown & McGill, 2005).

The muscle force and muscle stiffness profiles were then used to calculate the potential energy of the muscles, which was in turn used to calculate the stability/stiffness of the spine.

The stability/stiffness of the spine was measured via the EVs at each of the six lumbar joints and three rotational axes, resulting in 18 EVs. The potential energy of the linear springs, or muscles (U_L), was calculated from the individual muscle force, stiffness and length profiles, while the potential energy of the torsional springs, or passive tissues (U_T), was calculated from the lumbar spine geometry and kinematics as the spine deviated from neutral elastic equilibrium. These potential energies were compared to the work (W) performed from a “perturbation” ($V = U_L + U_T - W$), where negative values indicated insufficient stiffness to reveal unstable behaviour. The second partial derivatives of V were arranged into an 18 x 18 Hessian matrix that was symmetrical about the main diagonal. The Hessian matrix was then

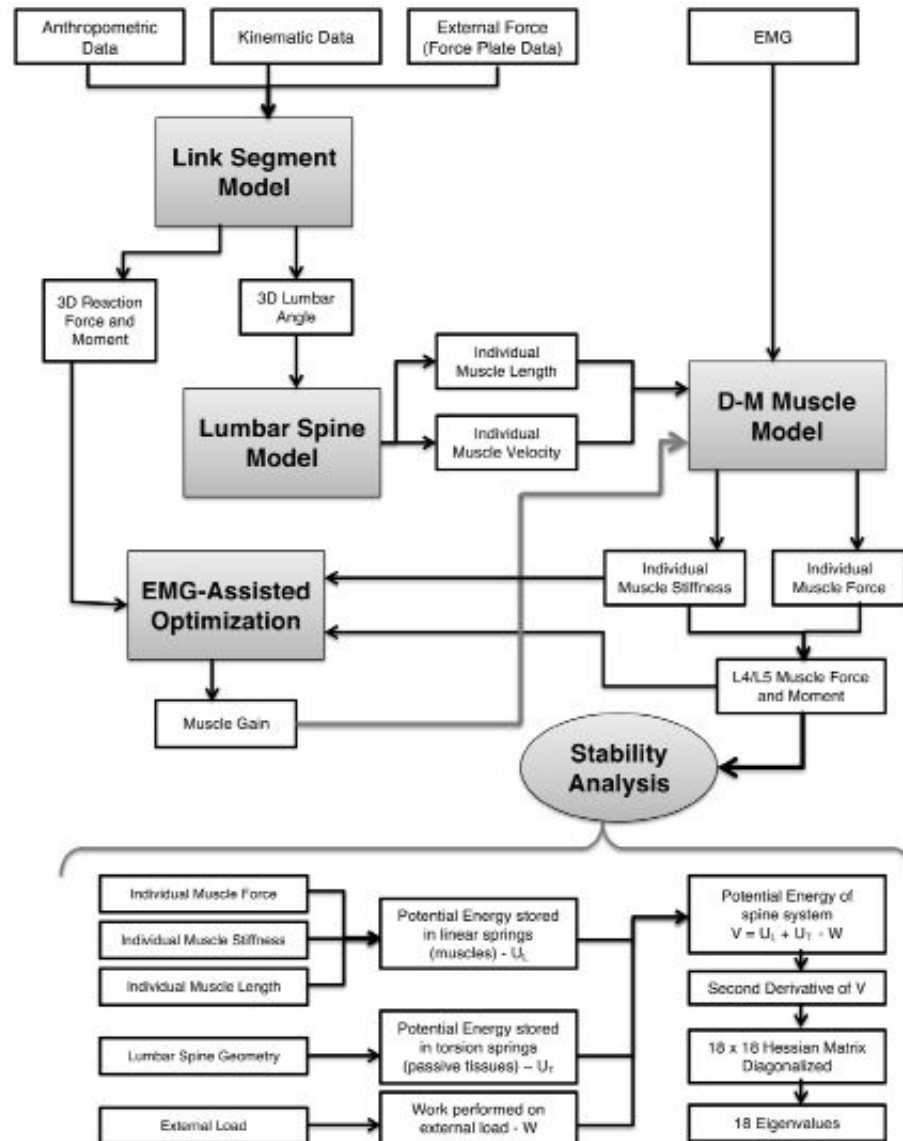
diagonalized to determine the associated 18 EVs. Further mathematical detail on the EV calculation can be found in Howarth et al. (2004). The three EVs (flexion/extension, lateral bend and axial twist) at the L4 lumbar level were used to represent the stability/stiffness of the system for this study, given that the greatest anatomical robustness was represented at this level. Typically in stability analysis, the smallest EV would indicate the first-to-occur buckling mode and thus have the greatest influence on overall stability. However, the focus here was to see if specific muscles affect specific EVs, which if true, may assist clinical efforts.

To assess possible influence of individual muscles on EVs, the first stage of “sensitivity testing” was conducted using a muscle knockout approach. Muscle activity of all muscles was set to 50% MVC. One at a time, the muscles were systematically knocked out to 0% MVC. This was repeated for each lumbar spine posture that altered one spine angle axis in iterations of 10° each. Iterations about the flexion axis ranged from -30° to 50°, about the lateral bend axis from -30° to 30° and about the axial twist axis from -40° to 40°, for a total of 23 postures. These angles were chosen to represent the approximate reasonable lumbar spine range of motion. Using this approach, twelve special cases were tested, including all muscles active, followed by the removal of bilateral rectus abdominis (RA), external oblique (EO), internal oblique (IO), pars lumborum (Pars), iliocostalis lumborum (Ilio), longissimus (Long), quadratus lumborum (QL), latissimus dorsi (LD), multifidus (Mult), psoas major (Psoas) and transverse abdominis (TrA). Finally, these twelve special cases were repeated, except the muscle was artificially activated to 100% MVC.

The EVs were calculated for each trial and the percent difference from the initial condition was calculated. To evaluate the effect of muscle, the initial condition was when all muscles were active to 50% MVC, while the neutral posture was the base initial condition to evaluate the effect of

Assessing Joint Stability from Eigenvalues Obtained from Multi-Channel EMG

Figure 1. Flow chart of the anatomically detailed spine model and steps required leading up to the stability analysis and the output of EVs. Abbreviations: D-M: Distribution-Moment



posture. A difference of 10% or greater in the EV was considered to be the biologically significant threshold.

The second stage replaced the synthesized activation and lumbar spine posture with actual data collected from individuals performing a load-carrying task. The subjects were asked to walk while carrying a bucket with 15 kg in each

hand. A linked segment model utilized foot contact forces obtained from a force plate and 3D kinematic data obtained with a VICON motion capture system (Vicon Motion systems, Oxford, UK) to determine 3D lumbar spine angles and L4/L5 joint forces and moments, as described by Ikeda and McGill (2012).

Surface electromyography (EMG) was recorded using Ag-Ag/Cl (Covidien Meditrace, Mansfield, USA) self-adhesive surface electrode pairs, spaced approximately 25 mm apart in a bipolar configuration. Twelve bilateral muscle locations were: rectus abdominis (RA), internal oblique (IO), external oblique (EO), latissimus dorsi (LD), upper erector spinae (UES) and lower erector spine (LES), after Grenier and McGill (2007). EMG signals were amplified using a Bortec amplifier (Bortec Biomedical, Calgary, Canada) and A/D converted using a 16-bit, 64-channel A/D converter at a sample rate of 2160 Hz. Two resting trials were conducted, one prone and one supine, followed by a MVC for each muscle to normalize the amplitude. For the abdominal muscles (RA, EO and IO), each participant adopted a sit up posture at approximately 45 degrees of hip flexion and was manually braced by a research assistant. The participant was instructed to produce a maximal isometric flexor moment followed sequentially by a right and left lateral bend moment and a right and left twist moment. For the spine extensors (LES and UES) and LD muscles, a resisted maximum extension in the Biering-Sorensen position was performed for normalization (Biering-Sørensen, 1984). The LD muscles were cued by instructing the participants to pull their shoulder blades back and down during extension. These contractions were performed according to established lab protocol (Grenier & McGill, 2007).

EMG was bandpass filtered from 30-500 Hz, full-wave rectified and low-pass filtered with a single-pass second order Butterworth filter at a cut-off frequency of 2.5 Hz to mimic the frequency response of torso muscle and enable muscle force prediction (Brereton & McGill, 1998). The zero bias from the resting trial was removed from all trials to account for bias. Finally, all trials were normalized to the maximum EMG amplitudes obtained during the MVC procedure and the signals were down sampled to 60 Hz to allow for syncing of the EMG and kinematic data. This was completed using custom LabView software

(National Instruments Corporation, Austin, TX, USA).

Results

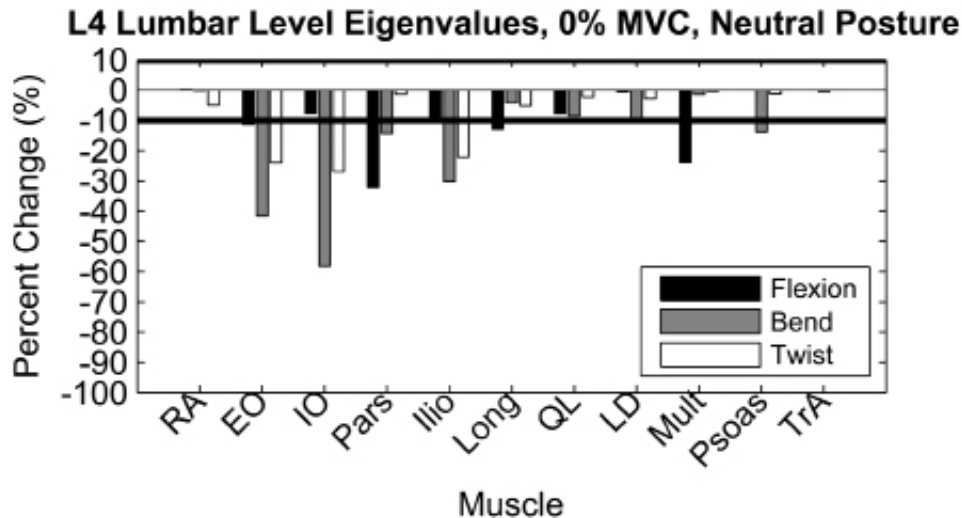
Altering muscle activation bilaterally resulted in the same effect on EVs in the right and left bend postures as well as the right and left twist postures. In other words, symmetric muscle intervention resulted in symmetric EV change. For this reason, only the degree of bend and twist, not the direction, was examined. The TrA muscle was also found to never result in a biologically significant change, therefore it was not discussed here. Also notable is the fact that the greatest anatomical detail is at the L4/L5 level such that results at this level are probably the most robust.

Hypothesis 1: Effect of Muscles on Eigenvalues and Hypothesis 2: Effect of Specific Muscles on Plane of Stability/Stiffness

Although posture had interactions with muscles in their effect on EVs, it was clear that single muscles did affect multiple levels of spine stability/stiffness and stability/stiffness at one segmental level was affected by multiple muscles. For the L1F EV, the Mult muscle had the largest effect followed by the Pars, Ilio and Long muscles in their contribution. On average across all postures, when removed, the Mult muscle resulted in a $67.3\% \pm 6.5\%$ (mean \pm SD) change, the Pars muscle resulted in a $53.2\% \pm 8.5\%$ change, the Ilio muscle resulted in a $31.7\% \pm 6.8\%$ change and the Long muscle resulted in a $24.0\% \pm 6.2\%$ change for the L1F EV. Similar results were found for the L1B and L1T EVs. The Mult, Pars, Ilio, Long and Psoas muscles were also the only muscles that affected the L2 level EVs. The Pars muscle was the only muscle that resulted in a biologically significant change for all postures for the L3F EV. The Mult, Ilio and IO muscles also resulted in biologically significant changes for most postures. For the

Assessing Joint Stability from Eigenvalues Obtained from Multi-Channel EMG

Figure 2. Percent change in the L4 level EVs when reducing single muscle activation to 0% MVC while all other muscles remained active to 50% MVC for the neutral posture. Negative change represents a lower EV when a single muscle's activity was reduced to 0% MVC. The thick black line highlights the point where changes were considered biologically significant (10% change). Abbreviations: RA: rectus abdominis; EO: external oblique; IO: internal oblique; Pars: pars lumborum; Ilio: iliocostalis lumborum; Long: longissimus; QL: quadratus lumborum; LD: latissimus dorsi; Mult: multifidus; TrA: transverse abdominis

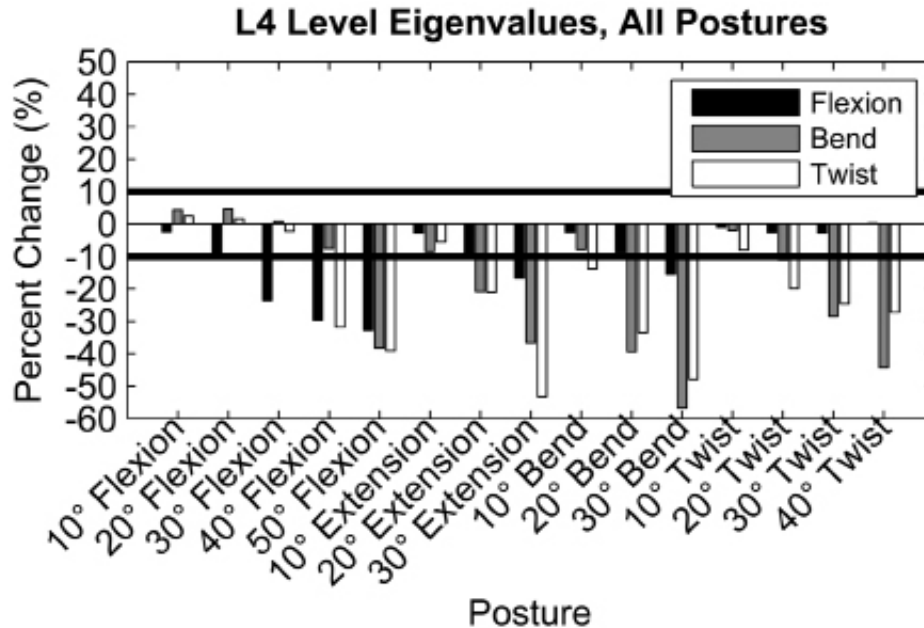


L3B EV, when averaged across all postures, the Mult muscle resulted in an $11.5\% \pm 6.1\%$ change in the L3B EV, while the Ilio muscle always had less than a 15% change in the EV. For the L3T EV, when averaged across all postures, the Pars muscle resulted in a $29.7\% \pm 6.3\%$ change, while the Ilio muscle resulted in a $26.0\% \pm 5.6\%$ change in the L3T EV. The Mult and QL muscles also caused biologically significant changes for most postures, with changes of $17.6\% \pm 7.7\%$ and $13.9\% \pm 4.2\%$ in the L3T EV, respectively, when averaged across all postures (average absolute values in table 3 for all EVs).

The Pars muscle was the only muscle that resulted in a biologically significant change for all postures when examining the L4F EV with a change in the EV of $30.9\% \pm 5.0\%$ when averaged across all postures. The Mult and Long muscles were also biologically significant for most postures. When averaged across all postures, the

Mult muscle had a change of $17.1\% \pm 6.9\%$ and the Long muscle had a change of $12.9\% \pm 2.4\%$ in the L4F EV. The IO and EO muscles became the most influential muscles for the L4B EV, while the Mult muscle no longer had a biologically significant effect. When averaged across all postures, the EO muscle resulted in a $38.8\% \pm 10.6\%$ change, while the IO muscle resulted in a $40.3\% \pm 18.4\%$ change in the L4B EV. The Ilio muscle caused a biologically significant effect for most postures, resulting in a $20.3\% \pm 10.2\%$ change in the L4B EV when averaged across all postures. For the L4T EV, the muscle that had the largest biological significant effect varied between the EO, IO and Ilio muscles. For the L5F EV, the IO, Ilio, Pars and Long muscles all caused biological significance for the majority of postures. When averaged across all postures, the Ilio muscle had a $28.2\% \pm 11.2\%$ change, the IO muscle caused a $20.8\% \pm 7.0\%$ change, the

Figure 3. Percent change in the L4 level EVs when comparing various postures to the neutral posture when all muscles were active to 50% MVC. Negative change represents a lower EV in the measured posture. The thick black line highlights the point where changes were considered biologically significant (10% change)



Long muscle had a $16.6\% \pm 7.7\%$ change and the Pars muscle resulted in a $14.6\% \pm 6.0\%$ change. The EO and RA muscles were the only other muscles that resulted in a biologically significant change. For the L5B EV, when averaged across all postures, the IO muscle resulted in a $30.2\% \pm 14.1\%$ change, the RA muscle resulted in a $21.8\% \pm 9.2\%$ change and the EO muscle caused a $13.8\% \pm 6.7\%$ change. It was also noted for the L5B EV that the Mult muscle resulted in a $1.4\% \pm 0.9\%$ change when averaged across all postures. Finally, for the L5T EV, the abdominal muscles caused the greatest influence on the EV, but the LD muscle had a small influence resulting in less than a 13% change in the EV for the neutral and extension postures. The effect of the RA muscle was also small, with a change in the L5T EV of less than 15%. The EO muscle resulted in a biologically significant change for all postures, with an average of a $23.9\% \pm 10.3\%$ change in the

EV. The IO muscle resulted in a $26.4\% \pm 9.4\%$ change when averaged across all postures. It was also noted for the L5T EV that the Mult muscle resulted in a $0.2\% \pm 0.2\%$ change when averaged across all postures (average absolute values in Table 3 for all EVs).

In summary, the erector spinae muscles influenced the upper lumbar level EVs (L1, L2 and L3 levels), more than the abdominal muscles, while the opposite occurred for the lower lumbar level EVs (L4 and L5 levels), than the erector spinae muscles. In addition, single muscles did affect multiple levels of spine stability/stiffness and stability/stiffness at one segmental level was influenced by multiple muscles.

Assessing Joint Stability from Eigenvalues Obtained from Multi-Channel EMG

Table 1. EV magnitudes (J/rad²) for the neutral posture. Abbreviations: RA: rectus abdominis; EO: external oblique; IO: internal oblique; Pars: pars lumborum; Ilio: iliocostalis lumborum; Long: longissimus; QL: quadratus lumborum; LD: latissimus dorsi; Mult: multifidus; TrA: transverse abdominis; F: flexion axis; B: bend axis; T: twist axis

	L1F	L1B	L1T	L2F	L2B	L2T	L3F	L3B	L3T	L4F	L4B	L4T	L5F	L5B	L5T
All	316.4	352.2	415.7	423.3	467.9	501.7	590.7	620.5	852.2	1075.3	2611.1	3581.7	4425.8	8036.5	9064.7
RA	332.4	355.3	424.0	434.8	468.9	503.5	536.0	598.8	862.0	1076.5	2605.3	3399.9	4069.8	5660.6	8183.0
EO	335.5	352.1	414.1	436.5	466.1	497.2	530.6	579.9	840.7	953.2	1523.6	2720.6	4346.6	6732.6	7625.6
IO	339.1	351.0	410.5	425.4	433.6	467.6	511.8	597.5	819.4	992.8	1091.9	2616.7	3562.8	4447.8	7349.0
Pars	136.0	263.8	307.0	344.4	346.0	409.0	442.3	470.2	626.2	729.8	2236.3	3529.6	3651.5	7971.2	9059.4
Ilio	200.1	244.5	308.0	320.2	385.0	419.9	466.9	605.7	618.9	980.9	1822.4	2786.0	3405.5	8043.7	8642.9
Long	232.4	306.4	312.8	372.4	380.7	430.4	555.3	604.9	786.4	937.8	2499.4	3396.3	3492.8	7988.0	8986.9
QL	289.3	348.5	388.2	415.4	450.6	473.5	572.7	605.5	719.9	991.9	2389.9	3498.2	4370.6	7912.2	8525.1
LD	327.6	353.2	413.5	423.8	466.2	495.2	574.5	624.6	830.8	1069.1	2358.4	3478.9	4385.5	7876.8	8142.3
Mult	87.3	204.7	343.0	388.4	413.1	441.6	460.4	573.0	748.5	818.5	2572.7	3569.5	4139.6	7948.1	9064.0
Psoas	301.2	318.4	372.3	415.5	435.9	449.8	531.7	609.6	758.8	1075.2	2249.7	3536.2	4426.6	8036.5	9060.5
TrA	316.3	348.3	415.5	420.2	463.4	498.4	587.9	620.1	845.5	1075.0	2600.3	3579.8	4425.3	8036.4	9064.6

Hypothesis 2: Effect of Specific Muscles on Plane of Stability/Stiffness

Muscles do appear to be related to specific planes of stability/stiffness. The L4 lumbar level will be discussed in detail because the L4 lumbar level contains the most anatomical robustness. In the neutral posture, the influence of muscles on the L4 lumbar level EVs depended on the axis of rotation (Figure 2). The Pars, Mult, Long and EO muscles had a biologically significant effect on the L4 flexion axis EV (L4F), with the Pars muscle having the largest influence (decreasing 32.1% when Pars was removed - see absolute values in Table 1). The IO and EO muscles had the greatest influence on the lateral bend axis EV (L4B) (decreased 58.2% when IO was removed, while the EV decreased 41.6% when EO was removed - see absolute values in Table 1), followed by the Ilio, Pars and Psoas muscles (Figure 2). The IO, EO and Ilio muscles had a biologically significant effect for the twist EV (L4T) (decreased 26.9% when IO was removed, decreased 24.0% when EO

was removed and decreased 22.2% when Ilio was removed - see absolute values in Table 1). At the upper lumbar levels (L1 to L3), the erector spinae and Mult muscles had the greatest influence on the EVs, while the abdominal muscles did not have a biologically significant effect (absolute values in Table 1). Similar trends were seen in all other postures.

In summary, the major findings regarding the plane of stability at the L4 lumbar level were that muscles preferentially influence different planes of stability/stiffness, assuming that a 10% change in the EV indicated biological significance. With most postures, the erector spinae and Mult muscles most influenced the flexion axis, while the abdominal muscles had the greatest influence on the bend axis and occasionally the twist axis.

Hypothesis 3: Effect of Posture on Eigenvalues

When determining if EVs were affected by posture, all postures were compared to the neutral posture

for the condition where all muscles were active to 50% MVC. Similar to the previous comparisons, a change of 10% or greater between the neutral posture and posture of interest was considered biologically significant. A negative change indicated that the EV for the posture being examined was smaller than that of the neutral posture and vice versa.

Postures that were close to neutral rarely resulted in a biologically significant change in the EVs. Sensitivity testing revealed that large posture changes were required to produce biological significance (Figure 3). For example, the largest EV changes were seen in the 50° flexion posture for the L4F EV (32.8% from 1080.6 J/rad² to 726.5 J/rad²), the 30° bend posture for the L4B EV (56.8% from 2628.7 J/rad² to 1134.3 J/rad²) and the 30° extension posture for the L4T EV (53.3% from 3596.5 J/rad² to 1680.1 J/rad²). Similar results were found with all other EVs.

In summary, postures close to neutral resulted in little change in the EVs. The postures further from neutral resulted in decreased EVs, indicating less stability/stiffness. The lowest EVs were found in the 30° extension, 50° flexion and 30° bend postures.

Hypothesis 4: Effect of 100% Muscle Activation on Eigenvalues

Boosting muscle activity from 50% MVC to 100% MVC, in most cases, had little effect on the EVs. In the neutral posture, the IO muscle with the twist EV at the L4 lumbar level was the only muscle to meet the criterion for biological significance (Figure 4), illustrating the influence of the non-linearity of the activation-stiffness relationship.

Hypothesis 5: Effect of Actual Data on EVs

The carrying task resulted in low levels of muscle activation (< 13% MVC), with average lumbar spine angles of 7.1° ± 1.9° flexion, 4.0° ± 2.2°

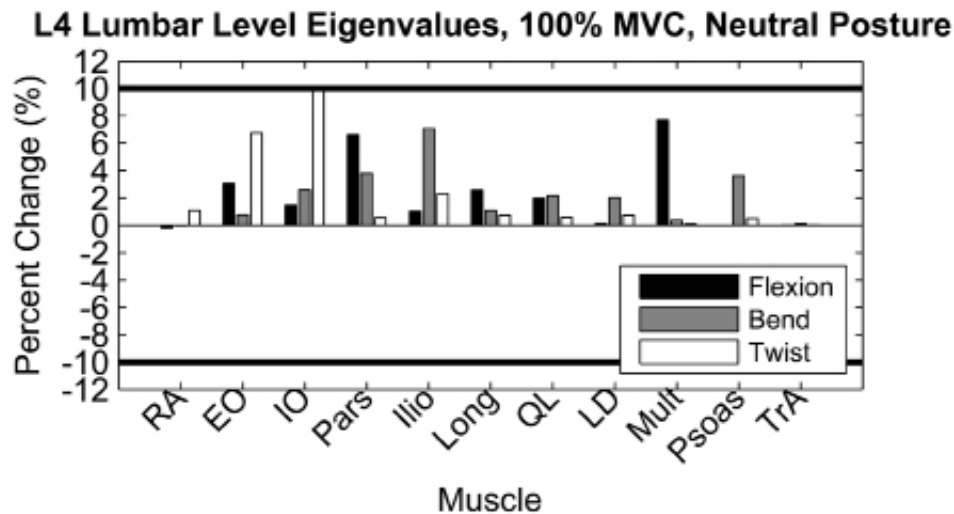
left bend and 4.0° ± 2.9° right twist, therefore comparisons were made between the 10° flexion posture in simulation and the actual data. There were few biologically and statistically significant changes when comparing the 0% MVC condition to the actual EMG condition. However, when comparing the 100% MVC condition to the actual EMG condition, the erector spinae and Mult muscles influenced most EVs, while the abdominal muscles only influenced the L4 and L5 level EVs. In most situations, the single muscles affected all planes of stability/stiffness, but the abdominal and Ilio muscles typically had a larger influence on the bend and twist axes than the flexion axis, while the erector spinae and Mult muscles typically had a greater influence on the flexion axis EVs. These results were similar to the results found using simulated muscle activity.

Discussion

The main objective of this study was to evaluate the EVs for information content. They appear to be more sensitive to muscle activation changes of lower %MVC than higher, which is consistent with the previously documented non-linear activation/stiffness relationship described about the ankle joint (Hoffer & Andreassen, 1981) and the spine (Brown & McGill, 2005). Is the knowledge of an EV helpful for those working to modulate stability in a patient? The answer is a qualified yes. The first hypothesis, that specific muscles are linked with specific EVs, has qualified support in that the erector spinae muscles (especially the shorter Mult whose stiffness is highly sensitive to length change given its short length) affect the L1, L2 and L3 level EVs, while the abdominal muscles were the most important at the L4 and L5 lumbar level. It was also important to note that the TrA muscle never resulted in a biologically significant change, and in the L4B, L4T and L5 level EVs, the Mult muscle did not cause a biologically significant change. These broad results support the idea that activating all torso muscles via an abdominal

Assessing Joint Stability from Eigenvalues Obtained from Multi-Channel EMG

Figure 4. Percent change in the L4 level EVs when increasing single muscle activation to 100% MVC while all other muscles remained active to 50% MVC for the neutral posture. Positive change represents a higher EV when a single muscle's activity was increased to 100% MVC. The thick black line highlights the point where changes were considered biologically significant (10% change). Abbreviations: RA: rectus abdominis; EO: external oblique; IO: internal oblique; Pars: pars lumborum; Ilio: iliocostalis lumborum; Long: longissimus; QL: quadratus lumborum; LD: latissimus dorsi; Mult: multifidus; TrA: transverse abdominis



brace (a clinical term to describe activation of the abdominal muscles that are consciously contracted to various levels to reduce pain) has a broad influence on spine stability/stiffness. The brace activates the obliques and the erectors. This is in contrast with some clinical objectives to activate individual muscles, such as the TrA muscle, via the abdominal hollowing method. Richardson et al. (1992) suggested this as a clinical corrective exercise focusing on TrA, in an attempt to influence spine stability. Note that the TrA did not directly influence any EV, which is consistent with the findings of the quantitative stability analysis of Stokes et al. (2011), although it is linked with the generation of intra-abdominal pressure, which adds stiffness to the spine in a global sense. Thus it appears that clinicians are not offered any insight into specific muscle targets for intervention based on knowledge of the individual EVs, except that if an individual has LBP associated with instability in the lumbar spine, they will most likely benefit

more from strengthening the torso muscles than focusing on strengthening the TrA and Mult muscles alone. These results agree with the results found by Grenier and McGill (2007) and Stanton and Kawchuk (2008).

The notion of the existence of “global” and “local” stability, which is popular among some clinical groups who do not quantify stability, is an interesting discussion topic. Quantifying stability via the EVs points out the concept that overall stability is influenced by the lowest EV. Thus addressing the location of the joint and mode most likely to experience unstable behavior would be the only way to enhance overall stability. Short muscles could do this acting to influence a single joint – these would be considered local stabilizers. Re-analysis would reveal the next lowest EV. Perhaps a larger muscle would have addressed both EVs. Thus the interaction of muscles clouds the practice of discussing stability in local and global terms.

Consistent with anatomical intuition, sagittal muscles influenced the flexion EV while lateral muscles influenced the lateral bend and twist EVs, supporting the second hypothesis. Posture was found to have a biologically significant effect on the EVs when compared to neutral, supporting the third hypothesis. A common approach to reduce low back pain is to reduce spine posture deviation, which enhances load tolerance in compressive and shear modes, reduces passive tissue stress and avoids the bending necessary for disc herniation (McGill, 2007). The data presented here add to this general notion as postures further from neutral resulted in larger decreases in stability/stiffness than those close to neutral, with the greatest compromise during extreme flexion, extension and bend.

It has been previously found that spine mechanics and load carrying abilities are affected by the degree of lordosis. For example, there is a smaller moment arm for the extensor muscles (Tveit, Daggfeldt, Hetland, & Thorstensson, 1994) and a decreased tolerance to compression (Gunning, Callaghan, & McGill, 2001) with a more flexed posture. In addition, flexion angles over 75% of the full range resulted in significantly higher intradiscal pressure (Adams, McNally, Chinn, & Dolan, 1994). It has also been found that in flexed postures the load is transferred from muscles to passive tissue, increasing the likelihood of a disc herniation (McGill 1997). Further, McGill, Hughson, and Parks (2000) found that flexing the lumbar spine reduces the cosine of the Long and Ilio muscles, which diminishes the ability of these muscles to resist the anterior shear forces introduced during flexion. This implies that there would be a larger shear load when in flexed postures than neutral postures.

Extension of the lumbar spine also causes changes in spine mechanics. First, extended postures cause an articulation of the spinous processes that result in transmission of high compressive forces (Adams, Dolan, & Hutton, 1988). Further,

due to the load-bearing apophyseal joints in extension, damage could occur at compressive loads as low as 500 N (Adams et al., 1994). These authors also found that the distribution of compressive stress is shifted from a peak in the anterior annulus during neutral postures to a large peak in the posterior annulus. In addition, there is a 40% decrease in nucleus pressure when in extension than in neutral postures (Adams et al., 1994). It has also been found that degenerated discs in extension usually showed an increase in compressive stress in the posterior annulus, but occasionally decreased the compressive stress (Adams, May, Freeman, Morrison, & Dolan, 2000). Further, extended discs show a decrease in foramen area increasing the likelihood of nerve root compression (Inufusa et al. 1996), which is one source of pain in individuals with LBP. This implies that extended postures may be detrimental for most individuals, but beneficial for others.

Extremes of muscle activation form an interesting situation. Increasing the muscle activation of single muscles from 50% MVC to 100% MVC did not have a major effect on most EVs, but when there was an effect, there was an increase in the EV, thus hypothesis 4 was refuted. Brown and McGill (2005) found that the contribution to stability of an individual muscle peaks at a critical force level, after which it may even be detrimental to stability. Here, force runs ahead of concomitant stiffness, actually causing a buckled spine. Fortunately, this behavior was not observed in the “live” portion of this study. Simulating increased activation from 50% MVC to 100% MVC may have been over this critical force level for most muscles. However, force was not evaluated here, thus no comment on risk could be made.

The results from the actual data and simulated data in the 10° flexion posture were similar, supporting hypothesis 5. Due to the low levels of muscle activation with the actual data set, it is not surprising that reducing the muscle activity to 0% MVC did not have a biologically significant

effect on most EVs. When there was a biologically significant change between actual EMG and 0% MVC, it was most often seen in the L4 and L5 EVs, indicating that these EVs are most sensitive, as would be expected given the anatomical robustness of the model at the L4 and L5 lumbar levels. The results also imply that activating all muscles to 50% MVC does not have a large influence on the interpretation of which EVs and muscles are linked. Although this study only tested one posture with actual EMG, it is not anticipated that there would be a large difference between the theoretical and actual data sets in different postures.

Limitations

There are a number of limitations for interpreting the data of this study. The choice of a 10% change in the EV as the criterion value for biological significance, although arbitrary, had several implications. Modulating muscle activity from a clinical perspective during daily activity is imprecise. However, changes smaller than 10% are probably difficult for an individual to perceive. Further, 10% appeared to be a natural cut-off point when reviewing the data. Thus, one could argue that the choice of change could be 8% or 15%, but the overall conclusions would be unaffected. Even so, as the 18 EVs are nonlinear, any single criterion would be influenced by their magnitude. A larger EV indicates a higher stable state, but not “how much” higher. Furthermore, changing activation levels of a single muscle would upset static moment equilibrium. Since the exercise conducted here was to assess single muscles on their role to influence EVs, this could not have been done had other muscle activation values been altered to achieve moment equilibrium.

Summary

This study provides evidence that increasing the activation of the abdominal wall and ensuring a more neutral spine posture results in an increase

in stiffness and by default stability. Thus, EVs appear to give insight into variables that influence stability/stiffness. However, the analysis conducted here of altering individual muscle activation levels suggests that the magnitude of individual EVs do not indicate the “amount” of change in stability/stiffness, nor does it appear that specific EVs reveal unique information about specific muscles. Thus, this approach does not appear to have potential to assist clinical decisions regarding muscle activation patterns to address specific modes of spine instability.

FUTURE RESEARCH DIRECTIONS

Future directions could involve further investigation into the information content of the individual EVs. In addition, it is important to determine if specific muscles have an effect on other aspects of spinal stability. For example, it was found that the TrA muscle does not affect any individual EV, but if it has a large effect on intra-abdominal pressure, the global stability may be affected. Therefore, it would also be beneficial to research the effect of individual muscles on global spine stability.

This EMG-assisted model of the spine only takes into account the torso muscles. However, clinical observations have shown that hip motion and muscle activity appears to be related to the spine. Further development of the model to include the interaction between the lumbar spine and hip would enhance the understanding of spine forces, moments and stability and the relationship between the hip and spine. In a more generic sense, the role of EVs throughout a multi-articular linkage may prove to render more information.

CONCLUSION

The approach of assessing joint stability with EVs does not appear to have potential to assist clinical decisions regarding muscle activation

patterns, at least with the spine example tested here. In terms of adding insight into spine muscle function, the approach did provide insight into the role of shorter muscles. In clinical terms for a spine specific context, the broad results support the idea that activating all torso muscles via an abdominal brace influences stability/stiffness. Thus, the EMG signal, appropriately processed to render EVs, appears to be useful in providing global insight into joint stability analysis.

REFERENCES

- Adams, M. A., Dolan, P., & Hutton, W. C. (1988). The lumbar spine in backward bending. *Spine*, *13*(9), 1019–1026. doi:10.1097/00007632-198809000-00009 PMID:3206295
- Adams, M. A., May, S., Freeman, B. J., Morrison, H. P., & Dolan, P. (2000). Effects of backward bending on lumbar intervertebral discs. Relevance to physical therapy treatments for low back pain. *Spine*, *25*(4), 431–437. doi:10.1097/00007632-200002150-00007 PMID:10707387
- Adams, M. A., McNally, D. S., Chinn, H., & Dolan, P. (1994). Posture and the compressive strength of the lumbar spine. *Clinical Biomechanics (Bristol, Avon)*, *9*(1), 5–14. doi:10.1016/0268-0033(94)90052-3 PMID:23916072
- Bergmark, A. (1989). Stability of the lumbar spine. A study in mechanical engineering. *Acta Orthopaedica Scandinavica. Supplementum*, *230*, 1–54. doi:10.3109/17453678909154177 PMID:2658468
- Biering-Sørensen, F. (1984). Physical measurements as risk indicators for low-back trouble over a one-year period. *Spine*, *9*(2), 106–119. PMID:6233709
- Brereton, L. C., & McGill, S. M. (1998). Frequency response of spine extensors during rapid isometric contractions: effects of muscle length and tension. *Journal of Electromyography and Kinesiology*, *8*(4), 227–232. doi:10.1016/S1050-6411(98)00009-1 PMID:9779396
- Brown, S. H. M., & McGill, S. M. (2005). Muscle force-stiffness characteristics influence joint stability: a spine example. *Clinical Biomechanics (Bristol, Avon)*, *20*(9), 917–922. doi:10.1016/j.clinbiomech.2005.06.002 PMID:16055250
- Cholewicki, J., & McGill, S. M. (1994). EMG assisted optimization: a hybrid approach for estimating muscle forces in an indeterminate biomechanical model. *Journal of Biomechanics*, *27*(10), 1287–1289. doi:10.1016/0021-9290(94)90282-8 PMID:7962016
- Cholewicki, J., & McGill, S. M. (1996). Mechanical stability of the in vivo lumbar spine: implications for injury and chronic low back pain. *Clinical Biomechanics (Bristol, Avon)*, *11*(1), 1–15. doi:10.1016/0268-0033(95)00035-6 PMID:11415593
- Cholewicki, J., McGill, S. M., & Norman, R. W. (1995). Comparison of muscle forces and joint load from an optimization and EMG assisted lumbar spine model: towards development of a hybrid approach. *Journal of Biomechanics*, *28*(3), 321–331. doi:10.1016/0021-9290(94)00065-C PMID:7730390
- Gardner-Morse, M. G., Stokes, I. A. F., & Huston, D. R. (2006). On the implications of interpreting the stability index: a spine example. *Journal of Biomechanics*, *39*(2), 391–392, author reply 393–394. doi:10.1016/j.jbiomech.2005.08.020 PMID:16256126

- Grenier, S. G., & McGill, S. M. (2007). Quantification of lumbar stability by using 2 different abdominal activation strategies. *Archives of Physical Medicine and Rehabilitation*, 88(1), 54–62. doi:10.1016/j.apmr.2006.10.014 PMID:17207676
- Gunning, J. L., Callaghan, J. P., & McGill, S. M. (2001). Spinal posture and prior loading history modulate compressive strength and type of failure in the spine: a biomechanical study using a porcine cervical spine model. *Clinical Biomechanics (Bristol, Avon)*, 16(6), 471–480. doi:10.1016/S0268-0033(01)00032-8 PMID:11427289
- Hoffer, J. A., & Andreassen, S. (1981). Regulation of soleus muscle stiffness in premaxillary cats: intrinsic and reflex components. *Journal of Neurophysiology*, 45(2), 267–285. PMID:6780665
- Howarth, S. J., Allison, A. E., Grenier, S. G., Cholewicki, J., & McGill, S. M. (2004). On the implications of interpreting the stability index: A spine example. *Journal of Biomechanics*, 37(8), 1147–1154. doi:10.1016/j.jbiomech.2003.12.038 PMID:15212919
- Ikeda, D. M., & McGill, S. M. (2012). Can altering motions, postures, and loads provide immediate low back pain relief: A study of 4 cases investigating spine load, posture, and stability. *Spine*, 37(23), E1469–E1475. doi:10.1097/BRS.0b013e31826c97e5 PMID:22872216
- Inufusa, A., An, H. S., Lim, T. H., Hasegawa, T., Haughton, V. M., & Nowicki, B. H. (1996). Anatomic changes of the spinal canal and intervertebral foramen associated with flexion-extension movement. *Spine*, 21(21), 2412–2420. doi:10.1097/00007632-199611010-00002 PMID:8923625
- Lucas, D. B., & Bresler, B. (1961). *Stability of the ligamentous spine* (Tech report No. 40). San Francisco: Biomechanics Laboratory, University of California, CA.
- McGill, S. M. (1992). A myoelectrically based dynamic three-dimensional model to predict loads on lumbar spine tissues during lateral bending. *Journal of Biomechanics*, 25(4), 395–414. doi:10.1016/0021-9290(92)90259-4 PMID:1533860
- McGill, S. M. (1997). The biomechanics of low back injury: Implications on current practice in industry and the clinic. *Journal of Biomechanics*, 30(5), 465–475. doi:10.1016/S0021-9290(96)00172-8 PMID:9109558
- McGill, S. M. (2007). *Low back disorders: Evidence-based prevention and rehabilitation*. Champaign, IL: Human Kinetics.
- McGill, S. M., Hughson, R. L., & Parks, K. (2000). Changes in lumbar lordosis modify the role of the extensor muscles. *Clinical Biomechanics (Bristol, Avon)*, 15(10), 777–780. doi:10.1016/S0268-0033(00)00037-1 PMID:11050362
- McGill, S. M., & Norman, R. W. (1986). Partitioning of the L4-L5 dynamic moment into disc, ligamentous, and muscular components during lifting. *Spine*, 11(7), 666–677. doi:10.1097/00007632-198609000-00004 PMID:3787338
- Richardson, C. A., Jull, G. A., Toppenberg, R., & Comerford, M. (1992). Techniques for active lumbar stabilisation for spinal protection: A pilot study. *The Australian Journal of Physiotherapy*, 38, 105–112. doi:10.1016/S0004-9514(14)60555-9
- Stanton, T., & Kawchuk, G. (2008). The effect of abdominal stabilization contractions on posteroanterior spinal stiffness. *Spine*, 33(6), 694–701. doi:10.1097/BRS.0b013e318166e034 PMID:18344865
- Stokes, I. A. F., & Gardner-Morse, M. G. (2001). Lumbar spinal muscle activation synergies predicted by multi-criteria cost function. *Journal of Biomechanics*, 34(6), 733–740. doi:10.1016/S0021-9290(01)00034-3 PMID:11470110

Stokes, I. A. F., Gardner-Morse, M. G., & Henry, S. M. (2011). Abdominal muscle activation increases lumbar spinal stability: Analysis of contributions of different muscle groups. *Clinical Biomechanics (Bristol, Avon)*, 26, 797–803. doi:10.1016/j.clinbiomech.2011.04.006 PMID:21571410

Tveit, P., Daggfeldt, K., Hetland, S., & Thorstenson, A. (1994). Erector spinae lever arm length variations with changes in spinal curvature. *Spine*, 19(2), 199–204. doi:10.1097/00007632-199401001-00015 PMID:8153831

KEY TERMS AND DEFINITIONS

Abdominal Brace: The technique of activating all the torso muscles to create a guy wire support system for the spine.

Eigenvalue (EV): A measure of spine stability, derived from the segmental stiffness and potential energy of the spinal column and joints.

EMG-Assisted Model: A mathematical model using electromyographic activity to drive the calculation of muscle forces and therefore joint moments and loads.

Sensitivity Analysis: A technique to determine the impact of an independent variable on a dependent variable, accomplished through systematically changing the values of the independent variable.

Spine Posture: The angle between the position of the bottom of the thoracic spine and top of the lumbar spine (T12/L1) level relative to the position of the pelvis.

Stability: The ability to withstand a perturbation by returning to its pre-perturbed state.

Chapter 10

Endurance Time Prediction using Electromyography

Sébastien Boyas

Université du Maine, France

Arnaud Guével

Université de Nantes, France

ABSTRACT

The purpose of endurance time (T_{lim}) prediction is to determine the exertion time of a fatiguing muscle contraction before it occurs. T_{lim} prediction would then allow the evaluation of muscle capacities while limiting fatigue and deleterious effects associated with exhaustive exercises. Fatigue is a progressive phenomenon which manifestations can be observed since the beginning of the exercise using electromyography (EMG). Studies have reported significant relationships between T_{lim} and changes in EMG signal suggesting that T_{lim} could be predicted from early EMG changes recorded during the first half of the fatiguing contraction. However some methodological factors can influence the reliability of the relationships between T_{lim} and EMG changes. The aim of this chapter is to present the methodology used to predict T_{lim} from early changes in EMG signal and the factors that may influence its feasibility and reliability. It will also present the possible uses and benefits of the T_{lim} prediction.

INTRODUCTION

Neuromuscular fatigue is a very complex phenomenon (Boyas & Guevel, 2011b). This phenomenon is progressive (Bigland-Ritchie, 1981) and induces changes in the electromyographic (EMG) signal (De Luca, 1984). Moreover, it has been illustrated that changes in the EMG signal occur before any mechanical manifestations of muscle fatigue (Lindstrom, Kadefors, & Petersen, 1977). This

suggests that EMG changes could provide useful information about the early manifestations of neuromuscular fatigue. The endurance time (T_{lim}) can be defined as the maximal duration during which an individual can sustain the required level of force. Several studies have reported significant relationships between T_{lim} and indicators characterizing the changes in the EMG signal (e.g. Dolan, Mannion, & Adams, 1995; Hagberg, 1981; Hagberg & Kvarnstrom, 1984; Mannion & Dolan,

DOI: 10.4018/978-1-4666-6090-8.ch010

1994, 1996; van Dieen, Oude Vrielink, Housheer, Lotters, & Toussaint, 1993). However, few studies have investigated the possibility of predicting the Tlim using the early changes in the EMG signal (Bouillard, Frere, Hug, & Guevel, 2012; Boyas & Guevel, 2011a; Boyas, Maisetti, & Guevel, 2009; Dolan et al., 1995; Maisetti, Guevel, Legros, & Hogrel, 2002a; Mannion & Dolan, 1994; Merletti & Roy, 1996; van Dieen, Heijblom, & Bunkens, 1998). This may be due to the fact that some factors influence the feasibility and reliability of the Tlim prediction such as the experimental conditions (contraction intensity (Boyas & Guevel, 2011a) and/or number of muscles involved (Boyas et al., 2009)) and physiological phenomena (putative compensations between muscles (Kouzaki, Shinohara, Masani, Kanehisa, & Fukunaga, 2002) and/or non-homogenous distribution of EMG activity within a muscle (Zijdewind, Kernell, & Kukulka, 1995)). However, this domain of research is relevant due to the multiple uses and benefits it can provide to clinical and sport fields.

The objectives of this chapter are *i*) to describe the methodology used to predict the endurance time of a muscle contraction using EMG; *ii*) to present the studies that have investigated endurance prediction during isometric and dynamic conditions and discuss the factors that may influence the feasibility and reliability of the endurance time prediction; *iii*) to depict the possible benefits of the endurance time prediction. The main studies in the field of endurance time prediction are presented in table 1.

BACKGROUND

Tlim Prediction Methodology

The study of relationships between the changes in the EMG signal and the Tlim of a muscle contraction requires the continuous recording of the EMG signal emanating from the muscles involved in the fatiguing contraction, from the beginning

to the end of the contraction (Tlim). Then, EMG parameters classically used to characterize the changes in neuromuscular function, such as the Root Mean Square (RMS), the Mean Power Frequency (MPF), the Median Frequency (MF) and the frequency bands (i.e. power of the signal in a given energy band - FB) are calculated. These EMG parameters are calculated as follow:

$$RMS = \sqrt{\frac{1}{T} \int_0^T x^2(t) dt}$$

In this equation, x is the EMG signal and T the duration of the calculation window.

$$MPF = \frac{\sum_{i=1}^M f_i P_i}{\sum_{i=1}^M f_i}$$

In this equation, P is the Power Spectral Density (PSD), M the number of samples of this PSD.

$$\sum_{i=1}^{MF} P_i = \sum_{i=MF}^M P_i = \frac{1}{2} \sum_{i=1}^M P_i$$

In this equation, P is the Power Spectral Density (PSD), M the number of samples of this PSD.

What is called frequency bands (FB) in this chapter represent the relative power of the signal in a given energy band that is determined by the researcher (e.g. between 6 and 30 Hz). Consequently, it is a percentage of the total power of the signal that is 100%.

Merletti et al. (1991) have illustrated the evolution of the EMG parameters during a submaximal contraction (figure 1). The changes in these parameters during time are then characterized thank to mathematical models which provides indicators illustrating their evolution. Afterwards, relationships between the Tlim and the indicators representing the changes in EMG signal

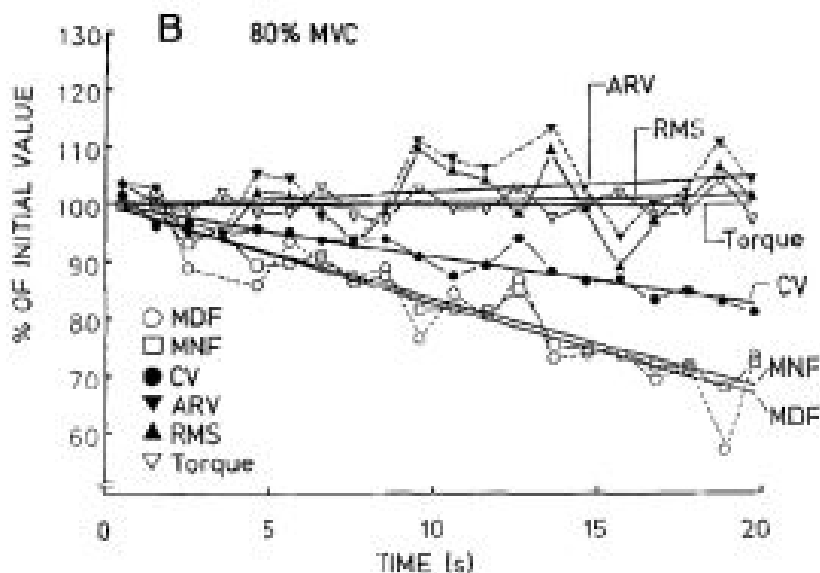
Endurance Time Prediction using Electromyography

Table 1. Studies that have investigated EMG signal-Tlim relationships and Tlim prediction

Authors	Year	Subjects number	Investigated muscles	Contraction intensity	Average Tlim	Tested EMG parameters	Indicators used	Main results
Hagberg et al.	1981	9	Forearm flexors	15 to 50% MVC	20 seconds to more than 15 minutes	RMS, MPF	Time constant and slope	EMG changes related to Tlim
Hagberg and Kvarnström	1984	10	Arm abductors (injured and sound)	Arm weight	207 s and 347 s	RMS, MPF	Time constant	EMG changes related to Tlim
Badier et al.	1993	3	Thumb adductors, leg extensors, respiratory muscles	20 to 80% MVC	15 to 36 s at 80%	FB 10-50 Hz / FB 80-400 Hz, MPF	Time constant	EMG changes related to Tlim
van Dieen et al.	1993	9	Trunk extensors	25 and 40% MVC	711 s at 25%, 463 s at 40%	RA-EMG, MPF, MDF	Time constant	EMG changes related to Tlim
Mannion and Dolan	1994	24	Trunk extensors	Body weight \approx 50% MVC	139 s	MDF	Slope	Tlim prediction possible since 50% Tlim
Dolan et al.	1995	9	Trunk extensors	60% MVC	91 s	FB 5-30 Hz, MDF	Slope	Tlim prediction possible since 50% Tlim
Mannion and Dolan	1996	10	Leg extensors	20 to 60% MVC	78 s	MDF	Slope	EMG changes related to Tlim
Merletti and Roy	1996	6	Ankle dorsiflexors	50 to 80% MVC	20-32 s at 80%, 40-55 s at 70%, 62-79 s at 60%, 84-140 s at 50%	MDF, APCV	Slope	Tlim prediction possible since 25-45% Tlim
van Dieen et al.	1998	5	Trunk extensors	25, 50 and 75% MVC	606 s at 25%, 144 s at 50%, 54 s at 75%	MPF	Slope	Tlim prediction possible since 50% Tlim
Maisetti et al.	2002	14	Leg extensors	50% MVC	78,8 s	RMS, MDF, MPF, APCV, FB 6-30 Hz	Slope and area ratio	Tlim prediction possible since 20 - 40% Tlim
Boyas et al.	2009	18	Trunk flexors, hip flexors, leg extensors, ankle flexors	50% MVC	315.4 s for hikers, 224.7 s for controls	RMS, MPF	Slope and area ratio	No correlations between EMG changes and Tlim
Boyas and Guével	2011	15	Leg extensors	20 and 50% MVC	79.6 to 316.8 s	RMS, MPF, FB 6-30 Hz	Slope and area ratio	Tlim prediction possible since 50% Tlim
Bouillard et al.	2012	30	Index abductor	35 and 50% MVC	144.6 and 63.0 s	RMS, MPF, FB 6-30 Hz, Wavelet	Slope and area ratio	Tlim prediction possible since 35% Tlim

MPF: Mean Power Frequency. FB: power in the frequency band. RA-EMG: Rectified-Average EMG. APCV: Action Potential Conduction Velocity.

Figure 1. Changes in EMG parameters with time during a sustained contraction of the tibialis anterior at 80% of maximal contraction. MVC: maximal voluntary contraction, ARV: averaged rectified value, RMS: root mean square, MNF: mean power frequency, MDF: median frequency. From Merletti et al. (Merletti, Lo Conte, & Orizio, 1991)



can be tested using linear regressions. In case of significant relationships, Tlim prediction can be evaluated from the correlations obtained between the changes in EMG signal calculated during time periods inferior to the Tlim. Three indicators have been used to characterize the changes in EMG signal parameters during time. These indicators are the time constant of the exponential model, the absolute slope of the linear regression and the area ratio index.

Time Constant of the Exponential Model

The time constant (τ) is an index characterizing the evolution speed of an EMG signal parameter:

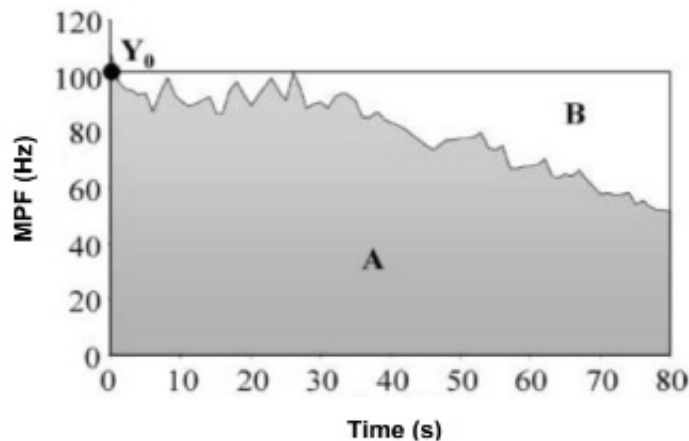
$$y = ae^{-bt} + c$$

In this equation, a is the change from initial value ($a + c$), and $b = 1/\tau$, τ is the time constant. Here, The decrement a from the initial value ($a + c$) to the asymptotic value c could describe the

overall amount of decrease of y but would provide no information about the time course or the rate of such decrease (Merletti et al., 1991). Several studies show that the changes in the EMG signal characterized by the time constant are related to the Tlim (Hagberg, 1981; Hagberg & Kvarnstrom, 1984; van Dieen et al., 1993). However, this indicator presents certain drawbacks relatively to the prediction of the Tlim (Merletti et al., 1991; Merletti & Roy, 1996). According to Merletti et al. (1991) the time constant gives intelligence on the evolution speed of a parameter, but does not give any quantitative information on the changes in the EMG parameter. More, the calculation of this index requires a time period equal or greater to the Tlim in order to characterize the changes in EMG parameter. Consequently, the time constant is not adapted to the prediction of the Tlim which objective is to estimate the Tlim from the early changes in EMG signal recorded at the beginning of the exercise in order to avoid the performance of exhaustive contractions.

Endurance Time Prediction using Electromyography

Figure 2. Illustration of the different areas considered in the calculation of the area ratio index for the MPF parameter. Here, the Y_0 value was calculated for the first two seconds of the signal. From Maisetti et al., (Maisetti, Guevel, et al., 2002a)



Slope of the Linear Regression

The linear regression is a model classically used to describe the changes in the EMG signal. The slope of this model constitutes an indicator allowing the characterization of the changes in EMG parameters:

$$y = ax + b$$

In this equation, a is the slope of the linear regression and b is the y-intercept. This indicator presents the advantage of being independent of the duration of the contraction. So, it is possible to determine the slope of the linear regression since the first seconds of the test and adjust its value as the contraction goes on. However, the validity of the linear regression as model representing the kinetic of the EMG parameters depends on the linearity of their evolution (Merletti et al., 1991). Consequently, the slope of the linear regression would not be a reliable indicator of the changes in EMG parameters if their evolutions are too different from the linear model.

Area Ratio Index

The third indicator aiming at characterizing the changes in EMG parameters is the area ratio index (figure 2). This index has been suggested by Merletti et al. (1991) after these authors described and discussed the relevance of the different regressive models.

The area ratio index is calculated as $B/(A+B)$ where A is the area beneath the EMG parameter-time relationship and $(A+B)$ is the sum of the area beneath and above the EMG parameter time course delimited by a signal reference value (Y_0). Area ratio index = $1 - A/R$, where R is the reference rectangle defined as the product of Y_0 by the total duration (figure 2). So, a decreasing pattern, as the power spectrum shifts towards a lower frequency, would result in a positive area ratio index of less than 1. For an increasing pattern, the area ratio index would be negative. This index is dimensionless and is not affected by fluctuations in the values in the experiment except for Y_0 which defines the reference area.

The advantage of the area ratio index is that this index is not regressive, meaning that it is not calculated from a predetermined model or

shape. Moreover, it can be calculated early and continuously during the contraction (Merletti et al., 1991). Finally, the area ratio index can be used to quantify a parameter during a contraction, but also as time-dependent variable illustrating the evolution of fatigue. However, the area ratio index is influenced by the value of Y_0 which is determined by the investigator. Usually, this value is the mean of the values recorded during the first two seconds of the contraction.

MAIN FOCUS OF THE CHAPTER

Possible Use and Benefits of the Tlim Prediction

The endurance time of a muscle contraction is dependent of physiological and psychological factors as motivation and pain tolerance (De Luca, 1997; Enoka & Stuart, 1992; Merletti & Roy, 1996). Then, Tlim prediction using EMG signal represents an objective methods to evaluate fatigue while limiting the influence of psychological factors (Mannion & Dolan, 1994; Merletti & Roy, 1996). Evaluation of fatigue tests are often performed in the clinical, research and sport fields. For example, it is used to characterize fatigue characteristics of patients with myopathy and to assess changes of the muscle status. In the sport field, it is used to determine athletes abilities in the performance of a specific fatiguing task that is a factor in performance such as the ability to maintain the hiking position in dinghy sailing (Maisetti, Boyas, & Guevel, 2006).

The performance of submaximal contractions while predicting the Tlim would present several advantages for the clinical and sport fields. The first interest of this method would be to limit the influence of psychological factors involved in the maintenance of a contraction sustained until exhaustion. Indeed, these psychological factors cannot be manipulated by the investigator whereas they may influence the subjects' ability to sustain

the fatigue task during time, which alters the objectivity of the fatigue evaluation (Mannion & Dolan, 1996; Merletti & Roy, 1996; van Dieen et al., 1998). The use of the Tlim prediction would then allow improving the evaluation of the capacities of the subjects to resist to fatigue. The second interest would be to reduce the time of effort and so limit the deleterious risks associated with the performance of contractions performed until exhaustion. This is very important in the clinical field during the evaluation of functional capabilities of older adults or of patients with pathologies (Agre & Sliwa, 2000; Moore & Kowalske, 2000). Indeed, monitoring disease progression and studying the effect of programs of therapy or rehabilitation require an objective and precise method allowing clinicians to evaluate muscle capacities (Bouillard et al., 2012). In the field of sport training, limiting the duration of fatigue trials would allow the evaluation of the ability to resist to fatigue while avoiding to exhaust the athletes, which could be very important in pre-competition period. It would be also useful to repeat fatigue tests, for example to determine the benefits of a training program. The Tlim prediction could also be used in the domain of the overtraining detection.

Establishment of Relationships between Changes in the EMG Signal and Tlim

The first studies in the field of endurance time prediction focused on establishing the relationships between the Tlim and the changes in the EMG signal characterized by some indicators.

The precursor was Hagberg who led several studies in the 1980s (Hagberg, 1981; Hagberg & Kvarnstrom, 1984) (table 1). This author used the time constant of the exponential model to characterize the changes in the EMG signal (Lindstrom et al., 1977; Merletti et al., 1991). Hagberg's first study (Hagberg, 1981) involved the forearm flexor muscles during isometric contractions performed between 15 and 50% of the maximal voluntary con-

Endurance Time Prediction using Electromyography

traction (MVC). Results indicate that the changes in RMS and MPF characterized by the values of the time constant were correlated to the T_{lim} of the contraction. Hence, the shorter the contraction time is, the lower the time constant and the faster the EMG parameters changes are. The same author also worked on the shoulder muscles (trapezius and supraspinatus) of patients with myofascial shoulder pain (Hagberg & Kvarnstrom, 1984). In this study, the load was the weight of the arm. Authors reported significant relationships between the T_{lim} and the time constant illustrating the MPF decrease and the RMS increase occurring during fatigue. Another interesting finding was that these relationships were not dependant of the characteristics of the tested muscles (sound or pathologic) which is encouraging for the application of this method with both healthy and non-healthy individuals.

Van Dieen et al. (1993) have also established significant relationships between T_{lim} and the time constant of some EMG parameters (e.g. MPF, MF) during isometric contractions of the trunk extensors between 25 and 40% MVC (table 1). Authors added that the reliability of these relationships depends on the consideration of the electrical activity of the most fatigable muscles involved in the contraction (i.e. those with the highest percentage of fast twitch fibers). Badier et al., (1993) focused on the fatigue of skeletal (adductor pollicis, vastus lateralis and vastus medialis) and respiratory (diaphragm and rectus abdominis) muscles during isometric contractions performed between 20 and 80% MVC. These authors used the power of the signal in two frequency bands (80-400 and 10-50 Hz) as EMG parameters. Their results indicate that the reliability of the relationships between T_{lim} and changes in EMG signal varied according to the function and so to the fatigability of the tested muscle, which is in accordance with the work of van Dieen (van Dieen et al., 1993). Finally, Mannion et al., (Mannion & Dolan, 1994) asked participants to perform isometric trunk extensions

against gravity by placing their trunk horizontally which was estimated to be equivalent to a 50% MVC contraction. Authors reported that the linear model was more appropriate than the exponential model to characterize the changes in MF. More, the logarithm of the maximal slope characterizing the changes in MF was significantly correlated to the logarithm of the T_{lim} ($r = -0.69, p < 0.001$). The maximal slope, associated with the most reliable relationships, was obtained for the most fatigable vertebral muscle.

In conclusion, we can state that the first prerequisite of T_{lim} prediction using EMG, which is that relationships exist between T_{lim} and the changes in EMG signal, is validated by the literature. Moreover, another prerequisite has been answered by the study of Maisetti et al., (2002b) which reported that the prior knowledge of the duration of a fatiguing contraction (until exhaustion vs. shorter duration) did not influence the changes in EMG signal. So, the next part will present the studies that have worked on the T_{lim} prediction, i.e. that have used the early changes in the EMG signal to estimate the T_{lim} of fatiguing contractions. It will also deal with the factors that may influence T_{lim} prediction.

Use of the Early Changes in EMG Signal to Predict T_{lim}

The findings of significant EMG signal-T_{lim} relationships enabled several authors to study the possibility of using the early changes in EMG parameters to predict the endurance time of a muscle contraction (Bouillard et al., 2012; Boyas & Guevel, 2011a; Boyas et al., 2009; Dolan et al., 1995; Maisetti, Guevel, et al., 2002a; Mannion & Dolan, 1994; Merletti & Roy, 1996; van Dieen et al., 1998).

First, Mannion and Dolan (Mannion & Dolan, 1994) worked on isometric trunk extensions. The load was determined by the weight of the upper body that subjects had to sustain until exhaustion. Authors showed that the maximal

slope of the linear regression characterizing the evolution of the MF determined over submaximal contraction duration allowed to predict the Tlim. Indeed, the logarithm of the maximal MF slope was significantly correlated to the logarithm of the Tlim when the slope was calculated over the first 60 seconds (45% Tlim) of the contraction ($r = -0.83$, $r^2 = 0.58$) or the first half (50% Tlim) of the fatigue test ($r^2 = 0.69$). The work led by van Dieen et al. (1998) on the same muscle groups also indicated that the prediction of the Tlim is possible using the changes in MPF illustrated by the slope of the linear regression and measured over the first half of the fatigue test (50% Tlim) for intensities between 25 and 75% MVC (table 1). However, in this study, the contraction intensity influenced the period of time necessary to the prediction of the Tlim. Tlim prediction was possible after 60 or 30s for the contractions performed at 50 and 75% MVC, but not when considering the contractions performed at 25% MVC, for which a longer time period was required. Moreover, the Tlim prediction was more reliable ($r > 0.85$, $r^2 > 0.72$) for the most active muscles reinforcing the importance of the most solicited/fatigable muscle in the relationships between Tlim and EMG. Always focusing on isometric trunk extensions (at 60% MVC), Dolan et al. (1995) reported that the slope of the linear regression characterizing the changes in the power of the signal present in the 5-30 Hz energy band, calculated over the first 46 s of the contraction (50% Tlim), allowed to predict Tlim ($r = 0.52$, $r^2 = 0.27$). These authors used the slope of the linear regression to characterize the changes in the frequency energy bands.

On distal muscles, Merletti and Roy (1996) showed that the slope of the changes in MF calculated over the first 30 seconds (i.e. 25 and 45% Tlim for contractions at 50 and 60% MVC, respectively) permitted to predict Tlim ($r > 0.85$, $r^2 > 0.74$) of isometric foot flexions performed until exhaustion. These authors explained that a 30 s period appears to be a good compromise between a time period too short which could

lead to estimation errors of the slope and of the Tlim, and a too long time period that would not be submaximal for high-intensity contractions. Considering isometric leg extensors, Maisetti et al. (2002a) indicated that only the early changes in the power of the 6-30 Hz energy band characterized by the area ratio index allowed a reliable prediction of the Tlim ($r = 0.82$, $r^2 = 0.67$). The prediction was then possible after contraction durations of 15 to 30 s, so approximately 20 to 40% Tlim. On the same muscles and for the same contraction mode, Boyas et al. (2011a) indicated that Tlim can be predicted ($r = 0.83$, $r^2 = 0.69$) using the EMG changes in the FB 6-30Hz characterized by the area ratio and monitored over a period of time shorter than 50% Tlim (table 1). These relationships are illustrated in figure 3. They also found greater relationships with the muscle for which EMG parameters evolved the most. These authors revealed that the associated error in Tlim prediction was $14.7 \pm 8.1\%$ of Tlim, i.e. 11.7 ± 8.4 s for a mean Tlim of 79.6 ± 28.4 s. More recently, Bouillard et al. (2012), using the area ratio and the slope of the linear regression reported significant relationships between Tlim and the early changes in the MPF of the EMG signal during isometric contractions of the first dorsal interosseous. These authors found greater coefficients of determination at 50% MVC ($r^2 = 0.56$) than at 35% MVC ($r^2 = 0.22$) using the early changes in EMG signal monitored for duration equal or lower than 50% Tlim. The error associated with the Tlim prediction was $36.2 \pm 38.0\%$ of Tlim (42.4 ± 34.4 s) for the 35% MVC task and $21.6 \pm 15.0\%$ of Tlim (12.6 ± 9.2 s) for the 50% MVC task compared with the real Tlim duration.

To our knowledge, only one study investigated Tlim prediction using EMG signal during a multi-joint task (Boyas et al., 2009). However, this study indicated that Tlim prediction was not possible in these specific conditions. This is probably due to the fact that the studied task involved numerous muscles crossing several joints which may lead to some variability in the contribution of synergist

Endurance Time Prediction using Electromyography

muscles impairing the Tlim prediction based on a single-muscle method.

All the aforementioned studies involved isometric contractions. To our knowledge, only three studies focused on the EMG signal-Tlim relationships during dynamic contractions (Hagberg, 1981; Kankaanpaa, Taimela, Webber, Airaksinen, & Hanninen, 1997; Maisetti, 2002). First, Hagberg (1981) reported significant relationships between the Tlim and the changes in RMS and MPF characterized by the time constant during isoinertial contractions of arm flexors. However, this author did not fully exploit these results to test the Tlim prediction. Considering trunk extensions, Kankaanpaa et al. (1997) indicated that the MPF and MF normalized slopes from paraspinal muscles were related to the Tlim. The slopes of these parameters calculated over submaximal durations (60 and 90 s) were significantly correlated to the Tlim ($0.62 < r < 0.89$ for the MPF, and $0.63 < r < 0.86$ for the MF). However, authors did not mention the Tlim of the contraction, and so we cannot determine which percentage of the Tlim was associated with the submaximal calculation periods (60 and 90 s). Maisetti (2002) studied the fatigue of the leg extensors during repeated isokinetic contractions. Results indicated the early changes (after 40% Tlim) in RMS and MPF illustrated with the area ratio index allowed the prediction of the Tlim of these contractions ($r^2 < 0.5$). This low determination coefficients may be due to the inter-individual differences in terms of quantity of work produced during leg extensions and the influence of methodological factors on EMG signal. However, the fact that the results were found for the rectus femoris confirms the importance of studying this muscle during leg extensions.

These studies show that Tlim prediction is possible and that some factors influence the feasibility and reliability of the prediction such as the complexity of the task, the muscles monitored and the exercise intensity. Moreover, only few studies presented the Tlim prediction error that remains

relatively high and may restrain the use of this method. These questions will be discussed in the following part.

Solutions and Recommendations

The number of studies about Tlim prediction is limited and some points relative to the optimal experimental conditions that would optimize the Tlim prediction have to be specified.

First, the complexity of the task (i.e. involving one or several joints) and the number of synergist muscles that can contribute to the task have to be considered. About that, Boyas et al. (2009) clearly demonstrated that the Tlim prediction method presented in this chapter is not adapted to multi-joint tasks. Indeed, as the number of joints increases the number of muscles increases similarly. This raises the number of possible combinations offered to the neuromuscular system to produce a specific amount of force (Prilutsky, 2000). The presence of compensations across synergist muscles can also happen during mono-articular tasks. Indeed, alternating recruitment of different synergists has been reported during an isometric task performed until exhaustion (Kouzaki, Shinohara, Masani, & Fukunaga, 2004; Kouzaki et al., 2002). These findings were obtained during contractions performed at low intensities. On the other hand, high exercise intensity also seems to limit the ability of the nervous system to modulate the muscle activity between synergists (Ebenbichler et al., 1998; Kouzaki et al., 2002; Sirin & Patla, 1987).

So, the contraction intensity is the second factor to consider in the field of Tlim prediction. Tlim prediction has been mainly illustrated during contractions performed at exercise intensities higher or equal to 50% MVC (Bouillard et al., 2012; Boyas & Guevel, 2011a; Dolan et al., 1995; Maisetti, Guevel, et al., 2002a; Mannion & Dolan, 1996; Merletti & Roy, 1996; van Dieen et al., 1998). Only three studies investigated Tlim prediction at lower exercise intensities (Bouillard et al., 2012; Boyas & Guevel, 2011a; van Dieen

et al., 1998). These studies reported that the reliability of the Tlim prediction increased when contraction intensity increased. Several factors may, at least partly, explain the higher accuracy of Tlim prediction with higher exercise intensities. First of all, one can suppose that the more the failure of the fatigue test would be of central origin, the less the ability to predict Tlim using early changes in sEMG parameters, as suggested by Dolan et al. (1995). The fact that it has been shown that the influence of central fatigue on force production is be inversely proportional to exercise intensity (Kent-Braun, 1999; Schillings, Hoefsloot, Stegeman, & Zwarts, 2003; Smith, Martin, Gandevia, & Taylor, 2007) supports the idea that Tlim prediction should be performed for contraction at medium to high intensities. Afterwards, a higher contraction intensity would be associated with a shorter exercise time, which would limit the contribution of the psychological factors in the performance (Dolan et al., 1995). One can also imagine that it is easier for a subject to perceive the time where she is not able to sustain the required force level when the intensity is high. For low intensities, pain tolerance and psychological factors have more influence on the Tlim. Finally, as mentioned earlier, when the contraction intensity increases, the modulation of the activity between muscles decreases (Kouzaki et al., 2002; Mullany, O'Malley, St Clair Gibson, & Vaughan, 2002). Considering the method used to predict Tlim (i.e., using EMG changes of each muscle individually), we can suppose that any modulation of the distribution of activity between the synergists may impair the accuracy of the prediction.

Third, numerous articles in the literature specified that Tlim prediction was more reliable when considering the EMG activity of the muscle which displayed the greatest EMG signal changes, often described as the most fatigable muscle studies (Boyas & Guevel, 2011a; Maisetti, Guevel, Iachkine, Legros, & Brisswalter, 2002; Mannion &

Dolan, 1996; van Dieen et al., 1998). This makes sense as this same muscle represents the limiting factor of the muscle contraction. So, when the most fatigable muscle gets exhausted, it becomes very difficult for the subject to sustain the contraction. However, this muscle is not necessarily the same for all the individuals, especially if they have different characteristics. This requires that investigators make sure to record the main synergist muscles involved in the task and then focus on the one with the greatest EMG signal changes.

Fourth, few indicators allowing the characterization of EMG signal changes have been used to predict Tlim. The slope of the linear regression was used to predict the Tlim for different muscle groups (Bouillard et al., 2012; Dolan et al., 1995; Mannion & Dolan, 1994; Merletti & Roy, 1996; van Dieen et al., 1998). However, the reliability of this indicator depends on the linearity of the EMG changes (Merletti et al., 1991). Other studies obtained better results using the area ratio index, a regression-free index not influenced by the shape of the changes in the EMG signal (Bouillard et al., 2012; Boyas & Guevel, 2011a; Maisetti, Guevel, et al., 2002a). However, this may depends on the muscle group tested. So, we think that it is better to work on Tlim prediction using the slope and the area ratio index. Considering the drawbacks of the time constant about the calculation time, this indicator is not relevant for Tlim prediction.

Fifth, several EMG parameters have been tested in the Tlim prediction field. Studies have reported that Tlim prediction was possible and/or more reliable with frequency parameters (i.e. MPF, MF, FB) (Boyas & Guevel, 2011a; Dolan et al., 1995; Maisetti, Guevel, et al., 2002a; van Dieen et al., 1998). This could be due to the fact that these parameters particularly illustrate peripheral fatigue phenomena which are the ones that mostly contribute to fatigue during high-intensity contractions. Consequently, we suggest the use of the frequency band parameter as this parameter characterizes the motor unit recruitment modality

and the changes in their discharge rate. Moreover, the changes in this parameter are close to those of the MF (Allison & Fujiwara, 2002) and seem to be related to the muscle typological profile and their fatigability, which is very important in the field of Tlim prediction (Badier et al., 1993; Komi & Tesch, 1979; Mannion & Dolan, 1996).

FUTURE RESEARCH DIRECTIONS

The prediction of the endurance time from non-exhausting exercise is important for subjects who cannot or don't want to achieve exhausting muscular tasks. The literature on this topic reveals that Tlim prediction using electromyography is possible when respecting some conditions. However, as illustrated by the latest studies of Boyas et al. (Boyas & Guevel, 2011a) and Bouillard et al. (Bouillard et al., 2012) the reliability remains sometimes moderate and future investigations could try to study other fatigue indices, such as changes in the force variability that occur during sustained isometric contraction (Keen, Yue, & Enoka, 1994) or a multifactorial model using, for instance, mechanical and EMG parameters, to predict Tlim (Rudroff, Christou, Poston, Bojsen-Moller, & Enoka, 2007). Interesting information would also be gathered by studies on pathological individuals that may have altered fatigue resistance capabilities (e.g. after a stroke or a traumatic brain injury). It is also important to keep in mind that there are important psychological factors that may impact Tlim measurement.

CONCLUSION

In conclusion, literature has shown that Tlim prediction was possible for several muscle groups. However, some experimental factors have to be respected to optimize the reliability of the Tlim prediction. Tlim prediction should be investigated

for simple mono-articular isometric contractions. The main muscles involved should be monitored, especially the one that is supposed to be the most fatigable. Contraction intensity should be equal or higher than 50% MVC. In terms of EMG parameters, frequency parameters (MPF, MF, FB) should be preferred to temporal parameters, but one can consider that monitoring one extra parameter, i.e. RMS, can be easily done and could be beneficial. Changes in these EMG parameters should be characterized with the area ratio and the slope of the linear regression. Tlim prediction may be improved using a multifactorial model combining EMG and mechanical parameters. Tlim prediction presents several interests in both clinical and sport fields. The first is to limit the influence of psychological factors in the characterization of fatigue abilities. The second is to reduce the time of effort and so limit the deleterious risks associated with the performance of contractions performed until exhaustion. All this is relevant for athletes and patients, especially those who are prevented from performing exhaustive contractions but whom muscle capacities should be regularly monitored such as patients with neuromuscular degenerative pathologies.

REFERENCES

- Agre, J. C., & Sliwa, J. A. (2000). Neuromuscular rehabilitation and electrodiagnosis. 4. Specialized neuropathy. *Arch Phys Med Rehabil*, 81(3 Suppl 1), S27-31, S36-44.
- Allison, G. T., & Fujiwara, T. (2002). The relationship between EMG median frequency and low frequency band amplitude changes at different levels of muscle capacity. *Clinical Biomechanics (Bristol, Avon)*, 17(6), 464-469. doi:10.1016/S0268-0033(02)00033-5 PMID:12135548

- Badier, M., Guillot, C., Lagier-Tessonier, F., Burnet, H., & Jammes, Y. (1993). EMG power spectrum of respiratory and skeletal muscles during static contraction in healthy man. *Muscle & Nerve*, *16*(6), 601–609. doi:10.1002/mus.880160605 PMID:8502257
- Bigland-Ritchie, B. (1981). EMG and fatigue of human voluntary and stimulated contractions. *Ciba Foundation Symposium*, *82*, 130–156. PMID:6913468
- Bouillard, K., Frere, J., Hug, F., & Guevel, A. (2012). Prediction of time-to-exhaustion in the first dorsal interosseous muscle from early changes in surface electromyography parameters. [Evaluation Studies]. *Muscle & Nerve*, *45*(6), 835–840. doi:10.1002/mus.23253 PMID:22581537
- Boyas, S., & Guevel, A. (2011a). Influence of exercise intensity and joint angle on endurance time prediction of sustained submaximal isometric knee extensions. *European Journal of Applied Physiology*, *111*(6), 1187–1196. doi:10.1007/s00421-010-1731-0 PMID:21127901
- Boyas, S., & Guevel, A. (2011b). Neuromuscular fatigue in healthy muscle: underlying factors and adaptation mechanisms. *Ann Phys Rehabil Med*, *54*(2), 88–108. doi:10.1016/j.rehab.2011.01.001 PMID:21376692
- Boyas, S., Maisetti, O., & Guevel, A. (2009). Changes in sEMG parameters among trunk and thigh muscles during a fatiguing bilateral isometric multi-joint task in trained and untrained subjects. *Journal of Electromyography and Kinesiology*, *19*(2), 259–268. doi:10.1016/j.jelekin.2007.09.002 PMID:17964184
- De Luca, C. J. (1984). Myoelectrical manifestations of localized muscular fatigue in humans. *Critical Reviews in Biomedical Engineering*, *11*(4), 251–279. PMID:6391814
- De Luca, C. J. (1997). The use of surface electromyography in biomechanics. *Journal of Applied Biomechanics*, *13*(2), 135–163.
- Dolan, P., Mannion, A. F., & Adams, M. A. (1995). Fatigue of the erector spinae muscles. A quantitative assessment using frequency banding of the surface electromyography signal. *Spine*, *20*(2), 149–159. doi:10.1097/00007632-199501150-00005 PMID:7716619
- Ebenbichler, G., Kollmitzer, J., Quittan, M., Uhl, F., Kirtley, C., & Fialka, V. (1998). EMG fatigue patterns accompanying isometric fatiguing knee-extensions are different in mono- and bi-articular muscles. *Electroencephalography and Clinical Neurophysiology*, *109*(3), 256–262. doi:10.1016/S0924-980X(98)00015-0 PMID:9741792
- Enoka, R. M., & Stuart, D. G. (1992). Neurobiology of muscle fatigue. *Journal of Applied Physiology (Bethesda, Md.)*, *72*(5), 1631–1648. PMID:1601767
- Hagberg, M. (1981). Muscular endurance and surface electromyogram in isometric and dynamic exercise. *Journal of Applied Physiology: Respiratory, Environmental and Exercise Physiology*, *51*(1), 1–7. PMID:7263402
- Hagberg, M., & Kvarnstrom, S. (1984). Muscular endurance and electromyographic fatigue in myofascial shoulder pain. *Archives of Physical Medicine and Rehabilitation*, *65*(9), 522–525. PMID:6477084
- Kankaanpaa, M., Taimela, S., Webber, C. L. Jr, Airaksinen, O., & Hanninen, O. (1997). Lumbar paraspinal muscle fatigability in repetitive isoinertial loading: EMG spectral indices, Borg scale and endurance time. *European Journal of Applied Physiology and Occupational Physiology*, *76*(3), 236–242. doi:10.1007/s004210050242 PMID:9286603
- Keen, D. A., Yue, G. H., & Enoka, R. M. (1994). Training-related enhancement in the control of motor output in elderly humans. *Journal of Applied Physiology (Bethesda, Md.)*, *77*(6), 2648–2658. PMID:7896604

Endurance Time Prediction using Electromyography

- Kent-Braun, J. A. (1999). Central and peripheral contributions to muscle fatigue in humans during sustained maximal effort. *European Journal of Applied Physiology and Occupational Physiology*, 80(1), 57–63. doi:10.1007/s004210050558 PMID:10367724
- Komi, P. V., & Tesch, P. (1979). EMG frequency spectrum, muscle structure, and fatigue during dynamic contractions in man. *European Journal of Applied Physiology and Occupational Physiology*, 42(1), 41–50. PMID:499196
- Kouzaki, M., Shinohara, M., Masani, K., & Fukunaga, T. (2004). Force fluctuations are modulated by alternate muscle activity of knee extensor synergists during low-level sustained contraction. *Journal of Applied Physiology (Bethesda, Md.)*, 97(6), 2121–2131. doi:10.1152/jappphysiol.00418.2004 PMID:15208288
- Kouzaki, M., Shinohara, M., Masani, K., Kanehisa, H., & Fukunaga, T. (2002). Alternate muscle activity observed between knee extensor synergists during low-level sustained contractions. *Journal of Applied Physiology (Bethesda, Md.)*, 93(2), 675–684. PMID:12133879
- Lindstrom, L., Kadefors, R., & Petersen, I. (1977). An electromyographic index for localized muscle fatigue. *Journal of Applied Physiology: Respiratory, Environmental and Exercise Physiology*, 43(4), 750–754. PMID:583632
- Maisetti, O. (2002). *Manifestations myoélectriques de la fatigue comme prédicteurs de la capacité de travail musculaire local* (Thèse de doctorat STAPS). Université de la méditerranée.
- Maisetti, O., Boyas, S., & Guevel, A. (2006). Specific neuromuscular responses of high skilled laser sailors during a multi-joint posture sustained until exhaustion. *International Journal of Sports Medicine*, 27(12), 968–975. doi:10.1055/s-2006-923893 PMID:16761219
- Maisetti, O., Guevel, A., Iachkine, P., Legros, P., & Brisswalter, J. (2002). Le maintien de la position de rappel en dériveur solitaire. Aspects théoriques et propositions méthodologiques d'évaluation de la fatigue musculaire. *Science & Sports*, 17, 234–246. doi:10.1016/S0765-1597(02)00170-3
- Maisetti, O., Guevel, A., Legros, P., & Hogrel, J. Y. (2002a). Prediction of endurance capacity of quadriceps muscles in humans using surface electromyogram spectrum analysis during submaximal voluntary isometric contractions. *European Journal of Applied Physiology*, 87(6), 509–519. doi:10.1007/s00421-002-0645-x PMID:12355190
- Maisetti, O., Guevel, A., Legros, P., & Hogrel, J. Y. (2002b). SEMG power spectrum changes during a sustained 50% maximum voluntary isometric torque do not depend upon the prior knowledge of the exercise duration. *Journal of Electromyography and Kinesiology*, 12(2), 103–109. doi:10.1016/S1050-6411(02)00010-X PMID:11955982
- Mannion, A. F., & Dolan, P. (1994). Electromyographic median frequency changes during isometric contraction of the back extensors to fatigue. *Spine*, 19(11), 1223–1229. doi:10.1097/00007632-199405310-00006 PMID:8073313
- Mannion, A. F., & Dolan, P. (1996). Relationship between myoelectric and mechanical manifestations of fatigue in the quadriceps femoris muscle group. *European Journal of Applied Physiology and Occupational Physiology*, 74(5), 411–419. PMID:8954288
- Merletti, R., Lo Conte, L., & Orizio, C. (1991). Indices of muscles fatigue. *Journal of Electromyography and Kinesiology*, 1, 20–33. doi:10.1016/1050-6411(91)90023-X PMID:20719592
- Merletti, R., & Roy, S. H. (1996). Myoelectrical and mechanical manifestations of muscle fatigue in voluntary contractions. *The Journal of Orthopaedic and Sports Physical Therapy*, 24(6), 342–353. doi:10.2519/jospt.1996.24.6.342 PMID:8938600

Moore, D. P., & Kowalske, K. J. (2000). Neuro-muscular rehabilitation and electrodiagnosis. 5. Myopathy. *Arch Phys Med Rehabil*, 81(3 Suppl 1), S32-35, S36-44.

Mullany, H., O'Malley, M., St Clair Gibson, A., & Vaughan, C. (2002). Agonist-antagonist common drive during fatiguing knee extension efforts using surface electromyography. *Journal of Electromyography and Kinesiology*, 12(5), 375–384. doi:10.1016/S1050-6411(02)00048-2 PMID:12223170

Prilutsky, B. I. (2000). Coordination of two- and one-joint muscles: Functional consequences and implications for motor control. *Motor Control*, 4(1), 1–44. PMID:10675807

Rudroff, T., Christou, E. A., Poston, B., Bojsen-Moller, J., & Enoka, R. M. (2007). Time to failure of a sustained contraction is predicted by target torque and initial electromyographic bursts in elbow flexor muscles. *Muscle & Nerve*, 35(5), 657–666. doi:10.1002/mus.20752 PMID:17294440

Schillings, M. L., Hoefsloot, W., Stegeman, D. F., & Zwarts, M. J. (2003). Relative contributions of central and peripheral factors to fatigue during a maximal sustained effort. *European Journal of Applied Physiology*, 90(5-6), 562–568. doi:10.1007/s00421-003-0913-4 PMID:12905050

Sirin, A. V., & Patla, A. E. (1987). Myoelectric changes in the triceps surae muscles under sustained contractions. Evidence for synergism. *European Journal of Applied Physiology and Occupational Physiology*, 56(2), 238–244. PMID:3569232

Smith, J. L., Martin, P. G., Gandevia, S. C., & Taylor, J. L. (2007). Sustained contraction at very low forces produces prominent supraspinal fatigue in human elbow flexor muscles. *Journal of Applied Physiology (Bethesda, Md.)*. doi:10.1152/jappphysiol.00220.2007

van Dieen, J. H., Heijblom, P., & Bunkens, H. (1998). Extrapolation of time series of EMG power spectrum parameters in isometric endurance tests of trunk extensor muscles. *Journal of Electromyography and Kinesiology*, 8(1), 35–44. doi:10.1016/S1050-6411(97)00003-5 PMID:9667032

van Dieen, J. H., Oude Vrielink, H. H., Housheer, A. F., Lotters, F. B., & Toussaint, H. M. (1993). Trunk extensor endurance and its relationship to electromyogram parameters. *European Journal of Applied Physiology and Occupational Physiology*, 66(5), 388–396. doi:10.1007/BF00599610 PMID:8330605

Zijdewind, I., Kernell, D., & Kukulka, C. G. (1995). Spatial differences in fatigue-associated electromyographic behaviour of the human first dorsal interosseus muscle. [Research Support, Non-U.S. Gov't]. *The Journal of Physiology*, 483(Pt 2), 499–509. PMID:7650617

ADDITIONAL READING

Basmajian, J. V., & De Luca, C. J. (1985). *Muscles Alive: Their Functions Revealed by Electromyography*. Baltimore: Williams & Wilkins.

KEY TERMS AND DEFINITIONS

Early Changes in EMG Signal: Changes occurring in the EMG signal at the beginning of the contraction.

Electromyography (EMG): Technique for assessing the electrical activity of muscles.

EMG Parameter: Value calculated from the raw EMG signal that characterizes it in terms of amplitude or frequency.

Endurance Time (T_{lim}): Maximal duration during which an individual can sustain the required level of force.

Endurance Time Prediction using Electromyography

Indicator of EMG Changes: Mathematical model used to characterize the changes in the EMG signal in terms of amplitude and/or speed.

Neuromuscular Fatigue: Exercise-induced reduction in force production capacity.

Time Prediction: Technique aiming at determining the exertion time of a fatiguing muscle contraction before it occurs.

Chapter 11

EMG Activation Pattern during Voluntary Bending and Donning Safety Shoes

P. K. Nag

National Institute of Occupational Health, India

Varsha Chorsiya

National Institute of Occupational Health, India

Anjali Nag

National Institute of Occupational Health, India

ABSTRACT

Posture control is a well-coordinated interplay of sensory-motor system and forms the basis of voluntary movements. The daily activities and occupational task involves voluntary bending in different directions, which if falls beyond the limit of stability can cause slipping, tripping and falling. Further, these accidents are very common in industries where workers have to wear safety shoes to protect their feet from hazards of the work environment. The study elucidates the muscular activation patterns in light of electromyographic (EMG) findings for voluntary bending within limits of stability and with donning of safety shoes. The aim of this chapter is to potentially contribute to occupational health and safety at workplaces. The present findings have implications regarding the viability of muscle adaptability as a putative postural control in preventing postural instability and avoiding injuries.

INTRODUCTION

A well-functioning control of posture represents an essential prerequisite for the human being to successfully perform activities of daily living and occupational activity, including large body excursion even to critical limits in different direction.

The neuromuscular system responds according to the central nervous system (CNS) identifying and selectively focussing on the sensory inputs (visual, vestibular, proprioceptive) that provide functionality to the most reliable signals (Allum, Bloem, Carpenter, Hulliger, & Hadders-Algra, 1998). Muscle fatigue may decrease the reliability of the

DOI: 10.4018/978-1-4666-6090-8.ch011

EMG Activation Pattern during Voluntary Bending and Donning Safety Shoes

proprioceptive signals (Allen & Proske, 2006) and therefore, the CNS might down-weight these sensory input and/or up-weight proprioceptive signals of other muscles to control posture (Brumagne, Cordo, & Verschueren, 2004; Carver, Kiemel, & Jeka, 2006). Upright stance is inherently unstable with two-thirds of the body mass is distributed at two-thirds height above the ground (Gage, Winter, Frank, & Adkin, 2004; Winter, 1995), and further, it becomes a challenging postural demand at critical limits of body excursion. Today, footwear (e.g., dress wear, safety/industrial shoe, athletic shoe) has become our basic requisite for safety, comfort and fashion, however, the footwear may influence postural instability and cause falls and accidents (Chang & Grönqvist, 2003; Hsiao & Simeonov, 2001). The dimensional and functional characteristics of footwear influence the interface between the locomotive system of the wearer and one's physical environment (Wunderlich & Cavanagh, 2001), and accordingly induce adaptation in the motion of the joints of the lower extremities, change in the reaction force, and modification in the electrical activity of the muscles involved. Literature elucidates the biomedical perspective of barefoot versus shoe running with reference

to mechanics, kinematics, kinetics, loading rates, and impact on the lower limbs (Lieberman et al., 2010; Benno Nigg, 2009), however, the studies are scanty on the effects of footwear on muscle activity (Gage et al., 2004; Gollhofer & Komi, 1987; BM Nigg & Wakeling, 2001; Wakeling, Pascual, & Nigg, 2002). With the understanding of potential implication of occupational health and safety at workplaces, the present contribution elucidates (a) the pattern of muscle activation of lower extremity and trunk muscles manifested in voluntary bending to critical limits of body stability (anterior, posterior, left and right direction) and (b) the muscle activity of lower extremity, trunk and neck muscles in bipedal stance (barefoot as well as wearing shoes).

METHOD AND MATERIALS

A total of thirty-five volunteers, who were free from any neurological, orthopaedic, hearing or vestibular problem, participated in the study. Informed consent for participation in the study was obtained from each volunteer, as per the ethical

Figure 1. Limits of stability in (a) forward, (b) backward, (c) right lateral bending and (d) left lateral bending

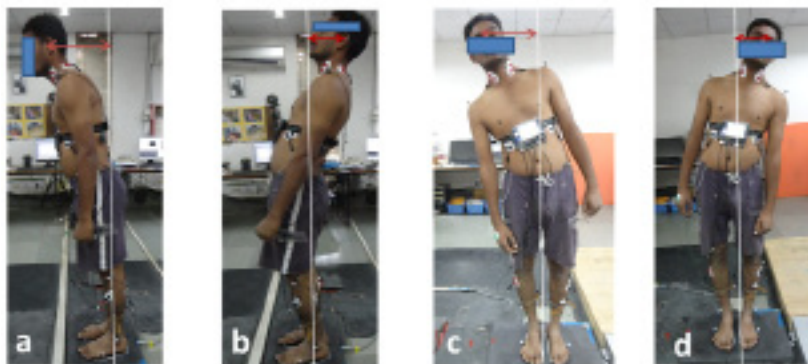
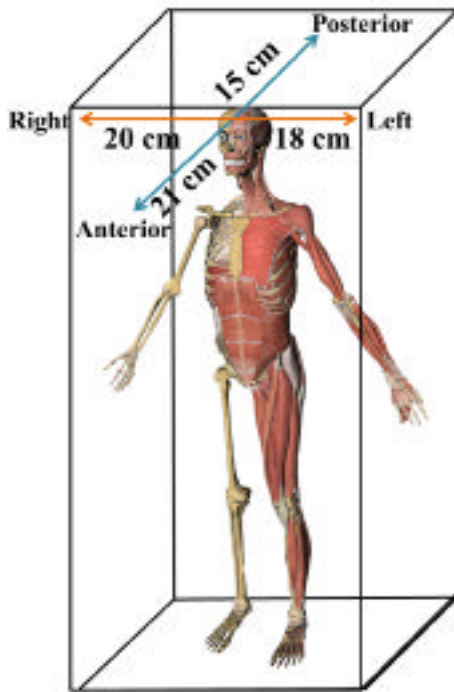


Figure 2. Range of excursion within the limit of stability during voluntary bending in antero-posterior, and right-left direction



guidelines of Indian Council of Medical Research (ICMR, 2000).

EMG Recording

For the research objectives indicated above, the experimental set up included a 16-channel Portable and Wi-Fi enabled EMG Machine (BTS Bioengineering, Italy) for recording of electrical activity of muscles. Bilateral electromyographic recording of lower extremity, trunk and neck muscles, [tibialis anterior (TA), medial gastrocnemius (GS), quadriceps (QUADS), biceps femoris (BF), trapezius upper fibers (TRAP), erector spinae (ES) and obliquus abdominis (ABD)] was undertaken, according to the European recommendations for

Surface ElectroMyoGraphy (Hermens, Freriks, Disselhorst-Klug, & Rau, 2000). The EMG signals were acquired by surface electrodes (Swaromed, Ag/AgCl pre-gelled), placed on the respective muscles with a 20 mm inter-electrode distance. The electrode placements were done along the direction of the muscle fibers. A reference electrode was placed on the dorsum of the right hand. Prior to electrode placement the skin was shaved and lightly abraded to decrease the skin impedance, below 5 k Ω .

The recorded EMG signals were A-D converted with 12-bit accuracy in ± 5 V range and before sampling, the surface EMG signals were analogue high-pass and low-pass filtered at 10 Hz and 500 Hz using Butterworth filter, in order to remove unwanted noise and movement artifacts. For relative reference of muscle activity of a given task, the maximum voluntary contractions (MVCs) were recorded which was used for EMG signal normalization, i.e., the RMS values of the EMG signals of trial conditions were expressed as the ratio of the activity level to that of the reference MVCs of the respective muscles. The EMG signals of muscles were captured by SMART capture software (BTS Bioengineering, Italy) and analyzed off-line using MYOLAB software (BTS Bioengineering, Italy).

Task Investigated

The experiments were conducted to gain insight about the patterns of muscle activations under intrinsic and extrinsic conditions, and its role in postural control. A human body usually moves as an inverted pendulum in cone of stability on mainly two fulcrum points at ankle and hip. The subject was asked to move voluntarily in four directions: anteriorly, posteriorly, right and left within their limits of stability (critical point), and to stay in each position for 60 seconds maintaining the knee extended; this was followed by a pre- and post-neutral erect standing position of 15 seconds each.

EMG Activation Pattern during Voluntary Bending and Donning Safety Shoes

The limit of body excursion was the critical limit beyond which subject may not be able to maintain the position and is measured using a plumb line as depicted in Figure 1. Before the trial was initiated, the plumb line was set passing through the vertex of the tragus of the ear to anterior of medial malleolus in sagittal view and in frontal plane passing through glabella to midpoint of line joining both feet. The anterior and posterior limit was measured as the distance between plumb line and tragus of ear when the subject had attained his/her critical limit of stability in anterior and posterior direction respectively. The right and left limit was measured as the distance between plumb line and glabella when the subject attained his/her critical limit of stability in right and left direction respectively. Average excursion within limits of stability was calculated for all the volunteers in anterior/forward, posterior/backward, right and left lateral bending directions (Figure 2), with simultaneous capturing of the muscle activity.

The second experiment was undertaken to compare muscle activations between conditions of with and without donning of industrial safety shoes. The shoe acts as the medium for extrinsic perturbation, influenced by the dimensional, functional and design characteristics of the shoes. Prior to the testing, the volunteers underwent task familiarization and a 12 minutes warm-up consisting of 6 minutes of walking at their preferred gait speed and 6 minutes of non-stressful muscle stretching was performed. The subjects' task consisted of maintaining an upright bilateral stance posture (barefoot and with industrial safety shoes), as immobile as possible, for duration of 120 seconds of the EMG signal capture period. The subjects were instructed to (1) keep their body straight, (2) hang their arms loosely by their sides and (3) looking straight ahead in front at eye level. Between successive trials, the subjects were given a rest break of 10 minutes to regain stable

conditions. Eight pairs of shoes were selected in the present study, as illustrated in Table 1.

RESULTS









The average physical characteristics of the volunteers were: age 31.5 ± 1.4 years; BMI 19.8 ± 2.6 ; spine length 57 ± 7.1 cm; leg length 90 ± 5.7 cm and foot length 27.1 ± 1.5 cm respectively. The spine length was measured from the anatomical landmarks of C7 (the most prominent spinous process of cervical vertebra) to the mid-point of the line joining the dimples of Venus by placing a flexi curve along the mid-line of a spine (Miller, Mayer, Cox, & Gatchel, 1992). As per the first part of the experiment, as shown in Figure 2, the body excursion (internal perturbation) within limits of stability, keeping the knee extended in antero-posterior direction was 21 ± 7 cm in anterior or forward direction and 15 ± 5.3 cm in posterior or backward direction, respectively. The motion in frontal plane consisted of right and left lateral bending keeping the knee extended in medial-lateral direction, with 20 ± 5.6 cm in right lateral bending and 18 ± 5.6 cm in left lateral bending respectively; that is, the body excursion was ~40% more in forward direction and about ~10% more in right lateral bending, as compared to backward direction and left lateral bending, respectively.

Muscle Activation in Maximal Antero-Posterior Movement

The pattern of muscle activation of TA and GS, along the sagittal plane movement in antero-posterior direction is shown in Figure 3a. In forward-anterior excursion, the RMS EMG amplitude of GS muscle appeared to be more, as compared to the TA; however, the activations of left GS and left TA were higher, as compared to the muscles of the right side. A reverse pattern was noted in

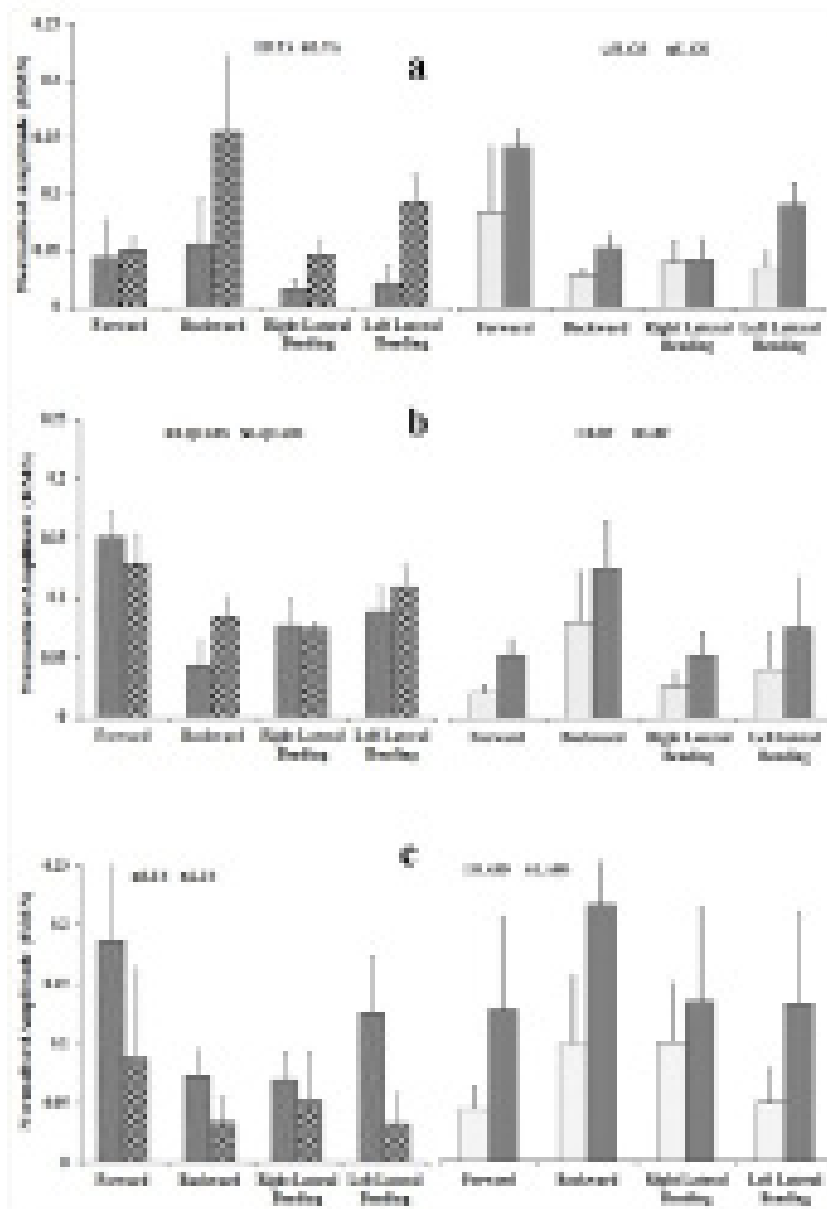
EMG Activation Pattern during Voluntary Bending and Donning Safety Shoes

Table 1. Industrial footwear used in the experimental study

Code	Footwear weight (gm)	Footwear sole	Footwear Toe	Upper Leather	Ankle type	Pictures
AS1	1000	Single density PU sole	Steel Toe Cap	Black Barton Leather	Low ankle	
BS3	1080	Double density PU sole	With Fiber Toe Cap	Black Barton Leather	High ankle	
CC1	1200	Nitrile rubber sole	Steel Toe Cap	Black Barton Leather	Low ankle	
CCL	1000	Single density PU sole	Without Steel toe cap	CG Leather	Low ankle	
CS1	1200	Nitrile PVC	Steel Toe Cap	PVC	High ankle	
GB1	2000	Nitrile PVC	Steel Toe Cap	PVC	High ankle	
NRH	1000	Single density PU sole	Steel Toe Cap	Black Barton Leather	High ankle	
OX1	1220	Double density PU sole	Steel Toe Cap	Neobuck Leather	High ankle	

EMG Activation Pattern during Voluntary Bending and Donning Safety Shoes

Figure 3. Normalized EMG of muscles of ankle joint (TA and GS), hip joint (QUADS and BF) and trunk (ES and ABD) at limits of stability. Values are means \pm SEM. (R- right; L- left)



backward - posterior excursion, where RMS EMG amplitude of TA surpassed the relative activation of GS, with higher levels of RMS amplitude being showed in both the muscles of the left side.

The RMS EMG of QUADS, as shown in Figure 3b, showed dominance in forward bending, as compared to the BF, whereas a reverse pattern was observed in backward - posterior excursion. The EMG activity of the ES and ABD, as presented in Figure 3c, indicates that in forward bending, the ES manifested relatively greater RMS EMG, as compared to its antagonist abdominals. The pattern of activity of the muscles had a reverse trend when movement direction changed from forward to backward excursion. Overall, the trunk muscles showed the maximum RMS amplitude in antero-posterior excursions, however, the normalized activation level of the muscles largely remained less than 15% of MVC.

Muscle Activation in Maximal Lateral Bending

The motion in the frontal plane, however, exhibited an asymmetric pattern of muscle activity during right and left lateral bending, with relatively higher RMS EMG amplitude of the TA, GS of the left side, as compared to the muscles of the right side (Figure 3a). In lateral bending either to right or left, the QUADS exceeded the relative level of activation of the BF. The latter exhibited more asymmetric behaviour, showing higher RMS EMG in the left muscle (Figure 3b).

With lateral bending to the right, the ES of the right side exhibited higher amplitude as compared to left side; however, the level of activity was relatively less in relation to its antagonist abdominal of the same side (Figure 3c). Similarly, in left lateral bending, the EMG activity of the left ABD dominated over the left ES. The activation pattern of the trunk muscles is indicative of typical muscle synergy that might be responsible for spinal coupling, i.e., trunk axial rotation and lateral flexion are associated with each other.

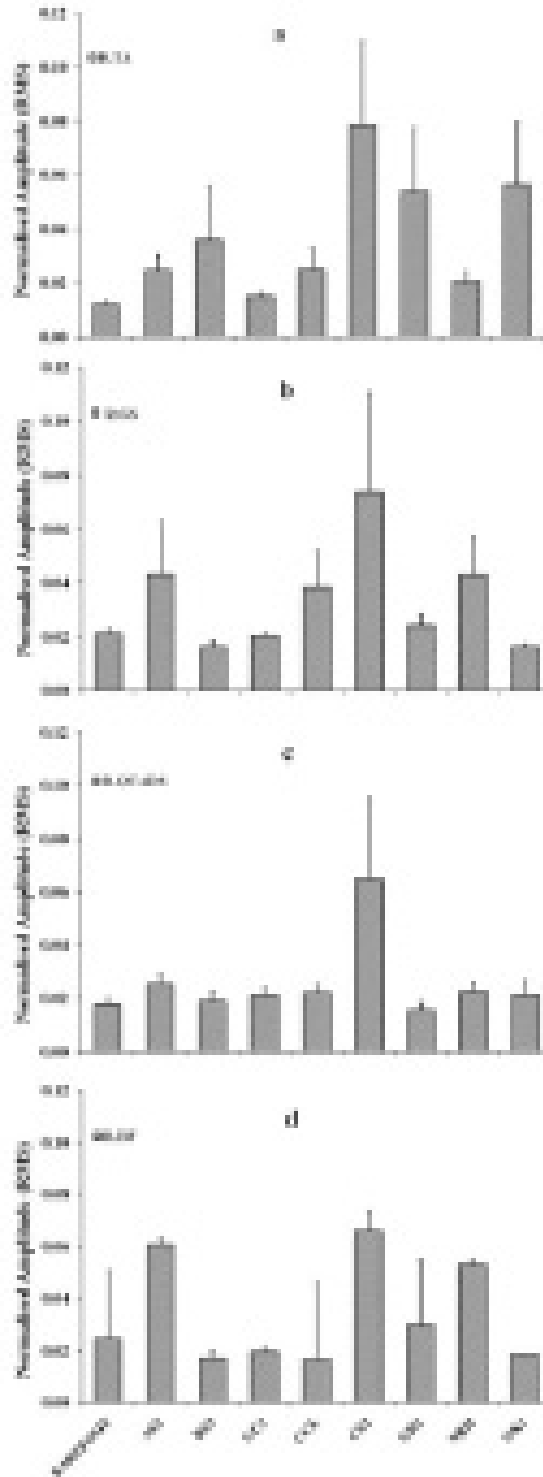
Muscle Activity in Standing and Walking (Barefoot vs. Safety Shoe)

The RMS EMG amplitude of bilateral TA, GS, QUADS, BF, TRAPS and ES in barefoot standing and walking and with 8 pairs of industrial shoes (AS1, BS3, CC1, CCL CS1, NRH, OX1) are represented in Figures 4 through 9. While standing, the EMG activities of TA increased several fold with wearing shoes (e.g., BS3, CS1, GB1, NRH and OX1) as compared to barefoot standing, with bilateral difference in RMS EMG, as observed high activity in left TA in case of CS1 and NRH. The recruitment of GS remained very similar in barefoot and with shoes, in contrast to those of TA, however, high activity observed with CS1 for right GS and BS3 for left GS, respectively. The hip joint muscles, i.e., QUADS and BF showed nearly similar level of activity in case of most of the shoes, excepting ~2.5 times higher activation for the right BF for the shoes - AS1, CS1 and NRH. Also bilateral TRAP showed increased activity for AS1 and CS1. The left ES showed higher levels of activation for GB1 and CS1.

The repeated measure of MANOVA was applied to compare RMS EMG amplitudes of muscles in relation to barefoot standing and wearing different types of shoes (Table 2), and the significant p values are marked as bold. Analysis yielded that bilateral activity of the muscles under study behaved differently with the types of shoes, in comparison to barefoot standing. The muscle load (right and left TA, right GS, right QUADS, right BF, right and left TRAP) during standing was distinctively high for the shoe code CS1, which is a high ankle type of shoe that weighs 1.2 Kg, with PVC sole and body, and steel toe cap. The shoe type, AS1 a low ankle shoe weighing ~1 Kg, with single density PU sole, and body from black Barton leather with steel toe cap, exerted significant load on right BF, as well as right and left TRAP, during standing. Other shoe types (e.g., CCL - a low ankle shoe, weighing ~1 Kg, with single density PU sole, and body from CG

EMG Activation Pattern during Voluntary Bending and Donning Safety Shoes

Figure 4. Normalized EMG amplitude of ankle and hip joint, and trunk muscles in standing barefoot and with industrial safety shoes. Values are means \pm SEM. (R- right; L- left)



leather without steel toe cap; GB1 - a high ankle gum boot, weighing 2 Kg, with nitrile PVC sole, and body from PVC with steel toe cap) showed significant load on left QUADS.

During walking, however, the muscle loads with different types of shoes were not consistent to those observed during standing. The levels of activity of the muscles during walking were much higher than observed with barefoot walking. The bilateral TA and BF activities were about 2 to 4 times higher with safety shoes, as compared to barefoot walking. The left GS showed 3 to 5 times more activity for OX1 and BS3 shoe respectively. Higher activation of right TRAP and ES were observed with the safety shoes than the muscles of the counter side. The repeated measure of MANOVA compared RMS EMG amplitudes of muscles in relation to walking barefoot and wearing shoes, as given in Table 3. The shoe AS1 (low ankle shoe) manifested significantly high muscle load on right BF, as well as right and left TRAP during walking. The shoe code BS3, which is a high ankle type of shoe that weighs ~1.1 Kg, with double density PU sole, body of black barton leather, and fiber toe cap had significantly higher activation during walking for right and left TA, left GS, right and left QUADS, right and left BF. The shoe type, GB1 (high ankle gum boot) exerted significantly high load on right and left TA, left QUADS and left ES. The exertion of load during walking with NRH - a high ankle shoe, weighing ~1 Kg, with single density PU sole, and body of black Barton leather, with steel toe cap was significantly high in right and left TA, and right BF, and in case of OX1 - a high ankle shoe, weighing ~1.2 Kg, with double density PU sole, and body of Neoback leather, with steel toe cap, significantly high muscle load was observed in case of right TA, right and left GS and left QUADS.

Time Trend of MDF of EMG in Standing Barefoot and with Safety Shoes

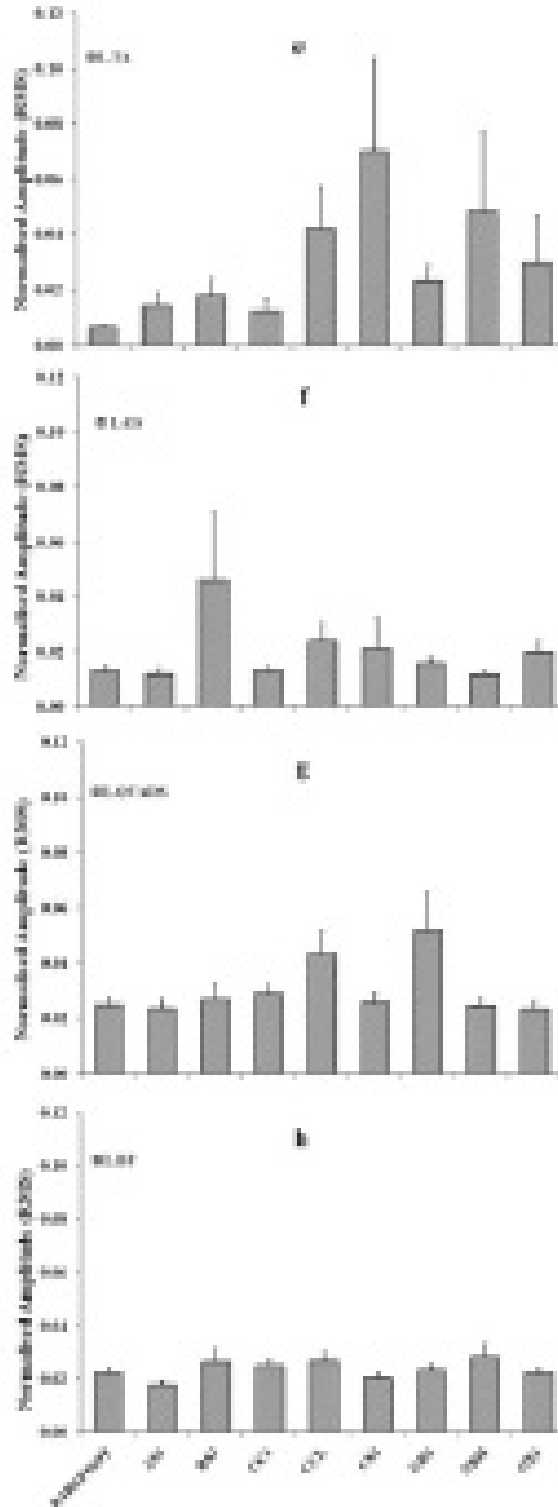
Figure 10 illustrates the time trend of average MDF of EMG activity different muscles in relation to standing barefoot and with safety shoes. Among other shoes, two high ankle type of shoes (BS3, weighing 1.1 Kg, double density PU sole, body of black barton leather, and fiber toe cap; CS1, weighing 1.2 Kg, PVC sole and body, steel toe cap) were chosen in the analysis, taking into account of its overall higher dominance of RMS EMG amplitudes during standing and walking. The sampling period of recording being 120 sec from the start of stance position, this remains the limitation to observe MDF trend over a longer period. Irrespective of stance position, either barefoot or with safety shoes, the MDF tended to build-up over the sampling duration, indicating continual recruitment of motor units in maintaining the stance. The MDF values of tibialis anterior ranged between 120 to 175 Hz, gastrocnemius (130 to 190 Hz), quadriceps (110 to 200 Hz), bicep femoris (110 to 145 Hz), erector spinae (80 to 140 Hz), and trapezius (60 to 150 Hz) respectively. A gradual plateau phase of the MDF values of BF was noted, and distinctively with CS1 safety shoe, indicating early attaining of the high level of MDF within the first min, followed by plateau phase. This might suggest of relatively more fatiguing trend of the BF during standing CS1 safety shoe.

DISCUSSION

The organization of the postural response with the muscle activation depends on the direction and intensity of external demand exerted on the body. The goal of our study was to investigate the pattern of activation exhibited in the bilateral group of muscles (ankle and hip joints, and trunk) during voluntary bending at the maximal anterior-posterior, and lateral positions. Further, the study

EMG Activation Pattern during Voluntary Bending and Donning Safety Shoes

Figure 5. Normalized EMG amplitude of ankle and hip joint, and trunk muscles in standing barefoot and with industrial safety shoes. Values are means \pm SEM. (R- right; L- left)



EMG Activation Pattern during Voluntary Bending and Donning Safety Shoes

Table 2. Pairwise comparison (MANOVA) of RMS EMG in standing barefoot and with safety shoes (p values); statistically significant ones are marked as Bold

Shoe codes	TA		GS		QUADS		BF		TRAP		ES	
	Right	Left	Right	Left	Right	Left	Right	Left	Right	Left	Right	Left
AS1	0.42	0.61	0.13	0.87	0.51	0.72	0.03	0.64	0.02	0.04	0.90	0.35
BS3	0.25	0.53	0.82	0.00	0.90	0.75	0.70	0.69	0.87	0.55	0.78	0.69
CC1	0.89	0.76	0.97	0.98	0.81	0.50	0.83	0.81	0.66	0.56	0.62	0.89
CCL	0.56	0.03	0.50	0.11	0.73	0.00	0.69	0.62	0.64	0.46	0.75	0.81
CS1	0.00	0.00	0.00	0.38	0.00	0.91	0.00	0.84	0.00	0.00	0.35	0.08
GB1	0.01	0.34	0.92	0.70	0.86	0.00	0.77	0.94	0.78	0.58	0.66	0.01
NRH	0.68	0.02	0.41	0.87	0.72	0.90	0.12	0.57	0.95	0.86	0.80	0.94
OX1	0.04	0.20	0.83	0.47	0.79	0.78	0.80	0.99	0.78	0.62	0.90	0.91

compared the activation pattern of muscles during standing and walking barefoot and donning industrial safety shoes. In industrial arena, the safety shoes are essential requisites as personal protective equipment. With reference to the design characteristics of the shoes that might act as the medium for extrinsic perturbation to the wearer, the relative muscle activation with the types of safety shoes were examined.

The experimentation, as illustrated in Figure 1, yielded that the average body excursion of selected adult males ranged about 21 cm in ante-

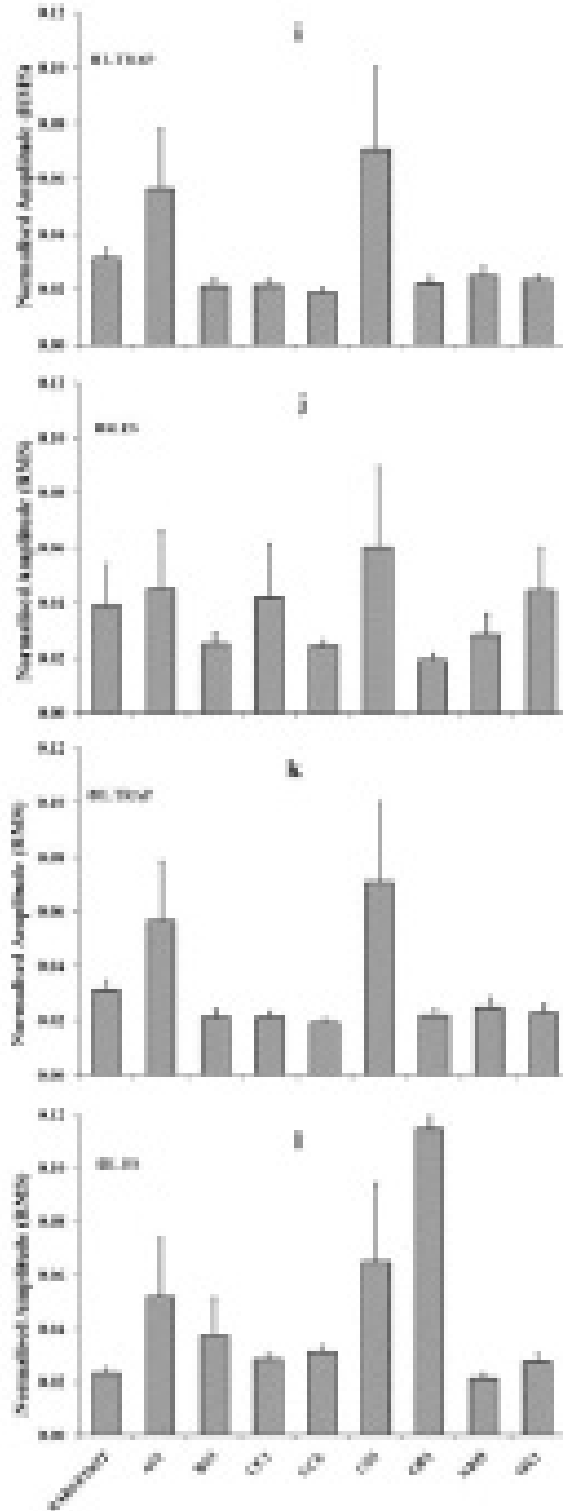
rior or forward direction and 15 cm in posterior or backward direction in sagittal plane, and the lateral bending ranged about 20 cm to the right and 18 cm to the left from the mid-line, e.g., the excursion was ~40% more in forward direction and ~10% more in right lateral bending. It was noted that 32 out of 35 volunteers were right dominant. The excursion limits in accordance with the optimal muscle activation behaviour have utility for ergonomic designing of safe work station. The EMG activity of the muscles of lower limbs and trunk showed asymmetric behaviour in recruitment

Table 3. Pairwise comparison (MANOVA) of RMS EMG in walking barefoot and with safety shoes (p values); statistically significant ones are marked as Bold

Shoe codes	TA		GS		QUADS		BF		TRAP		ES	
	Right	Left	Right	Left	Right	Left	Right	Left	Right	Left	Right	Left
AS1	0.10	0.08	0.91	0.71	0.85	0.78	0.03	0.95	0.003	0.03	0.73	0.25
BS3	0.003	0.05	0.34	0.001	0.05	0.01	0.05	0.002	0.93	0.76	0.83	0.80
CC1	0.51	0.08	0.92	0.77	0.68	0.53	0.32	0.50	0.002	0.83	0.07	0.77
CCL	0.27	0.03	0.35	0.40	0.71	0.04	0.49	0.03	0.04	0.81	0.99	0.44
CS1	0.37	0.17	0.92	0.83	0.06	0.68	0.27	0.34	0.001	0.001	0.04	0.10
GB1	0.04	0.013	0.86	0.26	0.99	0.001	0.06	0.33	0.10	0.27	0.43	0.004
NRH	0.01	0.03	0.41	0.88	0.29	0.71	0.04	0.63	0.56	0.98	0.78	0.96
OX1	0.001	0.08	0.383	0.004	0.02	0.001	0.98	0.64	0.38	0.96	0.88	0.25

EMG Activation Pattern during Voluntary Bending and Donning Safety Shoes

Figure 6. Normalized EMG amplitude of ankle and hip joint, and trunk muscles in standing barefoot and with industrial safety shoes. Values are means \pm SEM. (R- right; L- left)



and activation, suggesting the possible role of the side dominance in postural control.

The spinal coupling has been defined as the motion in which rotation or translation of a body about or along one axis is consistently associated with simultaneous rotation or translation about another axis. Our results indicated that the activation pattern of the trunk muscles manifest typical synergy that might be responsible for spinal coupling, i.e., trunk axial rotation and associated lateral flexion. It can be viewed that a set of muscle synergies might be identified that coactivate muscle groups of the limbs and trunk during bipedal standing (Torres-Oviedo, 2007). The muscle synergy does not necessarily result into a specific strategy, but the postural responses are evidently triggered by sensory information and transformed to motor output via specific muscle synergies (Chvatal, Torres-Oviedo, Safavynia, & Ting, 2011). As presented in Figure 3, the ES manifested relatively greater EMG amplitude in forward bending, as compared to its antagonist abdominals, and the pattern reversed when the direction of movement changed from forward to backward bending. Also, the pattern of activation of TA and GS was characteristic along the sagittal plane movement, with the EMG amplitude of GS appeared to be more than the TA in forward - anterior excursion; accordingly, a reverse was noted in backward - posterior excursion that EMG amplitude of TA surpassed the GS, with higher activation of both the muscles of the left side in comparison to the right side. Compared to the activation of BF, the QUADS showed dominance in forward bending and reverse was the case in backward - posterior excursion.

The lateral bending to the right exhibited higher activity of the right ES, however, the level of activity was relatively less in relation to its antagonist abdominal of the same side. In lateral bending to the left, the EMG activity of the left ABD dominated over the left ES. In lateral bending either to right or left, the QUADS exceeded the level of activation of the BF. The observation might

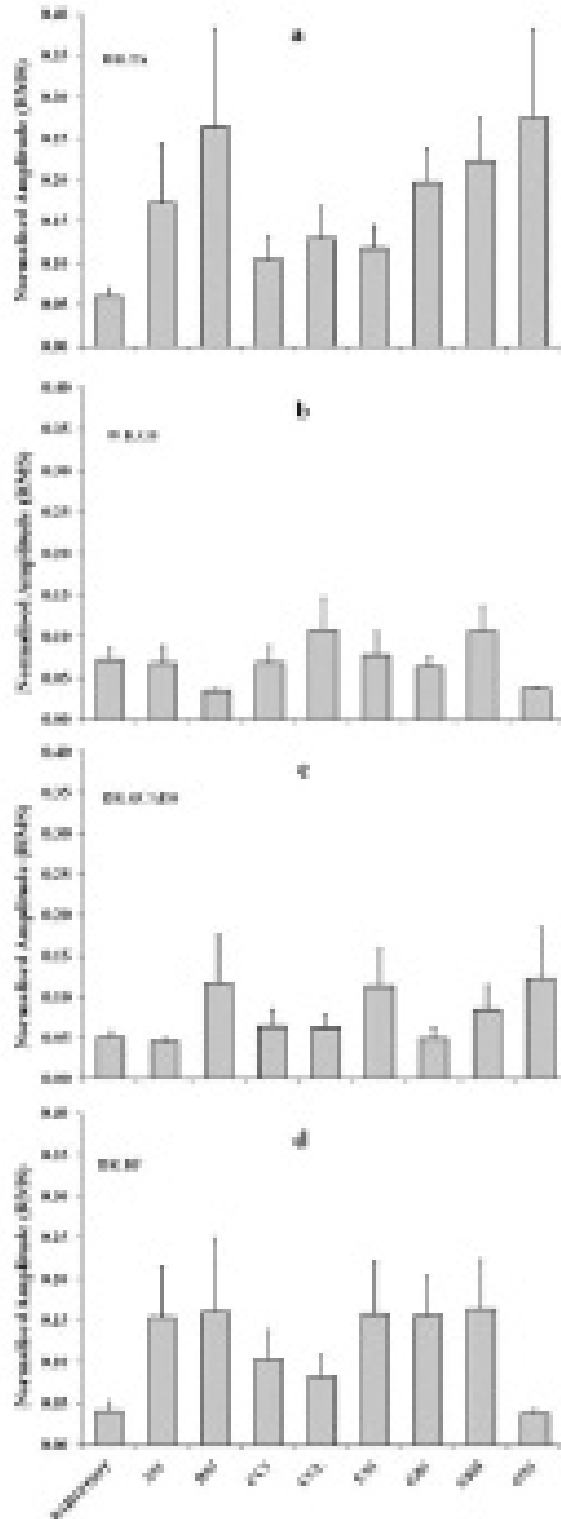
support that starting from the neutral position of a lumbar spine, the coupling of lateral flexion with rotation might be occurring in opposite directions, as evident from RMS EMG amplitudes of ABD and ES in frontal plane motion (Al-Eisa, Egan, Deluzio, & Wassersug, 2006).

The present study further revealed an efficient co-activation in agonist and antagonist muscles to adapt to the external load imposed through different types of safety shoes, with probable change in the person-shoe-ground interface. Nigg et al., (2003) showed specific changes in the intensity of muscle activation before heel strike in running shoes. Our study amply indicated that bilateral activity of the muscles under study behaved differently with the types of shoes, in comparison to barefoot standing. The muscle loads imposed with donning different shoes were not consistent during standing or walking, suggesting that changes in activation are influenced the shoe characteristics, such as, weight, material construction as regard to footwear sole, toe, toe cap, ankle height, etc. With reference to eight pairs of safety shoes investigated, high ankle shoe (CS1, weighing 1.2 Kg, PVC sole and body, and steel toe cap) resulted in significantly high muscle load (right and left TA, right GS, right QUADS, right BF, right and left TRAP) during standing.

Our results are consistent that the muscle activations during walking with shoes were manifold higher to that of barefoot walking. The bilateral TA and BF activities were about 2 to 4 times higher with safety shoes, as compared to barefoot walking. Nigg et al., (2003) postulated that the proximal muscles would be less required than the distal ones, and found that the TA activity increased more than that of BF. The authors viewed that the body reacts to changes in input signal to adapt muscle activity to reduce vibration of the soft tissues. Among other shoes analyzed in the present study, walking with high ankle shoe (BS3 weighing 1.1 Kg, double density PU sole, black Barton leather body, fibre toe cap) caused significantly higher activation bilaterally to TA,

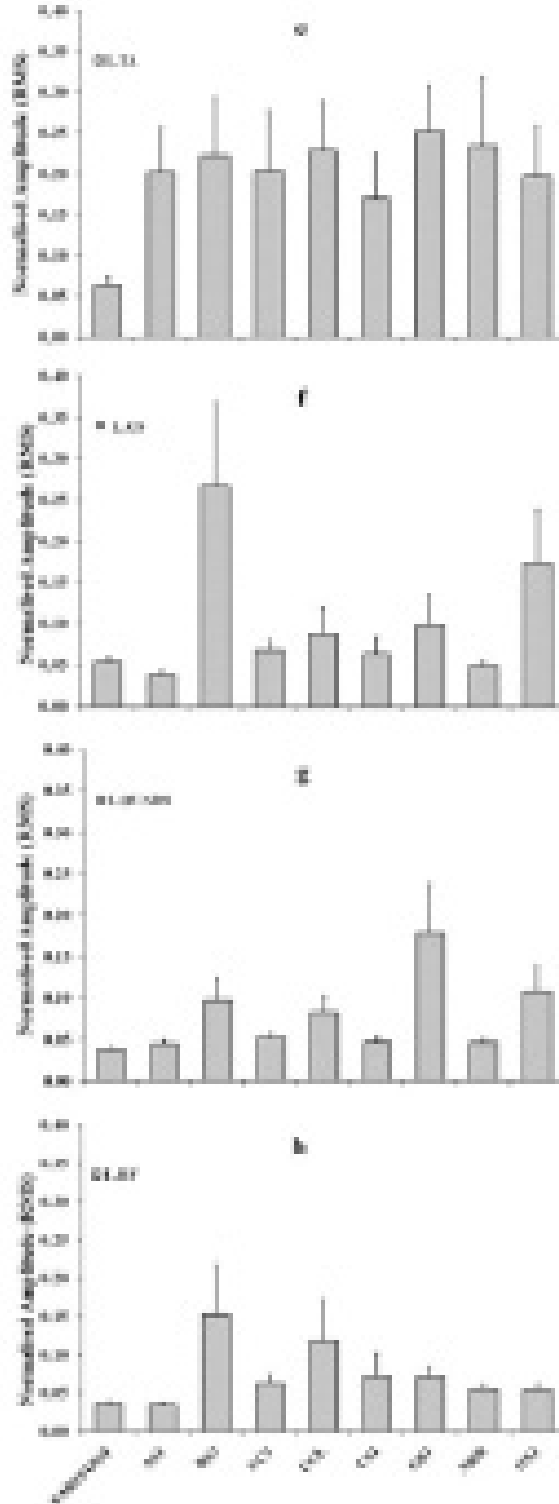
EMG Activation Pattern during Voluntary Bending and Donning Safety Shoes

Figures 7. Normalized EMG amplitude of ankle and hip joint, and trunk muscles in walking barefoot and with industrial safety shoes. Values are means \pm SEM. (R- right; L- left)



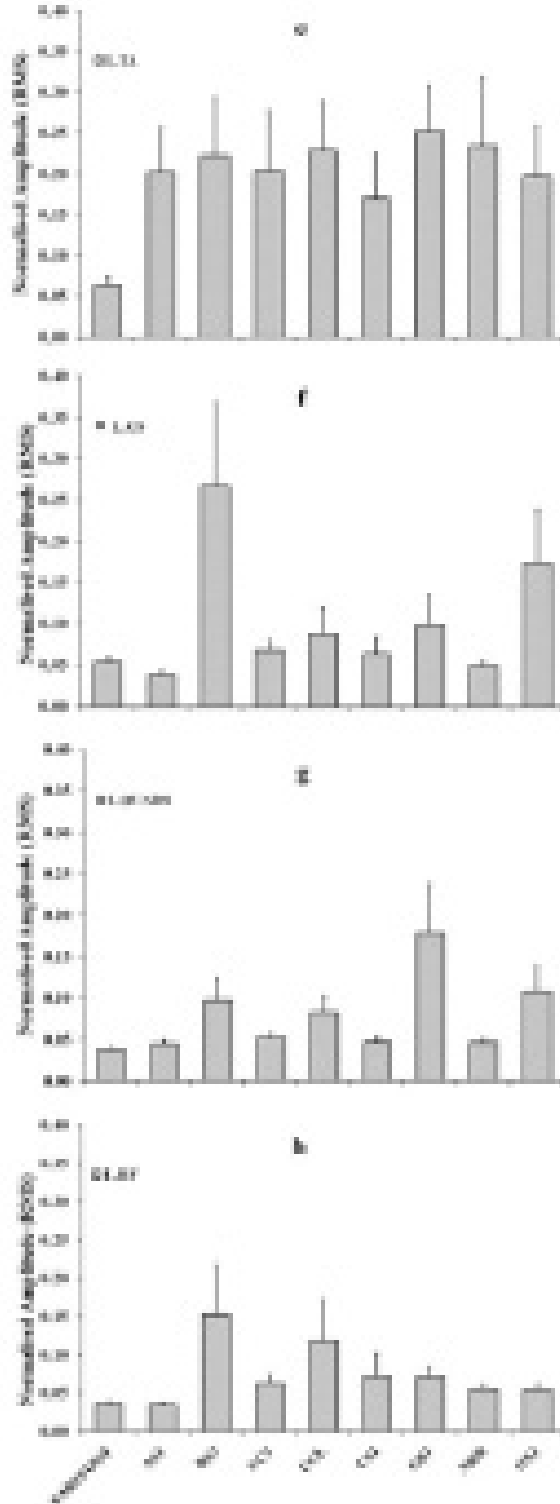
EMG Activation Pattern during Voluntary Bending and Donning Safety Shoes

Figures 8. Normalized EMG amplitude of ankle and hip joint, and trunk muscles in walking barefoot and with industrial safety shoes. Values are means±SEM. (R- right; L- left)



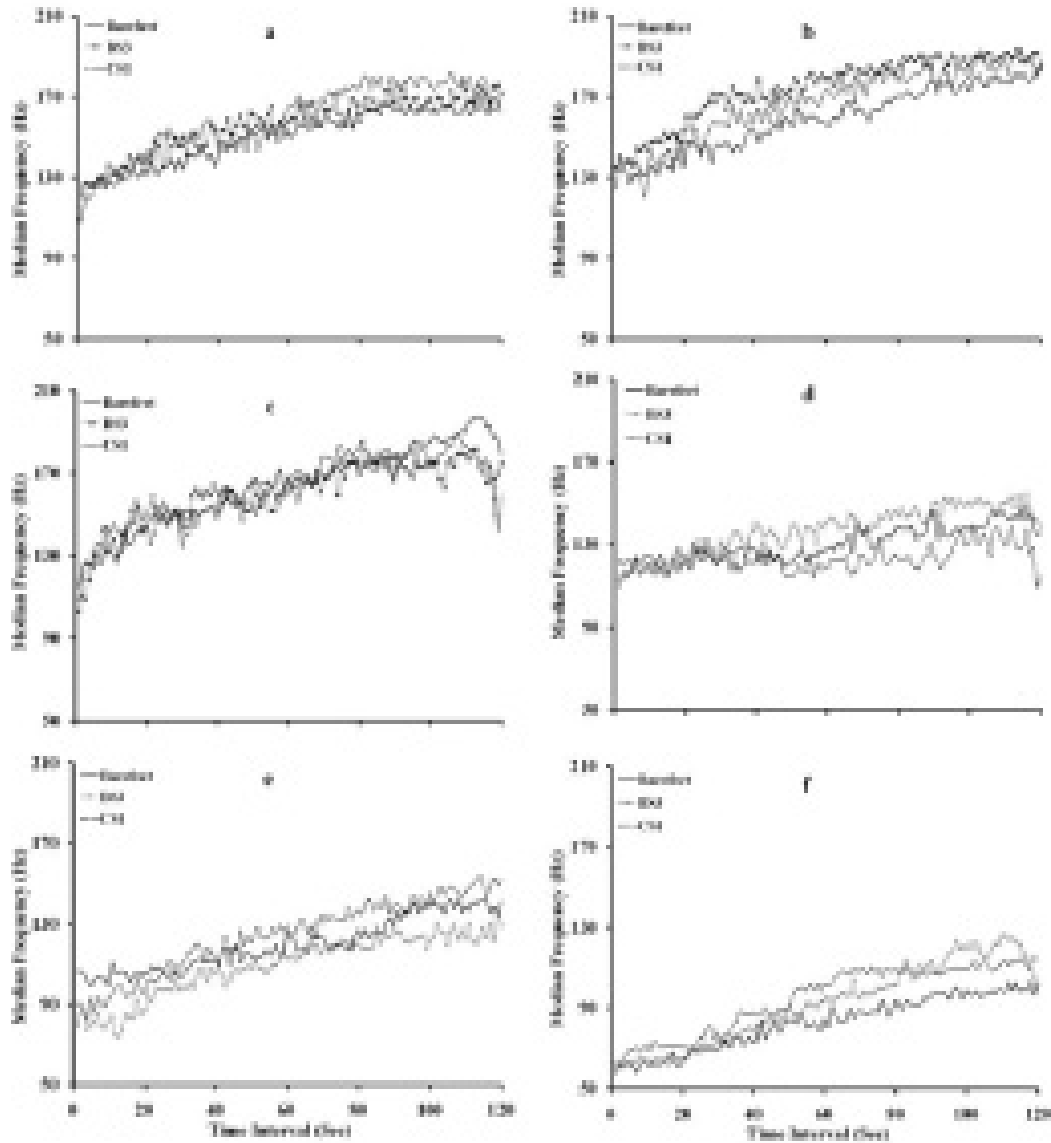
EMG Activation Pattern during Voluntary Bending and Donning Safety Shoes

Figures 9. Normalized EMG amplitude of ankle and hip joint, and trunk muscles in walking barefoot and with industrial safety shoes. Values are means \pm SEM. (R- right; L- left)



EMG Activation Pattern during Voluntary Bending and Donning Safety Shoes

Figures 10. Time trend of MDF of EMG of (a) *Tibialis anterior*, (b) *Gastrocnemius*, (c) *Quadriceps*, and (d) *Bicep femoris*, (e) *Erector spinae* and (f) *Trapezius* during standing barefoot and with safety shoes (type: BS3 and CS1)



EMG Activation Pattern during Voluntary Bending and Donning Safety Shoes

BF, QUADS, and also GS. Other high ankle shoes, such as GB1 (gum boot), NRH and OX1 exerted significantly high load on the TA, QUADS, BF, GS, and also on ES, emphasizing that trunk and muscles of hip and ankle contributed in characteristic manner to adapting the external demand arising from donning of different safety shoes.

Several indicators of muscle fatigue, e.g., increase in EMG signal amplitude expressed as RMS EMG, downward shifts in mean and median frequency, and upper frequency limit, decrease in zero crossings, increase in tremor in the frequency domain and physiological response, decrease in force generating capacity and subjective response have been described. Researchers have viewed that the median frequency of EMG (MDF) derived from Fast Fourier Transform on epochs of EMG data, is a more reproducible measure of muscle fatigue than the mean frequency (Al-Mulla, Sepulveda, & Colley, 2011; Oskoei & Hu, 2008; Phinyomark, Limsakul, & Phukpattaranont, 2009) As shown in Figure 6, the MDF values of muscles tended to build-up over the sampling duration, indicating recruitment of motor units during stance, either barefoot or with safety shoes. The MDF values of ankle joint (TA and GS) varied between 120 to 190 Hz, hip joint (quadriceps and bicep femoris) between 110 to 200 Hz, and trunk (erector spinae and trapezius) between 60 to 150 Hz), respectively. The gradual plateau phase of the MDF values of BF might suggest the ensuing trend of fatigue during standing with CS1 safety shoe.

In the overall analysis of the present study, the voluntary bending movements to the critical limit of stability exhibited characteristic behaviour in muscle activation. The trunk muscles (erector spinae and obliquus abdominis) manifested typical synergy for spinal coupling, i.e., trunk axial rotation and lateral flexion. During anterior-posterior movement in the sagittal plane, the muscles of the left ankle joints (TA and GS) had relatively higher activation in comparison to the right side. At the hip joint, the quadriceps showed dominance in activation in forward and lateral bending. As

an extrinsic variable, the shoe characteristics (industrial safety shoes) exerted extra demand on the muscles and joints in maintaining stance or during walking. The extent of muscle loading and fatigue due to the characteristics of shoes has the potential to influence the synchrony of the sensory-motor system. Our analysis with eight pair of shoes indicated that the design characteristics significantly modified muscle activation and fatigue (Wakeling, et al., 2003). Among other shoes, high ankle shoes (namely, BS3 and CS1) caused higher dominance of muscle activation during standing and walking, which in turn might alter the postural control and cause body instability.

CONCLUSION

Intrinsic and extrinsic mechanisms for sensory-motor integration are pivotal to postural control. The present findings emphasize on the muscular co-activation during voluntary bending in anterior-posterior and lateral direction to the critical points of stability. Data on excursion limits, optimized over a larger sample size, have essential utility in the ergonomics of workplace design. The study further highlights that the shoe characteristics (industrial safety shoes), as extrinsic factors, exert demand differently on the muscles either in maintaining stance or during walking. The extent of muscle loading and fatigue has the potential to affect the synchrony of the sensory-motor system that makes industrial safety shoes as the cause for slips, trips and falls. The features like heavy weight, steel toe cap, and shoes with high ankle had distinctive influence on the pattern of muscular recruitment and loading, attributing to movement restriction and discomforts of the wearer. The study findings have implication regarding the viability of muscle adaptability as a putative postural control in preventing postural instability and avoiding injuries.

REFERENCES

- Al-Eisa, E., Egan, D., Deluzio, K., & Wassersug, R. (2006). Effects of pelvic asymmetry and low back pain on trunk kinematics during sitting: A comparison with standing. *Spine*, *31*(5), 135–143. doi:10.1097/01.brs.0000201325.89493.5f PMID:16508537
- Al-Mulla, M. R., Sepulveda, F., & Colley, M. (2011). A review of non-invasive techniques to detect and predict localised muscle fatigue. *Sensors (Basel, Switzerland)*, *11*(4), 3545–3594. doi:10.3390/s110403545 PMID:22163810
- Allen, T., & Proske, U. (2006). Effect of muscle fatigue on the sense of limb position and movement. *Experimental Brain Research*, *170*(1), 30–38. doi:10.1007/s00221-005-0174-z PMID:16328298
- Allum, J., Bloem, B., Carpenter, M., Hulliger, M., & Hadders-Algra, M. (1998). Proprioceptive control of posture: A review of new concepts. *Gait & Posture*, *8*(3), 214–242. doi:10.1016/S0966-6362(98)00027-7 PMID:10200410
- Brumagne, S., Cordo, P., & Verschueren, S. (2004). Proprioceptive weighting changes in persons with low back pain and elderly persons during upright standing. *Neuroscience Letters*, *366*(1), 63–66. doi:10.1016/j.neulet.2004.05.013 PMID:15265591
- Carver, S., Kiemel, T., & Jeka, J. J. (2006). Modeling the dynamics of sensory reweighting. *Biological Cybernetics*, *95*(2), 123–134. doi:10.1007/s00422-006-0069-5 PMID:16639582
- Chang, W. R., & Grönqvist, R. (2003). *Measuring slipperiness: Human locomotion and surface factors*. Boca Raton, FL: CRC Press. doi:10.4324/9780203301913
- Chvatal, S. A., Torres-Oviedo, G., Safavynia, S. A., & Ting, L. H. (2011). Common muscle synergies for control of center of mass and force in nonstepping and stepping postural behaviors. *Journal of Neurophysiology*, *106*(2), 999–1015. doi:10.1152/jn.00549.2010 PMID:21653725
- Gage, W. H., Winter, D. A., Frank, J. S., & Adkin, A. L. (2004). Kinematic and kinetic validity of the inverted pendulum model in quiet standing. *Gait & Posture*, *19*(2), 124–132. doi:10.1016/S0966-6362(03)00037-7 PMID:15013500
- Gollhofer, A., & Komi, P. (1987). Measurement of man-shoe-surface interaction during locomotion. *Medicine and Sport Science*, *26*.
- Hermens, H. J., Freriks, B., Disselhorst-Klug, C., & Rau, G. (2000). Development of recommendations for SEMG sensors and sensor placement procedures. *Journal of Electromyography and Kinesiology*, *10*(5), 361–374. doi:10.1016/S1050-6411(00)00027-4 PMID:11018445
- Hsiao, H., & Simeonov, P. (2001). Preventing falls from roofs: A critical review. *Ergonomics*, *44*(5), 537–561. doi:10.1080/00140130110034480 PMID:11345496
- ICMR. (2000). *Ethical guidelines for biomedical research on human subject* (pp. 1–77). New Delhi, India: Indian Council of Medical Research.
- Lieberman, D. E., Venkadesan, M., Werbel, W. A., Daoud, A. I., D’Andrea, S., Davis, I. S., & Pitsiladis, Y. (2010). Foot strike patterns and collision forces in habitually barefoot versus shod runners. *Nature*, *463*(7280), 531–535. doi:10.1038/nature08723 PMID:20111000
- Miller, S. A., Mayer, T., Cox, R., & Gatchel, R. J. (1992). Reliability problems associated with the modified Schober technique for true lumbar flexion measurement. *Spine*, *17*(3), 345–348. doi:10.1097/00007632-199203000-00017 PMID:1533063

Nigg, B. (2009). Biomechanical considerations on barefoot movement and barefoot shoe concepts. *Footwear Science*, 1(2), 73–79. doi:10.1080/19424280903204036

Nigg, B., & Wakeling, J. (2001). Impact forces and muscle tuning: A new paradigm. *Exercise and Sport Sciences Reviews*, 29(1), 37–41. doi:10.1097/00003677-200101000-00008 PMID:11210446

Nigg, B. M., Bahlsen, A. H., Denoth, J., Luethi, S. M., & Stacoff, A. (1986). Factors influencing kinetic and kinematic variables in tuning. In B. Nigg (Ed.), *Biomechanics of running shoes*. Champaign, IL: Human Kinetics Publishers.

Nigg, B. M., Stefanyshyn, D., Cole, G., Stergiou, P., & Miller, J. (2003). The effect of material characteristics of shoe soles on muscle activation and energy aspects during running. *Journal of Biomechanics*, 36(4), 569–575. doi:10.1016/S0021-9290(02)00428-1 PMID:12600347

Oskoei, M. A., & Hu, H. (2008). Support vector machine-based classification scheme for myoelectric control applied to upper limb. *IEEE Transactions on Bio-Medical Engineering*, 55(8), 1956–1965. doi:10.1109/TBME.2008.919734 PMID:18632358

Phinyomark, A., Limsakul, C., & Phukpattaranont, P. (2009). *A novel feature extraction for robust EMG pattern recognition*. Retrieved from <http://arxiv.org/ftp/arxiv/papers/0912/0912.3973.pdf>

Wakeling, J. M., Pascual, S. A., & Nigg, B. M. (2002). Altering muscle activity in the lower extremities by running with different shoes. *Medicine and Science in Sports and Exercise*, 34(9), 1529–1532. doi:10.1097/00005768-200209000-00021 PMID:12218750

Winter, D. A. (1995). Human balance and posture control during standing and walking. *Gait & Posture*, 3(4), 193–214. doi:10.1016/0966-6362(96)82849-9

Wunderlich, R. E., & Cavanagh, P. R. (2001). Gender differences in adult foot shape: Implications for shoe design. *Medicine and Science in Sports and Exercise*, 33(4), 605–611. doi:10.1097/00005768-200104000-00015 PMID:11283437

ADDITIONAL READING

For a thorough and extensive understanding of other different aspects the following works help the reader: Alexandrov, A. V., Frolov, A. A., & Massion, J. (2001). Biomechanical analysis of movement strategies in human forward trunk bending. I. Modeling. *Biological Cybernetics*, 84(6), 425–434. doi:10.1007/PL00007986 PMID:11417054

Alexandrov, A. V., Frolov, A. A., & Massion, J. (2001). Biomechanical analysis of movement strategies in human forward trunk bending. II. *Experimental study*. *Biological Cybernetics*, 84(6), 435–443. doi:10.1007/PL00007987 PMID:11417055

Aruin, A. S. (2006). The effect of asymmetry of posture on anticipatory postural adjustments. *Neuroscience Letters*, 401(1), 150–153. doi:10.1016/j.neulet.2006.03.007 PMID:16569481

Borg, F., Finell, M., Hakala, I., & Herrala, M. (2007). Analyzing gastrocnemius EMG-activity and sway data from quiet and perturbed standing. *Journal of Electromyography and Kinesiology*, 17(5), 622–634. doi:10.1016/j.jelekin.2006.06.004 PMID:16890458

Callaghan, J. P., & McGill, S. M. (2001). Low back joint loading and kinematics during standing and unsupported sitting. *Ergonomics*, 44(3), 280–294. doi:10.1080/00140130118276 PMID:11219760

- Carpenter, M. G., Frank, J. S., Silcher, C. P., & Peysar, G. W. (2001). The influence of postural threat on the control of upright stance. *Experimental Brain Research*, 138(2), 210–218. doi:10.1007/s002210100681 PMID:11417462
- Cham, R., & Redfern, M. S. (2001). Effect of flooring on standing comfort and fatigue. *Human Factors: The Journal of the Human Factors and Ergonomics Society*, 43(3), 381–391. doi:10.1518/001872001775898205 PMID:11866194
- Dolan, P., & Adams, M. A. (1993). The relationship between EMG activity and extensor moment generation in the erector spinae muscles during bending and lifting activities. *Journal of Biomechanics*, 26(4), 513–522. doi:10.1016/0021-9290(93)90013-5 PMID:8478353
- Fransson, P. A., Gomez, S., Patel, M., & Johansson, L. (2007). Changes in multi-segmented body movements and EMG activity while standing on firm and foam support surfaces. *European Journal of Applied Physiology*, 101(1), 81–89. doi:10.1007/s00421-007-0476-x PMID:17503068
- Hansen, L., Winkel, J., & Jørgensen, K. (1998). Significance of mat and shoe softness during prolonged work in upright position: based on measurements of low back muscle EMG, foot volume changes, discomfort and ground force reactions. *Applied Ergonomics*, 29(3), 217–224. doi:10.1016/S0003-6870(97)00062-8 PMID:9676339
- Jorgensen, K., Hansen, L., Lundager, K., & Winkel, J. (1993). Low back muscle reactions to constrained standing in relation to shock absorbing properties of floor and shoes. *Advances in industrial ergonomics and safety*, 279–283.
- King, P. M. (2002). A comparison of the effects of floor mats and shoe in-soles on standing fatigue. *Applied Ergonomics*, 33(5), 477–484. doi:10.1016/S0003-6870(02)00027-3 PMID:12236657
- Landry, S. C., Nigg, B. M., & Tecante, K. E. (2010). Standing in an unstable shoe increases postural sway and muscle activity of selected smaller extrinsic foot muscles. *Gait & Posture*, 32(2), 215–219. doi:10.1016/j.gaitpost.2010.04.018 PMID:20547062
- Lee, C. M., Jeong, E. H., & Freivalds, A. (2001). Biomechanical effects of wearing high-heeled shoes. *International Journal of Industrial Ergonomics*, 28(6), 321–326. doi:10.1016/S0169-8141(01)00038-5
- McGill, S. M. (1992). A myoelectrically based dynamic three-dimensional model to predict loads on lumbar spine tissues during lateral bending. *Journal of Biomechanics*, 25(4), 395–414. doi:10.1016/0021-9290(92)90259-4 PMID:1533860
- Nigg, B. M., MacIntosh, B. R., & Mester, J. (2000). *Biomechanics and biology of movement*. Human Kinetics.
- Nurse, M. A., Hulliger, M., Wakeling, J. M., Nigg, B. M., & Stefanyshyn, D. J. (2005). Changing the texture of footwear can alter gait patterns. *Journal of Electromyography and Kinesiology*, 15(5), 496–506. doi:10.1016/j.jelekin.2004.12.003 PMID:15935961
- Rietdyk, S., Patla, A. E., Winter, D. A., Ishac, M. G., & Little, C. E. (1999). Balance recovery from medio-lateral perturbations of the upper body during standing. *Journal of Biomechanics*, 32(11), 1149–1158. doi:10.1016/S0021-9290(99)00116-5 PMID:10541064
- Shumway-Cook, A., Ciol, M. A., Hoffman, J., Dudgeon, B. J., Yorkston, K., & Chan, L. (2009). Falls in the Medicare population: incidence, associated factors, and impact on health care. *Physical Therapy*, 89(4), 324–332. doi:10.2522/ptj.20070107 PMID:19228831

Shumway-Cook, A., & Woollacott, M. H. (2007). *Motor control: translating research into clinical practice*. Wolters Kluwer Health.

Stuart-Buttle, C., Marras, W. S., & Kim, J. Y. (1993, October). The influence of anti-fatigue mats on back and leg fatigue. In *Proceedings of the Human Factors and Ergonomics Society Annual Meeting* (Vol. 37, No. 10, pp. 769-773). SAGE Publications.

Thomas, K., & Lee, R. Y. (2000). Fatigue of abdominal and paraspinal muscles during sustained loading of the trunk in the coronal plane. *Archives of Physical Medicine and Rehabilitation*, 81(7), 916–920. doi:10.1053/apmr.2000.5577 PMID:10896004

Wakeling, J. M., Pascual, S. A., & Nigg, B. M. (2002). Altering muscle activity in the lower extremities by running with different shoes. *Medicine and Science in Sports and Exercise*, 34(9), 1529–1532. doi:10.1097/00005768-200209000-00021 PMID:12218750

Winter, D. A., Patla, A. E., Ishac, M., & Gage, W. H. (2003). Motor mechanisms of balance during quiet standing. *Journal of Electromyography and Kinesiology*, 13(1), 49–56. doi:10.1016/S1050-6411(02)00085-8 PMID:12488086

Winter, D. A., Patla, A. E., Rietdyk, S., & Ishac, M. G. (2001). Ankle muscle stiffness in the control of balance during quiet standing. *Journal of Neurophysiology*, 85(6), 2630–2633. PMID:11387407

Woollacott, M. H., & Shumway-Cook, A. (1990). Changes in posture control across the life span—a systems approach. *Physical Therapy*, 70(12), 799–807. PMID:2236223

KEY TERMS AND DEFINITIONS

Electromyography: Closely associated with the generation of force by a muscle, is the generation of an electrical signal that can be observed by placing electrodes on the skin surface to detect underlying electrical activity displaying the associated waveform on a computer monitor. This process is called electromyography (EMG) and the waveform is the electromyogram.

Industrial Safety Shoes: Occupational Safety and Health Administration (OSHA) defines and describes safety shoes in their regulations as the most common type of foot “Personal Protective Equipment (PPE)” that provides many different ways of protecting the workers’ feet, such as from heat, impact, or electrical shock.

Limits of Stability (LOS): Boundaries of an area of space in which the body can maintain its position without changing its base of support (BOS).

Muscular Load: The extra demand of the force of contraction which is superimposed on the muscle to perform an action or overcome the resistance (ground reaction force, frictional force, external load etc.) which is mostly accomplished by recruitment of more motor units.

Postural Stability: The ability to maintain or control the center of mass (COM) in relation to the base of support (BOS) to prevent falls and complete desired movements.

Spinal Loading: Generated by a combination of body weight, muscle activity, pre-tension in ligament and external forces which might also result due to maintenance or alterations in the body postures.

Voluntary Bending: In the context of the experiment, voluntary bending is forward and backward movement of the body in the sagittal plane and right & left lateral bending in frontal

EMG Activation Pattern during Voluntary Bending and Donning Safety Shoes

plane within stability limits and keeping both the feet fix to the ground.

Chapter 12

Tongue Movement Estimation Based on Suprahyoid Muscle Activity

Makoto Sasaki
Iwate University, Japan

ABSTRACT

The motor function of the tongue often remains intact even in cases of severe movement paralysis. Therefore, tongue movements offer great potential for the design of highly efficient human-machine interfaces for alternative communication and control. This chapter introduces a novel method for tongue movement estimation based on analysis of surface electromyography (EMG) signals from the suprahyoid muscles, which usually function to open the mouth and to control the hyoid position.

1. INTRODUCTION

To support independent living of people with severe quadriplegia caused by cervical cord injury or muscular dystrophy, it is important to understand one's intention from biological signals that can be measured noninvasively. Electroencephalography (Wolpaw et al., 2002; Scherer et al., 2004), head movement (Harwin et al., 1990; Nguyen et al., 2004), jaw movement (Jacobs et al., 1997; Niikawa et al., 2006), eye movement (LaCourse et al., 1990; Duchowski, 2002), voice (Clark et al., 1977; Simpson et al., 2002), and breathing have all been used for the communication of intentions by people with severe dis-

abilities. Each intention-communication method entails benefits and shortcomings. For example, although the social expectations for implementing electroencephalography are high, its use requires high levels of concentration over long periods in real-life environments, where a person receives various external stimuli. Although voluntary movements of the head and jaw can readily express one's intentions, they might not be applicable to a person with cervical cord injury because of insufficient cervical stability. Furthermore, although intention communication by eye movement or voice is effective under environments in which external disturbances are removed or controlled to the greatest extent possible, precise isolation and

DOI: 10.4018/978-1-4666-6090-8.ch012

extraction of these signals is difficult when, for example, one is driving an electric wheelchair in an urban setting. Examining many methods of intention communication including those described above, we must develop them and improve their precision to prepare several alternatives that are readily applicable and which are convenient for individuals with various disabilities.

Against this background, intentional tongue movement is attracting attention in recent years. The motor function of the tongue often remains intact even in cases of severe movement paralysis. Therefore, tongue movements offer great potential for the design of novel highly efficient human-machine interfaces for alternative communication and control. Numerous approaches for deriving control signals from intentional tongue motions have been proposed: detection of the tongue position via measurement of magnetic fields of a permanent magnet attached to the tongue (Sonoda, 1974; Huo et al., 2008), detection of lingual proximity by light-emitting diodes and photodiodes placed on an artificial palate plate (Wrench et al., 1998; Saponas et al., 2009), measurement of the tongue force applied to a force sensor array mounted on an artificial palate plate (Ichinose et al., 2003; Terashima et al., 2010), and direct tongue manipulation of a joystick or switch inserted into the oral cavity (Niikawa et al., 2006). However, such methods require the insertion of a measuring instrument into the oral cavity, which entails certain risks and discomfort to the patient such as increased psychological stress, oral health problems, obstruction of speaking and drinking, battery fluid leakage, electric shock, and suffocation by accidental ingestion. Therefore, we have been developing a novel intention-communication method based on surface electromyography (EMG) signals (Sasaki et al., 2012a, 2012b, 2013a, 2013b).

Today, EMG signals are used widely for pattern recognition of human motions such as hand motions (Englehart et al., 2001, 2003; Zecca et

al., 2002; Kiguchi et al., 2008; Naik, et al., 2010). The same approach is applicable to the estimation of tongue movements without inserting a measuring instrument into the oral cavity. Tongue motions result from contractions of lingual muscles. However, the detection of the EMG activities of the lingual muscles requires the installation of surface electrodes or needle electrodes within the oral cavity, which can entail severe difficulties for the practical application of such approaches. For that reason, we have specifically examined surface EMG signals that are observable at the underside of the jaw. Such electromyograms include signal components related to the activity of the suprahyoid muscles, the function of which is to open the mouth and to control the position of the hyoid (base of the tongue) when the tongue moves. This chapter introduces a novel method for tongue movement estimation based on the analysis of EMG signals from suprahyoid muscles.

2. TONGUE MOVEMENT MECHANISM

Tongue movements are produced by the coordinated actions of the lingual muscles, which include the intrinsic muscles of the tongue (superior longitudinal muscle of tongue, inferior longitudinal muscle of tongue, transverse muscle of the tongue, vertical muscle of tongue) and extrinsic muscles of the tongue (genioglossus muscle, styloglossus muscle, hyoglossus muscle, palatoglossus muscle) (Figure 1) (Ide et al., 2004). The intrinsic muscles of the tongue control the tongue shape and the direction of tongue tip, and the extrinsic muscles of the tongue control the tongue position in anterior direction and move the tongue downward and backward. Detection of the EMG activities of the lingual muscles requires the installation of surface electrodes or needle electrodes within the oral cavity. For that reason, we decided to examine the EMG signals

of the suprahyoid muscles specifically (digastric muscle, stylohyoid muscle, mylohyoid muscle, and geniohyoid muscle), which are observable at the underside of the jaw. The primary function of the suprahyoid muscles is to open the mouth or to initiate swallowing movements. However, some of these muscles also support the hyoid (base of the tongue) during tongue movement and the EMG signals measured at the underside of the jaw change when the tongue position changes. That fact is useful for estimation of tongue movements from the EMG signals. The mylohyoid muscle supports the hyoid when the tongue moves laterally. The geniohyoid muscle supports the hyoid when the tongue moves in anterior direction. The hyoid is supported by the stylohyoid muscle when the tongue is crimped to the palate. Coordinated voluntary tongue movements cause contractions of the suprahyoid muscles that can be detected in the surface EMG and which are useful as control commands for assistive devices.

3. FEASIBILITY STUDY OF TONGUE MOVEMENT ESTIMATION

This section presents a description of the possibility of estimating tongue movement using EMG signals of the suprahyoid muscles. The effects of multi-channel electrode configuration and physiological movements such as swallowing on the precision of estimation are evaluated.

3.1. Estimation Algorithm

An algorithm for tongue movement estimation using EMG signals of the suprahyoid muscles is presented in Figure 2. For measuring EMG signals, a multi-channel electrode with nine detection electrodes was attached to the underside of the jaw. An indifferent electrode and a detection electrode were also attached to each earlobe. EMG signals between a detection electrode at earlobe

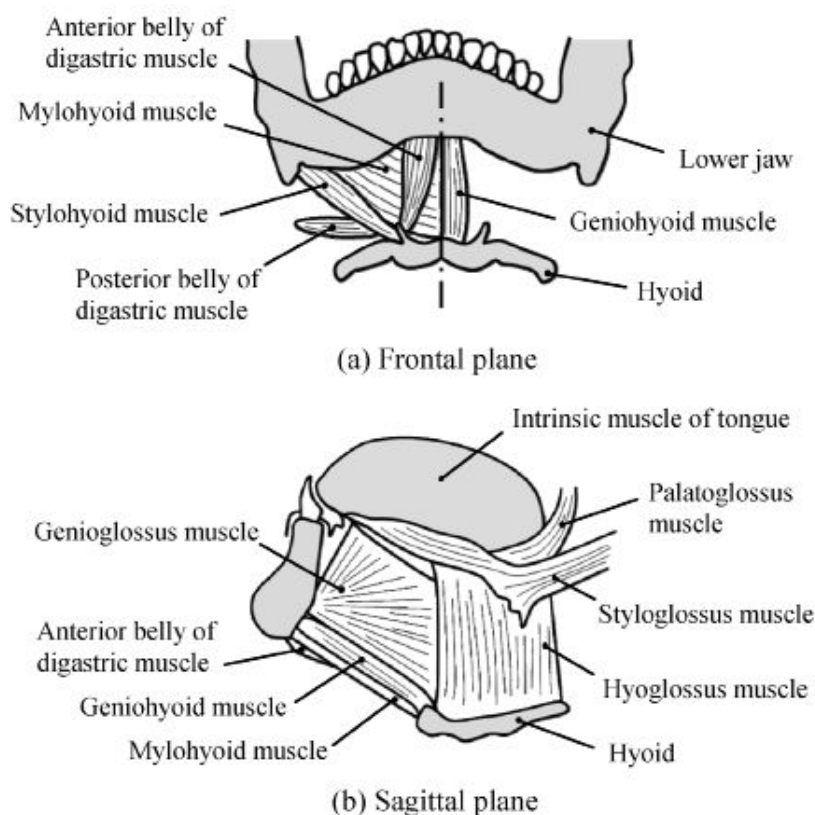
and each detection electrode at the underside of the jaw were measured using bipolar leads. The potential differences between every two signals for all combinations (${}_9C_2$) of EMG signals were calculated. By obtaining several EMG signals with different distances between electrodes, we can use for the estimation of tongue movement both the signals generated by nearby muscles (crosstalk components) and the signal with which crosstalk components were removed. Our configuration using a multi-channel electrode to measure muscle activities over the whole underside of the jaw obviates the need for professional knowledge and skill at electrode positioning. Furthermore, our configuration uses far fewer electrodes and bio-amplifiers than are generally used for bipolar leads. When we place nine electrodes at equal intervals, 36 ($= {}_9C_2$) channels of EMG signals are provided using nine bio-amplifiers. In contrast, using the general bipolar leads, four times as many bio-amplifiers are necessary to obtain similar information.

The hierarchical neural network used for pattern recognition of the tongue movement has three layers: input, middle, and output. Its inputs are the root mean square (RMS) of EMG signals of all 36 signals, which are features extracted with particular attention devoted to amplitude as

$$RMS = \sqrt{\frac{1}{n} \sum_{i=1}^n EMG^2} \quad (1)$$

where n is the smoothing number of signals. The outputs and teaching signals of neural network are information related to voluntary tongue movement, and movement identification signals such as swallowing, yawning, and mouth opening, which cause misrecognition. The weights of the connections among all neurons in the network were learned using the backpropagation learning algorithm to connect tongue movements with muscle activity of the whole underside of the jaw. Then those

Figure 1. Lingual muscles and hyoid muscles. (©2012, IEEE. Used with permission)



voluntary tongue movements which are useful for intention communication were extracted.

3.2. Measurement Conditions

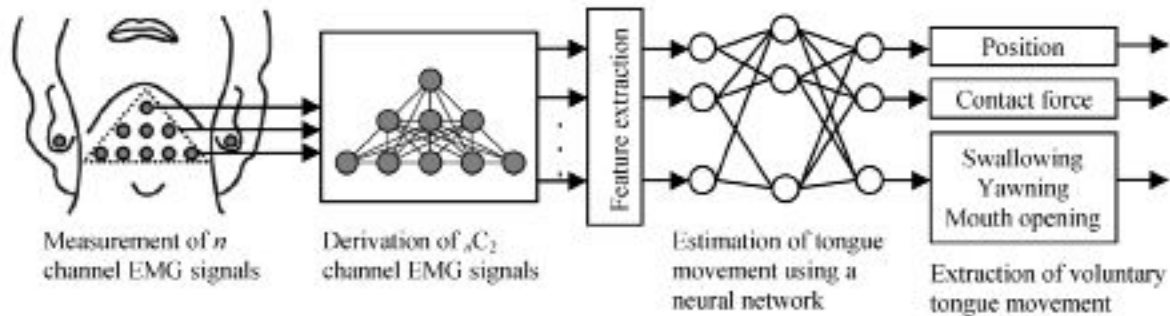
By inserting connectors of nine disposable electrodes (SMP-300; Mets Inc.) into a thin transparent sheet with nine holes 20 mm distant from each other, a multi-channel triangular electrode was prepared for the measurement of EMG signals of the suprahyoid muscles. By connecting lead electrodes (BR-331S; Nihon Kohden Corp.) to disposable electrodes, EMG signals were measured through a bio-amplifier (NB6101HS; Nabtesco Corp.) of gain 1,950. The cut-off frequencies of the bio-amplifier were 2.3 Hz for the high-pass filter and 320 Hz for the low-pass filter.

Although obtaining teaching signals for tongue positioning and contact force without inserting measuring instruments into the oral cavity is our ultimate purpose, as the first step of evaluating possibility of estimating tongue movement, we decided to measure tongue movement directly because that simplified our data processing. An upper jaw mouthpiece equipped with six thin-film force sensors (flexiforce; Nitta Corp.) 0.2 mm thick, with ϕ 9.5 mm of the force-sensitive part was produced to detect the tongue position and contact force, as depicted in Figure 3.

Teaching signals of swallowing, yawning, and mouth opening were defined as voltage signals to identify each action. Push-button switches were produced to output DC 5 V synchronized signals corresponding to those actions. In addition, the EMG signals of the suprahyoid muscles and

Tongue Movement Estimation Based on Suprahyoid Muscle Activity

Figure 2. Tongue position and contact force estimation algorithm. (©2012, IEEE. Used with permission)



teaching signals were measured simultaneously at a sampling frequency of 2,000 Hz through an analog-to-digital converter (AIO-163202FX-USB; Contec Co. Ltd.).

The subjects of this experiment were three healthy men with normal tongue function (22.3 ± 0.6 years old, 169.3 ± 5.1 cm, 66.0 ± 7.9 kg, mean \pm SD). They were examined using a multi-channel electrode and a mouthpiece carrying sensors for the upper jaw.

Each subject pushed the three positions of “right,” “left,” and “front,” as depicted in Figure 3 with the tongue tip for one second in sequence. They repeated these voluntary activities four times. Subjects were asked to perform intentional activities of saliva swallowing, yawning, and mouth opening while operating the push button switch to output identification signal of DC 5 V using a finger. They repeated these voluntary activities four times.

Among the four sets of measurement data, one set was used for learning neural networks. The rest were used for tongue movement estimation. The input to the neural network was the features related to the amplitude extracted from EMG signals by the root mean square (RMS). The smoothing number n was set to 200.

The output signals of the neural network were the estimated contact force of tongue when pushed to the right, left, and front sensors and the estimated identification signals corresponding to

swallowing, yawning, and mouth opening. For this study, two indices were adopted to evaluate the estimation precision. One is the correlation coefficient. The other is the root mean square (RMS) error. The closer to unity the correlation coefficient is and the closer to 0% the RMS error is, the better the precision of estimation is.

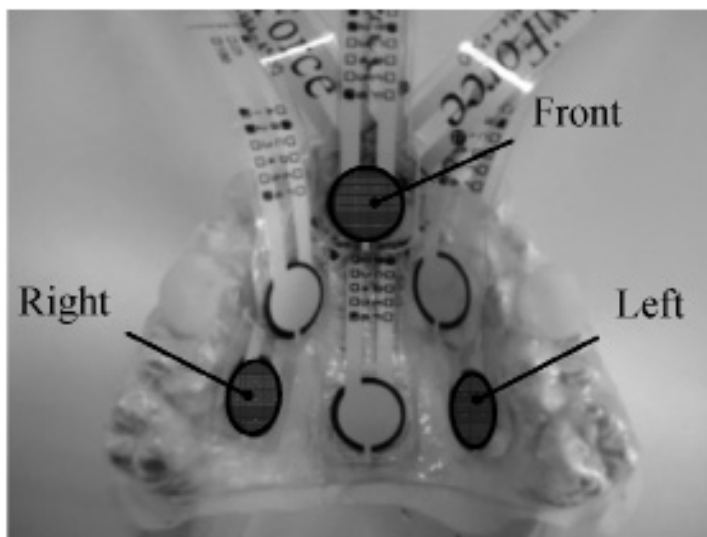
3.3. Results and Discussion

3.3.1. Effects of Electrode Configuration

When estimation precision is almost equal, the use of fewer electrodes is desired in order to reduce the burden of the wearer and the number of calculation steps. In addition, when the number of electrodes is limited, it is necessary to find optimal configuration of electrodes to obtain more features related to tongue movements. Therefore, we evaluated the precision of estimation for the configurations portrayed in Figure 4.

Of these multi-channel triangular electrode configurations from (a)-(d), (a) comprises nine electrodes (Tri-9), (b) eight electrodes (Tri-8), (c) six electrodes (Tri-6), and (d) four electrodes (Tri-4). Of those, (e) is a multi-channel rectangular electrode configuration with six electrodes (Rec-6); (f) is one with four electrodes (Rec-4). They are to be compared with Tri-6 and Tri-4. The pair of Rec-6 and Tri-6 and that of Rec-4 and Tri-4 have equal numbers of electrodes, but they have

Figure 3. Upper jaw mouthpiece equipped with six thin-film force sensors. (©2012, IEEE. Used with permission)



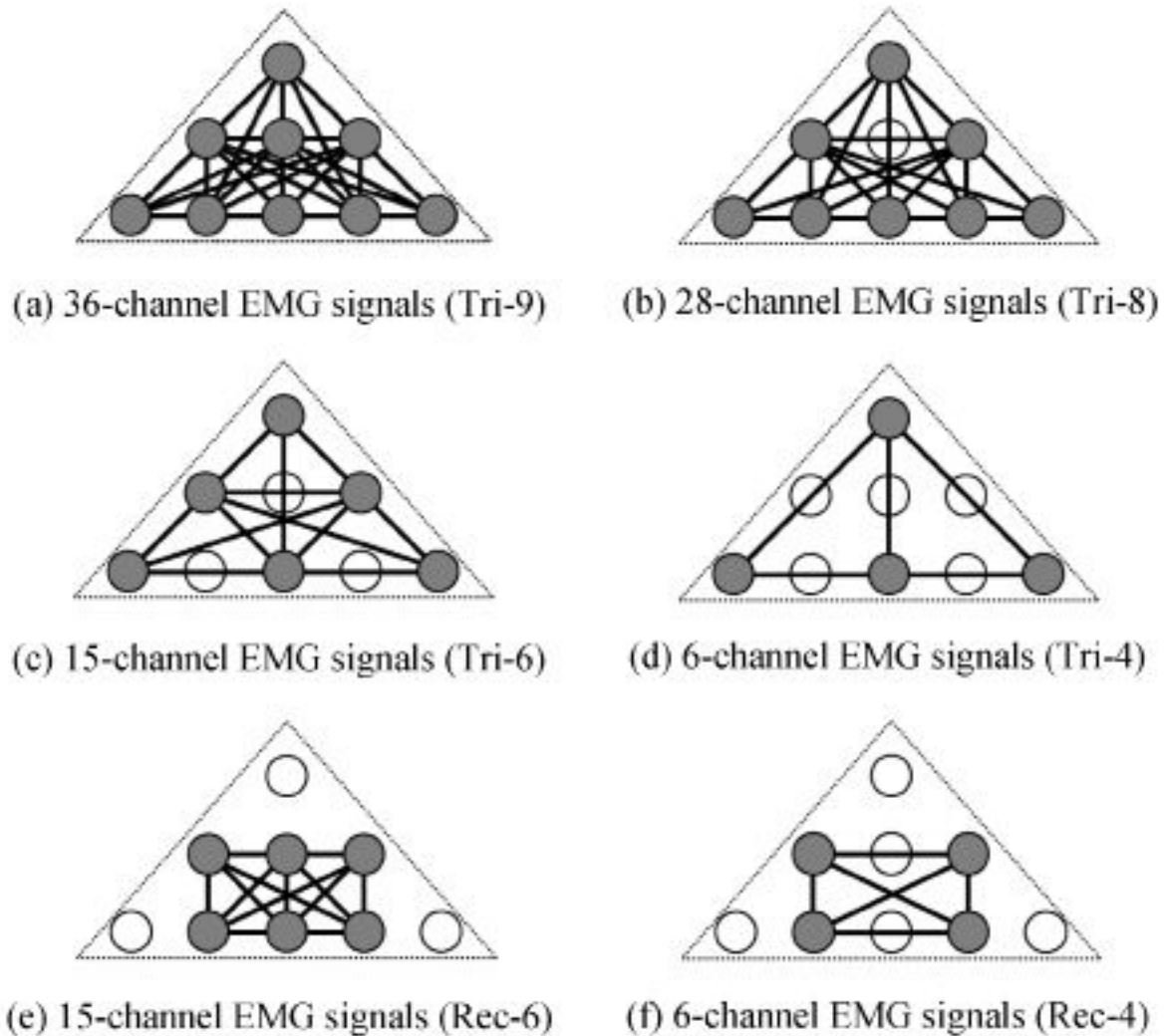
different geometries of positioning. Therefore, these pairs play an important role in examination of the effects of electrode positioning.

An example of estimating tongue movements from the electrode configuration Tri-9 is presented in Figure 5. In addition, the overall values of precision of estimating voluntary tongue movement for these three positions of right, left, and front are depicted in Figure 6. These reveal that the greater the number of electrodes in multi-channel electrodes, the greater the correlation coefficient and the smaller the RMS error. The coefficient of correlation is greater than 0.9, with RMS errors smaller than 10% for Tri-9, Tri-8, and Tri-6. These imply high precision of estimating voluntary tongue movement. In all these configurations, electrodes are arranged in a triangular shape. Results of *t*-tests for the pair of Tri-6 and Rec-6 (six electrodes) and the pair of Tri-4 and Rec-4 (four electrodes) show a significant advantage of triangular positioning over rectangular positioning for the precision of estimation (*: $p < 0.05$). Therefore, when the electrodes are fewer, they should be distributed over the whole underside of the jaw to detect crosstalk actively.

Because the usual function of suprahyoid muscles is to open the mouth and to control the hyoid position, false estimates can occur, as presented in Figure 7, during physiological motions such as swallowing, yawning, and mouth opening in neural networks that have learned to recognize voluntary tongue movement. For that reason, we added EMG signals of the suprahyoid muscles during swallowing, yawning, and mouth opening in learning procedures of neural networks to remove these false signals. By performing mask processing in estimation of voluntary tongue movement, the estimation error by swallowing, yawning, and mouth opening was reduced.

Results of mask processing for a series of movements of swallowing, yawning, and mouth opening are presented in Figure 8 for electrode configurations of Tri-9, Tri-8, and Tri-6. We applied multiple comparison of Tukey-Kramer test at each comparison, assigning a “*” mark in figures when a statistically significant difference was found ($p < 0.05$). For Tri-6, the estimation error after mask processing is significantly greater than that of other electrode configurations, yielding insufficient reduction of estimation error. In

Figure 4. Multi-channel electrodes configurations. (©2012, IEEE. Used with permission)



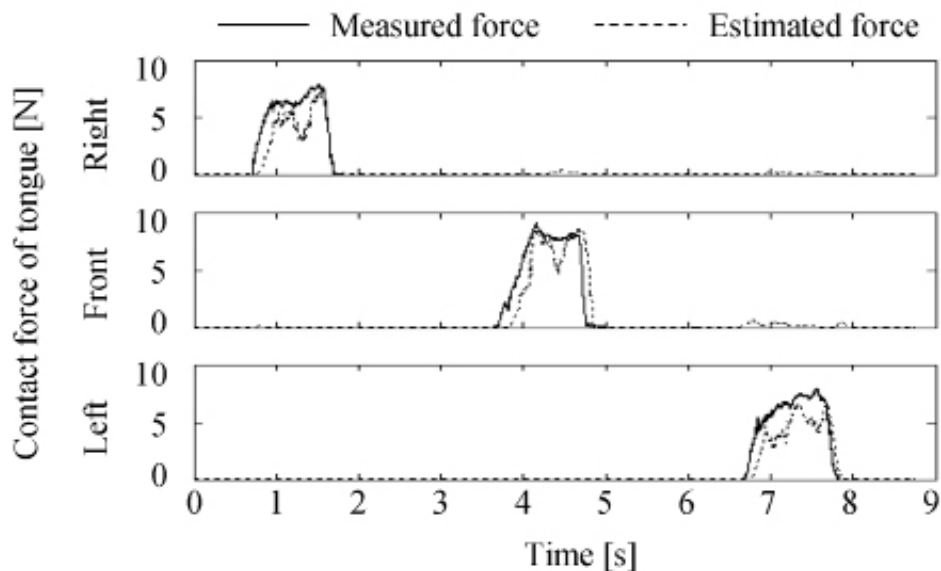
contrast, error reduction of 95% or more was obtained for Tri-9, with the greatest number of electrodes. Tri-9 showed a low RMS error of less than 1% for voluntary tongue movement after mask processing.

These results confirmed the possibility of precise extraction of only the signal of voluntary tongue movement from EMG signals of the suprahyoid muscles obtainable from the underside of the jaw.

4. ADVANCED ESTIMATION METHOD OF TONGUE MOVEMENT

The previous section presented confirmation of the feasibility of tongue movement estimation. To develop a safe and practical estimation method, we used tongue movement identification signals created artificially from the summation of RMS signals as teaching signals of the neural network instead of measurement data obtained from force sensors on the upper jaw mouthpiece. Tongue

Figure 5. Examples of tongue movement estimation using Tri-9 electrode configuration. (©2012, IEEE. Used with permission)



movements will be identifiable solely from the EMG signals of the suprahyoid muscles. This section introduces an advanced tongue movement estimation method based on principal component analysis (PCA) and artificial neural networks. Then the estimation precision and speed of this method are evaluated.

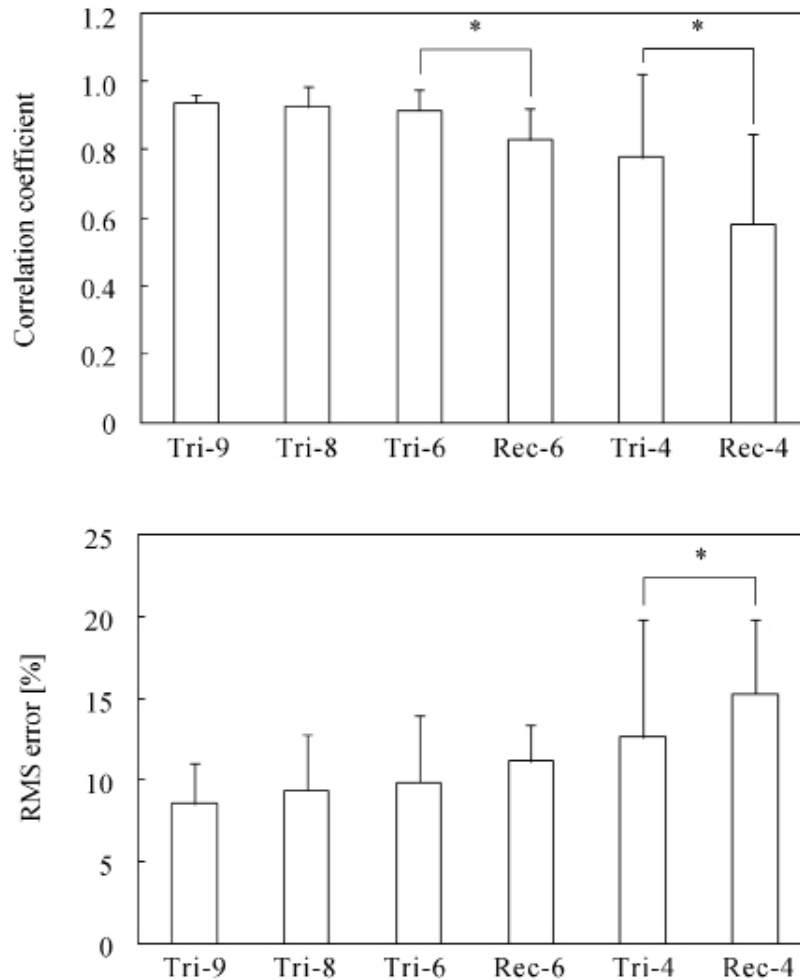
The EMG signal processing is explained below (Figure 9). The EMG signals of 36-channels were calculated using the method described in a previous section. To extract the feature quantities, the root mean square (RMS) of all 36 signals were calculated using the equation. The smoothing numbers n were set sequentially to 100, 300 and 500.

In doing so, we composed a feature quantity $Y(t) = [RMS_{100}, RMS_{300}, RMS_{500}]^t$. $Y(t)$ is 108-dimensional quantity (36 channels \times 3 values for n). The 108-dimensional feature quantity $Y(t)$ was reduced to a new, 10-dimensional quantity $Z(t)$ using PCA. The input signals to the neural network were determined from the last three sequential samples $F(t) = [Z(t), Z(t-1), Z(t-2)]$

[†]. Thereby, the tendency of time change of the feature vectors was examined. Signals used for teaching the neural network on the identifying tongue movements were generated by summation of RMS signals from all 32 channels and threshold processing. Tongue movements were linked with the feature vector $F(t)$ by adjustment of the connection weights of the neurons in the network via using a backpropagation learning algorithm. The output signals from the neural network were binarized using threshold processing. Finally, the tongue movement was determined by application of the majority rule among k recent estimations.

The subjects of this experiment were five adult men with normal tongue function (21.8 ± 0.8 years old, 169.0 ± 4.8 cm, 63.0 ± 7.0 kg, mean \pm SD). The EMG signals of suprahyoid muscles were measured for three voluntary tongue movements. Subjects were asked to push the tongue in the mouth cavity sequentially to the right, the left, and the front side. Apart from the voluntary tongue movements, the participants were also asked to perform one action of saliva swallowing. These

Figure 6. Effects of electrode configurations on estimation precision. (©2012, IEEE. Used with permission)



four measurements constituted one set of operations. Each subject was asked to perform eight sets of tasks. Each action needed to be completed within one second. Subjects were asked to rest for one second before they started the next action. The EMG signals of the suprahyoid muscles were digitalized at sampling frequency of 2,000 Hz.

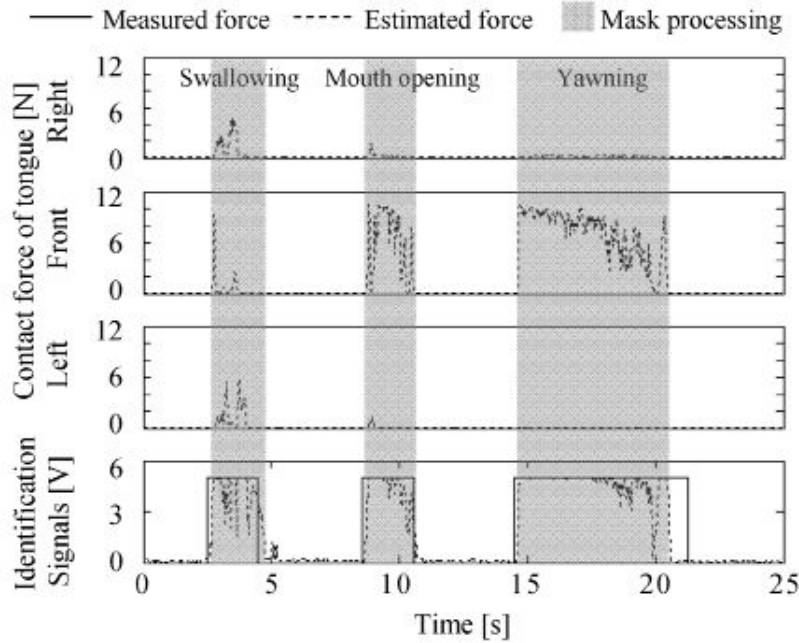
Four of these eight sets of data were used for the neural network learning processes. The remaining four sets were used for estimation of the tongue movements. The estimation precision was tested for the frame shift periods d of 0.5, 2.5, 5.0, 10,

and 25 ms. The numbers of votes for majority rule of k were 1, 5, 10, 20, and 50.

Additionally, we explored how $Y(t)$ influences the accuracy of the tongue movement estimation algorithm. For that purpose, we studied the estimation accuracy of the proposed algorithm for four values of $Y(t)$, namely: $Y(t) = RMS_{100}$, $Y(t) = RMS_{300}$, $Y(t) = RMS_{500}$, $Y(t) = [RMS_{100}, RMS_{300}, RMS_{500}]^T$.

The following two indices were used to evaluate the precision and speed of estimation of the developed algorithm.

Figure 7. Mask processing to remove false estimates caused by movements of swallowing, yawning, and mouth opening. (©2012, IEEE. Used with permission)



1. Rate of correct identification of movement (Rate of correct identification R_{ci})

$$R_{ci} = \frac{\text{Number of correct identifications}}{\text{Total number of identifications}} \times 100[\%] \quad (2)$$

2. Time from the start of the movement until the identification (Response time t_r)

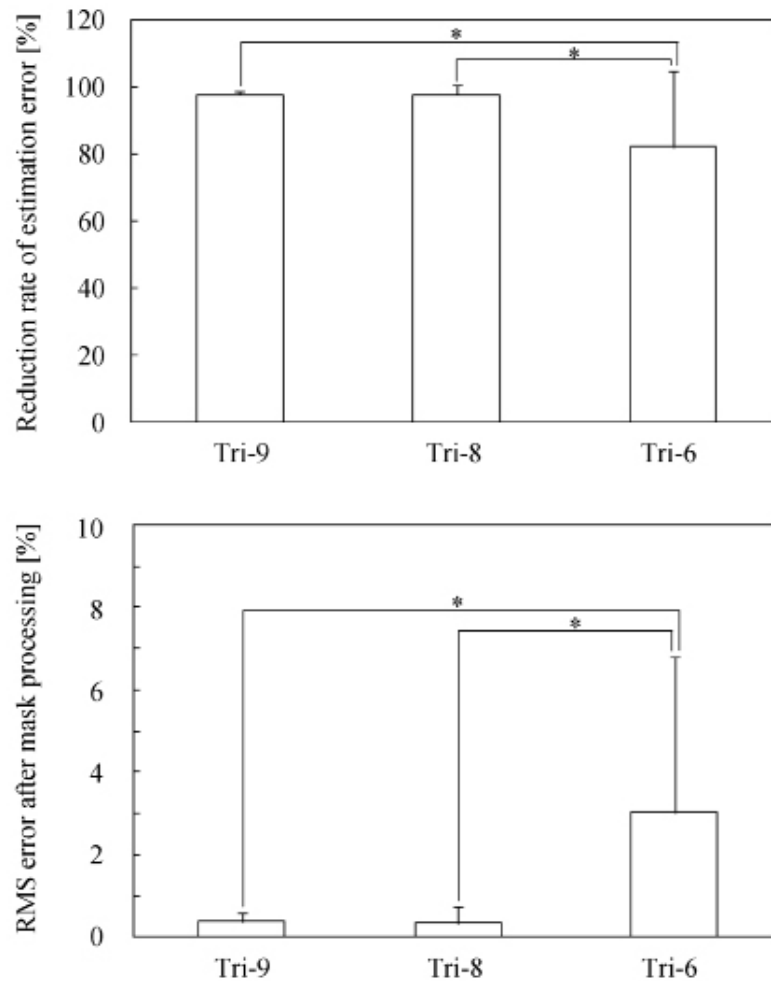
The average rates of correct identification and response times for all five subjects are presented respectively in Figures 10(a) and 10(b). Figure 11 presents the estimation results using the proposed algorithm for conditions A, B, and C in Figure 10. The increased frame shift period d and the increased number of votes for the majority rule of k indicate that the rate of correct identification was improved. As shown in the same figure, the initial rates of correct identification of 33.8% in

(C) ($d = 0.5$, $k = 1.5$), were improved to 98.8% in (A) ($d = 25$, $k = 50$). However, the response time increased from 0.04 s to 0.69 s, suggesting a tradeoff relation.

The effect of the frame shift period d was discussed previously by Kelvin et al., (2003). Our experiments also confirmed the estimation accuracy can be improved by choosing a long shift period. Although an increased number of votes for rule of majority k prolongs the response time from the start of movement to the completion of the estimation, it stabilizes the output signal and improves the estimation accuracy (Figure 10).

Table 1 presents a relation between feature quantity $Y(t)$ and accuracy of estimation (frame shift period d is 25 ms, and the quantities of votes for majority rule of k is 50). Results also show that the accuracy of estimation for RMS_{500} is higher than the accuracy of the procedure when $Y(t) = RMS_{100}$ or $Y(t) = RMS_{300}$ was used, which suggests

Figure 8. Reduction effect of estimation error by mask processing. (©2012, IEEE. Used with permission)



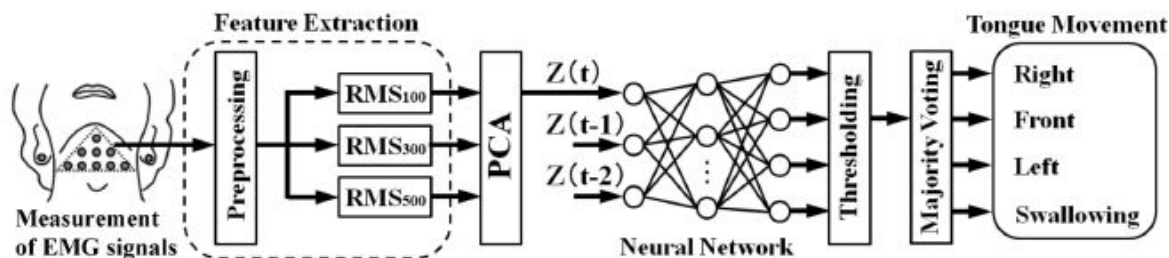
a trend by which a greater number of samplings engenders a higher accuracy of estimation. In addition, estimation by all three RMSs $Y(t) = [RMS_{100}, RMS_{300}, RMS_{500}]^T$ provided the best accuracy of estimation, with an identification rate of $98.8 \pm 2.8\%$ and response time of 0.67 ± 0.09 s.

RMS processing has the same effect as that of a low pass filter, where the degree of smoothing was determined by the number of samples n . By defining numerous signal components as feature

quantities of the EMG signals, we can attain high accuracy of estimation of the tongue motions.

Results showed that the initially obtained 108-dimensional feature quantity included signal components that do not contribute to the accuracy of estimation but which unnecessarily increase the amount of calculations. Therefore, to reduce the number of the feature quantity and to ignore the components that do not contribute to the estimation accuracy, we applied PCA to the input signal of the neural network. Although the average

Figure 9. Advanced tongue movement estimation algorithm. (©2013, IEEE. Used with permission)



response time for estimation of the tongue movements is greater than the response time of some other human motions (which is approximately 0.2 s), the accuracy and the speed of recognition of the tongue movements are sufficient for most cases of control of assistive devices by people with severe disabilities. In our future work, we intend to examine the response time and the accuracy of user's commands derived by the procedure presented herein in tasks for tongue control of assistive devices.

5. CONCLUSION

This chapter introduced a novel estimation method for voluntary tongue movements based on surface EMG signals. Although many studies using EMG signals to estimate movements of hands, legs, etc. have been reported to date, research estimating the tongue movement, as we have done, has never been reported. The main reasons are the following.

1. The relation between the muscle activity and the generated movement is complicated compared to that of a hand, a leg, etc.
2. Measurement of EMG signals of the lingual muscles, which control the position and direction of tongue tip, require the installation of surface electrodes or needle electrodes within the oral cavity, which might cause severe problems for a subject.

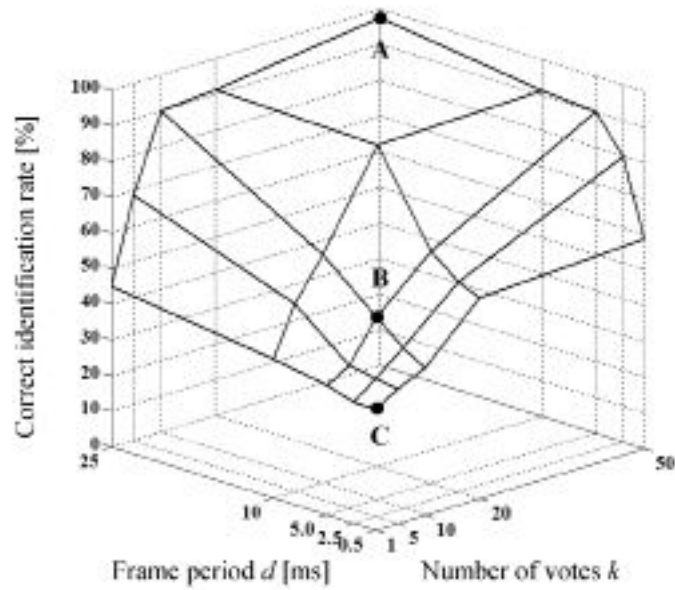
3. It has remained unknown whether tongue movement can be estimated from EMG signals of suprahyoid muscles, which function to open the mouth and to control the hyoid position (base of the tongue) or not.
4. EMG signals of the suprahyoid muscles are observed not only during voluntary movements but also during physiological movements related to swallowing or yawning. Therefore, it is necessary to isolate them and extract only those voluntary movements which are associated with intentional communication from EMG signals precisely.

Against these problems, this session demonstrated for the first time that the proposed method enables the precise estimation of the tongue movements and that it can identify the voluntary movement and the physiological movement respectively with identification rate greater than 98%. However, the following examinations are necessary for reduction of the calculation time and for an increase in the number of tongue movements that are classifiable as necessary to control assistive devices such as intention-communication devices and electric wheelchairs.

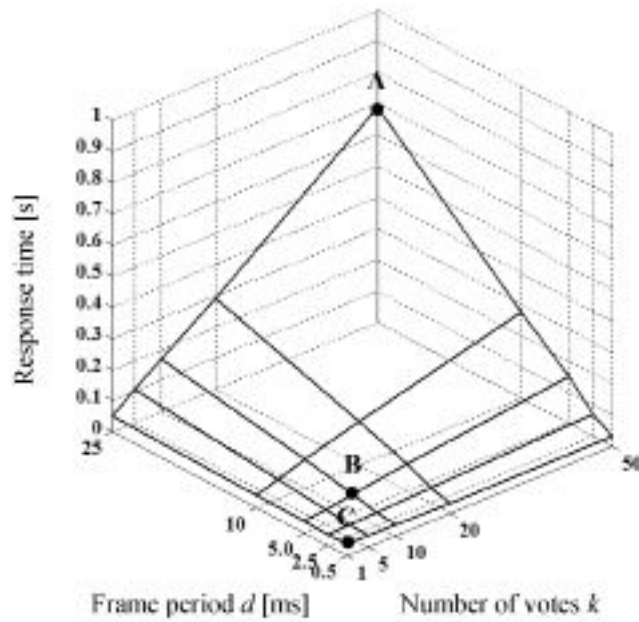
1. Selection of optimal feature quantities in the time or frequency domain (Zecca et al., 2002; Oseki, 2007)
2. Evaluation of estimation ability using other methods such as Bayesian pattern classi-

Tongue Movement Estimation Based on Suprahyoid Muscle Activity

Figure 10. Tongue movement estimation results (A: $d = 25$ ms, $k = 50$; B: $d = 1.0$ ms, $k = 20$; C: $d = 0.5$ ms, $k = 10$). (©2013, IEEE. Used with permission)



(a) Rate of Correct identification



(b) Response time

Table 1. Rate of correct identification. (©2013, IEEE. Used with permission)

$Y(t)$	Correct identification rate [%]	Response time [s]
RMS_{100}	93.8 ± 4.4	0.75 ± 0.10
RMS_{300}	93.8 ± 6.3	0.70 ± 0.10
RMS_{500}	96.3 ± 3.4	0.67 ± 0.12
All	98.8 ± 2.8	0.67 ± 0.09

fiers, Support vector machines (Graupe et al., 1982; Corinna et al., 1995; Huang et al., 2005; Shenoy, et al., 2008)

3. Optimization of the electrode configurations and the number of electrodes (Lal et al., 2004; Shibasaki et al., 2009)

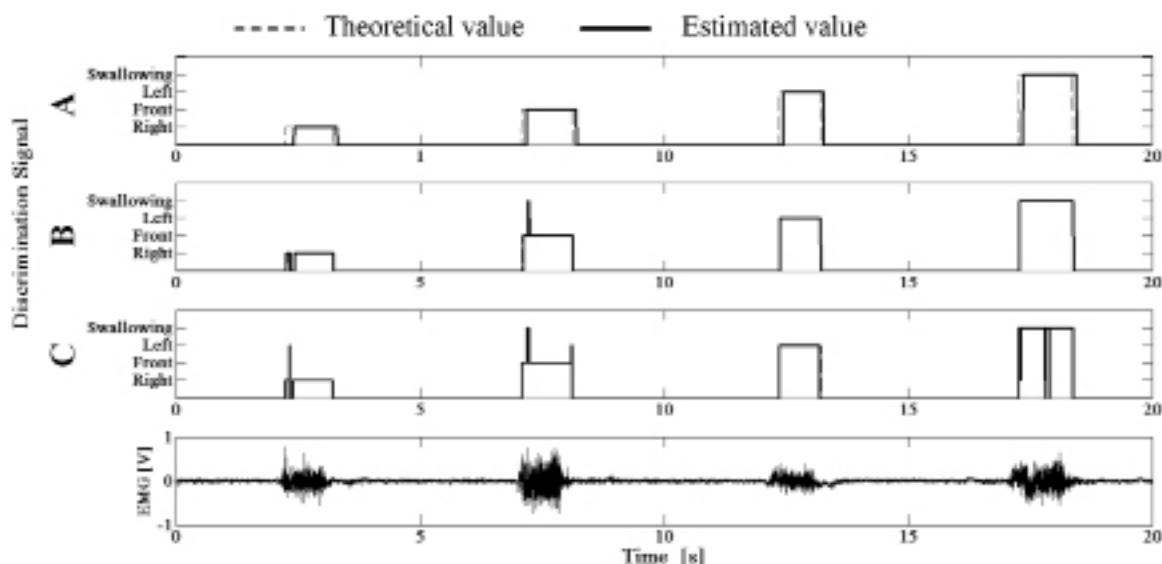
We are sure that the support of the independent living of persons with movement disabilities and elderly people is realizable in the future from development of studies of this area. We fervently

hope that the contents introduced in this chapter can contribute to the further development of this effort.

ACKNOWLEDGMENT

This study was supported in part by the Japan Society of Promotion of Science, Japan (Grant-in-Aid for Scientific Research (C) 24500637).

Figure 11. Effects of frame period d and number of votes k on estimation precision (A: $d = 25$ ms, $k = 50$; B: $d = 1.0$ ms, $k = 20$; C: $d = 0.5$ ms, $k = 10$). (©2013, IEEE. Used with permission)



REFERENCES

- Clark, J. A., & Roemer, R. B. (1977). Voice controlled wheelchair. *Archives of Physical Medicine and Rehabilitation*, 58(4), 169–175. PMID:849131
- Corinna, C., & Vladimir, V. (1995). Support-vector networks. *Machine Learning*, 20, 273–297. doi:10.1007/BF00994018
- Duchowski, A. T. (2002). A breadth-first survey of eye-tracking applications. *Behavior Research Methods, Instruments, & Computers*, 34(4), 455–470. doi:10.3758/BF03195475 PMID:12564550
- Englehart, K., & Hudgins, B. (2003). A robust, real-time control scheme for multifunction myoelectric control. *IEEE Transactions on Bio-Medical Engineering*, 50(7), 848–854. doi:10.1109/TBME.2003.813539 PMID:12848352
- Englehart, K., Hudgins, B., & Parker, P. A. (2001). A wavelet-based continuous classification scheme for multifunction myoelectric control. *IEEE Transactions on Bio-Medical Engineering*, 48(3), 302–311. doi:10.1109/10.914793 PMID:11327498
- Graupe, D., Salahi, J., & Kohn, K. H. (1982). Multifunctional prosthesis and orthosis control via microcomputer identification of temporal pattern differences in single-site myoelectric signal. *Journal of Biomedical Engineering*, 4(1), 17–22. doi:10.1016/0141-5425(82)90021-8 PMID:7078136
- Harwin, W. S., & Jackson, R. D. (1990). Analysis of intentional head gestures to assist computer access by physically disabled people. *Journal of Biomedical Engineering*, 12(3), 193–198. doi:10.1016/0141-5425(90)90040-T PMID:2140869
- Huang, Y., Englehart, K. B., Hudgins, B., & Chan, A. D. (2005). A gaussian mixture model based classification scheme for myoelectric control of powered upper limb prostheses. *IEEE Transactions on Bio-Medical Engineering*, 52(11), 1801–1811. doi:10.1109/TBME.2005.856295 PMID:16285383
- Huo, X., Wang, J., & Ghovanloo, M. (2008). Introduction and preliminary evaluation of the tongue drive system: Wireless tongue-operated assistive technology for people with little or no upper-limb function. *Journal of Rehabilitation Research and Development*, 45(6), 921–930. doi:10.1682/JRRD.2007.06.0096 PMID:19009478
- Ichinose, Y., Wakumoto, M., Honda, K., Azuma, T., & Satou, J. (2003). Human interface using a wireless tongue-palate contact pressure sensor system and its application to the control of an electric wheelchair. *The Institute of Electronics, Information and Communication Engineers*, J86-D-II(2), 364–367 (in Japanese).
- Ide, Y., & Koide, K. (Eds.). (2004). *Fundamental of functional anatomy for chairside evaluation of stomatognathic functions*. Tokyo: Ishiyaku Publishers.
- Jacobs, R., Hendrickx, E., Van Mele, I., Edwards, K., Verheust, M., & Spaepen, A. et al. (1997). Control of a trackball by the chin for communication applications, with and without neck movements. *Archives of Oral Biology*, 42(3), 213–218. doi:10.1016/S0003-9969(96)00117-3 PMID:9188991
- Kiguchi, K., Rahman, M. H., Sasaki, M., & Teramoto, K. (2008). Development of a 3DOF mobile exoskeleton robot for human upper-limb motion assist. *Robotics and Autonomous Systems*, 56, 678–691. doi:10.1016/j.robot.2007.11.007

- LaCourse, J. R., & Hludik, F. C. Jr. (1990). An eye movement communication-control system for the disabled. *IEEE Transactions on Bio-Medical Engineering*, 37(12), 1215–1220. doi:10.1109/10.64465 PMID:2149712
- Lal, T. N., Schröder, M., Hinterberger, T., Weston, J., Bogdan, M., & Birbaumer, N. et al. (2004). Support vector channel selection in BCI. *IEEE Transactions on Bio-Medical Engineering*, 51(6), 1003–1010. doi:10.1109/TBME.2004.827827 PMID:15188871
- Naik, G. R., & Kumar, D. K., & Jayadeva. (2010). Twin SVM for gesture classification using the surface electromyogram. *IEEE Transactions on Information Technology in Biomedicine*, 14(2), 301–308. doi:10.1109/TITB.2009.2037752 PMID:20007054
- Nguyen, H. T., King, L. M., & Knight, G. (2004). Real-time head movement system and embedded Linux implementation for the control of power wheelchairs. In *Proceedings of the 26th Annual International Conference of the IEEE Engineering in Medicine and Biology Society* (pp. 4892-4895).
- Niikawa, T., & Kawachi, R. (2006). Human-computer interface using mandibular and tongue movement. [in Japanese]. *Japanese Society for Medical and Biological Engineering*, 44(1), 94–100.
- Oseki, M. A., & Hu, H. (2007). Myoelectric control systems—A survey. *Biomedical Signal Processing and Control*, 2, 275–294. doi:10.1016/j.bspc.2007.07.009
- Saponas, T. S., Kelly, D., Parviz, B. A., & Tan, D. S. (2009). Optically sensing tongue gestures for computer input. In *Proceedings ACM Symposium on User Interface Software and Technology* (pp. 177-180).
- Sasaki, M., Arakawa, T., Nakayama, A., Obinata, G., & Yamaguchi, M. (2012b). Estimation of tongue movement based on suprahyoid muscle activity. In *Proceedings of the 2011 IEEE International Symposium on Micro-Nano Mechatronics and Human Science* (pp. 433-438).
- Sasaki, M., Arakawa, T., Nakayama, A., & Yamaguchi, M. (2012a). Method of tongue movement estimation based on suprahyoid muscle coordination. [in Japanese]. *Transactions of Japanese Society for Medical and Biological Engineering*, 50(1), 31–37.
- Sasaki, M., Onishi, K., Arakawa, T., Nakayama, A., Stefanov, D., & Yamaguchi, M. (2013a). Real-time estimation of tongue movement based on suprahyoid muscle activity. In *Proceedings of the 35th Annual International Conference of the IEEE Engineering in Medicine and Biology Society* (pp. 4605-4608).
- Sasaki, M., Onishi, K., Nakayama, A., Kamata, K., Stefanov, D., & Yamaguchi, M. (2013b). A system for tongue motor function training. In *Proceedings of the SICE Annual Conference 2013* (pp. 1598-1599).
- Scherer, R., Muller, G. R., Neuper, C., Graimann, B., & Pfurtscheller, G. (2004). An asynchronously controlled EEG-based virtual keyboard: Improvement of the spelling rate. *IEEE Transactions on Bio-Medical Engineering*, 51(6), 979–984. doi:10.1109/TBME.2004.827062 PMID:15188868
- Shenoy, P., Miller, K. J., Crawford, B., & Rao, R. N. (2008). Online electromyographic control of a robotic prosthesis. *IEEE Transactions on Bio-Medical Engineering*, 55(3), 1128–1135. doi:10.1109/TBME.2007.909536 PMID:18334405

Tongue Movement Estimation Based on Suprahyoid Muscle Activity

Shibanoki, T., Shima, K., Tsuji, T., Otsuka, A., & Chin, T. (2009). A novel channel selection method based on partial KL information measure for EMG-based motion classification. *Proceedings of 13th International Conference on Biomedical Engineering*, 23, 694-698.

Simpson, R. C., & Levine, S. P. (2002). Voice control of a powered wheelchair. *IEEE Transactions on Neural Systems and Rehabilitation Engineering*, 10(2), 122-125. doi:10.1109/TN-SRE.2002.1031981 PMID:12236450

Sonoda, Y. (1974). Observation of tongue movements employing a magnetometer sensor. *IEEE Transactions on Magnetics*, 10, 954-957. doi:10.1109/TMAG.1974.1058464

Terashima, S. G., Satoh, E., Kotake, K., Sasaki, E., Ueki, K., & Sasaki, S. (2010). Development of a mouthpiece type remote controller for disabled persons. *Journal of Biomechanical Science and Engineering*, 5(1), 66-77. doi:10.1299/jbse.5.66

Wolpaw, J. R., Birbaumer, N., McFarland, D. J., Pfurtscheller, G., & Vaughan, T. M. (2002). Brain-computer interfaces for communication and control. *Clinical Neurophysiology*, 113(6), 767-791. doi:10.1016/S1388-2457(02)00057-3 PMID:12048038

Wrench, A., McIntosh, A. D., Watson, C., & Hardcastle, W. J. (1998). Optopalatograph: Real-time feedback of tongue movement in 3D. In *Proceedings of the Fifth International Conference on Spoken Language Processing* (pp. 1867-1870).

Zecca, M., Micera, S., Carrozza, M. C., & Dario, P. (2002). Control of multifunctional prosthetic hands by processing the electromyographic signal. *Critical Reviews in Biomedical Engineering*, 30(4-6), 459-485. doi:10.1615/CritRevBiomedEng.v30.i456.80 PMID:12739757

KEY TERMS AND DEFINITIONS

Neural Networks: Computational models inspired by animals' central nervous systems.

Suprahyoid Muscle: Four muscles running from the mandible to the hyoid bone.

Section 4

EMG for Prosthetic and HCI Applications

Chapter 13

Design of Myocontrolled Neuroprosthesis: Tricks and Pitfalls

Emilia Ambrosini

Politecnico di Milano, Italy

Simona Ferrante

Politecnico di Milano, Italy

Alessandro Pedrocchi

Politecnico di Milano, Italy

ABSTRACT

Recent studies suggest that the therapeutic effects of Functional Electrical Stimulation (FES) are maximized when the patterned electrical stimulation is delivered in close synchrony with the attempted voluntary movement. FES systems that modulate stimulation parameters based on the residual volitional muscle activity would assure this combination. However, the development of such a system might be not trivial, both from a hardware and a software point of view. This chapter provides an extensive overview of devices and filtering solutions proposed in the literature to estimate the residual volitional EMG signal in the presence of electrical stimulation. Different control strategies to modulate FES parameters as well as the results of the first studies involving neurological patients are also presented. This chapter provides some guidelines to help people who want to design innovative myocontrolled neuroprostheses and might favor the spread of these solutions in clinical environments.

INTRODUCTION

Functional Electrical Stimulation (FES) consists of the electrical stimulation of an intact lower motor neuron to activate paralyzed or paretic muscles in a precise sequence so as to directly accomplish

or support functional tasks (Meo & Post, 1962). Functional tasks may include standing, walking, or cycling, upper limb activities, such as grasping or reaching, and control of respiration and bladder function. With the term neuroprosthesis we refer to a system or a device that provides FES.

DOI: 10.4018/978-1-4666-6090-8.ch013

FES systems have been covering a wide range of assistive and therapeutic applications in neuro-rehabilitation for the last forty years (Sheffler & Chae, 2007); they have been used to restore or replace impaired or lost motor functions in people affected by many neurological disorders, such as Spinal Cord Injury (SCI) (Gater, 2011), stroke (Ambrosini, 2012; Ambrosini, 2011a; Ferrante, 2008; Pomeroy, 2006; Popović, 2009), multiple sclerosis (Barrett, 2009), or cerebral palsy (Cau-rough, 2010; Trevisi, 2011).

When the muscles are not completely paralyzed it is possible to use the neural information extracted from the EMG signals of the paretic limb to control the timing and the intensity of the stimulation (Jiang, 2010). Such a control scheme seems to be a promising solution from a clinical prospective since it involves the physiological neural pathway in the recovery of the impaired motor functions. In support of this hypothesis, recent neurophysiological studies (Barsi, 2008; Iftime-Nielsen, 2012; Rushton, 2003; Gandolla, 2012) suggested that the use of electrical stimulation co-incidentally with the voluntary drive enhances the plasticity of the central nervous system (CNS), so as to improve motor relearning. First evidences about the efficacy of myocontrolled FES in improving upper limb motor performance have been shown in post-stroke patients (Fujiwara et al., 2009; Shindo et al., 2011). However, a full demonstration of the superiority of this approach compared to a more conventional use of FES is still missing, as well as a system ready to be transferred in clinical settings.

To design a control system that modulates FES parameters based on the residual volitional activation of the stimulated muscle, technological challenges, both from a software and a hardware point of view, need to be addressed. Indeed, when a muscle contraction is generated by two different activation sources, volitional and electrical stimulation, the overall EMG signal is due to the combination of these two components and the

estimate of the volitional component might not be trivial.

This chapter focuses on FES systems that use the residual volitional EMG signal of the stimulated muscle to modulate the stimulation parameters. An extensive overview of the hardware and software solutions to estimate the volitional EMG in the presence of electrical stimulation, as well as the correspondent control strategies for FES are presented. Guidelines to support people who want to design innovative myocontrolled neuroprostheses are also provided. The Background section summarizes the neurophysiological principle and the therapeutic effects of FES both at peripheral and central level. The neurophysiological hypotheses that advocate the use of FES co-incidentally with the voluntary drive are also presented. The chapter is organized into five sections that guide the reader in the critical development of myocontrolled neuroprosthetic devices. The first section describes the characteristics of volitional and FES-induced EMG signals. The following section provides an overview of the current available hardware systems for EMG recording. The third section reviews digital signal processing methods for the estimate of the volitional EMG signal in the presence of FES-evoked EMG. The fourth section reviews the use of the volitional EMG as a control signal for modulating FES parameters. The final section of the chapter presents the results of early studies that tested myocontrolled neuroprostheses on people with neurological impairments. In closing, future and emerging research directions are presented.

BACKGROUND

When electrical pulses are delivered to the peripheral nervous tissue, repetitive depolarization of motor axons beneath the stimulation electrodes occurs and a muscle contraction is produced by signals travelling from the stimulation site to the neuromuscular junction. In this sense, FES substitutes for the normal voluntary drive

Design of Myocontrolled Neuroprosthesis

travelling along the anterior corticospinal tract. Since the threshold for eliciting a nerve fiber action potential is 100 to 1000 times less than the threshold for muscle fiber excitation (Mortimer, 2011), FES usually excites nervous fibers instead of muscular fibers, stimulating either the nerve directly or the motor point of the nerve proximal to the neuromuscular junction. For this reason, the clinical application of FES is presently limited to neurological injuries with lower motor neurons still functional from the anterior horns of the spinal cord to the neuromuscular junction. In the same way the motor axons are elicited during FES, sensory fibers are also depolarized, and the signals travelling back to the spinal cord can contribute to the electrically evoked muscle contraction through the synaptic recruitment of the motor neuron. Thus, FES-induced muscle contractions can be generated by a combination of a peripheral (depolarization of the motor axons) and central (depolarization of the sensory axons) recruitment (Bergquist, 2011).

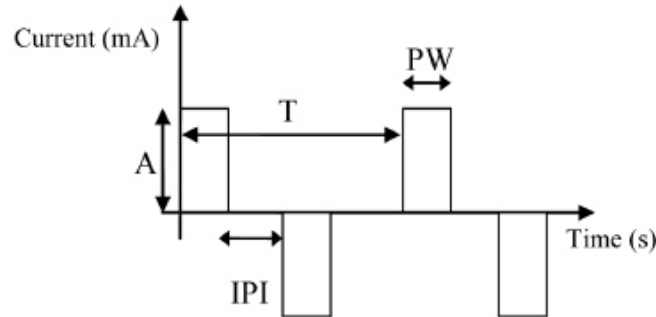
Electrical stimulation can be delivered through transcutaneous (surface) electrodes placed over the muscle belly, or through implanted (percutaneous, epimysial, epineural, intraneural, and cuff) electrodes. Surface electrodes are commonly preferred to implanted electrodes, especially for therapeutic applications (Benton, 1981) due to their minimal invasiveness and the ease of donning and doffing. For this reason, this chapter is focused on the use of surface electrodes for FES.

FES systems can be either voltage- or current-controlled. Voltage-controlled stimulators do not lead to dangerous high values of current density, in case that a partial detachment of surface electrodes occurs. However, the motor unit recruitment induced by voltage-controlled stimulators is less reliable than the one induced by current-controlled stimulators. Indeed, current-controlled stimulators are not affected by impedance variations due to electrode–skin interface changes and thus they are usually preferred in clinical applications.

FES is usually delivered as trains of current pulses, either monophasic or biphasic (see Figure 1). Biphasic pulses are preferred since they balance the charge delivered to the nerves. Among biphasic pulses, symmetrical (as the one shown in Figure 1) and unsymmetrical waveforms exist. Current pulses are characterized by three parameters: the pulse amplitude (A), the pulse width (PW), and the stimulation frequency. The strength of the resultant muscle contraction can be controlled by modulating these parameters. The product between the pulse amplitude and the pulse width defines the charge delivered by each pulse and determines the number of muscle fibers that are recruited (spatial summation): greater muscle force generation is accomplished by increasing either the pulse duration or the amplitude so as to activate fibers with a higher activation threshold (both smaller fibers and fibers at a greater distance from the stimulation electrodes). On the other hand, temporal summation is determined by the rate at which current pulses are applied to the muscle. The minimum stimulation frequency that generates a fused muscle response is about 12.5 Hz. Higher frequencies produce higher forces but result in an early onset of muscular fatigue (Sheffler & Chae, 2007). Usually, when electrical stimulation is provided through surface electrodes attached to the skin near the motor point, the stimulation frequency is fixed at a value ranging between 20 and 30 Hz, while the current pulses have a duration between 100 to 500 μ s and an amplitude between 10 and 125 mA.

The major limitation of FES applications is the rapid onset of muscular fatigue, which is due to the differences between physiological and FES-induced muscle contractions. First of all, FES induces a non-selective, spatially fixed, and temporally synchronous activation of the elicited fibers compared to the asynchronous activation that characterizes physiological muscle contractions. Synchronous activation of muscle fibers during conventional stimulation requires a higher stimulation frequency to achieve a smooth muscle

Figure 1. Current pulse waveforms (A: pulse amplitude; PW: pulse width; IPI: inter-pulse interval; T: stimulation period, i.e. the inverse of the stimulation frequency)



contraction thus causing the muscle to fatigue more quickly (Bickel, 2011). Another possible explanation for the quick onset of muscular fatigue is related to the recruitment order of the fibers. Skeletal muscle contains “fast” and “slow” muscle fibers that are distinguished on the basis of contraction kinetics into types I and II muscle fibers. Slow-twitch, oxidative type I fibers generate lower forces but are fatigue resistant; fast-twitch glycolytic type II fibers generate higher forces but fatigue more rapidly. During volitional muscle contractions, the motor unit recruitment order follows Henneman’s size principle: small size motor units (type I fibers) are recruited earlier than large size motor units (type II fibers) based on CNS drive. Conversely, during FES-induced contractions, two main factors affect the recruitment order:

- The size of the motor neuron and of the motor neuron branches, which is related to the excitability threshold (motor units with larger fibers are innervated by larger axons, which have a lower excitability threshold (Zajac & Faden, 1985))
- The location and orientation of the motor neuron branches in the electric field (Knaflitz, 1990).

Although a complete knowledge of the motor unit recruitment during FES-induced muscle contractions is still missing, it can be reasonably assumed that the artificial recruitment order turns out to be less efficient both in terms of force production and fatigue onset, than the natural one.

Clinical evidence demonstrates that FES induces peripheral benefits, such as the increase in muscle strength, changes in muscle length, bulk, type, and function, prevention and reversal of osteoporosis, enhancement of cardiorespiratory fitness, improvement in tissue oxygenation and peripheral hemodynamic function, reduction of spasticity, and increase in the range of motion (Gater, 2011; Glinsky, 2007; Popović, 2009).

When FES is applied on post-stroke patients, its efficacy in improving the ability to move voluntarily the affected limb and to use it in everyday life activities has been shown both for the upper (de Kroon & IJzerman, 2008; Popovic, 2004) and lower limb (Ambrosini, 2011a; Bogataj, 1995; Yan, 2005). Clinical evidence suggests that FES plays a major role in enhancing motor relearning after stroke (Sheffler & Chae, 2007), mainly if combined with goal-oriented repetitive movement therapy thanks to the combination of two motor learning principles in one protocol, i.e. repetition and sensorimotor integration (Krakauer, 2006). FES-induced afferent-efferent stimulation together with cutaneous and proprioceptive inputs

Design of Myocontrolled Neuroprosthesis

might increase activity in the spinal and cortical circuits that control the movements, facilitating the physiological reorganization occurring in the intact tissues adjacent to the brain lesion after stroke. Recent studies on central motor neuroplasticity have been conducted to investigate whether FES-induced motor recovery is related to changes in cortical activation or excitability. A dose-response relationship between FES delivered to the quadriceps muscle of the dominant limb and brain activation in sensory and motor regions contralateral to the stimulation side has been observed on a group of 10 healthy subjects (Smith, 2003). A recent fMRI study involving 12 healthy volunteers observed that a significantly greater number of voxels were activated during active and FES-induced ankle dorsi-flexion movements compared to passive ones in contralateral primary motor, primary sensory and secondary somatosensory areas, as well as in supplementary motor and cingulate motor areas, bilateral premotor areas and cerebellum (Francis, 2009). Comparing active and FES-induced movements, the authors observed a greater activation in brain areas responsible for motor planning, execution and visual-motor coordination when movements were performed voluntarily, whereas they showed a greater activation in bilateral secondary somatosensory areas and insula when movements were induced by FES, resulting from increased sensory integration, but also probably due to a nociceptive component of FES.

Recent neurophysiological studies advocated the use of FES co-incidentally with the voluntary drive to enhance the benefic effects of FES on the motor relearning process. In a study involving 25 healthy volunteers the effects of three training paradigms (passive FES of the finger flexors and extensors, voluntary movement with sensory stimulation, and FES-augmented voluntary activation) were compared in terms of cortical excitability (Barsi, 2008). The input-output relationship between transcranial magnetic stimulation intensity and the motor evoked potentials was investigated.

A significant increase in the magnitude of the motor evoked potentials was observed only during FES-augmented voluntary movements, suggesting an increased cortical excitability due to the cumulative effects of FES and voluntary activation. The authors concluded that the combination of voluntary effort and FES might have a greater potential to induce plasticity in the motor cortex and might represent a more effective training in the motor neuro-rehabilitation field.

In a more recent study (Iftime-Nielsen, 2012), fMRI cortical activity induced by FES combined with voluntary effort was compared to that produced when FES and voluntary activity were performed alone on a group of 17 healthy volunteers. FES plus voluntary effort revealed a greater cerebellar activity compared with FES alone and a reduced bilateral activity in the secondary somatosensory areas compared to voluntary effort alone. When a voluntary movement is present, the cerebellum predicts the sensory consequences of the movement and the reduced activity in the somatosensory areas might reflect a better match between the internal model and the actual sensory feedback due to the combination of FES and voluntary drive. The coactivation between the motor control regions and the sensory-feedback areas might be crucial in motor recovery at brain level.

It has been recently investigated the differential effect of FES applied with or without the volitional contribution of the subject in a 2x2 factorial design, with volitional intention (with the levels volitional and passive) and FES (with the levels present and absent) as factors (Gandolla, 2012). Right ankle dorsi-flexion was selected as motor task. The interaction contrast allowed to identify regions where the FES augmented proprioception – in the context of volitional intent – produced a higher activation than FES augmented proprioception in the absence of volitional movement. The authors demonstrated that the positive interaction was seen in both primary motor cortex (M1) and primary somatosensory cortex (S1); in other words, the effect of augmented proprioception depends on

volitional movement in both M1 and S1. The interaction mechanism between FES and voluntary effort could be therefore the mechanism by which FES leads to a clinically meaningful carryover effect in neurological patients.

Not only cortical but also spinal mechanisms might be involved in the potential positive effect of FES-augmented voluntary movements on motor recovery. It has been hypothesized that FES-mediated antidromic impulses, combined with coincident voluntary effort through a damaged pyramidal motor system, could provide an artificial means to synchronize pre-synaptic and post-synaptic activity in the affected population of the anterior horn cells, helping to promote restorative synaptic modifications at the spinal level (Rushton, 2003).

The results of these neurophysiological studies make interesting from a clinical prospective the development of myocontrolled neuroprosthesis that can assure the combination between the intended voluntary movement and the delivery of FES. Naturally, these systems require that the muscle to retrain is not completely paralyzed. Two different approaches have been proposed in the literature:

- The residual volitional EMG signal of the affected muscle can be detected and used to trigger the onset of a predetermined stimulation sequence applied in an open-loop modality to the same muscle used for control (Cauraugh, 2000; Kimberley, 2004; Saxena, 1995);
- The residual volitional EMG signal of the affected muscle can be detected and used to continuously control FES applied in a closed-loop modality to the same muscle used for control. Stimulation parameters, such as current amplitude and pulse width, are usually modulated (Fujiwara, 2009; Thorsen, 2001; Yeom & Chang, 2010).

Note that from the previous list we have excluded some studies which proposed to control FES based on the EMG signal of a muscle different from the stimulated one (such as Chen, 2010; Graupe & Kohn, 1987). Indeed, this approach does not guarantee the synchronization between FES-mediated activity and the voluntary motor drive.

Concerning the first approach, to trigger FES based on the residual volitional EMG signal of the stimulated muscle, advanced technological solutions are not needed since the EMG signal is measured only before the delivery of FES. When a volitional activation of the target muscle is detected, FES is delivered in an open-loop modality and the EMG signal is not measured anymore. Therefore, over the last 20 years different EMG-trigger FES systems have been developed and promising results have been achieved on neurological patients. EMG-triggered FES has been shown to improve wrist and finger extension movements in chronic post-stroke patients (Cauraugh, 2000). A 3-week home treatment of EMG-trigger FES applied on the extensors muscles of the impaired forearm significantly improved hand functions in chronic stroke patients (Kimberley, 2004). Improvements in the motor performance were also associated with an increased index of cortical intensity in the ipsilateral somatosensory cortex. A review investigating the variety of ways that can be used to apply FES to the hemiparetic upper extremity after stroke concluded that EMG-triggered FES may be more effective than non-triggered FES solutions (de Kroon, 2005). However, a recent systematic review to assess whether EMG-triggered FES applied to the extensor muscles of the forearm improves hand function after stroke was carried out and the authors did not find any statistically significant differences in the motor performance improvements between EMG-trigger FES and usual care (Meilink, 2008).

It is important to highlight that, EMG-trigger FES systems provide a predetermined stimulation sequence when the volitional EMG signal overcomes a certain threshold but the volitional

involvement of the patient in the exercise is not monitored anymore after the beginning of the stimulation phase. Therefore, the synchronization between the patterned electrical stimulation and the attempted voluntary movement might be assumed but not proved. To actually assure this synchronization, an on-line control of the volitional activity of the stimulated muscle is required. To design systems that continuously modulate stimulation parameters based on the residual volitional EMG signal, technological challenges need to be tackled, as described in the following sections.

MYOCONTROLLED NEUROPROSTHESIS: A TECHNOLOGICAL CHALLENGE

Characterization of Volitional and FES-Induced EMG Signal

During hybrid muscle activation, i.e. a muscle contraction generated by two different excitation sources, volitional and electrically induced (Langzam, 2006), the overall myoelectric signal is due to the combination of these two components.

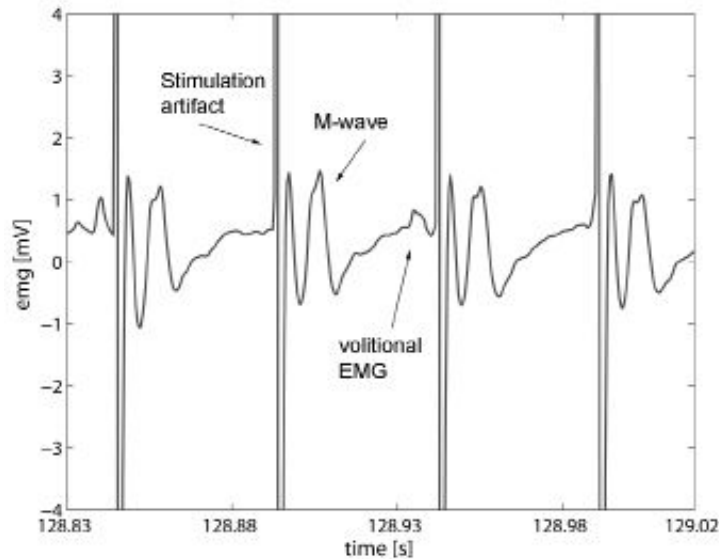
A typical muscle response to electrical stimulation includes the stimulation artifact and the M-wave. The stimulation artifact is due to the electric field generated in the tissue and the skin by the stimulation current. The artifact waveform is a spike followed by a decay composed of one or more exponential curves whose amplitude and time constant values are affected by the stimulator output characteristics, the inter-electrode impedance, and the relative geometry of stimulation and recording electrodes (Knaflitz & Merletti, 1988). The initial spike lasts about 3 ms and has an amplitude from one to three orders of magnitude greater than the M-wave. The decay, considerably smaller in amplitude with respect to the initial spike, lasts for a longer time interval and can be more or less superimposed with the M-wave,

depending on the distance of the detection point from the innervation zone (Mandrile, 2003). The M-wave represents the compound action potential due to the synchronous firing of the electrically elicited muscle fibers. It depends on many factors, such as the stimulation parameters, the position of both stimulation and recording electrodes, the properties of the muscle, the fatigue, the contraction level of the muscle, etc. (Merletti, 1992). The M-wave is usually in the range of some millivolts, starts few milliseconds after the electrical pulse and its main activity is concluded within the first 20 ms of the inter-pulse period. However, the M-wave can spread over most of the inter-pulse period, mainly at high stimulation intensities and frequencies.

Besides the M-wave, due to the orthodromic efferent volley, the electrically evoked motor response might be characterized by two other components: the H-reflex and the F-wave. The H-reflex is determined by the orthodromic sensory volley, that can recruit the motor neuron in the spinal cord, provoking a second muscle response visible on the EMG signal after the M-wave. To evoke the H-reflex, sensory fibers need to be depolarized and this requires a proper placement of the stimulation electrodes and a specific setting of the stimulation parameters (usually lower pulse amplitude and longer pulse duration are needed to preferentially recruit sensory axons (Bergquist, 2011)). The F-wave is a small, second compound action potential due to the antidromic efferent stimulus. This stimulus reaches the motor neuron, a small portion of the motor neuron backfires and orthodromic signal travels back down the nerve towards the muscle, evoking the F-wave. Strong electrical pulses are needed to evoke the F-wave.

Due to the asynchronous activation of the motor units during voluntary contractions, the volitional EMG is a stochastic signal, with an approximately Gaussian probability density function (Merletti, 1992) and an amplitude of at least one magnitude lower than the M-wave. During a hybrid muscle activation, the volitional EMG signal is usually

Figure 2. Example of a raw EMG signal acquired during a hybrid muscle activation (both volitional and FES-induced)



more visible in the second half of the inter-pulse period, when the main phase of the M-wave is concluded.

Figure 2 depicts an example of a typical EMG signal acquired during a hybrid muscle activation: the three main components, i.e. the stimulation artifact, the M-wave, and the volitional EMG, are shown. The stimulation frequency was set at 20 Hz, as it can be noticed by an inter-pulse period of 50 ms.

Figure 3 shows the overall EMG signal acquired during isometric and anisometric contractions. Each panel reports 20 consecutive inter-pulse periods measured during four different conditions: FES-induced isometric and anisometric contractions with no volitional contribution (panel (A) and (C), respectively); FES-induced and volitional isometric and anisometric contractions (panel (B) and (D), respectively). During short isometric contractions with fixed stimulation parameters (pulse amplitude of 18 mA and duration of 300 μ s in the example shown in the figure), the M-wave can be considered as a *quasi-deterministic*

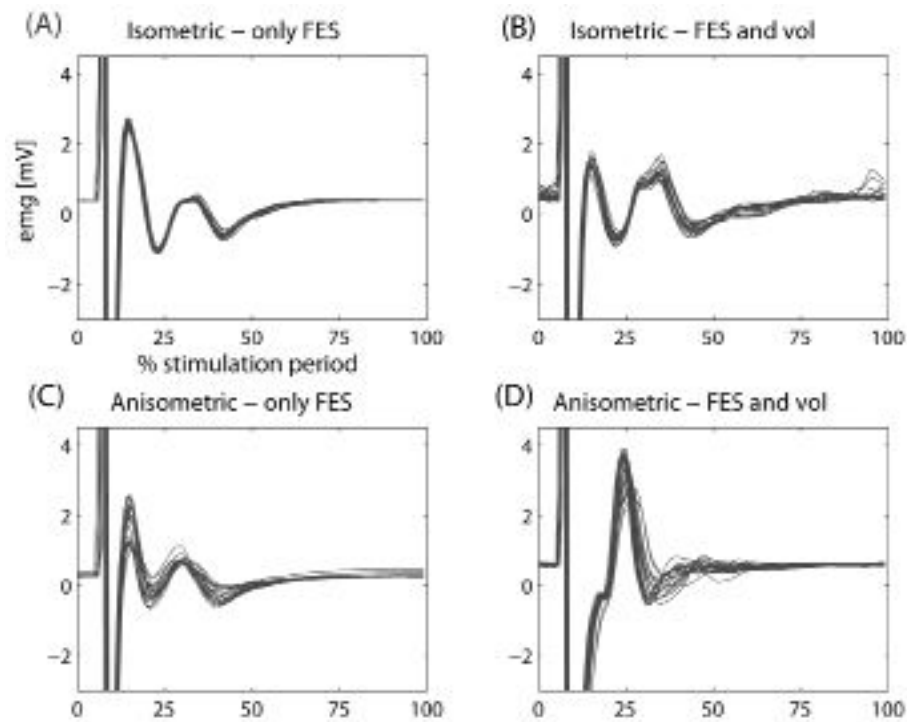
signal; indeed, low variations in the shape of the M-wave can be noticed in panels (A) and (B). On the other hand, during intermittent anisometric contractions (60° of elbow flex/extension) the shape of the M-wave changes, even in short term, due to the modifications of the relative position between the stimulation electrodes and the muscle fibers (Merletti, 1992). Indeed, panels (C) and (D) highlight higher variations in the shape of the M-wave compared to panels (A) and (B). The volitional EMG signal is represented by the low-amplitude pseudorandom noise that can be noticed mainly over the tail of the M-wave in both panels (B) and (D).

Devices for EMG Recordings during Electrical Stimulation

To acquire an EMG signal during FES, standard recording and stimulation electrodes are typically used. In most cases, the detection of the EMG signal from a single muscle requires to use up to five electrodes: two stimulation electrodes

Design of Myocontrolled Neuroprosthesis

Figure 3. Raw EMG signals acquired during four different conditions: FES-induced isometric and anisometric contractions with no volitional contribution (panel (A) and (C), respectively); FES-induced and volitional isometric and anisometric contractions (panel (B) and (D), respectively). In panels (C-D) a movement of about 60° of elbow flex/extension is shown. Each panel represents 20 consecutive inter-pulse periods



and three recording electrodes, two placed over the target muscle and one reference electrode. Surface self-adhesive electrodes (such as PALS® Platinum, Axelgaard) are placed over the muscle belly to deliver the stimulation. Different sizes of stimulation electrodes can be used depending on the target muscle. A size of about 50 x 50 mm is usually used for the stimulation of the arm muscles (e.g., the biceps or the triceps muscle), while 50 x 90 mm electrodes are usually attached over the thigh muscles (e.g., the quadriceps and the hamstrings muscles); rounded electrodes with a diameter of about 25 mm can be used for smaller muscles, such as the forearm or the face muscles. EMG signals are usually recorded using Ag/AgCl pre-gelled self-adhesive electrodes. A typical

contact size of 30 x 20 mm is used for both arm and leg muscles with an inter-electrode distance of about 3 cm following SENIAM indications (Hermens, 2000). The recording electrodes are usually placed between the stimulation electrodes and the reference EMG electrode is commonly placed away from the detection site.

Standard amplification units for EMG recordings cannot be used in the presence of electrical stimulation. Indeed, EMG recordings during hybrid muscle activation are problematic as large measurement artifacts occur. The stimulation artifact is the result of a potential difference developed by the stimulation current between the EMG recording electrodes. Indeed, this potential difference is a differential signal that can not be re-

jected from the differential amplifier. As described in the previous section the stimulation artifact is characterized by an initial spike lasting about 3 ms with an amplitude of one to three orders of magnitudes greater than the M-wave. Thus, this spike can drive the amplifier of a standard EMG circuit into saturation or even damage the amplifier.

Several studies in literature faced the problem of the suppression of the stimulation artifact and three main categories of solutions, here summarized in Figure 4, have been proposed. In all the flow diagrams reported in Figure 4, the reference EMG electrode is not shown for the sake of clarity. However, a reference electrode is always connected to a single reference generator (*driven-right-leg system*) to reduce the common mode disturbances at the measurement electrodes. The third solution, unlike the first two, uses only a single couple of electrodes for both stimulating and recording the EMG signal. In all the solutions, the cables can be equipped with active shielding, commonly used to reduce the effects of external noise and electrostatic interferences as well as effects of parasitic capacitances of the shielded cables. In the case of active shielding, the outer conductor (shielding) is driven at the average potential of the input terminals by using a buffer amplifier. Using active shielding, external interferences are suppressed through the low output impedance of the unity gain amplifier (Shalaby, 2011). Each cable has its own active shielding.

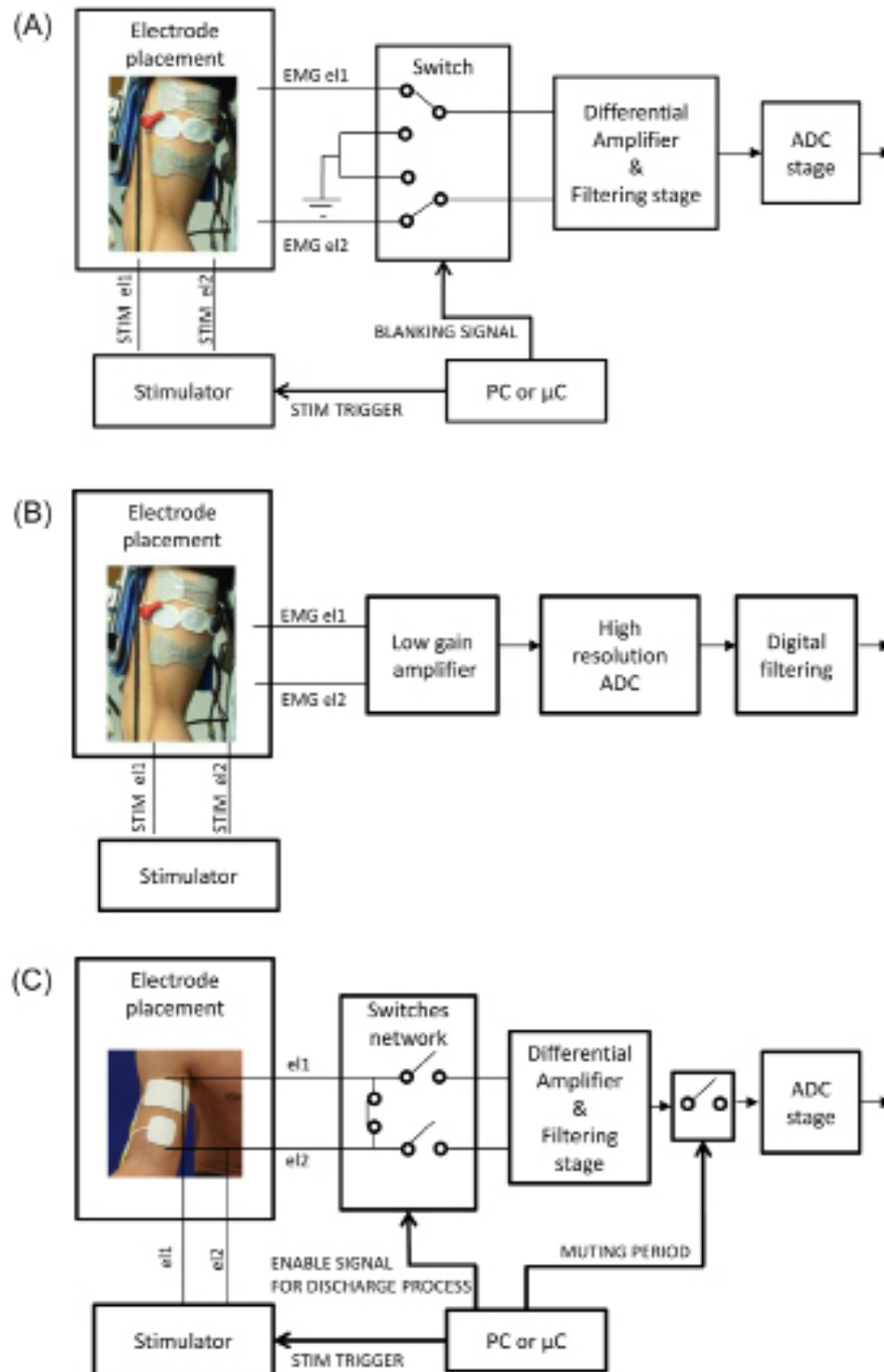
In the first type of solutions (Figure 4 - A), a switch (Knaflitz & Merletti, 1988; Minzly, 1993; Yeom & Chang, 2010) or a sample-and-hold circuit (Howson & Heule, 1980; H. Yeom & Chang, 2010) can be applied to disconnect the electrodes from the input of the conditioning circuit when the stimulation pulse is delivered. In this solution the switch or the sample-and-hold circuit must be synchronized to the stimulation signal. The blanking window starts with the stimulation pulse and has a width varying between 5 and 20 ms. If a long blanking window is used the acquired signal does not include the initial bigger part of

the M-wave widely used in literature as a fatigue indicator (Merletti, 1990). Some commercial EMG amplifiers such as the NeuroLog™ System by Digitimer, UK, are now available and can measure hybrid muscle activations because they offer a mute input for suppression or reduction of overload artifact signals. These commercial devices are EMG amplifiers that can be triggered and/or enabled from an external signal.

The second type of solutions does not require a blanking window or a synchronization with the stimulation pulse. A first example of device belonging to this category was proposed by Thorsen: the artifact suppression was achieved by using a fast recovery instrumentation amplifier (recovery time of about 1 ms after the stimulation artifact) and a nonlinear feedback loop for automatic compensation of changes in DC-offset mostly due to movement artifacts (Thorsen, 1999a). This EMG amplifier was specifically designed for EMG signals having an amplitude lower than 0.5 mV and a frequency range comprised between 20 and 500 Hz, stimulation artifacts having an amplitude lower than 3 V, a duration lower than 1 ms, and a repetition rate of about 20 Hz. The circuit was able to recover from a DC-offset change within the range of ± 0.1 V in less than 0.1 s. Given all these assumptions on the input signals, it was reported that this specific circuit was not robust enough; for instance, it was not sufficient for a complete rejection of the artifact when the recording electrodes were relatively close to the stimulation electrodes (Frigo, 2000). A more robust approach that still does not rely on the use of a blanking window and a synchronization with the stimulation pulse is schematically represented in Figure 4 - B. It consists of using a high resolution ADC to convert the signal from analog to digital soon after a first differential instrumentation amplifier with a very low gain. This amplifier does not require any blanking and is usually characterized by a very fast recovery from stimulation artifacts. Hence, both M-wave and volitional EMG during stimulation can be measured. However, digital

Design of Myocontrolled Neuroprosthesis

Figure 4. Three different solutions to measure the EMG signals during a hybrid muscle activation



filter algorithms must be implemented at the PC side to process the EMG signal. Nowadays, some commercial devices belonging to this category are available (e.g., the EMG/EEG amplifier Porti by Twente Medical Systems International (TMSI), characterized by a recovery time of less than 5 ms). This commercial solution robustly overcomes the problem of artifact suppression and can be widely applied in clinical settings.

When separate stimulation and recordings electrodes are used, the relative placement of the electrodes can affect the capability of the system to suppress the stimulation artifact and the electrically induced contribution (M-wave). Different relative placements of the recording electrodes with respect to the stimulation electrodes were evaluated (Frigo, 2000). The authors observed that when the recording electrodes are placed within the stimulation electrodes with an orientation of 90° with respect to the line of the stimulation electrodes, the signal to noise ratio was higher, thanks to the higher common mode component of the stimulation artifact that can be more easily rejected by the differential amplifiers. Thus, when separate stimulation and recording electrodes are used, a placement of the recording electrodes perpendicular to the muscle fiber direction, as shown in Figure 4, panels (A) and (B), should be preferred to the one proposed by SENIAM (Hermens, 2000), whether the objective is to acquire the volitional component of a hybrid muscle activation.

More recently, direct measurement of the EMG signals from stimulation electrodes have been also proposed (Muraoka, 2002; Shalaby, 2011). This approach simplifies electrodes placement (Figure 4 - C); indeed, only 3 electrodes, instead of 5, are needed for one EMG/stimulation channel, making this solution particularly interesting for small target muscles. However, when stimulation electrodes are used to record the EMG signal, another measurement artifact is introduced and needs to be eliminated. Indeed, when the electrical pulse is

delivered, an asymmetrical charge remains under the electrodes and ad-hoc hardware solutions are required to quickly eliminate this electric charge. A second artifact is caused by the discharging process; this artifact is even larger when big electrodes are used. Therefore, this solution requires a blanking circuit to avoid both the stimulation and the discharging artifacts (Figure 4 - C). A muting period longer than in the first approach (Figure 4 - A) is needed and, thus, an initial consistent part of the M-wave cannot be acquired. Both the blanking and the charge elimination circuits must be synchronous to the stimulation pulse.

The first device applying electrical stimulation via the EMG electrodes was designed by Kamono and colleagues for gait assistance (Kamono, 2002). They used a voltage-controlled stimulator working at 15 Hz, and a microcontroller (μ C) to switch the electrodes between the stimulation circuit and the EMG amplifier. A similar device was developed by Muraoka and colleagues; their device provided a good EMG signal for the second half of the stimulation period at a stimulation frequency of 20 Hz (Muraoka, 2002). Both these solutions were tested only on low stimulation frequencies and moderate intensities being the target muscles the ankle dorsi-flexor (Kamono, 2002) or upper limb muscles (Muraoka, 2002). In addition, Muraoka used a band pass filtering in the output stage in the range of 330-460 Hz, thus filtering out most of the volitional EMG information that typically has a bandwidth comprised between 30 and 500 Hz with a peak around 120 Hz (De Luca & Knaflitz, 1992).

Recently, Shalaby and colleagues developed a more robust device that can be used during 4-channel FES-induced cycling training (Shalaby, 2011). This device was compatible with a commercial 8-channel current-controlled stimulator (Rehastim™, Hasomed GmbH, Germany). Their novel device overcame the limitation of the previous devices in two main aspects: it could be used for higher stimulation intensities and it estimated

the volitional EMG component using a band pass filter in the range of 100-330 Hz. Their device included photo-MOS switches having very low on-resistance and capable to control voltage load up to 250 V. These switches protected the input circuit of the EMG pre-amplifier from any damage due to the electrical stimulation pulses and permitted a fast discharge process. The authors used a muting period of 30 ms for each stimulation period but they suggested that if smaller electrodes were used, less charge would be accumulated on the electrodes and thus shorter muting period could be used.

As a general recommendation, the devices that assure the highest flexibility in acquiring the EMG signal during hybrid muscle contractions are those belonging to the second category (Figure 4 - B). Indeed, they allow to measure both the M-wave and the volitional EMG so as to develop sophisticated control systems for FES. Besides the importance of the acquisition of the volitional EMG, that has been already mentioned in the Background, the acquisition of the M-wave might be interesting to assess the muscular fatigue induced by FES. It is generally accepted that the duration of the M-wave increases during sustained stimulation, and consequently characteristic spectral frequencies (mean and median frequency) decrease (Farina, 2004). On the other hand, the possibility to use the same electrodes for both stimulating and recording the EMG signal (Figure 4 - C) is very interesting for future clinical applications since it facilitates and shortens the donning procedure.

Filtering Techniques to Extract the Volitional EMG

Different solutions have been proposed over the last 15 years for removal of electrically induced components so as to estimate the volitional EMG signal during hybrid muscle activations.

Many solutions applied on the raw EMG signal a blocking window, that starts at the beginning of each stimulation pulse: the signal is zeroed for the

first 20 ms (Frigo, 2000; Thorsen, 2001) or 25 ms (Langzam, 2006; Muraoka, 2002) of each inter-pulse period to remove the stimulation artifact and the main part of the M-wave. The volitional EMG can then be estimated from the remaining part of the inter-pulse period. However, since the M-wave spreads over the most of the inter-pulse period, the use of a blocking window is not enough to completely eliminate the electrically evoked muscle response. Furthermore, it can be easily realized that high stimulation frequencies, above 40 Hz, can not be used.

Frigo and colleagues proposed to use a “comb” filter for estimating the volitional EMG component (Frigo, 2000). This filter is a finite impulse response filter characterized by the following equation:

$$EMG_v(n) = \frac{EMG_r(n) - EMG_r(n - N)}{\sqrt{2}} \quad (1)$$

where $EMG_v(n)$ is the estimated volitional EMG, $EMG_r(n)$ is the raw EMG signal, N is the number of samples of each inter-pulse period, and $\sqrt{2}$ is a scale factor required to keep the same power in the signal before and after filtering.

This filter is based on the assumption that the volitional EMG is a stochastic signal and the M-wave is a time-invariant deterministic signal with no variations occurring between two inter-pulse periods.

The authors applied the comb filter both alone and in combination with a blocking window of 20 ms and concluded that a better performance was achieved when a blocking window was used before the application of the comb filter. However, it is important to highlight that the assumption of time-invariance of the M-wave is not valid, mainly during anisometric contractions or when the stimulation intensity (both pulse amplitude and duration) changes.

Other authors have proposed to use a high-pass filter with a cut-off frequency between 100 to 330 Hz (Muraoka, 2002; Schauer, 2004; Thorsen, 2001) after the application of a blocking window. Indeed, about 20 to 30 ms after the stimulation pulse, only electrically induced muscle response with a low frequency content (tail of the M-wave) superposes the volitional EMG signal. However, it is important to highlight that the most of the spectral energy of the EMG signal is located between 30 and 300 Hz with a peak around 120 Hz (De Luca & Knaflitz, 1992). Thus, only high-frequency components of the volitional EMG signal are taken into account when such a high-pass filter is used.

Based on the assumption that the volitional EMG is a band-limited Gaussian signal and considering the time-variance of the M-wave, an adaptive linear prediction filter has been proposed for M-wave removal (Sennels, 1997). The filtering idea is to predict the current inter-pulse period ($M+1$) as a linear combination of M foregoing inter-pulse periods. If the prediction is good enough, subtracting the predicted inter-pulse period from the current one leaves a residual signal where the M-wave has been removed. The output of the filter is computed as:

$$EMG_v(n) = EMG_r(n) - \sum_{j=1}^M b_j EMG_r(n - jN) \quad (2)$$

where $EMG_v(n)$ is the volitional EMG estimated by the filter, $EMG_r(n)$ is the raw EMG signal, M is the number of previous inter-pulse periods used for prediction, N is the number of samples of each inter-pulse period, and b_j are the filter coefficients.

The optimal filter coefficients are calculated with a common least square algorithm where the output energy of the current inter-pulse period is minimized with respect to the filter coefficients. Each time a new inter-pulse period is acquired,

the optimal filter coefficients are updated and the output of the filter is computed. Thus, the filter adapts to the signal variations at a rate equal to the stimulation frequency.

The authors evaluated the performance of the filter using three different numbers of foregoing inter-pulses periods for prediction, both on simulated and real data. They concluded that 6 foregoing inter-pulses periods are enough to remove completely the electrically evoked muscle response.

Starting from the same filtering idea of Sennels and colleagues, in a more recent work a Gram-Schmidt prediction error filter was proposed (Yeom, 2004). This solution is particularly interesting for real-time processing on field programmable gate array (FPGA).

A method based on the Singular Value Decomposition (SVD) has been also proposed to eliminate the M-wave (Tabernig & Acevedo, 2008). After eliminating the stimulation artifact by means of a blanking process, the authors considered the raw EMG signal as a sum of the volitional EMG, the M-wave and the measurement noise. An $N \times M$ input matrix can be created: each column corresponds to the raw EMG signal acquired during an inter-pulse period, M is the number of inter-pulse periods considered, and N the number of sample for each inter-pulse period, with $N \geq M$. Based on the assumptions that the energy of the M-wave is larger than the energy of the volitional EMG, and that the M-wave and the volitional EMG are orthogonal with respect to the measurement noise, the singular values (SV) of the input matrix can be easily separated. The first two SVs can be considered as associated to the M-wave and the last four to the volitional EMG and the noise. Since the subspaces associated with the volitional EMG, the M-wave and the noise are orthogonal, it is possible to eliminate the M-wave projecting the raw EMG signal (input matrix) on the volitional EMG subspace. The algorithm demonstrated to

Design of Myocontrolled Neuroprosthesis

be robust in estimating the volitional EMG from real signals.

As a general guideline, most authors agreed on the application of a blocking window on the raw EMG signal to remove the main part of the stimulation artifact and the M-wave and then using an appropriate filtering solution for eliminating the residual electrically induced components (Frigo, 2000; Langzam, 2006). The blocking window should last about 20 ms starting from the stimulation pulse. The volitional EMG signal is then available only in the remaining part of the inter-pulse period. However, being the signal to noise ratio higher in the second half of the inter-pulse period, a more complete removal of all the electrically induced components can be assured.

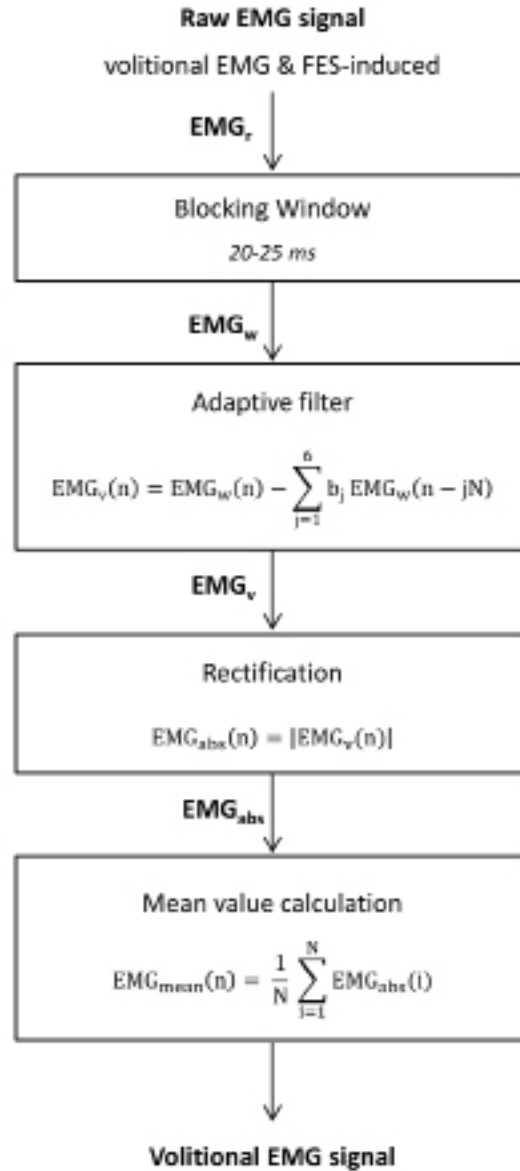
Concerning the filtering solution to apply after the blocking window, we suggest to use a method that does not rely on the assumption of time-invariance of the M-wave. Indeed, as we have seen in Figure 3, this assumption is not valid even in short term during anisometric contractions, that characterized real-life movements. Among the aforementioned solutions, two different approaches belonging to this category can be identified: a high-pass filter and an adaptive filter. Indeed, the method based on SVD can be considered adaptive if the input matrix is updated every M inter-pulse periods. To identify the best method to extract the volitional EMG, we conducted a study to compare the performance of these two approaches. A non-causal digital high-pass filter (Butterworth 2nd order, cut-off frequency of 200 Hz) was compared with a slightly modified version of the adaptive linear prediction filter proposed by Sennels and colleagues (1996). In particular, the M-wave was predicted as described in equation (2) and 6 foregoing inter-pulse periods were used for prediction as suggested by the authors, but, unlike Sennels and colleagues, we applied a blocking window of 20 ms before predicting the M-wave. The Cholesky decomposition was used to solve the least square algorithm so as to reduce

the computational cost and assure a real-time calculation. EMG signals acquired on a group of 10 healthy volunteers and 8 neurological patients during dynamic hybrid muscle activations of the biceps muscle were used for comparison. The results of the study demonstrated the superiority of the adaptive filter: different intensities of stimulation and variable stimulation did not affect the output of both filters, but only the adaptive filter was able to significantly distinguish a weak volitional activation from the residual noise. The results of this work have been recently submitted to the Journal of Electromyography and Kinesiology.

In conclusion, for on-line estimate of the volitional EMG component during dynamic hybrid muscle contractions, we suggest to use the processing scheme represented in Figure 5: first, a blocking window of at least 20 ms should be applied on the raw EMG signal, then the adaptive filter described by equation (2) should be used. This filter estimates the *quasi-deterministic* electrically induced components starting from 6 foregoing inter-pulse periods and subtracts them from the actual EMG signal to obtain the volitional contribution. To control the stimulation intensity a single value per each inter-pulse period is required. Thus, the volitional EMG signal is rectified and the mean value over the inter-pulse period is computed (Thorsen, 2001).

Figure 6 shows an example of the proposed processing scheme applied on a representative inter-pulse period. Panel (A) depicts the raw EMG signal and the applied blocking window. The blocking window lasts 20 ms that corresponds to half of the inter-pulse period, being the stimulation frequency set at 25 Hz in the example. Panel (B) reports the volitional EMG (black solid line), the rectified volitional EMG (grey solid line) and the averaged rectified EMG (gray dashed line).

Figure 5. Processing scheme of the raw EMG signal to estimate a low volitional component from dynamic hybrid muscle activations

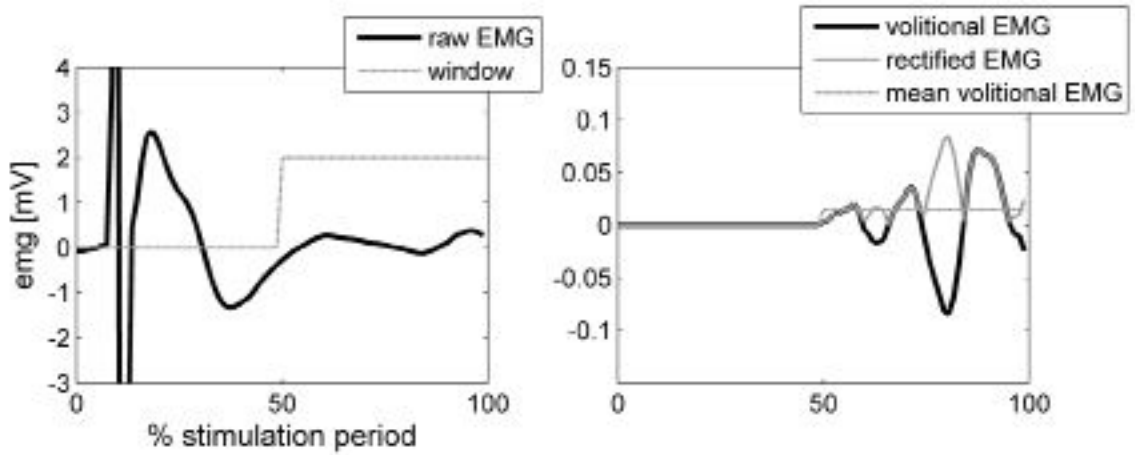


Control Strategies for Myocontrolled Neuroprostheses

Once the volitional EMG component is reliably estimated, it can be used to continuously control the stimulation intensity.

Control schemes for providing a stimulation intensity proportional to the residual volitional EMG have been proposed to support arm/hand functions (Ambrosini, 2011b; Fujiwara, 2009; Shindo, 2011; Thorsen, 2006; Thorsen, 2001) and ankle dorsi-flexion (Kamono, 2001; Yeom & Chang, 2010). In nearly all the reported cases

Figure 6. Example of the suggested processing scheme applied on a representative inter-pulse period during dynamic hybrid muscle activations



a single stimulation channel has been tested. The stimulation intensity was modulated in terms of pulse width (Ambrosini, 2011b; Kamono, 2001), current amplitude (Fujiwara, 2009; Shindo, 2011; Thorsen, 2006; Thorsen, 2001), and voltage amplitude (Yeom & Chang, 2010).

Figure 7 shows the principle of the EMG-based proportional controller for FES. In the example, the residual voluntary wrist extension is augmented by FES. The raw EMG signal is processed

with one of the method described in the previous section and the volitional EMG component, EMG_v in the figure, is estimated. Then, a low-pass filter is usually applied on the volitional EMG (EMG_{vf} in the figure is the filtered volitional EMG). The cut-off frequency of the filter must be carefully chosen to obtain a good compromise between smooth stimulation and acceptable delay between the patient's muscular activation and the stimulation response. The gain of the propor-

Figure 7 The principle of the EMG-based proportional controller for FES

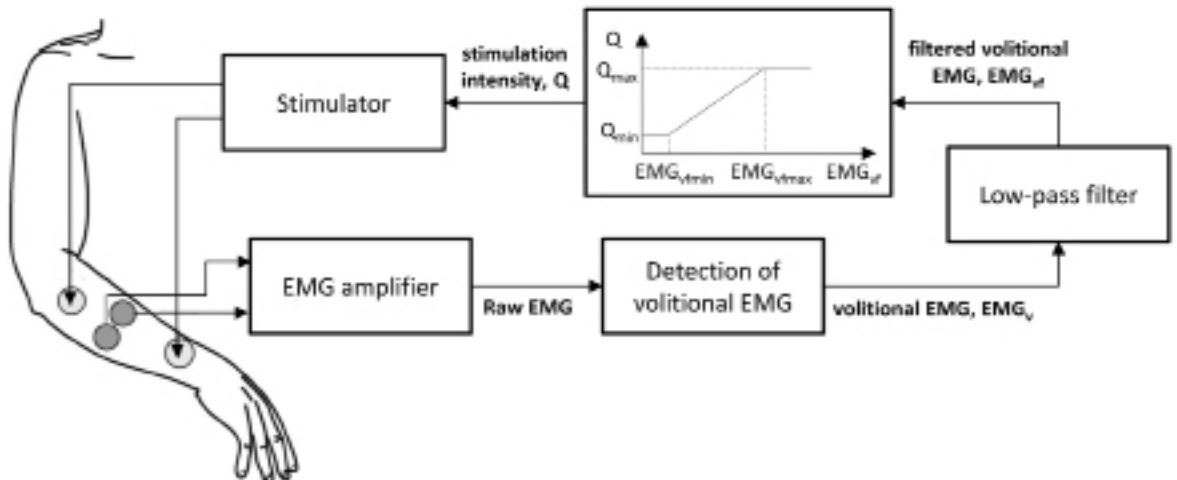
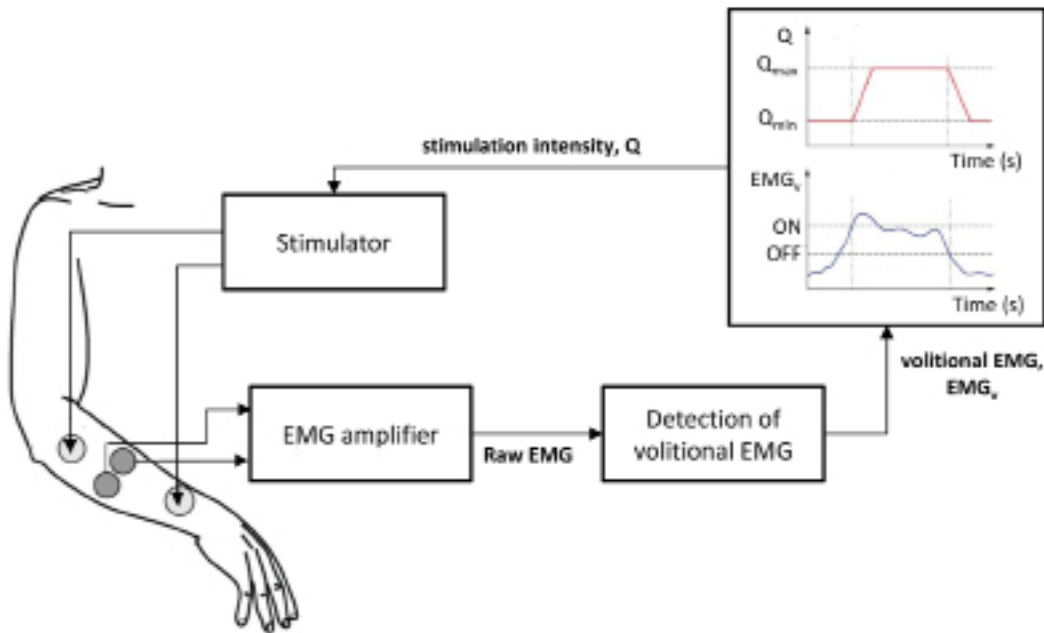


Figure 8 The principle of the EMG-based double threshold controller for FES



tional controller is defined by the saturation function shown in Figure 7, where $EMG_{v_{\max}}$ is the maximal residual filtered volitional EMG that the patient is able to generate and $EMG_{v_{\min}}$ is the baseline level of the filtered volitional EMG when the muscle is at rest. Usually, the value of $EMG_{v_{\min}}$ is computed at the maximal stimulation intensity with the subject who is supposed to be relaxed. Indeed, the higher is the stimulation intensity, the higher is the electrically induced muscle response and thus the higher are the potential residual components that remain on the estimated volitional EMG. The maximum stimulation intensity, Q_{\max} , is defined as the level of stimulation required to achieve a desired functional movement that the patient can not accomplish by using only his own residual muscle activity. The minimum stimulation intensity, Q_{\min} , represents the threshold of the motor unit recruitment curve above which a muscle contraction can be observed.

When patients are not able to generate smooth volitional contractions, an EMG-based proportional controller is not applicable due to risk of oscillation. For weak muscles, an on/off-control or a simple finite state control might be preferred (Sennels, 1997). Thus, to enlarge the number of subjects who could benefit from the system, we have recently proposed a double threshold control strategy. This approach can be seen as a compromise between EMG-triggered and EMG-proportional stimulation. The controller is characterized by a piece-wise linear input-output relationship, as shown in Figure 8: when the value of volitional EMG exceeds the upper threshold (ON), the stimulation intensity (Q in the figure) ramps up with slope K until the maximal stimulation intensity, Q_{\max} ; this stimulation level is kept constant until the muscle relaxes and the volitional EMG drops below the lower threshold (OFF); when this occurs, the stimulation intensity is reduced with slope $-K$ till the minimum

Design of Myocontrolled Neuroprosthesis

value, Q_{\min} . A calibration procedure to set appropriate values for the two thresholds is needed.

Both the presented solutions represent the most promising method to retrain the physiological neural pathway. Indeed, a physiologically appropriate control loop is provided to continually respond and enhance the volitional control of the affected muscle. This concept is aimed at reinforcing the natural control of the muscle activation. Furthermore, these myocontrolled neuroprostheses are able to maintain an active involvement of the patient during the exercise, thus facilitating the motor relearning process (Ferrante, 2011).

These myocontrolled neuroprostheses have also some potential limitations. Albeit controlled in a natural way, the subject has to be able to change the volitional muscle activity and also to relax the muscle when the stimulation is present. This can be still an unnatural task for the user. In particular, the relaxation of a stimulated muscle has shown to be difficult and requires special attention (Sennels, 1997). Furthermore, the level of the volitional EMG activation can be reduced in the presence of FES. This EMG reduction can be explained by the collision of antidromic and orthodromic motor impulse and the increased recurrent inhibition with increased stimulation intensity via the Renshaw cells (Taylor & Chappell, 2004; Yeom & Chang, 2010). Therefore, it might be possible that patients are not be able to generate adequate EMG amplitude or activation patterns to control the movement. This limitation might be solved through novel non-linear, non-proportional control or/and through a setting of control parameters more specific to the needs and abilities of each individual.

First Studies on Neurological Patients

While many clinical studies investigating the efficacy of EMG-trigger FES systems exist, only few clinical applications of neuroprostheses that

continuously modulate the stimulation intensity based on the residual volitional activation can be recorded. However, the technological advancements, both from a hardware and a software point of view, described in the previous sections, pave the way for assessing the effectiveness of this promising solution in the neuro-rehabilitation field.

First tests on neurological patients have been performed by the group of Thorsen (Thorsen, 1999b, 2001, 2006). All these studies were focused on the recovery of the hand functions, particularly grasping and wrist extension, and used a specifically designed device for both EMG recording and stimulation characterized by a fast recovery instrumentation amplifier for artifact suppression, as previously described (Thorsen, 1999a). Stimulation pulses with a current amplitude proportional to the residual volitional EMG signal were delivered. In the first study (Thorsen, 1999b), the EMG of the wrist extensors (extensor carpi radialis muscle) was used to control the thumb flexion. Three people with SCI performed some functional tasks with and without the device to assess its feasibility. A more extensive evaluation of the device was performed in a second study (Thorsen, 2001), where seven individuals with physical disabilities (six tetraplegia, one stroke) were involved. The residual volitional activity of the paretic wrist extensor was used to control the stimulation of the wrist extension (i.e., the stimulated muscle is the same used for control) in five people with SCI and the stimulation of the thumb flexion in the last two participants (one SCI, one stroke). The performances in tracking a trapezoidal target with and without the myocontrolled FES system were compared. Two subjects also carried out consecutive trials to evaluate the learning process. Three out of five people with a SCI, who had a weak volitional activation of the wrist extensors muscle, improved the tracking performance when using FES to control the wrist extension. The two subjects who preserved the highest natural contraction of the wrist extensors produced no

additional force when FES was applied. Thus, the authors concluded that subjects with a low residual natural force are good candidates for the device. One individual with an incomplete SCI tested the device to enhance thumb flexion over six training sessions; the authors observed a reduction of the tracking error thanks to a learning effect and an increase in the maximal augmented thumb force. Concerning the stroke patient, he showed some difficulties in controlling the thumb flexion but indicated the possibility of a carry-over effect after the first training session. In the last study of this set (Thorsen, 2006), the authors assessed again the possibility to use the residual EMG signal of the wrist extensors muscle to directly control the electrical stimulation of the extrinsic finger and thumb flexors. Five people with incomplete SCI tested the device during tasks involving three everyday objects (a videocassette, a bottle, and a pen). Without the device, none of the subjects were able to grasp any objects, but when myocontrolled FES was used all of the subject completed the required tasks. From the results of all these studies, it is possible to conclude that this control strategy is easy to be understood and no training is needed for the subjects to achieve an immediate improvement in motor performance. However, it is important to highlight that in most of the mentioned applications a stimulation site closed to the muscle used for EMG recordings was chosen. This is completely different from a motor control prospective than using the same muscle for both stimulation and EMG recordings: it is not the natural control of the affected muscle to be reinforced. The system proposed by the group of Thorsen might be more useful as an assistive device to improve the performance in activities of daily living, thus increasing independence and quality of life (e.g., for people with SCI), than as a treatment for enhancing motor relearning (e.g., for stroke patients).

Two more recent studies (Fujiwara, 2009; Shindo, 2011) evaluated the effectiveness of EMG-controlled FES in improving hand functions

in post-stroke patients. In both studies, the device developed by Muraoka and colleagues (2002) was used to stimulate the extensor digitorum communis: as previously described, this device allows to use the same electrodes for both stimulation and EMG recordings and provides a voltage amplitude proportional to the residual volitional EMG. In the first study (Fujiwara, 2009), 20 chronic stroke patients were involved in a 3-week training. Upper extremity motor function, spasticity, and functional scores were assessed before and after training. Furthermore, neurophysiological outcome measures, such as EMG activities, reciprocal inhibition with a H-reflex conditioning-test paradigm, and intracortical inhibition with a paired magnetic stimulation method, were also assessed. After training upper extremity motor function, spasticity, and functional scores significantly improved. EMG recordings showed a reduction in the co-contraction of the antagonist muscle (flexors). A partial restoration of the reciprocal inhibition was also observed. Finally, a change of intracortical circuitry in the motor cortex was assessed with the paired pulse paradigm: it was demonstrated that the paretic hemisphere short intracortical inhibition was reduced after intervention. This disinhibition of intracortical interneurons is supposed to play an important role in motor learning, reorganization and recovery after brain lesion. The authors concluded that EMG-controlled FES training increased corticospinal excitability, that resulted in motor function improvements. In another study (Shindo, 2011), the same training was assessed in a randomized controlled trial involving 24 post-acute stroke patients. Patients were randomly assigned to two groups, a control group, who performed 3-week of conventional training, and an experimental group, who underwent myocontrolled FES-induced training. Compared to the control group, the experimental group exhibited a significantly greater improvement in the upper extremity motor function after training. To summarize, these two studies provide some evidence that a myocon-

Design of Myocontrolled Neuroprosthesis

trolled FES-induced training might improve hand functions in patients with moderate to severe hand impairment both during early rehabilitation and chronic stage. Further investigations are actually needed to confirm these results; furthermore, the conventional use of FES should be compared with the use of EMG-controlled FES in order to evaluate the superiority of the latter approach.

All the aforementioned studies used a proportional control strategy to modulate the stimulation intensity. In a study recently submitted to the *Journal of Electromyography and Kinesiology*, we evaluated the feasibility of the EMG-based double threshold controller described in the previous section. The residual volitional EMG signal of the biceps muscle was used to control the elbow flexion, modulating the value of pulse width. Three people with an incomplete SCI were asked to flex the elbow while tracking a trapezoidal target with and without myocontrolled FES. All participants easily understood how to control the stimulation in a single session and improved their ability in reaching and maintaining a pre-defined level of elbow flexion when FES was added to the volitional effort. However, further investigations are needed to evaluate the efficacy of this method both for assistive and a rehabilitative purposes.

FUTURE RESEARCH DIRECTIONS

Once a clear neuropathological rationale is stated, to develop a neuro-rehabilitation treatment, the following key elements need to be fully addressed: 1) safe technology; 2) easy-to-use procedures; 3) outcome evidences. The latter two elements are still to be achieved to complete the clinical translation of myocontrolled neuroprostheses.

The current status of the bioengineering research applied to the design and development of myocontrolled neuroprostheses has achieved applicable solutions ready to be applied into clinical settings. The hardware components are now all available as commercial certificated devices and

proper signal processing and control strategies for FES have been designed and positively tested, as detailed in the chapter. However, to leave the research laboratories and reach the clinical settings, further technological improvements are needed: the procedures for settings the controller parameters should become faster, simpler, and independent of the operator. A compact and robust device, that does not require the use of an external computer for control and can exploit the same electrodes both for stimulation and EMG recordings, is also needed. These improvements are even more important to make this technology suitable for a home environment.

The next challenge is to define clear directions in the translation of the technology into the clinical practice. In our view, two are the main target populations who could mostly benefit of the use of myocontrolled neuroprostheses. On one hand, neurological patients, and, among all, people affected by muscle weakness and poor motor control, such as stroke survivors and people affected by multiple sclerosis. On the other hand, elderly people, to promote active ageing and to assure a longer period of healthy living. Different motor tasks could benefit of the combined volitional and FES-induced control, either for the upper and lower limbs. The possibility to combine more than one stimulation channel should be also assured in order to support more functional motor tasks. Treatments could be based on an intensive training during hospitalization but also continuous long term training at home. Adjustments to the hardware and software are then required to fit the specific requirements even if the core of the technology is common.

Another promising prospective for the near future might be the possibility to combine myocontrolled neuroprostheses with external (robotic) actuators in order to take advantages from the strength of each technology, overcoming the performances of each single approach (Moreno, 2011). The addition of FES to an exoskeleton system can take advantage of the muscle power

generation, reducing the power demand of the exoskeleton and allowing less powerful joint actuators, leading to a less heavy and power-demanding system. Also, the combination of FES and exoskeleton technologies can delay the onset of muscular fatigue induced by FES, thus prolonging the duration of the training and the consequent benefits, and can maximize the involvement of the patient in the exercise, thus enhancing motor learning. This combination might represent an interesting solution both from an assistive and a rehabilitative point of view.

Finally, EMG-controlled FES systems might also become an important tool to deeper investigate into the spinal and cortical mechanisms underlying the recovery of motor functions after a damage of the CNS.

CONCLUSION

In this chapter we have presented the most important elements to be considered to design a myocontrolled neuroprosthesis, intended as a device to produce a functional task thanks to the hybrid synchronous activation of the muscle. The combination of volitional residual muscle activations with FES-induced contractions requires specific hardware, which are now commercially available, and specific processing for real-time estimate of the volitional component and the consequent control of the stimulation parameters. As described, different approaches have been proposed in the literature and the most promising ones have been here compared to provide an overall evaluation and guidelines to identify the best solution. As usually happens, the best solution can be partially driven by the application itself, so detailed comments on the obtained results have been provided more than just a final solution.

From the neurophysiological point of view the combination of volitional control and FES-induced contraction is extremely promising since it allows to close the loop between intention, action, sen-

sory afferents and also subject reward, assuring task completion thanks to the amplification of the muscle contraction as provided by the artificial control. This loop is crucial to facilitate the best relearning process in neuro-rehabilitation, assuring the involvement of the subject into the exercises both from a cognitive and motivational point of view as well as from a physical neuromuscular point of view. At the same time, this loop could play a very important role also in the training of elderly people, where, even if the overall status is still healthy, a general functional decline involves the global neuromotor control function.

To conclude, it is noteworthy to spend a few words commenting the relevance of the use of myocontrolled neuroprostheses into the development of sustainable and personalized health care systems. Indeed, the possibility to have automatic system able to adapt on the single end-user and to allow the person to exercises without a one-to-one therapist assistance or even in a remote situation with a maximal safety and a promising re-learning outcome are crucial ingredients in view of the next societal challenges, such as the reduction of the hospitalization costs, the active ageing and the independent living.

REFERENCES

Ambrosini, E., Ferrante, S., Ferrigno, G., Molteni, F., & Pedrocchi, A. (2012). Cycling induced by electrical stimulation improves muscle activation and symmetry during pedaling in hemiparetic patients. *IEEE Transactions on Neural Systems and Rehabilitation Engineering*, 20, 320–330. doi:10.1109/TNSRE.2012.2191574 PMID:22514205

Design of Myocontrolled Neuroprosthesis

- Ambrosini, E., Ferrante, S., Pedrocchi, A., Ferrigno, G., & Molteni, F. (2011). Cycling induced by electrical stimulation improves motor recovery in postacute hemiparetic patients: A randomized controlled trial. *Stroke*, *42*, 1068–1073. doi:10.1161/STROKEAHA.110.599068 PMID:21372309
- Ambrosini, E., Ferrante, S., Tibiletti, M., Schauer, T., Klauer, C., Ferrigno, G., & Pedrocchi, A. (2011). An EMG-controlled neuroprosthesis for daily upper limb support: A preliminary study. In *Conference Proceedings of the Annual International Conference of the IEEE Engineering in Medicine and Biology Society* (pp. 4259–4262).
- Barrett, C. L., Mann, G. E., Taylor, P. N., & Strike, P. (2009). A randomized trial to investigate the effects of functional electrical stimulation and therapeutic exercise on walking performance for people with multiple sclerosis. *Multiple Sclerosis*, *15*, 493–504. doi:10.1177/1352458508101320 PMID:19282417
- Barsi, G. I., Popovic, D. B., Tarkka, I. M., Sinkjaer, T., & Grey, M. J. (2008). Cortical excitability changes following grasping exercise augmented with electrical stimulation. *Experimental Brain Research*, *191*, 57–66. doi:10.1007/s00221-008-1495-5 PMID:18663439
- Benton, L. A., Baker, L. L., Bowman, B. R., & Waters, R. L. (1981). *Functional electrical stimulation -- A practical clinical guide* (2nd ed.). Los Angeles, CA: Rehabilitation Engineering Center.
- Bergquist, A. J., Clair, J. M., Lagerquist, O., Mang, C. S., Okuma, Y., & Collins, D. F. (2011). Neuromuscular electrical stimulation: Implications of the electrically evoked sensory volley. *European Journal of Applied Physiology*, *111*, 2409–2426. doi:10.1007/s00421-011-2087-9 PMID:21805156
- Bickel, C. S., Gregory, C. M., & Dean, J. C. (2011). Motor unit recruitment during neuromuscular electrical stimulation: A critical appraisal. *European Journal of Applied Physiology*, *111*, 2399–2407. doi:10.1007/s00421-011-2128-4 PMID:21870119
- Bogataj, U., Gros, N., Kljajić, M., Aćimović, R., & Malezic, M. (1995). The rehabilitation of gait in patients with hemiplegia: A comparison between conventional therapy and multichannel functional electrical stimulation therapy. *Physical Therapy*, *75*, 490–502. PMID:7770495
- Cauraugh, J., Light, K., Kim, S., Thigpen, M., & Behrman, A. (2000). Chronic motor dysfunction after stroke: Recovering wrist and finger extension by electromyography-triggered neuromuscular stimulation. *Stroke*, *31*, 1360–1364. doi:10.1161/01.STR.31.6.1360 PMID:10835457
- Cauraugh, J. H., Naik, S. K., Hsu, W. H., Coombes, S. A., & Holt, K. G. (2010). Children with cerebral palsy: A systematic review and meta-analysis on gait and electrical stimulation. *Clinical Rehabilitation*, *24*, 963–978. doi:10.1177/0269215510371431 PMID:20685722
- De Kroon, J. R., & IJzerman, M. J. (2008). Electrical stimulation of the upper extremity in stroke: Cyclic versus EMG-triggered stimulation. *Clinical Rehabilitation*, *22*, 690–697. doi:10.1177/0269215508088984 PMID:18678569
- De Kroon, J. R., IJzerman, M. J., Chae, J., Lankhorst, G. J., & Zilvold, G. (2005). Relation between stimulation characteristics and clinical outcome in studies using electrical stimulation to improve motor control of the upper extremity in stroke. *Journal of Rehabilitation Medicine*, *37*, 65–74. doi:10.1080/16501970410024190 PMID:15788340

- Farina, D., Blanchietti, A., Pozzo, M., & Merletti, R. (2004). M-wave properties during progressive motor unit activation by transcutaneous stimulation. *Journal of Applied Physiology*, *97*, 545–555. doi:10.1152/jappphysiol.00064.2004 PMID:15121744
- Ferrante, S., Ambrosini, E., Ravelli, P., Guanziroli, E., Molteni, F., Ferrigno, G., & Pedrocchi, A. (2011). A biofeedback cycling training to improve locomotion: A case series study based on gait pattern classification of 153 chronic stroke patients. *Journal of Neuroengineering and Rehabilitation*, *8*, 47. doi:10.1186/1743-0003-8-47 PMID:21861930
- Ferrante, S., Pedrocchi, A., Ferrigno, G., & Molteni, F. (2008). Cycling induced by functional electrical stimulation improves the muscular strength and the motor control of individuals with post-acute stroke. *European Journal of Physical and Rehabilitation Medicine*, *44*, 159–167. PMID:18418336
- Francis, S., Lin, X., Aboushousah, S., White, T. P., Phillips, M., Bowtell, R., & Constantinescu, C. S. (2009). fMRI analysis of active, passive and electrically stimulated ankle dorsiflexion. *NeuroImage*, *44*, 469–479. doi:10.1016/j.neuroimage.2008.09.017 PMID:18950717
- Frigo, C., Ferrarin, M., Frasson, W., Pavan, E., & Thorsen, R. (2000). EMG signals detection and processing for on-line control of functional electrical stimulation. *Journal of Electromyography and Kinesiology*, *10*, 351–360. doi:10.1016/S1050-6411(00)00026-2 PMID:11018444
- Fujiwara, T., Kasashima, Y., Honaga, K., Muraoka, Y., Tsuji, T., & Osu, R. et al. (2009). Motor improvement and corticospinal modulation induced by hybrid assistive neuromuscular dynamic stimulation (HANDS) therapy in patients with chronic stroke. *Neurorehabilitation and Neural Repair*, *23*, 125–132. doi:10.1177/1545968308321777 PMID:19060131
- Gandolla, M., Pedrocchi, A., Ferrante, S., Guanziroli, E., Martegani, A., Ferrigno, G., & Ward, N. S. (2012). *Hypothesis for functional electrical stimulation mechanism of action: An fMRI study of cortical activations during ankle dorsiflexion in healthy subjects*. Paper presented at the 3rd Annual International Functional Electrical Stimulation Society UK and Ireland Chapter, Birmingham, UK.
- Gater, D. R. Jr, Dolbow, D., Tsui, B., & Gorgey, A. S. (2011). Functional electrical stimulation therapies after spinal cord injury. *NeuroRehabilitation*, *28*, 231–248. PMID:21558629
- Glinsky, J., Harvey, L., & Van Es, P. (2007). Efficacy of electrical stimulation to increase muscle strength in people with neurological conditions: A systematic review. *Physiotherapy Research International: The Journal for Researchers and Clinicians in Physical Therapy*, *12*, 175–194. doi:10.1002/pri.375 PMID:17624871
- Hermens, H. J., Freriks, B., Disselhorst-Klug, C., & Rau, G. (2000). Development of recommendations for SEMG sensors and sensor placement procedures. *Journal of Electromyography and Kinesiology*, *10*, 361–374. doi:10.1016/S1050-6411(00)00027-4 PMID:11018445
- Howson, D. C., & Heule, J. E. (1980). Electronic circuit permitting simultaneous use of stimulating and monitoring equipment.
- Iftime-Nielsen, S. D., Christensen, M. S., Vingborg, R. J., Sinkjaer, T., Roepstorff, A., & Grey, M. J. (2012). Interaction of electrical stimulation and voluntary hand movement in SII and the cerebellum during simulated therapeutic functional electrical stimulation in healthy adults. *Human Brain Mapping*, *33*, 40–49. doi:10.1002/hbm.21191 PMID:21591025

Design of Myocontrolled Neuroprosthesis

- Jiang, N., Falla, D., d'Avella, A., Graitmann, B., & Farina, D. (2010). Myoelectric control in neurorehabilitation. *Critical Reviews in Biomedical Engineering*, 38, 381–391. doi:10.1615/CritRev-BiomedEng.v38.i4.30 PMID:21133839
- Kamono, A., Muraoka, Y., Shimaoka, H., Uchida, S., & Ota, T. (2002). Development of EMG-controlled functional electrical stimulation system. In *Proceedings of the 41st SICE Annual Conference IEEE* (Vol. 3, pp. 2022–2027).
- Kamono, K. Y., & Tomita, Y. (2001). *Development of gait assist device for foot drop patients*. Paper presented at the 6th Annual Conference of the International Functional Electrical Stimulation Society, Cleveland, OH.
- Kimberley, T. J., Lewis, S. M., Auerbach, E. J., Dorsey, L. L., Lojovich, J. M., & Carey, J. R. (2004). Electrical stimulation driving functional improvements and cortical changes in subjects with stroke. *Experimental Brain Research*, 154, 450–460. doi:10.1007/s00221-003-1695-y PMID:14618287
- Knaflitz, M., & Merletti, R. (1988). Suppression of stimulation artifacts from myoelectric-evoked potential recordings. *IEEE Transactions on Bio-Medical Engineering*, 35, 758–763. doi:10.1109/10.7278 PMID:3169829
- Knaflitz, M., Merletti, R., & De Luca, C. J. (1990). Inference of motor unit recruitment order in voluntary and electrically elicited contractions. *Journal of Applied Physiology*, 68, 1657–1667. PMID:2347805
- Krakauer, J. W. (2006). Motor learning: Its relevance to stroke recovery and neurorehabilitation. *Current Opinion in Neurology*, 19, 84–90. doi:10.1097/01.wco.0000200544.29915.cc PMID:16415682
- Langzam, E., Isakov, E., & Mizrahi, J. (2006). Evaluation of methods for extraction of the volitional EMG in dynamic hybrid muscle activation. *Journal of Neuroengineering and Rehabilitation*, 3, 27. doi:10.1186/1743-0003-3-27 PMID:17123447
- Luca, C. J. D., & Knaflitz, M. (1992). *Surface Electromyography: What's New?* Torino, Italy: CLUT.
- Mandrile, F., Farina, D., Pozzo, M., & Merletti, R. (2003). Stimulation artifact in surface EMG signal: effect of the stimulation waveform, detection system, and current amplitude using hybrid stimulation technique. *IEEE Transactions on Neural Systems and Rehabilitation Engineering*, 11, 407–415. doi:10.1109/TNSRE.2003.819791 PMID:14960117
- Meilink, A., Hemmen, B., Seelen, H. A. M., & Kwakkel, G. (2008). Impact of EMG-triggered neuromuscular stimulation of the wrist and finger extensors of the paretic hand after stroke: A systematic review of the literature. *Clinical Rehabilitation*, 22, 291–305. doi:10.1177/0269215507083368 PMID:18390973
- Meo, J. H., & Post, H. W. (1962). Functional electrical stimulation for ambulation in hemiplegia. *The Journal-Lancet*, 82, 285–288. PMID:14474974
- Merletti, R., Knaflitz, M., & De Luca, C. J. (1990). Myoelectric manifestations of fatigue in voluntary and electrically elicited contractions. *Journal of Applied Physiology*, 69, 1810–1820. PMID:2272975
- Merletti, R., Knaflitz, M., & DeLuca, C. J. (1992). Electrically evoked myoelectric signals. *Critical Reviews in Biomedical Engineering*, 19, 293–340. PMID:1563271

- Minzly, J., Mizrahi, J., Hakim, N., & Liberson, A. (1993). Stimulus artefact suppressor for EMG recording during FES by a constant-current stimulator. *Medical & Biological Engineering & Computing*, *31*, 72–75. doi:10.1007/BF02446897 PMID:8326768
- Moreno, J. C., Del Ama, A. J., de Los Reyes-Guzmán, A., Gil-Agudo, A., Ceres, R., & Pons, J. L. (2011). Neurobotic and hybrid management of lower limb motor disorders: A review. *Medical & Biological Engineering & Computing*, *49*, 1119–1130. doi:10.1007/s11517-011-0821-4 PMID:21847596
- Mortimer, J. T. (2011). Motor prostheses. In *Comprehensive Physiology*. John Wiley & Sons, Inc. Retrieved from <http://onlinelibrary.wiley.com/doi/10.1002/cphy.cp010205/abstract>
- Muraoka, Y. (2002). Development of an EMG recording device from stimulation electrodes for functional electrical stimulation. *Frontiers of Medical and Biological Engineering*, *11*, 323–333. doi:10.1163/156855701321138969 PMID:12735431
- Pomeroy, V. M., King, L., Pollock, A., Baily-Hallam, A., & Langhorne, P. (2006). Electrostimulation for promoting recovery of movement or functional ability after stroke. *Cochrane Database of Systematic Reviews (Online)*, CD003241.
- Popovic, D. B., Popovic, M. B., Sinkjaer, T., Stefanovic, A., & Schwirtlich, L. (2004). Therapy of paretic arm in hemiplegic subjects augmented with a neural prosthesis: a cross-over study. *Canadian Journal of Physiology and Pharmacology*, *82*, 749–756. doi:10.1139/y04-057 PMID:15523532
- Popović, D. B., Sinkaer, T., & Popović, M. B. (2009). Electrical stimulation as a means for achieving recovery of function in stroke patients. *NeuroRehabilitation*, *25*, 45–58. PMID:19713618
- Rushton, D. N. (2003). Functional electrical stimulation and rehabilitation--An hypothesis. *Medical Engineering & Physics*, *25*, 75–78. doi:10.1016/S1350-4533(02)00040-1 PMID:12485788
- Saxena, S., Nikolic, S., & Popovic, D. (1995). An EMG-controlled grasping system for tetraplegics. *Journal of Rehabilitation Research and Development*, *32*, 17–24. PMID:7760263
- Schauer, T., Salbert, R., Negård, N.-O., & Raisch, J. (2004). Detection and filtering of EMG for assessing voluntary muscle activity during FES. In *Proceedings of 9th Annual Conference of the International FES Society* (pp. 1–3). Bournemouth, UK.
- Sennels, S., Biering-Sorensen, F., Andersen, O. T., & Hansen, S. D. (1997). Functional neuromuscular stimulation controlled by surface electromyographic signals produced by volitional activation of the same muscle: adaptive removal of the muscle response from the recorded EMG-signal. *IEEE Transactions on Rehabilitation Engineering*, *5*, 195–206. doi:10.1109/86.593293 PMID:9184905
- Shalaby, R., Schauer, T., Liedecke, W., & Raisch, J. (2011). Amplifier design for EMG recording from stimulation electrodes during functional electrical stimulation leg cycling ergometry. *Biomedical Engineering*, *56*, 23–33. doi:10.1515/bmt.2010.055 PMID:21162696
- Sheffler, L. R., & Chae, J. (2007). Neuromuscular electrical stimulation in neurorehabilitation. *Muscle & Nerve*, *35*, 562–590. doi:10.1002/mus.20758 PMID:17299744
- Shindo, K., Fujiwara, T., Hara, J., Oba, H., Hotta, F., & Tsuji, T. et al. (2011). Effectiveness of hybrid assistive neuromuscular dynamic stimulation therapy in patients with subacute stroke: A randomized controlled pilot trial. *Neurorehabilitation and Neural Repair*, *25*, 830–837. doi:10.1177/1545968311408917 PMID:21666139

Design of Myocontrolled Neuroprosthesis

- Smith, G. V., Alon, G., Roys, S. R., & Gullapalli, R. P. (2003). Functional MRI determination of a dose-response relationship to lower extremity neuromuscular electrical stimulation in healthy subjects. *Experimental Brain Research*, *150*, 33–39. PMID:12698214
- Tabernig, C. B., & Acevedo, R. C. (2008). M-wave elimination from surface electromyogram of electrically stimulated muscles using singular value decomposition: preliminary results. *Medical Engineering & Physics*, *30*, 800–803. doi:10.1016/j.medengphy.2007.09.001 PMID:17981071
- Taylor, & Chappell, P. (2004). Variation in system gain when using voluntary EMG to control electrical stimulation of the same muscle. In D. Wood (Ed.), *Proceedings of 9th Annual Conference of the International Functional Electrical Stimulation Society*. Bournemouth, UK.
- Thorsen, R. (1999). An artefact suppressing fast-recovery myoelectric amplifier. *IEEE Transactions on Bio-Medical Engineering*, *46*, 764–766. doi:10.1109/10.764955 PMID:10356884
- Thorsen, R., Ferrarin, M., Spadone, R., & Frigo, C. (1999). Functional control of the hand in tetraplegics based on residual synergistic EMG activity. *Artificial Organs*, *23*, 470–473. doi:10.1046/j.1525-1594.1999.06362.x PMID:10378946
- Thorsen, R., Spadone, R., & Ferrarin, M. (2001). A pilot study of myoelectrically controlled FES of upper extremity. *IEEE Transactions on Neural Systems and Rehabilitation Engineering*, *9*, 161–168. doi:10.1109/7333.928576 PMID:11474969
- Thorsen, R. A., Occhi, E., Boccardi, S., & Ferrarin, M. (2006). Functional electrical stimulation reinforced tenodesis effect controlled by myoelectric activity from wrist extensors. *Journal of Rehabilitation Research and Development*, *43*, 247–256. doi:10.1682/JRRD.2005.04.0068 PMID:16847791
- Trevisi, E., Gualdi, S., De Conti, C., Salghetti, A., Martinuzzi, A., Pedrocchi, A., & Ferrante, S. (2011). Cycling induced by functional electrical stimulation in children affected by cerebral palsy: Case report. *European Journal of Physical and Rehabilitation Medicine*.
- Yan, T., Hui-Chan, C. W. Y., & Li, L. S. W. (2005). Functional electrical stimulation improves motor recovery of the lower extremity and walking ability of subjects with first acute stroke: A randomized placebo-controlled trial. *Stroke*, *36*, 80–85. doi:10.1161/01.STR.0000149623.24906.63 PMID:15569875
- Yeom, H., & Chang, Y. H. (2010). Autogenic EMG-controlled functional electrical stimulation for ankle dorsiflexion control. *Journal of Neuroscience Methods*, *193*, 118–125. doi:10.1016/j.jneumeth.2010.08.011 PMID:20713086
- Yeom, H. J., Park, Y. C., Yoon, Y. R., Shin, T. M., & Yoon, H. R. (2004). An adaptive M-wave canceler for the EMG controlled functional electrical stimulator and its FPGA implementation. In *Proceedings of 26th Annual International Conference of the IEEE Engineering in Medicine and Biology Society, 2004. IEMBS '04* (Vol. 2, pp. 4122–4125).
- Zajac, F. E., & Faden, J. S. (1985). Relationship among recruitment order, axonal conduction velocity, and muscle-unit properties of type-identified motor units in cat plantaris muscle. *Journal of Neurophysiology*, *53*, 1303–1322. PMID:2987433

ADDITIONAL READING

- Arabadzhev, T. I., Dimitrov, G. V., & Dimitrova, N. A. (2005). Simulation analysis of the performance of a novel high sensitive spectral index for quantifying M-wave changes during fatigue. *Journal of Electromyography and Kinesiology*, *15*, 149–158. doi:10.1016/j.jelekin.2004.08.003 PMID:15664145
- Bashir, S., Mizrahi, I., Weaver, K., Fregni, F., & Pascual-Leone, A. (2010). Assessment and modulation of neural plasticity in rehabilitation with transcranial magnetic stimulation. *PM & R: the journal of injury, function, and rehabilitation*, *2*, S253–268.
- Chae, J., Sheffler, L., & Knutson, J. (2008). Neuromuscular electrical stimulation for motor restoration in hemiplegia. *Topics in Stroke Rehabilitation*, *15*, 412–426. doi:10.1310/tsr1505-412 PMID:19008202
- Dietz, V., & Nef, T. (2012). Neurorehabilitation Technology. Rymer, William Zev (Eds.).
- Doucet, B. M., Lam, A., & Griffin, L. (2012). Neuromuscular electrical stimulation for skeletal muscle function. *The Yale Journal of Biology and Medicine*, *85*, 201–215. PMID:22737049
- Henneman, E., Somjen, G., & Carpenter, D. O. (1965). Functional significance of cell size in spinal motoneurons. *Journal of Neurophysiology*, *28*, 560–580. PMID:14328454
- Kandel, E. R., Schwartz, J., Jessell, T., Siegelbaum, S., & Hudspeth, A. J. (2012). *Principles of Neural Science* (5th ed.). McGraw Hill Professional.
- Langhorne, P., Coupar, F., & Pollock, A. (2009). Motor recovery after stroke: a systematic review. *The Lancet Neurology*, *8*, 741–754. doi:10.1016/S1474-4422(09)70150-4 PMID:19608100
- Lee, R. G., & van Donkelaar, P. (1995). Mechanisms underlying functional recovery following stroke. *The Canadian Journal of Neurological Sciences*, *22*, 257–263. PMID:8599767
- Liberson, W. T., Holmquest, H. J., Scot, D., & Dow, M. (1961). Functional electrotherapy: stimulation of the peroneal nerve synchronized with the swing phase of the gait of hemiplegic patients. *Archives of Physical Medicine and Rehabilitation*, *42*, 101–105. PMID:13761879
- Mandrile, F., Farina, D., Pozzo, M., & Merletti, R. (2003). Stimulation artifact in surface EMG signal: effect of the stimulation waveform, detection system, and current amplitude using hybrid stimulation technique. *IEEE transactions on neural systems and rehabilitation engineering: a publication of the IEEE Engineering in Medicine and Biology Society*, *11*, 407–415.
- McGill, K. C., Cummins, K. L., Dorfman, L. J., Berlizot, B. B., Luetkemeyer, K., Nishimura, D. G., & Widrow, B. (1982). On the Nature and Elimination of Stimulus Artifact in Nerve Signals Evoked and Recorded Using Surface Electrodes. *IEEE Transactions on Bio-Medical Engineering*, *BME-29*, 129–137. doi:10.1109/TBME.1982.325019 PMID:7056556
- Merletti, R., & Parker, P. J. (2004). *Electromyography: Physiology, Engineering, and Non-Invasive Applications*. Wiley. doi:10.1002/0471678384
- Peckham, P. H., & Knutson, J. S. (2005). Functional electrical stimulation for neuromuscular applications. *Annual Review of Biomedical Engineering*, *7*, 327–360. doi:10.1146/annurev.bioeng.6.040803.140103 PMID:16004574
- Penny, W. D., Friston, K. J., Ashburner, J. T., Kiebel, S. J., & Nichols, T. E. (Eds.). (2006). *Statistical Parametric Mapping: The Analysis of Functional Brain Images* (1st ed.). Academic Press.

Petrofsky, J. S., & Phillips, C. A. (1984). The use of functional electrical stimulation for rehabilitation of spinal cord injured patients. *Central nervous system trauma: journal of the American Paralysis Association*, 1, 57–74.

Popovic, M. R., Curt, A., Keller, T., & Dietz, V. (2001). Functional electrical stimulation for grasping and walking: indications and limitations. *Spinal Cord*, 39, 403–412. doi:10.1038/sj.sc.3101191 PMID:11512070

Popovic, M. R., Keller, T., Pappas, I. P., Dietz, V., & Morari, M. (2001). Surface-stimulation technology for grasping and walking neuroprosthesis. *IEEE engineering in medicine and biology magazine: the quarterly magazine of the Engineering in Medicine & Biology and Society*, 20, 82–93.

Rattay, F. (1990). *Electrical nerve stimulation: theory, experiments and applications*. Springer-Verlag. doi:10.1007/978-3-7091-3271-5

Rossini, P. M., Altamura, C., Ferreri, F., Melgari, J.-M., Tecchio, F., & Tombini, M. et al. (2007). Neuroimaging experimental studies on brain plasticity in recovery from stroke. *Europa Medico-fisica*, 43, 241–254. PMID:17589415

Ward, Nick S, & Cohen, L. G. (2004). Mechanisms underlying recovery of motor function after stroke. *Archives of Neurology*, 61, 1844–1848. doi:10.1001/archneur.61.12.1844 PMID:15596603

Ward, N. S. (2007). Future perspectives in functional neuroimaging in stroke recovery. *Europa Medico-fisica*, 43, 285–294. PMID:17525701

KEY TERMS AND DEFINITIONS

Functional Electrical Stimulation (FES): Electrical stimulation of an intact lower motor neuron to activate plegic or paretic muscle in a precise sequence so as to directly accomplish or support functional tasks.

Hybrid Muscle Activation: A muscle contraction generated by two different excitation sources, volitional and electrically induced.

Motor Relearning: The recovery of previously learned motor abilities that have been lost or substantially compromised due to a damage or a disease of the central nervous system.

M-Wave: The electrically evoked myoelectric signal due to the synchronous firing of the electrically elicited muscle fibers, resulting in a quasi-deterministic signal.

Myocontrolled Neuroprosthesis: A neuroprosthesis which is controlled by means of the residual volitional muscle activations.

Neuroprosthesis: A device based on FES to activate the neuromuscular system in order to improve or substitute motor or sensory functions of an impaired central nervous system.

Neuro-Rehabilitation: The process of helping neurological patients to regain the highest possible level of independence and quality of life. This process includes a set of interventions designed to facilitate the recovery, minimizing, and/or compensating for any functional alterations resulting from a nervous system injury.

Stimulation Artifact: The result of a potential difference induced by the stimulation current between the EMG recording electrodes.

Volitional EMG: The EMG signal acquired during voluntary contraction due to the asynchronous firing of the elicited muscle fibers, resulting in a pseudorandom signal.

Chapter 14

Design and Development of EMG Conditioning System and Hand Gesture Recognition Based on Principal Component Analysis Feature Reduction Technique

P. Geethanjali
VIT University, India

ABSTRACT

This chapter discusses design and development of a surface Electromyogram (EMG) signal detection and conditioning system along with the issues of gratuitous spurious signals such as power line interference, artifacts, etc., which make signals plausible. In order to construe the recognition of hand gestures from EMG signals, Time Domain (TD) and well as Autoregressive (AR) coefficients features are extracted. The extracted features are diminished using the Principal Component Analysis (PCA) to alleviate the burden of the classifier. A four-channel continuous EMG signal conditioning system is developed and EMG signals are acquired from 10 able-bodied subjects to classify the 6 unique movements of hand and wrist. The reduced statistical TD and AR features are used to classify the signal patterns through k Nearest Neighbour (k NN) as well as Neural Network (NN) classifier. Further, EMG signals acquired from a transradial amputee using 8-channel systems for the 6 amenable motions are also classified. Statistical Analysis of Variance (ANOVA) results on classification performance of able-bodied subject divulge that the performance TD-PCA features are more significant than the AR-PCA features. Further, no significant difference in the performance of NN classifier and k NN classifier is construed with TD reduced features. Since the average classification error of k NN classifier with TD features is found to be less, k NN classifier is implemented in off-line using the TMS2407eZdsp digital signal controller to study the actuation of three low-power DC drives in the identification of intended motion with an able-bodied subject.

DOI: 10.4018/978-1-4666-6090-8.ch014

INTRODUCTION

Analysis of muscular activity such as force developed for a specific movement, evaluation of fatigue, type of movement etc., can be divulged from Electromyogram (EMG) signals. EMG signals are electrical signals that are generated in all living beings, in particular human beings and are obtained from body movement through the contraction and relaxation of skeletal muscles. These EMG signals are utilized for exploratory or diagnostic purposes when the technology is inchoate. However, with the advancement of technology, EMG signals have found to be of paramount importance in different fields of applications such as rehabilitation medicine, ergonomics, sports and space medicine and neurophysiology. In order to divulge the information effectively from EMG signals in different fields of application, it is necessary to detect and condition the EMG signals for further processing. EMG signals are generated during contraction of muscles and can be detected either invasively or non invasively. Detection of EMG signals by inserting the electrodes in the muscles are known as intramuscular EMG. Surface EMG (sEMG) signals are obtained by fixing electrode over the skin surface. The sEMG is widely used method in research as it is simple and non-invasive. However, the procurement of the EMG signal acquisition system is still a problem especially in electrophysiological research which involves EMG. Due to the advancement in technology, it is possible to fabricate portable EMG signal conditioning system at an affordable cost. One of the problems with the recording of physiological signals is various sources of noises. The noises include both high frequency and low frequency components. In addition, the power line noise from the EMG system has been the focus of researchers for some time. Further, proper grounding and electrical shielding are suggested by the researchers to rectify the power line interference problem. The low frequency noises are generated

due to electrode polarization and electrode cable artifacts.

This EMG signal normally comprises two states i.e., (i) A transient state emanating from a burst of fibers (ii) A steady state during constantly maintained contractions in the muscle. Hudgins, Parker, and Scott, (1993) were the first to consider the information content in a transient signal that comes with the onset of a contraction. The main weakness in using a transient state in EMG control is that contractions should be initiated from rest and precludes switching from class to class in an effective or intuitive manner. Englehart, Hudgins, and Parker (2003) have shown that steady state data is classified more accurately than transient state. Hargrove, Losier, Englehart, and Hudgins (2007) have shown real-time performance of a clinically-supported classifier with transient and steady state is always better than that of either transient or steady state alone. The process of identifying the intended limb motion from stored digitized EMG data consists of three stages: feature extraction, feature reduction and classification. Several techniques such as time domain (TD) statistical features (Hudgins, Parker, & Scott, 1993), auto regressions (AR) coefficients (Huang, Liu, Liu, & Wong, 2003), frequency domain techniques (Yazama, Mitsukura, Fukumi, & Akamatsu, 2003), time-scale techniques (Englehart, Hudgins, & Parker, 2001; Chu, Moon, & Mun, 2005), spectral components (Du & Vuskovic, 2004) etc. have so far been utilized for feature extraction. These extracted features are used in a classifier, such as, artificial neural network (NN) (Hudgins, Parker, & Scott, 1993), fuzzy logic (Ajiboye & Weir, 2005), Neuro-fuzzy (Kiguchi, Iwami, Yasuda, Watanabe, & Fukuda, 2003), *k*NN (Geethanjali, Ray & Shanmuganathan, 2009), state vector machine (Naik, Kumar, & Jayadeva, 2010) etc. to classify the intention hidden in the EMG.

One of the intricacies in the development of EMG controlled prosthetic hand is the classification of copious amount of features. The classification of larger number of features will

procrastinate the control and also onus to the classifier. In order to alleviate the computational complexity of such a system, feature reduction techniques such as principal component analysis (PCA) (Hudgins, Parker, & Scott, 1993), integral component analysis, and genetic algorithm (Kwon, Lee, Shin, Jang, & Hong, 1998), mutual components (Khushaba & Kodagoda, 2012) are considered to overcome the limitations of EMG controlled prosthetic hand. This chapter focuses on the influence of principal component analysis in classification of TD statistical features and AR coefficients with the neural network as well as the k nearest neighbour classifiers.

The objective of this chapter is to fathom the issues in the detection of surface Electromyogram (EMG) signals and conditioning to enable the researchers to build their low-cost reliable EMG signal conditioning system. This chapter also demonstrates the hand gesture recognition and actuation of prosthetic DC drives from EMG signals of able-bodied subject in off-line. Time domain features extracted from EMG signals for the purpose of recognition are studied with PCA to understand the influence of feature reduction in classifying the intended motion. Similarly the performance of the 8-channel amputee EMG data is studied and the results are discussed.

EMG SIGNAL CONDITIONING SYSTEM

Varying accuracy in the classification techniques may be due to signal conditioning along with

the physiological condition of the subject. Most researchers have used commercially available signal acquisition systems for the benefit of high signal-to-noise ratio and applied advanced signal processing techniques to show classification results with good accuracy (Ajiboye & Weir, 2005). For actual use by the researchers, it is desirable that the EMG signal conditioning system should be simple in design, reliable and affordable.

After detecting the signals from a specific muscle location, EMG signal is usually sent to a high quality amplifiers with variable gains to improve the quality of the EMG signal measurement. EMG signal conditioning depends on the characteristics of the amplification process which may have several stages. The most important stage of conditioning is the pre-amplification, i.e., the first stage of amplification, which is close to the signal. Pre-amplification is the differential amplification which enabled the measurement of EMG signals of low noise and high signal fidelity. After pre-amplification, it is possible to measure effective bandwidth of the signal with preferred frequency ranges with variable second stage of amplification for discretization. High-pass filtering remove movement artifacts typically of 10Hz and low pass filtering remove high-frequency components to avoid signal aliasing. Power-line noise components can be removed by using notch filter. But the use of notch filtering leads to the loss of important EMG signal information, as EMG has large information at these and neighbouring frequencies. So, notch filtering is not preferred in general.

Figure 1. Block diagram of EMG signal conditioning system

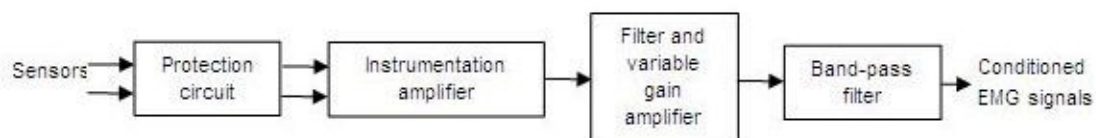
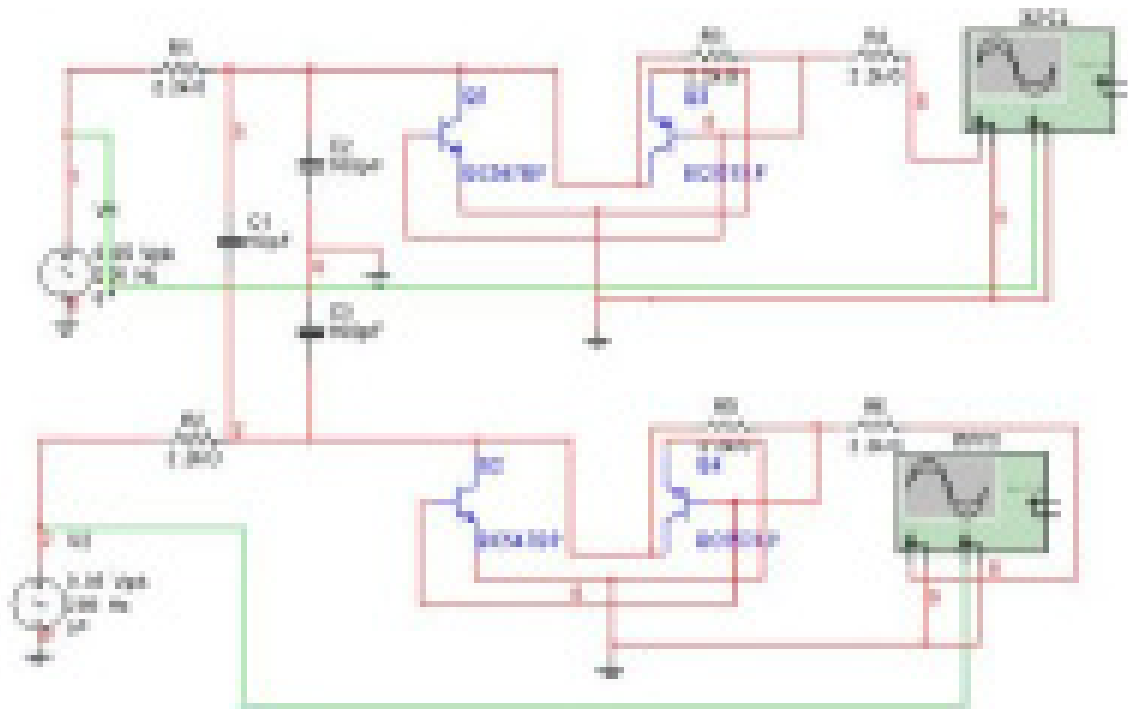


Figure 2. Protection Circuit



There are several important properties to be considered at each stage during the design of signal conditioning system for EMG signal acquisition. With the advent of modern technology, presently, there are many signal acquisition systems in particular for EMG signals that are commercially developed based on requirements. For the purpose of research work, the development of the EMG signal conditioning system is discussed.

This EMG data conditioning system comprises protection circuit, instrumentation amplifier, high pass filter for offset rejection, variable gain amplifier and band-pass filter as shown in Figure 1. The function of each stage is discussed in the subsequent subsections.

Protection Circuit

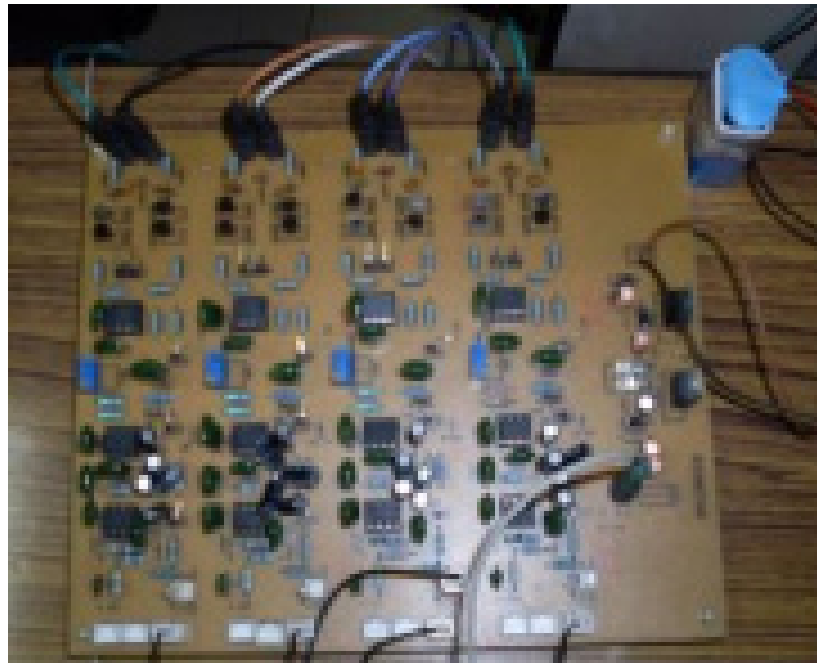
The protection circuit protects the user and the sensitive electronic circuit without any distortion

of the input signals. Figure 2 shows the protection circuit developed in Multisim software.

The initial stage is to subdue the high frequency radio signals, in the range of several hundred kHz that may enter the amplifier system through electrode cables. A RC suppression circuit with suitable values of R and C, is used to subdue the high frequency radio signals. The second stage consists of a clamping diode section which is a pair of matched NPN and PNP transistors (Engin, et al., 2007). Transistors begin to conduct at voltages exceeding $\pm\approx 0.58$ V. With a voltage above this level the transistors act as open circuits pulling all harmful currents down to the ground.

The protection circuit was simulated to verify the operation and found that it passes all the signals undistorted for amplitude $<\approx 550$ mV and frequency $<\approx 150$ kHz. Since the EMG signals of importance are less than 100 mV and in the frequency range of 0 to 1 kHz, the above mentioned circuit clearly meets the EMG data

Figure 3. Four channel EMG conditioning system



acquisition system requirements. This protection circuit is employed in the conditioning of EMG signals without any distortion as well as protecting the circuitry from the electrostatic discharge and maintains the comfort level of the subjects. The output of this stage is fed to the input of the pre-amplifier stage.

Pre-Amplification

Generally a differential amplifier is considered for pre-amplification depending on design requirements. It has the ability to eliminate the potentially much greater spurious signal from the power line sources. Differential amplifier subtracts the signals detected at two sites and then amplifies the difference.

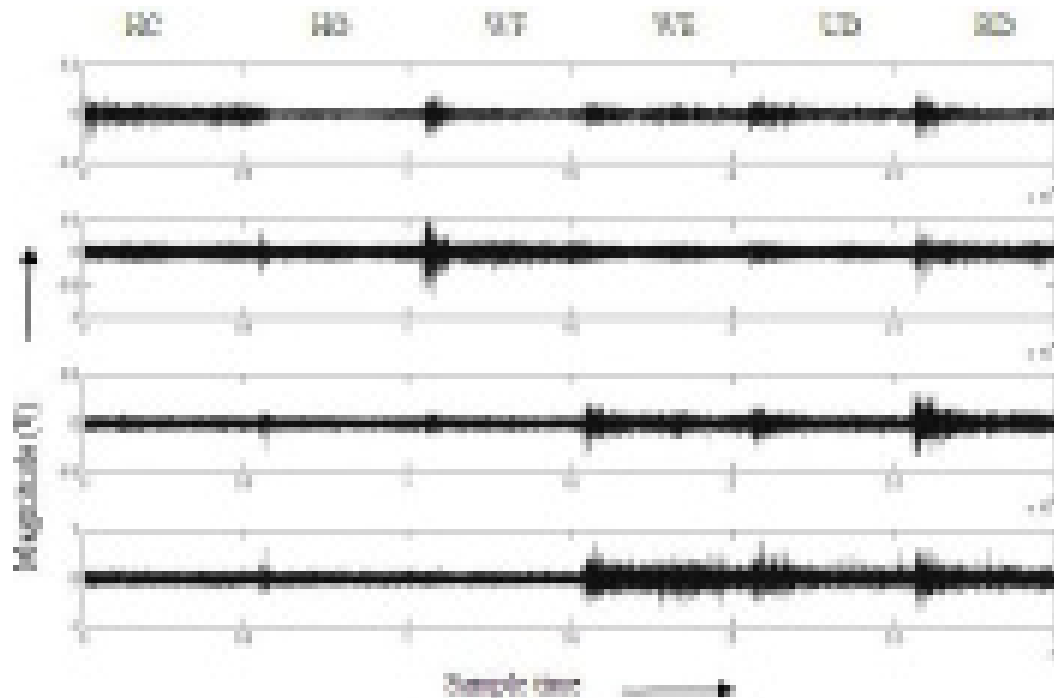
A suitable operational amplifier for this type of low-signal system is the instrumentation amplifier. The instrumentation amplifier for this type of application should have high common mode rejection ratio (CMRR), very high input impedance and low output impedance making it less

sensitive to noise. Based on these requirements instrumentation amplifiers may be chosen.

High Pass Filter

The high pass filter is connected after the pre-amplifier to prevent DC voltage offsets caused by skin impedance and chemical reaction between the skin and the electrode gel. Some electrode materials such as gold or silver are polarizable. This means that electric charge can accumulate on the surface of the electrode and build up a relatively large DC voltage. In this EMG conditioning system, a simple RC high pass filter circuit is used to overcome this problem. Since the usable energy of the EMG signal is dominant in the range of 20-500Hz, a cutoff frequency nearer to 10 Hz may be selected because it will not reject the necessary information of the EMG signals.

Figure 4. Four channel EMG signals for six movements of hand from able-bodied subject



Variable Gain Amplifier

The amplitude level of signal from the high pass filter is not sufficient enough for storing the EMG signals through data acquisition system. Thus the output from the high pass filter passes through the variable gain amplifier whose gain may be varied from 6 to 100 using high input impedance operational amplifiers.

Band Pass Filter

The final stage of the EMG signal conditioning system is the band pass filter which is a combination of low pass and high pass filter. The cutoff frequency of the filter may be 10-500Hz as most of the information is contained within this range.

A single-channel EMG conditioning circuit design can be extended to multichannel system. Figure 3 shows indigenously developed four channel EMG conditioning system in the laboratory.

EMG DATA ACQUISITION SYSTEM

The design of different blocks of single-channel EMG signal conditioning has been discussed in previous section. After experimental verification, conditioned signals are sent to analog to digital conversion process for further processing. This acquisition system may consist of multichannel A/D converters for multichannel systems.

The EMG signal quality is affected during A/D conversion process due to sampling and quantization. The sampling frequency should be chosen such that no information is lost during reconstruction. The sampling frequency need to be at least two times the signal frequency within the bandwidth. In case of multichannel A/D converter, the acquisition is not simultaneous but is shifted from channel to channel this must be accounted.

Further, the quantization is the process of expressing the analog value in terms of digital value. The amplitude of each sample is approximated due to a fixed number of bits available for quantifying

Figure 5. EMG signals acquisition from transradial amputee



the sample. This will add an additive noise in the signal. The quantization noise can be reduced by selection high precision A/D converter. The selection of A/D converter should also consider the gain and noise of the system along with a maximum output voltage of the system.

EXPERIMENTATION

In this work, four-channel EMG data corresponding to six different limb motions are obtained by using surface electrodes. To acquire the EMG signals, disc electrodes (Ag/AgCl) are placed at flexor digitorum superficialis, supinator, extensor digitorum communis and extensor indicis with a conductive paste on the surface of the skin for able-bodied subject. The EMG signal is acquired at a sample rate of 1000 Hz through DS1104 control board and dSPACE® software. The subject performed the following motions i.e., hand open (HO), hand close (HC), wrist flexion (WF), wrist extension (WE), ulnar deviation (UD) and radial deviation (RD) for 8 trials. Each motion continued

for 5 seconds. Figure 4 shows the EMG signals of an able-bodied subject from the indigenous system.

Similarly for a transradial amputee having shorter forearm, 8 channels Motion Lab acquisition (MA-300-XII) system is used for EMG signal acquisition due to difficulty in identifying the musculature. The signals are acquired with elbow resting on the table as shown in Figure 5.

Six classes of wrist and hand motions amenable and comfortable for the amputee are identified and performed in a sequential order i.e., hand supination, wrist flexion (WF), wrist extension (WE), radial deviation (RD), hand close (HC) and hand open (HO). Amputee subject is encouraged to move the phantom limb in a repeatable fashion to the best of his ability. Eight trials of data are collected. During all trials, subjects initiated the contraction from the hand supination. In each trial all motions are performed in sequential order and held for 5 sec, producing $(5 \times 6 = 30)$ 30 seconds of recording for all six motions. These signals are obtained from the forearm of the subject with a brief rest period of about 60 sec between each trial and without any report of fatigue from

Design and Development of EMG Conditioning System

the subject. These EMG signals are sampled at a frequency of 4 kHz and acquired in DATAQ (DI-720) to store it on a personal computer (PC) for further processing. Figure 6 shows the EMG signals acquired from the transradial amputee for six motions.

FEATURE EXTRACTION

From the EMG data, different information can be gathered by extracting different types of features. In this chapter, four time domain statistical features such as mean absolute value (MAV), zero crossings (ZC), slope sign changes (SSC) and waveform length (WL) as well as fourth order auto regressions (AR) coefficients are extracted using a rectangular windowing technique to identify the intended motions.

Two different feature vectors are obtained using TD statistical features and AR coefficients. From the signal the MAV and WL are calculated as in (1) and (2). ZC occurs when both (3) and (5) are satisfied. SSC occurs when conditions (4)-(6) are satisfied.

$$\text{MAV} = \frac{1}{L} \sum_{i=1}^L |y_i| \quad (1)$$

$$\text{WL} = \sum_{i=1}^L |y_i - y_{i-1}| \quad (2)$$

$$(y_i > 0 \ \& \ y_{i+1} < 0) \ || \ (y_i < 0 \ \& \ y_{i+1} > 0) \quad (3)$$

Figure 6. Eight channel EMG signals for six movements of hand from transradial amputee

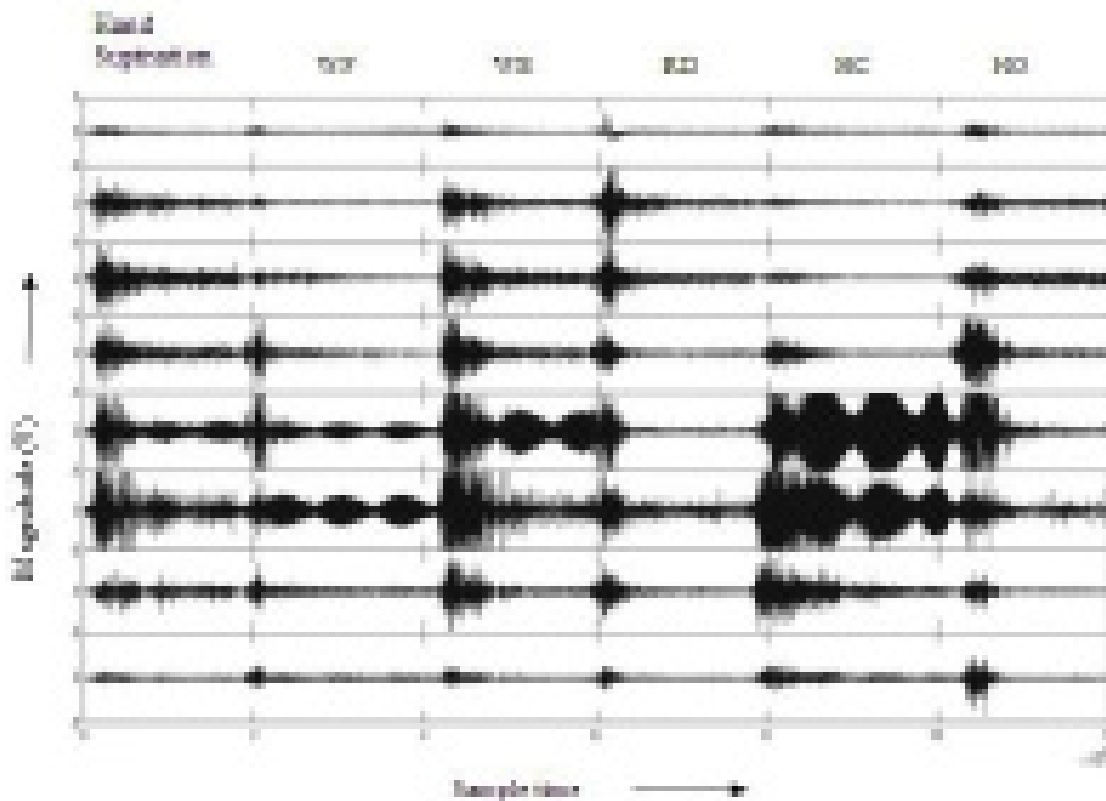


Table 1. Performance of classifiers with reduced TD statistical feature vector and AR feature vector

Subjects	kNN-TD	kNN-AR	NN-TD	NN-AR
Subject 1	89.3	60.9	86.8	61.8
Subject 2	83.6	50.7	82.7	55.9
Subject 3	78.3	52.7	78.3	68.2
Subject 4	84.8	58.5	83.9	59.7
Subject 5	89	56	87.9	69.4
Subject 6	83.2	60.7	70.2	64.2
Subject 7	87.2	55.6	71.3	63.9
Subject 8	79	66.5	77.4	73.4
Subject 9	81.2	61.3	82.7	53.8
Subject 10	87.2	67.9	86.3	65.1
Mean	84.3	59.1	80.8	63.5
SD	3.9	5.5	6.3	6.0

$$(y_i > y_{i-1} \ \& \ y_i > y_{i+1}) \ || \ (y_i < y_{i-1} \ \& \ y_i < y_{i+1}) \quad (4)$$

$$\left| y_i - y_{i+1} \right| \geq \varepsilon \quad (5)$$

$$\left| y_i - y_{i-1} \right| \geq \varepsilon \quad (6)$$

Auto regression models individual EMG signals as a linear autoregressive time series as given below.

$$y_k = \sum_{i=1}^p c_i y_{k-i} + e_k \quad (7)$$

- Where,
 L: Length of the sample
 y_i : i^{th} sample of signal
 ε : Threshold
 c_i : Autoregressive coefficient

- p: AR model order
 e_k : residual white noise

Features are computed from the EMG data stored in a personal computer using equations (1)-(7) from a segment (window), where a feature vector is engendered from each segment. Window size and increment in window size is chosen, considering the real-time constraint of the myoelectric hand control system which should be within 300 ms (Hudgins, B., Parker, P.A., & Scott, R.N., 1993). For real time EMG control, all processes including the generation to control must be completed within 300 ms. Therefore, analysis is performed on 256 ms window in all cases with a window increment of (overlap) 128 ms. A total of 234 time domain statistical feature vectors as well as 234 AR coefficient vector is obtained for six motions of hand and wrist for one trial of data. If four features were extracted on each channel per segment, the resulting feature vector will be of 16 features i.e., number of features/coefficients \times number of channels for able-bodied subject and 32 features for the transradial amputee.

Table 2. Confusion matrix of transradial amputee in recognition of different motions

Classifier	Motions	HC	HO	WF	WE	UD	RD	Sensitivity	Specificity
kNN-TD	HC	70	3	20	0	0	7	0.70	0.92
	HO	6	75	1	0	14	4	0.75	0.971
	WF	18	4.5	50.5	1	18.5	7.5	0.505	0.943
	WE	3.5	2	1	82	6	5.5	0.82	0.978
	UD	2	4.5	6	0	82.5	5	0.825	0.92
	RD	10.5	0.5	0.5	10	1.5	77	0.77	0.942
kNN-AR	HC	62.5	3	15.5	7	1	11	0.625	0.861
	HO	9.5	76.5	3	5	2	4	0.765	0.984
	WF	33	1.5	35	3.5	19	8	0.35	0.914
	WE	14	0	14.5	58.5	9	4	0.585	0.947
	UD	1	3	2	1.5	92.5	1	0.925	0.934
	RD	12	0.5	9	9.5	2	67	0.67	0.944
NN-TD	HC	62	8	28.5	0	0.5	1	0.62	0.951
	HO	2.5	81.5	1.5	0	13.5	1	0.815	0.964
	WF	9	4.5	64.5	1	16.5	4.5	0.645	0.909
	WE	2.5	0.5	0	86	6.5	4.5	0.86	0.979
	UD	1.5	1.5	14	0	82	1	0.82	0.922
	RD	9	3.5	1.5	9.5	2	74.5	0.745	0.976
NN-AR	HC	58.5	6.5	21.5	5.5	3.5	4.5	0.585	0.908
	HO	3.5	76.5	1.5	4	14.5	0	0.765	0.976
	WF	27	2.5	41	5.5	21.5	2.5	0.41	0.9
	WE	3	1	2	80.5	10	3.5	0.805	0.962
	UD	1.5	1	0.5	1.5	91.5	4	0.915	0.892
	RD	11	1	24.5	2.5	4.5	56.5	0.565	0.971

FEATURE REDUCTION

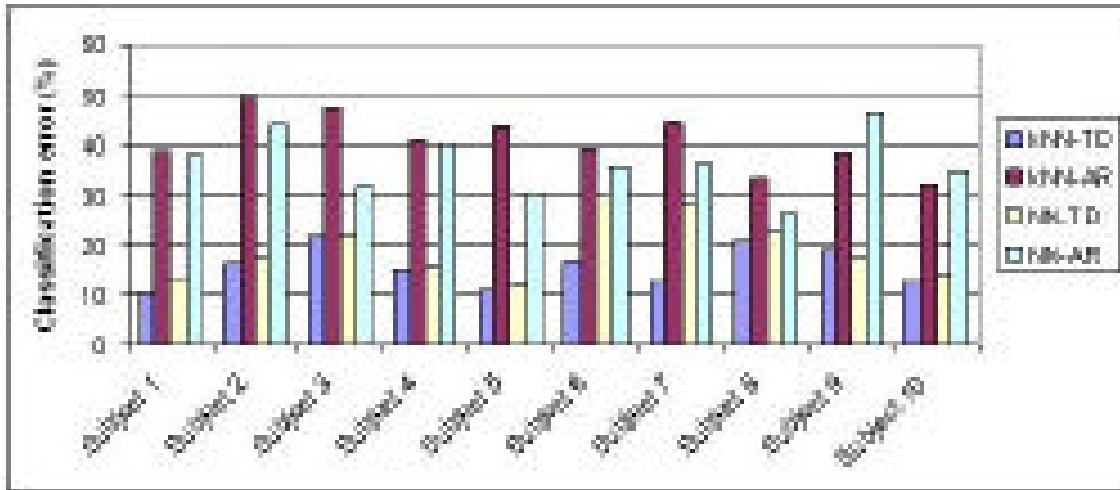
The objective of feature reduction is to consider the optimal features which contribute to effective classification for the purpose of reduction of burden to the classifier. Optimal features can be derived using feature selection and feature projection techniques. Feature selection methods may identify a best subset of features from the extracted feature set. However, this method does not utilize the class discrimination information that the discarded features carry.

On the other hand, feature projection method, project the complete feature set into smaller set without much loss of information. The most widely used feature projection technique is principal component analysis.

Principal Component Analysis

Principal component analysis is a linear transformation technique that transmutes p -dimension feature vector X into q -dimension vector Z with an objective of abating the redundancy of features.

Figure 7. NN and kNN classification error for able-bodied subjects with reduced TD and reduced AR feature vector



There are various ways of computing principal components. The simplest method of computation is identifications of projections with largest variance. Projections are obtained from the covariance matrix C of feature vector X . The eigenvalues of covariance matrix C represent the variance in the eigen-directions of feature space. The eigenvector corresponding to the largest eigenvalue have the strongest correlation with the feature set. The eigenvectors of the covariance matrix are referred as principal components of feature set. Having performed computation of eigenvector, the components are ranked with eigenvalue. A subset of the largest principal components may be chosen to obtain a reduced feature set. Unlike feature

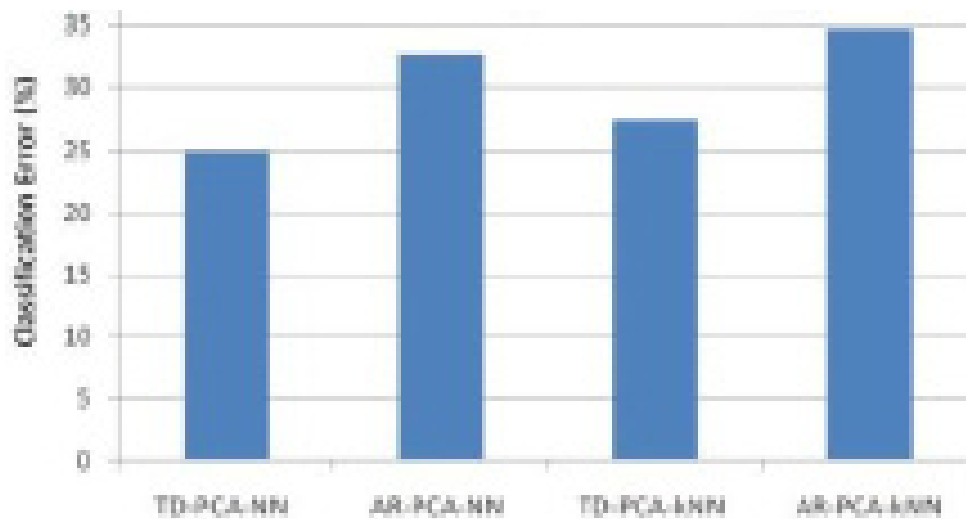
selection method, principal component analysis may be considered as unsupervised.

To abate feature input of the classifier, 16 features for each pattern are reduced to 4 features for able-bodied subjects using principal component analysis (PCA). PCA extracts the predominant data from the normalized input feature sets. From the normalized feature sets, the covariance matrix is calculated and from which eigenvalues and eigenvector are computed as mentioned above. A reduced feature set is obtained by multiplying the eigenvector corresponding to the four largest eigenvalue to the normalized feature set. However, for transradial amputee, 32 features are reduced to 8 features using PCA.

Table 3. Logic table for motor actuation using classifier signal

Class of Motion	Motor 1	Motor 2	Motor 3
Hand close	Forward	Off	Off
Hand open	Reverse	Off	Off
Wrist flexion	Off	Forward	Off
Wrist extension	Off	Reverse	On
Ulnar deviation	Off	Off	Forward
Radial deviation	Off	Off	Reverse

Figure 8. Pattern recognition performance of transradial amputee



CLASSIFICATION

The classification performance is studied with transmuted statistical TD features and AR coefficients to identify the user's intention. Here two different types of simple classifiers are used. One is the neural network (NN) classifier, and the other is the k nearest neighbour (k NN) classifier. In this classification, the multichannel EMG data for segment of size 256 is transformed 4 features in able-bodied subjects and 8 in transradial amputee. A total of 39 patterns of size 39×4 is obtained for each class from every trial in able-bodied subjects and 39×8 for transradial amputee. Three trials of the transmuted feature vectors 234×4 for every classes are used for training the NN and as a reference data set in the k NN technique for able-bodied and 234×8 for transradial amputee.

Neural Network Classifier

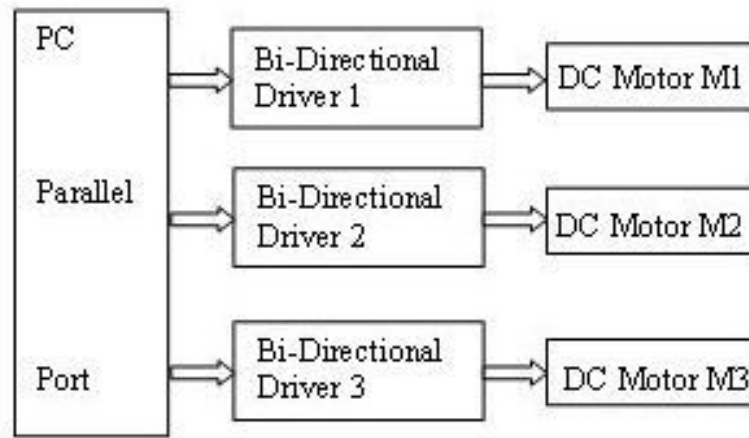
Two different multilayer neural networks are built for PCA reduced TD statistical data and PCA reduced AR coefficients. Since feature vector 16 has been reduced to 4 using PCA, the neural network is composed of 5 input neurons including

threshold and six output neurons for able-bodied subject. The neural network is built using WEKA software with default parameters. Similarly NN has been built with 9 input neurons for the transradial amputee. The classification was divided into two stages: the training stage and the testing stage. Three trials of all six motions out of 8 trials have been considered in training. During testing, the remaining five trials of six motions are used.

k Nearest Neighbour Classifier

Three trials of four channel reduced feature vectors are amalgamated to form reduced feature vector space. The transmuted reference vector space contains 702 reduced feature vector. In this vector space, the classification is carried out by measuring Euclidean distance between new reduced feature vector containing all the transmuted features to that of reference vectors. The distance of unknown test sample to the k nearest neighbor determines its class by obtaining a majority vote from k . With an arbitrary value of k , the performance of the classifier is studied. The best class is represented by majority voting amongst k nearest neighbor using MATLAB. The best result is obtained with

Figure 9. Block diagram of interfacing motor with a personal computer



k chosen as 9 in both the statistical reduced data and reduced AR coefficients.

RESULTS AND DISCUSSION

The classification performance of k NN classifier and NN classifier with the reduced statistical data and reduced AR coefficients is shown in Table 1 for able-bodied subjects. The confusion matrix of transradial amputee for different hand motions with sensitivity and specificity is shown in Table 2. The average percentage classification errors obtained from classifier for the reduced two different types of feature vector is shown in Figure 7 for ten able-bodied subjects. Figure 8 shows the average classification error in percentage for different methods of recognition of hand motions in transradial amputee.

In both the classifier it has been observed that the rate of classification error is more in the transient region. This may be due to the fact that the change of motions could not be performed exactly after every 5 seconds by the subject. From Figure 8 the average percentage classification error is less for TD features. Further, k NN classifier with reduced time domain statistical performs better than NN classifier. But the performance of the

transradial amputee is different from able-bodied subjects and it is difficult to generalize the results with respect to one amputee. Also k NN do not require any training and classification efficiency is more compared to NN classifier.

The statistical analysis of variance (ANOVA) test was performed on classification accuracy and it was found that the TD-reduced features ($p < 0.05$) significantly outperforms AR features in both the classifiers. The p -value of NN with k NN is > 0.05 with TD reduced features and divulged no significant difference.

Considering the efficiency of reduced TD statistical data with k NN and NN classifier, TD statistical data with k NN classifier may be considered to be a better choice for classification of continuous EMG signals to actuate the prosthetic drive. In the inchoate of development of prosthetic hand, the authors implemented the k NN classifier for actuation of three DC motors to manifest six motions of the hand.

DC MOTOR ACTUATION

The control signal obtained from the classifier is applied to actuate the drives through three bi-directional drivers as shown in Figure 9. All the six

motions are thus realized to perform the intended limb motions by driving three DC motors in both the direction. Logic for actuation of the drive is shown in Table 3.

FUTURE RESEARCH DIRECTIONS

The surface EMG signals based pattern recognition has been of great interest to researchers for several years. Many pattern recognition algorithms have been developed with different combination of feature extraction, feature reduction and classification for prosthetic hand control. These pattern recognition strategies have been developed for single degree of control. However, obtaining simultaneous control of multiple movements with EMG signals is one of the challenging tasks. Another direction of research is the identification of individual and combined finger control of surface EMG signals with less number of electrodes. Further, the development of robust classifier which is capable of classifying motions for practical prostheses is crucial.

Further, few researchers have shown that hand area of motor cortex stimulation enables movement of fingers to provide dexterity in prosthetics. But these are more invasive. Recently researchers have been attempting to use the peripheral nervous system in controlling prosthetics due to the less invasiveness compared to brain computer interface.

CONCLUSION

This chapter elucidates the method of detection and conditioning of surface EMG signals along with the actuation of prosthetic drive in off-line with DSP controller. At first, the design of an EMG signal conditioning system based on various factors that influence the detection of sEMG signals are explained. In experimental studies, four channel EMG signals are acquired with reduced

noise and the interference effect from able-bodied subject through surface electrodes. Also EMG signals are acquired from a transradial amputee using the 8 channel acquisition system. From the acquired EMG signals, the intended motions are identified through TD statistical features and AR coefficients. These features are reduced using a feature reduction technique through PCA. These reduced features are used in the classifiers to identify the user's intention. It is evident from the results that TD features outperform AR features in both the classifiers. Also the Performance analysis shows *k*NN classifier is better at classifying the EMG signal in identifying the user's intention than the NN classifier with TD statistical features. But *k*NN classifier requires more memory for classification compared to NN classifiers for storing the reference data. This may be suitable for less number of degrees of freedom.

ACKNOWLEDGMENT

I am thankful to Department of science and technology, Government of India, who has funded the research project (No.SR/S3/MERC/041/2009).

REFERENCES

- Ajiboye, A. B., & Weir, R. F. (2005). A heuristic fuzzy logic approach to EMG pattern recognition for multifunctional prosthetic control. *IEEE Transactions on Neural Systems and Rehabilitation Engineering*, 13(3), 280–291. doi:10.1109/TNSRE.2005.847357 PMID:16200752
- Chu, J. U., Moon, I., & Mun, M. (2005). A real-time EMG pattern recognition based on linear-nonlinear feature projection for multifunction myoelectric hand. In *Proceedings of International Conference on Rehabilitation Robotics* (pp. 295-298).

- Du, S., & Vuskovic, M. (2004). Temporal Vs spectral approach to feature extraction from prehensile EMG signals. In *Proceedings of IEEE International Conference on Information Reuse and Integration* (pp. 344-350).
- Engin, M., Dalbasti, T., Gulduren, M., Davasli, E., & Engin, Z. (2007). A prototype portable system for EEG measurements. *Measurement: Journal of the International Measurement Confederation*, 40(9-10), 936–942. doi:10.1016/j.measurement.2006.10.018
- Englehart, K., Hudgins, B., & Parker, P. A. (2001). A wavelet-based continuous classification scheme for multifunction myoelectric control. *IEEE Transactions on Bio-Medical Engineering*, 48(3), 302–311. doi:10.1109/10.914793 PMID:11327498
- Englehart, K., Hudgins, B., & Parker, P. A. (2003). A robust real-time control scheme for multifunction myoelectric control. *IEEE Transactions on Bio-Medical Engineering*, 50(7), 168–180. doi:10.1109/TBME.2003.813539 PMID:12665030
- Geethanjali, P., Ray, K. K., & Shanmuganathan, P. V. (2009). Actuation of prosthetic drive using EMG signal. In *Proceedings of IEEE International Conference TENCON*, (pp. 1-6), Singapore.
- Hargrove, L., Losier, Y., Englehart, K., & Hudgins, B. (2007). A real-time pattern recognition based myoelectric control usability study implemented in a virtual environment. In *Proceedings of 29th Annual International Conference of the IEEE Engineering Medicine Biological Society* (pp.4842-4845).
- Huang, H. P., Liu, Y. H., Liu, L. W., & Wong, C. S. (2003). EMG classification for prehensile posture using cascaded architecture of neural networks with self-organizing maps. In *Proceedings of IEEE International Conference Robotics and Automation* (pp. 1497–1502).
- Hudgins, B., Parker, P. A., & Scott, R. N. (1993). A new strategy for multifunction myoelectric control. *IEEE Transactions on Bio-Medical Engineering*, 40(1), 82–94. doi:10.1109/10.204774 PMID:8468080
- Khushaba, R. N., & Kodagoda, S. (2012). Electromyogram (EMG) feature reduction using mutual components analysis for multifunction prosthetic fingers control. In *Proceedings of International Conference on Control Automation Robotics & Vision* (pp.1534-1539), Guangzhou, China.
- Kiguchi, K., Iwami, K., Yasuda, M., Watanabe, K., & Fukuda, T. (2003). An exoskeletal robot for human shoulder joint motion assist. *IEEE/ASME Transactions on Mechatronics*, 8, 125–135. doi:10.1109/TMECH.2003.809168
- Kwon, J., Lee, S., Shin, C., Jang, Y., & Hong, S. (1998). Signal hybrid HMM-GA-MLP classifier for continuous EMG classification purpose. In *Proceedings of 20th Annual International Conference of the IEEE Engineering Medicine, Biology and Society*, 20(3), 1404–1407.
- Naik, G. R., & Kumar, D. K., & Jayadeva. (2010). Twin SVM for gesture classification using the surface electromyogram. *IEEE Transactions on Information Technology in Biomedicine*, 14(2), 301–308. doi:10.1109/TITB.2009.2037752 PMID:20007054
- Yazama, Y., Mitsukura, Y., Fukumi, M., & Akamatsu, N. (2003). Feature analysis for the EMG signals based on the class distance. In *Proceedings of International Symposium of the IEEE Computational Intelligence in Robotics and Automation* (pp.860-863).

ADDITIONAL READING

Ahmad, S. A., & Chappell, P. H. (2007). Surface EMG classification using moving approximate entropy. *Proceedings of International Conference on Intelligent and Advanced Systems*, (pp. 1163-1167), Malaysia.

Ajiboye, A. B., & Weir, R. F. (2005). A heuristic fuzzy logic approach to EMG pattern recognition for multifunctional prosthesis control. *IEEE Transactions on Neural Systems and Rehabilitation Engineering*, 13(3), 280–291. doi:10.1109/TNSRE.2005.847357 PMID:16200752

Ando, T. J., Okamoto, M., & Fujie, M. G. (2009). Optimal design of a micro macro neural network to recognize rollover movement. *Proceedings of IEEE/RSJ International Conference on Intelligent Robots and Systems*, (pp. 1615-1620), Missouri.

Baker, J. J., Scheme, E., Englehart, K., Hutchinson, D. T., & Greger, B. (2010). Continuous detection and decoding of dexterous finger flexions with implantable myoelectric sensors. *IEEE Transactions on Neural Systems and Rehabilitation Engineering*, 18(4), 424–432. doi:10.1109/TNSRE.2010.2047590 PMID:20378481

Bu, N., Okamoto, M., & Tsuji, T. (2009). A hybrid motion classification approach for EMG-based human robot interfaces using Bayesian and neural networks. *IEEE Transactions on Robotics*, 25(3), 502–511. doi:10.1109/TRO.2009.2019782

Farrell, T. R., & Weir, R. F. (2007). The optimal controller delay for myoelectric prostheses. *IEEE Transactions on Neural Systems and Rehabilitation Engineering*, 15(1), 111–118. doi:10.1109/TNSRE.2007.891391 PMID:17436883

Geethanjali, P., & Ray, K. K. (2011). Identification of motion from multi-channel EMG signals for control of prosthetic hand. *Australasian Physical & Engineering Sciences in Medicine*, 34(3), 419–427. doi:10.1007/s13246-011-0079-z PMID:21667211

Geethanjali, P., & Ray, K.K. (2013). Statistical Pattern Recognition Technique for Improved Real-Time Myoelectric Signal Classification. *Biomedical Engineering: Applications, Basis and Communications*, 25(4).

Li, D., Pedrycz, W., & Pizzi, N. J. (2005). Fuzzy wavelet packet based feature extraction method and its application to biomedical signal classification. *IEEE Transactions on Bio-Medical Engineering*, 52(6), 1132–1139. doi:10.1109/TBME.2005.848377 PMID:15977743

Light, C. M., Chappell, P. H., Hudgins, B., & Englehart, K. (2002). Intelligent multifunction myoelectric control of hand prostheses. *Journal of Medical Engineering & Technology*, 26(4), 139–146. doi:10.1080/03091900210142459 PMID:12396328

Lucas, M.-F., Gouffriaux, A., Pascual, S., Doncarli, C., & Farina, D. (2008). Multi-channel surface EMG classification using support vector machines and signal-based wavelet optimization. *Journal of Biomedical Signal Processing and Control*, 3(2), 169–174. doi:10.1016/j.bspc.2007.09.002

Maitrot, A., Lucas, M.-F., Doncarli, C., & Farina, D. (2005). Signal-dependent wavelets for electromyogram classification. *Journal of Medical and Biological Engineering and Computing*, 43(4), 487–492. doi:10.1007/BF02344730 PMID:16255431

Merlo, A., Farina, D., & Merletti, R. (2003). A fast and reliable technique for muscle activity detection from surface EMG signals. *IEEE Transactions on Bio-Medical Engineering*, 50(3), 316–323. doi:10.1109/TBME.2003.808829 PMID:12669988

Naik, G. R., Kumar, D. K., & Palaniswami, M. (2008). Multi run ICA and surface EMG based signal processing system for recognizing hand gestures. *Proceedings of IEEE International Conference on Computer and Information Technology*, (pp. 700-705), North South Wales.

Naik, G. R., Kumar, D. K., Weghorn, H., & Palaniswami, M. (2007). Subtle hand gesture identification for HCI using temporal decorrelation source separation BSS of surface EMG. *Proceedings of 9th Biennial Conference of the Australian Pattern Recognition Society on Digital Image Computing Techniques and Applications* (pp. 30-37), Australia.

Oskoei, M. A., & Hu, H. (2007). Myoelectrical control systems- A survey. *Journal of Biomedical Signal Processing and Control*, 2(4), 275–294. doi:10.1016/j.bspc.2007.07.009

Scheme, E. J., Hudgins, B., & Parker, P. A. (2007). Myoelectric signal classification for phoneme-based speech recognition. *IEEE Transactions on Bio-Medical Engineering*, 54(4), 694–699. doi:10.1109/TBME.2006.889175 PMID:17405376

Sensinger, J. W., Lock, B. A., & Kuiken, T. A. (2009). Adaptive pattern recognition of myoelectric signals: Exploration of conceptual framework and practical algorithms. *IEEE Transactions on Neural Systems and Rehabilitation Engineering*, 17(3), 270–278. doi:10.1109/TN-SRE.2009.2023282 PMID:19497834

Tenore, F. V. G., Ramos, A., Fahmy, A., Acharya, S., Etienne-cummings, R., & Thakor, N. T. (2009). Decoding of individuated finger movements using surface electromyography. *IEEE Transactions on Bio-Medical Engineering*, 56(5), 1427–1434. doi:10.1109/TBME.2008.2005485 PMID:19473933

Tkach, D., Huang, H., & Kuiken, T. A. (2010). Study of stability of time-domain features for electromyographic pattern recognition. *Journal of Neuroengineering and Rehabilitation*, 7(1), 1–13. doi:10.1186/1743-0003-7-21 PMID:20064261

Vuskovic, M., & Du, S. (2002). Classification of prehensile EMG patterns with simplified fuzzy ARTMAP networks. *Proceedings of International Joint Conference on Neural Networks*, (pp. 2539-2544), Hawaii.

KEY TERMS AND DEFINITIONS

Classification: Identification of a category/class from the input feature vector.

Electromyogram (EMG): A record of the electrical activity of the muscle.

Feature Extraction: The process of defining meaningful and efficient information from the raw data.

Feature Reduction: The process of reducing number of extracted features to optimal numbers to identify a category/class of data.

Neural Network: A computing system made up of a number of simple, highly interconnected processing elements which process information by their dynamic state response to external inputs.

Pattern Recognition: The process of identification of category/class of the pattern from the raw data.

Prosthetic Hand: An artificial hand that replaces the missing hand.

Signal Conditioning: Performing operations such as amplification, filtering etc to make it suitable for further processing.

Chapter 15

The Relationship between Anthropometric Variables and Features of Electromyography Signal for Human-Computer Interface

Angkoon Phinyomark

University Joseph Fourier, France & University of Grenoble, France

Franck Quaine

University Joseph Fourier, France

Yann Laurillau

University of Grenoble, France

ABSTRACT

Muscle-computer interfaces (MCIs) based on surface electromyography (EMG) pattern recognition have been developed based on two consecutive components: feature extraction and classification algorithms. Many features and classifiers are proposed and evaluated, which yield the high classification accuracy and the high number of discriminated motions under a single-session experimental condition. However, there are many limitations to use MCIs in the real-world contexts, such as the robustness over time, noise, or low-level EMG activities. Although the selection of the suitable robust features can solve such problems, EMG pattern recognition has to design and train for a particular individual user to reach high accuracy. Due to different body compositions across users, a feasibility to use anthropometric variables to calibrate EMG recognition system automatically/semi-automatically is proposed. This chapter presents the relationships between robust features extracted from actions associated with surface EMG signals and twelve related anthropometric variables. The strong and significant associations presented in this chapter could benefit a further design of the MCIs based on EMG pattern recognition.

DOI: 10.4018/978-1-4666-6090-8.ch015

INTRODUCTION

Surface electromyography (EMG) signals are measured by surface electrodes that are placed on the target muscles. During muscle contractions, a compound of the whole motor unit action potentials (MUAPs) occurred in the muscles. These MUAPs are the useful information for numerous fields, e.g. rehabilitation engineering, biomechanics, ergonomics, and human-computer interfaces (HCIs) (Merletti & Parker, 2004). Surface EMG signals can also be used in a medical decision support system, e.g. the diagnosis of neuromuscular disorders (Subasi, 2012, 2013). In this chapter, we focus on the development of the HCIs based on surface EMG signals, as called “muscle-computer interfaces or MCIs” (Saponas, Tan, Morris, & Balakrishnan, 2008). These interfaces can widely use in controlling many external devices, e.g. prosthetic limbs, electric-power wheelchairs, interactive surfaces, a virtual computer mouse or keyboard, a portable music player, and in-car electronic equipment (e.g. Barreto, Scargle, & Adjouadi, 2000; Benko, Saponas, Morris, & Tan, 2009; Khushaba, Kodagoda, Liu, & Dissanayake, 2013; Saponas et al., 2009; Shenoy, Miller, Crawford, & Rao, 2008; Wei, Hu, & Zhang, 2011; Yang, Lin, Lin, & Lee, 2013).

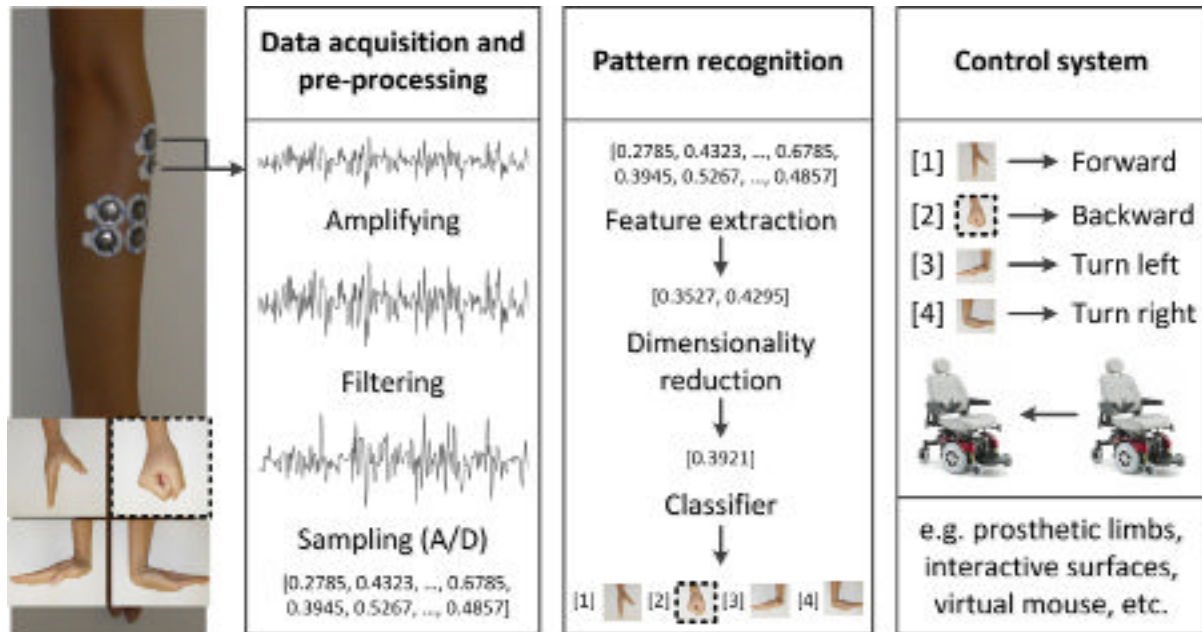
MCIs generally consist of three main modules, as shown in Figure. 1. The first module composes of two sub-modules: surface EMG signal acquisition (hardware) and data pre-processing (software). In the data acquisition sub-module, surface EMG signals are firstly amplified with an amplifier due to small EMG amplitude, and may be filtered by hardware filters, i.e., notch, high pass and/or low pass filters. Then, continuous surface EMG signals are sampled using an analog-to-digital converter. In case of no hardware filters, the raw EMG data can be filtered by software filters, before the EMG data go to the next module, the pattern recognition module. Different patterns of surface EMG signals are classified and matched to the control commands in this module. The second

module can be divided into three sub-modules: feature extraction, dimensionality reduction, and classification algorithms. All sub-modules are in the software part. The pre-processed surface EMG data from the first module are segmented into small time slot length using an adjacent or an overlapped windowing technique, and then some features are extracted in order to emphasize the relevant structures in the EMG signals and remove noises/irrelevant parts. A feature vector is formed and can be sent directly to a classifier, or the dimension of a feature vector is reduced by the dimensionality reduction technique before sending it to the classifier. The classifier maps the extracted features (the representative of the actions associated with surface EMG signals) to the target classes (the control commands for an external device). After the control commands were generated based on the mathematical functions in the second module, the third module is a control system, which serves as an interface between the software and hardware. In other words, an output command is converted from a digital code to an analog signal for controlling an external device. In this chapter, we focus on the second module, particularly the extraction of EMG features.

Nearly all previous studies on MCIs based on EMG pattern recognition concentrate on improving recognition rate together with increasing the number of discriminated motions. Currently, the recognition rate is more than 90% in discriminating 4-12 finger, wrist, hand, and forearm motions. It should be noted that the recognition rate or the classification accuracy is calculated as a ratio of the number of correct classifications to the total number of classifications. More details about many previous studies on MCIs based on EMG pattern recognition concentrate on improving recognition rate can be found in additional readings in the Additional Reading Section. However, the high recognition rates reported are usually based in single-session experiments conducted in research laboratories (Tkach, Huang, & Kuiken, 2010). On the other hand, in clinics when the context

The Relationship between Anthropometric Variables

Figure 1. Three main modules of MCIs: the surface EMG acquisition and pre-processing, the pattern recognition, and the control system



of the real-world requirements have been given attention, there are many issues that have to find the solutions, e.g. the robustness against a variety of noises (Boostani & Moradi, 2003; Zardoshti-Kermani, Wheeler, Badie, & Hashemi, 1995), the robustness over time—between sessions (Oskouei, Paulin, & Carman, 2013; Sensinger, Lock, & Kuiken, 2009) and between days (Boschmann, Kaufmann, Platzner, & Winkler, 2010; Zhang et al., 2008)—due to EMG electrode location shift (Young, Hargrove, & Kuiken, 2011, 2012), muscle fatigue, and/or variation in muscle contraction effort (Tkach et al., 2010), or the robustness in limb position variations (Chen, Geng, & Li, 2011; Fougner et al., 2011; Jiang, Muceli, Graimann, & Farina, 2013).

Among such issues, the problem of the cross-user classification is far from being a practical one (Cannan & Hu, 2011; Saponas et al., 2008). The proposed systems in the literature were trained and tested independently on the EMG signals from each user. In other words, EMG-based MCIs

have to design and create for each user. Based on a preliminary study of Saponas et al., (2008), when the classifier is trained on the data from all subjects in the database except the testing subject, the classification accuracy computed from the testing subject data is about 50%, reducing from about 95% using the independent training and testing system. It should be noted that their system classifies five single-finger motions based on three time-domain and frequency-domain features extracted from eight EMG channels placed around the upper forearm (Saponas et al., 2008). Moreover, based on our preliminary experiments, the selection of the robust EMG features is not an efficient solution to reduce the variability of surface EMG signals between users, like other previous mentioned problems.

This is due to the different compositions of the body across users, which result in the different muscle types with varying architecture characteristics. This factor prevents the development of standard MCIs that are compatible with

almost any user, and MCIs based on EMG pattern recognition have never really reached the general population. Being able to solve this problem, in our previous work (Phinyomark et al., 2013a) a feasibility to use anthropometric variables, a measurable characteristic of the human body, to calibrate the EMG pattern recognition systems is presented. The anthropometric variables are used to compensate for discrepancies between user body compositions (Cannan & Hu, 2011), which are based on the relationship between the EMG signal, muscle force, and muscle size consisting of cross-sectional area and length (Hof, Pronk, & van Best, 1987; Marras & Sommerich, 1991; see our preliminary work—Phinyomark et al., 2013a—for more details about this relationship). They can automatically or semi-automatically calibrate a system. As a result of the proposed technique, EMG-based MCIs that require little or no user-specific training EMG data are possible. It is important to note that it is easy to measure anthropometric variables, and some variables can be measured directly together with surface EMG signals via an armband device (Cannan & Hu, 2011; Saponas et al., 2008). It is also possible to obtain estimated anthropometric variables from the anthropometric table, which can be found in many sources including academic books (e.g. De Leva, 1996; Winter, 1990). It means that there is no need to measure all anthropometric variables and may need only a few simple variables, i.e., gender, age, body mass, or standing height. However, at the beginning all anthropometric variables proposed in this chapter are measured directly from the volunteers.

For simple MCI systems that use a thresholding technique, a maximum voluntary contraction (MVC) can be used as an additional input to calibrate and adapt the classification system from one user to another user. In order to use MVC normalization technique, it is important that the linear relationship between force generated and EMG level should be held for the muscle of interest up

to the maximum force/EMG level (Bolgia & Uhl, 2007; Vera-Garcia, Moreside, & McGill, 2010). Although the linear relationship has been found in many previous works (e.g. Kamavuako, Farina, Yoshida, & Jensen, 2009; Woods & Bigland-Ritchie, 1983), several researchers have found a non-linear relationship between force generated and EMG muscle activity (e.g. Lawrence & De Luca, 1983; Woods & Bigland-Ritchie, 1983). The relationship is more complicated in case of a dynamic muscle contraction, i.e., a muscle is free to change length and a joint is free to move (Oatis, 2008). Several anthropometric variables have been found to have a strong relationship with the MVC and several maximum force/EMG measurement techniques, such as hand circumference has the strong correlation with the maximal grip strength (MGS) and can be used to predict the MGS using a simple regression equation in the study of Li, Hewson, Duchene, & Hogrel (2010), or in the study of Marras & David (2001) several linear regression equations developed from five of the fifteen anthropometric variables are used to predict the EMC (Expected Maximum Contraction) of trunk muscles.

However, for advanced MCI systems, features extracted from surface EMG signals are the important stage, and only the MVC, related with only muscle force, is not enough to be used alone. Other additional useful information is needed, which should have strong relationships with many EMG features, extracted not only force level information but also other useful information such as complexity and frequency. So some additional inputs should be used to calibrate the machine learning and pattern recognition instead of the simple thresholding technique. Forearm circumference is an anthropometric variable that has already been proposed to be used as a calibrating variable in an EMG recognition system in previous works (Anakwe, Huntley, & Mceachan, 2007; Cannan & Hu, 2011). However, the relationship between EMG and forearm circumference is not

strong enough, therefore further anthropometric variables were evaluated their relationships with surface EMG features in this chapter. All relationships between EMG features and anthropometric variables that are strong and significant could benefit a further design of the EMG-based MCIs. It could semi-automatically/automatically adapt the setting of the EMG recognition systems to a wider population. It can be used in two different ways: 1) a normalized value for EMG features, and 2) a weighting factor for a classifier. Moreover, wearable and wireless EMG devices are already commercially available, e.g. MYO (see www.thalmic.com/myo/) and has been developed rapidly, so using anthropometric variables to calibrate the EMG recognition system would become more practical and important in the near future.

EMG FEATURE EXTRACTION

Definition of Feature Extraction

Feature extraction is a technique to transform raw EMG signals into a reduced representation set of features as called “a feature vector.” A transformation is usually based on mathematical functions, which highlights relevant structures in surface EMG signals and rejects irrelevant parts. If the extracted features are carefully selected, the feature vector will contain effective and relevant information drawn from the whole set of raw EMG data, which can be used to represent the desired actions. Training an EMG classifier on raw EMG signal patterns requires high computational cost and their testing classification performances are very poor (Phinyomark, Phukpattaranont, & Limsakul, 2012e). Therefore, the extraction of EMG features is very important step in EMG-based gesture recognition. It is noted in the literature that the success of the EMG pattern recognition systems almost entirely depends on the choice of

features (Kendall et al., 2012; Hudgins, Parker, & Scott, 1993).

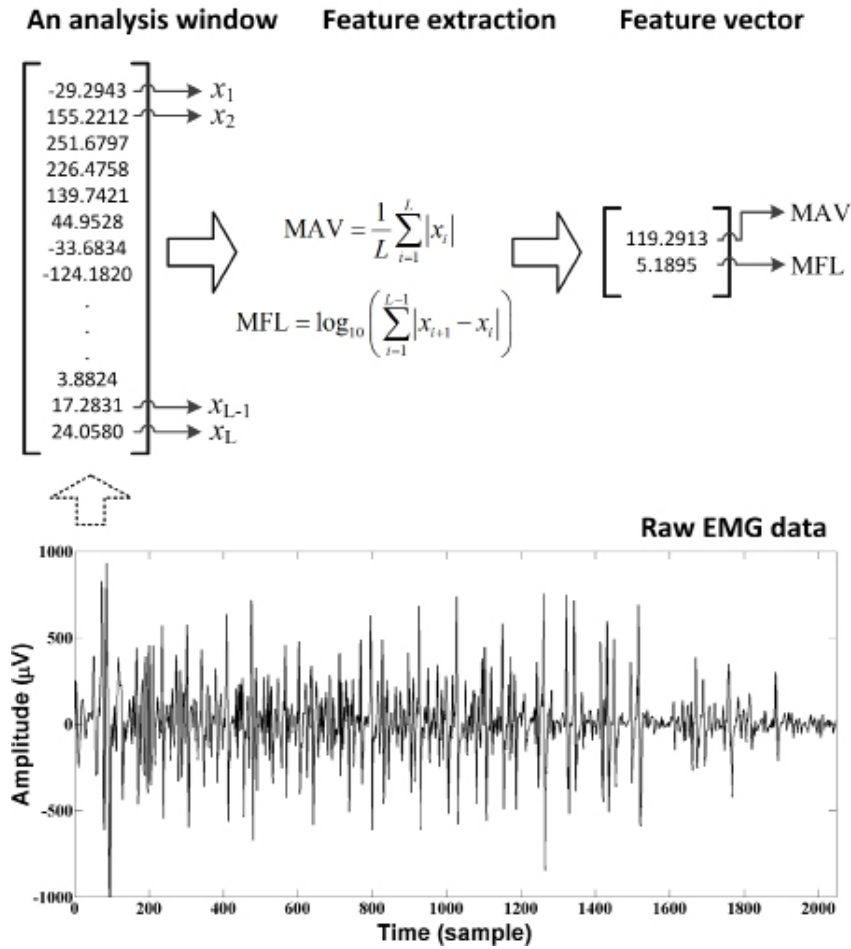
EMG feature extraction can be computed in three domains: 1) time domain, 2) frequency domain, and 3) time-frequency or time-scale domain (Boostani & Moradi, 2003). Time domain features are widely used in EMG pattern recognition due to the low complexity and computational cost, which can be implemented and computed using a simple hardware processor, i.e., a mobile device or a microprocessor (Hudgins et al, 1993; Kundu, Mazumder, & Bhaumik, 2011). Moreover, time domain features can be successfully used as a dimensionality reduction technique for time-frequency/time-scale features, i.e., the coefficients of short-time Fourier transform, discrete wavelet transform, and wavelet packet transform (Phinyomark, Nuidod, Phukpattaranont, & Limsakul, 2012b). Hence, in this chapter, features in time domain are mainly focused, and time-frequency/time-scale features are not considered. A number of frequency domain features are considered to be used in developing the robust MCI systems and to provide additional information.

Computation of EMG Feature Extraction

A basic idea about the computation of EMG feature extraction is illustrated in Figure. 2. Following is a brief description of all robust EMG features, which were investigated and discussed in the present chapter. In each, x_i is the i_{th} sample of surface EMG signal amplitude and L is the length of the analysis window for computing the features.

Willison Amplitude (WAMP) is a number of times resulting from the difference between two consecutive EMG amplitudes in a time segment becomes more than a predefined threshold thr . In other words, WAMP is a number of times that the length of the EMG waveform in a time seg-

Figure 2. An example of EMG feature extraction procedure in time domain



ment exceeds a predefined threshold thr , which can be expressed as

$$WAMP = \sum_{i=1}^{L-1} [f(|x_{i-1} - x_i|)];$$

$$f(x) = \begin{cases} 1, & \text{if } x \geq thr \\ 0, & \text{otherwise} \end{cases} \quad (1)$$

Myopulse Percentage Rate (MYOP) is an average number of times that the absolute value

of EMG amplitude, i.e., myopulse output, exceeds a predefined threshold thr , and the calculation is defined as

$$MYOP = \frac{1}{L} \sum_{i=1}^L [f(|x_i|)];$$

$$f(x) = \begin{cases} 1, & \text{if } x \geq thr \\ 0, & \text{otherwise} \end{cases} \quad (2)$$

The Relationship between Anthropometric Variables

Slope Sign Change (SSC) or the number of turns (NT) is a number of times that the slope of the EMG waveform changes sign. This method uses three consecutive EMG signal amplitudes to detect the EMG waveform slope, which is calculated as

$$\text{SSC} = \sum_{i=2}^{L-1} \left[f \left[(x_i - x_{i-1}) \times (x_i - x_{i+1}) \right] \right];$$

$$f(x) = \begin{cases} 1, & \text{if } x \geq thr \\ 0, & \text{otherwise} \end{cases} \quad (3)$$

Zero Crossing (ZC) is a number of times that the EMG waveform crosses the zero amplitude axes. Several works used this value without implementing threshold condition (Boostani & Moradi, 2003; Zardoshti-Kermani et al., 1995). However, a predefined threshold thr should be included in the ZC computation to reduce the effect of noise (Hudgins et al., 1993). ZC can be defined as

$$\text{ZC} = \sum_{i=1}^{L-1} \left[\text{sgn}(x_{i+1} \times x_i) \cap |x_{i+1} - x_i| \geq \right]$$

$$\text{sgn}(x) = \begin{cases} 1, & \text{if } x < 0 \\ 0, & \text{otherwise} \end{cases} \quad (4)$$

A suitable predefined threshold to reduce noise is dependent on a system gain value and a background noise level. We can roughly estimate a predefined threshold if we know both values (Hudgins et al, 1993). For example, assuming a system gain of 1000 and a background noise of 4 μV peak to peak, the threshold can be calculated to be ± 2 mV. It is normally chosen between 50 μV and 100 mV (Philipson & Larsson, 1988). However, to obtain a high quality feature space, the suitable threshold could be defined based on taking some offline trial-and-error classifications.

Detrended Fluctuation Analysis (DFA) is a modified root mean square analysis of a random

walk (Peng, Havlin, Stanley, & Goldberger, 1995). A slope of the line relating the logarithm of the RMS fluctuation of the profiles $y_k(F_n)$ to the logarithm of the predefined box size (n) is used as a feature value (\pm). This value indicates the presence of the power law (fractal) scaling, as can be expressed as

$$\pm = \frac{\left[\Delta \log_{10}(F_n) \right]}{\left[\Delta \log_{10}(n) \right]};$$

$$F_n = \sqrt{\frac{1}{L} \sum_{k=1}^L (y_k - y_{nk})^2};$$

$$y_k = \sum_{i=1}^k \left[\left\{ x_i \right\} - x_i \right]^{\Delta}$$

$$k = 1, \dots, L \quad (5)$$

Based on our previous work (Phinyomark, Phukpattaranont, Limsakul, & Phothisonothai, 2011d), the minimum box size n_{\min} is set at four, the maximum box size n_{\max} is set at one-tenth of the signal length, and the box size increment is based on a power of two. A least-square fit, which is applied to the profiles y_k , is the quadratic polynomial fit.

Higuchi method (HG) is another fractal dimension estimator (Higuchi, 1988), which performs well in the classification of surface EMG signals and the simulated signals (Arjunan & Kumar, 2010; Esteller, Vachtsevanos, Echaz, & Litt, 2001). For $k = 1, 2, \dots, k$, a negative slope of the line relating the logarithm of the length of the curve (L_{mk}) to the logarithm of the discrete time interval between points (k) is used as a feature value (D). Based on the finding of Phothisonothai and Nakagawa (2007), the maximum time inter-

val k_{\max} is set at 128. This value is from the relationship $L_k \propto k^D$, which can be given by

$$L_{mk} = \frac{1}{k} \left\{ \left[\sum_{j=1}^{\frac{L-m}{k}} |x_{m+jk} - x_{m+(j-1)k}| \right] \cdot \frac{L-1}{\frac{L-m}{k} \cdot k} \right\};$$

$$X_m^k = \left\{ x_m, x_{m+k}, x_{m+2k}, \dots, x_{m+\frac{L-m}{k} \cdot k} \right\}$$

(6)

Integrated EMG (IEMG) is a summation of the absolute value of the EMG signal amplitude over the time segment, which can be expressed as

$$\text{IEMG} = \sum_{i=1}^L |x_i|$$

(7)

Waveform Length (WL) is a cumulative length of the EMG waveform over the time segment. It is the IEMG of the EMG wavelength. A number of previous studies call this feature as the “wavelength,” which provides simple waveform complexity information. It can be calculated by

$$\text{WL} = \sum_{i=1}^{L-1} |x_{i+1} - x_i|$$

(8)

Maximum Fractal Length (MFL) is proposed as a feature, which can measure EMG signal patterns at low level muscle contraction (Arjunan, 2008). It is defined as the average fractal length of the signal measured at the smallest scale from the HG method in Eq. (6). If the smallest scale is set at one, MFL can be defined as the modification of the WL using a logarithm function as follows

$$\text{MFL} = \log_{10} \left(\sum_{i=1}^{L-1} |x_{i+1} - x_i| \right)$$

(9)

Mean Absolute Value (MAV) is an average of the absolute value of the EMG signal amplitude. There are many ways to call this feature, e.g. averaged absolute value, average rectified value, integral of absolute value, integrated absolute value, and the first order of the ν -Order feature. It can be given by

$$\text{MAV} = \frac{1}{L} \sum_{i=1}^L |x_i|$$

(10)

Difference Absolute Mean Value (DAMV) is an average of the absolute value of the difference between the adjacent EMG amplitudes over the time segment (Kim, Choi, Moon, & Mun, 2011; Park & Lee, 1998; Yu, Jeong, Hong, & Lee, 2012). It can be seen as the MAV of the EMG wavelength and sometimes is called as the “Average Amplitude Change (AAC)” (Fougner, 2007). It is given by

$$\text{DAMV} = \frac{1}{L} \sum_{i=1}^{L-1} |x_{i+1} - x_i|$$

(11)

Variance of EMG (VAR) is an average of the square value of the EMG signal amplitude. This is due to a mean value of surface EMG signals is close to zero, in which the equation is defined as

$$\text{VAR} = \frac{1}{L-1} \sum_{i=1}^L x_i^2$$

(12)

Root Mean Square (RMS) is a square root of the average of the square of the EMG signal amplitude values. In other words, it has a similar value to the standard deviation of EMG signal amplitude. It can be defined as the modification of the VAR using a square root function as follows

$$\text{RMS} = \sqrt{\frac{1}{L} \sum_{i=1}^L x_i^2}$$

(13)

The Relationship between Anthropometric Variables

Difference Absolute Standard Deviation Value (DASDV) is a square root of the average of the square of the difference between the adjacent EMG amplitudes over the time segment. It is the RMS of the EMG wavelength, as can be formulated as

$$\text{DASDV} = \sqrt{\frac{1}{L-1} \sum_{i=1}^{L-1} (x_{i+1} - x_i)^2} \quad (14)$$

Approximation Entropy (ApEn) and Sample Entropy (SampEn) are techniques used to quantify the unpredictability of fluctuations in EMG signal amplitudes over the time segment (Zhao et al., 2006a, 2006b). They provide the waveform similarity or complexity information. SampEn is developed from ApEn to avoid the bias caused by self-matching. Both methods use two input parameters: m and r , where m is the pattern length and r is the criterion of similarity (Zhang & Zhou, 2012). The basic idea is about the estimation of the conditional probability that the patterns of the EMG signal amplitude, which are similar to each other within a predefined tolerance r , will remain similar for the next comparison point (Richman & Moorman, 2000).

Mean Frequency (MNF) is an average frequency, which is calculated as a sum of the product of the EMG power spectrum and the frequency divided by a total sum of the EMG power spectrum. There are other ways to call this feature, such as central frequency and the spectral center of gravity. It can be defined as

$$\text{MNF} = \frac{\sum_{j=1}^M f_j P_j}{\sum_{j=1}^M P_j} \quad (15)$$

where f_j is the frequency of the spectrum at a frequency bin j , P_j is the EMG power spectrum at a frequency bin j , and M is the length of whole frequency bin.

Median Frequency (MDF) is a frequency at which the EMG power spectrum is divided into two areas with an equal total power, as can be expressed as

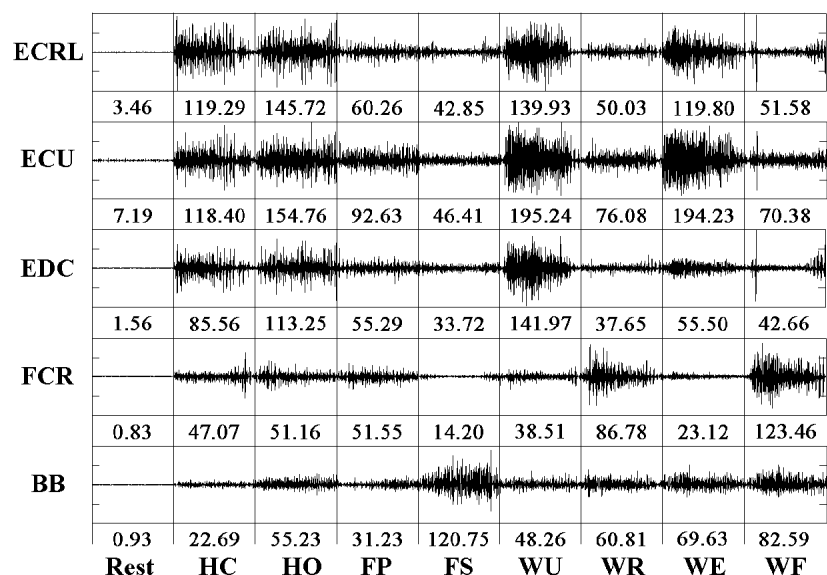
$$\sum_{j=1}^{\text{MDF}} P_j = \sum_{j=\text{MDF}}^M P_j = \frac{1}{2} \sum_{j=1}^M P_j \quad (16)$$

Experimental Data for Extracting EMG Features

All features are computed from the EMG data, which are recorded from 20 subjects (10 males and 10 females). The subjects were asked to perform 8 motions consisting of forearm pronation (FP), forearm supination (FS), wrist flexion (WF), wrist extension (WE), wrist radial deviation (WR), wrist ulnar deviation (WU), hand open (HO), and hand close (HC), and maintain for 2 s. Each motion was repeated 15 trails per day for four separate days. EMG data were measured from 4 forearm muscles and an upper arm muscle: extensor carpi radialis longus (ECRL), extensor carpi ulnaris (ECU), extensor digitorum communis (EDC), flexor carpi radialis (FCR), and biceps brachii (BB). More details about data acquisition and experiments can be found in Phinyomark et al., (2011d).

To briefly explain the relationship between actions associated with surface EMG signals and EMG features, the amplitude shape of surface EMG signals acquired from all the muscles and motions from a trial in time domain is shown in Figure. 3, together with one extracted feature: MAV. It is clearly shown in the figure that the EMG amplitude shapes from all muscles are significantly different according to the direction of the eight motions. For instance, we can observe that the EMG magnitudes of WE are very high in two extensor muscles, i.e., ECRL and ECU. These two muscles are the corresponding muscles to produce wrist extension, i.e., high contraction level. On the other hand, the EMG magnitudes of WF are low in both extensor muscles but are very

Figure 3. An example of surface EMG signals in time domain from the first trail in the first day of subject 1 (5 muscles and 8 motions with a rest state) and the extracted MAV features



high in the flexor muscle or FCR. As we know that the MAV feature is used to estimate the EMG amplitude/magnitude level, so MAV features of WE extracted from ECRL and ECU are higher than the other muscles. In the same way, the MAV feature of WF extracted from FCR is relatively higher than the other muscles.

ANTHROPOMETRIC VARIABLES

Definition of Anthropometric Variables

Anthropometry is a measurement of the dimensions of the different parts of human body. There are two types of measurement: 1) static dimension and 2) dynamic dimension. In order to use anthropometric variables to calibrate the EMG-based MCI systems, only static dimensions are considered. There are many anthropometric variables, e.g. overhead reach height and breadth, shoulder circumference and length, and waist front and back length. However, only twelve related variables are chosen for the experiments in this chapter.

Computation of Anthropometric Variables

Following is a brief description of all anthropometric variables, which were investigated and discussed for this chapter.

Body mass is measured in kilograms (kg). It is defined as a subject's weight or mass, which can be measured by the balance type scales. A subject stands on the center of the scale platform.

Stature or standing height is measured in centimeters (cm). It is defined as the distance from the bottom of the feet to the top of the head of a subject, which can be measured by a stadiometer. A subject stands erect on the center of the base plate with heels together, and head in the Frankfort plane.

BMI or body mass index is a roughly estimation of human body fat based a subject's weight and height in kilograms/meters² (kg/m²). It can be defined as

$$\text{BMI} = \frac{\text{body mass}}{(\text{stature})^2} \quad (17)$$

The Relationship between Anthropometric Variables

The remaining anthropometric variables are measured in centimeters (cm), as shown in Figure 4, using a tape for biceps and forearm circumferences, a sliding or small bone caliper for hand breadth and length, a wide sliding torso caliper for elbow-hand grip length, elbow-fingertip length, shoulder-elbow length and bi-deltoid breadth, and a measuring block with tape measure for forward grip reach. The specific locations are defined as the following.

Biceps circumference is a linear distance around the upper arm when subject stands. The upper arm is extended forward horizontally and the elbow is flexed about 90° (the arm is abducted). It is measured at the level of the drawn biceps point landmark, which is the point of maximum quiet inspiration.

Forearm circumference is a linear distance around the lower arm with the same posture as measured the biceps circumference. It is usually measured at the level of maximum forearm circumference.

For hand breadth, subject sits with right hand flats on a table and the fingers are together and straight. Hand breadth is measured from metacarpalphalangeal joint II to metacarpalphalangeal joint V.

Hand length is measured from the wrist landmark to dactylion with the same posture as the hand breadth.

Elbow-hand grip length is measured from the posterior tip of the olecranon process to the center of grip during holding a pencil. It can be called as the elbow to center of grip.

Elbow-fingertip length is measured from the posterior tip of the olecranon process to dactylion.

Shoulder-elbow length is measured from the right acromion landmark to the inferior tip of the olecranon process of the right elbow.

Forward grip reach or functional reach is measured from the back wall to the tip of the thumb.

Bi-deltoid breadth is measured across the body at the level of the deltoid landmarks.

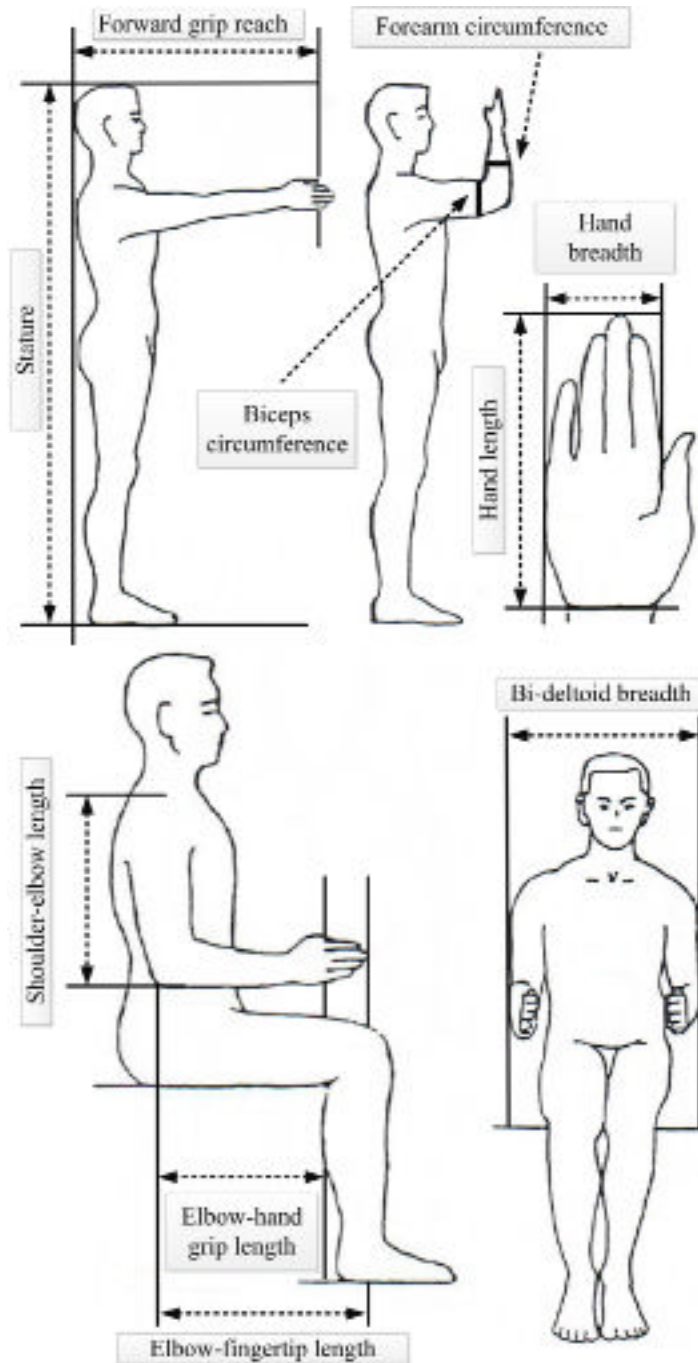
Experimental Anthropometric Data

It should be noted that the anthropometric variables are measured in the same day for all twenty subjects from the right arm of the subject using the standard instruments (Centurion Kit, Rosscraft). Due to the significant difference of muscle size and force between male and female subjects, anthropometric variables have usually been investigated and discussed by gender: male and female (Anakwe et al., 2007; Holzbaur, Murray, Gold, & Delp, 2007). In our experiments, the difference of anthropometric variables between male and female subjects is statistically significant at $p < 0.01$ for 8 parameters (body weight, stature, biceps circumference, forearm circumference, hand breadth, hand length, elbow-fingertip length, and forward grip reach) and significant at $p < 0.10$ for the remainders (BMI, elbow-hand grip length, shoulder-elbow length, and bi-deltoid breadth). In addition, to avoid the effect of ages we used the subjects from the same age, around 21 years old (no significant difference, $p = 0.458$). Twelve anthropometric variables from 10 males and 10 females are reported respectively in Table 1 and Table 2.

STATISTICAL ANALYSIS

Correlation analysis is used as an evaluating function in the study. It measures a relationship between two parameters and provides a statistic known as the correlation r coefficient. This coefficient shows the degree of a linear relationship between two measured variables. Correlation coefficients can interpret as the weak or low correlation when $r \leq 0.35$, the modest or moderate correlation when $0.35 < r \leq 0.67$, and the strong or high correlation when $0.67 < r \leq 1$ (Taylor, 1990). Actually, the r value contains both a magnitude and a direction (positive and negative) of the relationship. However, in our experiment only the magnitude of correlation coefficient (the absolute

Figure 4. Anthropometric measurements: stature, forward grip reach, biceps circumference, forearm circumference, hand breadth, hand length, shoulder-elbow length, elbow-hand grip length, elbow-fingertip length, and bi-deltoid breadth



The Relationship between Anthropometric Variables

Table 1. Twelve anthropometric variables of 10 male subjects (M1-M10) with the mean and the standard deviation (SD) of each variable

Subjects Variables	M1	M2	M3	M4	M5	M6	M7	M8	M9	M10	Mean	SD
Body weight	49.0	62.0	65.0	74.0	73.0	58.0	57.0	55.0	63.0	54.0	61.0	8.1
Stature	166.5	170.0	173.0	177.0	172.0	170.0	170.0	167.5	167.0	164.0	169.7	3.7
BMI	17.7	21.5	21.7	23.6	24.7	20.1	19.7	19.6	22.6	20.1	21.1	2.1
Biceps circumference	23.1	26.2	27.5	32.6	32.4	30.7	26.1	23.6	26.7	25.6	27.5	3.4
Forearm circumference	22.5	22.4	25.2	29.1	28.2	26.8	23.4	23.1	24.3	22.7	24.8	2.5
Hand breadth	7.4	7.2	8.4	9.1	8.9	12.6	11.7	7.5	7.8	7.6	8.8	1.9
Hand length	17.2	17.8	15.5	18.2	18.9	19.1	19.3	17.4	18.3	17.1	17.9	1.1
Elbow-hand grip length	34.4	35.1	37.6	39.3	39.7	33.9	33.8	36.0	38.5	38.4	36.7	2.3
Elbow-fingertip length	46.8	49.7	52.2	52.2	52.6	46.2	46.2	47.2	50.0	49.7	49.3	2.5
Shoulder-elbow length	37.7	33.6	36.9	37.8	38.2	35.7	38.4	35.4	38.3	36.6	36.9	1.6
Forward grip reach	75.6	74.5	80.7	89.0	80.4	74.3	75.7	72.6	83.5	78.1	78.4	5.0
Bi-deltoid breadth	39.3	46.4	44.6	54.7	47.3	37.4	30.4	42.1	45.9	47.4	43.6	6.7

value of average r coefficient) is used. Moreover, due to a small number of subjects n (less than 20), the significant level is set at $p < 0.05$ and is tested using t -test, as can be defined by

$$t = r \sqrt{\frac{n-2}{1-r^2}} \quad (18)$$

It should be noted that degrees of freedom for entering the t -distribution is defined as $n - 2$.

Table 2. Twelve anthropometric variables of 10 female subjects (F1-F10) with the mean and the SD of each variable

Subjects Variables	F1	F2	F3	F4	F5	F6	F7	F8	F9	F10	Mean	SD
Body weight	47.0	45.0	53.0	46.0	54.0	45.0	43.0	56.0	50.0	49.0	48.8	4.4
Stature	150.0	160.0	156.0	155.0	160.0	146.0	159.0	163.0	167.0	162.0	157.8	6.3
BMI	20.9	17.6	21.8	19.1	21.1	21.1	17.0	21.1	17.9	18.7	19.6	1.8
Biceps circumference	24.4	19.8	27.6	24.2	24.8	25.5	22.6	24.9	22.3	21.5	23.8	2.2
Forearm circumference	21.6	19.1	22.9	21.5	22.2	21.9	19.7	22.7	20.6	20.9	21.3	1.2
Hand breadth	7.4	6.4	7.3	7.5	6.9	6.6	6.9	8.1	7.4	7.2	7.2	0.5
Hand length	15.6	16.7	16.8	16.6	16.4	14.7	16.1	15.2	17.1	17.2	16.2	0.8
Elbow-hand grip length	32.8	35.0	34.8	34.6	34.4	32.6	34.3	35.2	38.4	36.2	34.8	1.6
Elbow-fingertip length	43.3	46.8	46.4	46.4	46.2	39.1	46.2	47.1	49.0	47.7	45.8	2.8
Shoulder-elbow length	34.9	35.3	36.1	35.8	33.1	34.2	33.0	37.1	37.8	36.0	35.3	1.6
Forward grip reach	65.1	72.0	60.8	68.1	75.7	65.2	70.2	63.3	74.4	70.6	68.5	4.9
Bi-deltoid breadth	41.9	36.8	43.4	41.2	41.0	37.8	36.9	37.0	37.2	38.7	39.2	2.5

Only the combinations between EMG features extracted from a muscle and anthropometric variables that have the strong and significant correlations in at least 4 motions are considered for the next stage.

RELATIONSHIP BETWEEN EMG FEATURE AND ANTHROPOMETRIC VARIABLE

To reach the high potential of EMG-based MCIs in the context of real-world requirements, the proposed anthropometric variables have been investigated the relationship with robust EMG features, which are divided into 4 groups as follows:

1. **Noise Tolerance:** WAMP, MYOP, SSC, and ZC;
2. **Low-Level and High-Level Surface EMG Signals:** DFA, HG, MFL, DAMV, DASDV, WL, VAR, IEMG, MAV, and RMS;
3. **Fluctuating EMG Signals Over Time:** SampEn and ApEn;
4. **Muscle Fatigue:** MNF and MDF.

It should be noted that the relationship between anthropometric variables and the Hudgins' time domain feature set, i.e. SSC, ZC, WL, MAV and mean absolute value slope, is presented and discussed in detail in our previous study (Phinyomark et al., 2013b).

Feature Set 1: Noise Tolerance

Noise is one of the major problems in the analysis of surface EMG signals. Zardoshti-Kermani et al., (1995) proposed that the robustness of EMG features is one of the three major properties for evaluating high-quality features. In their study, the definition of robustness is limited to the tolerance of noise. Artificial white noise at different noise levels was used to evaluate the robustness of features. The cluster separability of feature spaces

should be preserved as much as possible in a noisy environment. This property is important because both biological and environmental resources can generate noise and artifact. It is difficult to record only a pure signal component without noise. For this reason, noise removal or noise reduction is an important step before performing feature extraction in most of MCI systems. Many noise removal tools have been proposed, e.g. notch filter, band pass filter, adaptive filter, and wavelet filter (Jindapetch, Chewae, & Phukpattaranont, 2012; Phinyomark, Phukpattaranont, & Limsakul, 2011c). Unfortunately, there are not any filters that can remove one hundred percent of noise. Sometimes it removes some important parts of real EMG signals (De Luca, Gilmore, Kuznetsov, & Roy, 2010; Li, Li, Yu, & Geng, 2011). So EMG features that have high tolerance for biological and environmental noises should increase the ability of EMG-based gesture recognition.

Noises contaminated in surface EMG signal can be categorized into four major types: 1) ambient noise, 2) motion artifact, 3) the inherent instability of surface EMG signals, and 4) the in-herece in electronic components in the detection and recording equipment (De Luca, 2002; Reaz, Hussain, & Mohd-Yasin, 2006). The first three types have a specific band of frequencies, but the last noise type has a broaden frequency band and falls in a usable energy band of surface EMG signals. In the literature, four noisy EMG signals that consist of baseline noise, movement artifact, power-line interference, and random noise, i.e., white Gaussian noise, have been simulated and used to develop robust EMG methods (Phinyomark, Phukpattaranont, & Limsakul, 2012f). First two simulated noises, i.e., baseline noise and movement artifact have a narrow frequency band below 20 Hz, which ranges outside the EMG energy band. We can use a high-pass filter at a cut-off frequency of 20 Hz to remove these kinds of noise (De Luca et al., 2010). On the other hand, power-line interference (50/60 Hz) and random noise (0-1000 Hz) have a frequency band in a

The Relationship between Anthropometric Variables

Table 3. Correlation coefficients $|r|$ between anthropometric variables and EMG features (WAMP, MYOP, SSC, and ZC) in cases of strong and significant relationships (at least 4 movements for a muscle) based on 10 males and/or 10 females

Feature	Gender	Anthropometric variable	Muscle position	Movements	Average $ r $ (min- max)
WAMP	Male	Bi-deltoid breadth	ECU	FP, WE, WF, WU, HC	0.75 (0.72-0.78)
	Female	Bi-deltoid breadth	BB	FP, FS, WF, WR	0.72 (0.69-0.77)
MYOP	Male	Bi-deltoid breadth	ECU	FP, WE, WF, WU, HC	0.77 (0.76-0.77)
	Female	Bi-deltoid breadth	BB	FP, WF, WR, WU	0.72 (0.68-0.81)
SSC	Female	Bi-deltoid breadth	BB	FP, FS, WF, WU, HC	0.80 (0.70-0.86)
ZC	Male	Biceps circumference	BB	FP, FS, WF, HO	0.76 (0.69-0.85)
	Female	Bi-deltoid breadth	BB	FP, FS, WF, WU, HC	0.77 (0.70-0.84)

range of usable EMG energy band (20-500 Hz), therefore such noises can be only reduced to a predictable level or cannot be entirely removed.

In our previous works (Phinyomark, Limsakul, & Phukpattaranont, 2008, 2009), nine time domain and frequency domain features: RMS, WL, ZC, SSC, WAMP, HIST, AR, MDF, and MNF, were evaluated the robust performance based on two noise types: 50-Hz interference and white Gaussian noise, at different signal-to-noise ratios (0-20 dB SNRs). The experimental results showed that, on average WAMP is the most robust feature, followed by ZC and SSC features. These features are in the same feature group, together with MYOP, which compute in time domain and provide frequency information (Phinyomark, Phukpattaranont, & Limsakul, 2012c). All features in this group have a threshold parameter, which can be used to avoid some noises (Hudgins et al., 1993). In addition, the distribution of feature spaces in this group is similar to each other, particularly for WAMP and ZC.

From Table 3, all four features extracted from the BB muscle have a strong relationship with the bi-deltoid breadth for female subjects. For male subjects, there are two relationships: 1) WAMP

and MYOP from the ECU muscle and bi-deltoid breadth, and 2) ZC from the BB muscle and biceps circumference. All relationships share the motions of FP and WF.

Although the SSC feature has a higher average $|r|$ value than other three features for female subjects, it does not have a strong relationship with any anthropometric variables for male subjects. SSC and ZC are the members of the Hudgins' time domain feature set (Hudgins et al., 1993) and their classification performances are not influenced by the variation in muscle contraction effort (Tkach et al., 2010). Other features in Hudgins' time domain feature set are MAV, WL, and mean absolute value slope. Chan et al., (2000) re-evaluated the classification performance of the Hudgins' feature set using fuzzy approach. The SSC feature does not improve classification performance and in some subjects the classification accuracy decreases. So SSC is not recommended for developing robust MCI system.

Based on the similar distribution of feature spaces of ZC and WAMP (Phinyomark et al., 2012c), one of them should be selected in order to avoid the information redundancy in an EMG feature vector. The selection depends on the choice

of the system. If the automatically calibrated system is preferred, the ZC feature is recommended. On the other hand, if the semi-automatically calibrated system is acceptable, WAMP is a suitable feature. WAMP and MYOP have the same associations with the anthropometric variables, whereas WAMP is the most robust feature against noises. Moreover, WAMP has higher classification accuracy than other three features in the classification of upper-limb motions based on a robust linear discriminant analysis (LDA) classifier with and without periodic retraining scheme (Phinyomark et al., 2011a, in press b). WAMP is also successful in the classification of lower-limb exercise activities for the elderly (Phinyomark et al., 2012a) and in the estimation of muscle force levels (Kamavuako et al., 2013).

Feature Set 2: Low-Level and High-Level Surface EMG Signals

If the low-noise EMG signals are obtained from an EMG recording system with/without noise removal algorithms, the next challenge in EMG-based gesture recognition is about weak measured EMG signals. Simple MCI systems use the potential of a large difference between a high EMG magnitude at strong muscle contractions and a very low magnitude (close to zero) at the rest of the contractions. EMG amplitude estimators, i.e., RMS and MAV are sufficient enough for classifying the proposed activities (Clancy & Hogan, 1999). However, such systems often offer a few control schemes with a single speed of actuation based on a few EMG channels. To increase the number of control commands, a variety of motions and EMG channels have been proposed for the recognition system. In that case, it is not possible to get only strong EMG signals. Weak or low-level EMG signals (low SNR signals) must be measured. There are two cases: 1) a weak EMG signal is measured from a major corresponding muscle when a user performs a low force motion or a little movement (Arjunan, 2008) and 2) a

weak EMG signal is measured from a minor corresponding muscle when a user performs a high force motion or a strong movement (Phinyomark, Phukpattaranont, & Limsakul, 2012d).

To deal with the analysis of low-level EMG signals, a fractal analysis is used. Fractals refer to signal patterns, which exhibit self-similarity, that have fractal dimension. Fractal dimension of surface EMG signals is found under different types and levels of muscle contraction using several fractal methods, e.g. box-counting method (Gupta, Suryanarayanan, & Reddy, 1997), correlation dimension method (Hu, Wang, & Ren, 2005), critical exponent analysis (Phinyomark, Phothisonothai, Phukpattaranont, & Limsakul, 2011b), and Katz method (Gitter & Czerniecki, 1995). Based on the finding in previous studies, a fractal dimension of EMG signals depends on the level of muscle contraction during strong or high level activities (Gupta et al., 1997; Hu et al., 2005). For the low level of muscle contraction, fractal dimension does not change with change in the level of muscle contraction. It is a measure of the size and complexity of the muscles (Arjunan, 2008).

In our previous work (Phinyomark et al., 2012d), a fractal dimension estimator DFA was examined the performance in the classification of low-level EMG signal patterns compared with another fractal estimator HG (Arjunan & Kumar, 2010). The experimental results showed that, DFA has better cluster separability than HG (Phinyomark et al., 2011d), as well as classification performance (Phinyomark et al., 2012d). On the other hand, features based on a magnitude detector provide better performance in the classification of high-level EMG signal patterns than fractal features. So a combination of fractal and magnitude features is recommended (Arjunan & Kumar, 2011).

The past several years, magnitude features extracted from the first-order difference of EMG time series, i.e., MFL, DAMV, DASDV, and WL, present higher accuracy than magnitude features

The Relationship between Anthropometric Variables

extracted from the original time series, i.e., VAR, IEMG, MAV, and RMS (Brzostowski & Zieba, 2011; Kim et al., 2011; Kim, Jeong, Lee, & Song, 2012; Yu et al., 2012). In addition, the distribution of feature spaces in both groups is similar to each other for some motions and muscles.

Features in Table 4 can be divided into three feature groups based on the explanation above. Due to a large difference of feature spaces of the fractal features compared to the magnitude features, anthropometric variables that have strong associations with fractal features are different to other magnitude features. DFA computed from the FCR muscle has a strong relationship with the stature and elbow-fingertip length for female subjects. On the other hand, HG computed from the EDC muscle has a strong relationship with the BMI for male subjects. Both DFA and HG features estimate the fractal dimension of surface EMG signals, so the selection of fractal features is dependent on the gender of target users. On average DFA is more accurate than HG about 2%-5% (Phinyomark et al., 2012d).

For magnitude features, strong associations are found only with the bi-deltoid breadth. For female subjects, only features extracted from the BB muscle have a strong relationship with the variable. All relationships share the motions of FP, FS, and WR. For male subjects, two muscles have the strong relationships: ECU and BB muscles. Although feature space distribution of features extracted from the original and the first-order difference of EMG signals is similar to each other for some motions and muscles, the best feature from each group is usually selected in many previous studies to be a member of an optimal multiple feature set based on the feature selection scheme (Phinyomark et al., 2013b).

For the first-order differencing magnitude features, MFL outperforms others, followed respectively by DAMV, DASDV, and WL, based on many state-of-the-art classifiers, i.e., the LDA, the quadratic discriminant analysis (QDA), the artificial neural network (ANN), the k-nearest

neighbor (k-NN), and the maximum likelihood estimation (MLE), with and without the periodic retraining scheme (Arjunan & Kumar, 2010; Kim et al., 2011; Phinyomark et al., 2013b; Yu et al., 2012). Although WL performs the best in accuracy, stability, and computation load among the single features in several previous studies (Oskoei & Hu, 2008; Phinyomark et al., 2010), it is because of its popularity and other first-order differencing features were not included in the evaluating studies. In total, MFL is recommended to be used as a representative feature in this group instead of WL.

For the original magnitude features, all features have the same relationship with the anthropometric variable. Due to its similarity of IEMG to MAV and its similarity of VAR to RMS, the IEMG and VAR features should be excluded, because in comparison IEMG and VAR result in weaker performance in classification than MAV and RMS (Oskoei & Hu, 2008; Phinyomark et al., 2012c). For MAV and RMS, both features are close together in the success rate of classification, as well as the computational cost. The selection of MAV and RMS should be based on the probability density function (PDF) of the measured EMG signals. If the EMG PDF is close to the Gaussian density, an optimal EMG amplitude estimator is RMS (Hogan & Mann, 1980) based on both theoretically and experimentally. On the other hand, if the EMG PDF is close to the Laplacian density, an optimal EMG amplitude estimator is MAV (Clancy & Hogan, 1999). Moreover, MAV and RMS performance in the estimation of muscle force is similar to the performance of WAMP and WL features (Kamavuako et al., 2013).

Feature Set 3: Fluctuating EMG Signals over Time

Multifunction EMG pattern recognition systems that allow high recognition rate in research laboratories are usually based in single-session experiments. Most of related works collected EMG data only from a single day. A next major problem

The Relationship between Anthropometric Variables

Table 4. Correlation coefficients $|r|$ between anthropometric variables and EMG features (DFA, HG, MFL, DAMV, DASDV, WL, VAR, IEMG, MAV, and RMS) in cases of strong and significant relationships (at least 4 movements for a muscle) based on 10 males and/or 10 females

Feature	Gender	Anthropometric variable	Muscle position	Movements	Average $ r $ (min- max)
DFA	Female	Stature	FCR	FP, WF, WR, WU, HO	0.74 (0.67-0.83)
	Female	Elbow-fingertip length	FCR	WF, WU, HO, HC	0.73 (0.68-0.79)
HG	Male	BMI	EDC	FP, WU, HO, HC	0.72 (0.67-0.81)
MFL	Male	Bi-deltoid breadth	ECU	FP, WE, WF, WU, HC	0.75 (0.70-0.78)
	Both	Bi-deltoid breadth	BB	WE, WR, WU, HC	0.69 (0.68-0.69)
	Female	Bi-deltoid breadth	BB	FP, FS, WF, WR, WU, HC	0.76 (0.70-0.78)
DAMV	Male	Bi-deltoid breadth	ECU	FP, WE, WF, WU, HC	0.72 (0.67-0.75)
	Male	Bi-deltoid breadth	BB	WE, WR, WU, HC	0.69 (0.68-0.70)
	Female	Bi-deltoid breadth	BB	FP, FS, WR, HC	0.73 (0.68-0.78)
DASDV	Male	Bi-deltoid breadth	ECU	FP, WE, WF, WU	0.72 (0.67-0.75)
	Male	Bi-deltoid breadth	BB	WE, WR, WU, HC	0.70 (0.70-0.71)
	Female	Bi-deltoid breadth	BB	FP, FS, WF, WR	0.72 (0.67-0.75)
WL	Male	Bi-deltoid breadth	BB	WE, WR, WU, HC	0.69 (0.68-0.70)
	Female	Bi-deltoid breadth	BB	FP, FS, WF, WR, HC	0.75 (0.72-0.83)
VAR	Male	Bi-deltoid breadth	ECU	FP, WE, WF, HC	0.71 (0.68-0.76)
IEMG	Male	Bi-deltoid breadth	ECU	FP, WE, WF, WU, HC	0.77 (0.73-0.82)
MAV	Male	Bi-deltoid breadth	ECU	FP, WE, WF, WU, HC	0.77 (0.73-0.82)
RMS	Male	Bi-deltoid breadth	ECU	FP, WE, WF, WU, HC	0.76 (0.71-0.82)

is about the fluctuation of surface EMG signals over time. It is widely known that EMG signals measured in one day are relatively different from the EMG signals measured in another day, even on the same muscle and also same subject (Jain et al., 2012; Kaufmann, Englehart, & Platzner, 2010). This can be due to many factors, such as the EMG electrode location shift, the variation in muscle contraction effort, or change in the architecture characteristics of the subject (Saponas

et al., 2010; Tkach et al., 2010). So it is possible that features extracted from the initial training data (one day) and the present testing data (another day) are significant difference, which will degrade the performance of the pattern matching algorithms. In order to implement the MCIs based on EMG pattern recognition in clinics, the robustness over time of the system (i.e., feature extraction and classification algorithm) is very important.

The Relationship between Anthropometric Variables

In the literature, however, this problem has rarely been evaluated. Sensinger et al., (2009) and Jain et al., (2012) found that the performance of the EMG pattern recognition systems can degrade within hours after initial classifier training. Zhang et al., (2007) studied the effect of the number of days used as the training data sets. They found that if the data used for training the classifier decrease, the classification accuracy also decreases based on EMG signals recorded from five different days. Kaufmann et al., (2010) evaluated the performance of five state-of-the-art classifiers: support vector machine (SVM), decision tree (DT), the ANN, k-NN, and LDA, in the classification of surface EMG signals recorded from 21 days. They also found that the performance of the EMG pattern recognition systems degrades with increasing time difference between initial classifier training and testing data for all studied classifiers (about 8%-15%), except the LDA (about 3.6%) using the Hudgins' time domain feature set.

Using the same EMG data recorded during 21 days, fifty state-of-the-art EMG features in time domain and frequency domain were evaluated in one of our previous works (Phinyomark et al., 2013b). Among the single features, SampEn performed the highest classification accuracy (93.37%) by training the LDA classifier using EMG from only the first day without any retraining classifier again, followed by ApEn (84.68%) and MFL (82.07%). The EMG data were recorded from four surface EMG channels on the forearm for 21 days with 5-6 trials per day, and in each trial 11 wrist and finger motions were performed (Kaufmann et al., 2010).

SampEn and ApEn features extracted from the FCR muscle have a strong relationship with the forward grip reach for female subjects. Both relationships share the four motions of FP, FS, HO, and HC. In addition to the robustness over time, SampEn can use to detect the onset of EMG activity while suppressing spurious background spikes (Zhang & Zhou, 2012).

Feature Set 4: Muscle Fatigue

Muscle fatigue is generally resulted when a user performs the repetitive proposed motions for a long time and cannot produce the certain level of force with the muscle (De Luca, 1984). Generally, muscle fatigue results in an increase in EMG signal amplitude and a downward shift of EMG frequency spectrum (Cifrek, Medved, Tonković, & Ostojić, 2009). However, Tkach et al., (2010) reported that the effect of muscle fatigue on the classification performance of eleven time domain features (i.e., WAMP, ZC, SSC, WL, VAR, MAV, ν -Order, log-Detector, EMG histogram, autoregressive coefficients, and cepstrum coefficients) is very weak. On the other hand, for frequency domain features, MNF and MDF have been hailed so far as the gold standard for the muscle fatigue detection with surface EMG signals (Al-Mulla, Sepulveda, & Colley, 2011).

The experimental results showed that MDF does not have a strong relationship with any anthropometric variables, whereas MNF extracted from the FCR muscle of female subjects has a strong relationship with the hand length for four motions: FS, WU, HO, and HC at the average correlation coefficient $|r|$ of 0.76 (in range of 0.71-0.87). Further, MNF performs better performance in the classification of upper-limb motions than MDF and other frequency domain features, i.e., peak frequency, frequency ratio, power spectrum ratio, and the variance of central frequency (Phinyomark et al., 2012c, 2013b). The modified MNF can also be used to estimate muscle force like time domain features (Phinyomark et al., 2012g; Thongpanja, Phinyomark, Phukpattaranont, & Limsakul, 2013). If EMG frequency information is needed in developing EMG-based MCIs, the MNF feature is recommended to be used as an optimal frequency domain feature for both the classification of actions-based EMG signal and the assessment of muscle fatigue during actions.

Table 5. Correlation coefficients $|r|$ between anthropometric variables and EMG features (SampEn, ApEn) in cases of strong and significant relationships (at least 4 movements for a muscle) based on 10 males and/or 10 females

Feature	Gender	Anthropometric variable	Muscle position	Movements	Average $ r $ (min- max)
SampEn	Female	Forward grip reach	FCR	FP, FS, WU, HO, HC	0.75 (0.69-0.86)
ApEn	Female	Forward grip reach	FCR	FP, FS, HO, HC	0.76 (0.67-0.89)

SEMI-AUTOMATIC AND AUTOMATIC CALIBRATION SYSTEMS

As mentioned in the Introduction section, we can use the anthropometric variables to calibrate the systems in two different ways: a weighting factor for a classifier and a normalizing value for EMG features. Both ways can be used for adapting the system automatically. However, the difference between semi-automatic and automatic calibration systems is about the way to measure anthropometric variables. From twelve proposed anthropometric variables, only two variables: forearm and biceps circumferences can measure directly from an EMG measuring armband device, which is composed of surface EMG electrodes and the circumference measurement (Cannan & Hu, 2011). They can be used as calibrated inputs for an automatic calibration system. On the other hand, the remaining variables cannot measure directly from the EMG measuring armband device. These variables need to be measured manually, so they can be used as calibrated inputs for a semi-automatic calibration system. From the experiments, 7 out of the 12 proposed variables have strong relationships with EMG features, which can be divided into two groups: 1) the bi-deltoid breadth, stature, elbow-fingertip length, BMI, forward grip reach, and hand length for a semi-automatic calibration system, and 2) the biceps circumference for an automatic calibration system.

Among the seven variables, the bi-deltoid breadth has more associations with EMG features than other variables. It can be used to calibrate many robust EMG features consisting of WAMP, MFL, MAV, and RMS. The use of a feature vector of WAMP, MFL, and MAV/RMS would result in the high classification accuracy under robust conditions such as noisy environment, variation in muscle contraction effort, and low-and-high-level muscle contractions. For instance, using this EMG multiple feature set produced $89.97 \pm 7.34\%$ accuracy when classified the EMG data recorded from 21 days without the retraining classifier scheme (Kaufmann et al., 2010) and only the bi-deltoid breadth variable is used to calibrate the recognition system. However, if the system is not limited by a low processor, the multiple robust feature sets with respect to all studied robust conditions, which consisted of some robust features: WAMP, MFL, MAV/RMS, DFA, SampEn, and MNF, would result in high classification accuracy and could be used across users by calibrating with the correspond anthropometric variables. Hence, in future works, the stability of the possible multiple feature sets with respect to several studied robust conditions should be evaluated their performance together with the development of calibration techniques using the correspond anthropometric variables.

On the other hand, only a combination of the ZC and the biceps circumference has a strong relationship, which can be used for an automatic

The Relationship between Anthropometric Variables

calibration system. However, due to a rapid increased number of EMG wearable devices and a success of classifying motions associated with surface EMG recorded from the armband, new EMG features and other useful motions/muscles should be evaluated their associations with forearm and biceps circumferences in future studies. In addition to both the circumferences, hand circumference may be a useful anthropometric variable, because it is possible to record surface EMG signals using electrode sensor ring around the hand. This variable was also found that it has a strong relationship with the maximal grip strength and can use to create a simple model to predict the maximal grip strength (Li et al., 2010). In order to explore the potential use of automatic calibration systems, a review of the EMG pattern recognition using electrode arm bands is presented in the following sub-section.

EMG Sensor Arm Bands

To measure wrist and finger actions associated with surface EMG signals, traditionally, multiple surface electrodes need to be placed right above all the corresponding muscles. However, it is difficult to identify the exact position of the muscles (Kendall et al., 2012; Vigreux, Cnockaert, & Pertuzon, 1979). Because users typically have no detailed knowledge of human anatomy hence the EMG system is limited to only medical applications, and several muscles are closely together so it is not possible to acquire EMG from some specific single muscles. Moreover, the placing electrodes in this way require more time consuming. Errors in electrode placement degrade the classification accuracy of EMG-based MCIs (Tkach et al., 2010; Young et al., 2011, 2012).

Recent studies have designed and developed multichannel sensor rings/armbands to solve this problem. In this way, end-users will not have expertise and time to work on the electrode placement. It can be clearly seen from a recent commercial EMG sensor armband (i.e., MYO armband, see www.getmyo.com).

The MYO armband is composed of a large amount of small active electrodes in a form of sensor ring and can transfer the EMG data over a wireless network, which is feasible for use outside the laboratory. This device is easy to set up and configure by a user, and provides an always-available and highly personalized input interface with is a low cost (inexpensive). It could be like a watch, wristband, jewelry, or concealed beneath clothing in the near future, which is unobtrusive. Many wireless EMG systems have also become commercially available, such as ZeroWire EMG (see www.aurion.it), BTS FREEEMG 100RT/300 (see www.btsbioengineering.com), Wave Plus EMG (see www.cometasystems.com), and MYON 320 (see www.myon-prophysics.ch).

There are two useful positions on the forearm that have been proposed in related works on EMG pattern recognition:

1. Lower forearm positions, i.e., around the wrist (Rhee, You, & Shin, 2011; Tang, Liu, Lv, & Sun, 2012; You, Rhee, & Shin, 2010, 2011);
2. Upper forearm positions, i.e., below the elbow (Andews, Morin, & McLean, 2009; Benko et al., 2009; Du, Lin, Shyu, & Chen, 2010; Du, Shyu, & Hu, 2006; Khushaba & Kodagoda, 2012; Khushaba et al., 2013; Mogk & Keir, 2003; Saponas et al., 2008; Shyu, Chen, Tatn, & Hu, 2002; Smith, Huberdeau, Tenore, & Thakor, 2009; Smith et al., 2008; Tenore et al, 2007, 2009).

For the placement of the EMG electrodes around the forearm, there are two possible ways:

1. An adapted scheme, i.e., the distances between every two channels of electrodes are changed and dependent on the forearm sizes of the users (Andews et al., 2009; Benko et al., 2009; Saponas et al., 2008; Tang et al., 2012);

2. A fixed scheme, i.e., the distances between every two channels of electrodes are fixed, except one pair of electrodes in which the distance is varied depending on forearm circumference, e.g. one pair across the ulnar border (Du et al., 2006, 2010; Mogk & Keir, 2003; Shyu et al., 2002; Smith et al., 2008, 2009). In this scheme, however, there is no guarantee that electrodes are placed over the same muscles in all users.

For lower forearm positions, the EMG electrodes are designed to place on one side of the forearm: anterior forearm or posterior forearm, as a half wristband. In You et al., (2010, 2011) and Rhee et al., (2011), four EMG channels are placed on the anterior side of the forearm (flexor muscles). The recognition system is used to classify all five single finger motions and three multi-finger motions (index-middle fingers, middle-ring fingers, and hand close) and provides the average accuracy of about 95%-97%. On the other hand, Tang et al., (2012) used six EMG channels placed on the posterior side of the forearm (extensor muscles) instead of the anterior forearm to recognize three single finger motions (thumb, index finger, middle finger), and eight multi-finger motions. The success recognition rate is higher than 89%. Tang et al., (2012) mentioned that six channels are enough to cover the circumference of the posterior side and cover all useful extensor muscles: extensor digitorum, extensor pollicis longus and brevis, extensor indicis, and extensor digiti minimi.

For upper forearm positions, the EMG electrodes are designed to place on both sides of the forearm. The number of EMG channels placed in a narrow uniform band/ring, which is proposed in the literature, is seven sensors (Du et al., 2006, 2010; Mogk & Keir, 2003; Shyu et al., 2002) and eight sensors (Andrews et al., 2009; Khushaba & Kodagoda, 2012; Khushaba et al., 2013; Saponas et al., 2008; Smith et al., 2009). When multiple sets of sensors were placed around the forearm, reasonable EMG signals with useful information

could be acquired from the armband even the sensors are only approximately placed (Saponas et al., 2008). The landmark sensor armband is placed below the elbow in several conditions, e.g. approximately one third of the distance from the proximal end of a line from medial epicondyle to the distal head of the radius (Andrews et al., 2009; Mogk & Keir, 2003), or approximately two inches or five centimeters below the elbow (Du et al., 2006, 2010; Shyu et al., 2002; Smith et al., 2009). For the landmark of the starting electrode pair, there are several ways, such as placing just superior to the ulna (Andrews et al., 2009) or over the flexor carpi radialis (Mogk & Keir, 2003). On average, the proposed systems achieve more than 90%-95% accuracy.

Tenore et al., (2009, 2007) reported that there is no statistically significant difference ($p < 0.05$) in the classification accuracy using 32 electrodes placed on upper and lower forearm (6 sensor rings) and 19 electrodes placed on only upper forearm (3 sensor rings). The accuracy in classifying ten single flexed and extended finger motions is greater than 90% even in a transradial amputee. It means that the multi-channel sensor ring may be a kind of redundant sensor. Mogk and Keir (2003) found that the EMG signal amplitudes between adjacent electrode pairs (3 cm apart) share 40% common signal (or crosstalk), and the common signal is reduced to about 10% at 6 cm spacing and 2.5% at 9 cm, while only 2% common signal or crosstalk is found between flexor and extensor electrode pairs. On the other hand, we could place a similar sensor band on the other forearm to provide even more input possibilities (Saponas et al., 2008).

CONCLUSION AND FUTURE WORKS

This chapter presents the relationships between robust EMG features and twelve related anthropometric variables for MCIs. In feature extraction view point, the robust EMG feature is recom-

The Relationship between Anthropometric Variables

mended for each feature set 1-4, which is based on robust conditions in the context of real-world requirements. It can be summarized, as the following:

1. WAMP is the most robust feature against a variety of noises, i.e., random noise and power-line interference, followed by ZC. WAMP is also an optimal feature to estimate muscle force. It has a strong relationship with bi-deltoid breadth.
2. DFA, a fractal (complexity) feature, is the suitable feature for the classification of low-level EMG signals, and MFL and MAV/RMS are the optimal magnitude features for the classification of high-level EMG signals. DFA has a strong relationship with the stature and the elbow-fingertip length variables, whereas MFL and MAV/RMS have strong relationships with bi-deltoid breadth.
3. SampEn is the most robust feature for the variability of the muscle contraction over time. It is not only reliable for long-term usage but also for noise tolerance, i.e., spurious background spikes. SampEn has a strong relationship with forward grip reach.
4. MNF is used as a standard muscle fatigue detector. It is reliable for a noisy environment and can provide additional information in frequency domain. It has a strong relationship with hand length.

The optimal robust features mentioned above have strong relationships with several experimental anthropometric variables, i.e., biceps circumference, bi-deltoid breadth, standing height, elbow-fingertip length, forward grip reach, and hand length. These variables can be used to calibrate the MCI systems in two ways. The first way is a manual calibrated input system or a semi-automatic calibration, which can be implemented using all anthropometric variables. In this way, the system can develop using many robust features,

for instance, a robust multiple EMG feature set may consist of WAMP, DFA, MFL, MAV/RMS, SampEn, and MNF, and each feature can be calibrated by its related anthropometric variables. The second way is as an auto-calibration system. Based on this condition, forearm and bicep circumferences are two out of twelve variables that can be measured directly from wearable EMG device and used automatically to adapt the recognition system. However, in our experiments (eight upper-limb motions and five muscle positions) only the ZC feature has a strong and significant relationship with the biceps circumference. In future works, new features and/or other motions and muscles should be evaluated their associations with anthropometric variables.

In addition to the measured anthropometric data, we mentioned in the Introduction Section that it is possible to get the estimated anthropometric data from the published anthropometric tables. So in future works the estimated anthropometric data should be evaluated their relationships with EMG features too. If there are the strong and significant relationships between them, it means that we can add the anthropometric tables into the classification system and use this information to calibrate the system without measuring the anthropometric variables directly from the user. Further, the calibration techniques using the anthropometric variables: a weighting factor for a classifier and/or a normalizing value for EMG features should be developed and evaluated in future works. A simple idea for using anthropometric variables as a normalizing value for EMG features can be found in our preliminary study (Phinyomark et al., 2013a).

ACKNOWLEDGMENT

This work was funded by the FI MSTIC University Joseph Fourier Grenoble 1 (TIGRE project).

REFERENCES

- Al-Mulla, M. R., Sepulveda, F., & Colley, M. (2011). A review of non-invasive techniques to detect and predict localised muscle fatigue. *Sensors (Basel, Switzerland)*, *11*(4), 3545–3594. doi:10.3390/s110403545 PMID:22163810
- Anakwe, R. E., Huntley, J. S., & Mceachan, J. E. (2007). Grip strength and forearm circumference in a healthy population. *The Journal of Hand Surgery, European Volume*, *32*(2), 203–209. doi:10.1016/j.jhsb.2006.11.003 PMID:17197064
- Andrews, A., Morin, E., & McLean, L. (2009). Optimal electrode configurations for finger movement classification using EMG. *Proceedings of the 31st Annual International Conference of the IEEE EMBS*, Minneapolis, MN (pp. 2987-2990).
- Arjunan, S. P. (2008). *Fractal features of surface electromyogram: A new measure for low level muscle activation* (Ph.D. Dissertation). RMIT University, Melbourne, Australia.
- Arjunan, S. P., & Kumar, D. K. (2010). Decoding subtle forearm flexions using fractal features of surface electromyogram from single and multiple sensors. *Journal of Neuroengineering and Rehabilitation*, *7*(53). PMID:20964863
- Arjunan, S. P., & Kumar, D. K. (2011). Fractal properties of surface electromyogram for classification of low-level hand movements from single-channel forearm muscle activity. *Journal of Mechanics in Medicine and Biology*, *11*(3), 581–590. doi:10.1142/S0219519411003867
- Barreto, A. B., Scargle, S. D., & Adjouadi, M. (2000). A practical EMG-based human-computer interface for users with motor disabilities. *Journal of Rehabilitation Research and Development*, *37*(1), 53–64. PMID:10847572
- Benko, H., Saponas, T. S., Morris, D., & Tan, D. (2009). Enhancing input on and above the interactive surface with muscle sensing. In *Proceedings of the ACM International Conference on Interactive Tabletops and Surfaces*, Banff, Canada (pp. 93-100).
- Bolglia, L. A., & Uhl, T. L. (2007). Reliability of electromyographic normalization methods for evaluating the hip musculature. *Journal of Electromyography and Kinesiology*, *17*(1), 102–111. doi:10.1016/j.jelekin.2005.11.007 PMID:16423539
- Boostani, R., & Moradi, M. H. (2003). Evaluation of the forearm EMG signal features for the control of a prosthetic hand. *Physiological Measurement*, *24*(2), 309–319. doi:10.1088/0967-3334/24/2/307 PMID:12812417
- Boschmann, A., Kaufmann, P., Platzner, M., & Winkler, M. (2009). Towards multi-movement hand prostheses: Combining adaptive classification with high precision sockets. In *Proceedings of 2nd European Conference Technically Assisted Rehabilitation*, Berlin (pp. 1-4).
- Brzostowski, K., & Zieba, M. (2011). Analysis of human arm motions recognition algorithms for system to visualize virtual arm. In *Proceedings of the 21st International Conference on Systems Engineering*, Las Vegas, NV (pp. 422-426).
- Cannan, J. A. R., & Hu, H. (2011). Automatic circumference measurement for aiding in the estimation of maximum voluntary contraction (MVC) in EMG systems. In *Proceedings of the 4th international conference on Intelligent Robotics and Applications*, Aachen, Germany (pp. 202-211).
- Chan, F. H. Y., Yang, Y. S., Lam, F. K., Zhang, Y. T., & Parker, P. A. (2000). Fuzzy EMG classification for prosthesis control. *IEEE Transactions on Rehabilitation Engineering*, *8*(3), 305–311. doi:10.1109/86.867872 PMID:11001510

The Relationship between Anthropometric Variables

- Chen, L., Geng, Y., & Li, G. (2011). Effect of upper-limb positions on motion pattern recognition using electromyography. In *Proceedings of 4th International Congress on Image and Signal Processing*, Shanghai, China (pp. 139-142).
- Cifrek, M., Medved, V., Tonković, S., & Ostojić, S. (2009). Surface EMG based muscle fatigue evaluation in biomechanics. *Clinical Biomechanics (Bristol, Avon)*, 24(4), 327–340. doi:10.1016/j.clinbiomech.2009.01.010 PMID:19285766
- Clancy, E. A., & Hogan, N. (1999). Probability density of the surface electromyogram and its relation to amplitude detectors. *IEEE Transactions on Bio-Medical Engineering*, 46(6), 730–739. doi:10.1109/10.764949 PMID:10356879
- De Leva, P. (1996). Adjustments to Zatsiorsky-Seluyanov's segment inertia parameters. *Journal of Biomechanics*, 29(9), 1223–1230. doi:10.1016/0021-9290(95)00178-6 PMID:8872282
- De Luca, C. J. (1984). Myoelectrical manifestations of localized muscular fatigue in humans. *Critical Reviews in Biomedical Engineering*, 11(4), 254–279. PMID:6391814
- De Luca, C. J. (2002). *Surface electromyography: Detection and recording*. Retrieved from http://www.delsys.com/Attachments_pdf / WP_SEMGintro.pdf
- De Luca, C. J., Gilmore, L. D., Kuznetsov, M., & Roy, S. H. (2010). Filtering the surface EMG signal: Movement artifact and baseline noise contamination. *Journal of Biomechanics*, 43(8), 1573–1579. doi:10.1016/j.jbiomech.2010.01.027 PMID:20206934
- Du, Y. C., Lin, C. H., Shyu, L. Y., & Chen, T. (2010). Portable hand motion classifier for multi-channel surface electromyography recognition using gray relational analysis. *Expert Systems with Applications*, 37(6), 4283–4291. doi:10.1016/j.eswa.2009.11.072
- Du, Y. C., Shyu, L. Y., & Hu, W. (2006). The effect of combining stationary wavelet transform and independent component analysis in the multichannel SEMGs hand motion identification system. *Journal of Medical and Biological Engineering*, 26(1), 9–14.
- Esteller, R., Vachtsevanos, G., Echaz, J., & Litt, B. (2001). A comparison of waveform fractal dimension algorithms. *IEEE Transactions on Circuits and Systems. I, Fundamental Theory and Applications*, 48(2), 177–1831. doi:10.1109/81.904882
- Fougner, A., Scheme, E., Chan, A. D. C., Englehart, K., & Staudahl, Ø. (2011). Resolving the limb position effect in myoelectric pattern recognition. *IEEE Transactions on Neural Systems and Rehabilitation Engineering*, 19(6), 644–651. doi:10.1109/TNSRE.2011.2163529 PMID:21846608
- Fougner, A. L. (2007). *Proportional myoelectric control of a multifunction upper-limb prosthesis* (Master thesis). Norwegian University of Science and Technology, Norway.
- Gitter, J. A., & Czerniecki, M. J. (1995). Fractal analysis of the electromyographic interference pattern. *Journal of Neuroscience Methods*, 58(1-2), 103–108. doi:10.1016/0165-0270(94)00164-C PMID:7475215
- Gupta, V., Suryanarayanan, S., & Reddy, N. P. (1997). Fractal analysis of surface EMG signals from the biceps. *International Journal of Medical Informatics*, 45(3), 185–192. doi:10.1016/S1386-5056(97)00029-4 PMID:9291030
- Higuchi, T. (1988). Approach to an irregular time series on the basis of the fractal theory. *Physica D. Nonlinear Phenomena*, 31(2), 277–283. doi:10.1016/0167-2789(88)90081-4

- Hof, A. L., Pronk, C. N. A., & van Best, J. A. (1987). Comparison between EMG to force processing and kinetic analysis for the calf muscle moment in walking and stepping. *Journal of Biomechanics*, *20*(2), 167–178. doi:10.1016/0021-9290(87)90308-3 PMID:3571297
- Hogan, N., & Mann, R. W. (1980). Myoelectric signal processing: Optimal estimation applied to electromyography—Part I: Deviation of the optimal myoprocessor. *IEEE Transactions on Bio-Medical Engineering*, *BME-27*(7), 382–395. doi:10.1109/TBME.1980.326652
- Holzbaur, K. R., Murray, W. M., Gold, G. E., & Delp, S. L. (2007). Upper limb muscle volumes in adult subjects. *Journal of Biomechanics*, *40*(4), 742–749. doi:10.1016/j.jbiomech.2006.11.011 PMID:17241636
- Hu, X., Wang, Z., & Ren, X. (2005). Classification of surface EMG signal with fractal dimension. *Journal of Zhejiang University. Science. B.*, *6*(8), 844–848. doi:10.1631/jzus.2005.B0844 PMID:16052721
- Hudgins, B., Parker, P., & Scott, R. N. (1993). A new strategy for multifunction myoelectric control. *IEEE Transactions on Bio-Medical Engineering*, *40*(1), 82–94. doi:10.1109/10.204774 PMID:8468080
- Jain, S., Singhal, G., Smith, R. J., Kaliki, R., & Thakor, N. (2012). Improving long term myoelectric decoding, using an adaptive classifier with label correction. In *Proceedings of the 4th IEEE RAS/EMBS International Conference on Biomedical Robotics and Biomechatronics*, Rome (pp. 532-537).
- Jiang, N., Muceli, S., Graitmann, B., & Farina, D. (2013). Effect of arm position on the prediction of kinematics from EMG in amputees. *Medical & Biological Engineering & Computing*, *51*(1-2), 143–151. doi:10.1007/s11517-012-0979-4 PMID:23090099
- Jindapetch, N., Chewae, S., & Phukpattaranont, P. (2012). FPGA implementations of an ADALINE adaptive filter for power-line noise cancellation in surface electromyography signals. *Measurement*, *45*(3), 405–414. doi:10.1016/j.measurement.2011.11.004
- Kamavuako, E. N., Farina, D., Yoshida, K., & Jensen, W. (2009). Relationship between grasping force and features of single-channel intramuscular EMG signals. *Journal of Neuroscience Methods*, *185*(1), 143–150. doi:10.1016/j.jneumeth.2009.09.006 PMID:19747943
- Kamavuako, E. N., Rosenvang, J. C., Bøg, M. F., Smidstrup, A., Erkocevic, E., Niemeier, M. J., & Farina, D. (2013). Influence of the feature space on the estimation of hand grasping force from intramuscular EMG. *Biomedical Signal Processing and Control*, *8*(1), 1–5. doi:10.1016/j.bspc.2012.05.002
- Kaufmann, P., Englehart, L., & Platzner, M. (2010). Fluctuating EMG signals: Investigating long-term effects of pattern matching algorithms. *Proceedings of the 32nd Annual International Conference of the IEEE Engineering in Medicine and Biology Society*, Buenos Aires, Argentina (pp. 6357-6360).
- Kendall, C., Lemaire, E. D., Losier, Y., Chan, A., & Hudgins, B. (2012). A novel approach to surface electromyography: An exploratory study of electrode-pair selection based on signal characteristics. *Journal of Neuroengineering and Rehabilitation*, *9*(24).
- Khushaba, R. N., & Kodagoda, S. (2012). Electromyogram (EMG) feature reduction using mutual components analysis for multifunction prosthetic fingers control. In *Proceedings of the 12th International Conference on Control, Automation, Robotics and Vision*, Guangzhou, China (pp. 1534-1539).

The Relationship between Anthropometric Variables

- Khushaba, R. N., Kodagoda, S., Liu, D., & Dis-sanayake, G. (2013). Muscle computer interfaces for driver distraction reduction. *Computer Methods and Programs in Biomedicine*, *110*(2), 137–149. doi:10.1016/j.cmpb.2012.11.002 PMID:23290462
- Kim, K. S., Choi, H. H., Moon, C. S., & Mun, C. W. (2011). Comparison of k-nearest neighbor, quadratic discriminant and linear discriminant analysis in classification of electromyogram signals based on the wrist-motion directions. *Current Applied Physics*, *11*(3), 740–745. doi:10.1016/j.cap.2010.11.051
- Kim, S. J., Jeong, E. C., Lee, S. M., & Song, Y. R. (2012). Improvements of multi-features extraction for EMG for estimating wrist movements. *The Transactions of the Korean Institute of Electrical Engineers*, *61*(5), 757–762. doi:10.5370/KIEE.2012.61.5.757
- Kundu, A. S., Mazumder, O., & Bhaumik, S. (2011). Design of wearable, low power, single supply surface EMG extractor unit for wireless monitoring. In *Proceedings of the 2nd International Conference on Nanotechnology and Biosensors*, Dubai, United Arab Emirates (pp. 69-74).
- Lawrence, J. H., & De Luca, C. J. (1983). Myoelectric signal versus force relationship in different human muscles. *Journal of Applied Physiology*, *54*(6), 1653–1659. PMID:6874489
- Li, G., Li, Y., Yu, L., & Geng, Y. (2011). Conditioning and sampling issues of EMG signals in motion recognition of multifunctional myoelectric prostheses. *Annals of Biomedical Engineering*, *39*(6), 1779–1787. doi:10.1007/s10439-011-0265-x PMID:21293972
- Li, K., Hewson, D. J., Duchene, J., & Hogrel, J.-Y. (2010). Predicting maximal grip strength using hand circumference. *Manual Therapy*, *15*(6), 579–585. doi:10.1016/j.math.2010.06.010 PMID:20708427
- Marras, W. S., & Davis, K. G. (2001). A non-MVC EMG normalization technique for the trunk musculature: Part 1. Method development. *Journal of Electromyography and Kinesiology*, *11*(1), 1–9. doi:10.1016/S1050-6411(00)00039-0 PMID:11166603
- Marras, W. S., & Sommerich, C. M. (1991). A three-dimensional motion model of loads on the lumbar spine: I. Model structure. *Human Factors*, *33*(2), 123–137. PMID:1860700
- Merletti, R., & Parker, P. J. (Eds.). (2004). *Electromyography: Physiology, engineering, and non-invasive applications*. Hoboken, NJ: John Wiley & Sons. doi:10.1002/0471678384
- Mogk, J. P. M., & Keir, P. J. (2003). Crosstalk in surface electromyography of the proximal forearm during gripping tasks. *Journal of Electromyography and Kinesiology*, *13*(1), 63–71. doi:10.1016/S1050-6411(02)00071-8 PMID:12488088
- Oatis, C. A. (2008). *Kinesiology: The mechanics and pathomechanics of human movement*. Philadelphia, PA: Lippincott Williams & Wilkins.
- Oskoei, M. A., & Hu, H. (2008). Support vector machine-based classification scheme for myoelectric control applied to upper limb. *IEEE Transactions on Bio-Medical Engineering*, *55*(8), 1956–1965. doi:10.1109/TBME.2008.919734 PMID:18632358
- Oskoei, A. H., Paulin, M. G., & Carman, A. B. (2013). Intra-session and inter-day reliability of forearm surface EMG during varying hand grip forces. *Journal of Electromyography and Kinesiology*, *23*(1), 216–222. doi:10.1016/j.jelekin.2012.08.011 PMID:22999075
- Park, S. H., & Lee, S. P. (1998). EMG pattern recognition based on artificial intelligence techniques. *IEEE Transactions on Rehabilitation Engineering*, *6*(4), 400–405. doi:10.1109/86.736154 PMID:9865887

- Peng, C. K., Havlin, S., Stanley, H. E., & Goldberger, A. L. (1995). Quantification of scaling exponents and crossover phenomena in non-stationary heartbeat time series. *Chaos (Woodbury, N.Y.)*, 5(1), 82–87. doi:10.1063/1.166141 PMID:11538314
- Philipson, L., & Larsson, P. G. (1988). The electromyographic signal as a measure of muscular force: A comparison of detection and quantification techniques. *Electromyography and Clinical Neurophysiology*, 28(2-3), 141–150. PMID:3416804
- Phinyomark, A., Chujit, G., Phukpattaranont, P., Limsakul, C., & Hu, H. (2012a). A preliminary study assessing time-domain EMG features of classifying exercises in preventing falls in the elderly. In *Proceedings of the 9th International Conference on Electrical Engineering/Electronics, Computer, Telecommunications and Information Technology*, Phetchaburi, Thailand (pp. 1-4).
- Phinyomark, A., Hirunviriyaya, S., Nuidod, A., Phukpattaranont, P., & Limsakul, C. (2011a). Evaluation of EMG feature extraction for movement control of upper limb prostheses based on class separation index. In *Proceedings of the 5th Kuala Lumpur International Conference on Biomedical Engineering*, Kuala Lumpur, Malaysia (pp. 750-754).
- Phinyomark, A., Hirunviriyaya, S., Phukpattaranont, P., & Limsakul, C. (2010). Evaluation of EMG feature extraction for hand movement recognition based on Euclidean distance and standard deviation. In *Proceedings of the 7th International Conference on Electrical Engineering/Electronics, Computer, Telecommunications and Information Technology*, Chiang Mai, Thailand (pp. 856-860).
- Phinyomark, A., Limsakul, C., & Phukpattaranont, P. (2008). EMG feature extraction for tolerance of white Gaussian noise. In *Proceedings of the International Workshop and Symposium on Science and Technology*, Nong Khai, Thailand (pp. 178-183).
- Phinyomark, A., Limsakul, C., & Phukpattaranont, P. (2009). EMG feature extraction for tolerance of 50 Hz interference. In *Proceedings of the 4th International Conference on Engineering Technologies*, Novi Sad, Serbia (pp. 289-293).
- Phinyomark, A., Nuidod, A., Phukpattaranont, P., & Limsakul, C. (2012b). Feature extraction and reduction of wavelet transform coefficients for EMG pattern classification. *Elektronika ir Elektrotechnika*, 122(6), 27-32.
- Phinyomark, A., Phothisonothai, M., Phukpattaranont, P., & Limsakul, C. (2011b). Critical exponent analysis applied to surface electromyography (EMG) signals for gesture recognition. *Metrology and Measurement Systems*, 18(4), 645–658. doi:10.2478/v10178-011-0061-9
- Phinyomark, A., Phukpattaranont, P., & Limsakul, C. (2011c). Wavelet-based denoising algorithm for robust EMG pattern recognition. *Fluctuation and Noise Letters*, 10(2), 157–167. doi:10.1142/S0219477511000466
- Phinyomark, A., Phukpattaranont, P., & Limsakul, C. (2012c). Feature reduction and selection for EMG signal classification. *Expert Systems with Applications*, 39(8), 7420–7431. doi:10.1016/j.eswa.2012.01.102
- Phinyomark, A., Phukpattaranont, P., & Limsakul, C. (2012d). Fractal analysis features for weak and single-channel upper-limb EMG signal. *Expert Systems with Applications*, 39(12), 11156–11163. doi:10.1016/j.eswa.2012.03.039
- Phinyomark, A., Phukpattaranont, P., & Limsakul, C. (2012e). Investigating long-term effects of feature extraction methods for continuous EMG pattern classification. *Fluctuation and Noise Letters*, 11(4), 1250028. doi:10.1142/S0219477512500289

The Relationship between Anthropometric Variables

Phinyomark, A., Phukpattaranont, P., & Limsakul, C. (2012f). The usefulness of wavelet transform to reduce noise in the SEMG signal. In M. Schwartz (Ed.), *EMG methods for evaluating muscle and nerve function* (pp. 107–132). Rijeka, Croatia: InTech. doi:10.5772/25757

Phinyomark, A., Phukpattaranont, P., Limsakul, C., & Phothisonothai, M. (2011d). Electromyography (EMG) signal classification based on detrended fluctuation analysis. *Fluctuation and Noise Letters*, 10(3), 281–301. doi:10.1142/S0219477511000570

Phinyomark, A., Quaine, F., Charbonnier, S., Serviere, C., Tarpin-Bernard, F., & Laurillau, Y. (2013a). A feasibility study on the use of anthropometric variables to make muscle-computer interface more practical. *Engineering Applications of Artificial Intelligence*, 26(7), 1681–1688. doi:10.1016/j.engappai.2013.01.004

Phinyomark, A., Quaine, F., Charbonnier, S., Serviere, C., Tarpin-Bernard, F., & Laurillau, Y. (2013b). EMG feature evaluation for improving myoelectric pattern recognition robustness. *Expert Systems with Applications*, 40(12), 4832–4840. doi:10.1016/j.eswa.2013.02.023

Phinyomark, A., Thongpanja, S., Hu, H., Phukpattaranont, P., & Limsakul, C. (2012g). The usefulness of mean and median frequencies in electromyography analysis. In G. R. Naik (Ed.), *Computational intelligence in electromyography analysis - A perspective on current applications and future challenges* (pp. 195–220). Rijeka, Croatia: InTech. doi:10.5772/50639

Phothisonothai, M., & Nakagawa, M. (2007). Fractal-based EEG data analysis of body parts movement imagery tasks. *The Journal of Physiological Sciences; JPS*, 57(4), 217–226. doi:10.2170/physiolsci.RP006307 PMID:17637165

Reaz, M. B. I., Hussain, M. S., & Mohd-Yasin, F. (2006). Techniques of EMG signal analysis: Detection, processing, classification and applications. *Biological Procedures Online*, 8(1), 11–35. doi:10.1251/bpo115 PMID:16799694

Rhee, K. W., You, K. J., & Shin, H. C. (2011). Recognition of finger motion with sEMG and gyrosensor signals. *Journal of Measurement Science and Instrumentation*, 2(2), 136–139.

Richman, J. S., & Moorman, J. R. (2000). Physiological time series analysis using approximate entropy and sample entropy. *American Journal of Physiology. Heart and Circulatory Physiology*, 278(6), H2039–H2049. PMID:10843903

Saponas, T. S., Tan, D. S., Morris, D., & Balakrishnan, R. (2008). Demonstrating the feasibility of using forearm electromyography for muscle-computer interfaces. In *Proceedings of the SIGCHI Conference on Human Factors in Computing Systems*, Florence, Italy (pp. 515–524).

Saponas, T. S., Tan, D. S., Morris, D., Balakrishnan, R., Turner, J., & Landay, J. A. (2009). Enabling always-available input with muscle-computer interfaces. In *Proceedings of the ACM Symposium on User Interface Software and Technology*, Victoria, Canada (pp. 167–176).

Saponas, T. S., Tan, D. S., Morris, D., Turner, J., & Landay, J. A. (2010). Making muscle-computer interfaces more practical. In *Proceedings of the SIGCHI Conference on Human Factors in Computing Systems*, Atlanta, GA (pp. 851–854).

Sensinger, J. W., Lock, B. A., & Kuiken, T. A. (2009). Adaptive pattern recognition of myoelectric signals: exploration of conceptual framework and practical algorithms. *IEEE Transactions on Neural Systems and Rehabilitation Engineering*, 17(3), 270–278. doi:10.1109/TN-SRE.2009.2023282 PMID:19497834

- Shenoy, P., Miller, K. J., Crawford, B., & Rao, R. P. N. (2008). Online electromyographic control of a robotic prosthesis. *IEEE Transactions on Bio-Medical Engineering*, 55(3), 1128–1135. doi:10.1109/TBME.2007.909536 PMID:18334405
- Shyu, L. Y., Chen, J. Y., Tatn, R. W., & Hu, W. (2002). A new electrode system for hand action discrimination. *Journal of Medical and Biological Engineering*, 22(4), 211–217.
- Smith, R. J., Huberdeau, D., Tenore, F., & Thakor, N. V. (2009). Real-time myoelectric decoding of individual finger movements for a virtual target task. In *Proceedings of the 31st Annual International Conference of the IEEE EMBS*, Minneapolis, MN (pp. 2376-2379).
- Smith, R. J., Tenore, F., Huberdeau, D., Etienne-Cummings, R., & Thakor, N. V. (2008). Continuous decoding of finger position from surface EMG signals for the control of powered prostheses. In *Proceedings of the 30th Annual International Conference of the IEEE EMBS*, Vancouver, Canada (pp. 197-200).
- Subasi, A. (2012). Medical decision support system for diagnosis for neuromuscular disorders using DWT and fuzzy support vector machines. *Computers in Biology and Medicine*, 42(8), 806–815. doi:10.1016/j.compbiomed.2012.06.004 PMID:22763356
- Subasi, A. (2013). Classification of EMG signals using PSO optimized SVM for diagnosis of neuromuscular disorders. *Computers in Biology and Medicine*, 43(5), 576–586. doi:10.1016/j.compbiomed.2013.01.020 PMID:23453053
- Tang, X., Liu, Y., Lv, C., & Sun, D. (2012). Hand motion classification using a multi-channel surface electromyography sensor. *Sensors (Basel, Switzerland)*, 12(2), 1130–1147. doi:10.3390/s120201130 PMID:22438703
- Taylor, R. (1990). Interpretation of the correlation coefficient: A basic review. *Journal of Diagnostic Medical Sonography*, 6(1), 35–39. doi:10.1177/875647939000600106
- Tenore, F. V. G., Ramos, A., Fahmy, A., Acharya, S., Etienne-Cummings, R., & Thakor, N. V. (2007). Towards the control of individual fingers of a prosthetic hand using surface EMG signals. In *Proceedings of the 29th Annual International Conference of the IEEE EMBS*, Lyon, France (pp. 6145-6148).
- Tenore, F. V. G., Ramos, A., Fahmy, A., Acharya, S., Etienne-Cummings, R., & Thakor, N. V. (2009). Decoding of individual finger movements using surface electromyography. *IEEE Transactions on Bio-Medical Engineering*, 56(5), 1427–1434. doi:10.1109/TBME.2008.2005485 PMID:19473933
- Thongpanja, S., Phinyomark, A., Phukpattaranont, P., & Limsakul, C. (2013). Mean and median frequency of EMG signal to determine muscle force based on time-dependent power spectrum. *Elektronika ir Elektrotechnika*, 19(3), 51-56.
- Tkach, D., Huang, H., & Kuiken, T. A. (2010). Study of stability of time-domain features for electromyographic pattern recognition. *Journal of Neuroengineering and Rehabilitation*, 7(21). PMID:20492713
- Vera-Garcia, F. J., Moreside, J. M., & McGill, S. M. (2010). MVC techniques to normalize trunk muscle EMG in healthy women. *Journal of Electromyography and Kinesiology*, 20(1), 10–16. doi:10.1016/j.jelekin.2009.03.010 PMID:19394867
- Vigreux, B., Cnockaert, J. C., & Pertuzon, E. (1979). Factors influencing quantified surface EMGs. *European Journal of Applied Physiology and Occupational Physiology*, 41(2), 119–129. doi:10.1007/BF00421659 PMID:467411

The Relationship between Anthropometric Variables

- Wei, L., Hu, H., & Zhang, Y. (2011). Fusing EMG and visual data for hands-free control of an intelligent wheelchair. *International Journal of Humanoid Robotics*, 8(4), 707–724. doi:10.1142/S0219843611002629
- Winter, D. A. (1990). *Biomechanics and motor control of human movement*. New York: Wiley & Sons.
- Woods, J. J., & Bigland-Ritchie, B. (1983). Linear and non-linear surface EMG/force relationships in human muscles. An anatomical/functional argument for the existence of both. *American Journal of Physical Medicine*, 62(6), 287–299. PMID:6650674
- Yang, S. W., Lin, C. S., Lin, S. K., & Lee, C. H. (2013). Design of virtual keyboard using blink control method for the severely disabled. *Computer Methods and Programs in Biomedicine*, 111(2), 410–418. doi:10.1016/j.cmpb.2013.04.012 PMID:23702128
- You, K. J., Rhee, K. W., & Shin, H. C. (2010). Finger motion decoding using EMG signals corresponding various arm postures. *Experimental Neurology*, 19(1), 54–61. PMID:22110342
- You, K. J., Rhee, K. W., & Shin, H. C. (2011). Finger flexion motion inference from sEMG signals. *Journal of Measurement Science and Instrumentation*, 2(2), 140–143.
- Young, A. J., Hargrove, L. J., & Kuiken, T. A. (2011). The effects of electrode size and orientation on the sensitivity of myoelectric pattern recognition systems to electrode shift. *IEEE Transactions on Bio-Medical Engineering*, 58(9), 2537–2544. doi:10.1109/TBME.2011.2159216 PMID:21659017
- Young, A. J., Hargrove, L. J., & Kuiken, T. A. (2012). Improving myoelectric pattern recognition robustness to electrode shift by changing interelectrode distance and electrode configuration. *IEEE Transactions on Bio-Medical Engineering*, 59(3), 645–652. doi:10.1109/TBME.2011.2177662 PMID:22147289
- Yu, S., Jeong, E., Hong, K., & Lee, S. (2012). Classification of nine directions using the maximum likelihood estimation based on electromyogram of both forearms. *Biomedical Engineering Letters*, 2(2), 129–137. doi:10.1007/s13534-012-0063-x
- Zardoshti-Kermani, M., Wheeler, B. C., Badie, K., & Hashemi, R. M. (1995). EMG feature evaluation for movement control of upper extremity prostheses. *IEEE Transactions on Rehabilitation Engineering*, 3(4), 324–333. doi:10.1109/86.481972
- Zhang, X., Chen, X., Zhao, Z. Y., Li, Q., Yang, J. H., Lantz, V., & Wang, K. Q. (2008). An adaptive feature extractor for gesture SEMG recognition. In *Proceedings of the 1st International Conference on Medical Biometrics*, Hong Kong (pp. 83-90).
- Zhang, X., & Zhou, P. (2012). Sample entropy analysis of surface EMG for improved muscle activity onset detection against spurious background spikes. *Journal of Electromyography and Kinesiology*, 22(6), 901–907. doi:10.1016/j.jelekin.2012.06.005 PMID:22800657
- Zhao, J., Jiang, L., Cai, H., Liu, H., & Hirzinger, G. (2006a). A novel EMG motion pattern classifier based on wavelet transform and nonlinearity analysis method. In *Proceedings of IEEE International Conference on Robotics and Biomimetics*, Kunming, China (pp. 1494-1499).

Zhao, J., Xie, Z., Jiang, L., Cai, H., Liu, H., & Hirzinger, G. (2006b). EMG control for a five-fingered underactuated prosthetic hand based on wavelet transform and sample entropy. In *Proceedings of IEEE/RSJ International Conference on Intelligent Robots and Systems*, Beijing, China (pp. 3215-3220).

ADDITIONAL READING

Ahsan, Md. R., Ibrahimy, M. I., & Khalifa, O. O. (2009). EMG signal classification for human computer interaction: A review. *European Journal of Scientific Research*, 33(3), 480–501.

Franti, E., Milea, L., Butu, V., Cismas, S., Lungu, M., & Schiopu, P. et al. (2012). Methods of acquisition and signal processing for myoelectric control of artificial arms. *Romanian Journal of Information Science and Technology*, 15(2), 91–105.

Herle, S., & Man, S. (2009). Processing surface electromyographical signals for myoelectric control. In T. Y. Kheng (Ed.), *Rehabilitation engineering* (pp. 223–244). Rijeka: InTech. doi:10.5772/7383

Li, G. (2011). Electromyography pattern-recognition-based control of powered multifunctional upper-limb prostheses. In J. Mizrahi (Ed.), *Advances in applied electromyography* (pp. 99–116). Rijeka: InTech. doi:10.5772/22876

Micera, S., Carpaneto, J., & Raspopovic, S. (2010). Control of hand prostheses using peripheral information. *IEEE Reviews in Biomedical Engineering*, 3, 48–68. doi:10.1109/RBME.2010.2085429 PMID:22275201

Oskoei, M. A., & Hu, H. (2007). Myoelectric control systems – A survey. *Biomedical Signal Processing and Control*, 2(4), 275–294. doi:10.1016/j.bspc.2007.07.009

Peerdeman, B., Boere, D., Witteveen, H., In 't Veld, R. H., Hermens, H., & Stramigioli, S. et al. (2011). Myoelectric forearm prostheses: State of the art from a user-centered perspective. *Journal of Rehabilitation Research and Development*, 48(6), 719–738. doi:10.1682/JRRD.2010.08.0161 PMID:21938658

Phinyomark, A., Phukpattaranont, P., & Limsakul, C. (2011). A review of control methods for electric power wheelchairs based on electromyography (EMG) signals with special emphasis on pattern recognition. *IETE Technical Review*, 25(4), 316–326. doi:10.4103/0256-4602.83552

Zecca, M., Micera, S., Carrozza, M. C., & Dario, P. (2002). Control of multifunctional prosthetic hands by processing the electromyographic signal. *Critical Reviews in Biomedical Engineering*, 30(4-6), 459–485. doi:10.1615/CritRevBiomedEng.v30.i456.80 PMID:12739757

KEY TERMS AND DEFINITIONS

Anthropometry: A measurement of the dimensions of the different parts of body.

Bi-Deltoid Breadth: Measured from the maximum horizontal breadth across the body at the level of the deltoid landmarks (shoulder breadth).

Electromyography (EMG) Signal: An electrophysiological signal which is measured from the proposed muscle by electrodes during movements.

Feature Extraction: A technique to transform original signal into a reduced set of features, which highlight the relevant structures and discard the irrelevant parts in the original signal.

Forearm Circumference: The linear distance around the forearm, which is usually measured at the level of maximum forearm circumference.

Gesture Recognition: A technique to interpret and classify the human gestures via mathematical algorithms.

The Relationship between Anthropometric Variables

Multifunction Myoelectric Control: An advanced technique concerned with the preprocessing, feature extraction, dimensionality reduction, and pattern classification of myoelectric (or EMG) signals to control external devices with many functions.

Muscle-Computer Interface: An interface between users based on EMG signals via muscles and computers.

Compilation of References

- Abernethy, B., Neal, R. J., Moran, M. J., & Parker, A. W. (1990). Science and golf: Proceedings of the First World Scientific Congress of Golf. In A. J. Cochran (Ed.), *Expert-novice differences in muscle activity during the golf swing* (pp. 54-60). London: E. & F. N. Spon.
- Acosta, A. M., Kirsch, R. F., & Perreault, E. J. (2000). A robotic manipulator for the characterization of two-dimensional dynamic stiffness using stochastic displacement perturbations. *Journal of Neuroscience Methods*, *102*(2), 177–186. doi:10.1016/S0165-0270(00)00307-1 PMID:11040414
- Adams, M. A., Dolan, P., & Hutton, W. C. (1988). The lumbar spine in backward bending. *Spine*, *13*(9), 1019–1026. doi:10.1097/00007632-198809000-00009 PMID:3206295
- Adams, M. A., May, S., Freeman, B. J., Morrison, H. P., & Dolan, P. (2000). Effects of backward bending on lumbar intervertebral discs. Relevance to physical therapy treatments for low back pain. *Spine*, *25*(4), 431–437. doi:10.1097/00007632-200002150-00007 PMID:10707387
- Adams, M. A., McNally, D. S., Chinn, H., & Dolan, P. (1994). Posture and the compressive strength of the lumbar spine. *Clinical Biomechanics (Bristol, Avon)*, *9*(1), 5–14. doi:10.1016/0268-0033(94)90052-3 PMID:23916072
- Adrian, R. H. (1976). The propagation of excitation in striated muscle. (1976). Voluntary control of human motor units. In M. Shahani (Ed.), *The motor system: Neurophysiology and muscle mechanisms* (pp. 15–24). Amsterdam, The Netherlands: Elsevier.
- Agre, J. C., & Sliwa, J. A. (2000). Neuromuscular rehabilitation and electrodiagnosis. 4. Specialized neuropathy. *Arch Phys Med Rehabil*, *81*(3 Suppl 1), S27–31, S36–44.
- Agur, A. M., Ng-Thow-Hing, V., Ball, K. A., Fiume, E., & McKee, N. H. (2003). Documentation and three-dimensional modelling of human soleus muscle architecture. *Clinical Anatomy (New York, N.Y.)*, *16*(4), 285–293. doi:10.1002/ca.10112 PMID:12794910
- Ajiboye, A. B., & Weir, R. F. (2005). A heuristic fuzzy logic approach to EMG pattern recognition for multifunctional prosthetic control. *IEEE Transactions on Neural Systems and Rehabilitation Engineering*, *13*(3), 280–291. doi:10.1109/TNSRE.2005.847357 PMID:16200752
- Akaike, N. (1978). Resting and action potentials in white muscle of potassium deficient rats. *Comparative Biochemistry and Physiology. Part A, Physiology*, *61*, 629–633. doi:10.1016/0300-9629(78)90140-8
- Albers, B. A., Put, J. H., Wallinga, W., & Wirtz, P. (1989). Quantitative analysis of single muscle fiber action potentials recorded at known distances. *Electroencephalography and Clinical Neurophysiology*, *73*(3), 245–253. doi:10.1016/0013-4694(89)90125-9 PMID:2475329
- Albuquerque, E. X., & Thesleff, S. (1968). A comparative study of membrane properties of innervated and chronically denervated fast and slow skeletal muscles of the rat. *Acta Physiologica Scandinavica*, *73*, 471–480. PMID:5708174
- Al-Eisa, E., Egan, D., Deluzio, K., & Wassersug, R. (2006). Effects of pelvic asymmetry and low back pain on trunk kinematics during sitting: A comparison with standing. *Spine*, *31*(5), 135–143. doi:10.1097/01.brs.0000201325.89493.5f PMID:16508537
- Allen, T., & Proske, U. (2006). Effect of muscle fatigue on the sense of limb position and movement. *Experimental Brain Research*, *170*(1), 30–38. doi:10.1007/s00221-005-0174-z PMID:16328298

Compilation of References

- Allison, G. T. (2003). Trunk muscle onset detection technique for EMG signals with ECG artefact. *Journal of Electromyography and Kinesiology*, 13(3), 209–216. doi:10.1016/S1050-6411(03)00019-1 PMID:12706601
- Allison, G. T., & Fujiwara, T. (2002). The relationship between EMG median frequency and low frequency band amplitude changes at different levels of muscle capacity. *Clinical Biomechanics (Bristol, Avon)*, 17(6), 464–469. doi:10.1016/S0268-0033(02)00033-5 PMID:12135548
- Allum, J., Bloem, B., Carpenter, M., Hulliger, M., & Hadders-Algra, M. (1998). Proprioceptive control of posture: A review of new concepts. *Gait & Posture*, 8(3), 214–242. doi:10.1016/S0966-6362(98)00027-7 PMID:10200410
- Al-Mulla, M. R., Sepulveda, F., & Colley, M. (2011). A review of non-invasive techniques to detect and predict localised muscle fatigue. *Sensors (Basel, Switzerland)*, 11(4), 3545–3594. doi:10.3390/s110403545 PMID:22163810
- Ambrosini, E., Ferrante, S., Tibiletti, M., Schauer, T., Klauer, C., Ferrigno, G., & Pedrocchi, A. (2011). An EMG-controlled neuroprosthesis for daily upper limb support: A preliminary study. In *Conference Proceedings of the Annual International Conference of the IEEE Engineering in Medicine and Biology Society* (pp. 4259–4262).
- Ambrosini, E., Ferrante, S., Ferrigno, G., Molteni, F., & Pedrocchi, A. (2012). Cycling induced by electrical stimulation improves muscle activation and symmetry during pedaling in hemiparetic patients. *IEEE Transactions on Neural Systems and Rehabilitation Engineering*, 20, 320–330. doi:10.1109/TNSRE.2012.2191574 PMID:22514205
- Ambrosini, E., Ferrante, S., Pedrocchi, A., Ferrigno, G., & Molteni, F. (2011). Cycling induced by electrical stimulation improves motor recovery in postacute hemiparetic patients: A randomized controlled trial. *Stroke*, 42, 1068–1073. doi:10.1161/STROKEAHA.110.599068 PMID:21372309
- Aminoff, M. J. (1992). Clinical electromyography. In M. J. Aminoff (Ed.), *Electrodiagnosis in clinical neurology* (pp. 249–283). New York: Churchill Livingstone Inc.
- Anakwe, R. E., Huntley, J. S., & Mceachan, J. E. (2007). Grip strength and forearm circumference in a healthy population. *The Journal of Hand Surgery, European Volume*, 32(2), 203–209. doi:10.1016/j.jhsb.2006.11.003 PMID:17197064
- Anders, C., Wagner, H., Puta, C., Grassme, R., Petrovitch, A., & Scholle, H. C. (2007). Trunk muscle activation patterns during walking at different speeds. *Journal of Electromyography and Kinesiology*, 17(2), 245–252. doi:10.1016/j.jelekin.2006.01.002 PMID:16517182
- Anderson, F. C., & Pandy, M. G. (2001). Dynamic optimization of human walking. *Journal of Biomechanical Engineering: ASME*, 123, 381–390. doi:10.1115/1.1392310 PMID:11601721
- Andrews, A., Morin, E., & McLean, L. (2009). Optimal electrode configurations for finger movement classification using EMG. *Proceedings of the 31st Annual International Conference of the IEEE EMBS*, Minneapolis, MN (pp. 2987–2990).
- Arabadzhev, T. I., Dimitrov, G. V., Dimitrov, A. G., Chakarov, V. E., & Dimitrova, N. A. (2008). Factors affecting the turns analysis of the interference EMG signal. *Biomedical Signal Processing and Control*, 3(4), 145–153. doi:10.1016/j.bspc.2007.07.003
- Arasaki, K., Tamaki, M., Hosoya, Y., & Kudo, N. (1997). Validity of electromyograms and tension as a means of motor unit number estimation. *Muscle & Nerve*, 20(5), 552–560. doi:10.1002/(SICI)1097-4598(199705)20:5<552::AID-MUS3>3.0.CO;2-8 PMID:9140361
- Arellano, C. J., & Kram, R. (2011). The effects of step width and arm swing on energetic cost and lateral balance during running. *Journal of Biomechanics*, 44(7), 1291–1295. doi:10.1016/j.jbiomech.2011.01.002 PMID:21316058
- Arjunan, S. P. (2008). *Fractal features of surface electromyogram: A new measure for low level muscle activation* (Ph.D. Dissertation). RMIT University, Melbourne, Australia.
- Arjunan, S. P., & Kumar, D. K. (2010). Decoding subtle forearm flexions using fractal features of surface electromyogram from single and multiple sensors. *Journal of Neuroengineering and Rehabilitation*, 7(53). PMID:20964863

- Arjunan, S. P., & Kumar, D. K. (2011). Fractal properties of surface electromyogram for classification of low-level hand movements from single-channel forearm muscle activity. *Journal of Mechanics in Medicine and Biology*, *11*(3), 581–590. doi:10.1142/S0219519411003867
- Badier, M., Guillot, C., Lagier-Tessonier, F., Burnet, H., & Jammes, Y. (1993). EMG power spectrum of respiratory and skeletal muscles during static contraction in healthy man. *Muscle & Nerve*, *16*(6), 601–609. doi:10.1002/mus.880160605 PMID:8502257
- Ballesteros, M. L. F., Buchthal, F., & Rosenfalck, P. (1965). The pattern of muscular activity during the arm swing of natural walking. *Acta Physiologica Scandinavica*, *63*, 296–310. doi:10.1111/j.1748-1716.1965.tb04069.x PMID:14329151
- Balter, J. E., & Zehr, E. P. (2007). Neural coupling between the arms and legs during rhythmic locomotor-like cycling movement. *Journal of Neurophysiology*, *97*(2), 1809–1818. doi:10.1152/jn.01038.2006 PMID:17065245
- Barreto, A. B., Scargle, S. D., & Adjouadi, M. (2000). A practical EMG-based human-computer interface for users with motor disabilities. *Journal of Rehabilitation Research and Development*, *37*(1), 53–64. PMID:10847572
- Barrett, C. L., Mann, G. E., Taylor, P. N., & Strike, P. (2009). A randomized trial to investigate the effects of functional electrical stimulation and therapeutic exercise on walking performance for people with multiple sclerosis. *Multiple Sclerosis*, *15*, 493–504. doi:10.1177/1352458508101320 PMID:19282417
- Barsi, G. I., Popovic, D. B., Tarkka, I. M., Sinkjaer, T., & Grey, M. J. (2008). Cortical excitability changes following grasping exercise augmented with electrical stimulation. *Experimental Brain Research*, *191*, 57–66. doi:10.1007/s00221-008-1495-5 PMID:18663439
- Barthelemy, D., & Nielsen, J. B. (2010). Corticospinal contribution to arm muscle activity during human walking. *The Journal of Physiology*, *588*(6), 967–979. doi:10.1113/jphysiol.2009.185520 PMID:20123782
- Bawa, P., & Calancie, B. (1983). Repetitive doublets in human flexor carpi radialis muscle. *Journal of Physiology*, (London), *339*, 123–132.
- Bawa, P., & Lemon, R. N. (1993). Recruitment of motor units in response to transcranial magnetic stimulation in man. *Journal of Physiology*, (London), *471*, 445–464.
- Bawa, P., & Jones, K. E. (1999). Do lengthening contractions represent a case of preferential recruitment of large motor units. *Progress in Brain Research*, *123*, 215–220. doi:10.1016/S0079-6123(08)62858-7 PMID:10635718
- Bawa, P., Pang, P., Olesen, K., & Calancie, B. (2006). Rotation of motoneurons during prolonged isometric contractions in humans. *Journal of Neurophysiology*, *96*(3), 1135–1140. doi:10.1152/jn.01063.2005 PMID:16775202
- Bawa, P., & Tatton, W. G. (1979). Motor units responses in muscles stretched by imposed displacements of the monkey wrist. *Experimental Brain Research*, *37*, 417–438. doi:10.1007/BF00236815 PMID:118044
- Becher, J. G., Harlaar, J., Lankhorst, G. J., & Vogelaar, T. W. (1998). Measurement of impaired muscle function of the gastrocnemius, soleus, and tibialis anterior muscles in spastic hemiplegia: A preliminary study. *Journal of Rehabilitation Research and Development*, *35*, 314–326. PMID:9704315
- Bechler, J., Jobe, F., Pink, M., Perry, J., & Ruwe, P. (1995). Electromyographic analysis of the hip and knee during the golf swing. *Clinical Journal of Sport Medicine*, *5*(3), 162–165. doi:10.1097/00042752-199507000-00005 PMID:7670971
- Bellemare, F., Woods, J. J., Johansson, R., & Bigland-Ritchie, B. (1983). Motor-unit discharge rates in maximal voluntary contractions of three human muscles. *Journal of Neurophysiology*, *50*(6), 1380–1392. PMID:6663333
- Benko, H., Saponas, T. S., Morris, D., & Tan, D. (2009). Enhancing input on and above the interactive surface with muscle sensing. In *Proceedings of the ACM International Conference on Interactive Tabletops and Surfaces*, Banff, Canada (pp. 93–100).
- Benoit, D. L., & Dowling, J. J. (2006). In vivo assessment of elbow flexor work and activation during stretch-shortening cycle tasks. *Journal of Electromyography and Kinesiology*, *16*, 352–364. doi:10.1016/j.jelekin.2004.07.006 PMID:16263310

Compilation of References

- Benton, L. A., Baker, L. L., Bowman, B. R., & Waters, R. L. (1981). *Functional electrical stimulation -- A practical clinical guide* (2nd ed.). Los Angeles, CA: Rehabilitation Engineering Center.
- Bergmark, A. (1989). Stability of the lumbar spine. A study in mechanical engineering. *Acta Orthopaedica Scandinavica. Supplementum*, 230, 1–54. doi:10.3109/17453678909154177 PMID:2658468
- Bergquist, A. J., Clair, J. M., Lagerquist, O., Mang, C. S., Okuma, Y., & Collins, D. F. (2011). Neuromuscular electrical stimulation: Implications of the electrically evoked sensory volley. *European Journal of Applied Physiology*, 111, 2409–2426. doi:10.1007/s00421-011-2087-9 PMID:21805156
- Bickel, C. S., Gregory, C. M., & Dean, J. C. (2011). Motor unit recruitment during neuromuscular electrical stimulation: A critical appraisal. *European Journal of Applied Physiology*, 111, 2399–2407. doi:10.1007/s00421-011-2128-4 PMID:21870119
- Biering-Sørensen, F. (1984). Physical measurements as risk indicators for low-back trouble over a one-year period. *Spine*, 9(2), 106–119. PMID:6233709
- Bigland-Ritchie, B. (1981). EMG and fatigue of human voluntary and stimulated contractions. *Ciba Foundation Symposium*, 82, 130–156. PMID:6913468
- Blevins, F. (1997). Rotator cuff pathology in athletes. *Sports Medicine (Auckland, N.Z.)*, 24(3), 205–220. doi:10.2165/00007256-199724030-00009 PMID:9327536
- Bodine-Fowler, S., Garfinkel, A., Roland, R. R., & Edgerton, V. R. (1990). Spatial distribution of muscle fibres within the territory of a motor unit. *Muscle & Nerve*, 13(12), 1133–1145. doi:10.1002/mus.880131208 PMID:1702521
- Bogataj, U., Gros, N., Kljajić, M., Aćimović, R., & Malezic, M. (1995). The rehabilitation of gait in patients with hemiplegia: A comparison between conventional therapy and multichannel functional electrical stimulation therapy. *Physical Therapy*, 75, 490–502. PMID:7770495
- Bohannon, R. W., & Smith, M. B. (1987). Interrater reliability of a modified Ashworth scale of muscle spasticity. *Physical Therapy*, 67, 206–207. PMID:3809245
- Bolgia, L. A., & Uhl, T. L. (2007). Reliability of electromyographic normalization methods for evaluating the hip musculature. *Journal of Electromyography and Kinesiology*, 17(1), 102–111. doi:10.1016/j.jelekin.2005.11.007 PMID:16423539
- Boostani, R., & Moradi, M. H. (2003). Evaluation of the forearm EMG signal features for the control of a prosthetic hand. *Physiological Measurement*, 24(2), 309–319. doi:10.1088/0967-3334/24/2/307 PMID:12812417
- Boschmann, A., Kaufmann, P., Platzner, M., & Winkler, M. (2009). Towards multi-movement hand prostheses: Combining adaptive classification with high precision sockets. In *Proceedings of 2nd European Conference Technically Assisted Rehabilitation*, Berlin (pp. 1-4).
- Bouillard, K., Frere, J., Hug, F., & Guevel, A. (2012). Prediction of time-to-exhaustion in the first dorsal interosseous muscle from early changes in surface electromyography parameters. [Evaluation Studies]. *Muscle & Nerve*, 45(6), 835–840. doi:10.1002/mus.23253 PMID:22581537
- Boyas, S., & Guevel, A. (2011a). Influence of exercise intensity and joint angle on endurance time prediction of sustained submaximal isometric knee extensions. *European Journal of Applied Physiology*, 111(6), 1187–1196. doi:10.1007/s00421-010-1731-0 PMID:21127901
- Boyas, S., & Guevel, A. (2011b). Neuromuscular fatigue in healthy muscle: underlying factors and adaptation mechanisms. *Ann Phys Rehabil Med*, 54(2), 88–108. doi:10.1016/j.rehab.2011.01.001 PMID:21376692
- Boyas, S., Maisetti, O., & Guevel, A. (2009). Changes in sEMG parameters among trunk and thigh muscles during a fatiguing bilateral isometric multi-joint task in trained and untrained subjects. *Journal of Electromyography and Kinesiology*, 19(2), 259–268. doi:10.1016/j.jelekin.2007.09.002 PMID:17964184
- Brackley, H. M., & Stevenson, J. M. (2004). Are children's backpack weight limits enough? A critical review of the relevant literature. *Spine*, 29(19), 2184–2190. doi:10.1097/01.brs.0000141183.20124.a9 PMID:15454714

- Brereton, L. C., & McGill, S. M. (1998). Frequency response of spine extensors during rapid isometric contractions: effects of muscle length and tension. *Journal of Electromyography and Kinesiology*, 8(4), 227–232. doi:10.1016/S1050-6411(98)00009-1 PMID:9779396
- Brinkman, R. S. A., & Türker, K. S. (2003). A method for quantifying reflex responses from intra-muscular and surface electromyogram. *Journal of Neuroscience Methods*, 122, 179–193. doi:10.1016/S0165-0270(02)00321-7 PMID:12573477
- Brown, B. H., Lawford, P. W., Smallwood, R. H., Hose, D. R., & Barber, D. C. (1999). *Medical physics and biomedical engineering*. London: IOP Publishing Ltd. doi:10.1887/0750303689
- Brown, S. H. M., & McGill, S. M. (2005). Muscle force-stiffness characteristics influence joint stability: a spine example. *Clinical Biomechanics (Bristol, Avon)*, 20(9), 917–922. doi:10.1016/j.clinbiomech.2005.06.002 PMID:16055250
- Bru, B., & Amarantini, D. (2008). Influence of sporting expertise on the EMG–torque relationship during isometric contraction in man. *Computer Methods in Biomechanics and Biomedical Engineering*, 11(1), 43–44. doi:10.1080/10255840802296806
- Brumagne, S., Cordo, P., & Verschueren, S. (2004). Proprioceptive weighting changes in persons with low back pain and elderly persons during upright standing. *Neuroscience Letters*, 366(1), 63–66. doi:10.1016/j.neulet.2004.05.013 PMID:15265591
- Bryan, A. (1998). Electromyography: Recording methods and signal processing techniques. *Current Anaesthesia and Critical Care*, 9(3), 110–116. doi:10.1016/S0953-7112(98)80003-3
- Brzostowski, K., & Zieba, M. (2011). Analysis of human arm motions recognition algorithms for system to visualize virtual arm. In *Proceedings of the 21st International Conference on Systems Engineering*, Las Vegas, NV (pp. 422–426).
- Buchanan, T. S., Lloyd, D. G., Manal, K., & Besier, T. F. (2004). Neuromusculoskeletal modeling: Estimation of muscle forces and joint moments and movements from measurements of neural command. *Journal of Applied Biomechanics*, 20, 367–395. PMID:16467928
- Buchanan, T. S., Lloyd, D. G., Manal, K., & Besier, T. F. (2005). Estimation of muscle forces and joint moments using a forward-inverse dynamics model. *Medicine and Science in Sports and Exercise*, 37, 1911–1916. doi:10.1249/01.mss.0000176684.24008.6f PMID:16286861
- Buchthal, F., & Fernandez-Ballesteros, M. L. (1965). Electromyographic study of the muscles of the upper arm and shoulder during walking in patients with Parkinson's disease. *Brain*, 88, 875–896. doi:10.1093/brain/88.5.875 PMID:5864465
- Buchthal, F., Guld, C., & Rosenfalck, P. (1954b). Action potential parameters in normal human muscle and their dependence on physical variables. *Acta Physiologica Scandinavica*, 32, 200–218. doi:10.1111/j.1748-1716.1954.tb01167.x PMID:13228109
- Buchthal, F., & Pinelli, P. (1953). Action potentials in muscular atrophy of neurogenic origin. *Neurology*, 3(8), 591–603. doi:10.1212/WNL.3.8.591 PMID:13087579
- Buchthal, F., Pinelli, P., & Rosenfalck, P. (1954a). Action potential parameters in normal human muscle and their physiological determinants. *Acta Physiologica Scandinavica*, 32(2), 219–229. doi:10.1111/j.1748-1716.1954.tb01168.x PMID:13228110
- Bulbulian, R., Ball, K., & Seaman, D. (2001). The short golf backswing effects on performance and spinal health implications. *Journal of Manipulative Physiological Therapy*, 24(9), 569–575. doi:10.1067/mmt.2001.118982 PMID:11753330
- Buller, N. P., Garnett, R., & Stephens, J. A. (1980). The reflex responses of single motor units in human hand muscles following muscle afferent stimulation. *The Journal of Physiology*, 193, 141–160. PMID:7431236
- Burden, A. (2010). How should we normalize electromyograms obtained from healthy participants? What we have learned from over 25 years of research. *Journal of Electromyography and Kinesiology*, 20(6), 1023–1035. doi:10.1016/j.jelekin.2010.07.004 PMID:20702112
- Burke, R. E. (1981). Motor units: Anatomy, physiology, and functional organization. In V. B. Brooks (Ed.), *Handbook of physiology* (Vol. I, pp. 345–422). Bethesda, MD: American Physiological Society.

Compilation of References

- Burke, R. E., Dum, R. P., Fleshman, J. W., Glenn, L. L., Lev-Tov, A., O'Donovan, M. J., & Pinter, M. J. (1982). An HRP study of the relation between cell size and motor unit type in cat ankle extensor motoneurons. *The Journal of Comparative Neurology*, *209*, 17–28. doi:10.1002/cne.902090103 PMID:7119171
- Cabri, J., Sousa, J. P., Kots, M., & Barreiros, J. (2009). Injuries in golf: A systematic review. *European Journal of Sport Science*, *9*(6), 353–366. doi:10.1080/17461390903009141
- Calancie, B., & Bawa, P. (1985). Voluntary and reflexive recruitment of flexor carpi radialis motor units in man. *Journal of Neurophysiology*, *53*, 1194–1200. PMID:3998806
- Calancie, B., & Bawa, P. (1986). Limitations of the spike triggered averaging technique for obtaining motor unit twitch profiles. *Muscle & Nerve*, *9*, 78–83. doi:10.1002/mus.880090113 PMID:3951484
- Calancie, B., & Bawa, P. (1990). Motor unit recruitment in humans. In M. D. Binder, & L. M. Mendell (Eds.), *The segmental motor system* (pp. 75–111). New York: Oxford University Press.
- Calancie, B., Nordin, M., Wallin, U., & Hagbarth, K.-E. (1987). Motor-unit responses in human wrist flexor and extensor muscles to transcranial cortical stimuli. *Journal of Neurophysiology*, *58*, 1168–1185. PMID:3694249
- Callaghan, J. P., Patla, A. E., & McGill, S. M. (1999). Low back three-dimensional joint forces, kinematics, and kinetics during walking. *Clinical Biomechanics (Bristol, Avon)*, *14*(3), 203–216. doi:10.1016/S0268-0033(98)00069-2 PMID:10619108
- Cannan, J. A. R., & Hu, H. (2011). Automatic circumference measurement for aiding in the estimation of maximum voluntary contraction (MVC) in EMG systems. In *Proceedings of the 4th international conference on Intelligent Robotics and Applications*, Aachen, Germany (pp. 202–211).
- Cappellini, G., Ivanenko, Y. P., Dominici, N., Poppele, R. E., & Lacquaniti, F. (2010). Migration of motor pool activity in the spinal cord reflects body mechanics in human locomotion. *Journal of Neurophysiology*, *104*(6), 3064–3073. doi:10.1152/jn.00318.2010 PMID:20881204
- Cappellini, G., Ivanenko, Y. P., Poppele, R. E., & Lacquaniti, F. (2006). Motor patterns in human walking and running. *Journal of Neurophysiology*, *95*(6), 3426–3437. doi:10.1152/jn.00081.2006 PMID:16554517
- Carpinella, I., Crenna, P., Rabuffetti, M., & Ferrarin, M. (2010). Coordination between upper- and lower-limb movements is different during overground and treadmill walking. *European Journal of Applied Physiology*, *108*(1), 71–82. doi:10.1007/s00421-009-1168-5 PMID:19756711
- Carr, H. J. (2003). *Stroke rehabilitation guidelines for exercise and training to optimize motor skill*. New York: Elsevier Science Ltd.
- Carver, S., Kiemel, T., & Jeka, J. J. (2006). Modeling the dynamics of sensory reweighting. *Biological Cybernetics*, *95*(2), 123–134. doi:10.1007/s00422-006-0069-5 PMID:16639582
- Cauraugh, J. H., Naik, S. K., Hsu, W. H., Coombes, S. A., & Holt, K. G. (2010). Children with cerebral palsy: A systematic review and meta-analysis on gait and electrical stimulation. *Clinical Rehabilitation*, *24*, 963–978. doi:10.1177/0269215510371431 PMID:20685722
- Cauraugh, J., Light, K., Kim, S., Thigpen, M., & Behrman, A. (2000). Chronic motor dysfunction after stroke: Recovering wrist and finger extension by electromyography-triggered neuromuscular stimulation. *Stroke*, *31*, 1360–1364. doi:10.1161/01.STR.31.6.1360 PMID:10835457
- Ceccato, J. C., de Sèze, M., Azevedo, C., & Cazalets, J. R. (2009). Comparison of trunk activity during gait initiation and walking in humans. *PLoS ONE*, *4*(12), e8193. doi:10.1371/journal.pone.0008193 PMID:19997606
- Chae, J., Yang, G., Park, R. K., & Labatia, I. (2002). Muscle weakness and cocontraction in upper limb hemiparesis: Relationship to motor impairment and physical disability. *Neurorehabilitation and Neural Repair*, *16*, 241–248. doi:10.1177/154596830201600303 PMID:12234087
- Challis, J. (1999). A procedure for the automatic determination of filter cutoff frequency for the processing of biomechanical data. *Journal of Applied Biomechanics*, *15*(3), 303–317.

- Chan, F. H. Y., Yang, Y. S., Lam, F. K., Zhang, Y. T., & Parker, P. A. (2000). Fuzzy EMG classification for prosthesis control. *IEEE Transactions on Rehabilitation Engineering*, 8(3), 305–311. doi:10.1109/86.867872 PMID:11001510
- Chang, W. R., & Grönqvist, R. (2003). *Measuring slipperiness: Human locomotion and surface factors*. Boca Raton, FL: CRC Press. doi:10.4324/9780203301913
- Chang, Y. W., Su, F. C., Wu, H. W., & An, K. N. (1999). Optimum length of muscle contraction. *Clinical Biomechanics (Bristol, Avon)*, 14, 537–542. doi:10.1016/S0268-0033(99)00014-5 PMID:10521638
- Chan, K. M., Doherty, T. J., & Brown, W. F. (2001). Contractile properties of human motor units in health, aging, and disease. *Muscle & Nerve*, 24(9), 1113–1133. doi:10.1002/mus.1123 PMID:11494264
- Chan, R. C., & Hsu, T. C. (1991). Quantitative comparison of motor unit potential parameters between monopolar and concentric needles. *Muscle & Nerve*, 14(10), 1028–1032. doi:10.1002/mus.880141015 PMID:1944402
- Chardon, M. K., Suresh, N. L., & Rymer, W. Z. (2010). An evaluation of passive properties of spastic muscles in hemiparetic stroke survivors. In *Conference Proceedings 32th IEEE Engineering Medical Biology Society*, (pp. 2993-2996).
- Chastan, N., Westby, G. W. M., Yelnik, J., Bardinet, E., Do, M. C., Agid, Y., & Welter, M. L. (2009). Effects of nigral stimulation on locomotion and postural stability in patients with Parkinson's disease. *Brain*, 132(1), 172–184. doi:10.1093/brain/awn294 PMID:19001482
- Chaudry, V., & Crawford, T. O. (1999). Stimulation single-fiber EMG in infant botulism. *Muscle & Nerve*, 22(10), 1698–1703. doi:10.1002/(SICI)1097-4598(199912)22:12<1698::AID-MUS12>3.0.CO;2-K PMID:10567083
- Chen, L., Geng, Y., & Li, G. (2011). Effect of upper-limb positions on motion pattern recognition using electromyography. In *Proceedings of 4th International Congress on Image and Signal Processing*, Shanghai, China (pp. 139-142).
- Chiovetto, E. (2011). The motor system plays the violin: a musical metaphor inferred from the oscillatory activity of the α -motoneuron pools during locomotion. *Journal of Neurophysiology*, 105(4), 1429–1431. doi:10.1152/jn.011119.2010 PMID:21273310
- Chleboun, G. S., France, A. R., Crill, M. T., Braddock, H. K., & Howell, J. N. (2001). In vivo measurement of fascicle length and pennation angle of the human biceps femoris muscle. *Cells, Tissues, Organs*, 169, 401–409. doi:10.1159/000047908 PMID:11490120
- Cho, K. K., Kim, Y. S., & Kim, E. J. (2006). The comparative analysis of kinematic and EMG on power walking and normal gait. *Korean Journal of Sport Biomechanics*, 16(2), 85–95. doi:10.5103/KJSB.2006.16.2.085
- Cholewicki, J., & McGill, S. M. (1994). EMG assisted optimization: a hybrid approach for estimating muscle forces in an indeterminate biomechanical model. *Journal of Biomechanics*, 27(10), 1287–1289. doi:10.1016/0021-9290(94)90282-8 PMID:7962016
- Cholewicki, J., & McGill, S. M. (1996). Mechanical stability of the in vivo lumbar spine: implications for injury and chronic low back pain. *Clinical Biomechanics (Bristol, Avon)*, 11(1), 1–15. doi:10.1016/0268-0033(95)00035-6 PMID:11415593
- Cholewicki, J., McGill, S. M., & Norman, R. W. (1995). Comparison of muscle forces and joint load from an optimization and EMG assisted lumbar spine model: towards development of a hybrid approach. *Journal of Biomechanics*, 28(3), 321–331. doi:10.1016/0021-9290(94)00065-C PMID:7730390
- Christe, B. L. (2009). *Introduction to biomedical instrumentation: the technology of patient Care*. New York: Cambridge University Press. doi:10.1017/CBO9780511808937
- Chu, J. U., Moon, I., & Mun, M. (2005). A real-time EMG pattern recognition based on linear-nonlinear feature projection for multifunction myoelectric hand. In *Proceedings of International Conference on Rehabilitation Robotics* (pp. 295-298).
- Chu, E., & George, A. (2010). *Inside the FFT black box, serial and parallel fast Fourier transform algorithms*. Boca Raton, FL: CRC Press.

Compilation of References

- Chvatal, S. A., Torres-Oviedo, G., Safavynia, S. A., & Ting, L. H. (2011). Common muscle synergies for control of center of mass and force in nonstepping and stepping postural behaviors. *Journal of Neurophysiology*, *106*(2), 999–1015. doi:10.1152/jn.00549.2010 PMID:21653725
- Cifrek, M., Medved, V., Tonković, S., & Ostojić, S. (2009). Surface EMG based muscle fatigue evaluation in biomechanics. *Clinical Biomechanics (Bristol, Avon)*, *24*(4), 327–340. doi:10.1016/j.clinbiomech.2009.01.010 PMID:19285766
- Clancy, E. A., Bida, O., & Rancourt, D. (2006). Influence of advanced electromyogram (EMG) amplitude processors on EMG-to-torque estimation during constant-posture, force-varying contractions. *Journal of Biomechanics*, *36*(14), 2690–2698. doi:10.1016/j.jbiomech.2005.08.007 PMID:16243341
- Clancy, E. A., & Hogan, N. (1999). Probability density of the surface electromyogram and its relation to amplitude detectors. *IEEE Transactions on Bio-Medical Engineering*, *46*(6), 730–739. doi:10.1109/10.764949 PMID:10356879
- Clancy, E. A., Lukai, L., Liu, P., & Moyer, D. V. Z. (2012). Identification of constant-posture EMG–torque relationship about the elbow using nonlinear dynamic models. *IEEE Transactions on Bio-Medical Engineering*, *59*(1), 205–212. doi:10.1109/TBME.2011.2170423 PMID:21968709
- Clark, B. D., Dacko, S. M., & Cope, T. C. (1993). Cutaneous stimulation fails to alter motor units recruitment in the decerebrate cat. *Journal of Neurophysiology*, *70*(4), 1433–1439. PMID:8283206
- Clark, J. A., & Roemer, R. B. (1977). Voice controlled wheelchair. *Archives of Physical Medicine and Rehabilitation*, *58*(4), 169–175. PMID:849131
- Clark, J., & Plonsey, R. (1966). A mathematical evaluation of the core conductor model. *Biophysical Journal*, *6*(1), 95–112. doi:10.1016/S0006-3495(66)86642-0 PMID:5903155
- Clark, J., & Plonsey, R. (1968). The extracellular potential field of the single active nerve fibre in a volume conductor. *Biophysical Journal*, *8*(7), 842–864. doi:10.1016/S0006-3495(68)86524-5 PMID:5699809
- Cole, M. H., & Grimshaw, P. N. (2008a). Electromyography of the trunk and abdominal muscles in golfers with and without low back pain. *Journal of Science and Medicine in Sport*, *11*(2), 174–181. doi:10.1016/j.jsams.2007.02.006 PMID:17433775
- Cole, M. H., & Grimshaw, P. N. (2008b). Trunk muscle onset and cessation in golfers with and without low back pain. *Journal of Biomechanics*, *41*(13), 2829–2833. doi:10.1016/j.jbiomech.2008.07.004 PMID:18718596
- Collins, S. H., Adamczyk, P. G., & Kuo, A. D. (2009). Dynamic arm swinging in human walking. *Proceedings. Biological Sciences*, *276*, 3679–3688. doi:10.1098/rspb.2009.0664 PMID:19640879
- Corinna, C., & Vladimir, V. (1995). Support-vector networks. *Machine Learning*, *20*, 273–297. doi:10.1007/BF00994018
- Cotterill, R. M. J. (2002). *Biophysics: An introduction*. Hoboken, NJ: John Wiley & Sons Inc.
- Cram, J. R., & Kasman, G. S. (2001). The basics of surface electromyography. In E. Criswell (Ed.), *Cram's introduction to surface electromyography* (pp. 1–173). Sudbury, MA: Jones and Bartlett Publishers.
- Crenna, P., Carpinella, I., Lopiano, L., Marzegan, A., Rabuffetti, M., & Rizzone, M. et al. (2008). Influence of basal ganglia on upper limb locomotor synergies. Evidence from deep brain stimulation and L-DOPA treatment in Parkinson's disease. *Brain*, *131*(12), 3410–3420. doi:10.1093/brain/awn272 PMID:18952669
- Daube, J. R. (2006). Motor unit number estimates—From A to Z. *Journal of the Neurological Sciences*, *242*(1), 23–35. doi:10.1016/j.jns.2005.11.011 PMID:16423366
- Daube, J. R., & Rubin, D. I. (2009). *Needle electromyography (Contemporary neurology)* (pp. 475–492). Oxford, UK: Oxford University Press.
- De Kroon, J. R., & IJzerman, M. J. (2008). Electrical stimulation of the upper extremity in stroke: Cyclic versus EMG-triggered stimulation. *Clinical Rehabilitation*, *22*, 690–697. doi:10.1177/0269215508088984 PMID:18678569

- De Kroon, J. R., Ijzerman, M. J., Chae, J., Lankhorst, G. J., & Zilvold, G. (2005). Relation between stimulation characteristics and clinical outcome in studies using electrical stimulation to improve motor control of the upper extremity in stroke. *Journal of Rehabilitation Medicine*, *37*, 65–74. doi:10.1080/16501970410024190 PMID:15788340
- De Leva, P. (1996). Adjustments to Zatsiorsky-Seluyanov's segment inertia parameters. *Journal of Biomechanics*, *29*(9), 1223–1230. doi:10.1016/0021-9290(95)00178-6 PMID:8872282
- De Luca, C. J. (2002). *Surface electromyography: Detection and recording*. Retrieved from http://www.delsys.com/Attachments_pdf/WP_SEMGintro.pdf
- De Luca, C. J. (1984). Myoelectrical manifestations of localized muscular fatigue in humans. *Critical Reviews in Biomedical Engineering*, *11*(4), 251–279. PMID:6391814
- De Luca, C. J. (1997). The use of surface electromyography in biomechanics. *Journal Applied Biomechanics*, *13*, 135–163. Escamilla, R., & Andrews, J. (2009). Shoulder muscle recruitment patterns and related biomechanics during upper extremity sports. *Sports Medicine (Auckland, N.Z.)*, *39*(7), 569–590.
- De Luca, C. J., Adam, A., Wotiz, R., Gilmore, L. D., & Nawab, S. H. (2006). Decomposition of surface EMG signals. *Journal of Neurophysiology*, *96*(3), 1646–1657. doi:10.1152/jn.00009.2006 PMID:16899649
- De Luca, C. J., & Contessa, P. (2012). Hierarchical control of motor units in voluntary contractions. *Journal of Neurophysiology*, *107*(1), 178–195. doi:10.1152/jn.00961.2010 PMID:21975447
- De Luca, C. J., & Erim, Z. (1994). Common drive of motor units in the regulation of muscle force. *Trends in Neurosciences*, *17*(7), 299–305. doi:10.1016/0166-2236(94)90064-7 PMID:7524216
- De Luca, C. J., Gilmore, L. D., Kuznetsov, M., & Roy, S. H. (2010). Filtering the surface EMG signal: Movement artifact and baseline noise contamination. *Journal of Biomechanics*, *43*(8), 1573–1579. doi:10.1016/j.jbiomech.2010.01.027 PMID:20206934
- De Luca, C. J., Kuznetsov, M., Gilmore, L. D., & Roy, S. H. (2012). Inter-electrode spacing of surface EMG sensors: Reduction of crosstalk contamination during voluntary contractions. *Journal of Biomechanics*, *45*(3), 555–561. doi:10.1016/j.jbiomech.2011.11.010 PMID:22169134
- De Luca, G. (2003). *Fundamental concepts in EMG signal acquisition*. Boston: DelSys Inc.
- De Séze, M., Falgairolle, M., Viel, S., Assaiante, C., & Cazalets, J. R. (2008). Sequential activation of axial muscles during different forms of rhythmic behavior in man. *Experimental Brain Research*, *185*(2), 237–247. doi:10.1007/s00221-007-1146-2 PMID:17940760
- de Vlugt, E., Schouten, A. C., & van der Helm, F. C. (2003). Closed-loop multivariable system identification for the characterization of the dynamic arm compliance using continuous force disturbances: a model study. *Journal of Neuroscience Methods*, *122*(2), 123–140. doi:10.1016/S0165-0270(02)00303-5 PMID:12573472
- Dean, C. M., & Shepherd, R. B. (1997). Task-related training improves performance of seated reaching tasks after stroke. *Stroke*, *28*, 722–728. doi:10.1161/01.STR.28.4.722 PMID:9099186
- Debicki, D. B., & Gribble, P. L. (2004). Inter-joint coupling strategy during adaptation to novel viscous loads in human arm movement. *Journal of Neurophysiology*, *92*(1), 754–765. doi:10.1152/jn.00119.2004 PMID:15056688
- Dempster, W. T. (1955). *Space requirements of the seated operator: Geometrical, kinematics, and mechanical aspects of the body with special reference to the limbs* (Wright Air Development Center Tech. Rep. No. 55-159). Dayton, OH: Wright-Patterson Air Force Base, WADC. (National Technical Information Service No. AD-087892).
- Denny-Brown, D. (1949). Interpretation of the electromyogram. *Archives of Neurology and Psychiatry*, *61*(2), 99–128. doi:10.1001/archneurpsyc.1949.02310080003001 PMID:18152778
- Desmedt, J. E. (1981). The size principle of motoneuron recruitment in ballistic or ramp voluntary contractions in man. In J. E. Desmedt (Ed.), *Motor unit types, recruitment and plasticity in health and disease* (Progress in clinical neurophysiology, Vol. 9) (pp. 97-136). Basel, Switzerland: Karger.

Compilation of References

- Desmedt, J. E., & Godaux, E. (1978). Mechanism of the vibration paradox: Excitatory and inhibitory effects of tendon vibration on single soleus motor units in man. *Journal of Physiology*, (London), 285, 197-207.
- Desmedt, J. E., & Godaux, E. (1977). Fast motor units are not preferentially activated in rapid voluntary contractions in man. *Nature*, 267(5613), 717-719. doi:10.1038/267717a0 PMID:876393
- Dietz, V. (2002). Do human bipeds use quadrupedal coordination? *Trends in Neurosciences*, 25(9), 462-467. doi:10.1016/S0166-2236(02)02229-4 PMID:12183207
- Dietz, V., & Michel, J. (2009). Human bipeds use quadrupedal coordination during locomotion. *Annals of the New York Academy of Sciences*, 1164, 97-103. doi:10.1111/j.1749-6632.2008.03710.x PMID:19645886
- Dimitrova, N. A., & Dimitrov, G. V. (2002). Amplitude-related characteristics of motor unit and M-wave potentials during fatigue. A simulation study using literature data on intracellular potential changes found in vitro. *Journal of Electromyography and Kinesiology*, 12, 339-349. doi:10.1016/S1050-6411(02)00046-9 PMID:12223166
- Dimitrova, N. A., & Dimitrov, G. V. (2006). Electromyography (EMG) modeling. In A. Metin (Ed.), *Wiley encyclopedia of biomedical engineering*. Hoboken, NJ: John Wiley & Sons. doi:10.1002/9780471740360.ebs0656
- Dimitrov, G. V., & Dimitrova, N. A. (1998). Precise and fast calculation of the motor unit potentials detected by a point and rectangular plate electrode. *Medical Engineering & Physics*, 20, 374-381. doi:10.1016/S1350-4533(09)00014-9 PMID:9773690
- Diószeghy, P. (2002). Scanning electromyography. *Muscle & Nerve*, 25(S11), S66-S71. doi:10.1002/mus.10150 PMID:12116288
- Diószeghy, P., Egerhazi, A., Molnar, M., & Mechler, F. (1996). Turn-amplitude analysis in neuromuscular diseases. *Electromyography and Clinical Neurophysiology*, 36(8), 463-468. PMID:8985673
- Dolan, J. M., Friedman, M. B., & Nagurka, M. L. (1993). Dynamic and loaded impedance components in the maintenance of human arm posture. *IEEE Transactions on Systems, Man, and Cybernetics*, 23(3), 698-709. doi:10.1109/21.256543
- Dolan, P., Mannion, A. F., & Adams, M. A. (1995). Fatigue of the erector spinae muscles. A quantitative assessment using frequency banding of the surface electromyography signal. *Spine*, 20(2), 149-159. doi:10.1097/00007632-199501150-00005 PMID:7716619
- Donker, S. F., Mulder, T., Nienhuis, B., & Duysens, J. (2002). Adaptation in arm movements for added mass to wrist or ankle during walking. *Experimental Brain Research*, 145, 26-31. doi:10.1007/s00221-002-1145-2
- Du, S., & Vuskovic, M. (2004). Temporal Vs spectral approach to feature extraction from prehensile EMG signals. In *Proceedings of IEEE International Conference on Information Reuse and Integration* (pp. 344-350).
- Duchowski, A. T. (2002). A breadth-first survey of eye-tracking applications. *Behavior Research Methods, Instruments, & Computers*, 34(4), 455-470. doi:10.3758/BF03195475 PMID:12564550
- Dumitru, D. (1994). The biphasic morphology of voluntary and spontaneous SFAPs. *Muscle & Nerve*, 17, 1301-1307. doi:10.1002/mus.880171109 PMID:7935552
- Dumitru, D., King, J. C., & Rogers, W. E. (1999). Motor unit action potential components and physiologic duration. *Muscle & Nerve*, 22(6), 733-741. doi:10.1002/(SICI)1097-4598(199906)22:6<733::AID-MUS10>3.0.CO;2-6 PMID:10366227
- Dumitru, D., King, J. C., & Rogers, W. E. (2000). Physiologic basis of potentials recorded in electromyography. *Muscle & Nerve*, 23(11), 1667-1685. doi:10.1002/1097-4598(200011)23:11<1667::AID-MUS2>3.0.CO;2-H PMID:11054745
- Du, Y. C., Lin, C. H., Shyu, L. Y., & Chen, T. (2010). Portable hand motion classifier for multi-channel surface electromyography recognition using gray relational analysis. *Expert Systems with Applications*, 37(6), 4283-4291. doi:10.1016/j.eswa.2009.11.072
- Du, Y. C., Shyu, L. Y., & Hu, W. (2006). The effect of combining stationary wavelet transform and independent component analysis in the multichannel SEMGs hand motion identification system. *Journal of Medical and Biological Engineering*, 26(1), 9-14.

- Ebenbichler, G., Kollmitzer, J., Quittan, M., Uhl, F., Kirtley, C., & Fialka, V. (1998). EMG fatigue patterns accompanying isometric fatiguing knee-extensions are different in mono- and bi-articular muscles. *Electroencephalography and Clinical Neurophysiology*, *109*(3), 256–262. doi:10.1016/S0924-980X(98)00015-0 PMID:9741792
- Eke-Okoro, S. T., Gregoric, M., & Larsson, L. E. (1997). Alterations in gait resulting from deliberate changes of arm-swing amplitude and phase. *Clinical Biomechanics (Bristol, Avon)*, *12*(7-8), 516–521. doi:10.1016/S0268-0033(97)00050-8 PMID:11415762
- Ekstedt, J. (1964). Human single fibre action potentials. *Acta Physiologica Scandinavica*, *61*(226), 1–96. PMID:14168041
- Ekstedt, J., Nilsson, G., & Stålberg, E. (1974). Calculation of the electromyographic jitter. *Journal of Neurology, Neurosurgery, and Psychiatry*, *37*(5), 526–539. doi:10.1136/jnnp.37.5.526 PMID:4836748
- Elftman, H. (1939). The function of the arms in walking. *Human Biology*, *11*(4), 529–535.
- Ellaway, P. H. (1978). Cumulative sum technique and its application to the analysis of peristimulus time histograms. *Electroencephalography and Clinical Neurophysiology*, *45*, 302–304. doi:10.1016/0013-4694(78)90017-2 PMID:78843
- Engin, M., Dalbasti, T., Gulduren, M., Davasli, E., & Engin, Z. (2007). A prototype portable system for EEG measurements. *Measurement: Journal of the International Measurement Confederation*, *40*(9-10), 936–942. doi:10.1016/j.measurement.2006.10.018
- Englehart, K., & Hudgins, B. (2003). A robust, real-time control scheme for multifunction myoelectric control. *IEEE Transactions on Bio-Medical Engineering*, *50*(7), 848–854. doi:10.1109/TBME.2003.813539 PMID:12848352
- Englehart, K., Hudgins, B., & Parker, P. A. (2001). A wavelet-based continuous classification scheme for multifunction myoelectric control. *IEEE Transactions on Bio-Medical Engineering*, *48*(3), 302–311. doi:10.1109/10.914793 PMID:11327498
- Enoka, R. M., & Stuart, D. G. (1992). Neurobiology of muscle fatigue. *Journal of Applied Physiology (Bethesda, Md.)*, *72*(5), 1631–1648. PMID:1601767
- Ertas, M., Baslo, M. B., Yıldız, N., Yazıcı, J., & Öge, E. (2000). Concentric needle electrode for neuromuscular jitter analysis. *Muscle & Nerve*, *23*(5), 715–719. doi:10.1002/(SICI)1097-4598(200005)23:5<715::AID-MUS8>3.0.CO;2-V PMID:10797394
- Esteller, R., Vachtsevanos, G., Echauz, J., & Litt, B. (2001). A comparison of waveform fractal dimension algorithms. *IEEE Transactions on Circuits and Systems. I, Fundamental Theory and Applications*, *48*(2), 177–1831. doi:10.1109/81.904882
- Falgairolle, M., de Sèze, M., Juvin, L., Morin, D., & Cazalets, J. R. (2006). Coordinated network functioning in the spinal cord: an evolutionary perspective. *Journal of Physiology, Paris*, *100*(5-6), 304–316. doi:10.1016/j.jphysparis.2007.05.003 PMID:17658245
- Farber, A., Smith, J., Kvitne, R., Mohr, K., & Shin, S. (2009). Electromyographic analysis of forearm muscles in professional and amateur golfers. *The American Journal of Sports Medicine*, *37*(2), 396–401. doi:10.1177/0363546508325154 PMID:19022991
- Farina, D., Blanchietti, A., Pozzo, M., & Merletti, R. (2004). M-wave properties during progressive motor unit activation by transcutaneous stimulation. *Journal of Applied Physiology*, *97*, 545–555. doi:10.1152/jappphysiol.00064.2004 PMID:15121744
- Farina, D., & Merletti, R. (2000). Comparison of algorithms for estimation of EMG variables during voluntary isometric contractions. *Journal of Electromyography and Kinesiology*, *10*(5), 337–349. doi:10.1016/S1050-6411(00)00025-0 PMID:11018443
- Farina, D., Merletti, R., & Enoka, R. M. (2004). The extraction of neural strategies from the surface EMG. *Journal of Applied Physiology*, *96*(1), 1486–1495. doi:10.1152/jappphysiol.01070.2003 PMID:15016793
- Farrugia, M. A., & Kenet, R. P. (2005). Turns amplitude analysis of the orbicularis oculi and oris muscles. *Clinical Neurophysiology*, *116*(11), 2550–2559. doi:10.1016/j.clinph.2005.07.018 PMID:16221560

Compilation of References

- Fasoli, S. E., Krebs, H. I., Stein, J., Frontera, W. R., & Hogan, N. (2003). Effects of robotic therapy on motor impairment and recovery in chronic stroke. *Archives of Physical Medicine and Rehabilitation*, 84, 477–482. doi:10.1053/apmr.2003.50110 PMID:12690583
- Faulkner, J. A. (2003). Terminology for contractions of muscles during shortening, while isometric, and during lengthening. *Journal of Applied Physiology*, 95(2), 455–459. PMID:12851415
- Ferrante, S., Ambrosini, E., Ravelli, P., Guanziroli, E., Molteni, F., Ferrigno, G., & Pedrocchi, A. (2011). A biofeedback cycling training to improve locomotion: A case series study based on gait pattern classification of 153 chronic stroke patients. *Journal of Neuroengineering and Rehabilitation*, 8, 47. doi:10.1186/1743-0003-8-47 PMID:21861930
- Ferrante, S., Pedrocchi, A., Ferrigno, G., & Molteni, F. (2008). Cycling induced by functional electrical stimulation improves the muscular strength and the motor control of individuals with post-acute stroke. *European Journal of Physical and Rehabilitation Medicine*, 44, 159–167. PMID:18418336
- Ferris, D. P., Huang, H. J., & Kao, P. C. (2006). Moving the arms to activate the legs. *Exercise and Sport Sciences Reviews*, 34(3), 113–120. doi:10.1249/00003677-200607000-00005 PMID:16829738
- Finsterer, J. (2001). EMG-interference pattern analysis. *Journal of Electromyography and Kinesiology*, 11(4), 231–246. doi:10.1016/S1050-6411(01)00006-2 PMID:11532594
- Fleisher, S. M. (1984). Comparative analysis of modeled extracellular potentials. *Medical & Biological Engineering & Computing*, 22, 440–447. doi:10.1007/BF02447704 PMID:6482532
- Ford, M. P., Wagenaar, R. C., & Newell, K. M. (2007). Arm constraint and walking in healthy adults. *Gait & Posture*, 26(1), 135–141. doi:10.1016/j.gaitpost.2006.08.008 PMID:16997561
- Fortune, E., & Lowery, M. M. (2009). Effect of extracellular potassium accumulation on muscle fiber conduction velocity: A simulation study. *Annals of Biomedical Engineering*, 37(10), 2105–2117. doi:10.1007/s10439-009-9756-4 PMID:19588250
- Fougner, A.L. (2007). *Proportional myoelectric control of a multifunction upper-limb prosthesis* (Master thesis). Norwegian University of Science and Technology, Norway.
- Fougner, A., Scheme, E., Chan, A. D. C., Englehart, K., & Stavaahl, Ø. (2011). Resolving the limb position effect in myoelectric pattern recognition. *IEEE Transactions on Neural Systems and Rehabilitation Engineering*, 19(6), 644–651. doi:10.1109/TNSRE.2011.2163529 PMID:21846608
- Francis, S., Lin, X., Aboushoushah, S., White, T. P., Phillips, M., Bowtell, R., & Constantinescu, C. S. (2009). fMRI analysis of active, passive and electrically stimulated ankle dorsiflexion. *NeuroImage*, 44, 469–479. doi:10.1016/j.neuroimage.2008.09.017 PMID:18950717
- Franklin, D. W., Leung, F., Kawato, M., & Milner, T. E. (2003). Estimation of multijoint limb stiffness from EMG during reaching movements. In *Proceedings of IEEE EMBS Asian-Pacific Conference on Biomedical Engineering* (pp. 224-225).
- Frigo, C., & Crenna, P. (2009). Multichannel SEMG in clinical gait analysis: A review and state-of-the-art. *Clinical Biomechanics (Bristol, Avon)*, 24(3), 236–245. doi:10.1016/j.clinbiomech.2008.07.012 PMID:18995937
- Frigo, C., Ferrarin, M., Frasson, W., Pavan, E., & Thorsen, R. (2000). EMG signals detection and processing for on-line control of functional electrical stimulation. *Journal of Electromyography and Kinesiology*, 10, 351–360. doi:10.1016/S1050-6411(00)00026-2 PMID:11018444
- Fuglevand, A. J., Winter, D. A., & Patla, A. E. (1993). . *Journal of Neurophysiology*, 70(6), 2470–2488. PMID:8120594
- Fuglsang-Frederiksen, A. (2006). The role of different EMG methods in evaluating myopathy. *Clinical Neurophysiology*, 117(6), 1173–1189. doi:10.1016/j.clinph.2005.12.018 PMID:16516549
- Fujiwara, T., Kasashima, Y., Honaga, K., Muraoka, Y., Tsuji, T., & Osu, R. et al. (2009). Motor improvement and corticospinal modulation induced by hybrid assistive neuromuscular dynamic stimulation (HANDS) therapy in patients with chronic stroke. *Neurorehabilitation and Neural Repair*, 23, 125–132. doi:10.1177/1545968308321777 PMID:19060131

- Fukunaga, T., Kawakami, Y., Kuno, S., Funato, K., & Fukashiro, S. (1997). Muscle architecture and function in humans. *Journal of Biomechanics*, *30*, 457–463. doi:10.1016/S0021-9290(96)00171-6 PMID:9109557
- Gage, W. H., Winter, D. A., Frank, J. S., & Adkin, A. L. (2004). Kinematic and kinetic validity of the inverted pendulum model in quiet standing. *Gait & Posture*, *19*(2), 124–132. doi:10.1016/S0966-6362(03)00037-7 PMID:15013500
- Gandolla, M., Pedrocchi, A., Ferrante, S., Guanziroli, E., Martegani, A., Ferrigno, G., & Ward, N. S. (2012). *Hypothesis for functional electrical stimulation mechanism of action: An fMRI study of cortical activations during ankle dorsiflexion in healthy subjects*. Paper presented at the 3rd Annual International Functional Electrical Stimulation Society UK and Ireland Chapter, Birmingham, UK.
- Ganong, W. F. (2001). *Review of medical physiology*. New York: McGraw-Hill.
- Gao, F., Grant, T. H., Roth, E. J., & Zhang, L. Q. (2009). Changes in passive mechanical properties of the gastrocnemius muscle at the muscle fascicle and joint levels in stroke survivors. *Archives of Physical Medicine and Rehabilitation*, *90*, 819–826. doi:10.1016/j.apmr.2008.11.004 PMID:19406302
- Gardner-Morse, M. G., Stokes, I. A. F., & Huston, D. R. (2006). On the implications of interpreting the stability index: a spine example. *Journal of Biomechanics*, *39*(2), 391–392, author reply 393–394. doi:10.1016/j.jbiomech.2005.08.020 PMID:16256126
- Gater, D. R. Jr, Dolbow, D., Tsui, B., & Gorgey, A. S. (2011). Functional electrical stimulation therapies after spinal cord injury. *NeuroRehabilitation*, *28*, 231–248. PMID:21558629
- Gath, I., & Stålberg, E. (1978). The calculated radial decline of the extracellular action potential compared with in situ measurements in the human brachial biceps. *Electroencephalography and Clinical Neurophysiology*, *44*(5), 547–552. doi:10.1016/0013-4694(78)90121-9 PMID:77760
- Geethanjali, P., Ray, K. K., & Shanmuganathan, P. V. (2009). Actuation of prosthetic drive using EMG signal. In *Proceedings of IEEE International Conference TENCON*, (pp. 1-6), Singapore.
- Giat, Y., Mizrahi, J., Levine, W. A., & Chen, J. (1994). Simulation of distal tendon transfer of the biceps brachii and the brachialis muscles. *Journal of Biomechanics*, *27*, 1005–1014. doi:10.1016/0021-9290(94)90217-8 PMID:8089155
- Gillette, J. C., Stevermer, C. A., Miller, R. H., Meardon, S. A., & Schwab, C. V. (2010). The effects of age and type of carrying task on lower extremity kinematics. *Ergonomics*, *53*(3), 355–364. doi:10.1080/00140130903402234 PMID:20191410
- Gitter, J. A., & Czerniecki, M. J. (1995). Fractal analysis of the electromyographic interference pattern. *Journal of Neuroscience Methods*, *58*(1-2), 103–108. doi:10.1016/0165-0270(94)00164-C PMID:7475215
- Glazebrook, M., Curwin, S., Islam, M., Kozey, J., & Stanish, W. (1994). Medial epicondylitis. An electromyographic analysis and an investigation of intervention strategies. *The American Journal of Sports Medicine*, *22*(5), 674–679. doi:10.1177/036354659402200516 PMID:7810792
- Glinsky, J., Harvey, L., & Van Es, P. (2007). Efficacy of electrical stimulation to increase muscle strength in people with neurological conditions: A systematic review. *Physiotherapy Research International: The Journal for Researchers and Clinicians in Physical Therapy*, *12*, 175–194. doi:10.1002/pri.375 PMID:17624871
- Goker, I., Baslo, B., Ertas, M., & Ulgen, Y. (2009). Design of an experimental system for scanning electromyography method to investigate alterations of motor units in neurological disorders. *Digest Journal of Nanomaterials and Biostructures*, *4*(1), 133–139.
- Goker, I., Baslo, B., Ertas, M., & Ulgen, Y. (2010). Large motor unit territories by scanning electromyography in patients with juvenile myoclonic epilepsy. *Journal of Clinical Neurophysiology*, *27*(3), 212–215. doi:10.1097/WNP.0b013e3181e0b228 PMID:20461011
- Goker, I., Osman, O., Ozekes, S., Baslo, M. B., Ertas, M., & Ulgen, Y. (2012). Classification of juvenile myoclonic epilepsy data acquired through scanning electromyography with machine learning algorithms. *Journal of Medical Systems*, *36*(5), 2705–2711. doi:10.1007/s10916-011-9746-6 PMID:21681512

Compilation of References

- Gollhofer, A., & Komi, P. (1987). Measurement of man-shoe-surface interaction during locomotion. *Medicine and Sport Science*, 26.
- Gomi, H., & Osu, R. (1998). Task-dependent viscoelasticity of human multijoint arm and its spatial characteristics for interaction with environments. *The Journal of Neuroscience*, 18(21), 8965–8978. PMID:9787002
- Gonzalez, R. V., Buchanan, T. S., & Delp, S. L. (1997). How muscle architecture and moment arms affect wrist flexion-extension moment. *Journal of Biomechanics*, 30, 705–712. doi:10.1016/S0021-9290(97)00015-8 PMID:9239550
- Gonzalez, R. V., Hutchins, E. L., Barr, R. E., & Abraham, L. D. (1996). Development and evaluation of a musculoskeletal model of the elbow joint complex. *Journal of Biomechanical Engineering: ASME*, 118, 32–40. doi:10.1115/1.2795943 PMID:8833072
- Gootzen, T. H. J. M., Vingerhoest, D. J. M., & Stegeman, D. F. (1992). A study of motor unit structure by means of scanning EMG. *Muscle & Nerve*, 15(3), 349–357. doi:10.1002/mus.880150314 PMID:1557083
- Gordon, A. M., Huxley, A. F., & Julian, F. J. (1996). The variation in isometric tension with sarcomere length in vertebrate muscle fibres. *The Journal of Physiology*, 184, 170–192.
- Gordon, T., Thomas, C. K., Munson, J. B., & Stein, R. B. (2004). The resilience of the size principle in the organization of motor unit properties in normal and reinnervated adult skeletal muscle. *Canadian Journal of Physiology and Pharmacology*, 82(8-9), 645–661. doi:10.1139/y04-081 PMID:15523522
- Gossman, M. R., Sahrman, S. A., & Rose, S. J. (1982). Review of length-associated changes in muscle: experimental evidence and clinical implications. *Physical Therapy*, 62, 1799–1808. PMID:6755499
- Grasso, R., Bianchi, L., & Lacquaniti, F. (1998). Motor patterns for human gait: backward versus forward locomotion. *Journal of Neurophysiology*, 80(4), 1868–1885. PMID:9772246
- Graupe, D., Salahi, J., & Kohn, K. H. (1982). Multifunctional prosthesis and orthosis control via microcomputer identification of temporal pattern differences in single-site myoelectric signal. *Journal of Biomedical Engineering*, 4(1), 17–22. doi:10.1016/0141-5425(82)90021-8 PMID:7078136
- Grenier, S. G., & McGill, S. M. (2007). Quantification of lumbar stability by using 2 different abdominal activation strategies. *Archives of Physical Medicine and Rehabilitation*, 88(1), 54–62. doi:10.1016/j.apmr.2006.10.014 PMID:17207676
- Grillner, S. (1981). Control of locomotion in bipeds, tetrapods, and fish. In V. Brooks (Ed.), *Handbook of physiology-the nervous system II* (pp. 1179–1236). Baltimore: Waverly Press.
- Grillner, S. (2011). Neuroscience. Human locomotor circuits conform. *Science*, 334(6058), 912–913. doi:10.1126/science.1214778 PMID:22096178
- Grimbergen, C. A., Metting van Rijn, A. C., & Peper, A. (1991). Influence of isolation on interference in bioelectric recordings. *Annual International Conference of the IEEE Engineering in Medicine and Biology Society*, 13(4), 1720–1721.
- Grimby, L., & Hannerz, J. (1968). Recruitment order of motor units in voluntary contractions: Changes induced by proprioceptive afferent activity. *Journal of Neurology, Neurosurgery, and Psychiatry*, 31(6), 565–564. doi:10.1136/jnnp.31.6.565 PMID:5709842
- Grimby, L., Hannerz, J., & Hedman, B. (1981). The fatigue and voluntary discharge properties of single motor units in man. *The Journal of Physiology*, 316, 545–554. PMID:7320881
- Grimshaw, P., & Burden, A. (2000). Case report: Reduction of low back pain in professional golfer. *Medicine & Science in Sports & Medicine*, 32(10), 1667–1673.
- Gunning, J. L., Callaghan, J. P., & McGill, S. M. (2001). Spinal posture and prior loading history modulate compressive strength and type of failure in the spine: a biomechanical study using a porcine cervical spine model. *Clinical Biomechanics (Bristol, Avon)*, 16(6), 471–480. doi:10.1016/S0268-0033(01)00032-8 PMID:11427289

- Gupta, V., Suryanarayanan, S., & Reddy, N. P. (1997). Fractal analysis of surface EMG signals from the biceps. *International Journal of Medical Informatics*, 45(3), 185–192. doi:10.1016/S1386-5056(97)00029-4 PMID:9291030
- Gustaffson, B., & Pinter, M. J. (1985). On factors determining orderly recruitment of motor units: a role for intrinsic membrane properties. *Trends in Neurosciences*, 8, 431–433. doi:10.1016/0166-2236(85)90152-3
- Guyton, A. C., & Hall, J. E. (2000). *Textbook of medical physiology*. West Philadelphia, PA: W. B. Saunders Company.
- Gydikov, A. (1991). Biophysics of the skeletal muscle extracellular potentials. *Bulgarian Academy of Sciences*, 132, 60–100.
- Hagberg, M. (1981). Muscular endurance and surface electromyogram in isometric and dynamic exercise. *Journal of Applied Physiology: Respiratory, Environmental and Exercise Physiology*, 51(1), 1–7. PMID:7263402
- Hagberg, M., & Kvarnstrom, S. (1984). Muscular endurance and electromyographic fatigue in myofascial shoulder pain. *Archives of Physical Medicine and Rehabilitation*, 65(9), 522–525. PMID:6477084
- Hakelius, L., & Stålberg, E. (1974). Electromyographical studies of free autogenous muscle transplants in man. *Scandinavian Journal of Plastic and Reconstructive Surgery*, 8, 211–219. doi:10.3109/02844317409084397 PMID:4458046
- Halar, E. M., Stolov, W. C., Venkatesh, B., Brozovich, F. V., & Harley, J. D. (1978). Gastrocnemius muscle belly and tendon length in stroke patients and able-bodied persons. *Archives of Physical Medicine and Rehabilitation*, 59, 476–484. PMID:718411
- Hamner, S. R., & Delp, S. L. (2013). Muscle contributions to fore-aft and vertical body mass center accelerations over a range of running speeds. *Journal of Biomechanics*, 46(4), 780–787. doi:10.1016/j.jbiomech.2012.11.024 PMID:23246045
- Hamner, S. R., Seth, A., & Delp, S. L. (2010). Muscle contributions to propulsion and support during running. *Journal of Biomechanics*, 43(14), 2709–2716. doi:10.1016/j.jbiomech.2010.06.025 PMID:20691972
- Hanson, J. (1974). Effects of repetitive stimulation on membrane potentials and twitch in human and rat intercostal muscle fibres. *Acta Physiologica Scandinavica*, 92, 238–248. doi:10.1111/j.1748-1716.1974.tb05741.x PMID:4138188
- Hanson, J., & Persson, A. (1971). Changes in the action potential and contraction of isolated frog muscle after repetitive stimulation. *Acta Physiologica Scandinavica*, 81, 340–348. doi:10.1111/j.1748-1716.1971.tb04908.x PMID:5550516
- Hargrove, L., Losier, Y., Englehart, K., & Hudgins, B. (2007). A real-time pattern recognition based myoelectric control usability study implemented in a virtual environment. In *Proceedings of 29th Annual International Conference of the IEEE Engineering Medicine Biological Society* (pp.4842-4845).
- Harper, M. C. (2009). Single fiber electromyography. In J. R. Daube, & D. I. Rubin (Eds.), *Clinical neurophysiology* (pp. 475–491). New York: Oxford University Press.
- Harwin, W. S., & Jackson, R. D. (1990). Analysis of intentional head gestures to assist computer access by physically disabled people. *Journal of Biomedical Engineering*, 12(3), 193–198. doi:10.1016/0141-5425(90)90040-T PMID:2140869
- Haykin, S., & Liu, R. (2009). *Handbook on array processing and sensor networks*. Hoboken, NJ: John Wiley and Sons, Inc.
- Heckman, C. J., & Binder, M. D. (1988). Analysis of effective synaptic currents generated by homonymous Ia afferent fibers in motoneurons of the cat. *Journal of Neurophysiology*, 60(6), 1946–1966. PMID:3236057
- Henneberg, K. A. (2000). Principles of electromyography. In J. D. Bronzino (Ed.), *The biomedical engineering handbook* (pp. 14.1–14.3). Boca Raton, FL: Taylor and Francis Group.
- Henneman, E. (1985). The size principle: A deterministic output emerges from a set of probabilistic connections. *The Journal of Experimental Biology*, 115, 105–112. PMID:3161974

Compilation of References

- Henneman, E., Clamann, H. P., Gillies, J. D., & Skinner, R. D. (1974). Rank order of motoneurons within a pool: Law of combination. *Journal of Neurophysiology*, *37*(6), 1338–1349. PMID:4436704
- Henneman, E., & Mendell, L. M. (1981). Functional organization of motoneuron pool and its inputs. In V. B. Brooks (Ed.), *Handbook of physiology* (Vol. I, pp. 423–507). Bethesda, MD: American Physiological Society.
- Henneman, E., Shahani, B. T., & Young, R. R. (1976). Voluntary control of human motor units. In M. Shahani (Ed.), *The motor system: Neurophysiology and muscle mechanisms* (pp. 73–78). Amsterdam, The Netherlands: Elsevier.
- Henneman, E., Somjen, G., & Carpenter, D. (1965). Functional significance of cell size in spinal motoneurons. *Journal of Neurophysiology*, *28*, 599–620. PMID:5835487
- Herbert, R. D., & Gandevia, S. C. (1995). Changes in pennation with joint angle and muscle torque: in vivo measurements in human brachialis muscles. *The Journal of Physiology*, *484*, 523–532. PMID:7602542
- Hermens, H. J., Freriks, B., Disselhorst-Klug, C., & Rau, G. (2000). Development of recommendations for SEMG sensors and sensor placement procedures. *Journal of Electromyography and Kinesiology*, *10*(5), 361–374. doi:10.1016/S1050-6411(00)00027-4 PMID:11018445
- Hess, C. W., Mills, K. R., & Murray, N. M. (1987). Responses in small hand muscles from magnetic stimulation of the human brain. *Journal of Physiology*, (London), *388*, 397–419.
- Hicks, A., & McComas, A. J. (1989). Increased sodium pump activity following repetitive stimulation of rat soleus muscles. *The Journal of Physiology*, *414*, 337–349. PMID:2558169
- Higuchi, T. (1988). Approach to an irregular time series on the basis of the fractal theory. *Physica D. Nonlinear Phenomena*, *31*(2), 277–283. doi:10.1016/0167-2789(88)90081-4
- Hilton-Brown, P., & Stålberg, E. (1983a). Motor unit size in muscular dystrophy, a macro EMG and scanning EMG study. *Journal of Neurology, Neurosurgery, and Psychiatry*, *46*(11), 996–1005. doi:10.1136/jnnp.46.11.996 PMID:6655485
- Hilton-Brown, P., & Stålberg, E. (1983b). Motor unit size in muscular dystrophy, a single fiber EMG and scanning EMG study. *Journal of Neurology, Neurosurgery, and Psychiatry*, *46*(11), 981–996. doi:10.1136/jnnp.46.11.981 PMID:6655484
- Hinrichs, R. N. (1990). Whole body movement: Coordination of arms and legs in walking and running. In J. M. Winters, & S. L. Y. Woo (Eds.), *Multiple muscle systems: Biomechanics and movement organization* (pp. 694–705). New York: Springer. doi:10.1007/978-1-4613-9030-5_45
- Hirashima, M., Kadota, H., Sakurai, S., Kudo, K., & Ohtsuki, T. J. (2002). Sequential muscle activity and its functional role in the upper extremity and trunk during overarm throwing. *Sports Science*, *20*(4), 301–310. doi:10.1080/026404102753576071 PMID:12003275
- Hodges, P. W. (2001). Changes in motor planning of feedforward postural responses of the trunk muscles in low back pain. *Experimental Brain Research*, *141*(2), 261–266. doi:10.1007/s002210100873 PMID:11713638
- Hodges, P. W., & Bui, B. H. (1996). A comparison of computer-based methods for the determination of onset of muscle contraction using electromyography. *Electroencephalography and Clinical Neurophysiology*, *101*(6), 511–519. doi:10.1016/S0013-4694(96)95190-5 PMID:9020824
- Hodges, P. W., Pengel, L. H. M., Herbert, R. D., & Gandevia, S. C. (2003). Measurement of muscle contraction with ultrasound imaging. *Muscle & Nerve*, *27*, 682–692. doi:10.1002/mus.10375 PMID:12766979
- Hof, A. L., Elzinga, H., Grimmius, W., & Halbertsma, J. P. (2002). Speed dependence of averaged EMG profiles in walking. *Gait & Posture*, *16*(1), 78–86. doi:10.1016/S0966-6362(01)00206-5 PMID:12127190
- Hof, A. L., Pronk, C. N. A., & van Best, J. A. (1987). Comparison between EMG to force processing and kinetic analysis for the calf muscle moment in walking and stepping. *Journal of Biomechanics*, *20*(2), 167–178. doi:10.1016/0021-9290(87)90308-3 PMID:3571297
- Hoffer, J. A., & Andreassen, S. (1981). Regulation of soleus muscle stiffness in premammillary cats: intrinsic and reflex components. *Journal of Neurophysiology*, *45*(2), 267–285. PMID:6780665

- Hoffer, J. A., Loeb, G. E., Sugano, N., Marks, W. B., O'Donovan, M. J., & Pratt, C. A. (1987). Cat hindlimb motoneurons during locomotion. III. Functional segregation in Sartorius. *Journal of Neurophysiology*, *57*(2), 554–562. PMID:3559692
- Hogan, N. (1984). Adaptive control of mechanical impedance by coactivation of antagonist muscles. *IEEE Transactions on Automatic Control*, *29*(8), 681–690. doi:10.1109/TAC.1984.1103644
- Hogan, N. (1985). Impedance control: An approach to manipulation, parts i, ii, iii. *Transactions of the ASME. Journal of Dynamic Systems, Measurement, and Control*, *107*(1), 1–24. doi:10.1115/1.3140702
- Hogan, N., & Mann, R. W. (1980). Myoelectric signal processing: Optimal estimation applied to electromyography—Part I: Deviation of the optimal myoprocessor. *IEEE Transactions on Bio-Medical Engineering, BME-27*(7), 382–395. doi:10.1109/TBME.1980.326652
- Hogue, R. E. (1969). Upper-extremity muscular activity at different cadences and inclines during normal gait. *Physical Therapy*, *49*(9), 963–972. PMID:5802700
- Holzbour, K. R. S., Murray, W. R., & Delp, S. L. (2005). A model of the upper extremity for simulating musculoskeletal surgery and analyzing neuromuscular control. *Annals of Biomedical Engineering*, *33*, 829–840. doi:10.1007/s10439-005-3320-7 PMID:16078622
- Holzbour, K. R., Murray, W. M., Gold, G. E., & Delp, S. L. (2007). Upper limb muscle volumes in adult subjects. *Journal of Biomechanics*, *40*(4), 742–749. doi:10.1016/j.jbiomech.2006.11.011 PMID:17241636
- Horton, J. F., Lindsay, D. M., & Macintosh, B. R. (2001). Abdominal muscle activation of elite male golfers with chronic low back pain. *Medicine and Science in Sports and Exercise*, *33*(10), 1647–1654. doi:10.1097/00005768-200110000-00006 PMID:11581547
- Howarth, S. J., Allison, A. E., Grenier, S. G., Cholewicki, J., & McGill, S. M. (2004). On the implications of interpreting the stability index: A spine example. *Journal of Biomechanics*, *37*(8), 1147–1154. doi:10.1016/j.jbiomech.2003.12.038 PMID:15212919
- Howson, D. C., & Heule, J. E. (1980). Electronic circuit permitting simultaneous use of stimulating and monitoring equipment.
- Hsiao, H., & Simeonov, P. (2001). Preventing falls from roofs: A critical review. *Ergonomics*, *44*(5), 537–561. doi:10.1080/00140130110034480 PMID:11345496
- Huang, H. P., Liu, Y. H., Liu, L. W., & Wong, C. S. (2003). EMG classification for prehensile posture using cascaded architecture of neural networks with self-organizing maps. In *Proceedings of IEEE International Conference Robotics and Automation* (pp. 1497–1502).
- Huang, Y., Englehart, K. B., Hudgins, B., & Chan, A. D. (2005). A gaussian mixture model based classification scheme for myoelectric control of powered upper limb prostheses. *IEEE Transactions on Bio-Medical Engineering*, *52*(11), 1801–1811. doi:10.1109/TBME.2005.856295 PMID:16285383
- Hudgins, B., Parker, P. A., & Scott, R. N. (1993). A new strategy for multifunction myoelectric control. *IEEE Transactions on Bio-Medical Engineering*, *40*(1), 82–94. doi:10.1109/10.204774 PMID:8468080
- Hug, F. (2011). Can muscle coordination be precisely studied by surface electromyography? *Journal of Electromyography and Kinesiology*, *21*, 1–12. doi:10.1016/j.jelekin.2010.08.009 PMID:20869882
- Huijing, P. A., & Baan, G. S. (1992). Stimulation level dependent length-force and architecture characteristics of rat gastrocnemius muscle. *Journal of Electromyography and Kinesiology*, *2*, 112–120. doi:10.1016/1050-6411(92)90022-B PMID:20719604
- Huo, X., Wang, J., & Ghovanloo, M. (2008). Introduction and preliminary evaluation of the tongue drive system: Wireless tongue-operated assistive technology for people with little or no upper-limb function. *Journal of Rehabilitation Research and Development*, *45*(6), 921–930. doi:10.1682/JRRD.2007.06.0096 PMID:19009478
- Hu, X., Wang, Z., & Ren, X. (2005). Classification of surface EMG signal with fractal dimension. *Journal of Zhejiang University. Science. B.*, *6*(8), 844–848. doi:10.1631/jzus.2005.B0844 PMID:16052721

Compilation of References

- Huxley, A. F. (1957). Muscle structure and theories of contraction. *Progress in Biochemistry and Biophysics*, 7, 255–318. PMID:13485191
- Ichinose, Y., Wakumoto, M., Honda, K., Azuma, T., & Satou, J. (2003). Human interface using a wireless tongue-palate contact pressure sensor system and its application to the control of an electric wheelchair. *The Institute of Electronics, Information and Communication Engineers*, J86-D-II(2), 364-367 (in Japanese).
- ICMR. (2000). *Ethical guidelines for biomedical research on human subject* (pp. 1–77). New Delhi, India: Indian Council of Medical Research.
- Ide, Y., & Koide, K. (Eds.). (2004). *Fundamental of functional anatomy for chairside evaluation of stomatognathic functions*. Tokyo: Ishiyaku Publishers.
- Iftime-Nielsen, S. D., Christensen, M. S., Vingborg, R. J., Sinkjaer, T., Roepstorff, A., & Grey, M. J. (2012). Interaction of electrical stimulation and voluntary hand movement in SII and the cerebellum during simulated therapeutic functional electrical stimulation in healthy adults. *Human Brain Mapping*, 33, 40–49. doi:10.1002/hbm.21191 PMID:21591025
- Ikeda, D. M., & McGill, S. M. (2012). Can altering motions, postures, and loads provide immediate low back pain relief: A study of 4 cases investigating spine load, posture, and stability. *Spine*, 37(23), E1469–E1475. doi:10.1097/BRS.0b013e31826c97e5 PMID:22872216
- Inufusa, A., An, H. S., Lim, T. H., Hasegawa, T., Haughton, V. M., & Nowicki, B. H. (1996). Anatomic changes of the spinal canal and intervertebral foramen associated with flexion-extension movement. *Spine*, 21(21), 2412–2420. doi:10.1097/00007632-199611010-00002 PMID:8923625
- Ivanenko, Y. P., Cappellini, G., Poppele, R. E., & Lacquaniti, F. (2008). Spatiotemporal organization of alpha-motoneuron activity in the human spinal cord during different gaits and gait transitions. *The European Journal of Neuroscience*, 27(12), 3351–3368. doi:10.1111/j.1460-9568.2008.06289.x PMID:18598271
- Jackson, K. M. (1979). Fitting of mathematical functions to biomechanical data. *IEEE Transactions on Bio-Medical Engineering*, BME-26(2), 122–124. doi:10.1109/TBME.1979.326551 PMID:761932
- Jackson, K. M., Joseph, J., & Wyard, S. J. (1978). A mathematical model of arm swing during human locomotion. *Journal of Biomechanics*, 11(6-7), 277–289. doi:10.1016/0021-9290(78)90061-1 PMID:711777
- Jackson, K. M., Joseph, J., & Wyard, S. J. (1983a). The upper limbs during human walking. Part I: Sagittal movement. *Electromyography and Clinical Neurophysiology*, 23(6), 425–434. PMID:6641598
- Jackson, K. M., Joseph, J., & Wyard, S. J. (1983b). The upper limbs during human walking. Part 2: Function. *Electromyography and Clinical Neurophysiology*, 23(6), 435–446. PMID:6641599
- Jacobs, R., Hendrickx, E., Van Mele, I., Edwards, K., Verheust, M., & Spaepen, A. et al. (1997). Control of a trackball by the chin for communication applications, with and without neck movements. *Archives of Oral Biology*, 42(3), 213–218. doi:10.1016/S0003-9969(96)00117-3 PMID:9188991
- Jain, S., Singhal, G., Smith, R. J., Kaliki, R., & Thakor, N. (2012). Improving long term myoelectric decoding, using an adaptive classifier with label correction. In *Proceedings of the 4th IEEE RAS/EMBS International Conference on Biomedical Robotics and Biomechanics*, Rome (pp. 532-537).
- Jennings, D., Flint, A., Turton, B. C. H., & Nokes, L. D. M. (1995). *Introduction to medical electronics applications*. London: Hodder Headline PLC.
- Jiang, N., Falla, D., d'Avella, A., Graitmann, B., & Farina, D. (2010). Myoelectric control in neurorehabilitation. *Critical Reviews in Biomedical Engineering*, 38, 381–391. doi:10.1615/CritRevBiomedEng.v38.i4.30 PMID:21133839
- Jiang, N., Muceli, S., Graitmann, B., & Farina, D. (2013). Effect of arm position on the prediction of kinematics from EMG in amputees. *Medical & Biological Engineering & Computing*, 51(1-2), 143–151. doi:10.1007/s11517-012-0979-4 PMID:23090099
- Jindapetch, N., Chewae, S., & Phukpattaranont, P. (2012). FPGA implementations of an ADALINE adaptive filter for power-line noise cancellation in surface electromyography signals. *Measurement*, 45(3), 405–414. doi:10.1016/j.measurement.2011.11.004

- Jobe, F., Moynes, D., & Antonelli, D. (1986). Rota-tor cuff functions during a golf swing. *The American Journal of Sports Medicine*, 14(5), 388–392. doi:10.1177/036354658601400509 PMID:3777315
- Jobe, F., Perry, J., & Pink, M. (1989). EMG shoulder activity in men and women professional golfers. *The American Journal of Sports Medicine*, 17(6), 782–787. doi:10.1177/036354658901700611 PMID:2624291
- Johnson, M. A., Polgar, J., Weightman, D., & Appleton, D. (1973). Data on the distribution of fibre types in thirty-six human muscles. An autopsy study. *Journal of the Neurological Sciences*, 18, 111–129. doi:10.1016/0022-510X(73)90023-3 PMID:4120482
- Jöllnbeck, J. (2000). Methodological limitations of EMG-based bio-mechanical motion analysis. In *ISBS Conference Proceedings Archive, 18th International Symposium on Biomechanics in Sports*. Hong Kong, China.
- Jones, K. E., & Bawa, P. (1997). Computer simulations of responses of human motoneurons to composite Ia EPSPs: Effects of background firing rate. *Journal of Neurophysiology*, 77, 405–420. PMID:9120581
- Jones, K. E., & Bawa, P. (1999). A comparison of human motoneuron data to simulated data using cat motoneuron models. *Journal of Physiology, Paris*, 93, 43–59. doi:10.1016/S0928-4257(99)80135-1 PMID:10084708
- Jones, K. E., Bawa, P., & McMillan, A. S. (1993). Recruitment of motor units in human flexor carpi ulnaris. *Brain Research*, 602, 354–356. doi:10.1016/0006-8993(93)90702-O PMID:8448677
- Jones, K. E., Lyons, M., Bawa, P., & Lemon, R. N. (1994). Recruitment of motoneurons during various behavioural tasks. *Experimental Brain Research*, 100(3), 503–508. doi:10.1007/BF02738409 PMID:7813686
- Joynt, R. L., Erlandson, R. F., Wu, S. J., & Wang, C. M. (1991). Electromyography interference pattern decomposition. *Archives of Physical Medicine and Rehabilitation*, 72(8), 567–572. PMID:2059134
- Juel, C. (1988). Muscle action potential propagation velocity changes during activity. *Muscle & Nerve*, 11(7), 714–719. doi:10.1002/mus.880110707 PMID:2457155
- Ju, M. S., Lin, C. C. K., Chen, J., Cheng, H. S., & Lin, C. W. (2002). Performance of elbow tracking under constant torque disturbance in normotonic stroke patients and normal subjects. *Clinical Biomechanics (Bristol, Avon)*, 17, 640–649. doi:10.1016/S0268-0033(02)00131-6 PMID:12446160
- Kamavuako, E. N., Farina, D., Yoshida, K., & Jensen, W. (2009). Relationship between grasping force and features of single-channel intramuscular EMG signals. *Journal of Neuroscience Methods*, 185(1), 143–150. doi:10.1016/j.jneumeth.2009.09.006 PMID:19747943
- Kamavuako, E. N., Rosenvang, J. C., Bøg, M. F., Smidstrup, A., Erkocevic, E., Niemeier, M. J., & Farina, D. (2013). Influence of the feature space on the estimation of hand grasping force from intramuscular EMG. *Biomedical Signal Processing and Control*, 8(1), 1–5. doi:10.1016/j.bspc.2012.05.002
- Kamono, A., Muraoka, Y., Shimaoka, H., Uchida, S., & Ota, T. (2002). Development of EMG-controlled functional electrical stimulation system. In *Proceedings of the 41st SICE Annual Conference IEEE* (Vol. 3, pp. 2022–2027).
- Kamono, K. Y., & Tomita, Y. (2001). *Development of gait assist device for foot drop patients*. Paper presented at the 6th Annual Conference of the International Functional Electrical Stimulation Society, Cleveland, OH.
- Kanda, K., & Desmedt, J. E. (1983). Cutaneous facilitation of large motor units and motor control of human fingers in precision grip. In J. E. Desmedt (Ed.), *Motor control mechanisms in health and disease*. (Advances in neurology, vol. 39) (pp. 253–261). New York: Raven Press.
- Kanda, K., Burke, R. E., & Walmsley, B. (1977). Differential control of fast and slow twitch motor units in the decerebrate cat. *Experimental Brain Research*, 29(1), 57–74. doi:10.1007/BF00236875 PMID:891681
- Kankaanpää, M., Taimela, S., Webber, C. L. Jr, Airaksinen, O., & Hanninen, O. (1997). Lumbar paraspinal muscle fatigability in repetitive isoinertial loading: EMG spectral indices, Borg scale and endurance time. *European Journal of Applied Physiology and Occupational Physiology*, 76(3), 236–242. doi:10.1007/s004210050242 PMID:9286603

Compilation of References

- Kao, J., Pink, M., Jobe, F., & Perry, J. (1995). EMG analysis of the scapular muscles during a golf swing. *The American Journal of Sports Medicine*, 23(1), 19–23. doi:10.1177/036354659502300104 PMID:7726345
- Katirji, B. (2007). *Electromyography in clinical practice. A case study approach*. Philadelphia, PA: Mosby Elsevier.
- Kaufmann, P., Englehart, L., & Platzner, M. (2010). Fluctuating EMG signals: Investigating long-term effects of pattern matching algorithms. *Proceedings of the 32nd Annual International Conference of the IEEE Engineering in Medicine and Biology Society*, Buenos Aires, Argentina (pp. 6357–6360).
- Kawakami, Y., Abe, T., & Fukunaga, T. (1993). Muscle-fiber pennation angle are greater in hypertrophied than in normal muscles. *Journal of Applied Physiology*, 74, 2740–2744. PMID:8365975
- Kawato, M. (1999). Internal models for motor control and trajectory planning. *Current Opinion in Neurobiology*, 9(1), 718–727. doi:10.1016/S0959-4388(99)00028-8 PMID:10607637
- Kearney, R. E., & Hunter, I. W. (1990). System identification of human joint dynamics. *Critical Reviews in Biomedical Engineering*, 18, 55–87. PMID:2204515
- Keen, D. A., Chou, L.-W., Nordstrom, M. A., & Fuglevand, A. J. (2012). Short-term synchrony in diverse motor nuclei presumed to receive different extents of direct cortical input. *Journal of Neurophysiology*, 108, 3264–3275. doi:10.1152/jn.01154.2011 PMID:23019009
- Keen, D. A., Yue, G. H., & Enoka, R. M. (1994). Training-related enhancement in the control of motor output in elderly humans. *Journal of Applied Physiology (Bethesda, Md.)*, 77(6), 2648–2658. PMID:7896604
- Kendall, C., Lemaire, E. D., Losier, Y., Chan, A., & Hudgins, B. (2012). A novel approach to surface electromyography: An exploratory study of electrode-pair selection based on signal characteristics. *Journal of Neuroengineering and Rehabilitation*, 9(24).
- Kent-Braun, J. A. (1999). Central and peripheral contributions to muscle fatigue in humans during sustained maximal effort. *European Journal of Applied Physiology and Occupational Physiology*, 80(1), 57–63. doi:10.1007/s004210050558 PMID:10367724
- Kernell, D., Bakels, R., & Copray, J. C. (1999). Discharge properties of motoneurons: How are they matched to the properties and use of their muscle units? *Journal of Physiology, Paris*, 93, 87–96. doi:10.1016/S0928-4257(99)80139-9 PMID:10084712
- Kernell, D., & Hultborn, H. (1990). Synaptic effects on recruitment gain: A mechanism of importance for the input-output relations of motoneuron pools? *Brain Research*, 507, 176–179. doi:10.1016/0006-8993(90)90542-J PMID:2302576
- Kester, W. (2005). *The data conversion handbook*. Norwood, MA: Analog Devices, Inc.
- Khushaba, R. N., & Kodagoda, S. (2012). Electromyogram (EMG) feature reduction using mutual components analysis for multifunction prosthetic fingers control. In *Proceedings of the 12th International Conference on Control, Automation, Robotics and Vision*, Guangzhou, China (pp. 1534–1539).
- Khushaba, R. N., Kodagoda, S., Liu, D., & Dissanayake, G. (2013). Muscle computer interfaces for driver distraction reduction. *Computer Methods and Programs in Biomedicine*, 110(2), 137–149. doi:10.1016/j.cmpb.2012.11.002 PMID:23290462
- Kiguchi, K., Iwami, K., Yasuda, M., Watanabe, K., & Fukuda, T. (2003). An exoskeletal robot for human shoulder joint motion assist. *IEEE/ASME Transactions on Mechatronics*, 8, 125–135. doi:10.1109/TMECH.2003.809168
- Kiguchi, K., Rahman, M. H., Sasaki, M., & Teramoto, K. (2008). Development of a 3DOF mobile exoskeleton robot for human upper-limb motion assist. *Robotics and Autonomous Systems*, 56, 678–691. doi:10.1016/j.robot.2007.11.007
- Kimberley, T. J., Lewis, S. M., Auerbach, E. J., Dorsey, L. L., Lojovich, J. M., & Carey, J. R. (2004). Electrical stimulation driving functional improvements and cortical changes in subjects with stroke. *Experimental Brain Research*, 154, 450–460. doi:10.1007/s00221-003-1695-y PMID:14618287
- Kim, D., Millett, P., Warner, J., & Jobe, F. (2004). Shoulder injuries in golf. *The American Journal of Sports Medicine*, 32(5), 1324–1330. doi:10.1177/0363546504267346 PMID:15262661

- Kim, K. S., Choi, H. H., Moon, C. S., & Mun, C. W. (2011). Comparison of k-nearest neighbor, quadratic discriminant and linear discriminant analysis in classification of electromyogram signals based on the wrist-motion directions. *Current Applied Physics*, *11*(3), 740–745. doi:10.1016/j.cap.2010.11.051
- Kim, S. J., Jeong, E. C., Lee, S. M., & Song, Y. R. (2012). Improvements of multi-features extraction for EMG for estimating wrist movements. *The Transactions of the Korean Institute of Electrical Engineers*, *61*(5), 757–762. doi:10.5370/KIEE.2012.61.5.757
- Kimura, J. (1989). *Electrodiagnosis in diseases of nerve and muscle*. Philadelphia, PA: Davis.
- Kimura, J. (2001). *Electrodiagnosis in the disease of nerve and muscle*. New York: Oxford University Press.
- Kleissen, R. F. M., Buurke, J. H., Harlaar, J., & Zilvold, G. (1998). Electromyography in the biomechanical analysis of human movement and its clinical application. *Gait & Posture*, *8*(2), 143–158. doi:10.1016/S0966-6362(98)00025-3 PMID:10200405
- Klimstra, M. D., Thomas, E., Stoloff, R. H., Ferris, D. P., & Zehr E. P. (2009) Neuromechanical considerations for incorporating rhythmic arm movement in the rehabilitation of walking. *Chaos* *19*(2), 026102 1-14.
- Knaflitz, M., & Merletti, R. (1988). Suppression of simulation artifacts from myoelectric-evoked potential recordings. *IEEE Transactions on Bio-Medical Engineering*, *35*, 758–763. doi:10.1109/10.7278 PMID:3169829
- Knaflitz, M., Merletti, R., & De Luca, C. J. (1990). Inference of motor unit recruitment order in voluntary and electrically elicited contractions. *Journal of Applied Physiology*, *68*, 1657–1667. PMID:2347805
- Komi, P. V., & Tesch, P. (1979). EMG frequency spectrum, muscle structure, and fatigue during dynamic contractions in man. *European Journal of Applied Physiology and Occupational Physiology*, *42*(1), 41–50. PMID:499196
- Konrad, P., Schmitz, K., & Denner, A. (2001). Neuro-muscular evaluation of trunk-training exercises. *Journal of Athletic Training*, *36*(2), 109–118. PMID:12937449
- Koo, T. K. K., & Mak, A. F. T. (2005). Feasibility of using EMG driven neuromusculoskeletal model for prediction of dynamic movement of the elbow. *Journal of Electromyography and Kinesiology*, *15*, 12–26. doi:10.1016/j.jelekin.2004.06.007 PMID:15642650
- Koo, T. K. K., Mak, A. F. T., & Hung, L. K. (2002). In vivo determination of subject-specific musculodenton parameters: Applications to the prime elbow flexors in normal and hemiparetic subject. *Clinical Biomechanics (Bristol, Avon)*, *17*, 390–399. doi:10.1016/S0268-0033(02)00031-1 PMID:12084544
- Kouzaki, M., Shinohara, M., Masani, K., & Fukunaga, T. (2004). Force fluctuations are modulated by alternate muscle activity of knee extensor synergists during low-level sustained contraction. *Journal of Applied Physiology (Bethesda, Md.)*, *97*(6), 2121–2131. doi:10.1152/jappphysiol.00418.2004 PMID:15208288
- Kouzaki, M., Shinohara, M., Masani, K., Kanehisa, H., & Fukunaga, T. (2002). Alternate muscle activity observed between knee extensor synergists during low-level sustained contractions. *Journal of Applied Physiology (Bethesda, Md.)*, *93*(2), 675–684. PMID:12133879
- Krakauer, J. W. (2006). Motor learning: Its relevance to stroke recovery and neurorehabilitation. *Current Opinion in Neurology*, *19*, 84–90. doi:10.1097/01.wco.0000200544.29915.cc PMID:16415682
- Kubo, M., Wagenaar, R. C., Saltzman, E., & Holt, K. G. (2004). Biomechanical mechanism for transitions in phase and frequency of arm and leg swing during walking. *Biological Cybernetics*, *91*(2), 91–98. doi:10.1007/s00422-004-0503-5 PMID:15351887
- Kuhtz-Buschbeck, J. P., Brockmann, K., Gilster, R., Koch, A., & Stolze, H. (2008). Asymmetry of arm-swing not related to handedness. *Gait & Posture*, *27*(3), 447–454. doi:10.1016/j.gaitpost.2007.05.011 PMID:17616462
- Kuhtz-Buschbeck, J. P., & Jing, B. (2012). Activity of upper limb muscles during human walking. *Journal of Electromyography and Kinesiology*, *22*(2), 199–206. doi:10.1016/j.jelekin.2011.08.014 PMID:21945656

Compilation of References

- Kukulka, C. G., & Clamann, H. P. (1981). Comparison of the recruitment and discharge properties of motor units in human brachial biceps and adductor pollicis during isometric contractions. *Brain Research*, *219*, 45–55. doi:10.1016/0006-8993(81)90266-3 PMID:7260629
- Kundu, A. S., Mazumder, O., & Bhaumik, S. (2011). Design of wearable, low power, single supply surface EMG extractor unit for wireless monitoring. In *Proceedings of the 2nd International Conference on Nanotechnology and Biosensors*, Dubai, United Arab Emirates (pp. 69-74).
- Kutch, J. J., & Buchanan, T. S. (2001). Human elbow joint torque is linearly encoded in electromyographic signals from multiple muscles. *Neuroscience Letters*, *311*(1), 97–100. doi:10.1016/S0304-3940(01)02146-2 PMID:11567787
- Kwon, J., Lee, S., Shin, C., Jang, Y., & Hong, S. (1998). Signal hybrid HMM-GA-MLP classifier for continuous EMG classification purpose. In *Proceedings of 20th Annual International Conference of the IEEE Engineering Medicine, Biology and Society*, *20*(3), 1404–1407.
- LaCourse, J. R., & Hludik, F. C. Jr. (1990). An eye movement communication-control system for the disabled. *IEEE Transactions on Bio-Medical Engineering*, *37*(12), 1215–1220. doi:10.1109/10.64465 PMID:2149712
- Lacquiniti, F., Ivanenko, Y. P., & Zago, M. (2012). Patterned control of human locomotion. *The Journal of Physiology*, *590*(10), 2189–2199. doi:10.1113/jphysiol.2011.215137 PMID:22411012
- Lal, T. N., Schröder, M., Hinterberger, T., Weston, J., Bogdan, M., & Birbaumer, N. et al. (2004). Support vector channel selection in BCI. *IEEE Transactions on Bio-Medical Engineering*, *51*(6), 1003–1010. doi:10.1109/TBME.2004.827827 PMID:15188871
- Lange, D. J. (1992). Single fiber electromyography in normal subjects: Reproducibility, variability, and technical considerations. *Electromyography and Clinical Neurophysiology*, *32*(7), 397–402. PMID:1526222
- Langzam, E., Isakov, E., & Mizrahi, J. (2006). Evaluation of methods for extraction of the volitional EMG in dynamic hybrid muscle activation. *Journal of Neuroengineering and Rehabilitation*, *3*, 27. doi:10.1186/1743-0003-3-27 PMID:17123447
- Larson, S. G., & Stern, J. T. (2007). Humeral retractor EMG during quadrupedal walking in primates. *The Journal of Experimental Biology*, *210*(7), 1204–1215. doi:10.1242/jeb.002337 PMID:17371919
- Lawrence, J. H., & De Luca, C. J. (1983). Myoelectric signal versus force relationship in different human muscles. *Journal of Applied Physiology*, *54*(6), 1653–1659. PMID:6874489
- Leedham, J. S., & Dowling, J. J. (1995). Force-length, torque-angle and EMG-joint angle relationships of the human in vivo biceps brachii. *Archives of Physical Medicine and Rehabilitation*, *70*, 421–426. PMID:7671877
- Lee, J., Jung, M. Y., & Kim, S. H. (2001). Reliability of spike and turn variables of surface EMG during isometric voluntary contractions of the biceps brachii muscle. *Journal of Electromyography and Kinesiology*, *21*(1), 119–127. doi:10.1016/j.jelekin.2010.08.008 PMID:20833563
- Lemay, M. A., & Crago, P. E. (1996). A dynamic model for simulating movements of the elbow, forearm, and wrist. *Journal of Biomechanics*, *29*, 1319–1330. doi:10.1016/0021-9290(96)00026-7 PMID:8884477
- Lewek, M. D., Poole, R., Johnson, J., Halawa, O., & Huang, X. (2010). Arm swing magnitude and asymmetry during gait in the early stages of Parkinson's disease. *Gait & Posture*, *31*(2), 256–260. doi:10.1016/j.gaitpost.2009.10.013 PMID:19945285
- Lieberman, D. E., Venkadesan, M., Werbel, W. A., Daoud, A. I., D'Andrea, S., Davis, I. S., & Pitsiladis, Y. (2010). Foot strike patterns and collision forces in habitually barefoot versus shod runners. *Nature*, *463*(7280), 531–535. doi:10.1038/nature08723 PMID:20111000
- Lieber, R. L. (2010). *Skeletal muscle structure, function, and plasticity*. Baltimore, MD: Lippincott Williams & Wilkins.
- Lieber, R. L., Fazeli, B. M., & Botte, M. J. (1990). Architecture of selected wrist flexor and extensor muscles. *The Journal of Hand Surgery*, *15A*, 244–250. doi:10.1016/0363-5023(90)90103-X PMID:2324452

- Lieber, R. L., Jacobson, M. D., Fazeli, B. M., Abrams, R. A., & Botte, M. J. (1992). Architecture of selected muscles of the arm and forearm: Anatomy and implications for tendon transfer. [American Volume]. *The Journal of Hand Surgery*, 17A, 787–798. doi:10.1016/0363-5023(92)90444-T PMID:1401782
- Li, G., Li, Y., Yu, L., & Geng, Y. (2011). Conditioning and sampling issues of EMG signals in motion recognition of multifunctional myoelectric prostheses. *Annals of Biomedical Engineering*, 39(6), 1779–1787. doi:10.1007/s10439-011-0265-x PMID:21293972
- Li, K., Hewson, D. J., Duchene, J., & Hogrel, J.-Y. (2010). Predicting maximal grip strength using hand circumference. *Manual Therapy*, 15(6), 579–585. doi:10.1016/j.math.2010.06.010 PMID:20708427
- Li, L., & Tong, K. Y. (2011). An introduction to biomechatronics. In K. Y. Tong (Ed.), *Biomechatronics in medicine and health care* (pp. 1–8). Singapore: Pan Stanford Publishing Pte Ltd. doi:10.1201/b11402-2
- Li, L., Tong, K. Y., & Hu, X. L. (2007a). The effect of poststroke impairments on brachialis muscle architecture as measured by ultrasound. *Archives of Physical Medicine and Rehabilitation*, 88, 243–250. doi:10.1016/j.apmr.2006.11.013 PMID:17270524
- Li, L., Tong, K. Y., Song, R., & Koo, T. K. K. (2007b). Is maximum isometric muscle stress the same among prime elbow flexors? *Clinical Biomechanics (Bristol, Avon)*, 22, 874–883. doi:10.1016/j.clinbiomech.2007.06.001 PMID:17681653
- Lindsay, D., & Horton, J. (2002). Comparison of spine motion in elite golfers with and without low back pain. *Journal of Sports Sciences*, 20(8), 599–605. doi:10.1080/026404102320183158 PMID:12190279
- Lindsay, D., Horton, J., & Vandervoort, A. (2000). A review of injury characteristics, aging factors and prevention programmes for the older golfer. *Sports Medicine (Auckland, N.Z.)*, 30(2), 89–103. doi:10.2165/00007256-200030020-00003 PMID:10966149
- Lindstrom, L., Kadefors, R., & Petersen, I. (1977). An electromyographic index for localized muscle fatigue. *Journal of Applied Physiology: Respiratory, Environmental and Exercise Physiology*, 43(4), 750–754. PMID:583632
- Lin, Y. D., Tsai, C. D., Huang, H. H., Chiou, D. C., & Wu, C. P. (1999). Preamplifier with a second-order high-pass filtering characteristic. *IEEE Transactions on Bio-Medical Engineering*, 46(5), 609–612. doi:10.1109/10.759062 PMID:10230140
- Li, X., Zhou, P., & Aruin, A. S. (2007). Teager-Kaiser energy operation of surface EMG improves muscle activity onset detection. *Annual Biomedicine Engineer*, 35(9), 1532–153. doi:10.1007/s10439-007-9320-z PMID:17473984
- Li, Y., Wang, W., Crompton, R. H., & Gunther, M. M. (2001). Free vertical moments and transverse forces in human walking and their role in relation to arm-swing. *The Journal of Experimental Biology*, 204(1), 47–58. PMID:11104710
- Ljung, L. (1999). *System identification: Theory for the user* (2nd ed.). Englewood Cliffs, NJ: Prentice-Hall.
- Loeb, G. E., & Ghez, C. (2006). The motor unit and muscle action. In E. R. Kandel, J. H. Schwartz, & T. M. Jessell (Eds.), *Principles of neural science* (pp. 674–695). New York: McGraw-Hill.
- Luca, C. J. D., & Knaflitz, M. (1992). *Surface Electromyography: What's New?* Torino, Italy: CLUT.
- Lucas, D. B., & Bresler, B. (1961). *Stability of the ligamentous spine* (Tech report No. 40). San Francisco: Biomechanics Laboratory, University of California, CA.
- Ludin, H. (1973). Action potentials of normal and dystrophic human muscle fibres. In J. E. Desmedt (Ed.), *New development in electromyography and clinical neurophysiology* (pp. 400–406). Basel, Switzerland: Karger.
- Lum, P. S., Taub, E., Schwandt, D., Postman, M., Hardin, P., & Uswatte, G. (2004). Automated constraint-induced therapy extension (AutoCITE) for movement deficits after stroke. *Journal of Rehabilitation Research and Development*, 41, 249–258. doi:10.1682/JRRD.2003.06.0092 PMID:15543442
- Maganaris, C. N. (2004). A predictive model of moment-angle characteristics in human skeletal muscle: Application and validation in muscles across the ankle joint. *Journal of Theoretical Biology*, 230, 89–98. doi:10.1016/j.jtbi.2004.04.025 PMID:15276003

Compilation of References

- Maganaris, C. N., Baltzopoulos, V., & Sargeant, A. J. (1998). In vivo measurement of the triceps surae complex architecture in man: implications for muscle function. *The Journal of Physiology*, *512*, 603–614. doi:10.1111/j.1469-7793.1998.603be.x PMID:9763648
- Mainardi, L. T., Bianchi, A. M., & Cerutti, S. (2006). Digital biomedical signal acquisition and processing. In J. D. Bronzino (Ed.), *Medical devices and systems* (pp. 2–24). Boca Raton, FL: CRC Press Taylor & Francis Group. doi:10.1201/9781420003864.ch2
- Maisetti, O. (2002). *Manifestations myoélectriques de la fatigue comme prédicteurs de la capacité de travail musculaire local* (Thèse de doctorat STAPS). Université de la méditerranée.
- Maisetti, O., Boyas, S., & Guevel, A. (2006). Specific neuromuscular responses of high skilled laser sailors during a multi-joint posture sustained until exhaustion. *International Journal of Sports Medicine*, *27*(12), 968–975. doi:10.1055/s-2006-923893 PMID:16761219
- Maisetti, O., Guevel, A., Iachkine, P., Legros, P., & Brisswalter, J. (2002). Le maintien de la position de rappel en dériveur solitaire. Aspects théoriques et propositions méthodologiques d'évaluation de la fatigue musculaire. *Science & Sports*, *17*, 234–246. doi:10.1016/S0765-1597(02)00170-3
- Maisetti, O., Guevel, A., Legros, P., & Hogrel, J. Y. (2002a). Prediction of endurance capacity of quadriceps muscles in humans using surface electromyogram spectrum analysis during submaximal voluntary isometric contractions. *European Journal of Applied Physiology*, *87*(6), 509–519. doi:10.1007/s00421-002-0645-x PMID:12355190
- Maisetti, O., Guevel, A., Legros, P., & Hogrel, J. Y. (2002b). SEMG power spectrum changes during a sustained 50% maximum voluntary isometric torque do not depend upon the prior knowledge of the exercise duration. *Journal of Electromyography and Kinesiology*, *12*(2), 103–109. doi:10.1016/S1050-6411(02)00010-X PMID:11955982
- Manal, K., & Buchanan, T. S. (2005). Use of an EMG-driven biomechanical model to study virtual injuries. *Medicine and Science in Sports and Exercise*, *37*, 1917–1923. doi:10.1249/01.mss.0000176685.35442.6b PMID:16286862
- Mandrile, F., Farina, D., Pozzo, M., & Merletti, R. (2003). Stimulation artifact in surface EMG signal: effect of the stimulation waveform, detection system, and current amplitude using hybrid stimulation technique. *IEEE Transactions on Neural Systems and Rehabilitation Engineering*, *11*, 407–415. doi:10.1109/TNSRE.2003.819791 PMID:14960117
- Manning, C. D., Miller, T. A., Burnham, M. L., Murnaghan, C. D., Calancie, B., & Bawa, P. (2010). Recovery of human motoneurons during rotation. *Experimental Brain Research*, *204*, 139–144. doi:10.1007/s00221-010-2295-2 PMID:20490783
- Manning, C. D., Tolhurst, S. A., & Bawa, P. (2012). Proprioceptive reaction times and long-latency reflexes in humans. *Experimental Brain Research*, *221*, 155–166. doi:10.1007/s00221-012-3157-x PMID:22766848
- Mannion, A. F., & Dolan, P. (1994). Electromyographic median frequency changes during isometric contraction of the back extensors to fatigue. *Spine*, *19*(11), 1223–1229. doi:10.1097/00007632-199405310-00006 PMID:8073313
- Mannion, A. F., & Dolan, P. (1996). Relationship between myoelectric and mechanical manifestations of fatigue in the quadriceps femoris muscle group. *European Journal of Applied Physiology and Occupational Physiology*, *74*(5), 411–419. PMID:8954288
- Marieb, E. N. (1995). *Human anatomy and physiology*. Redwood City, CA: Benjamin/Cummings.
- Marras, W. S., & Davis, K. G. (2001). A non-MVC EMG normalization technique for the trunk musculature: Part 1. Method development. *Journal of Electromyography and Kinesiology*, *11*(1), 1–9. doi:10.1016/S1050-6411(00)00039-0 PMID:11166603
- Marras, W. S., & Sommerich, C. M. (1991). A three-dimensional motion model of loads on the lumbar spine: I. Model structure. *Human Factors*, *33*(2), 123–137. PMID:1860700

- Marshall, P., & Murphy, B. (2003). The validity and reliability of surface EMG to assess the neuromuscular response of the abdominal muscles to rapid limb movement. *Journal of Electromyography and Kinesiology*, 13, 477–489. doi:10.1016/S1050-6411(03)00027-0 PMID:12932422
- Marta, S., Silva, L., Vaz, J., Bruno, P., & Pezarat-Correia, P. (in press). Electromyographic analysis of trunk muscles during the golf swing performed with two different clubs. *Annual Review of Golf Coaching supplement of the International Journal of Sports Science & Coaching*.
- Marta, S., Silva, L., Castro, M. A., Pezarat-Correia, P., & Cabri, J. (2012). Electromyography variables during the golf swing: A literature review. *Journal of Electromyography and Kinesiology*, 22(6), 803–813. doi:10.1016/j.jelekin.2012.04.002 PMID:22542769
- Martin, D. C., Medri, M. K., Chow, R. S., Oxorn, V., Leekam, R. N., Agur, A. M., & McKee, N. H. (2001). Comparing human skeletal muscle architectural parameters of cadavers with in vivo ultrasonographic measurements. *Journal of Anatomy*, 199(4), 429–434. doi:10.1046/j.1469-7580.2001.19940429.x PMID:11693303
- Martini, F. H. (1995). *Fundamentals of anatomy and physiology*. Englewood, NJ: Prentice Hall.
- Matthews, P. B. C. (1991). The human stretch reflex and the motor cortex. *Trends in Neurosciences*, 14, 87–91. doi:10.1016/0166-2236(91)90064-2 PMID:1709536
- Matthews, P. B. C. (1996). Relationship of firing intervals of human motor units to the trajectory of post-spike after-hyperpolarization and synaptic noise. *The Journal of Physiology*, 492(2), 597–628. PMID:9019553
- Maurel, W., & Thalman, D. (1998). A case study on human upper limb modelling for dynamic simulation. *Computer Methods in Biomechanics and Biomedical Engineering*, 2, 65–82. doi:10.1080/10255849908907979 PMID:11264819
- Mcardle, J., Michelson, L., & D'Alonzo, A. J. (1980). Action potentials in fast- and slow- twitch mammalian muscles during reinnervation and development. *The Journal of General Physiology*, 75, 655–672. doi:10.1085/jgp.75.6.655 PMID:7391811
- McComas, A. J. (1995). Motor unit estimation: Anxieties and achievements. *Muscle & Nerve*, 18(4), 369–379. doi:10.1002/mus.880180402 PMID:7715621
- McCommas, et al. (1971). Electrophysiological estimation of the number of motor units within a human muscle. *Journal of Neurology, Neurosurgery, and Psychiatry*, 34(2), 121–131. doi:10.1136/jnnp.34.2.121 PMID:5571599
- Mccrea, P. H., Eng, J. J., & Hodgson, A. J. (2003). Time and magnitude of torque generation is impaired in both arms following stroke. *Muscle & Nerve*, 28, 46–53. doi:10.1002/mus.10397 PMID:12811772
- McGill, K. C. (2002). Optimal resolution of superimposed action potentials. *IEEE Transactions on Bio-Medical Engineering*, 49(7), 640–650. doi:10.1109/TBME.2002.1010847 PMID:12083298
- McGill, K. C., Cummins, K. L., & Dorfman, L. J. (1985). Automatic decomposition of the clinical electromyogram. *IEEE Transactions on Bio-Medical Engineering*, 32(7), 470–477. doi:10.1109/TBME.1985.325562 PMID:3839488
- McGill, K. C., Lateva, Z. C., & Marateb, H. R. (2005). EMGLAB: An interactive EMG decomposition program. *Journal of Neuroscience Methods*, 149(2), 121–133. doi:10.1016/j.jneumeth.2005.05.015 PMID:16026846
- McGill, S. M. (1992). A myoelectrically based dynamic three-dimensional model to predict loads on lumbar spine tissues during lateral bending. *Journal of Biomechanics*, 25(4), 395–414. doi:10.1016/0021-9290(92)90259-4 PMID:1533860
- McGill, S. M. (1997). The biomechanics of low back injury: Implications on current practice in industry and the clinic. *Journal of Biomechanics*, 30(5), 465–475. doi:10.1016/S0021-9290(96)00172-8 PMID:9109558
- McGill, S. M. (2007). *Low back disorders: Evidence-based prevention and rehabilitation*. Champaign, IL: Human Kinetics.
- McGill, S. M., Chaimberg, J. D., Frost, D. M., & Fenwick, C. M. (2010). Evidence of a double peak in muscle activation to enhance strike speed and force: an example with elite mixed martial arts fighters. *Journal of Strength and Conditioning Research*, 24(2), 348–357. doi:10.1519/JSC.0b013e3181cc23d5 PMID:20072065

Compilation of References

- McGill, S. M., Hughson, R. L., & Parks, K. (2000). Changes in lumbar lordosis modify the role of the extensor muscles. *Clinical Biomechanics (Bristol, Avon)*, *15*(10), 777–780. doi:10.1016/S0268-0033(00)00037-1 PMID:11050362
- McGill, S. M., & Norman, R. W. (1986). Partitioning of the L4-L5 dynamic moment into disc, ligamentous, and muscular components during lifting. *Spine*, *11*(7), 666–677. doi:10.1097/00007632-198609000-00004 PMID:3787338
- McHardy, A., & Pollard, H. (2005a). Muscle activity during the golf swing. *British Journal of Sports Medicine*, *39*(11), 799–804. doi:10.1136/bjism.2005.020271 PMID:16244187
- McHardy, A., & Pollard, H. (2005b). Golf and upper limb injuries: A summary and review of the literature. *Chiropractic & Osteopathy*, *13*(7). PMID:15967021
- McHardy, A., Pollard, H., & Luo, K. (2006). Golf injuries: A review of the literature. *Sports Medicine (Auckland, N.Z.)*, *36*, 171–187. doi:10.2165/00007256-200636020-00006 PMID:16464124
- McMahon, T. A. (1984). *Muscles, reflexes, and locomotion*. Princeton, NJ: Princeton University Press.
- Meakin, J. (2003). *The beginner's guide to power walking*. Hauppauge, NY: Barron's Educational Series.
- Meilink, A., Hemmen, B., Seelen, H. A. M., & Kwakkel, G. (2008). Impact of EMG-triggered neuromuscular stimulation of the wrist and finger extensors of the paretic hand after stroke: A systematic review of the literature. *Clinical Rehabilitation*, *22*, 291–305. doi:10.1177/0269215507083368 PMID:18390973
- Meo, J. H., & Post, H. W. (1962). Functional electrical stimulation for ambulation in hemiplegia. *The Journal-Lancet*, *82*, 285–288. PMID:14474974
- Merletti, R., & Farina, D. (2009). Analysis of intramuscular electromyogram signals. *Philosophical Transactions of the Royal Society A*, *367*, 357–368. doi:10.1098/rsta.2008.0235
- Merletti, R., Knaflitz, M., & De Luca, C. J. (1990). Myoelectric manifestations of fatigue in voluntary and electrically elicited contractions. *Journal of Applied Physiology*, *69*, 1810–1820. PMID:2272975
- Merletti, R., Knaflitz, M., & DeLuca, C. J. (1992). Electrically evoked myoelectric signals. *Critical Reviews in Biomedical Engineering*, *19*, 293–340. PMID:1563271
- Merletti, R., Lo Conte, L., & Orizio, C. (1991). Indices of muscles fatigue. *Journal of Electromyography and Kinesiology*, *1*, 20–33. doi:10.1016/1050-6411(91)90023-X PMID:20719592
- Merletti, R., & Parker, P. J. (Eds.). (2004). *Electromyography: Physiology, engineering, and non-invasive applications*. Hoboken, NJ: John Wiley & Sons. doi:10.1002/0471678384
- Merletti, R., & Roy, S. H. (1996). Myoelectrical and mechanical manifestations of muscle fatigue in voluntary contractions. *The Journal of Orthopaedic and Sports Physical Therapy*, *24*(6), 342–353. doi:10.2519/jospt.1996.24.6.342 PMID:8938600
- Metoki, N., Sato, Y., Satoh, K., Okumura, K., & Iwamoto, J. (2003). Muscular atrophy in the hemiplegic thigh in patients after stroke. *American Journal of Physical Medicine & Rehabilitation*, *82*, 862–865. doi:10.1097/01.PHM.0000091988.20916.EF PMID:14566154
- Metting van Rijn, A. C., Kuiper, A. P., Linnenbank, A. C., & Grimbergen, C. A. (1993). Patients isolation in multichannel bioelectric recordings by digital transmission through a single optical fiber. *IEEE Transactions on Bio-Medical Engineering*, *40*(3), 302–307. doi:10.1109/10.216416 PMID:8335335
- Meyns, P., Bruijn, S. M., & Duysens, J. (2013). (in press). The how and why of arm swing during human walking. *Gait & Posture*; Epub ahead of print. doi:10.1016/j.gaitpost.2013.02.006 PMID:23489950
- Micera, S., Sabatini, A. M., & Dario, P. (1998). An algorithm for detecting the onset of muscle contraction by EMG signal processing. *Medicine Engennier Physical*, *20*(3), 211–215. doi:10.1016/S1350-4533(98)00017-4 PMID:9690491

- Miller-Larsson, A. (1980). A model of spatial distribution of muscle fibres of a motor unit in normal human limb muscles. *Electroencephalography and Clinical Neurophysiology*, *20*, 281–298. PMID:7418648
- Miller, S. A., Mayer, T., Cox, R., & Gatchel, R. J. (1992). Reliability problems associated with the modified Schober technique for true lumbar flexion measurement. *Spine*, *17*(3), 345–348. doi:10.1097/00007632-199203000-00017 PMID:1533063
- Mills, K. R. (2005). The basics of electromyography. *Journal of Neurology, Neurosurgery, and Psychiatry*, *76*(Supplement II), ii32–ii35. doi:10.1136/jnnp.2005.069211 PMID:15961866
- Milner-Brown, H. S., Stein, R. B., & Yemm, R. (1973a). The orderly recruitment of human motor units during voluntary isometric contractions. *The Journal of Physiology*, *230*, 359–370. PMID:4350770
- Milner-Brown, H. S., Stein, R. B., & Yemm, R. (1973b). Changes in firing rate of human motor units during linearly changing voluntary contractions. *The Journal of Physiology*, *230*, 371–390. PMID:4708898
- Minzly, J., Mizrahi, J., Hakim, N., & Liberson, A. (1993). Stimulus artefact suppressor for EMG recording during FES by a constant-current stimulator. *Medical & Biological Engineering & Computing*, *31*, 72–75. doi:10.1007/BF02446897 PMID:8326768
- Mochizuki, G., Ivanova, T. D., & Garland, S. J. (2005). Synchronization of motor units in human soleus muscle during standing postural tasks. *Journal of Neurophysiology*, *94*, 62–69. doi:10.1152/jn.01322.2004 PMID:15744004
- Mogk, J. P. M., & Keir, P. J. (2003). Crosstalk in surface electromyography of the proximal forearm during gripping tasks. *Journal of Electromyography and Kinesiology*, *13*(1), 63–71. doi:10.1016/S1050-6411(02)00071-8 PMID:12488088
- Monster, A. W., & Chan, H. (1977). Isometric force production by motor units of the extensor digitorum communis muscle in man. *Journal of Neurophysiology*, *40*, 1432–1443. PMID:925737
- Monti, R. J., Roy, R. R., & Edgerton, V. R. (2001). Role of motor unit structure in defining function. *Muscle & Nerve*, *24*(7), 848–866. doi:10.1002/mus.1083 PMID:11410913
- Moore, D. P., & Kowalske, K. J. (2000). Neuromuscular rehabilitation and electrodiagnosis. 5. Myopathy. *Arch Phys Med Rehabil*, *81*(3 Suppl 1), S32–35, S36–44.
- Moreno, J. C., Del Ama, A. J., de Los Reyes-Guzmán, A., Gil-Agudo, A., Ceres, R., & Pons, J. L. (2011). Neurobotic and hybrid management of lower limb motor disorders: A review. *Medical & Biological Engineering & Computing*, *49*, 1119–1130. doi:10.1007/s11517-011-0821-4 PMID:21847596
- Moritani, T., Stegeman, D., & Merletti, R. (2004). Basic physiology and biophysics of EMG signal generation. In R. Merletti, & P. A. Parker (Eds.), *Electromyography, physiology, engineering and noninvasive applications* (pp. 1–27). Hoboken, NJ: John Wiley and Sons. doi:10.1002/0471678384.ch1
- Mortimer, J. T. (2011). Motor prostheses. In *Comprehensive Physiology*. John Wiley & Sons, Inc. Retrieved from <http://onlinelibrary.wiley.com/doi/10.1002/cphy.cp010205/abstract>
- Moynes, D., Perry, J., Antonelli, D., & Jobe, F. (1986). Electromyography and motion analysis of the upper extremity in sports. *Physical Therapy*, *66*(12), 1905–1911. PMID:3786421
- Mullany, H., O'Malley, M., St Clair Gibson, A., & Vaughan, C. (2002). Agonist-antagonist common drive during fatiguing knee extension efforts using surface electromyography. *Journal of Electromyography and Kinesiology*, *12*(5), 375–384. doi:10.1016/S1050-6411(02)00048-2 PMID:12223170
- Muraoka, Y. (2002). Development of an EMG recording device from stimulation electrodes for functional electrical stimulation. *Frontiers of Medical and Biological Engineering*, *11*, 323–333. doi:10.1163/156855701321138969 PMID:12735431
- Murphy, S., & Robertson, D. G. E. (1994). Construction of a high-pass digital filter from a low-pass digital filter. *Journal of Applied Biomechanics Biomechanics*, *10*, 374–381.
- Murray, M. P. (1967). Gait as a total pattern of movement. *American Journal of Physical Medicine*, *46*(1), 290–333. PMID:5336886

Compilation of References

- Murray, W. M., Buchanan, T. S., & Delp, S. L. (2000). The isometric functional capacity of muscles that cross the elbow. *Journal of Biomechanics*, 33, 943–952. doi:10.1016/S0021-9290(00)00051-8 PMID:10828324
- Nagel, J. (2006). Biopotential amplifiers. In J. D. Bronzino (Ed.), *The biomedical engineering handbook, medical devices and systems* (pp. 52.1–52.14). Boca Raton, FL: CRC Press Taylor & Francis Group.
- Naik, G. R., & Kumar, D. K., & Jayadeva. (2010). Twin SVM for gesture classification using the surface electromyogram. *IEEE Transactions on Information Technology in Biomedicine*, 14(2), 301–308. doi:10.1109/TITB.2009.2037752 PMID:20007054
- Nandedkar, S. D., & Sanders, D. B. (1990). Measurement of the amplitude of the envelope. *Muscle & Nerve*, 13(10), 933–938. doi:10.1002/mus.880131008 PMID:2233851
- Nandedkar, S., & Stålberg, E. (1983). Simulation of single muscle fibre action potentials. *Medical & Biological Engineering & Computing*, 21, 158–165. doi:10.1007/BF02441531 PMID:6887989
- Nardone, A., Romanò, C., & Schieppatti, A. (1989). Selective recruitment of high-threshold human motor units during voluntary isotonic lengthening of active muscles. *The Journal of Physiology*, 409, 451–471. PMID:2585297
- Narici, M. V., Binzoni, T., Hiltbrand, E., Fasel, J., Terrier, F., & Cerretelli, P. (1996). In vivo human gastrocnemius architecture with changing joint angle at rest and during graded isometric contraction. *The Journal of Physiology*, 496, 287–297. PMID:8910216
- Navallas, J., & Stålberg, E. (2009). Studying motor end-plate topography by means of scanning-electromyography. *Clinical Neurophysiology*, 120(7), 1335–1341. doi:10.1016/j.clinph.2009.05.014 PMID:19535290
- Neptune, R. R., Kautz, S. A., & Hull, M. L. (1998). Evaluation of performance criteria for simulation of submaximal steady-state cycling using a forward dynamic model. *Journal of Biomechanical Engineering: ASME*, 120, 334–341. doi:10.1115/1.2797999 PMID:10412400
- Neptune, R. R., Kautz, S. A., & Zajac, F. E. (2000). Muscle contributions to specific biomechanical functions do not change in forward versus backward pedaling. *Journal of Biomechanics*, 33, 155–164. doi:10.1016/S0021-9290(99)00150-5 PMID:10653028
- Neuman, M. R. (2010). Biopotential amplifiers. In J. G. Webster (Ed.), *Medical instrumentation: Application and design* (pp. 241–292). Hoboken, NJ: John Wiley & Sons.
- Neuman, M. R. (2010). Biopotential electrodes. In J. G. Webster (Ed.), *Medical instrumentation: Application and design* (pp. 189–241). Hoboken, NJ: John Wiley & Sons.
- Nguyen, H. T., King, L. M., & Knight, G. (2004). Real-time head movement system and embedded Linux implementation for the control of power wheelchairs. In *Proceedings of the 26th Annual International Conference of the IEEE Engineering in Medicine and Biology Society* (pp. 4892–4895).
- Nicola, T. L., & Jewison, D. J. (2012). The anatomy and biomechanics of running. *Clinics in Sports Medicine*, 31(2), 187–201. doi:10.1016/j.csm.2011.10.001 PMID:22341011
- Nielsen, J. B. (2003). How we walk: Central control of muscle activity during human walking. *The Neuroscientist*, 9(3), 195–204. doi:10.1177/1073858403009003012 PMID:15065815
- Nigg, B. (2009). Biomechanical considerations on barefoot movement and barefoot shoe concepts. *Footwear Science*, 1(2), 73–79. doi:10.1080/19424280903204036
- Nigg, B. M., Bahlsen, A. H., Denoth, J., Luethi, S. M., & Stacoff, A. (1986). Factors influencing kinetic and kinematic variables in tuning. In B. Nigg (Ed.), *Biomechanics of running shoes*. Champaign, IL: Human Kinetics Publishers.
- Nigg, B. M., Stefanyshyn, D., Cole, G., Stergiou, P., & Miller, J. (2003). The effect of material characteristics of shoe soles on muscle activation and energy aspects during running. *Journal of Biomechanics*, 36(4), 569–575. doi:10.1016/S0021-9290(02)00428-1 PMID:12600347
- Nigg, B., & Wakeling, J. (2001). Impact forces and muscle tuning: A new paradigm. *Exercise and Sport Sciences Reviews*, 29(1), 37–41. doi:10.1097/00003677-200101000-00008 PMID:11210446

- Niikawa, T., & Kawachi, R. (2006). Human-computer interface using mandibular and tongue movement.[in Japanese]. *Japanese Society for Medical and Biological Engineering*, 44(1), 94–100.
- Northrop, R. B. (2002). *Noninvasive instrumentation and measurement in medical diagnosis*. Boca Raton, FL: CRC Press.
- Oatis, C. A. (2008). *Kinesiology: The mechanics and pathomechanics of human movement*. Philadelphia, PA: Lippincott Williams & Wilkins.
- Oh, S. J. (2003). *Clinical electromyography: Nerve conduction studies*. Philadelphia, PA: Lippincott Williams and Wilkins.
- Ortega, J. D., Fehlman, L. A., & Farley, C. T. (2008). Effects of aging and arm swing on the metabolic cost of stability in human walking. *Journal of Biomechanics*, 41(16), 3303–3308. doi:10.1016/j.jbiomech.2008.06.039 PMID:18814873
- Oseki, M. A., & Hu, H. (2007). Myoelectric control systems—A survey. *Biomedical Signal Processing and Control*, 2, 275–294. doi:10.1016/j.bspc.2007.07.009
- Oskoei, M. A., & Hu, H. (2008). Support vector machine-based classification scheme for myoelectric control applied to upper limb. *IEEE Transactions on Bio-Medical Engineering*, 55(8), 1956–1965. doi:10.1109/TBME.2008.919734 PMID:18632358
- Oskouei, A. H., Paulin, M. G., & Carman, A. B. (2013). Intra-session and inter-day reliability of forearm surface EMG during varying hand grip forces. *Journal of Electromyography and Kinesiology*, 23(1), 216–222. doi:10.1016/j.jelekin.2012.08.011 PMID:22999075
- Osu, R., & Gomi, H. (1999). Multijoint muscle regulation mechanisms examined by measured human arm stiffness and EMG signals. *Journal of Neurophysiology*, 81(4), 1458–1468. PMID:10200182
- Osu, R., Kamimura, N., Iwasaki, H., Nakano, E., Harris, C. M., Wada, Y., & Kawato, M. (2004). Optimal impedance control for task achievement in the presence of signal-dependent noise. *Journal of Neurophysiology*, 92(2), 1199–1215. doi:10.1152/jn.00519.2003 PMID:15056685
- Oya, T., Riek, S., & Cresswell, A. G. (2009). Recruitment and rate coding organisation for soleus motor units across entire range of voluntary isometric plantar flexions. *The Journal of Physiology*, 587(19), 4737–4748. doi:10.1113/jphysiol.2009.175695 PMID:19703968
- Padua, L., Aprile, I., Monaco, M., Fenicia, L., Anniballi, F., Pauri, F., & Tonali, P. (1999). Neurophysiological assessment in the diagnosis of botulism: Usefulness of single-fiber EMG. *Muscle & Nerve*, 22(10), 1388–1392. doi:10.1002/(SICI)1097-4598(199910)22:10<1388::AID-MUS8>3.0.CO;2-3 PMID:10487905
- Pandy, M. G. (2001). Computer modeling and simulation of human movement. *Annual Review of Biomedical Engineering*, 3, 245–273. doi:10.1146/annurev.bioeng.3.1.245 PMID:11447064
- Park, J. (2008). Synthesis of natural arm swing motion in human bipedal walking. *Journal of Biomechanics*, 41(7), 1417–1426. doi:10.1016/j.jbiomech.2008.02.031 PMID:18417138
- Park, S. H., & Lee, S. P. (1998). EMG pattern recognition based on artificial intelligence techniques. *IEEE Transactions on Rehabilitation Engineering*, 6(4), 400–405. doi:10.1109/86.736154 PMID:9865887
- Parsaei, H., Stashuk, D. W., Rasheed, S., Farkas, C., & Hamilton-Wright, A. (2010). Intramuscular EMG signal decomposition. *Critical Reviews in Biomedical Engineering*, 38(5), 435–465. doi:10.1615/CritRevBiomedEng.v38.i5.20 PMID:21175408
- Pasquet, B., Carpentier, A., & Duchateau, J. (2006). Specific modulation of motor unit discharge for a similar change in fascicle length during shortening and lengthening contractions in humans. *The Journal of Physiology*, 577(2), 753–765. doi:10.1113/jphysiol.2006.117986 PMID:16959853
- Patten, C., Lexell, J., & Brown, H. E. (2004). Weakness and strength training in persons with poststroke hemiplegia: Rationale, method, and efficacy. *Journal of Rehabilitation Research and Development*, 41, 293–312. doi:10.1682/JRRD.2004.03.0293 PMID:15543447
- Payan, J. (1978). The blanket principle: a technical note. *Muscle & Nerve*, 1, 423–426. doi:10.1002/mus.880010517 PMID:263984

Compilation of References

- Peng, C. K., Havlin, S., Stanley, H. E., & Goldberger, A. L. (1995). Quantification of scaling exponents and crossover phenomena in nonstationary heartbeat time series. *Chaos (Woodbury, N.Y.)*, 5(1), 82–87. doi:10.1063/1.166141 PMID:11538314
- Perreault, E. J., Crago, P. E., & Kirsch, R. F. (2000). Estimation of intrinsic and reflex contributions to muscle dynamics: A modeling study. *IEEE Transactions on Bio-Medical Engineering*, 47(11), 1413–1421. doi:10.1109/TBME.2000.880092 PMID:11077734
- Person, R. S., & Kudina, L. P. (1972). Discharge frequency and discharge pattern of human motor units during voluntary contraction of muscle. *Electroencephalography and Clinical Neurophysiology*, 32, 471–483. doi:10.1016/0013-4694(72)90058-2 PMID:4112299
- Philipson, L., & Larsson, P. G. (1988). The electromyographic signal as a measure of muscular force: A comparison of detection and quantification techniques. *Electromyography and Clinical Neurophysiology*, 28(2-3), 141–150. PMID:3416804
- Phinyomark, A., Chujit, G., Phukpattaranont, P., Limsakul, C., & Hu, H. (2012a). A preliminary study assessing time-domain EMG features of classifying exercises in preventing falls in the elderly. In *Proceedings of the 9th International Conference on Electrical Engineering/Electronics, Computer, Telecommunications and Information Technology*, Phetchaburi, Thailand (pp. 1-4).
- Phinyomark, A., Hirunviriyaya, S., Nuidod, A., Phukpattaranont, P., & Limsakul, C. (2011a). Evaluation of EMG feature extraction for movement control of upper limb prostheses based on class separation index. In *Proceedings of the 5th Kuala Lumpur International Conference on Biomedical Engineering*, Kuala Lumpur, Malaysia (pp. 750-754).
- Phinyomark, A., Hirunviriyaya, S., Phukpattaranont, P., & Limsakul, C. (2010). Evaluation of EMG feature extraction for hand movement recognition based on Euclidean distance and standard deviation. In *Proceedings of the 7th International Conference on Electrical Engineering/Electronics, Computer, Telecommunications and Information Technology*, Chiang Mai, Thailand (pp. 856-860).
- Phinyomark, A., Limsakul, C., & Phukpattaranont, P. (2008). EMG feature extraction for tolerance of white Gaussian noise. In *Proceedings of the International Workshop and Symposium on Science and Technology*, Nong Khai, Thailand (pp. 178-183).
- Phinyomark, A., Limsakul, C., & Phukpattaranont, P. (2009). A novel feature extraction for robust EMG pattern recognition. Retrieved from <http://arxiv.org/ftp/arxiv/papers/0912/0912.3973.pdf>
- Phinyomark, A., Limsakul, C., & Phukpattaranont, P. (2009). EMG feature extraction for tolerance of 50 Hz interference. In *Proceedings of the 4th International Conference on Engineering Technologies*, Novi Sad, Serbia (pp. 289-293).
- Phinyomark, A., Nuidod, A., Phukpattaranont, P., & Limsakul, C. (2012b). Feature extraction and reduction of wavelet transform coefficients for EMG pattern classification. *Elektronika ir Elektrotehnika*, 122(6), 27-32.
- Phinyomark, A., Phothisonothai, M., Phukpattaranont, P., & Limsakul, C. (2011b). Critical exponent analysis applied to surface electromyography (EMG) signals for gesture recognition. *Metrology and Measurement Systems*, 18(4), 645–658. doi:10.2478/v10178-011-0061-9
- Phinyomark, A., Phukpattaranont, P., & Limsakul, C. (2011c). Wavelet-based denoising algorithm for robust EMG pattern recognition. *Fluctuation and Noise Letters*, 10(2), 157–167. doi:10.1142/S0219477511000466
- Phinyomark, A., Phukpattaranont, P., & Limsakul, C. (2012c). Feature reduction and selection for EMG signal classification. *Expert Systems with Applications*, 39(8), 7420–7431. doi:10.1016/j.eswa.2012.01.102
- Phinyomark, A., Phukpattaranont, P., & Limsakul, C. (2012d). Fractal analysis features for weak and single-channel upper-limb EMG signal. *Expert Systems with Applications*, 39(12), 11156–11163. doi:10.1016/j.eswa.2012.03.039
- Phinyomark, A., Phukpattaranont, P., & Limsakul, C. (2012e). Investigating long-term effects of feature extraction methods for continuous EMG pattern classification. *Fluctuation and Noise Letters*, 11(4), 1250028. doi:10.1142/S0219477512500289

- Phinyomark, A., Phukpattaranont, P., & Limsakul, C. (2012f). The usefulness of wavelet transform to reduce noise in the SEMG signal. In M. Schwartz (Ed.), *EMG methods for evaluating muscle and nerve function* (pp. 107–132). Rijeka, Croatia: InTech. doi:10.5772/25757
- Phinyomark, A., Phukpattaranont, P., Limsakul, C., & Phothisonothai, M. (2011d). Electromyography (EMG) signal classification based on detrended fluctuation analysis. *Fluctuation and Noise Letters*, *10*(3), 281–301. doi:10.1142/S0219477511000570
- Phinyomark, A., Quaine, F., Charbonnier, S., Serviere, C., Tarpin-Bernard, F., & Laurillau, Y. (2013a). A feasibility study on the use of anthropometric variables to make muscle-computer interface more practical. *Engineering Applications of Artificial Intelligence*, *26*(7), 1681–1688. doi:10.1016/j.engappai.2013.01.004
- Phinyomark, A., Quaine, F., Charbonnier, S., Serviere, C., Tarpin-Bernard, F., & Laurillau, Y. (2013b). EMG feature evaluation for improving myoelectric pattern recognition robustness. *Expert Systems with Applications*, *40*(12), 4832–4840. doi:10.1016/j.eswa.2013.02.023
- Phinyomark, A., Thongpanja, S., Hu, H., Phukpattaranont, P., & Limsakul, C. (2012g). The usefulness of mean and median frequencies in electromyography analysis. In G. R. Naik (Ed.), *Computational intelligence in electromyography analysis - A perspective on current applications and future challenges* (pp. 195–220). Rijeka, Croatia: InTech. doi:10.5772/50639
- Phothisonothai, M., & Nakagawa, M. (2007). Fractal-based EEG data analysis of body parts movement imagery tasks. *The Journal of Physiological Sciences; JPS*, *57*(4), 217–226. doi:10.2170/physiolsci.RP006307 PMID:17637165
- Pink, M., Jobe, F., & Perry, J. (1990). Electromyographic analysis of the shoulder during the golf swing. *The American Journal of Sports Medicine*, *18*(2), 137–140. doi:10.1177/036354659001800205 PMID:2343980
- Pink, M., Perry, J., & Jobe, F. (1993). EMG analysis of the trunk in golfers. *American Journal of Sports Medicine*, *21*(3), 385–388.
- Piotrkiewicz, M., & Miller-Larsson, A. (1987). A method of description of single muscle fiber activity. *Biological Cybernetics*, *56*, 237–245. doi:10.1007/BF00365218 PMID:3607099
- Pizzi, A., Carlucci, G., Falsini, C., Verdesca, S., & Grippo, A. (2005). Application of a volar static splint in poststroke spasticity of the upper limb. *Archives of Physical Medicine and Rehabilitation*, *86*, 1855–1859. doi:10.1016/j.apmr.2005.03.032 PMID:16181954
- Plonsey, R. (1974). The active fibre in a volume conductor. *IEEE Transactions on Bio-Medical Engineering*, *21*, 371–381. doi:10.1109/TBME.1974.324406 PMID:4461667
- Plonsey, R., & Barr, R. C. (2000). *Bioelectricity. A quantitative approach*. New York: Kluwer Academic. doi:10.1007/978-1-4757-3152-1
- Pomeroy, V. M., King, L., Pollock, A., Baily-Hallam, A., & Langhorne, P. (2006). Electrostimulation for promoting recovery of movement or functional ability after stroke. *Cochrane Database of Systematic Reviews (Online)*, CD003241.
- Pontzer, H., Holloway, J. H., Raichlen, D. A., & Lieberman, D. E. (2009). Control and function of arm swing in human walking and running. *The Journal of Experimental Biology*, *212*(4), 523–534. doi:10.1242/jeb.024927 PMID:19181900
- Popovic, D. B., Popovic, M. B., Sinkjaer, T., Stefanovic, A., & Schwirtlich, L. (2004). Therapy of paretic arm in hemiplegic subjects augmented with a neural prosthesis: a cross-over study. *Canadian Journal of Physiology and Pharmacology*, *82*, 749–756. doi:10.1139/y04-057 PMID:15523532
- Popović, D. B., Sinkaer, T., & Popović, M. B. (2009). Electrical stimulation as a means for achieving recovery of function in stroke patients. *NeuroRehabilitation*, *25*, 45–58. PMID:19713618
- Popovic, D., & Sinkjaer, T. (2000). *Control of movement for the physically disabled*. London: Springer-Verlag. doi:10.1007/978-1-4471-0433-9
- Powers, R. K., & Binder, M. D. (2001). Input-output functions of mammalian motoneurons. *Reviews of Physiology, Biochemistry and Pharmacology*, *143*, 137–263. doi:10.1007/BFb0115594 PMID:11428264

Compilation of References

- Pozzo, M., Farina, D., & Merletti, R. (2004). Electromyography: Detection, processing, and applications. In J. Moore, & G. Zouridakis (Eds.), *Biomedical technology and devices handbook* (pp. 4.1–4.60). Boca Raton, FL: CRC Press.
- Preston, D. C., & Shapiro, B. E. (2005). *Electromyography and neuromuscular disorders: Clinical-electrophysiologic correlation*. Philadelphia, PA: Butterworth-Heinemann.
- Prilutsky, B. I. (2000). Coordination of two- and one-joint muscles: Functional consequences and implications for motor control. *Motor Control*, 4(1), 1–44. PMID:10675807
- Prochazka, G. L., Clarac, F., Loeb, G. E., Rothwell, J. C., & Wolpaw, J. R. (2000). What do reflex and voluntary mean? Modern views on an ancient debate. *Experimental Brain Research*, 130(4), 417–432. doi:10.1007/s002219900250 PMID:10717785
- Prutchi, D., & Norris, M. (2005). *Design and development of medical electronic instrumentation*. Hoboken, NJ: John Wiley and Sons, Inc. doi:10.1002/0471681849
- Prutchi, D., & Norris, M. (2005). *Design and development of medical electronic instrumentation: A practical perspective of the design, construction, and test of medical devices*. Hoboken, NJ: John Wiley & Sons.
- Radicheva, N., Gerilovsky, L., & Gydikov, A. (1986). Changes in the muscle fibre extracellular action potentials in long-lasting (fatiguing) activity. *European Journal of Applied Physiology and Occupational Physiology*, 55(5), 545–552. doi:10.1007/BF00421651 PMID:3769911
- Reaz, M. B. I., Hussain, M. S., & Mohd-Yasin, F. (2006). Techniques of EMG signal analysis: Detection, processing, classification and applications. *Biological Procedures Online*, 8(1), 11–35. doi:10.1251/bpo115 PMID:16799694
- Rhee, K. W., You, K. J., & Shin, H. C. (2011). Recognition of finger motion with sEMG and gyrosensor signals. *Journal of Measurement Science and Instrumentation*, 2(2), 136–139.
- Richardson, C. A., Jull, G. A., Toppenberg, R., & Comerford, M. (1992). Techniques for active lumbar stabilisation for spinal protection: A pilot study. *The Australian Journal of Physiotherapy*, 38, 105–112. doi:10.1016/S0004-9514(14)60555-9
- Richman, J. S., & Moorman, J. R. (2000). Physiological time series analysis using approximate entropy and sample entropy. *American Journal of Physiology. Heart and Circulatory Physiology*, 278(6), H2039–H2049. PMID:10843903
- Riek, S., & Bawa, P. (1992). Recruitment of motor units in human forearm extensors. *Journal of Neurophysiology*, 68, 100–108. PMID:1517816
- Robertson, D. G. E., & Dowling, J. J. (2003). Design and responses of Butterworth and critically damped digital filters. *Journal of Electromyography and Kinesiology: Official Journal of the International Society of Electrophysiological Kinesiology*, 13(6), 569–573. doi:10.1016/S1050-6411(03)00080-4 PMID:14573371
- Rodriguez-Falces, J., Dimitrova, N., Dimitrov, G., & Gila, L. (2011c). Shape variability of potentials recorded by a single-fiber electrode and its effect on jitter estimation. *Annals of Biomedical Engineering*, 39(2), 812–823. doi:10.1007/s10439-010-0207-z PMID:21108004
- Rodriguez-Falces, J., Gila, L., & Dimitrova, N. A. (2012a). The morphology of single muscle fibre potentials - Part I: Simulation study of the distortion introduced by the distant-interfering potentials. *Journal of Electromyography and Kinesiology*, 23(1), 14–23. doi:10.1016/j.jelekin.2012.07.002 PMID:22863372
- Rodriguez-Falces, J., Gila, L., & Dimitrova, N. A. (2012b). The morphology of single muscle fibre potentials - Part II: Experimental findings. *Journal of Electromyography and Kinesiology*, 23(1), 24–32. doi:10.1016/j.jelekin.2012.07.003 PMID:22868038
- Rodriguez-Falces, J., Navallas, J., Gila, L., Dimitrova, N., & Malanda, A. (2011a). Estimating the duration of intracellular action potentials in muscle fibres from single-fiber extracellular potentials. *Journal of Neuroscience Methods*, 197, 221–230. doi:10.1016/j.jneumeth.2011.02.022 PMID:21396959
- Rodriguez-Falces, J., Navallas, J., Gila, L., Malanda, A., & Dimitrova, N. A. (2012c). Influence of the shape of intracellular potentials on the morphology of single-fiber extracellular potentials in human muscle fibers. *Medical & Biological Engineering & Computing*, 50(5), 447–460. doi:10.1007/s11517-012-0879-7 PMID:22447347

- Rodriguez-Falces, J., Navallas, J., Gila, L., Rodríguez, I., & Malanda, A. (2011b). The peak-to-peak ratio of single-fibre potentials is little influenced by changes in the electrode positions close to the muscle fibre. *Journal of Electromyography and Kinesiology*, *21*, 423–432. doi:10.1016/j.jelekin.2010.04.001 PMID:20451410
- Röhrle, O., Davidson, J. B., & Pullan, A. J. (2012). A physiologically based, multi-scale model of skeletal muscle structure and function. *Frontiers in Physiology*, *3*, 1–14. doi:10.3389/fphys.2012.00358 PMID:22275902
- Rubin, D. I. (2009). Assessing the neuromuscular junction with repetitive stimulation studies. In J. R. Daube, & D. I. Rubin (Eds.), *Clinical neurophysiology* (pp. 401–451). New York: Oxford University Press.
- Rudroff, T., Christou, E. A., Poston, B., Bojsen-Moller, J., & Enoka, R. M. (2007). Time to failure of a sustained contraction is predicted by target torque and initial electromyographic bursts in elbow flexor muscles. *Muscle & Nerve*, *35*(5), 657–666. doi:10.1002/mus.20752 PMID:17294440
- Ruiz, A. F., Brunetti, F. J., Rocon, E., Moreno, J. C., Bueno, L., & Pons, J. L. (2008). NeuroLab: A multimodal networked exoskeleton for neuromotor and biomechanical research. In *Proceedings of the International Conference on Biomedical Electronics and Devices - BioDevices*, *2*, (pp. 68-73).
- Rushton, D. N. (2003). Functional electrical stimulation and rehabilitation--An hypothesis. *Medical Engineering & Physics*, *25*, 75–78. doi:10.1016/S1350-4533(02)00040-1 PMID:12485788
- Sadeghi, H., Allard, P., Prince, F., & Labelle, H. (2000). Symmetry and limb dominance in able-bodied gait: A review. *Gait & Posture*, *12*(1), 34–45. doi:10.1016/S0966-6362(00)00070-9 PMID:10996295
- Sanders, D. B. (1987). The electrodiagnosis of myasthenia gravis. *Annals of the New York Academy of Sciences*, *505*, 539–556. doi:10.1111/j.1749-6632.1987.tb51322.x PMID:2825576
- Sanders, D. B., Howard, J. F., & Johns, T. R. (1979). Single-fiber electromyography in myasthenia gravis. *Neurology*, *29*(1), 68–76. doi:10.1212/WNL.29.1.68 PMID:218146
- Sanders, D. B., & Stålberg, E. (1996). Single-fibre electromyography. *Muscle & Nerve*, *19*, 1069–1083. doi:10.1002/(SICI)1097-4598(199609)19:9<1069::AID-MUS1>3.0.CO;2-Y PMID:8761262
- Saponas, T. S., Kelly, D., Parviz, B. A., & Tan, D. S. (2009). Optically sensing tongue gestures for computer input. In *Proceedings ACM Symposium on User Interface Software and Technology* (pp. 177-180).
- Saponas, T. S., Tan, D. S., Morris, D., & Balakrishnan, R. (2008). Demonstrating the feasibility of using forearm electromyography for muscle-computer interfaces. In *Proceedings of the SIGCHI Conference on Human Factors in Computing Systems*, Florence, Italy (pp. 515-524).
- Saponas, T. S., Tan, D. S., Morris, D., Balakrishnan, R., Turner, J., & Landay, J. A. (2009). Enabling always-available input with muscle-computer interfaces. In *Proceedings of the ACM Symposium on User Interface Software and Technology*, Victoria, Canada (pp. 167-176).
- Saponas, T. S., Tan, D. S., Morris, D., Turner, J., & Landay, J. A. (2010). Making muscle-computer interfaces more practical. In *Proceedings of the SIGCHI Conference on Human Factors in Computing Systems*, Atlanta, GA (pp. 851-854).
- Sasaki, M., Arakawa, T., Nakayama, A., Obinata, G., & Yamaguchi, M. (2012b). Estimation of tongue movement based on suprahyoid muscle activity. In *Proceedings of the 2011 IEEE International Symposium on Micro-Nano Mechatronics and Human Science* (pp. 433-438).
- Sasaki, M., Onishi, K., Arakawa, T., Nakayama, A., Stefanov, D., & Yamaguchi, M. (2013a). Real-time estimation of tongue movement based on suprahyoid muscle activity. In *Proceedings of the 35th Annual International Conference of the IEEE Engineering in Medicine and Biology Society* (pp. 4605-4608).
- Sasaki, M., Onishi, K., Nakayama, A., Kamata, K., Stefanov, D., & Yamaguchi, M. (2013b). A system for tongue motor function training. In *Proceedings of the SICE Annual Conference 2013* (pp. 1598-1599).
- Sasaki, M., Arakawa, T., Nakayama, A., & Yamaguchi, M. (2012a). Method of tongue movement estimation based on suprahyoid muscle coordination.[in Japanese]. *Transactions of Japanese Society for Medical and Biological Engineering*, *50*(1), 31–37.

Compilation of References

- Sawhney, G. S. (2007). *Fundamentals of biomedical engineering*. New Delhi, India: New Age International (P) Ltd. Publisher.
- Saxena, S., Nikolic, S., & Popovic, D. (1995). An EMG-controlled grasping system for tetraplegics. *Journal of Rehabilitation Research and Development*, *32*, 17–24. PMID:7760263
- Schauer, T., Salbert, R., Negård, N.-O., & Raisch, J. (2004). Detection and filtering of EMG for assessing voluntary muscle activity during FES. In *Proceedings of 9th Annual Conference of the International FES Society* (pp. 1–3). Bournemouth, UK.
- Scherer, R., Muller, G. R., Neuper, C., Graimann, B., & Pfurtscheller, G. (2004). An asynchronously controlled EEG-based virtual keyboard: Improvement of the spelling rate. *IEEE Transactions on Bio-Medical Engineering*, *51*(6), 979–984. doi:10.1109/TBME.2004.827062 PMID:15188868
- Schiaffino, S., & Reggiani, C. (2011). Fiber types in mammalian skeletal muscles. *Physiological Reviews*, *91*(4), 1447–1531. doi:10.1152/physrev.00031.2010 PMID:22013216
- Schillings, M. L., Hoefsloot, W., Stegeman, D. F., & Zwarts, M. J. (2003). Relative contributions of central and peripheral factors to fatigue during a maximal sustained effort. *European Journal of Applied Physiology*, *90*(5-6), 562–568. doi:10.1007/s00421-003-0913-4 PMID:12905050
- Schünke, M., Schulte, E., Schumacher, U., Voll, M., & Wesker, K. (2007). *Allgemeine Anatomie und Bewegungssystem. Prometheus. Lernatlas der Anatomie*. Stuttgart, Germany: Georg Thieme Verlag.
- Schwartz, M. S., & Stålberg, E. (1975). Myasthenia gravis with features of the myasthenic syndrome. An investigation with electrophysiologic methods including single-fiber electromyography. *Neurology*, *25*(1), 80–84. doi:10.1212/WNL.25.1.80 PMID:1167410
- Sejersted, O. M., & Sjogaard, G. (2000). Dynamics and consequences of potassium shifts in skeletal muscle and heart during exercise. *Physiological Reviews*, *80*(4), 1411–1481. PMID:11015618
- Sennels, S., Biering-Sorensen, F., Andersen, O. T., & Hansen, S. D. (1997). Functional neuromuscular stimulation controlled by surface electromyographic signals produced by volitional activation of the same muscle: adaptive removal of the muscle response from the recorded EMG-signal. *IEEE Transactions on Rehabilitation Engineering*, *5*, 195–206. doi:10.1109/86.593293 PMID:9184905
- Senn, W. K., Wyler, K., Clamann, H. P., Kleinle, J., Lüscher, H.-R., & Müller, L. (1997). Size principle and information theory. *Biological Cybernetics*, *76*, 11–22. doi:10.1007/s004220050317 PMID:9050202
- Sensinger, J. W., Lock, B. A., & Kuiken, T. A. (2009). Adaptive pattern recognition of myoelectric signals: exploration of conceptual framework and practical algorithms. *IEEE Transactions on Neural Systems and Rehabilitation Engineering*, *17*(3), 270–278. doi:10.1109/TNSRE.2009.2023282 PMID:19497834
- Shadmehr, R., & Mussa-Ivaldi, F. A. (1994). Adaptive representation of dynamics during learning of a motor task. *The Journal of Neuroscience*, *14*(1), 3208–3224. PMID:8182467
- Shalaby, R., Schauer, T., Liedecke, W., & Raisch, J. (2011). Amplifier design for EMG recording from stimulation electrodes during functional electrical stimulation leg cycling ergometry. *Biomedical Engineering*, *56*, 23–33. doi:10.1515/bmt.2010.055 PMID:21162696
- Sheffler, L. R., & Chae, J. (2007). Neuromuscular electrical stimulation in neurorehabilitation. *Muscle & Nerve*, *35*, 562–590. doi:10.1002/mus.20758 PMID:17299744
- Shefner, J. M. (2001). Motor unit number estimation in human neurological diseases and animal models. *Clinical Neurophysiology*, *112*(6), 955–964. doi:10.1016/S1388-2457(01)00520-X PMID:11377252
- Shenoy, P., Miller, K. J., Crawford, B., & Rao, R. N. (2008). Online electromyographic control of a robotic prosthesis. *IEEE Transactions on Bio-Medical Engineering*, *55*(3), 1128–1135. doi:10.1109/TBME.2007.909536 PMID:18334405
- Shibanoki, T., Shima, K., Tsuji, T., Otsuka, A., & Chin, T. (2009). A novel channel selection method based on partial KL information measure for EMG-based motion classification. *Proceedings of 13th International Conference on Biomedical Engineering*, *23*, 694–698.

- Shindo, K., Fujiwara, T., Hara, J., Oba, H., Hotta, F., & Tsuji, T. et al. (2011). Effectiveness of hybrid assistive neuromuscular dynamic stimulation therapy in patients with subacute stroke: A randomized controlled pilot trial. *Neurorehabilitation and Neural Repair*, 25, 830–837. doi:10.1177/1545968311408917 PMID:21666139
- Shyu, L. Y., Chen, J. Y., Tatn, R. W., & Hu, W. (2002). A new electrode system for hand action discrimination. *Journal of Medical and Biological Engineering*, 22(4), 211–217.
- Silva, L., Marta, S., Vaz, J., Fernandes, O., Castro, M. A., & Pezarat-Correia, P. (2013). Trunk muscle activation during golf swing: Baseline and threshold. *Journal of Electromyography and Kinesiology*, 23(5), 1174–1182.
- Silver, J. (2004). What Is EMG? In L. Weiss, J. K. Silver, & J. Weiss (Eds.), *Easy EMG* (pp. 1–5). China: Butterworth-Heinemann. doi:10.1016/B978-0-7506-7431-7.50006-3
- Simpson, R. C., & Levine, S. P. (2002). Voice control of a powered wheelchair. *IEEE Transactions on Neural Systems and Rehabilitation Engineering*, 10(2), 122–125. doi:10.1109/TNSRE.2002.1031981 PMID:12236450
- Sinha, U., Sinha, S., Hodgson, J. A., & Edgerton, R. V. (2011). Human soleus muscle architecture at different ankle joint angles from magnetic resonance diffusion tensor imaging. *Journal of Applied Physiology*, 110(3), 807–819. doi:10.1152/jappphysiol.00923.2010 PMID:21164150
- Sirin, A. V., & Patla, A. E. (1987). Myoelectric changes in the triceps surae muscles under sustained contractions. Evidence for synergism. *European Journal of Applied Physiology and Occupational Physiology*, 56(2), 238–244. PMID:3569232
- Slater-Hammel, A. T. (1948). Action current study of contraction-movement relationship in golf stroke. *Research Quarterly*, 19(3), 164–177. PMID:18887614
- Smith, R. J., Huberdeau, D., Tenore, F., & Thakor, N. V. (2009). Real-time myoelectric decoding of individual finger movements for a virtual target task. In *Proceedings of the 31st Annual International Conference of the IEEE EMBS*, Minneapolis, MN (pp. 2376–2379).
- Smith, R. J., Tenore, F., Huberdeau, D., Etienne-Cummings, R., & Thakor, N. V. (2008). Continuous decoding of finger position from surface EMG signals for the control of powered prostheses. In *Proceedings of the 30th Annual International Conference of the IEEE EMBS*, Vancouver, Canada (pp. 197–200).
- Smith, B. E. (2009). Quantitative electromyography. In J. R. Daube, & D. I. Rubin (Eds.), *Clinical neurophysiology* (pp. 451–475). New York: Oxford University Press.
- Smith, G. V., Alon, G., Roys, S. R., & Gullapalli, R. P. (2003). Functional MRI determination of a dose-response relationship to lower extremity neuromuscular electrical stimulation in healthy subjects. *Experimental Brain Research*, 150, 33–39. PMID:12698214
- Smith, J. L., Martin, P. G., Gandevia, S. C., & Taylor, J. L. (2007). Sustained contraction at very low forces produces prominent supraspinal fatigue in human elbow flexor muscles. *Journal of Applied Physiology (Bethesda, Md.)*. doi:10.1152/jappphysiol.00220.2007
- Smith, L. C., Zhong, T., & Bawa, P. (1995). Dynamic properties of human motoneurons. *Canadian Journal of Physiology and Pharmacology*, 73, 113–123. doi:10.1139/y95-016 PMID:7600441
- Søgaard, K., Christensen, H., Jansen, B. R., Finsen, L., & Sjøgaard, G. (1996). Motor control and kinetics during low level concentric and eccentric contractions in man. *Electroencephalography and Clinical Neurophysiology*, 101(5), 453–460. doi:10.1016/0924-980X(96)95629-5 PMID:8913200
- Solnik, S., DeVita, P., Rider, P., Long, B., & Hortobágyi, T. (2008). Teager-Kaiser Operator improves the accuracy of EMG onset detection independent of signal-to-noise ratio. *Acta Bioengener Biomechanics*, 10(2), 65–68. PMID:19032000
- Solnik, S., Rider, P., Steinweg, K., DeVita, P., & Hortobágyi, T. (2010). Teager-Kaiser energy operator signal conditioning improves EMG onset detection. *European Journal of Applied Physiology*, 110(3), 489–498. doi:10.1007/s00421-010-1521-8 PMID:20526612
- Sonoda, Y. (1974). Observation of tongue movements employing a magnetometer sensor. *IEEE Transactions on Magnetics*, 10, 954–957. doi:10.1109/TMAG.1974.1058464

Compilation of References

- Sonoo, M., & Stålberg, E. (1993). The ability of MUP parameters to discriminate between normal and neurogenic MUPs in concentric EMG: analysis of the MUP thickness and the proposal of size index. *Electroencephalography and Clinical Neurophysiology*, 89(5), 291–303. doi:10.1016/0168-5597(93)90068-Z PMID:7691568
- Sörnmo, L., & Laguna, P. (2005). *Bioelectrical signal processing in cardiac and neurological application*. New York: Elsevier Academic Press.
- Spaans, F., Vredevelde, J. W., Morre, H. H. E., Jacobs, B. C., & Debaets, M. H. (2003). Dysfunction at the motor end-plate and axon membrane in Guillain-Barré Syndrome: A single-fiber EMG study. *Muscle & Nerve*, 27(4), 426–434. doi:10.1002/mus.10334 PMID:12661043
- Stålberg, E. (1966). Propagation velocity in human muscle fibres in situ. *Acta Physiologica Scandinavica*, 70(287), 1–112.
- Stålberg, E. (1977). Electrogenesis in human dystrophic muscle. In L. P. Rowland (Ed.), *Pathogenesis of human muscular dystrophies* (pp. 570–587). Amsterdam, The Netherlands: Excerpta Medica.
- Stålberg, E. (1986). Single fiber EMG, macro EMG, and scanning EMG. New ways of looking at the motor unit. *CRC Critical Reviews in Clinical Neurobiology*, 2(2), 125–167. PMID:3536309
- Stålberg, E. (1987). New EMG methods to study the motor unit. *Electroencephalography and Clinical Neurophysiology. Supplement*, 39, 38–49. PMID:3308420
- Stålberg, E., Andreassen, S., Falck, B., Lang, H., Rosenfalck, A., & Trojaborg, W. (1986). Quantitative analysis of individual motor unit potentials: A proposition for standardized terminology and criteria for measurement. *Journal of Clinical Neurophysiology*, 3(4), 313–348. doi:10.1097/00004691-198610000-00003 PMID:3332279
- Stålberg, E., & Antoni, L. (1980). Electrophysiological cross section of the motor unit. *Journal of Neurology, Neurosurgery, and Psychiatry*, 43(6), 469–474. doi:10.1136/jnnp.43.6.469 PMID:7205287
- Stålberg, E., & Dioszeghy, P. (1991). Scanning EMG in normal muscle and in neuromuscular disorders. *Electroencephalography and Clinical Neurophysiology*, 81(6), 403–416. doi:10.1016/0168-5597(91)90048-3 PMID:1721580
- Stålberg, E., Ekstedt, J., & Broman, A. (1974). Neuro-muscular transmission in myasthenia gravis studied with single fibre electromyography. *Journal of Neurology, Neurosurgery, and Psychiatry*, 37(5), 540–547. doi:10.1136/jnnp.37.5.540 PMID:4366058
- Stålberg, E., & Eriksson, P. O. (1987). A scanning electromyographic study of the topography of human masseter single motor units. *Archives of Oral Biology*, 32(11), 793–797. doi:10.1016/0003-9969(87)90005-7 PMID:3482348
- Stålberg, E., & Falck, B. (1997). The role of EMG in neurology. *Electroencephalography and Clinical Neurophysiology*, 103(6), 579–598. doi:10.1016/S0013-4694(97)00138-7 PMID:9546485
- Stålberg, E., Falck, B., Sonoo, M., Stålberg, S., & As-tröm, M. (1995). Multi-MUP EMG analysis—A two year experience in daily clinical work. *Electroencephalography and Clinical Neurophysiology*, 97(3), 145–154. doi:10.1016/0924-980X(95)00007-8 PMID:7607102
- Stålberg, E., & Sanders, D. B. (2009). Jitter recordings with concentric needle electrodes. *Muscle & Nerve*, 40(3), 331–339. doi:10.1002/mus.21424 PMID:19705424
- Stålberg, E., & Trontelji, J. V. (1994). *Single fiber electromyography studies in healthy and diseased muscle*. New York: Raven Press.
- Stålberg, E., & Trontelj, J. (1979). *Single fibre electromyography*. Old Woking, UK: Raven Press.
- Stanton, T., & Kawchuk, G. (2008). The effect of abdominal stabilization contractions on posteroanterior spinal stiffness. *Spine*, 33(6), 694–701. doi:10.1097/BRS.0b013e318166e034 PMID:18344865
- Stashuk, D. W. (1999). Decomposition and quantitative analysis of clinical electromyographic signals. *Medical Engineering & Physics*, 21(6-7), 389–404. doi:10.1016/S1350-4533(99)00064-8 PMID:10624736

- Stauder, G., Flachenecker, C., & Wolf, W. (2001). Onset detection in surface electromyographic signals: A systematic comparison of methods. *EURASIP Journal on Applied Signal Processing*, 2, 67–81. doi:10.1155/S1110865701000191
- Staudenmann, D., Kingma, I., Daffertshofer, A., Stegeman, D. F., & van Dieën, J. H. (2009). Heterogeneity of muscle activation in relation to force direction: A multi-channel surface electromyography study on the triceps surae muscle. *Journal of Electromyography and Kinesiology*, 19, 882–895. doi:10.1016/j.jelekin.2008.04.013 PMID:18556216
- Stein, R. B., French, A. S., Mannard, A., & Yemm, R. (1972). New methods for analyzing motor function in man and animals. *Brain Research*, 40(1), 187–192. doi:10.1016/0006-8993(72)90126-6 PMID:5033795
- Stephenson, J. L., De Serres, S. J., & Lamontagne, A. (2010). The effect of arm movements on the lower limb during gait after a stroke. *Gait & Posture*, 31(1), 109–115. doi:10.1016/j.gaitpost.2009.09.008 PMID:19854654
- Stokes, I. A. F., & Gardner-Morse, M. G. (2001). Lumbar spinal muscle activation synergies predicted by multi-criteria cost function. *Journal of Biomechanics*, 34(6), 733–740. doi:10.1016/S0021-9290(01)00034-3 PMID:11470110
- Stokes, I. A. F., Gardner-Morse, M. G., & Henry, S. M. (2011). Abdominal muscle activation increases lumbar spinal stability: Analysis of contributions of different muscle groups. *Clinical Biomechanics (Bristol, Avon)*, 26, 797–803. doi:10.1016/j.clinbiomech.2011.04.006 PMID:21571410
- Stolze, H., Kuhtz-Buschbeck, J. P., Mondwurf, C., Boczek-Funcke, A., Jöhnk, K., Deuschl, G., & Illert, M. (1997). Gait analysis during treadmill and overground locomotion in children and adults. *Electroencephalography and Clinical Neurophysiology*, 105(6), 490–497. doi:10.1016/S0924-980X(97)00055-6 PMID:9448652
- Stotz, P. J., & Bawa, P. (2001). Motor unit recruitment during lengthening contractions of human wrist flexors. *Muscle & Nerve*, 24(11), 1535–1541. doi:10.1002/mus.1179 PMID:11745957
- Stroeve, S. (1999). Impedance characteristics of a neuro-musculoskeletal model of the human arm I. Posture control. *Biological Cybernetics*, 81(5-6), 475–494. doi:10.1007/s004220050577 PMID:10592022
- Subasi, A. (2012). Medical decision support system for diagnosis for neuromuscular disorders using DWT and fuzzy support vector machines. *Computers in Biology and Medicine*, 42(8), 806–815. doi:10.1016/j.compbiomed.2012.06.004 PMID:22763356
- Subasi, A. (2013). Classification of EMG signals using PSO optimized SVM for diagnosis of neuromuscular disorders. *Computers in Biology and Medicine*, 43(5), 576–586. doi:10.1016/j.compbiomed.2013.01.020 PMID:23453053
- Tabernig, C. B., & Acevedo, R. C. (2008). M-wave elimination from surface electromyogram of electrically stimulated muscles using singular value decomposition: preliminary results. *Medical Engineering & Physics*, 30, 800–803. doi:10.1016/j.medengphy.2007.09.001 PMID:17981071
- Tanaka, Y., Onishi, T., Tsuji, T., Yamada, N., Takeda, Y., & Masamori, I. (2007). Analysis and modeling of human impedance properties for designing a human-machine control system. In *Proceeding of the IEEE International Conference on Robotics and Automation* (pp. 3627–3632).
- Tang, X., Liu, Y., Lv, C., & Sun, D. (2012). Hand motion classification using a multi-channel surface electromyography sensor. *Sensors (Basel, Switzerland)*, 12(2), 1130–1147. doi:10.3390/s120201130 PMID:22438703
- Tanji, J., & Kato, M. (1972). Discharges of single motor units at voluntary contractions of abductor digiti minimi muscle in man. *Brain Research*, 45, 590–593. doi:10.1016/0006-8993(72)90488-X PMID:4634329
- Tanji, J., & Kato, M. (1973). Firing rate of individual motor units in voluntary contractions of abductor digiti minimi muscle in man. *Experimental Neurology*, 40, 771–783. doi:10.1016/0014-4886(73)90111-8 PMID:4353259
- Taylor, & Chappell, P. (2004). Variation in system gain when using voluntary EMG to control electrical stimulation of the same muscle. In D. Wood (Ed.), *Proceedings of 9th Annual Conference of the International Functional Electrical Stimulation Society*. Bournemouth, UK.

Compilation of References

- Taylor, R. (1990). Interpretation of the correlation coefficient: A basic review. *Journal of Diagnostic Medical Sonography*, 6(1), 35–39. doi:10.1177/875647939000600106
- Tenore, F. V. G., Ramos, A., Fahmy, A., Acharya, S., Etienne-Cummings, R., & Thakor, N. V. (2007). Towards the control of individual fingers of a prosthetic hand using surface EMG signals. In *Proceedings of the 29th Annual International Conference of the IEEE EMBS*, Lyon, France (pp. 6145–6148).
- Tenore, F. V. G., Ramos, A., Fahmy, A., Acharya, S., Etienne-Cummings, R., & Thakor, N. V. (2009). Decoding of individual finger movements using surface electromyography. *IEEE Transactions on Bio-Medical Engineering*, 56(5), 1427–1434. doi:10.1109/TBME.2008.2005485 PMID:19473933
- Ter Haar Romeny, B. M., Danier van der Gon, J. J., & Gielen, C. C. A. M. (1984). Relation between location of a motor unit in the human biceps brachii and its critical firing levels for different tasks. *Experimental Neurology*, 85, 631–650. doi:10.1016/0014-4886(84)90036-0 PMID:6468581
- Terashima, S. G., Satoh, E., Kotake, K., Sasaki, E., Ueki, K., & Sasaki, S. (2010). Development of a mouthpiece type remote controller for disabled persons. *Journal of Biomechanical Science and Engineering*, 5(1), 66–77. doi:10.1299/jbse.5.66
- Therriault, G., & Lachance, P. (1998). Golf injuries. An overview. *Sports Medicine (Auckland, N.Z.)*, 26(1), 43–57. doi:10.2165/00007256-199826010-00004 PMID:9739540
- Thongpanja, S., Phinyomark, A., Phukpattaranont, P., & Limsakul, C. (2013). Mean and median frequency of EMG signal to determine muscle force based on time-dependent power spectrum. *Elektronika ir Elektrotechnika*, 19(3), 51–56.
- Thorsen, R. (1999). An artefact suppressing fast-recovery myoelectric amplifier. *IEEE Transactions on Bio-Medical Engineering*, 46, 764–766. doi:10.1109/10.764955 PMID:10356884
- Thorsen, R. A., Occhi, E., Boccardi, S., & Ferrarin, M. (2006). Functional electrical stimulation reinforced tenodesis effect controlled by myoelectric activity from wrist extensors. *Journal of Rehabilitation Research and Development*, 43, 247–256. doi:10.1682/JRRD.2005.04.0068 PMID:16847791
- Thorsen, R., Ferrarin, M., Spadone, R., & Frigo, C. (1999). Functional control of the hand in tetraplegics based on residual synergistic EMG activity. *Artificial Organs*, 23, 470–473. doi:10.1046/j.1525-1594.1999.06362.x PMID:10378946
- Thorsen, R., Spadone, R., & Ferrarin, M. (2001). A pilot study of myoelectrically controlled FES of upper extremity. *IEEE Transactions on Neural Systems and Rehabilitation Engineering*, 9, 161–168. doi:10.1109/7333.928576 PMID:11474969
- Thorstensson, A. (1986). How is the normal locomotor program modified to produce backward walking? *Experimental Brain Research*, 61(3), 664–668. doi:10.1007/BF00237595 PMID:3956625
- Thorstensson, A., Carlson, H., Zomlefer, M. R., & Nilsson, J. (1982). Lumbar back muscle activity in relation to trunk movements during locomotion in man. *Acta Physiologica Scandinavica*, 116(1), 13–20. doi:10.1111/j.1748-1716.1982.tb10593.x PMID:7158389
- Tkach, D., Huang, H., & Kuiken, T. A. (2010). Study of stability of time-domain features for electromyographic pattern recognition. *Journal of Neuroengineering and Rehabilitation*, 7(21). PMID:20492713
- Togawa, T., Tamura, T., & Öberg, P. A. (1997). *Biomedical transducers and instruments*. Boca Raton, FL: CRC Press.
- Tortora, G. J., & Derrickson, B. (2009). *Principles of anatomy and physiology*. Hoboken, NJ: John Wiley & Sons, Inc.
- Tortora, G. J., & Derrickson, B. (2010). *Introduction to the human body*. Hoboken, NJ: John Wiley & Sons, Inc.
- Transnational College of LEX. (2006). *Who is Fourier? A mathematical adventure*. Language Research Foundation.

- Trevisi, E., Gualdi, S., De Conti, C., Salghetti, A., Martinuzzi, A., Pedrocchi, A., & Ferrante, S. (2011). Cycling induced by functional electrical stimulation in children affected by cerebral palsy: Case report. *European Journal of Physical and Rehabilitation Medicine*.
- Tsuji, T., Morasso, P. G., & Ito, K. (1995). Human hand impedance characteristics during maintained posture. *Biological Cybernetics*, 74(1), 475–485. doi:10.1007/BF00199890 PMID:7612720
- Tucker, K., Butler, J., Graven-Nielsen, T., Riek, S., & Hodges, P. (2009). Motor unit recruitment strategies are altered during deep-tissue pain. *The Journal of Neuroscience*, 29(35), 10820–10826. doi:10.1523/JNEUROSCI.5211-08.2009 PMID:19726639
- Tveit, P., Daggfeldt, K., Hetland, S., & Thorstensson, A. (1994). Erector spinae lever arm length variations with changes in spinal curvature. *Spine*, 19(2), 199–204. doi:10.1097/00007632-199401001-00015 PMID:8153831
- Umberger, B. R. (2008). Effects of suppressing arm swing on kinematics, kinetics, and energetics of human walking. *Journal of Biomechanics*, 41(11), 2575–2580. doi:10.1016/j.jbiomech.2008.05.024 PMID:18621376
- Vaisman, L., Zariffa, J., & Popovic, M. R. (2010). Application of singular spectrum-based change-point analysis to EMG-onset detection. *Journal of Electromyography and Kinesiology*, 20(4), 750–760. doi:10.1016/j.jelekin.2010.02.010 PMID:20303784
- Van Boxtel, G. J., Geraats, L. H., Van den Berg-Lenssen, M. M., & Brunia, C. H. (1993). Detection of EMG onset in ERP research. *Psychophysiology*, 30(4), 405–412. doi:10.1111/j.1469-8986.1993.tb02062.x PMID:8327626
- van der Helm, F. C. T., Schouten, A. C., de Vlugt, E., & Brouwn, G. G. (2002). Identification of intrinsic and reflexive components of human arm dynamics during postural control. *Journal of Neuroscience Methods*, 119(1), 1–14. doi:10.1016/S0165-0270(02)00147-4 PMID:12234629
- van der Horst, M. J., Metting van Rijn, A. C., Peper, A., & Grimbergen, C. A. (1998). High frequency interference effects in amplifiers for biopotential recordings. *Proceedings of the 20th Annual International Conference of the IEEE Engineering in Medicine and Biology Society*, 20(6), 3309–3312.
- van Dieen, J. H., Heijblom, P., & Bunkens, H. (1998). Extrapolation of time series of EMG power spectrum parameters in isometric endurance tests of trunk extensor muscles. *Journal of Electromyography and Kinesiology*, 8(1), 35–44. doi:10.1016/S1050-6411(97)00003-5 PMID:9667032
- van Dieen, J. H., Oude Vrielink, H. H., Housheer, A. F., Lotters, F. B., & Toussaint, H. M. (1993). Trunk extensor endurance and its relationship to electromyogram parameters. *European Journal of Applied Physiology and Occupational Physiology*, 66(5), 388–396. doi:10.1007/BF00599610 PMID:8330605
- Van Veen, B. K., Wolters, H., & Wallinga, W. (1993). The bioelectrical source in computing single muscle fibre action potentials. *Biophysical Journal*, 64, 1492–1498. doi:10.1016/S0006-3495(93)81516-9 PMID:8324186
- Van Zuylen, E. J., Cielen, C. C., & Denier van der Gon, J. J. (1988). Coordination and inhomogeneous activation of human muscles during isometric torques. *Journal of Neurophysiology*, 60, 1523–1548. PMID:3199172
- Vannozzi, G., Conforto, S., & D'Alessio, T. (2010). Automatic detection of surface EMG activation timing using a wavelet transform based method. *Journal of Electromyography and Kinesiology*, 20(4), 767–772. doi:10.1016/j.jelekin.2010.02.007 PMID:20303286
- Vera-Garcia, F. J., Moreside, J. M., & McGill, S. M. (2010). MVC techniques to normalize trunk muscle EMG in healthy women. *Journal of Electromyography and Kinesiology*, 20(1), 10–16. doi:10.1016/j.jelekin.2009.03.010 PMID:19394867
- Vieira, T. M., Loram, I. D., Muceli, S., & Merletti, R., & Farina. (2011). Postural activation of the human gastrocnemius muscle: Are the muscle units spatially localised. *The Journal of Physiology*, 589(2), 431–443. doi:10.1113/jphysiol.2010.201806 PMID:21115645

Compilation of References

- Vigreux, B., Cnockaert, J. C., & Pertuzon, E. (1979). Factors influencing quantified surface EMGs. *European Journal of Applied Physiology and Occupational Physiology*, 41(2), 119–129. doi:10.1007/BF00421659 PMID:467411
- Vredenberg, J., & Rau, G. (1973). Surface electromyography in relation to force, muscle length and endurance. In J. E. Desmede (Ed.), *New developments in EMG and clinical neurophysiology* (pp. 607–622). Basel, Switzerland: Karger.
- Wagenaar, R. C., & van Emmerik, R. E. (2000). Resonant frequencies of arms and legs identify different walking patterns. *Journal of Biomechanics*, 33(7), 853–861. doi:10.1016/S0021-9290(00)00020-8 PMID:10831760
- Wakeling, J. M., Pascual, S. A., & Nigg, B. M. (2002). Altering muscle activity in the lower extremities by running with different shoes. *Medicine and Science in Sports and Exercise*, 34(9), 1529–1532. doi:10.1097/00005768-200209000-00021 PMID:12218750
- Wallinga, W., Gielen, F. L. H., Wirtz, P., de Jong, P., & Broenink, J. (1985). The different intracellular action potentials of fast and slow muscle fibres. *Electromyography and Clinical Neurophysiology*, 60, 539–547. doi:10.1016/0013-4694(85)91115-0
- Watkins, R., Uppal, G., Perry, J., Pink, M., & Dinsay, J. (1996). Dynamic electromyographic analysis of trunk musculature in professional golfers. *The American Journal of Sports Medicine*, 24(4), 535–538. doi:10.1177/036354659602400420 PMID:8827315
- Webb, D., Tuttle, R. H., & Baksh, M. (1994). Pendular activity of human upper limbs during slow and normal walking. *American Journal of Physical Anthropology*, 93(4), 477–489. doi:10.1002/ajpa.1330930407 PMID:8048469
- Wei, L., Hu, H., & Zhang, Y. (2011). Fusing EMG and visual data for hands-free control of an intelligent wheelchair. *International Journal of Humanoid Robotics*, 8(4), 707–724. doi:10.1142/S0219843611002629
- Weinberg, D. H., Rizzo, J., Hayes, M. T., Knell, M. D., & Kelly, J. J. (1999). Ocular yasthenia gravis: Predictive value of single-fiber electromyography. *Muscle & Nerve*, 22(9), 1222–1227. doi:10.1002/(SICI)1097-4598(199909)22:9<1222::AID-MUS8>3.0.CO;2-R PMID:10454717
- Weiss, P. L., & St Pierre, D. (1983). Upper and lower extremity EMG correlations during normal human gait. *Archives of Physical Medicine and Rehabilitation*, 64(1), 11–15. PMID:6849627
- Westcott, P. (2000). *Stroke-questions and answers*. London: The Stroke Association.
- Westgaard, R. H., & De Luca, C. J. (1999). Motor unit substitution in long-duration contractions of the human trapezius muscle. *Journal of Neurophysiology*, 82, 501–504. PMID:10400978
- Winter, D. (2005). *Biomechanics and motor control of human movement* (3rd ed.). Hoboken, NJ: John Wiley and Sons, Inc.
- Winter, D. A. (1995). Human balance and posture control during standing and walking. *Gait & Posture*, 3(4), 193–214. doi:10.1016/0966-6362(96)82849-9
- Winter, D., & Webster, J. G. (1983). Driven right leg circuit design. *IEEE Transactions on Bio-Medical Engineering*, 30(1), 62–66. doi:10.1109/TBME.1983.325168 PMID:6826188
- Winters, J. M., & Stark, L. (1988). Estimated mechanical properties of synergistic muscles involved in movements of a variety of human joints. *Journal of Biomechanics*, 21, 1027–1041. doi:10.1016/0021-9290(88)90249-7 PMID:2577949
- Wirz, M., Colombo, G., & Dietz, V. (2001). Long term effects of locomotor training in spinal humans. *Journal of Neurology, Neurosurgery, and Psychiatry*, 71(1), 93–96. doi:10.1136/jnnp.71.1.93 PMID:11413270
- Wolpaw, J. R., Birbaumer, N., McFarland, D. J., Pfurtscheller, G., & Vaughan, T. M. (2002). Brain-computer interfaces for communication and control. *Clinical Neurophysiology*, 113(6), 767–791. doi:10.1016/S1388-2457(02)00057-3 PMID:12048038
- Woods, J. J., & Bigland-Ritchie, B. (1983). Linear and non-linear surface EMG/force relationships in human muscles. An anatomical/functional argument for the existence of both. *American Journal of Physical Medicine*, 62(6), 287–299. PMID:6650674

- Wrench, A., McIntosh, A. D., Watson, C., & Hardcastle, W. J. (1998). Optopalatograph: Real-time feedback of tongue movement in 3D. In *Proceedings of the Fifth International Conference on Spoken Language Processing* (pp. 1867-1870).
- Wunderlich, R. E., & Cavanagh, P. R. (2001). Gender differences in adult foot shape: Implications for shoe design. *Medicine and Science in Sports and Exercise*, 33(4), 605–611. doi:10.1097/00005768-200104000-00015 PMID:11283437
- Xu, Y. M., & Hollerbach, J. M. (1999). A robust ensemble data method for identification of human joint mechanical properties during movement. *IEEE Transactions on Bio-Medical Engineering*, 46(4), 409–419. doi:10.1109/10.752938 PMID:10217879
- Yang, S. W., Lin, C. S., Lin, S. K., & Lee, C. H. (2013). Design of virtual keyboard using blink control method for the severely disabled. *Computer Methods and Programs in Biomedicine*, 111(2), 410–418. doi:10.1016/j.cmpb.2013.04.012 PMID:23702128
- Yan, T., Hui-Chan, C. W. Y., & Li, L. S. W. (2005). Functional electrical stimulation improves motor recovery of the lower extremity and walking ability of subjects with first acute stroke: A randomized placebo-controlled trial. *Stroke*, 36, 80–85. doi:10.1161/01.STR.0000149623.24906.63 PMID:15569875
- Yazama, Y., Mitsukura, Y., Fukumi, M., & Akamatsu, N. (2003). Feature analysis for the EMG signals based on the class distance. In *Proceedings of International Symposium of the IEEE Computational Intelligence in Robotics and Automation* (pp.860-863).
- Yazıcıoğlu, R. F., Van Hoof, C., & Puers, R. (2009). *Biopotential readout circuits for portable acquisition systems*. Dordrecht, The Netherlands: Springer.
- Yeh, C. Y., Chen, J. J. J., & Tsai, K. H. (2004). Quantitative analysis of ankle hypertonia after prolonged stretch in subjects with stroke. *Journal of Neuroscience Methods*, 137, 305–314. doi:10.1016/j.jneumeth.2004.03.001 PMID:15262075
- Yeom, H. J., Park, Y. C., Yoon, Y. R., Shin, T. M., & Yoon, H. R. (2004). An adaptive M-wave canceler for the EMG controlled functional electrical stimulator and its FPGA implementation. In *Proceedings of 26th Annual International Conference of the IEEE Engineering in Medicine and Biology Society, 2004. IEMBS '04* (Vol. 2, pp. 4122–4125).
- Yeom, H., & Chang, Y. H. (2010). Autogenic EMG-controlled functional electrical stimulation for ankle dorsiflexion control. *Journal of Neuroscience Methods*, 193, 118–125. doi:10.1016/j.jneumeth.2010.08.011 PMID:20713086
- You, K. J., Rhee, K. W., & Shin, H. C. (2010). Finger motion decoding using EMG signals corresponding various arm postures. *Experimental Neurology*, 19(1), 54–61. PMID:22110342
- You, K. J., Rhee, K. W., & Shin, H. C. (2011). Finger flexion motion inference from sEMG signals. *Journal of Measurement Science and Instrumentation*, 2(2), 140–143.
- Young, A. J., Hargrove, L. J., & Kuiken, T. A. (2011). The effects of electrode size and orientation on the sensitivity of myoelectric pattern recognition systems to electrode shift. *IEEE Transactions on Bio-Medical Engineering*, 58(9), 2537–2544. doi:10.1109/TBME.2011.2159216 PMID:21659017
- Young, A. J., Hargrove, L. J., & Kuiken, T. A. (2012). Improving myoelectric pattern recognition robustness to electrode shift by changing interelectrode distance and electrode configuration. *IEEE Transactions on Bio-Medical Engineering*, 59(3), 645–652. doi:10.1109/TBME.2011.2177662 PMID:22147289
- Yu, S., Jeong, E., Hong, K., & Lee, S. (2012). Classification of nine directions using the maximum likelihood estimation based on electromyogram of both forearms. *Biomedical Engineering Letters*, 2(2), 129–137. doi:10.1007/s13534-012-0063-x
- Zajac, F. E., & Faden, J. S. (1985). Relationship among recruitment order, axonal conduction velocity, and muscle-unit properties of type-identified motor units in cat plantaris muscle. *Journal of Neurophysiology*, 53, 1303–1322. PMID:2987433

Compilation of References

- Zardoshti-Kermani, M., Wheeler, B. C., Badie, K., & Hashemi, R. M. (1995). EMG feature evaluation for movement control of upper extremity prostheses. *IEEE Transactions on Rehabilitation Engineering*, 3(4), 324–333. doi:10.1109/86.481972
- Zecca, M., Micera, S., Carrozza, M. C., & Dario, P. (2002). Control of multifunctional prosthetic hands by processing the electromyographic signal. *Critical Reviews in Biomedical Engineering*, 30(4-6), 459–485. doi:10.1615/CritRevBiomedEng.v30.i456.80 PMID:12739757
- Zehr, E. P., & Duysens, J. (2004). Regulation of arm and leg movement during human locomotion. *The Neuroscientist*, 10(4), 347–361. doi:10.1177/1073858404264680 PMID:15271262
- Zhang, X., Chen, X., Zhao, Z. Y., Li, Q., Yang, J. H., Lantz, V., & Wang, K. Q. (2008). An adaptive feature extractor for gesture SEMG recognition. In *Proceedings of the 1st International Conference on Medical Biometrics*, Hong Kong (pp. 83-90).
- Zhang, L. Q., & Rymer, W. Z. (1997). Simultaneous and nonlinear identification of mechanical and reflex properties of human elbow joint muscles. *IEEE Transactions on Bio-Medical Engineering*, 44(12), 1192–1209. doi:10.1109/10.649991 PMID:9401219
- Zhang, X. A., Ye, M., & Wang, C. T. (2010). Effect of unilateral load carriage on postures and gait symmetry in ground reaction force during walking. *Computer Methods in Biomechanics and Biomedical Engineering*, 13(3), 339–344. doi:10.1080/10255840903213445 PMID:20521188
- Zhang, X., & Zhou, P. (2012). Sample entropy analysis of surface EMG for improved muscle activity onset detection against spurious background spikes. *Journal of Electromyography and Kinesiology*, 22(6), 901–907. doi:10.1016/j.jelekin.2012.06.005 PMID:22800657
- Zhao, J., Jiang, L., Cai, H., Liu, H., & Hirzinger, G. (2006a). A novel EMG motion pattern classifier based on wavelet transform and nonlinearity analysis method. In *Proceedings of IEEE International Conference on Robotics and Biomimetics*, Kunming, China (pp. 1494-1499).
- Zhao, J., Xie, Z., Jiang, L., Cai, H., Liu, H., & Hirzinger, G. (2006b). EMG control for a five-fingered underactuated prosthetic hand based on wavelet transform and sample entropy. In *Proceedings of IEEE/RSJ International Conference on Intelligent Robots and Systems*, Beijing, China (pp. 3215-3220).
- Zijdewind, I., Kernell, D., & Kukulka, C. G. (1995). Spatial differences in fatigue-associated electromyographic behaviour of the human first dorsal interosseus muscle. [Research Support, Non-U.S. Gov't]. *The Journal of Physiology*, 483(Pt 2), 499–509. PMID:7650617
- Zuurbier, C. J., & Huijing, P. A. (1992). Influence of muscle geometry on shortening speed of fibre, aponeurosis and muscle. *Journal of Biomechanics*, 25, 1017–1026. doi:10.1016/0021-9290(92)90037-2 PMID:1517262

About the Contributors

Ganesh R. Naik received B.E. degree in Electronics and Communication Engineering from the University of Mysore, India, in 1997. He received his M.E. degree in Communication and Information Engineering from Griffith University, Brisbane, Australia, in 2002, and the PhD degree in the area of Electronics Engineering, specialised in Biomedical Engineering and Signal processing from RMIT University, Melbourne, Australia, in 2009. He is currently Chancellor's Post Doctoral Research Fellow at Faculty of Engineering and Information Technology (FEIT), UTS. As an early career researcher, he has edited 9 books, authored more than 80 papers in peer reviewed journals, conferences, and book chapters over the last five years. His research interests include EMG signal processing, Pattern recognition, Blind Source Separation (BSS) techniques, Biomedical signal processing, Human Computer Interface (HCI) and Audio signal processing. Currently he serves as an associate editor for two Springer journals (*Circuits, Systems, and Signal Processing* and *Australasian Physical & Engineering Sciences in Medicine*). He is also a reviewer and member of editorial board in several reputed journals. He is a recipient of the Baden-Württemberg Scholarship from the University of Berufsakademie, Stuttgart, Germany (2006–2007). In 2010, Dr. Naik is awarded with ISSI overseas fellowship from skilled Institute Victoria, Australia.

* * *

Emilia Ambrosini graduated cum laude in Biomedical Engineering in 2007 and obtained a PhD Degree cum laude in Bioengineering in 2011 from Politecnico di Milano. In 2009 she was a visiting PhD student at the Control System Group of the Technische Universität of Berlin. Since March 2011, she is a Research Fellow at Neuroengineering and medical robotics Laboratory (NearLab, www.biomed.polimi.it/nearlab) and she has been involved in the European project MUNDUS (FP7ICT-2009.7.2). Her research interest is about the design and clinical translation of safe, simple and immersive devices based on the integration of functional electrical stimulation and robotic systems for the rehabilitation and the daily life assistance of neurological patients.

Parveen Bawa received her undergraduate degree in Physics from Punjab University and M.Sc. from the University of Alberta. She switched to Physiology and received her Ph.D. (1975) from the University of Alberta. After her postdoctoral training in Neuroscience at the University of Calgary, she got a faculty position at Simon Fraser University in 1978 from where she retired in 2009. As Professor Emerita, she has continued her research, the main focus of which has been motor units and stretch reflexes. She enjoyed her sabbatical years at Harvard Medical School (Physiology), Cambridge University in UK, and State University of New York at Syracuse.

About the Contributors

Sébastien Boyas received the Ph.D. degree in 2007 in Sports Sciences from the University of Nantes, France. From 2008 to 2012 he was Professor at the School of Human Kinetics of the University of Ottawa, Ottawa, Canada. He was postdoctoral fellow and Research Associate at the Research Institute of the Elizabeth Bruyère Hospital of Ottawa from 2012 to 2013. He was a member of the Aging and Movement Research Laboratory directed by Martin Bilodeau from 2009 to 2013. In 2013, he joined the School of Sport Sciences of the University of Le Mans, France. His research interests focus on the human movement in the field of sport performance and health. He is interested in the influence of training, fatigue and aging on neuromuscular function, muscle activity, force production and postural control. He is a member of the Laboratory “Motricité, Interactions, Performance” (EA 4334).

Maria António Castro graduated in Physiotherapy in 1987 at Coimbra’s College of Health (ESTESC). PhD in Physiotherapy-Human Kinetics at the Faculdade de Motricidade Humana da Universidade Técnica de Lisboa –Portugal (2008). Currently, she is Adjunct Professor of Coimbra Health School where she teaches Human Movement, Manual Therapy and Exam and Evaluation. She is a researcher of University of Coimbra’s Mechanical Engineering Research Center. Physiotherapist of Women’s Basketball Senior National Team (1995 to 2005). Founder and president (1998 to 2005) of the Portuguese Physiotherapists’ Trade Union. Her research interests include movement analysis, sports injuries and injury prevention.

Varsha Chorsiya is Master of Physiotherapy with specialization in Neurology Jamia Hamdard University, New Delhi in 2011. She is working as Senior Research Fellow at National Institute of Occupational Health, Ahmedabad (Gujarat), a Ph.D scholar at Gujarat University, India, and as Assistant Professor at Manav Rachna International University. Her research and educational activities is on Physical therapy and Rehabilitation, Ergonomics, Occupational Health and Safety Management, Bio-mechanics and other allied areas.

Javier Rodriguez-Falces is a professor at the Department of Electrical and Electronic Engineering at the Public University of Navarra. He worked for the Higher Scientific Investigation Council of Spain during one year (2006). He obtained a PhD in Electromyography from the Public University of Navarra in 2007. Currently, he teaches courses in the Master of Biomedical Engineering and in the Bachelor Degree of Telecommunication at the Public University of Navarra. His research interests include biomedical signal processing, quantitative analysis of electromyographic signals, modelling of biological structures, and analysis of muscle electrical and mechanical responses and neuromuscular adaptations to exercise.

Simona Ferrante received the M.S. degree in Biomedical Engineering and the Ph.D. degree in Bioengineering from the Politecnico di Milano in 2002 and 2006, respectively. She is an Assistant Professor at the Electronics, Information and Bioengineering Department of the Politecnico di Milano. She currently works at the Neuroengineering and Medical Robotics Laboratory in the field of biomechanics in motor control, neuroengineering, and neurorehabilitation. Her research interests are related to the development of novel treatment in the rehabilitation of neurologic patients, in the quantitative assessment of motor recovery. She is author of about 26 papers in peer-reviewed international journals.

Antonia Frendel has studied medicine in Kiel, Germany. She started as a doctoral student at the Institute of Physiology (Kiel, Germany) in 2011, under the supervision of J.P. Kuhtz-Buschbeck. She has performed detailed experiments on the EMG activity of arm and trunk muscles during different forms of human locomotion.

P. Geethanjali received her B.E. degree in Electrical and Electronics Engineering from University of Madras, Tamilnadu, India in 2001. She obtained M. Tech in Electrical Drives and Control from Pondicherry Engineering College, Pondicherry University, Puducherry, India in 2004 and Ph. D from VIT University, Vellore in 2012. She is Associate Professor in School of Electrical Engineering, VIT University, Vellore, Tamilnadu, India. Her research interests include bio-signal processing using soft computing techniques, development of assistive devices, renewable energy, and applications of renewable energy.

İmran Göker received his MD degree from the Ege University, İzmir, Turkey in 1996, M.S. Degree from the Institute of Biomedical Engineering of Boğaziçi University, İstanbul in 2000 and his PhD degree from the Institute of Biomedical Engineering of Boğaziçi University, İstanbul in 2009. He was lecturer in the Department of Information Technology and he was the Head of Department of Dental Health in School of Vocational Studies in the same university between 2001 and 2010. He was teaching courses Medical Informatics, Statistics and Healthcare Informatics in Okan University, Istanbul between 2011 and 2013. He is lecturer in the Department of Biomedical Engineering in the Faculty of Engineering and Architecture of Istanbul Arel University teaching Introduction to Biomedical Engineering and Biostatistics. He is also Head of Department of Biomedical Engineering in the same university. His research is associated with Scanning EMG and Diagnosis of Neuromuscular Disorders.

Arnaud Guével received the Ph.D. degree in Sports Sciences from University of Méditerranée, Marseille, France, in 1997. He joined the Faculty of Sports Sciences from the University of Nantes in 1998. His research interests focus on the evaluation of neuromuscular fatigue based on the surface EMG analysis and on the investigation of sports performance and the effects of training on the neuromuscular function. He is a member of the Laboratory “Motricité, Interactions, Performance” (EA 4334) which he managed when it was created in 2004.

Huijing Hu got her PhD at Department of Physiology, the University of Hong Kong at Dec 2011. Then she joined the Guangdong Provincial Work Injury Rehabilitation Center as a physician and researcher. Now she is taking her post doctoral training at Department of Rehabilitation Medicine, First Affiliated Hospital, Sun Yat-sen University. Her research interests include neurorehabilitation, electrophysiology, bio-signal processing.

Dianne Ikeda is the research coordinator in the Dynamics of Human Motion Lab at Dalhousie University. She completed her Masters in Kinesiology (Biomechanics) at the University of Waterloo under the supervision of Dr. Stuart McGill. Her primary focus was on low back injury mechanisms and how they relate to spine stability, spine loading and spine mechanics. She has since become involved with investigating knee osteoarthritis and the influence of severity, obesity and gender, on lower limb muscle activity and mechanics during gait.

Bo Jing was born and raised in Peking, China. He studied medicine in Kiel, Germany, and graduated as a medical doctor from Christian-Albrechts-Universität in 2010. He worked as a research assistant at the Institute of Physiology, Kiel, where he completed his doctoral thesis on EMG activity of upper limb muscles during human gait. Meanwhile he is specializing in ophthalmology.

Kelvin Jones received his B.Sc. (1991) and Ph.D. (1996) degrees from Simon Fraser University, Canada. He joined the University of Alberta in 2002 after fellowships at Goteborg University (Sweden),

About the Contributors

the University of Manitoba (Canada) and the Institute of Neurology (UK). He is currently an Associate Professor in the Faculty of Physical Education and Recreation with adjunct positions in the Department of Biomedical Engineering and the Department of Computing Science. His current interests revolve around electrodiagnosis of neurodegenerative conditions and the effects of exercise on the progression of motor neuron disease.

Johann P. Kuhtz-Buschbeck graduated as a medical doctor in 1991, after finishing his studies of medicine at the Christian-Albrechts-Universität in Kiel (Germany). He qualified as a lecturer habilitated in medical physiology in 2000. Since 2005 he has been working as an extraordinary professor at the Institute of Physiology in Kiel. His field of research includes sensorimotor control, with studies of gait, hand function, and neurorehabilitation. A further focus of his research is neuroimaging.

Yann Laurillau is an assistant professor in computer science at the University of Grenoble in France, where he works in the LIG laboratory. His research interests include human-computer interaction and computer-supported cooperative work. Laurillau received a Ph.D. in computer science from the University of Grenoble. Based on an interdisciplinary approach, his recent work explores tangible gesture interaction based on EMG as an input modality. He claims that EMG is an interesting basis to design much more natural human-computer interactions. He envisions interactive systems able to adapt interaction to user's needs, and able to proactively assist users with their tasks thanks to gesture and intention recognition.

Le Li received his B.E. degree and M.E. degree in Biomedical Engineering in 2000 and 2003, respectively, from Xi'an JiaoTong University, Xi'an, China and Ph.D degree in the Department of Health Technology and Informatics, The Hong Kong Polytechnic University in 2007. After finishing his postdoctoral training at the Hong Kong Polytechnic University, he became an associate professor at the department of rehabilitation medicine, first affiliated hospital, Sun Yat-Sen University, Guangzhou, China. His research interests include neuromusculoskeletal modeling of normal and spastic subjects, biosignal processing and motor recovery research.

Sérgio Marta, born in 1974, graduated in Sport Science, received the Master degree in Young Athlete Training in 2007 from the Faculdade de Motricidade Humana from Universidade Técnica de Lisboa. A former professor of Anatomophysiology in the Portuguese Piaget Institute – Almada Campus (2000-2008), Sérgio Marta is currently a Human Kinetics Ph.D. student and an investigator of the research unit of the Faculdade de Motricidade Humana da Universidade de Lisboa, the Interdisciplinary Center for the Study of Human Performance (CIPER). His main interests are motion analysis, electromyography and kinesiology in sports.

Stuart McGill is a Professor of Spine Biomechanics at the University of Waterloo where he heads a laboratory that explores the issues of lumbar function, low back injury mechanisms, investigation of tissue loading during rehabilitation programs, the formulation of work-related injury avoidance strategies and high performance training. He has mentored over 35 graduate students. As a consultant, he has provided expertise on low back injury to various government agencies, many corporations and legal firms and professional/international athletes and teams worldwide. He is regularly referred special patient cases from the medical community for opinion.

Anjali Nag is Master of Science in Human Physiology with specialization in Biochemistry and Ph.D in Human Physiology from university of Calcutta, India. She was Head of the Occupational Physiology Department, National Institute of Occupational Health (Ahmedabad) 2007 to 2013. Her research and educational activities are on Women Health, Occupational Health and Safety Management and other allied areas.

P.K Nag is Master of Science in Human Physiology and Ph.D and D.Sc. in the specialty area of Ergonomics from the University of Calcutta, India. He was Director of the National Institute of Occupational Health (Ahmedabad) and regional Occupational Health centres at Bangalore and Kolkata from 2007 to 2013. His research and educational activities are on ergonomics, Occupational Health and Safety Management and other allied areas.

Alessandra Pedrocchi received the M.S. degree in Electrical Engineering and the Ph.D. degree in Bioengineering from the Politecnico di Milano in 1997 and 2001, respectively. Since June 2008, she is Assistant Professor in tenure track at the Department of Electronics Informatics and Bioengineering of the Politecnico di Milano, where she teaches Neuroengineering in the Master of Science in Biomedical Engineering. Her research activities are carried out at the NearLab in the field of biomechanics in motor control, neuroengineering and neurorehabilitation (www.nearlab.polimi.it). She has been the Project Manager of the MUNDUS project (FP7 ICT-2009.7.2) and she is the Politecnico PI for REALNET project (FP7 Obj ICT-2009.6).

Pedro Pezarat-Correia, born in 1958, obtained his PhD degree in Human Kinetics (Faculdade de Motricidade Humana da Universidade Técnica de Lisboa – Portugal) in 1995. Currently is Associated Professor of the Universidade de Lisboa where he is the coordinator of the Laboratory of Motor Behavior. He is the (co-) author of about 15 peer reviewed international publications. Research topics: electromyography, neuromuscular function and muscle coordination.

Angkoon Phinyomark is a postdoctoral research fellow at Running Injury Clinic, Faculty of Kinesiology, University of Calgary, Canada during September 2013-August 2015. He was a postdoctoral research fellow at GIPSA-lab and LIG-lab, University Joseph Fourier, France during September 2012-August 2013. He received a B.Eng. degree in Computer Engineering with First Class Honors in 2008 from Prince of Songkla University, Thailand, where he received a Ph.D. degree in Electrical Engineering in 2012. He has published over 50 papers during 6 years in refereed journals, books, and conference proceedings in the areas of biomechanical signals processing and pattern recognition notably EMG (electromyography signal), nonlinear (fractal) analysis, time-frequency (wavelet) analysis, image (texture) analysis, feature extraction and machine learning algorithms, and assistive and rehabilitative devices. He is a member of the IEEE.

Franck Quaine is an associated professor at the Grenoble University (France). He is in charge of the research team SAIGA (Signal and Automatic for surveillance, diaGnostics and BiomechANics) in GIPSA-lab in the Control system Department (<http://www.gipsa-lab.grenoble-inp.fr>). He graduated his Ph.D. in human movement sciences from Grenoble University in 1996. His work is focused on the evaluation of muscular tensions by coupling biomechanical models and electromyography signals (inverse dynamic, resolution of redundant system, optimization techniques, and signal processing). The main application areas are health and care, muscle computer interfaces and human movement.

About the Contributors

Dan Robbins received master's degrees in Soft Tissue Biomechanics from the University of Greenwich in 2007 and Biomechanics from the University of Manchester in 2008. After graduating, Dan worked in the department of Clinical Neurophysiology at the Royal National Orthopaedic Hospital before returning to the University of Greenwich to complete a PhD on the effect of Whole Body Vibration on the Neuromuscular System. Dan currently works as a lecturer in biomechanics and physiology within the division of Sports Therapy at the University of Bedfordshire (UK). Dan's main research interests are exercise science; neuromusculoskeletal biomechanics; vibration exercise; neuromuscular physiology and rehabilitation.

Andres F. Ruiz-Olaya received the Electronic Engineering degree from University of Valle (Colombia) and his Ph.D. degree from Carlos III University of Madrid (Spain). He is a full professor of the Faculty of Electronics and Biomedical Engineering at the Antonio Nariño University (Colombia), where he joined the Bioengineering Research Group. His research interests include rehabilitation robotics, multimodal human-robot interaction, bio-inspired control architectures and modelling of human motor control. Currently, he is working on several projects oriented to the development of neurorehabilitation devices to attend motor disabled people. Prof. Ruiz-Olaya is a member of IEEE. He has been author and co-author of multiple papers and has performed as reviewer of several international journals and conferences of relevance.

Makoto Sasaki received M.E. and Ph.D. degrees in Mechanical Engineering from Akita University, Japan respectively in 2002 and 2005. Since October 2009, he has been an Assistant Professor of the Biomedical Engineering and Robotics Laboratory, Graduate School of Engineering, Iwate University, Japan. His research interests include biorobotics, human interfaces, and medical and biological engineering. He has received several awards including the Young Engineers Award of the Japan Society of Mechanical Engineers in 2010, the Best Research Award of the Japanese Society for Medical and Biological Engineering in 2011, and the Young Scientist Award of the Society of Biomechanisms Japan in 2012. He is a member of the IEEE Engineering in Medicine and Biology Society, the Japan Society of Mechanical Engineers, the Society of Biomechanisms Japan, the Japanese Society for Medical and Biological Engineering, and the Society of Life Support Engineering.

Luís Silva is graduated in Sport Science –Physical Condition by the Sport Sciences School of Rio Maior, Management by the University Lusíada, and received the M. Sc. at the Faculdade de Motricidade Humana from Universidade Técnica de Lisboa - Portugal. He's currently a Ph. D. student and researcher in the Laboratory of Motor Behavior of the Faculdade de Motricidade Humana da Universidade de Lisboa (CIPER–Interdisciplinary Center for the Study of Human Performance), and professor of Anatomophysiology in University Lusíada. His research topics are electromyography, kinesiology and statistics.

João Rocha Vaz is graduated in Psychomotricity (2009) and in Physical Therapy (2013). Currently he is a PhD Student in Motor Behavior at the Faculdade de Motricidade Humana da Universidade de Lisboa. He has also been working as a research assistant at Laboratory of Motor Behaviour, since 2009. Research Topics: electromyography, muscle coordination, neuromuscular function, kinesiology.

Index

A

abdominal brace 212, 216, 218
 Acquisition Rate 27
 Action Potential (AP) 27
 angular momentum 131, 133, 139, 146, 155
 Anthropometry 321, 330, 352
 Applications of Surface Electromyography 114, 128

B

bi-deltoid breadth 321, 331-332, 335, 337, 340, 343, 352
 biological signals 95, 108, 257
 biomechanical modelling 114-115, 125, 128
 biomedical instrumentation 26, 58, 84-85, 93

C

Center of Mass (COM) of the Body 155
 Central Pattern Generator (CPG) for Locomotion 155
 Concentric Needle Electrode (CNE) 62, 93
 Conventional Electromyography 78, 80, 93

D

Double Stance Phase (=Double Support Phase) 155

E

EarlyChanges in EMG Signal 232
 Eigenvalue (EV) 218
 Elbow Joint Dynamics 114-115, 118, 121-122, 128
 electromyography (EMG) 27, 37, 52, 58, 60, 78, 116, 119, 129, 183, 208, 219, 232, 255, 257-258, 321-322, 348-349, 352
 EMG-Assisted Model 215, 218
 EMG-driven model 161, 165, 171-173, 179-180
 EMG parameter 222-223, 232
 Endurance Time (Tlim) 219, 232

F

feature extraction 200, 253, 305, 311, 317-322, 325-326, 334, 338, 342, 348, 352-353
 feature reduction 304-306, 313, 317-318, 320, 346, 348
 FFT 83, 95-96, 98-99, 111
 filter settings 29, 35, 45, 51, 57
 Firing Rate, Expressed As Impulses/s (imp 27
 forearm circumference 321, 324, 331-332, 342, 344, 352
 Functional Electrical Stimulation (FES) 275, 303

G

gesture recognition 304, 306, 325, 334, 336, 348, 352

H

human motor control 114-117, 125, 128
 hybrid muscle activation 281-283, 285-286, 299, 303

I

IAP spike duration 33, 36, 41, 57
 impedance control 126-128
 Indicator of EMG Changes 233
 Inter-Limb Coupling 155
 intracellular action potential 7, 28, 30-32, 34, 55-57

J

jitter estimation 28-29, 48-49, 51, 53, 57

L

lead 12, 68, 84, 186-187, 192, 201, 226, 260, 277
 Limits of Stability (LOS) 255

Index

M

Macro Electromyography 70, 80, 93
MatLab 95, 98-99, 101, 103, 105, 107-108, 110, 315
maximum voluntary contraction (MVC) 155, 204, 324, 344
mechanical impedance 114-118, 121-122, 125-126, 128, 173
motor control 23, 25, 51, 111, 114-117, 125, 127-128, 178, 180, 183, 232, 255, 279, 294-295, 297-298, 351
motor relearning 276, 278-279, 293-294, 303
motor unit 1-4, 6-10, 12-15, 17, 19-22, 24-29, 45-49, 52-53, 56, 59-60, 64-65, 68, 74, 76-88, 90, 92-93, 120, 164, 183, 228, 277-278, 292, 297-299, 322
motor unit action potential 8, 27, 60, 68, 76-77, 80-83, 85, 90, 93
multifunction myoelectric control 199-200, 271, 318-319, 346, 353
Muscle-Computer Interface 349, 353
Muscular Load 234, 255
musculoskeletal system 1, 59, 128, 205
musculotendon parameters 161, 163, 165, 173, 179-180
M-wave 52, 83, 173, 281-282, 284, 286-289, 298, 301-303
Myocontrolled Neuroprosthesis 275, 280-281, 296, 303

N

neural network 128, 180, 259, 261, 263-265, 267, 304-306, 315, 319-320, 337
Neuromuscular fatigue 219, 230, 233
Neuromusculoskeletal (NMS) Model 180
neuroprosthesis 275, 280-281, 296-297, 303
neuro-rehabilitation 276, 279, 293, 295-296, 303
noise 2, 6-7, 14, 17, 19, 21, 24, 29, 42, 49-50, 65-71, 84, 95-97, 106, 112, 127, 193, 236, 282, 284, 286, 288-289, 305-306, 308, 310, 312, 317, 321, 327, 334-336, 343, 345-346, 348-349

O

offset 12, 97-98, 101, 103-104, 106-109, 112, 181, 192, 201, 307
onset 4, 12, 14, 27, 34, 37, 76, 136-137, 139, 146, 149, 162, 173, 181, 191-199, 201, 277-278, 280, 296, 305, 339, 351

P

pattern recognition 83, 200, 253, 258-259, 315, 317-325, 337-339, 341, 345, 347-352
period 2, 9, 13, 16-17, 75, 77, 80, 96-99, 112, 137-138, 148, 190, 216, 222, 224, 226-227, 237, 242, 257, 265-266, 270, 278, 281-283, 286-289, 291, 295, 310, 336-337
Postural Stability 151, 234, 255
Propriospinal Pathways 133, 155

Q

Quantitative Electromyography (QEMG) 93

R

rectification 12, 14, 104, 106-107, 112, 120, 136, 169
RMS 95, 104-106, 108-111, 120, 122, 172, 220, 222, 225, 227, 229, 236-237, 240, 242, 244, 246, 251, 259, 261-267, 327-329, 334-338, 340, 343
Roll-Off 102, 112

S

scanning electromyography 80-81, 85-86, 93
Sensitivity Analysis 204, 218
SFAP Morphology 45, 57
SFAP third phase 35, 41, 46-47, 57
signal conditioning 9, 65, 68, 71, 84, 198, 304-307, 309, 317, 320
signal processing 65, 84-85, 88-89, 92, 95-97, 104, 106, 108, 193, 198, 200, 264, 272, 276, 295, 306, 319-320, 345-346, 352
single-fiber electromyography 54, 79, 89, 93-94
Single Fibre Action Potential (SFAP) 27, 31
spike triggered averaging 11-12, 14, 21, 27
Spinal Loading 255
spine posture 203-204, 206-207, 214-215, 218
stability 7, 49, 120, 128-129, 151, 153, 184, 200, 203-208, 210-218, 234-237, 239, 251, 255-257, 320, 337, 340, 350
step cycle 131, 133, 136-139, 143, 146, 149, 155-160
stimulation artifact 281-284, 286-289, 299, 302-303
suprahyoid muscle 257, 272-273
surface electromyography 25, 84-85, 90, 94, 114-116, 119, 126, 128, 178, 180, 190, 196, 199, 208, 230, 232, 236, 257-258, 299, 320-322, 345-348, 350

synergies 130, 143, 149, 151, 194-196, 198-199,
201, 217, 246, 252

T

threshold 7, 9-12, 18-19, 79, 181, 192-193, 198,
201, 207, 264, 277-278, 280, 292, 295, 312,
315, 325-327, 335

Tlim prediction 219-222, 224-229, 233

TTL or Transistor-Transistor-Logic Pulse 27

U

Ultrasonography 161, 165, 180

V

volitional EMG 275-276, 280-282, 284, 286-295,
299, 303

voluntary bending 234-236, 242, 251, 255

Z

zero offset 97-98, 101, 104, 106, 112